frontiers | Research Topics

Exploring the key targets and compounds that manipulate brain neurocircuits against mental disorders and psychiatric

Edited by
Weijie Xie, Yuan Li, Dereje Kebebe Borga, Song Zhang, Yuwei Wang and Zezhi Li

Published in
Frontiers in Pharmacology
Frontiers in Neuroscience

ISSN 1664-8714
ISBN 978-2-8325-4887-5
DOI 10.3389/978-2-8325-4887-5

About Frontiers

Frontiers is more than just an open access publisher of scholarly articles: it is a pioneering approach to the world of academia, radically improving the way scholarly research is managed. The grand vision of Frontiers is a world where all people have an equal opportunity to seek, share and generate knowledge. Frontiers provides immediate and permanent online open access to all its publications, but this alone is not enough to realize our grand goals.

Frontiers journal series

The Frontiers journal series is a multi-tier and interdisciplinary set of open-access, online journals, promising a paradigm shift from the current review, selection and dissemination processes in academic publishing. All Frontiers journals are driven by researchers for researchers; therefore, they constitute a service to the scholarly community. At the same time, the *Frontiers journal series* operates on a revolutionary invention, the tiered publishing system, initially addressing specific communities of scholars, and gradually climbing up to broader public understanding, thus serving the interests of the lay society, too.

Dedication to quality

Each Frontiers article is a landmark of the highest quality, thanks to genuinely collaborative interactions between authors and review editors, who include some of the world's best academicians. Research must be certified by peers before entering a stream of knowledge that may eventually reach the public - and shape society; therefore, Frontiers only applies the most rigorous and unbiased reviews. Frontiers revolutionizes research publishing by freely delivering the most outstanding research, evaluated with no bias from both the academic and social point of view. By applying the most advanced information technologies, Frontiers is catapulting scholarly publishing into a new generation.

What are Frontiers Research Topics?

Frontiers Research Topics are very popular trademarks of the *Frontiers journals series*: they are collections of at least ten articles, all centered on a particular subject. With their unique mix of varied contributions from Original Research to Review Articles, Frontiers Research Topics unify the most influential researchers, the latest key findings and historical advances in a hot research area.

Find out more on how to host your own Frontiers Research Topic or contribute to one as an author by contacting the Frontiers editorial office: frontiersin.org/about/contact

Exploring the key targets and compounds that manipulate brain neurocircuits against mental disorders and psychiatric

Topic editors

Weijie Xie – Tongji University, China
Yuan Li – Shanghai Jiao Tong University, China
Dereje Kebebe Borga – Jimma University, Ethiopia
Song Zhang – Shanghai Jiao Tong University, China
Yuwei Wang – SingHealth, Singapore
Zezhi Li – Guangzhou Medical University, China

Citation

Xie, W., Li, Y., Borga, D. K., Zhang, S., Wang, Y., Li, Z., eds. (2024). *Exploring the key targets and compounds that manipulate brain neurocircuits against mental disorders and psychiatric*. Lausanne: Frontiers Media SA. doi: 10.3389/978-2-8325-4887-5

Table of contents

frontiers | Frontiers in Pharmacology

TYPE Editorial
PUBLISHED 29 April 2024
DOI 10.3389/fphar.2024.1411528

OPEN ACCESS

EDITED AND REVIEWED BY
Nicholas M. Barnes,
University of Birmingham, United Kingdom

*CORRESPONDENCE
Song Zhang,
zhangsong1031@163.com

RECEIVED 03 April 2024
ACCEPTED 18 April 2024
PUBLISHED 29 April 2024

CITATION
Xie W and Zhang S (2024), Editorial: Exploring the key targets and compounds that manipulate brain neurocircuits against mental disorders and psychiatric.
Front. Pharmacol. 15:1411528.
doi: 10.3389/fphar.2024.1411528

Editorial: Exploring the key targets and compounds that manipulate brain neurocircuits against mental disorders and psychiatric

Weijie Xie[1] and Song Zhang[2]*

[1]Shanghai Pudong New Area Mental Health Center, Tongji University School of Medicine, Shanghai, China, [2]Renji Hospital, School of Medicine, Shanghai Jiao Tong University, Shanghai, China

KEYWORDS

neuropharmachology, neurocircuit, targets, brian network, molecular pathway

Editorial on the Research Topic
Exploring the key targets and compounds that manipulate brain neurocircuits against mental disorders and psychiatric

Neuropharmacology investigates how drugs influence the nervous system, with the goal of creating medications that can help individuals suffering from psychiatric and neurological disorders ranging from depression and anxiety to schizophrenia and chronic pain. However, neurons in the CNS do not operate in isolation; instead, they work within synaptically connected neural circuits and networks. With advances in neuroscience methods, such as genetic techniques, viral recombination, and *in vivo* imaging, scientists have been able to uncover the neural circuits that underlie neurological and psychiatric diseases. Furthermore, recent studies in *Science* and *Neuron* (Wang et al., 2020; Trieu et al., 2022) have provided a novel insight into the precise regulation of the neural circuit and brain network functions by small molecular compounds targeting the enriched molecules or receptors of these neural circuits, thereby treating psychiatric and neurological diseases. In this Research Topic, we present a collection of original research works from both basic and clinical researchers and reviews that explore the interactions between neural circuits and neuropharmacological approaches to intervene in psychiatric and neurological disorders.

Natural products and compounds are vital resources of exploring new treatments for mental disorders (Zhu et al., 2024). In this Research Topic entitled "*Exploring the Key Targets and Compounds That Manipulate Brain Neurocircuits Against Mental Disorders and Psychiatric*", there are four original research works that demonstrate the protective effects and therapeutic value for stress-induced psychiatric symptoms, including bioactive compound ginsenosides Rb1 and Rg1 (Jiang et al.), Fraxetin (Ahmed et al.), fresh *Gastrodia* products (Zhang et al.) and traditional Chinese drugs called *Chaihu-jia-Longgu-Muli-tang* (CLM, Zhao et al.). Herein, Rb1 and Rg1 significantly improve the impairment of spatial and associative learning and memory caused by microgravity-induced learning and memory dysfunction in a rat model of hindlimb suspension; administration of fraxetin can ameliorate chronic unpredictable stress-induced behavioral deficits and inhibit the increased corticosterone level; the use of Gastrodia noticeably reverses hindlimb unloading weightlessness-induced cognitive impairment. In additions, the data analysis of twenty-four RCTs shows that CLM treatment could improve the symptoms of anxiety and insomnia.

These positive effects of nature products are involved in the inhibition of oxidative stress and apoptosis, increase of synaptic plasticity and regulation of inflammatory factors. The molecular mechanisms involved might be related to the BDNF-TrkB, PI3K-Akt, MAPK, and NF-κB pathways, offering intriguing and insightful approaches for the prevention and treatment of mental disorders.

In contrast to traditional molecular pharmacology, which focuses on the modulatory effects of drug-target interactions, recent advancements in neuroscience have enabled manipulations at the level of brain neurocircuits and networks, allowing for more precise modulation of neurological and psychiatric disorders. The Research Topic section studies show that chronic stress induces the alteration of melatonin receptors and the circadian rhythm, presenting the sleep disorder-related symptoms (Xia et al.). In the nucleus accumbens, the dynamics and kinetics of dopamine release vary distinctly in response to different nicotine salts (Li et al.). In addition to the receptor and neurons, the optogenetic and chemogenetic manipulations of the medial septum (MS)→lateral hypothalamus (LH) glutamatergic projections suppress pain thresholds in the chronic constriction injury model, indicating MS glutamatergic neurons modulate nociception via the projections to LH (Fan et al.). Furthermore, another review dissects the roles of afferent and efferent projections of the rostral ventromedial medulla (RVM) and related neurotransmitters in pain modulation (Peng et al.). However, where to pharmacologically intervene at a larger scale of the brain neurocircuit and network is a common dilemma in the fields of neuropharmacology.

In this Research Topic, the included four clinical trials also provide some novel finding and clues between the molecular targets and clinical phenotypes. For instance, baseline BMI shows a significant correlation with the symptom improvements in schizophrenia (SZ, Chen et al.); cognitive improvement is associated with changes of carnitine metabolite levels after olanzapine monotherapy in CS (Zhao et al.). The clinical neuromodulation data further reveal some therapeutic effects (Zhu et al.) and potential biomarkers (Li et al.) for clinical psychiatrical assessment. In additions, the included two reviews further discuss and explore the dysregulation of copper (Chen et al.) and iron (Sousa et al.) behind neuropsychiatric deficits. These suggest that much work remains to be done in uncovering the neurocircuitry mechanisms and molecular targets underpin the clinical phenotypes of neuropsychiatric disorders in the future.

Overall, our collection of articles highlights the remarkable progress made in identifying potential compounds or natural products and key targets within brain neurocircuits that, when manipulated, offer new hope for individuals battling psychiatric and neurological disorders. Thus, the neurocircuit-regulatory pharmacology may become a future research hotspot. We hope that this Research Topic will inspire new research and well deserve discussion, and we look forward to publishing future advances in this important area of neuropharmacology.

Author contributions

WX: Conceptualization, Funding acquisition, Project administration, Writing–original draft, Writing–review and editing. SZ: Conceptualization, Funding acquisition, Project administration, Writing–original draft, Writing–review and editing.

Funding

The author(s) declare that financial support was received for the research, authorship, and/or publication of this article. This work was supported by the NSFC grant (82371536) to SZ, STI2030-Major Projects (2022ZD0206200) to SZ, the NSFC grant (82101622) to WX and the Outstanding Clinical Discipline Project of Shanghai Pudong (PWYgy 2021-02).

Acknowledgments

We express our profound thanks to all the authors, reviewers, and readers who have contributed to making this Research Topic a reality. Your dedication and passion for unraveling the mysteries of the brain inspire us all to continue this important work.

Conflict of interest

The authors declare that the research was conducted in the absence of any commercial or financial relationships that could be construed as a potential conflict of interest.

Publisher's note

References

Trieu, B. H., Remmers, B. C., Toddes, C., Brandner, D. D., Lefevre, E. M., Kocharian, A., et al. (2022). Angiotensin-converting enzyme gates brain circuit-specific plasticity via an endogenous opioid. *Science* 375, 1177–1182. doi:10.1126/science.abl5130

Wang, H., Dong, P., He, C., Feng, X. Y., Huang, Y., Yang, W. W., et al. (2020). Incerta-thalamic circuit controls nocifensive behavior via cannabinoid type 1 receptors. *Neuron* 107, 538–551. doi:10.1016/j.neuron.2020.04.027

Zhu, T., Liu, H., Gao, S., Jiang, N., Chen, S., and Xie, W. (2024). Effect of salidroside on neuroprotection and psychiatric sequelae during the COVID-19 pandemic: a review. *Biomed. Pharmacother.* 170, 115999. doi:10.1016/j.biopha.2023.115999

frontiers | Frontiers in Pharmacology

TYPE Original Research
PUBLISHED 23 March 2023
DOI 10.3389/fphar.2023.1135497

OPEN ACCESS

EDITED BY
Weijie Xie,
Shanghai Jiao Tong University, China

REVIEWED BY
Wladyslaw-Lason,
Maj Institute of Pharmacology, Polish Academy of Sciences, Poland
Juan Francisco Rodríguez-Landa,
Universidad Veracruzana, Mexico

*CORRESPONDENCE
Khalid Rauf,
khalidrauf@cuiatd.edu.pk

SPECIALTY SECTION
This article was submitted to Neuropharmacology, a section of the journal Frontiers in Pharmacology

RECEIVED 31 December 2022
ACCEPTED 14 March 2023
PUBLISHED 23 March 2023

CITATION
Ahmed Z, Tokhi A, Arif M, Rehman NU, Sheibani V, Rauf K and Sewell RDE (2023), Fraxetin attenuates disrupted behavioral and central neurochemical activity in a model of chronic unpredictable stress. *Front. Pharmacol.* 14:1135497. doi: 10.3389/fphar.2023.1135497

Fraxetin attenuates disrupted behavioral and central neurochemical activity in a model of chronic unpredictable stress

Zainab Ahmed[1], Ahmed Tokhi[1], Mehreen Arif[1], Naeem Ur Rehman[1,2], Vahid Sheibani[3], Khalid Rauf[1]* and Robert D. E. Sewell[4]

[1]Department of Pharmacy, COMSATS University Islamabad, Abbottabad campus, Abbottabad, Pakistan, [2]Faculty of Pharmacy, Gomal University, Dera Ismail Khan, KP, Pakistan, [3]Neuroscience Research Center, Institute of Neuropharmacology, Kerman University of MedicalSciences, Kerman, Iran, [4]Cardiff School of Pharmacy and Pharmaceutical Sciences, Cardiff University, Cardiff, United Kingdom

Purpose: Chronic unpredictable stress (CUS) induces long-term neuronal and synaptic plasticity with a neurohormonal disbalance leading to the development of co-existing anxiety, depression, and cognitive decline. The side effects and delayed onset of current clinically used antidepressants has prompted a quest for antidepressants with minimum drawbacks. Fraxetin is a natural coumarin derivative with documented antioxidant and neuroprotective activity though its effects on stress are unknown. This study therefore aimed to investigate any possible acute effect of fraxetin in behavioral tests including a CUS paradigm in correlation with brain regional neurochemical changes.

Methods: Mice were subjected to a series of mild stressors for 14 days to induce CUS. Furthermore, behavioral performance in the open field test, forced swim test (FST), Y-maze and elevated plus-maze were evaluated. *Postmortem* frontal cortical, hippocampal and striatal tissues were analyzed *via* high-performance liquid chromatography (HPLC) for neurochemical changes.

Result: Acute administration of fraxetin (20–60 mg/kg, orally) decreased depression-like behavior in the FST and behavioral anxiety in both the open field test and elevated plus-maze. Memory deficits induced during the CUS paradigm were markedly improved as reflected by enhanced Y maze performance. Concurrent biochemical and neurochemical analyses revealed that only the two higher fraxetin doses decreased elevated serum corticosterone levels while diminished serotonin levels in the frontal cortex, striatum and hippocampus were reversed, though noradrenaline was only raised in the striatum. Concomitantly, dopamine levels were restored by fraxetin at the highest dose exclusively in the frontal cortex.

Conclusion: Acute treatment with fraxetin attenuated CUS-induced behavioral deficits, ameliorated the increased corticosterone level and restored altered regional neurotransmitter levels and this may indicate a potential application of fraxetin in the management of anxiety and depression modeled by CUS. However, further studies are warranted regarding the chronic effects of fraxetin behaviorally and neurochemically.

KEYWORDS
fraxetin, chronic unpredictable stress, ELISA, corticosterone, HPLC

1 Introduction

Stress is generally a well-recognized and studied global problem of modern society (Carrasco and Van De Kar, 2003). It can be categorized as any state/threat, whether actual or perceived which may alter body homeostasis (Charmandari et al., 2005), and thus contribute to etiology and repetitive episodes of depression (Lee et al., 2002). It is well documented in clinical and preclinical studies that neuronal atrophy and decreased neurotransmitter levels may arise due to chronic stress in specific brain areas like the prefrontal cortex (PFC) and hippocampus, leading to both cognitive, affective and social decline (Rajkowska et al., 1999; Drevets et al., 2008; Sacher et al., 2012). Maintaining homeostasis in an aversive situation (involving stressors) requires the activation of a complex range of neurochemical, neuroendocrine and genetic factors coupled with perception and this is collectively termed the stress response. This results in several physiological and behavioral changes tending to increase survival chances in unfavorable conditions (Charmandari et al., 2005). Increased awareness, improved cognition and increased analgesia are the behavioral outcomes of acute stress, while increased cardiovascular tone, respiratory rate, decreased food intake, growth, immunity, and reproduction represent the physiological effects. Stress has dual consequences which may either be positive or negative in nature (Sapolsky et al., 2000; Habib et al., 2001). Acute stress usually occurs for a brief period and may protect the individual from any aversive condition by preparing the body for a "fight or flight" situation. In contrast, persistent and long-term stress may produce deleterious effects (Gold, 2015), *via* elevated cortisol levels that may result in dysregulated emotional, biological, as well as psychological ailments including anxiety, depression, stress-induced asthma, cardiomyopathy, irritable bowel syndrome, chronic headaches, and substance abuse (Stetler and Miller, 2011).

Stress is a normal body response to external or internal stressors identified by stress mediators implicating the endocrine, nervous and immune systems. Glucocorticoids and epinephrine play important roles in body homeostasis i.e., by adapting to the stressor response (Duman and Aghajanian, 2012). However, if this response persists for an extended episode, it not only disrupts normal homeostasis, but also undermines the body's ability to cope with the stressor ultimately leading to chronic-stress illnesses like anxiety, depression, and cognitive deficits (Nestler et al., 2002; Bondi et al., 2008). In this context, unpredictable stressful events may even predispose individuals to the development of neuropsychiatric disorders (Nestler et al., 2002; Moghaddam and Javitt, 2012).

The clinically used antidepressants increase the monoamine levels in the synaptic cleft, and they include, selective serotonin reuptake inhibitors (SSRIs), serotonin and noradrenaline reuptake inhibitors (SNRIs), monoamine oxidase inhibitors (MAOIs), and tricyclic antidepressants (TCAs). However, they have a slow onset of action, poor tolerability and severe adverse effects including insomnia, dependency, a withdrawal syndrome, weight gain, migraine and suicidal tendencies (Blackburn, 2019). These limitations necessitate the development of newer antidepressants with improved efficacy, fast onset of action, safety, tolerability, reduced or no withdrawal syndrome and a contribution to overall mental health (Blackburn, 2019).

In this respect, plant-based natural products may provide an alternative solution and one such phytochemical class are the coumarins with recognized therapeutic potentials in multiple neuropsychiatric illnesses through antioxidant, neuroprotective, neuromodulator and antidepressant actions(Skalicka-Woźniak et al., 2016; Abu-Aisheh et al., 2019; Pruccoli, 2019; Daliev et al., 2021; Koyiparambath et al., 2021; Sharifi-Rad et al., 2021; Kılıç, 2022). One particular coumarin derivative, fraxetin, is an *O*-methylated coumarin (An et al., 2020), present in many functional foods as well as several dietary supplements with a documented neuroprotective profile mediated primarily through inhibition of oxidative stress (Pruccoli, 2019; Qin et al., 2019; Zhang et al., 2021a). Although the antioxidant, anti-inflammatory, and neuroprotective activities of fraxetin have been described (Zhang et al., 2021a), its effects on stress have not been reported in the literature and remain unknown. Consequently, the present study was undertaken to investigate the effect of fraxetin (20, 40, and 60 mg/kg) in the CUS model which is a widely used animal model to investigate depressive-like behavior. The behavioral activity in the current study was then correlated with brain regional neurochemical parameters in mice.

2 Materials and methods

2.1 Animals

Adult male BALB/c mice (n = 6/group) ranging in weight from 22 to 26 g) were used during experimentation. All animals were kept at room temperature (22 ± 2°C) on a 12/12 h of light/dark cycle and access to food and water was available *ad libitum*. The experimental protocol and animal welfare were approved by the Ethical Committee COMSATS University Islamabad, Abbottabad campus (ethical approval number PHM.Eth/CS-M01-017-1017) with guidelines adherence to UK Animals (Scientific Procedures) Act 1986.

2.2 Chemicals

Fraxetin (CAS: 574-84-5) was purchased from Shandong Chuangying Chemical Co., Ltd. China. Fluoxetine (A.R. No: FP/FX/1905002) was gifted by Palam Pharma PVT. Ltd.

2.3 Experimental design

Fraxetin (20, 40 and 60 mg/kg) (Li et al., 2011; Murali et al., 2013) as well as fluoxetine (10 mg/kg), Kryst et al. (2022) were administered orally (p.o.) in a single dose 5 h after day 14 of the CUS protocol. All the drugs were freshly prepared prior to administration. Animals were randomly allocated to the following six treatment groups (n = 6/group): 1) Non-stressed +

TABLE 1 14 days schedule of stressors in the chronic unpredictable stress model.

Days	Stressor	Duration
1	Restrain	1.5 h
2	Cold Swim (15°C)	10 min
3	Wet sawdust bedding/box housing tilted (45°)	16 h
4	Inversion of light/dark cycle	16 h
5	Tail pinch	10 min
6	Swim (25°C)	6 min
7	Restrain	1.5 h
8	Food and water deprivation	16 h
9	Cold swim (15°C)	10 min
10	Wet sawdust bedding/box housing tilted (45°)	24 h
11	Inescapable shock (0.7 mA, 0.5 s/min)	3 min
12	Inversion of light/dark cycle	16 min
13	Tail pinch	10 min
14	Inescapable shock (0.7 mA, 0.3 s/min)	3 min

normal saline, 2) stressed + normal saline (CUS model group) 3) stressed + fluoxetine (10 mg/kg), 4) stressed + fraxetin (20 mg/kg), 5) stressed + fraxetin (40 mg/kg) and 6) stressed + fraxetin (60 mg/kg).

2.4 Chronic unpredictable stress procedure

The CUS protocol was composed of different stressors applied daily at a variable times of the day over a 14-day period and it was designed to avoid the predictability of each stressor (Table 1). There were two groups of animals; CUS (stressed) and control (non-stressed) mice. During the 14 days, non-stressed animals were kept in their home cage according to the standard protocol while the stressed animals underwent 14 days of the variable stress paradigm. On day 14, all the stressed groups received fraxetin, fluoxetine, or vehicle except for the CUS only model group and subsequently, behavioral parameters were assessed (Moretti et al., 2012). Separate groups were subjected to behavioral testing, one hour after acute administration of fluoxetine, fraxetin or vehicle. In addition, the dosing and testing procedure was executed 5 h after of the last stressor, in order to avoid any additional stress experienced during behavioral testing which occurred.

2.5 Behavioral assessment

All behavioral tests were evaluated manually from video recordings by an experimenter who was blind to the treatments.

2.5.1 Locomotor activity boxes (open field test)

The open-field test is a simple method used to assess underlying exploratory behavior in rodents. Each animal displayed simple movement or ambulation in an open field or more complex behaviors like rearing or thigmotaxis. Locomotor activity was assessed by placing the mice individually in an arena comprised of wooden monitor boxes divided internally by lines on the floor into equivalent quadrants 22.8 cm^2 each and surrounded externally by a 45.6 cm high wall. The locomotor activity of the test animals was measured for 30 min. A digital CAT-I camera installed 230 cm above the locomotor arena was used for locomotion recordings and locomotor activity (simple ambulation) was assessed in activity monitoring boxes (45.6 × 45.6 cm × 30 cm), internally divided into four quadrants measuring 22.8 cm^2 with floor line markings. After cleaning the arena with 70% alcohol, animals were introduced to the center of box, and the activity was recorded by a video camera mounted 230 cm above the box. The number of lines crossed in 30 min was noted (Moretti et al., 2011; Arif et al., 2022).

2.5.2 Elevated plus maze (EPM)

This method is used to investigate anxiogenic and anxiolytic drug effects in laboratory animals and it is based on the survival instinct that rodents are generally aversed to open spaces because of increased exposure risk to predation.

The apparatus consisted of a "plus-shaped" maze elevated above the floor with alternating open and enclosed arms and an open central area. The method relies on the fact that rodents are generally aversed to exploration in open spaces. Single animals were gently placed in the central area, allowed to roam freely for 5 min and the time spent in open and enclosed arms was recorded (Handley and Mithani, 1984).

2.5.3 Y-maze test (Y-maze)

The Y-maze is a widely used technique to study learning and short-term memory in rodents and it incorporates spontaneous alternation as a measure of spatial working memory.

The apparatus consisted of three equal-length arms positioned at an angle of 120° (21 cm long × 8.5 cm wide × 40 cm height). Each animal was positioned at the midpoint of the apparatus and permitted to freely explore all arms for 5 min. The time spent in each arm was recorded using a video camera and between each animal procedure, the apparatus was swabbed with 70% ethanol. Brain areas including the prefrontal cortex, hippocampus and basal forebrain are considered to be involved in this type of memory process. Following animal placement in the maze and consecutive arm entry, the percentage alternation between arms was calculated as follows:

$$\%\,\text{alternation} = (\text{total number of alternations}) / (\text{no of entry in each arm}) \times 100 \quad (1)$$

Distance, speed, and time spent in every arm was also recorded using a CAT-I video camera (Golub et al., 2015).

2.5.4 Forced swimming test (FST)

This test was originally developed by Porsolt et al. (1977) to screen compounds for prospective antidepressant activity in rodents. Mice were introduced individually into a cylindrical container (30 cm in height x 10 cm in diameter) and filled with water to a depth of 15 cm thereby presenting them with the challenge of forced swim. The test procedure is based on the assumption that under a stressful situation, each animal expresses escape mobility eventually adopting a characteristic immobile state that is readily identifiable and time recorded. The test was modified

such that animals were allowed to swim for 6 min only, the first minute instead of 2 min being considered an acclimatization period while the remaining 5 min were regarded as the test time (Porsolt et al., 1977) and only immobility was recorded.

2.5.5 Analysis of corticosterone serum concentration in parallel with behavioral assessment

The animals were euthanized by cervical dislocation and then decapitated to collect trunk blood in vacutainers without anticoagulant. All the animals in the groups were used to obtain blood samples and brain tissue. Since cervical dislocation was employed, cortical function and biological processes were inhibited as rapidly as possible i.e., 5–10 s (Cartner et al., 2007). Samples were allowed to clot undisturbed for 30–60 min. The clot was removed by centrifugation at 1,500 x g for 15 min at 4°C (5418 R centrifuge, Eppendorf, Hamburg, Germany). Serum samples were assayed immediately or stored at -20°C for subsequent analysis. Corticosterone concentrations were determined using an ELISA kit (Cayman Chemical Company, Ann Arbor, United States, catalogue number 501320), having an assay range of 8.2–5000 pg/ml and a sensitivity (80% B/B_0) of 30 pg/ml. The corticosterone concentrations in the samples were compared with a standard curve. All samples were thawed on ice and diluted 20-fold in ELISA buffer. A volume of 100 µL ELISA buffer was added to NSB wells (non-specific binding) and 50 µL to B_0 (maximum binding). A 50 µL corticosterone ELISA standard was then added to each well, followed by 50 µL of corticosterone AChE (Acetylcholinesterase) tracer except for the TA (total activity) and Blk (blank) wells. Finally, a 50 µL corticosterone antiserum was added to each well except for the TA, the NSB and the Blk wells. The plate was covered with plastic film (item No. 400012) and incubated overnight at 4°C. After incubation, each well was emptied and rinsed five times with wash buffer. Next, the wells were filled with Ellman's Reagent at a volume of 200 µL and 5 µL of tracer to the TA well. The plates were again covered. An orbital shaker equipped with a large flat cover was used to allow the plate to develop in the dark. After 120 min of incubation, the plates were read at 405 nm using a spectrophotometer (T80 + UV/VIS Spectrometer, PG Instruments Limited, Leicestershire, United Kingdom). For standard curve fitting and sample data analysis, a Cayman computer spreadsheet available at (www.caymanchem.com/analysis/elisa) and GraphPad Prism version 8.0 for Windows (GraphPad Software, San Diego, California, United States) were used.

2.6 Neurochemical analysis *via* high pressure liquid chromatography (HPLC)

2.6.1 Biological sample preparation

After behavioral experimentation, the mice were euthanized by cervical dislocation and decapitated. The *post mortem* brain regions (frontal cortex, striatum, and hippocampus) were dissected on ice chilled plates where they were accurately weighed and stored at -80°C. The tissues were homogenized *via* a Teflon-glass homogenizer (Ultra-Turax®T-50) in 0.2% ice-cold perchloric acid with rpm of 12,000. Eventually all samples were cold centrifuged (4°C) at 12,000 rpm (DLAB Scientific). Later, the supernatant was filtered with 0.45 mm filter (CNW technologies), which was then placed for analysis in an HPLC auto-sampler (Rehman et al., 2020).

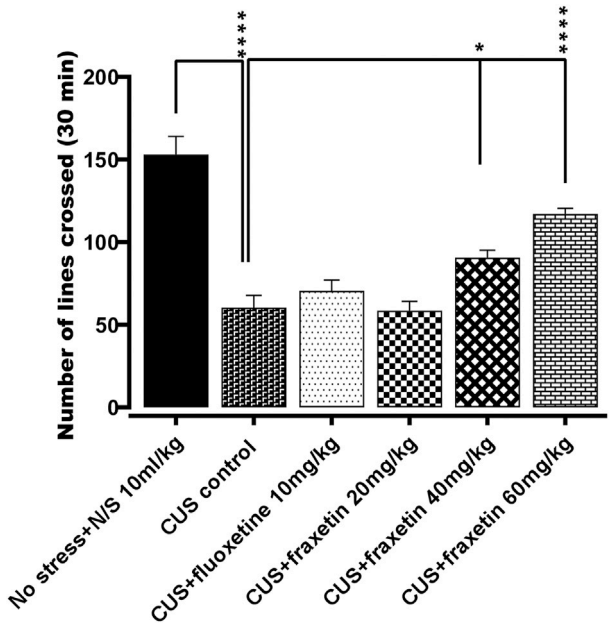

FIGURE 1
The action of fraxetin (20, 40, and 60 mg/kg, p.o.) or fluoxetine (STD; 10 mg/kg, p.o.) on CUS reduced locomotor activity compared to the vehicle alone treated animal group (saline). Values were expressed as mean ± SEM (n = 6/group), *$p < 0.05$, ****$p < 0.0001$ vs. CUS. One-way ANOVA was applied followed by *post hoc* Tukey's test.

2.6.2 Chromatographic conditions

Chromatography was performed (Waters Alliance e2695 separations module with 2998 PDA UV detector, and auto-sampler, United States), using a C18 stainless steel column (250 × 4.6 mm) (Waters X Select® HSS Ireland) with 5 µm particle size. The composition of mobile phase was methanol: HPLC grade water (DAEJUNG; Korea: 8585-2304) in a ratio of 5:95 v/v, plus 20 mM monobasic sodium phosphate (DAEJUNG; Korea: CAS: 7558-80-7) as a buffer. The detection wavelength was 280 nm with isocratic elution. The column temperature was 35°C and flow rate was 0.5 mL/min (Hou et al., 2019; Rehman et al., 2020).

2.6.3 Standard preparation

A standard stock solution of 1.0 mg of dopamine, serotonin, or norepinephrine was prepared by dissolving in 10 mL HPLC grade water. Five different concentrations of 100, 200, 300, 400, 500 ng/mL of stock solution of each neurotransmitter were made by serial dilutions, and then used for the calibration curve. Samples were placed in an HPLC auto-sampler with an injection volume of 20 µL set by software (Empower™). By using linear regression analysis, the calibration curve was plotted using the peak area of dopamine, serotonin, and noradrenaline (y) against the concentration of dopamine, serotonin, and norepinephrine (x) respectively (Rehman et al., 2020).

2.7 Statistical analysis

Results were evaluated using GraphPad Prism (version 8). Mean ± SEM was calculated for each group (n = 6/group).

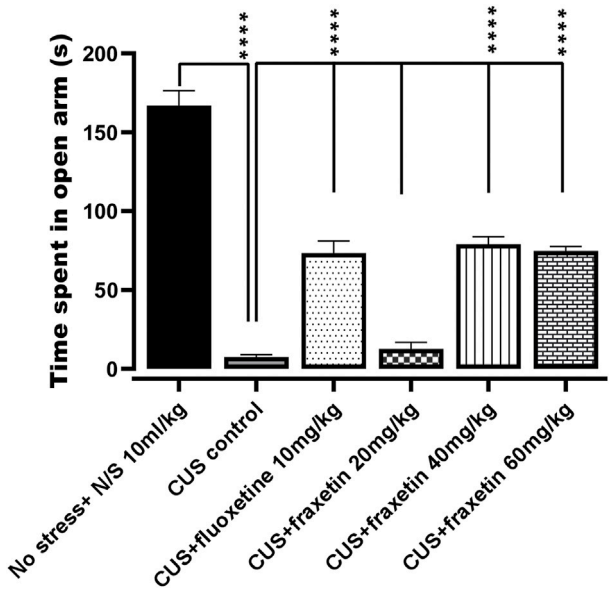

FIGURE 2
Action of fraxetin (20, 40, and 60 mg/kg, p.o.) or fluoxetine (10 mg/kg, p.o.) on CUS inhibited open arm entry compared to the vehicle alone treated control group (saline) in the EPM test. Values were expressed as mean ± SEM (n = 6/group), ****$p < 0.0001$ vs. CUS. One-way ANOVA was applied followed by post hot Tukey's test.

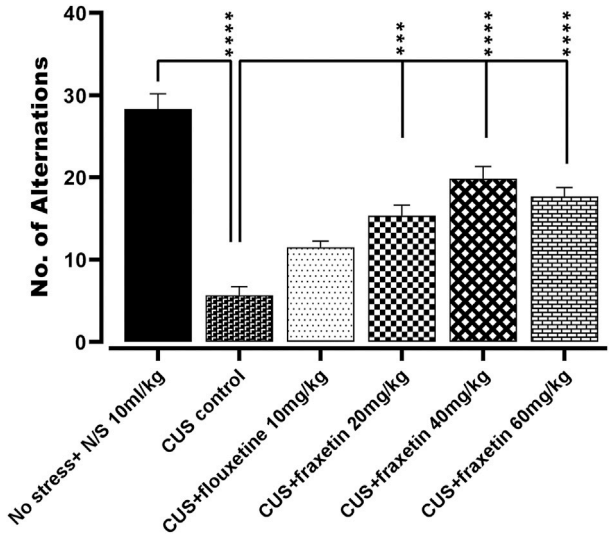

FIGURE 3
Action of fraxetin (20, 40, and 60 mg/kg, p.o.) or fluoxetine (10 mg/kg, p.o. STD) on CUS evoked reduction in spontaneous number of alternations compared to the vehicle alone treated control group (saline) in the Y-maze. Values were expressed as mean ± SEM (n = 6/group), *$p < 0.05$, ***$p < 0.001$, ****$p < 0.0001$ vs. CUS. One-way ANOVA was applied followed by post hot Tukey's test.

Analysis of variance, one-way ANOVA was used followed by *post hoc* Tukey's test. $p < 0.05$ was considered as a significant value.

3 Results

3.1 Behavioral analysis

3.1.1 Open field test

There was a substantial decrease in the locomotor activity evoked in the animals exposed to CUS compared to the vehicle alone control treated group (saline) However, this CUS locomotor activity suppression was at least partially restored to levels approaching those of controls by the CUS group co-administered fraxetin 40, and 60 mg/kg F (5, 30) = 29. 43 and $p <$ 0.0001. In contrast, there was no significant difference in the degree of locomotion expressed between the animal groups administered fluoxetine (10 mg/kg) as a standard antidepressant or fraxetin (20 mg/kg) (Figure 1).

3.1.2 Elevated plus maze (EPM)

In the animal group that underwent CUS, there was an almost total abolition of any time spent in the open EPM arms in comparison with the vehicle-treated controls (saline), and this outcome remained unmodified in the CUS animals co-treated with fraxetin (20 mg/kg). However, combined treatment with fluoxetine (STD) or the two higher doses of fraxetin partially but significantly (Figure 2: F (5, 30) = 98.13 and $p < 0.0001$) restored the CUS inhibition of entry time in the EPM open arms indicating an antianxiety-like effect.

3.1.3 *Y*-maze test (Y-maze)

In the animal group that experienced CUS, there was an extensive reduction in the number of spontaneous alternations versus the vehicle alone treated controls (saline) in Y-maze performance indicating an impairment of short-term working memory. Conversely, the CUS repressed incidence of Y-maze arm alternation was significantly redressed by concomitant administration of fluoxetine (STD; 10 mg/kg) and all three doses of fraxetin 10, 20, and 40 mg/kg (Figure 3: F (5, 30) = 35.11 and $p <$ 0.0001) reflecting an improvement of spatial memory.

3.1.4 Forced swim test (FST)

In the animal group that was subjected to CUS, it was observed that there was an extensive increase in the duration of immobility time (s) versus the vehicle alone treated controls (N/S or vehicle) in the forced swim test, indicating an increase in the behavioral despair. This immobility time duration was markedly reduced by fluoxetine treatment (STD, 10 mg/kg) and totally restored by all three doses of fraxetin to levels that were not significantly different from vehicle-treated controls (saline) Figure 4: F (5, 30) = 94.73 and $p < 0.0001$).

3.2 Neurochemical analysis *via* high-pressure liquid chromatography (HPLC)

3.2.1 Action of fraxetin on brain regional serotonin levels

In the CUS exposed group, serotonin levels in the frontal cortex, hippocampus and striatum were decreased significantly as compared with saline-treated non-stressed animals. However, fraxetin (40, and 60 mg/kg) and fluoxetine (10 mg/kg) caused an

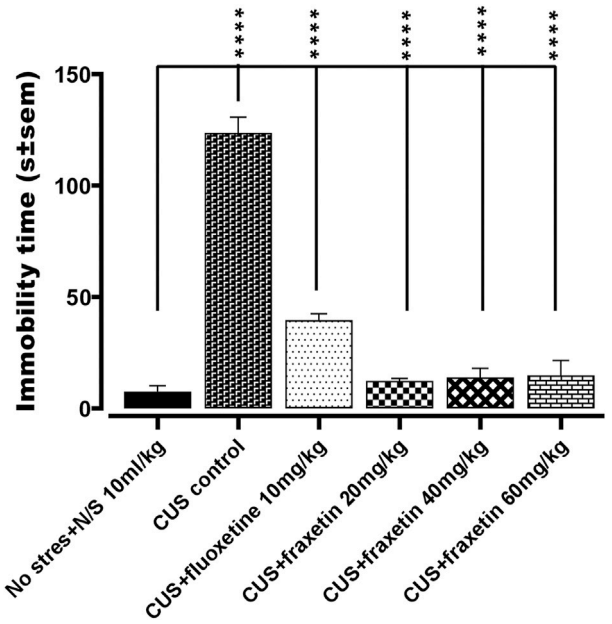

FIGURE 4
Action of fraxetin (20, 40, and 60 mg/kg, p.o.) or fluoxetine (10 mg/kg, p.o. STD) in the forced swim test (FST): immobility time compared to the vehicle alone treated control group (saline) in the forced swim test. Values were expressed as mean ± SEM (n = 6/group), ****p < 0.0001 vs. CUS. One-way ANOVA was applied followed by *post hoc* Tukey's test.

upsurge in CUS repressed serotonin level in the frontal cortex and striatum F (5, 30) = 50.77 and p < 0.0001, while in the hippocampus, fluoxetine (10 mg/kg) and only the highest dose of fraxetin (60 mg/kg) F (5, 30) = 49.92 and p < 0.0001 elevated serotonin concentration compared with the CUS group (Figures 5A,B,C).

3.2.2 Action of fraxetin on brain regional dopamine levels

In the group subjected to CUS, dopamine levels in the frontal cortex, hippocampus and striatum were significantly diminished compared with saline-treated non-stressed animals. There was no statistically significant change in the dopamine level in the striatum and hippocampus after treatment with either fraxetin (20, 40, and 60 mg/kg) or fluoxetine (10 mg/kg) in the CUS group, (Figures 6B,C). In contrast, fraxetin (60 mg/kg) and fluoxetine (10 mg/kg) both increased CUS suppressed dopamine concentrations in the frontal cortex to levels which were comparable to the non-stressed animals (Figure 6A: F (5, 30) = 80.58 and p < 0.0001).

3.2.3 Action of fraxetin on brain regional norepinephrine levels

In the CUS model group, norepinephrine levels in the frontal cortex, hippocampus, and striatum were markedly decreased compared with the saline-treated non-stressed animals. However, after treatment with fraxetin (40, and 60 mg/kg), norepinephrine levels were elevated in the striatum only (Figure 7B: F (5, 30) = 66.16 and p < 0.0001) while fluoxetine 10 mg/kg raised norepinephrine concentrations in both the hippocampus F (5, 30) = 79.26 and p < 0.0001 and striatum (Figures 7B,C) compared to the CUS positive control group (Figure 7B).

3.3 Corticosterone serum concentration parallel to behavioral assessment

There was a very highly significantly increased serum concentration of corticosterone in the CUS group compared to the non-stressed control animal group. However, this augmented level of corticosterone was significantly reversed by fraxetin (40 mg/kg and 60 mg/kg) but not by the 20 mg/kg dose (Figure 8: F (5, 30) = 19.51 and p < 0.0001).

4 Discussion

In the present study, our findings showed that fraxetin significantly attenuated CUS-induced anxiety and depressive-like behaviors in the open field test, elevated plus maze and forced swim test. Moreover, fraxetin also significantly improved spatial learning and working memory in the Y-maze.

Chronic unpredictable stress (CUS) can induce an impairment of cognition and adversely affect emotional aspects such as anxiety, depression, and irritability in addition to diminishing social interaction. Altered serotonergic activity occurring during stress in the central nervous system is a primary and crucial factor contributing to these symptoms. Moreover, a combination of autonomic symptoms including gastrointestinal problems, hyperactivity, restlessness plus paresthesia, and more centrally-mediated symptoms such as binge eating and sleep disorders may also develop. Stressful events are responsible for the release of corticotrophin-releasing factor (CRF) from the hypothalamic paraventricular nucleus (PVN) which in turn releases adrenocorticotropic hormone (ACTH) from the pituitary and ultimately stimulates the adrenal cortex to secrete cortisol in humans and corticosterone in rodents. In addition, stress can lead to perturbation of the blood-brain barrier (BBB) and induction of cellular and neuronal damage, leading to neuronal and cellular inflammation and ultimately death. All of these crucial influential elements can be instrumental in the disruption of cognitive processes (O'connor et al., 2000; Hughes et al., 2016; Sántha et al., 2016). The stress response is a consequence of sympathetic nervous system activation largely dependent on the intensity and duration of stressful events and also through activation of stress pathways in the hypothalamic-pituitary-adrenal axis (Mcewen, 2000; Kim and Diamond, 2002; Sántha et al., 2016; Cameron and Schoenfeld, 2018). Additionally, acute stress may increase memory consolidation by increasing glutamatergic neurotransmission thereby improving spatial memory (Lupien et al., 2002; Roozendaal et al., 2006). In this context, separate groups were run for each behavioral test and acute administration of fluoxetine, fraxetin or vehicle was given after 5 h of the last stressor in order to avoid any additional stress experienced during behavioral testing.

Coumarins and their derivatives have recently attracted much attention regarding their diverse biological and pharmacological

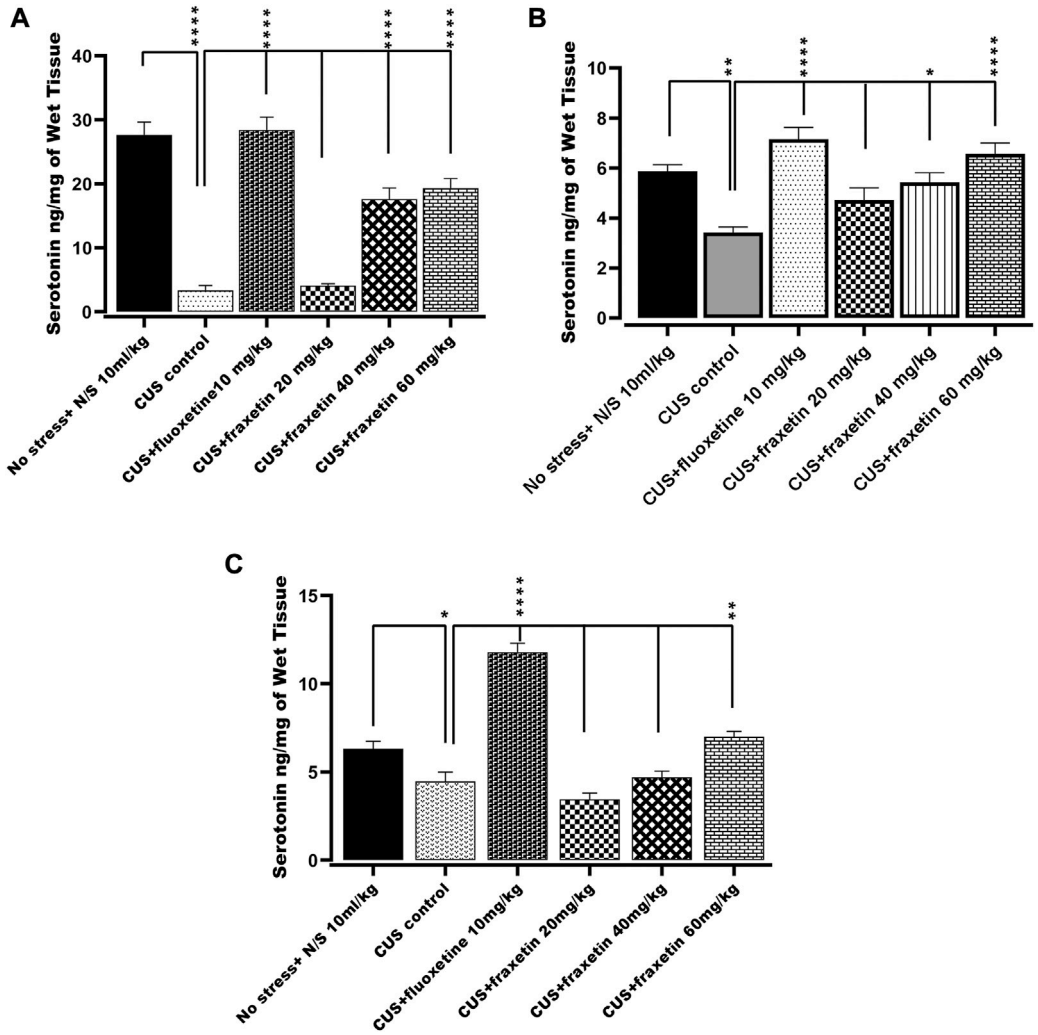

FIGURE 5
(A,B) and **(C)**. Action of fraxetin (20, 40, and 60 mg/kg p.o.) and fluoxetine (10 mg/kg p.o.) on serotonin levels in **(A)** frontal cortex, **(B)** striatum and **(C)** hippocampus in mice subjected to the CUS model. Data were expressed as mean ± SEM (? = 6/group). *$p < 0.05$, **$p < 0.01$, ***$p < 0.001$ and ****$p < 0.0001$ compared with the CUS model group. One-way ANOVA was applied with *post hoc* Tukey's test.

properties. On one hand, they offer microbial resistance against pathogens in plants while on the other hand in humans, they are thought to possess aptitude against cancer, pain and inflammation in addition to acting as antimicrobials, anti-Alzheimer, and anti-Parkinsonian agents (Hussain et al., 2019).

Fraxetin, a natural derivative of coumarin, is present in many functional foods and various dietary supplements (Gaur et al., 2017). Furthermore, it displays neuroprotective, biological scavenger/antioxidant, anti-hyperglycemic, antibacterial actions, and also inhibits platelet aggregation along with anti-osteoporotic properties (Sánchez-Reus et al., 2005; Kuo et al., 2006; Wang et al., 2020). Fraxetin readily crosses the blood-brain barrier, maintaining permeability and its antioxidant activity may well have potential in neurodegenerative disorders that stem from oxidative stress (Ng et al., 2000; Cui et al., 2022).

Bearing in mind its neuroprotective and antioxidant profile along with antidepressant properties, the effects of fraxetin were investigated in the CUS plus FST model for depression. Accordingly, CUS exhibited depressive-like behavior in the FST which was disclosed as an increase in the duration of immobility time. Subsequently, acute treatment with fraxetin reversed CUS induced depressive-like behavior as shown in (Figure 4). This finding may suggest that its pharmacological activity might have an overlap with fast-acting antidepressants such as ketamine and brexanolone rather than more conventional monoaminergic-based drugs (Li, 2020). The approval of fast-acting antidepressants i.e., S-ketamine and brexanolone by the FDA in 2019, has provided new insight into treating depression with new targets such as NMDA and $GABA_A$ agents (Li, 2020). NMDA receptors (NMDARs) are associated with glutamate-gated ion channels expressed throughout the entire central nervous system providing excitatory synaptic neurotransmission. NMDARs are heteromeric complexes comprising many homologous subunits (Neyton and Paoletti, 2006; Ide and Ikeda, 2020). In this connection, ketamine delivers a rapid and sustained

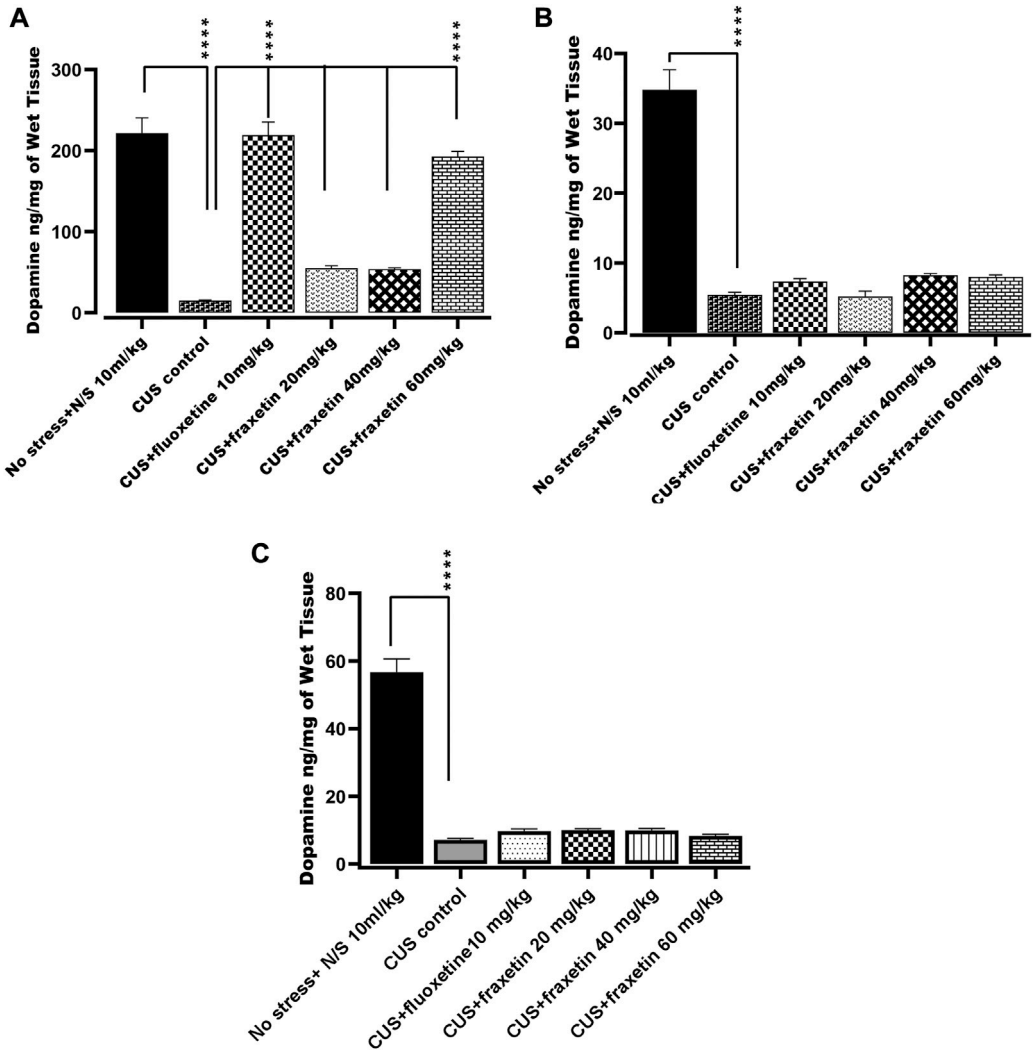

FIGURE 6
(A,B) and **(C)**. Action of fraxetin (20, 40, and 60 mg/kg, p.o.) and fluoxetine 10 mg/kg, p.o.) on dopamine level in **(A)** frontal cortex, **(B)** striatum and **(C)** hippocampus in mice subjected to the CUS model. Data was expressed as mean ± SEM (? = 6/group). *$p < 0.05$, **$p < 0.01$, ***$p < 0.001$ and ****$p < 0.0001$ compared with the CUS model group. One-way ANOVA followed by Tukey's Post hoc multiple comparison test was applied for statistical analysis.

antidepressant effect which is achieved primarily *via* NMDA receptor antagonism and this mechanism may well be shared by fraxetin during its acute antidepressant-like activity in the FST. This assertion is further substantiated by the fact that computationally, fraxetin is an NMDA antagonist at the glutamic acid position 236 and 106 and arginine at position 115 *via* hydrogen bonding, a possible consequence of which is that fraxetin's fast-acting antidepressant-like property might be ascribed to a selective antagonistic effect at the NMDA receptor (supplementary file attached).

The neuroprotective profile of fraxetin is well documented (Wang et al., 2020), and our findings confirm that acute treatment with all three doses of fraxetin (20, 40, and 60 mg/kg) attenuated CUS-induced memory impairment observed in Y-maze performance (Figure 3). The elevated plus maze (EPM) is a simple method used to assess anxiety, and what is more, it can also be used for the anxiogenic-like effect of pharmacological agents, hormones, and drugs of abuse. In the present study, acute administration of fraxetin (40 and 60 mg/kg) ameliorated CUS-induced anxiety-like behavior in the elevated plus-maze (EPM) implying the possible modulation of GABAergic neurotransmission (Figure 2). In relation to this finding, not only does CUS exacerbate memory loss and the accumulation of hippocampal senescent cells but CUS treatment with a senolytic cocktail containing another phytochemical agent, quercetin, alleviates this cognitive deficit (Lin et al., 2021).

The OFT is a classical approach/avoidance paradigm in which the novel environment concomitantly evokes both anxiety and exploration (Guo et al., 2009). Acute treatment with fraxetin allayed the anxiety-like behavior expressed by the CUS model and there was no stimulant effect of fraxetin on its own in naive mice (unpublished data) (see Figure 1).

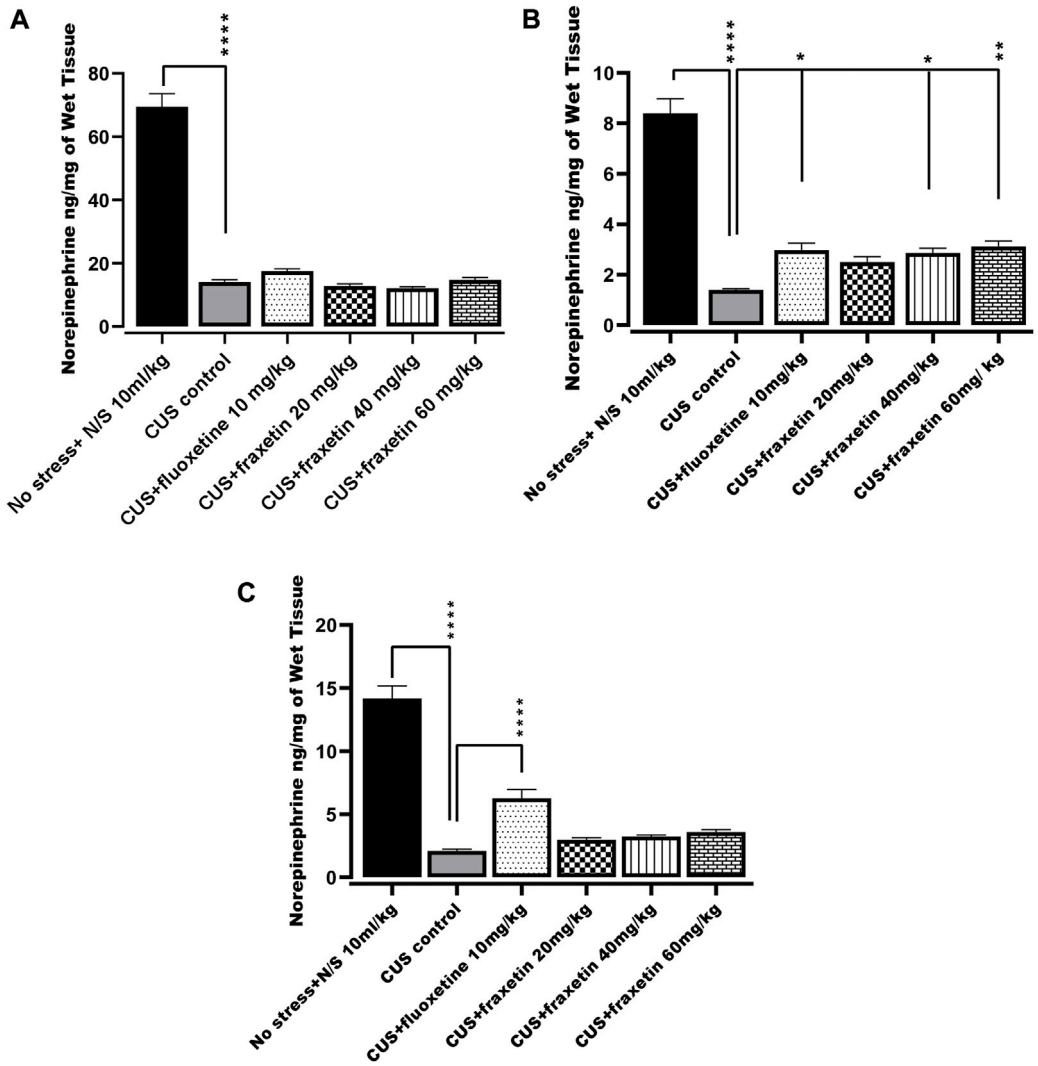

FIGURE 7
(A,B) and **(C)**. Action of fraxetin (20, 40, and 60 mg/kg p.o.) and fluoxetine (10 mg/kg p.o.) on norepinephrine level in **(A)** frontal cortex **(B)** striatum and **(C)** hippocampus in mice subjected to the CUS model. Data were expressed as mean ± SEM (? = 6/group). *$p < 0.05$, **$p < 0.01$, ***$p < 0.001$ compared with CUS model group. One-way ANOVA was applied followed by Tukey's multiple comparison test.

Altered monoaminergic neurotransmission involving serotonin, norepinephrine, and dopamine in the initiation and development of various psychiatric disorders, especially depression, has been well-documented (Elhwuegi, 2004; Krishnan and Nestler, 2008), and antidepressants tend to operate either directly or indirectly to restore monoamine levels (Krishnan and Nestler, 2008). The present study was intended to investigate the acute effect of fraxetin in the CUS model of depression for both behavioral as well neurochemical profiling. For this reason, the levels of serotonin, norepinephrine and dopamine were quantified in the frontal cortex, hippocampus, and striatum in animals exposed to CUS compared to those cotreated with fraxetin. These brain regions and neurotransmitters were selected for study because they are known to be involved in the pathogenesis of depression (Drevets et al., 2008).

It was found that in the CUS model, the levels of serotonin, norepinephrine and dopamine in the frontal cortex, hippocampus and striatum were all significantly decreased and these outcomes are consistent with earlier published findings (Yu et al., 2013; Natarajan et al., 2017; Malta et al., 2021). Furthermore, fraxetin and fluoxetine have been reported to activate the Akt/PKB signaling pathway, a serine/threonine-protein kinase that is a critical regulator of cell survival and proliferation including nutrient metabolism, cell growth and apoptosis. Additionally, regulation of this pathway also plays a role as an integrator of serotonin and dopamine neurotransmission with the function of genes linked to disorders of the CNS (Mo et al., 2019; Kitagishi et al., 2012; Beaulieu, 2012).

Acute treatment with fraxetin tended to restore CUS suppressed serotonin levels in the frontal cortex, striatum and hippocampus.

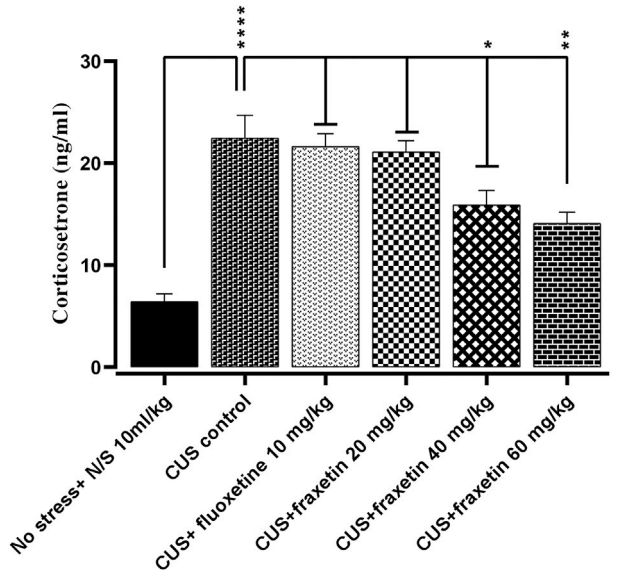

FIGURE 8
The effects of acute fraxetin (20 mg/kg, 40 mg/kg or 60 mg/kg) on 14 days chronic unpredictable stress on the serum corticosterone levels in mice. The data expressed as the means ± SEMs (N = 6/group). GraphPad Prism was used to analyze the data. $p < 0.05$ was the significance vale.

Serotonergic pathways throughout the CNS are altered in CUS and there is an imbalance between serotonin levels and receptor densities (Lages et al., 2021). The hippocampus is the main region where alteration of key neurotransmitter pathways and specified protein levels occur in response to CUS and the differential neurotransmitter modification is reflected by variable levels of behavioral expression (Zhang et al., 2021b). Additionally, it was notable that a similar behavioral and neurochemical pattern was seen with standard fluoxetine. These results confirm that acute fraxetin has a significant effect on brain serotonin levels in the frontal cortex, hippocampus and striatum at higher doses and this may explain its antidepressant-like behavior in the FST. Additionally fraxetin also increased norepinephrine concentrations in the striatum, but not in the frontal cortex or hippocampus, while at the same time, only at the highest dose, it did produce an upsurge in dopamine levels in the frontal cortex. Furthermore, sub-acute and chronic studies are warranted to investigate the effects of fraxetin and its interactions with serotoninergic, noradrenergic and dopaminergic receptors to further probe a more precise mechanism.

Together with the neurotransmitter alterations, there was a raised serum concentration of corticosterone in the CUS group compared to non-stressed animals, however, this augmented level of corticosterone was reversed by the higher doses of fraxetin. It is well documented that persistent and prolonged elevation of cortisol in humans can decrease levels of serotonin and a model of depression that has been employed in preclinical studies involves the use of cortisol. Conversely, the finding that fraxetin raised the CUS-suppressed serotonin level may in turn have had an effect resulting in a decline of serum corticosteroid in mice (Figure 8) (Moretti et al., 2012).

5 Conclusion

The identification of fast-acting antidepressants with minimal side effects has recently gained special attention in the treatment of depression. A worthwhile approach of this study was an investigation of antidepressant-like properties of fraxetin that might share a possible underlying mechanism with fluoxetine. Thus, we showed that acute fraxetin treatment can attenuate not only depressive- and anxiety-like behavior in the OFT, EPM, Y-maze, and FST paradigms, but also the raised corticosterone along with suppressed serotonin levels subsequent to a CUS protocol. Further, studies are warranted to explore the chronic effect of fraxetin at the molecular level in brain areas associated with depression, anxiety and stress.

Data availability statement

The original contributions presented in the study are included in the article/supplementary material, further inquiries can be directed to the corresponding author.

Ethics statement

The animal study was reviewed and approved by Ethical Committee of COMSATS university Islamabad, Abbottabad Campus.

Author contributions

The study conception and design by KR (Supervisor and corresponding author). Material preparation, data collection and analysis were performed by ZA (First Author). Data correction and validation by NR, MA, and AT. The first draft of the manuscript was written by ZA and thoroughly checked by KR and RS. The first draft was thoroughly checked by KR, RS and VS. The manuscript was critically checked for English correction as well as scientific input by RS. All authors commented on previous versions of the manuscript. All authors read and approved the final manuscript.

Acknowledgments

The author acknowledges the Higher Education Commission of Pakistan for granting Indigenous Scholarship *via* 17-5(Ph-II)/2BM2-177)/HEC/IS/2013 and the University of Balochistan for providing study leave.

Conflict of interest

The authors declare that the research was conducted in the absence of any commercial or financial relationships that could be construed as a potential conflict of interest.

Publisher's note

References

Abu-Aisheh, M. N., Al-Aboudi, A., Mustafa, M. S., El-Abadelah, M. M., Ali, S. Y., Ul-Haq, Z., et al. (2019). Coumarin derivatives as acetyl-and butyrylcholinestrase inhibitors: An *in vitro*, molecular docking, and molecular dynamics simulations study. *Heliyon* 5 (4), e01552. doi:10.1016/j.heliyon.2019.e01552

An, S. H., Choi, G.-S., and Ahn, J.-H. (2020). Biosynthesis of fraxetin from three different substrates using engineered *Escherichia coli*. *Appl. Biol. Chem.* 63 (1), 55–56. doi:10.1186/s13765-020-00543-9

Arif, M., Rauf, K., Rehman, N. U., Tokhi, A., Ikram, M., and Sewell, R. D. (2022). 6-Methoxyflavone and donepezil behavioral plus neurochemical correlates in reversing chronic ethanol and withdrawal induced cognitive impairment. *Drug Des. Dev. Ther.* 16, 1573–1593. doi:10.2147/DDDT.S360677

Blackburn, T. P. (2019). Depressive disorders: Treatment failures and poor prognosis over the last 50 years. *Pharmacol. Res. Perspect.* 7 (3), e00472. doi:10.1002/prp2.472

Bondi, C. O., Rodriguez, G., Gould, G. G., Frazer, A., and Morilak, D. A. (2008). Chronic unpredictable stress induces a cognitive deficit and anxiety-like behavior in rats that is prevented by chronic antidepressant drug treatment. *Neuropsychopharmacology* 33 (2), 320–331. doi:10.1038/sj.npp.1301410

Cameron, H. A., and Schoenfeld, T. J. (2018). Behavioral and structural adaptations to stress. *Front. Neuroendocrinol.* 49, 106–113. doi:10.1016/j.yfrne.2018.02.002

Carrasco, G. A., and Van de Kar, L. D. (2003). Neuroendocrine pharmacology of stress. *Eur. J. Pharmacol.* 463 (1-3), 235–272. doi:10.1016/s0014-2999(03)01285-8

Cartner, S. C., Barlow, S. C., and Ness, T. J. (2007). Loss of cortical function in mice after decapitation, cervical dislocation, potassium chloride injection, and CO2 inhalation. *Comp. Med.* 57 (6), 570–573.

Charmandari, E., Tsigos, C., and Chrousos, G. (2005). Endocrinology of the stress response. *Annu. Rev. Physiol.* 67, 259–284. doi:10.1146/annurev.physiol.67.040403.120816

Cui, Y., Liu, M., Zuo, L., Wang, H., and Liu, J. (2022). Fraxetin protects rat brains from the cerebral stroke via promoting angiogenesis and activating PI3K/Akt pathway. *Immunopharmacol. Immunotoxicol.* 44 (3), 400–409. doi:10.1080/08923973.2022.2052893

Daliev, B. B., Bychkov, E. R., Myznikov, L. V., Lebedev, A. A., and Shabanov, P. D. (2021). Anticompulsive effects of novel derivatives of coumarin in rats. *Rev. Clin. Pharmacol. Drug Ther.* 19 (3), 339–344. doi:10.17816/rcf193339-344

Drevets, W. C., Price, J. L., and Furey, M. L. (2008). Brain structural and functional abnormalities in mood disorders: Implications for neurocircuitry models of depression. *Brain Struct. Funct.* 213 (1-2), 93–118. doi:10.1007/s00429-008-0189-x

Duman, R. S., and Aghajanian, G. K. (2012). Synaptic dysfunction in depression: Potential therapeutic targets. *science* 338 (6103), 68–72. doi:10.1126/science.1222939

Elhwuegi, A. S. (2004). Central monoamines and their role in major depression. *Prog. Neuro-Psychopharmacology Biol. Psychiatry* 28 (3), 435–451. doi:10.1016/j.pnpbp.2003.11.018

Gaur, P., Singh, D. K., Luqman, S., and Shanker, K. (2017). Validated method for quality assessment of henna (Lawsonia inermis L.) leaves after postharvest blanching and its cosmetic application. *Industrial Crops Prod.* 95, 33–42. doi:10.1016/j.indcrop.2016.10.010

Gold, P. W. (2015). The organization of the stress system and its dysregulation in depressive illness. *Mol. psychiatry* 20 (1), 32–47. doi:10.1038/mp.2014.163

Golub, H. M., Zhou, Q. G., Zucker, H., McMullen, M. R., Kokiko-Cochran, O. N., Ro, E. J., et al. (2015). Chronic alcohol exposure is associated with decreased neurogenesis, aberrant integration of newborn neurons, and cognitive dysfunction in female mice. *Alcohol. Clin. Exp. Res.* 39 (10), 1967–1977. doi:10.1111/acer.12843

Guo, J.-Y., Li, C.-Y., Ruan, Y.-P., Sun, M., Qi, X.-L., Zhao, B.-S., et al. (2009). Chronic treatment with celecoxib reverses chronic unpredictable stress-induced depressive-like behavior via reducing cyclooxygenase-2 expression in rat brain. *Eur. J. Pharmacol.* 612 (1-3), 54–60. doi:10.1016/j.ejphar.2009.03.076

Habib, K. E., Gold, P. W., and Chrousos, G. P. (2001). Neuroendocrinology of stress. *Endocrinol. Metabolism Clin.* 30 (3), 695–728. doi:10.1016/s0889-8529(05)70208-5

Handley, S. L., and Mithani, S. (1984). Effects of alpha-adrenoceptor agonists and antagonists in a maze-exploration model of 'fear'-motivated behaviour. *Naunyn-Schmiedeberg's archives Pharmacol.* 327 (1), 1–5. doi:10.1007/BF00504983

Hou, X., Huang, W., Tong, Y., and Tian, M. (2019). Hollow dummy template imprinted boronate-modified polymers for extraction of norepinephrine, epinephrine and dopamine prior to quantitation by HPLC. *Microchim. Acta* 186 (11), 686–689. doi:10.1007/s00604-019-3801-2

Hughes, M. M., Connor, T. J., and Harkin, A. (2016). Stress-related immune markers in depression: Implications for treatment. *Int. J. Neuropsychopharmacol.* 19 (6), pyw001. doi:10.1093/ijnp/pyw001

Hussain, M. I., Syed, Q. A., Khattak, M. N. K., Hafez, B., Reigosa, M. J., and El-Keblawy, A. (2019). Natural product coumarins: Biological and pharmacological perspectives. *Biologia* 2019, 1–26. doi:10.2478/s11756-019-00242-x

Ide, S., and Ikeda, K. (2020). "Distinct roles of NMDA receptor GluN2 subunits in the effects of ketamine and its enantiomers," in *Ketamine* (Singapore: Springer), 157–173.

Kılıç, C. S. (2022). "Herbal coumarins in healthcare," in *Herbal biomolecules in healthcare applications* (Netherlands: Elsevier), 363–380.

Kim, J. J., and Diamond, D. M. (2002). The stressed hippocampus, synaptic plasticity and lost memories. *Nat. Rev. Neurosci.* 3 (6), 453–462. doi:10.1038/nrn849

Koyiparambath, V. P., Prayaga Rajappan, K., Rangarajan, T., Al-Sehemi, A. G., Pannipara, M., Bhaskar, V., et al. (2021). Deciphering the detailed structure–activity relationship of coumarins as monoamine oxidase enzyme inhibitors—an updated review. *Chem. Biol. Drug Des.* 98 (4), 655–673. doi:10.1111/cbdd.13919

Krishnan, V., and Nestler, E. J. (2008). The molecular neurobiology of depression. *Nature* 455 (7215), 894–902. doi:10.1038/nature07455

Kryst, J., Majcher-Maślanka, I., and Chocyk, A. (2022). Effects of chronic fluoxetine treatment on anxiety-and depressive-like behaviors in adolescent rodents–systematic review and meta-analysis. *Pharmacol. Rep.* 74 (5), 920–946. doi:10.1007/s43440-022-00420-w

Kuo, P.-L., Huang, Y.-T., Chang, C.-H., and Chang, J.-K. (2006). Fraxetin inhibits the induction of anti-Fas IgM, tumor necrosis factor-alpha and interleukin-1beta-mediated apoptosis by Fas pathway inhibition in human osteoblastic cell line MG-63. *Int. Immunopharmacol.* 6 (7), 1167–1175. doi:10.1016/j.intimp.2006.02.010

Lages, Y., Rossi, A., Krahe, T., and Landeira-Fernandez, J. (2021). Effect of chronic unpredictable mild stress on the expression profile of serotonin receptors in rats and mice: A meta-analysis. *Neurosci. Biobehav. Rev.* 124, 78–88. doi:10.1016/j.neubiorev.2021.01.020

Lee, A. L., Ogle, W. O., and Sapolsky, R. M. (2002). Stress and depression: Possible links to neuron death in the hippocampus. *Bipolar Disord.* 4 (2), 117–128. doi:10.1034/j.1399-5618.2002.01144.x

Li, J.-M., Zhang, X., Wang, X., Xie, Y.-C., and Kong, L.-D. (2011). Protective effects of cortex fraxini coumarines against oxonate-induced hyperuricemia and renal dysfunction in mice. *Eur. J. Pharmacol.* 666 (1-3), 196–204. doi:10.1016/j.ejphar.2011.05.021

Li, Y.-F. (2020). A hypothesis of monoamine (5-ht)–glutamate/GABA long neural circuit: Aiming for fast-onset antidepressant discovery. *Pharmacol. Ther.* 208, 107494. doi:10.1016/j.pharmthera.2020.107494

Lin, Y.-F., Wang, L.-Y., Chen, C.-S., Li, C.-C., and Hsiao, Y.-H. (2021). Cellular senescence as a driver of cognitive decline triggered by chronic unpredictable stress. *Neurobiol. stress* 15, 100341. doi:10.1016/j.ynstr.2021.100341

Lupien, S. J., Wilkinson, C. W., Brière, S., Ménard, C., Kin, N. N. Y., and Nair, N. (2002). The modulatory effects of corticosteroids on cognition: Studies in young human populations. *Psychoneuroendocrinology* 27 (3), 401–416. doi:10.1016/s0306-4530(01)00061-0

Malta, M. B., Martins, J., Novaes, L. S., dos Santos, N. B., Sita, L. V., Camarini, R., et al. (2021). Norepinephrine and glucocorticoids modulate chronic unpredictable stress-induced increase in the type 2 CRF and glucocorticoid receptors in brain structures related to the HPA axis activation. bioRxiv.

McEwen, B. S. (2000). The neurobiology of stress: From serendipity to clinical relevance. *Brain Res.* 886 (1-2), 172–189. doi:10.1016/s0006-8993(00)02950-4

Moghaddam, B., and Javitt, D. (2012). From revolution to evolution: The glutamate hypothesis of schizophrenia and its implication for treatment. *Neuropsychopharmacology* 37 (1), 4–15. doi:10.1038/npp.2011.181

Moretti, M., Colla, A., de Oliveira Balen, G., dos Santos, D. B., Budni, J., de Freitas, A. E., et al. (2012). Ascorbic acid treatment, similarly to fluoxetine, reverses depressive-like behavior and brain oxidative damage induced by chronic unpredictable stress. *J. psychiatric Res.* 46 (3), 331–340. doi:10.1016/j.jpsychires.2011.11.009

Moretti, M., de Freitas, A. E., Budni, J., Fernandes, S. C. P., de Oliveira Balen, G., and Rodrigues, A. L. S. (2011). Involvement of nitric oxide–cGMP pathway in the

antidepressant-like effect of ascorbic acid in the tail suspension test. *Behav. Brain Res.* 225 (1), 328–333. doi:10.1016/j.bbr.2011.07.024

Murali, R., Srinivasan, S., and Ashokkumar, N. (2013). Antihyperglycemic effect of fraxetin on hepatic key enzymes of carbohydrate metabolism in streptozotocin-induced diabetic rats. *Biochimie* 95 (10), 1848–1854. doi:10.1016/j.biochi.2013.06.013

Natarajan, R., Forrester, L., Chiaia, N. L., and Yamamoto, B. K. (2017). Chronic-stress-induced behavioral changes associated with subregion-selective serotonin cell death in the dorsal raphe. *J. Neurosci.* 37 (26), 6214–6223. doi:10.1523/JNEUROSCI.3781-16.2017

Nestler, E. J., Barrot, M., DiLeone, R. J., Eisch, A. J., Gold, S. J., and Monteggia, L. M. (2002). Neurobiology of depression. *Neuron* 34 (1), 13–25. doi:10.1016/s0896-6273(02)00653-0

Neyton, J., and Paoletti, P. (2006). Relating NMDA receptor function to receptor subunit composition: Limitations of the pharmacological approach. *J. Neurosci.* 26 (5), 1331–1333. doi:10.1523/JNEUROSCI.5242-05.2006

Ng, T., Liu, F., and Wang, Z. (2000). Antioxidative activity of natural products from plants. *Life Sci.* 66 (8), 709–723. doi:10.1016/s0024-3205(99)00642-6

O'connor, T., O'halloran, D., and Shanahan, F. (2000). The stress response and the hypothalamic-pituitary-adrenal axis: From molecule to melancholia. *Qjm* 93 (6), 323–333. doi:10.1093/qjmed/93.6.323

Porsolt, R., Bertin, A., and Jalfre, M. (1977). Behavioral despair in mice: A primary screening test for antidepressants. *Archives Int. de pharmacodynamie de Ther.* 229 (2), 327–336.

Pruccoli, L. (2019). Neuroprotective effects of coumarins in neurodegenerative disease models. *Science* 31, 8975. doi:10.48676/unibo/amsdottorato/8975

Qin, Z., Zhang, B., Yang, J., Li, S., Xu, J., Yao, Z., et al. (2019). The efflux mechanism of fraxetin-O-glucuronides in ugt1a9-transfected HeLa cells: Identification of multidrug resistance-associated proteins 3 and 4 (MRP3/4) as the important contributors. *Front. Pharmacol.* 10, 496. doi:10.3389/fphar.2019.00496

Rajkowska, G., Miguel-Hidalgo, J. J., Wei, J., Dilley, G., Pittman, S. D., Meltzer, H. Y., et al. (1999). Morphometric evidence for neuronal and glial prefrontal cell pathology in major depression. *Biol. psychiatry* 45 (9), 1085–1098. doi:10.1016/s0006-3223(99)00041-4

Rehman, N. U., Abbas, M., Al-Rashida, M., Tokhi, A., Arshid, M. A., Khan, M. S., et al. (2020). Effect of 4-fluoro-N-(4-Sulfamoylbenzyl) benzene sulfonamide on acquisition and expression of nicotine-induced behavioral sensitization and striatal adenosine levels. *Drug Des. Dev. Ther.* 14, 3777–3786. doi:10.2147/DDDT.S270025

Roozendaal, B., Okuda, S., Van der Zee, E. A., and McGaugh, J. L. (2006). Glucocorticoid enhancement of memory requires arousal-induced noradrenergic activation in the basolateral amygdala. *Proc. Natl. Acad. Sci.* 103 (17), 6741–6746. doi:10.1073/pnas.0601874103

Sacher, J., Neumann, J., Fünfstück, T., Soliman, A., Villringer, A., and Schroeter, M. L. (2012). Mapping the depressed brain: A meta-analysis of structural and functional alterations in major depressive disorder. *J. Affect. Disord.* 140 (2), 142–148. doi:10.1016/j.jad.2011.08.001

Sánchez-Reus, M. I., Peinado, I. I., Molina-Jiménez, M. F., and Benedí, J. (2005). Fraxetin prevents rotenone-induced apoptosis by induction of endogenous glutathione in human neuroblastoma cells. *Neurosci. Res.* 53 (1), 48–56. doi:10.1016/j.neures.2005.05.009

Sántha, P., Veszelka, S., Hoyk, Z., Mészáros, M., Walter, F. R., Tóth, A. E., et al. (2016). Restraint stress-induced morphological changes at the blood-brain barrier in adult rats. *Front. Mol. Neurosci.* 8, 88. doi:10.3389/fnmol.2015.00088

Sapolsky, R. M., Romero, L. M., and Munck, A. U. (2000). How do glucocorticoids influence stress responses? Integrating permissive, suppressive, stimulatory, and preparative actions. *Endocr. Rev.* 21 (1), 55–89. doi:10.1210/edrv.21.1.0389

Sharifi-Rad, J., Cruz-Martins, N., López-Jornet, P., Lopez, E. P.-F., Harun, N., Yeskaliyeva, B., et al. (2021). Natural coumarins: Exploring the pharmacological complexity and underlying molecular mechanisms. *Oxidative Med. Cell. Longev.* 2021, 6492346. doi:10.1155/2021/6492346

Skalicka-Woźniak, K., Orhan, I. E., Cordell, G. A., Nabavi, S. M., and Budzyńska, B. (2016). Implication of coumarins towards central nervous system disorders. *Pharmacol. Res.* 103, 188–203. doi:10.1016/j.phrs.2015.11.023

Stetler, C., and Miller, G. E. (2011). Depression and hypothalamic-pituitary-adrenal activation: A quantitative summary of four decades of research. *Psychosom. Med.* 73 (2), 114–126. doi:10.1097/PSY.0b013e31820ad12b

Wang, Q., Zhuang, D., Feng, W., Ma, B., Qin, L., and Jin, L. (2020). Fraxetin inhibits interleukin-1β-induced apoptosis, inflammation, and matrix degradation in chondrocytes and protects rat cartilage *in vivo*. *Saudi Pharm. J.* 28 (12), 1499–1506. doi:10.1016/j.jsps.2020.09.016

Yu, Y., Wang, R., Chen, C., Du, X., Ruan, L., Sun, J., et al. (2013). Antidepressant-like effect of trans-resveratrol in chronic stress model: Behavioral and neurochemical evidences. *J. psychiatric Res.* 47 (3), 315–322. doi:10.1016/j.jpsychires.2012.10.018

Zhang, T., Zhang, X., Liu, N., Ren, S., Xia, C., Yang, X., et al. (2021b). Comparative proteomic characterization of ventral Hippocampus in susceptible and resilient rats subjected to chronic unpredictable stress. *Front. Neurosci.* 15, 675430. doi:10.3389/fnins.2021.675430

Zhang, T., Zhou, B., Sun, J., Song, J., Nie, L., and Zhu, K. (2021a). Fraxetin suppresses reactive oxygen species-dependent autophagy by the PI3K/Akt pathway to inhibit isoflurane-induced neurotoxicity in hippocampal neuronal cells. *J. Appl. Toxicol.* 42, 617–628. doi:10.1002/jat.4243

frontiers | Frontiers in Pharmacology

TYPE Review
PUBLISHED 20 April 2023
DOI 10.3389/fphar.2023.1159753

OPEN ACCESS

EDITED BY
Yuan Li,
Shanghai Jiao Tong University, China

REVIEWED BY
Xinyou Lv,
Shanghai Mental Health Center, China
Jing Wang,
Central South University, China

*CORRESPONDENCE
Yinghui Fan,
fanyh86@hotmail.com
Weifeng Yu,
ywff808@yeah.net

†These authors have contributed equally to this work and share first authorship

RECEIVED 06 February 2023
ACCEPTED 10 April 2023
PUBLISHED 20 April 2023

CITATION
Peng B, Jiao Y, Zhang Y, Li S, Chen S, Xu S, Gao P, Fan Y and Yu W (2023), Bulbospinal nociceptive ON and OFF cells related neural circuits and transmitters. *Front. Pharmacol.* 14:1159753. doi: 10.3389/fphar.2023.1159753

Bulbospinal nociceptive ON and OFF cells related neural circuits and transmitters

Bingxue Peng[1,2†], Yingfu Jiao[1,2†], Yunchun Zhang[1,2], Shian Li[1,2], Sihan Chen[1,2], Saihong Xu[1,2], Po Gao[1,2], Yinghui Fan[1,2*] and Weifeng Yu[1,2*]

[1]Department of Anesthesiology, Renji Hospital, Shanghai Jiao Tong University School of Medicine, Shanghai, China, [2]Key Laboratory of Anesthesiology (Shanghai Jiao Tong University), Ministry of Education, Shanghai, China

The rostral ventromedial medulla (RVM) is a bulbospinal nuclei in the descending pain modulation system, and directly affects spinal nociceptive transmission through pronociceptive ON cells and antinociceptive OFF cells in this area. The functional status of ON and OFF neurons play a pivotal role in pain chronification. As distinct pain modulative information converges in the RVM and affects ON and OFF cell excitability, neural circuits and transmitters correlated to RVM need to be defined for an in-depth understanding of central-mediated pain sensitivity. In this review, neural circuits including the role of the periaqueductal gray, locus coeruleus, parabrachial complex, hypothalamus, amygdala input to the RVM, and RVM output to the spinal dorsal horn are discussed. Meanwhile, the role of neurotransmitters is concluded, including serotonin, opioids, amino acids, cannabinoids, TRPV1, substance P and cholecystokinin, and their dynamic impact on both ON and OFF cell activities in modulating pain transmission. Via clarifying potential specific receptors of ON and OFF cells, more targeted therapies can be raised to generate pain relief for patients who suffer from chronic pain.

KEYWORDS

rostral ventromedial medulla, pain, neural circuit, transmitter, ON cell, OFF cell

1 Introduction

Central sensitization plays a significant role in the endogenous modulation of nociceptive transmission (Woolf, 1983). The descending pain modulation system influences the sensitization of central nociceptive transmission predominantly by altering the interconnections with the rostral ventromedial medulla (RVM) (Francois et al., 2017). Therefore, it is essential to define a role for RVM in pain modulation.

Located in the lower bulbospinal area, the RVM mainly consists of the nucleus raphe magnus (NRM), the nucleus reticularis gigantocellularis-pars alpha, and the nucleus paragiganto-cellularis lateralis (Zhuo and Gebhart, 1990). Regarding its function, it has been reported that when experiencing noxious heat stimuli or continuous neuropathic pain, not only the contralateral RVM but also the ipsilateral/median RVM activity is increased, as indicated in a functional magnetic resonance imaging (fMRI) study of human supraspinal structures (Rempe et al., 2015; Mills et al., 2020). Furthermore, in opioid-mediated, attentional, and placebo analgesia, a significant increase in correlated voxels was observed primarily in the middle and ventral aspects of the RVM (Crawford et al., 2021;

Oliva et al., 2022). In addition, other investigations have subsequently conveyed the importance of the RVM in modulating descending pain in male and female animal models (Drake et al., 2007; M. M. Heinricher et al., 2009). These findings confirmed the distinctive role of the RVM as the main gatekeeper of descending pain modulation and facilitating bidirectional or inhibitory pain modulatory effects. Moreover, variations in RVM neuronal responses to nociceptive stimulation have been observed through classic extracellular recording (Fields et al., 1983). ON cell firing increases and OFF cell firing decreases, while Neutral cells exert no responses to nociceptive stimulus (M. M. Heinricher et al., 1987). Interestingly, other studies have suggested that Neutral cells could participate in the development of hyperalgesia by responding in an ON/OFF manner when applying noxious stimuli other than tail heat (Ellrich et al., 2000). Thus, ON and OFF cells are pivotal for RVM-related pain modulation.

Although studies have characterized the key role of the RVM in pain modulation, there are still several questions that remain unresolved in RVM-related pain modulation of neural networks, which impede the development of new analgesic approaches targeting the RVM and the corresponding pathways. These limitations include, but are not limited to: 1) neural circuits and neurotransmitters influencing the activities of RVM ON and OFF cells have not been precisely elucidated; 2) neurotransmitters participating in RVM ON and OFF cells driven spinal nociceptive modulation remain elusive.

In reality, the RVM is an integral relay point between high-level nerve systems and peripheral inputs in pain modulation. Nociceptive information is transmitted to the RVM through specific groups of spinal ascending neurons (Todd, 2010) and through connective neurons in supraspinal structures involved in pain modulation. The RVM receives nociceptive-related neural afferents, including the parabrachial complex (PB) (Roeder et al., 2016), locus coeruleus (LC) (Tanaka et al., 1996), midbrain (PAG) (Behbehani and Fields, 1979), hypothalamus (Gu and Wessendorf, 2007), and the amygdala (Mcgaraughty and Heinricher, 2002), and then projects to the trigeminal nucleus caudalis and the spinal dorsal horn via ventrolateral funiculus and spinal dorsolateral funiculus separately (Fields et al., 1995). Several key neurotransmitters have been demonstrated to be involved in RVM-related pain modulation, including opioids (Cheng et al., 1986; Lau et al., 2020), amino acids (Winkler et al., 2006), serotonin (Wei et al., 2010), and cannabinoids (Meng et al., 1998), which will also be discussed in this review. By providing an overview of the potential neural circuits and neurotransmitters corresponding to RVM ON and OFF cells, this review will deepen our current understanding of RVM-driven descending pain modulation.

2 Function and molecular characteristics of RVM ON and OFF cells

2.1 Functional definition of ON and OFF cells

According to cell discharge patterns and electroexcitation reactions in response to tail heat stimulation (Fields et al., 1983), Fields first confirmed that pronociceptive ON cells increased activity immediately before facilitation of the withdrawal response. Antinociceptive OFF cells decreased their relatively high spontaneous activity up to a pause, which triggered the nociceptive response. Neutral cells did not respond to painful stimuli. ON and OFF cells exert different activities and pain modulation effects under different circumstances. Under normal conditions, ON and OFF cells exhibit alternating periods of activity and silence (Barbaro et al., 1989). These synaptic interconnections within the RVM play an important role in modulating pain. Within the RVM, opioids directly inhibit the activities of ON cells, while indirectly increasing the activities of OFF cells, exerting analgesic effects (Cheng et al., 1986). Furthermore, when ON cells are inhibited and OFF cells are activated, this leads to responses of attentional analgesia (Oliva et al., 2021), placebo analgesia (Crawford et al., 2021), and stress-induced analgesia (Martenson et al., 2009). In the presence of nerve injury (Lopez-Canul et al., 2015) and in diabetic models (Silva et al., 2013; Palazzo et al., 2022) of hyperalgesia, increased ON cell activities and decreased OFF cell activities are observed, sustaining central sensitization and neuropathic pain responses. Therefore, any change in the balance of activity between ON and OFF cells produces bidirectional stimulatory or inhibitory modulatory effects on pain, regardless of normal circumstances or neuropathic and inflammatory situations.

2.2 Molecular expression characteristics of ON and OFF cells

Notwithstanding the electrophysiological properties of ON and OFF cells having been thoroughly investigated, the lack of specific cell markers encourages speculation into the neurotransmitters and receptors expressed by ON and OFF cells.

The RVM is considered the main site for opioid analgesia and opioid receptors are abundantly expressed in the RVM, including the μ-opioid receptor (MOR), κ-opioid receptor (KOR), δ-opioid receptor (DOR), and nociception/orphanin FQ receptors (NOPR), with especially high expression of MOR on ON cells. Previously, MOR has been considered a specific marker for ON cells (M. M. Heinricher et al., 1992). After injection of the micro-opioid MOR agonist DAMGO into the RVM *in vivo*, ON cell firing is directly inhibited through a postsynaptic mechanism (M. M. Heinricher et al., 1994). Indeed, MOR are positively expressed on part of OFF cells (Harasawa et al., 2016), and it has been assumed that the MOR agonists DAMGO activated OFF cells predominantly through two distinct mechanisms: one was direct activation via inducing glutamate release, while the other involved indirect disinhibition of RVM OFF cells by pre-synaptic inhibition of GABAergic terminals with the resulting release of endogenous opioids (M. M. Heinricher et al., 1992; M. M. Heinricher et al., 1994). KOR has limited expression on ON cells (approximately 13%) (Winkler et al., 2006). RVM microinjection of the KOR agonist U69593 did not affect tail flick latencies, although it did attenuate the ON cell burst (Meng et al., 2005), suggesting that OFF cells play a significant role in analgesia medicated by KOR. Approximately 86% of OFF cells are positive for KOR expression (Winkler et al., 2006), while functionally, administration of KOR agonists U69,593 into the RVM directly suppressed OFF cells activity through a postsynaptic

mechanism and inhibited glutamatergic input to OFF cells presynaptically, and thus could elicit mechanical hypersensitivity under normal conditions or following injuries (Winkler et al., 2006; Lau et al., 2020). Furthermore, KOR was found to be necessary and sufficient to mediate stress induced analgesia (SIA) since activation of KOR exerted similar effects as SIA, which were not enhanced by stress (Bagley and Ingram, 2020). Moreover, Nguyen et al. (2022) demonstrated that chemogenetic activation of KOR-positive neurons in the RVM increased thresholds of heat and mechanical pain and reversed hypersensitivity in acute and chronic pain states, which was consistent with presynaptic inhibition of excitatory inputs to ON cells and direct facilitation of OFF cells activity. Taken together, these results strongly indicate that KOR is expressed mainly on OFF cells but not on ON cells. After microinfusion of the DOR agonist DELT, ON cells activities decrease, while OFF cells activity is increased and behavioral antinociception is observed (Harasawa et al., 2000). Similar to MOR, the activation of DOR inhibits ON cells directly, disinhibits OFF cells, and induces analgesia. NOPR is co-expressed with MOR on ON cells, and both agonists exhibit the same suppression effects on ON cells, although the effects are not a crucial step in opioid-mediated analgesia (M. M. Heinricher et al., 1997). Previous studies have shown that under the circumstances of naloxone-precipitated withdrawal from opioids, infusing NOPR inhibited ON cell activity, removed the pronociceptive influence and counteracted the opioid withdrawal-induced hyperalgesia (Kaplan and Fields, 1991; Pan et al., 2000). Interestingly, NOPR activity induces pain-increasing effects via reversing the disinhibitory effect of facilitating OFF cells in the presence of stress stimulation, in which KOR participated (Pan et al., 2000). Thus, endogenous opioids interact with both ON and OFF cells, which fail to be identified as specific markers of any cell groups.

The effects of GABA and glutamate on RVM ON and OFF cells cannot be overlooked, as their dysfunction may represent a specific marker of ON or OFF cells. Approximately two-thirds of RVM ON cells contain express γ-aminobutyric acid (GABA) (Winkler et al., 2006). However, after administration of the $GABA_A$ receptor antagonist bicuculline methiodide, analgesic effects were observed, although ON cells did not show a consistent change in activity (M. M. Heinricher and Tortorici, 1994). Further research is still needed to determine whether other GABA receptors mediate ON cell modulation. Interestingly, RVM GABA transporter positive ($VGAT^+$) GABAergic neurons express immune-responsive MOR (MOR-ir), and approximately 67% of MOR-ir RVM neurons are vesicular $VGAT^+$ (Francois et al., 2017), indicating co-expression of MOR and GABA in ON cells. Activation of MOR or DOR produces a concentration-dependent decrease of GABA overflow in the RVM, reduces inhibitory GABAergic activity, and directly hyperpolarizes ON cells (Schepers et al., 2008; C. Zhang et al., 2020). Meanwhile, recent research by Jiao et al. (2022) confirmed that the G protein-coupled estrogen receptor (GPER) was expressed specifically in GABAergic ON cells, as activation of GPER caused depolarization of ON cells through modulation of MOR and potentiated pain. These findings may explain the major role of GABA and MOR in ON cell modulation, although GPER are found to be specific only in GABAergic groups. Furthermore, GAD67 (GABA markers) were identified in approximately 93% of OFF cells by immunostaining, indicating that OFF cells are also GABAergic neurons (Winkler et al., 2006). Since only 22% of $GABA_B$-expressing neurons in the RVM were retrogradely labeled, activating $GABA_B$ receptors at low doses facilitates OFF cells, while these were inhibited at high doses (Pinto et al., 2008). Following administration of the $GABA_A$ receptor antagonist bicuculline, OFF cells enter a prolonged period of continuous firing and exert behaviorally measurable antinociception (M. M. Heinricher and Tortorici, 1994), reiterating the importance of the OFF cell disinhibition on $GABA_A$ receptor-induced antinociception.

Regarding glutamate, repeated intramuscular injections increase the response of ON cells to glutamate by altering the activity of the N-methyl-D-aspartate receptor (NMDA), a glutamate receptor (Da Silva et al., 2010). By microinjecting the NMDA receptor antagonist AP5 into the RVM, Xu et al. (2007) found that only ON cell activities were inhibited, while activated OFF cells and Neutral cells were not affected, exerting a block of hyperalgesia. By applying the NMDA receptor antagonist ketamine to the RVM, ON cells were inhibited, which caused a reversal of chronic morphine-induced heat hypersensitivity (Viisanen et al., 2020). Moreover, the injection of low-dose glutamate into the RVM facilitated nociception in models of neuropathic and inflammatory pain, where the expression of cannabinoid receptor 1 (CB1R) and NMDA/AMPA receptors (glutamate receptors) on RVM ON cells was increased (Radhakrishnan and Sluka, 2009; Boadas-Vaello et al., 2016; Li et al., 2017). In general, we believe that NMDA receptors and glutamate in RVM could enhance ON cell activities and produce hyperalgesia. Conversely, OFF cells exert stronger activity and produce antinociceptive effects following application of glutamate or the specific activation of metabotropic receptors 8 (mGluR8) (Hosseini et al., 2021). Consequently, infusing the D-2-amino-5-phosophonopentanoic acid (NMDA) receptor antagonists into the RVM could attenuate or block the activation of OFF cells, which congruently confirmed the expression of glutamate receptors on OFF cells (M. M. Heinricher et al., 2001).

The transient receptor potential vanilloid-1 (TRPV1) is also expressed by both ON and OFF cells. Through immunoreactivity studies, Starowicz et al. (2007) found that in naïve rats, TRPV1/MOR was colocalized in 84% ± 5% of RVM neurons, while 21% ± 3% of TRPV1-labeled cells were surrounded by positive nerve terminals for VGAT, and of these, 80% ± 7% also expressed vesicular glutamate transporter 1 (VGLUT1). As MORs are mainly expressed in ON cells, we prefer to consider the existence of TRPV1 in ON cells under normal conditions. Interestingly, in the streptozotocin (STZ)-induced diabetic rat model, administering the capsaicin agonist TRPV1 increased TRPV1 expression and decreased hyperalgesia in the formalin test, with no effect in control animals (Silva et al., 2016). It is reasonable to suggest that during diabetic neuropathy, rats tend to be more sensitive to modulation of TRPV1 activity and changes in TRPV1 expression may be involved in glutamatergic circuits, namely OFF cells (Maione et al., 2009).

Microinjection of cholecystokinin (CCK) at low doses (10 ng/200 nL) attenuated opioid activation of OFF cells and blocked opioid-mediated analgesia; however, it exerted no direct effects on ON or OFF cells (Heinricher, 2001). Only administration of CCK at higher doses (30 ng/200 nL) selectively activated ON cells and produced behavioral hyperalgesia (M. M. Heinricher and Neubert, 2004). Therefore, the anti-opioid and pronociceptive

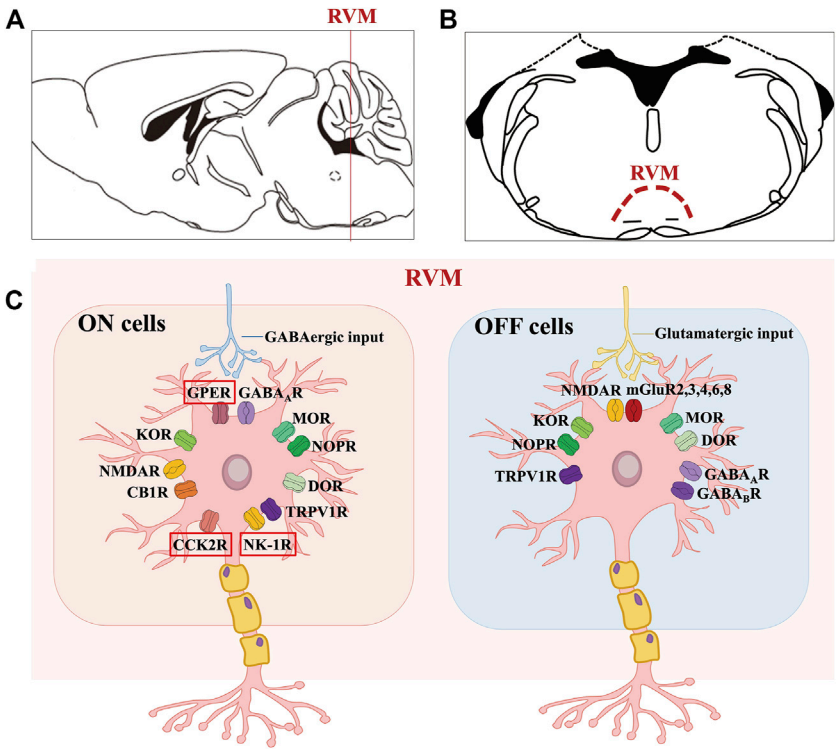

FIGURE 1
Molecular characteristics of the ON and OFF cells in RVM. **(A, B)** shows the anatomical location of the RVM nucleus in the mouse brain. **(C)** shows that GPER along with opioid, cannabinoid, GABA, TRPV1, glutamate, NK-1 and CCK2 receptors are expressed on ON cells, where GPER, CCK2R and NK-1R may be specific. Likewise, OFF cells mainly express opioid, cannabinoid, GABA, TRPV1 and glutamate receptors.

effects induced by CCK within the RVM are mediated by OFF and ON cells separately. Furthermore, Zhang et al. (2009) confirmed that 80% of RVM neurons co-expressed MOR and the CCK type 2 receptor (CCK2), and that MOR was specifically expressed in ON cells. After microinjecting L365,260 (a selective antagonist for CCK2) rather than a CCK1 antagonist into the RVM, the thermal hypersensitivity of rats with spinal injury was reversed (Kovelowski et al., 2000). Meanwhile, in female rats after plantar incision, injecting the CCK2 receptor agonist CCK-8 into the RVM produced hyperalgesia, while the CCK2 receptor antagonist YM022 decreased sensitivity to pain (Jiang et al., 2019). These studies provide evidence that CCK acts through CCK2 on ON cells and contributes to hyperalgesia under normal and pathological conditions. However, it remains unclear whether CCK2 can be regarded a specific marker of ON cells, as there has been no study investigating whether all ON cells express CCK2 and the direct effects on ON or OFF cells when facilitating or inhibiting CCK2.

Immunohistochemical studies have shown that the neurokinin-1 receptor (NK-1R) of substance P (SP) is co-expressed with NMDA receptors in RVM ON cells (Budai et al., 2007). Activation of NK-1R through microinjection of the NK-1R agonist SP or capsaicin actually improved ON cell responses evoked by NMDA receptors but not those of OFF cells and promoted hyperalgesia; these changes were attenuated by iontophoretic application of the NK-1R antagonist L-733,060 (Budai et al., 2007). However, NK-1R cannot be considered a specific marker of ON cells, although SP and NK-1R have been confirmed to promote descending facilitation and contribute to central sensitization and hyperalgesia. First, NK-1 positive neurons were a relatively small proportion of all neurons in the RVM, therefore, it is not clear whether all ON cells express NK-1R. Moreover, in the absence of inflammation, injecting L-733,060 or SP fails to change mechanical antinociception but alters thermal antinociception (Hamity et al., 2010). Meanwhile, pretreatment with L-733,060 in the RVM decreases nociception sensitivity only after injecting capsaicin, rather than complete Freud's adjuvant (CFA) (Hamity et al., 2010; Brink et al., 2012), indicating its limit in the processing of different pain stimuli (Khasabov et al., 2012).

Neurotensin (NT) is mainly expressed in the RVM and exerts nociceptive or antinociceptive effects in different states of pain (Feng et al., 2015). The low dose of NT in the RVM selectively activates the CCK2R in ON cells, increases the release of CCK, and produces thermal hyperalgesia, while high doses of NT recruit OFF cells and activate NT receptors, resulting in antinociception (Neubert et al., 2004; Li et al., 2021). Both the high-affinity NT receptor (NTR1) and the low-affinity NT receptor (NTR2) are expressed in RVM, of which NTR1 is predominantly co-expressed with 5-HT, whereas NTR2 is rarely expressed in 5-HTergic neurons. Antinociception produced by PD149163 (NTR1 agonists) is blocked by methysergide (non-selective serotonergic receptor antagonists) and is partially blocked by intrathecal yohimbine (NA receptor antagonists), although β-LT (NTR2 agonists) induced antinociception is only inhibited by yohimbine (Buhler et al., 2005; Buhler et al., 2008; Li

et al., 2021). Taken together, it is plausible that NTR1-mediated antinociception is mediated by noradrenaline (NA) and 5-HT release, while NTR2-mediated antinociception involves spinal release of NE alone. For the aim of pain relief, we conclude that through activating MOR, DOR, GPER and GABA, or inhibiting KOR, NMDA, TRPV1, CCK2R, CB1, NK-1R and NTR1, ON cells firing can be inhibited and OFF cells firing can be facilitated, leading to analgesia (Figure 1).

Although the role of neutral cells in pain modulation remains unknown, studies have suggested that they could develop ON or OFF cell-like properties under pathological conditions (Ellrich et al., 2000; Miki et al., 2002). Approximately 80% of neutral cells express GAD67, with a similar proportion expressing KOR (Winkler et al., 2006). In the RVM, approximately 23% of all neurons were found to be serotoninergic (5-HTergic), among which the vast majority were Neutral cells, while slightly fewer were OFF cells and the least were ON cells (Gu and Wessendorf, 2007; Lima et al., 2017). Serotonin (5-HT) has also been found to be expressed exclusively in a subset of neutral cells (36%), while none of ON or OFF cells exhibit 5-HT immunoreactivity (Winkler et al., 2006; Wang et al., 2017). It is worth paying closer attention to the exact function of 5-HTergic neutral cells in chronic pain modulation.

3 Neural circuits and neurotransmitters modulating RVM ON and OFF cells

3.1 Periaqueductal gray

3.1.1 Neural circuits involved in PAG-driven descending modulation of RVM

As the first discovered nuclei modulating descending pain in the brain, the periaqueductal gray (PAG) plays a key role in modulating descending pain, with direct projection to the RVM, and this projection terminates in superficial laminae (laminae I and II) of the spinal dorsal horn (Fields and Basbaum, 1978; Lau et al., 2020). Projections from PAG to RVM ON and OFF cells react to noxious stimuli and generated protective or defensive effects on pain sensation as defined using animal studies (M. M. Heinricher et al., 1987), which were also clearly confirmed by human brain imaging studies (Oliva et al., 2021). In-depth observations further provided stronger evidence indicating that opioid-triggered analgesia was mediated by ventrolateral projections of the PAG (vlPAG)-RVM, while non-opioid-triggered analgesia could be aroused by projections of the lateral PAG and the dorsolateral PAG (lPAG/dlPAG)-RVM (Crawford et al., 2021). As there have been no subsequent investigations, the delicate circuit constructions from the PAG to RVM for pain modulation are still far from being clarified.

3.1.2 Neurotransmitters mediating PAG-driven descending modulation of RVM

As the descending pain modulation circuit of the brain, the transmitters in the PAG-RVM projections have been comprehensively studied and include mainly GABA, glutamate, opioid, cannabinoid, and dopamine (DA) neurotransmitters. The vlPAG has direct GABAergic projections to RVM ON and OFF cells. Through immunochemistry studies, approximately 71% of the synapses in the PAG appeared to be GABAergic (containing GAD67 immunoreactivity), and directly projected to the RVM ON, OFF, and Neutral cells (Morgan et al., 2008). Microinjecting the $GABA_A$ receptor antagonist bicuculline into vlPAG, the spontaneous activity of OFF cells increased while that of ON cells decreased, resulting in pain inhibition (Moreau and Fields, 1986). When exposed to repeated restraint stress, GABA release into the RVM was increased, facilitating ON cells activity and inhibiting OFF cells activity, hence leading to mechanical hypersensitivity (Kohn et al., 2020). Several studies have suggested that GABA plays a major role in opioid and cannabinoid induced analgesia through the PAG-RVM pathway and is discussed below.

Glutamate also plays an important role in pain modulation via the PAG-RVM pathway with a pattern similar to that of GABA. Ho et al. (2013) found that when exposed to nerve injury, the α-amino-3-hydroxy-5-methyl-4-isoxazolepropionic acid (AMPA, another ionotropic transmembrane receptor for glutamate) receptor response was decreased, while the response of the NMDA receptor increased in vlPAG, decreasing the activities of OFF cells, thus initiating and facilitating hyperalgesia. Furthermore, the researchers identified eight subtypes of glutamate metabotropic receptors (mGluR1-8) in PAG exert different effects on nociception modulation, of which hyperalgesia was elicited by activating mGluR1 and mGluR5 (Group I), while activation of mGluR2, mGluR3 (Group II), and mGluR4, 6, 7, 8 (Group III) led to analgesia. Studies conducted by Hosseini et al. (2020) showed that after administration of mGluR8 agonists (S)-3,4-dicarboxyphenylglycine (DCPG) in PAG, glutamate transmission increased, then RVM ON cell firings were reduced and OFF cell activities were enhanced, and predominantly generated antinociceptive effects. However, Marabese et al. (2007) reported a disturbing finding in which intra-PAG microinjection of AMN082, a selective mGluR7 agonist, increased RVM ON cell activity while abrogating OFF cell activity and then induced hyperalgesia. It is plausible that hyperalgesia was attributed to the activation of mGluR7 in the PAG before that of mGluR4/8, which overlaps the antinociceptive effects triggered by mGluR4/8.

Opioid mediated analgesia mainly through PAG-RVM circuit. Via the presynaptic inhibition of PAG GABAergic interneurons and glutamatergic transmission, the microinjection of morphine into the PAG inhibited GABAergic projections to the RVM (Beitz, 1990; Park et al., 2010; Lau et al., 2020), indirectly activated (disinhibited) RVM OFF cells and directly inhibited ON cell activity, thereby leading to analgesia (Basbaum and Fields, 1984; M. M. Heinricher et al., 1987; Fang et al., 1989; M. M. Heinricher et al., 1994). Although opioids released from PAG to RVM play a pivotal role in endogenous analgesia, more in-depth studies are needed to clarify the expression of different opioid receptors in this system. Similar to the observations in the RVM, MOR, DOR, KOR, and NOPR were also prevalent in the PAG region (Gutstein et al., 1998). MOR expression in the PAG is located primarily in GABAergic projection neurons to the RVM (Commons et al., 2000). Vaughan et al. (1997) found that MOR coupled to a voltage-dependent K+ conductance in the GABAergic terminals via the PLA2/arachidonic acid/12-lipoxygenase cascade system, inhibits GABAergic interneurons in the PAG. G protein-coupled inwardly rectifying potassium channels (GIRKs) were also found to be activated by MOR, leading to hyperpolarization of PAG-RVM projections (Morgan et al.,

2020). These findings enhanced the reliability of the disinhibition theory. Regarding DOR, the mechanisms of pain modulation and the effects of DOR in the PAG-RVM circuit were similar to MOR, except for the indirect inhibition of GABAergic projections (Kalyuzhny and Wessendorf, 1998). Accumulating evidence suggests that DOR is located mainly in terminals containing enkephalins of the PAG, and when released, glutamatergic inputs to GABAergic projections in the vlPAG would be inhibited, including the metabolic pathways involving CB1R and phospholipase A (Commons et al., 2001; Z. Zhang and Pan, 2012; Bushlin et al., 2012). NOPR can presynaptically inhibit GABAergic and glutamatergic neurons in the vlPAG and postsynaptically inhibit PAG-RVM projections, leading to hyperalgesia and reverse opioid-induced analgesia (Morgan et al., 1997; Vaughan et al., 1997; Lu et al., 2010).

Interestingly, the PAG-RVM opioidergic projections are closely related to the sexual dimorphism of pain modulation. Studies have shown that antinociceptive effects of morphine were reduced in intact gonadal females compared to males, while MOR and KOR agonists were more potent or effective in one sex or the other in more than 60% of cases (Craft, 2003). Additionally, Tonsfeldt et al. (2016) observed that antagonists or negative allosteric modulators of the $GABA_A$ receptor appeared to be more efficient in morphine-induced analgesia of female rats compared to that of male rats during continuous inflammation. Therefore, it is reasonable to suspect that sexually dependent neurotransmitters may modulate opioid-mediated analgesia. Craft et al. (2004) suggested that compared to males, morphine-mediated antinociception could be attributed at least in part to higher levels of estradiol in females, since in female rats the baseline ON cell burst and OFF cell pause were depressed. Meanwhile, researchers found that estrogen receptor alpha was required for estrogen-induced internalization of MOR (Micevych et al., 2003). Loyd et al. (2007) further demonstrated that the PAG-RVM projections contained less MOR immunoreactivity in vlPAG in females compared to males, resulting in the attenuation of opioid-mediated analgesia. Furthermore, reproductive hormone levels have been found to influence the distribution of KOR in RVM, which, in turn, modulates opioid-mediated analgesia (Drake et al., 2007). All of these results have confirmed the crucial role of the opioid system in PAG-RVM projections to mediate pain-related sexual dimorphism.

Endocannabinoid also participates in analgesia through PAG-RVM pathway. The endocannabinoid system consists of the endogenous synthesis enzyme lipid signals 2-arachidonoylglycerol and the degraded enzyme anandamide, and also the cannabinoid receptors. Except in some cortex regions, PAG is a key nucleus that synthesizes endocannabinoids, which are in turn released to the RVM. The projections of the PAG-RVM mediate cannabinoid-induced analgesia and contribute to SIA (Ossipov et al., 2010). Microinjection of cannabinoid receptor agonists WIN55,212-2 into the RVM decreased the firing of ON cells while increased ongoing OFF cells activities, thus increasing the rat tail-flick latency (Rea et al., 2007; Ossipov et al., 2010). Therefore, the endogenous cannabinoids can modulate the tonic increase in OFF cells activity and diminish ON cells firing, modulating baseline nociceptive thresholds and exerting antinociceptive effects. Cannabinoid receptors consist of cannabinoid receptor 1 and 2 (CB1R, CB2R), among which CB1R is expressed in approximately one-third of PAG neurons and is co-expressed with MOR. Activation of PAG CB1R decreases GABA release and activates mGlu5R, leading to the inhibition of ON cells and disinhibition of OFF cells, ultimately resulting in SIA, as well as analgesia in both normal and neuropathic pain situations (Novellis et al., 2005; Rea et al., 2007; Ossipov et al., 2010). However, CB2R expression appears to be highly dynamic and depends on the microenvironment, since CB2R expression increases in inflammation and neuropathic pain (Bouchet and Ingram, 2020). Through *in vivo* recording assays, the CB1R agonists SR141716 activated OFF cells, which was consistent with their analgesic effects on pain behavior, while through *ex vivo* slice recording, SR141716 significantly decreased the frequency of miniature inhibitory postsynaptic potential (mIPSC, related to GABA release) frequency and inhibited GABA release to ON cells (Li et al., 2015; Bouchet and Ingram, 2020; Milligan et al., 2020). Of note, CB2R agonists AM1241 and GW405833 inhibited presynaptic GABA release and ON cell activities in the RVM in CFA-treated but not in naïve rats (Bouchet and Ingram, 2020). Alternatively, it has been fully demonstrated that endogenous cannabinoids activate opioid-insensitive SIA predominantly through the CB1R rather than the CB2R, and inhibiting endogenous cannabinoids hydrolysis in the RVM can enhance SIA (Ossipov et al., 2010).

Compared to opioid-related analgesia, the contribution of PAG dopaminergic neurons (DAergic) to pain modulation via the vlPAG-RVM pathway is obscure. To our knowledge, there are indeed DAergic neurons in vlPAG, but no direct DAergic projections from the PAG to RVM (Li et al., 2016). However, DA may activate the dopamine receptor 2 (D2R), which was expressed in PAG GABAergic neurons (Li et al., 2016; Ferrari et al., 2021). Meyer et al. (2009) determined that injection of the D2R agonist quinpirole but not dopamine receptor 1 (D1R) agonists chloro-APB into the vlPAG modulated PAG-RVM projections, and increased the threshold for the paw-withdrawal response and generating protective reactions to pain, while suppressing DAergic neurons reduced opioid-mediated analgesia (Ferrari et al., 2021). Li et al. (2016) determined D2R activation blocked MOR-induced inhibition of GABAergic neurons and reduced presynaptic GABAergic neurotransmission, leading to a decrease in inhibitory input to vlPAG DA neurons and antinociception. In contrast, the administration of D-amphetamine to vlPAG led to an inhibition of RVM ON cells by PAG GABAergic neurons, although increased PAG glutamatergic projections to RVM OFF cells were not involved in antinociception effects (Ferrari et al., 2021). Collectively, it has been speculated that the analgesic effects of PAG DA neurons are mediated by indirect modulation of the RVM, mainly by interfering with the opioid- and GABA-mediated descending pathway of PAG-RVM.

Melatonin (MLT) participates in analgesia across different states of abnormal pain. Specifically, MLT acts primarily through melatonin 2 (MT2) receptors in vlPAG, inhibiting ON cell activities and facilitating OFF cells, leading to analgesia (Lopez-Canul et al., 2015). Interestingly, researchers found that only 0.2% of MOR was co-expressed with melatonin 2 (MT2) receptors in vlPAG, but all MT2 receptors, which did not show expression in RVM, required MOR to exert antinociceptive effects (Posa et al., 2022) (Figure 2).

3.2 Parabrachial complex

3.2.1 Neural circuits involved in PB-driven descending modulation of RVM

The parabrachial complex (PB) functions as a significant supraspinal relay region in the midbrain for nociceptive transmission, not only under normal situations but also under pathological pain conditions. PB was shown to project directly to the RVM using bulk tracer methods (Verner et al., 2008). Interestingly, electrophysiological investigations determined that during the PB block, the extent of OFF cell pauses and ON cell bursts was attenuated, but not eliminated, suggesting a modest rather than robust decisive contribution to modulation to RVM ON and OFF cell activities in the pain process. Additionally, optogenetic inhibition of archaerhodopsin (ArchT) expressing PB terminals in the RVM can substantially attenuate ON cell (62%) and OFF cell (71%) activity during *in vivo* recording, leading to antinociception (Chen et al., 2017). Furthermore, blocking contralateral PB, but not ipsilateral PB, significantly attenuated the burst of ON cells and the pause of OFF cells in the first hour after CFA injection and substantially reversed mechanical hypersensitivity, while during the ~1–6 days after CFA injection, blocking the contralateral PB did not alter the firing of ON or OFF cells and did not exert any effects on hyperalgesia. In contrast, during the ~5–6 days after CFA administration, only activating the ipsilateral PB interfered with the evoked responses in the RVM, which resulted in an increase in overall ON cell firing and a reduction in OFF cell activities, exacerbating the inflamed hind paw, and ultimately improving and maintaining pain hypersensitivity (Chen and Heinricher, 2019b). Altogether, the general consensus indicates that PB receives substantial projections from nociceptive neurons in the contralateral superficial dorsal horn, and less dense inputs from the ipsilateral superficial dorsal horn and deeper lamina, more specifically, the PB projects directly to RVM ON and OFF cells. Under physiological conditions and when exposed to acute pain stimuli, it is the contralateral PB that transmits projections to the RVM ON and OFF cells and then triggers acute hyperalgesia, while the ipsilateral PB is involved in the RVM ON and OFF cells-induced modulation of persistent inflammation and chronic pain.

3.2.2 Neurotransmitters mediating PB-driven descending modulation of RVM

PB-RVM circuits exert hyperalgesia mainly through GABAergic and glutamatergic projections. Most PB neurons were glutamatergic (72%) or GABAergic (28%) (Geerling et al., 2017; Chiang et al., 2019). In particular, by whole cell patch clamp recordings, Chen et al. found that light stimulation of PB neuron terminals that expressed ChR2 in RVM slices elicited synaptic currents in 29 neurons, of which 21 neurons were blocked by glutamate antagonists KA or NBQX, while the remaining 8 neurons were inhibited by bicuculine, a $GABA_AR$ antagonist. Furthermore, the GABAergic inputs observed in slice experiments formed inhibitory nociceptive inputs to OFF cells, while the glutamatergic inputs corresponded to excitatory projections to ON cells and some were concomitant with Neutral cells (Chen et al., 2017). Importantly, under stress, lPB neurons, specifically those projecting onto RVM GABAergic neurons (that is, ON cells), cooperate with cannabinoids and CB2R and participated in hyperalgesia (Francois et al., 2017) (Figure 2).

3.3 Locus coeruleus

As an important mental stress-responsive nucleus, the locus coeruleus (LC) is also a pivotal region involved in the modulation of descending pain, mainly through direct spinal cord projections and effects on RVM activity via NAergic projections. Through a retrograde tracing study, Braz et al. (2009) found that ventrally located LC neurons were labeled after injecting pseudorabies virus (PRV) into the RVM, which is consistent with the results that in attentional analgesia, an fMRI parameter of LC-RVM connections was improved (Tanaka et al., 1996; Hickey et al., 2014; Oliva et al., 2022). Moreover, studies by Dehkordi. et al., 2019 demonstrated that stimulation of LC NAergic neurons increased the release of NA and increased 1-adrenoceptor concentrations of α1-adrenoceptors (NAα1R) in NRM, leading to analgesia (Dehkordi. et al., 2019). In contrast, it was also possible that LC-NRM projecting NAergic neurons induced hyperalgesia by activating NRM NAα1R. As Bie et al. (2003) showed, during opioid withdrawal, administration of the NAα1R antagonist prazosin in NRM significantly decreased the activities of NAergic projections of the LC and suppressed hyperalgesia. RVM ON cells received NAergic inputs from LC and contained NAα1R, which contributed to hyperalgesia during opioid withdrawal, while inhibition of NAα2R-expressed ON cells by clonidine suppressed DAMGO-mediated analgesia instead of modulating hyperalgesia during opioid withdrawal. OFF cells also received dense NAergic input from the LC, and mainly expressed NAα1R and some co-expressed NAα2R (Bie et al., 2003). Overall, these results suggest that LC-RVM projections on NAergic neurons trigger not only antinociceptive but also pronociceptive effects by modulating RVM ON and OFF cells, although the precise role of LC-RVM projections in different pain conditions requires further investigation (Figure 2).

3.4 Hypothalamus

Hypothalamus-RVM circuits participate in pain modulation mainly in dorsal medial hypothalamus (DMH) via endomorphin-2 and CCK containing projections. After microinjection of Fluoro-Gold (FG) into the RVM, retrogradely labeled neurons were detected in the hypothalamus, the majority of which were present in the lateral hypothalamus (LH) and DMH (Gu and Wessendorf, 2007). DMH stimulation directly induced robust activation of ON cells along with suppression of OFF cell firing, leading to behavioral hyperalgesia, in contrast to other research showing that stimulation of the hypothalamus produced analgesia that could be inhibited by systemic naloxone (Adams and Hosobuchi, 1977; Martenson et al., 2009). Hyperalgesia induced by DMH stimulation recruits ON cells under mild and persistent stress, a response known as stress-induced hyperalgesia (SIH). However, microinjection of lidocaine into the RVM potentiates hypothalamic-mediated analgesia, as observed by the increase in

the pain threshold and inhibition of the tail flick reflex (Gu and Wessendorf, 2007). Collectively, these findings confirm that the hypothalamus projects directly to the RVM and influences the activities of ON and OFF cells; thus, exerting bidirectional pain modulation. In terms of neurotransmitters and receptors, endomorphin-2 (EM-2, an endogenous ligand of MOR) containing neurons exist primarily in the DMH and project to the RVM, and EM-2 has been found to participate in hypothalamus stimulation-induced analgesia, replicating its antinociceptive effects through MOR and endogenous opioids (Gu and Wessendorf, 2007; Bagley and Ingram, 2020). Furthermore, in stress states, DMH has been identified as the only supraspinal source of CCK input to the RVM, acting with CCK2R in ON cells and can elicit hyperalgesia as observed experimentally under abundant abnormal pain states via retrograde tract tracing combined with electrophysiological and immunohistochemistry (Wagner et al., 2013). Moreover, infusion of 1 nmol excitatory amino acid receptor cytonurenate into the RVM blocked the DMH-induced ON cell activation and suppression of OFF cells, alleviating hyperalgesia. Similar results can also be observed after infusion of the $GABA_A$ receptor agonist muscimol (Martenson et al., 2009). In conclusion, the hypothalamus-RVM projection modulates pain sensitivity primarily through endogenous opioid synaptic transmission and communicates with CCK2R and MOR (Figure 2).

3.5 Amygdala

The amygdala is characterized by direct and indirect projections to the RVM, and participates in pain modulation. After microinjection of morphine into different sites of the amygdala, several significant findings suggest that its analgesic effects were mainly attributed to the direct projections from the amygdala to the RVM, for instance: 1) infusing morphine into the basolateral nuclei increased OFF cell activity, modestly decreased ON cell activity, remarkably attenuated the OFF cell pause, and increased tail flick latency; 2) administering morphine into the cortical and medial nuclei exerted smaller effects on ON and OFF cells than infusion directly into basolateral nuclei, but did not significantly eliminate the OFF cell pause and only the increased tail flick latency to a small degree; 3) introducing morphine within the central, medial, and dorsal lateral nuclei failed to modulate activities of the RVM ON and OFF cells and the tail flick latency (Mcgaraughty and Heinricher, 2002). In fact, the basolateral nucleus of the amygdala is relayed

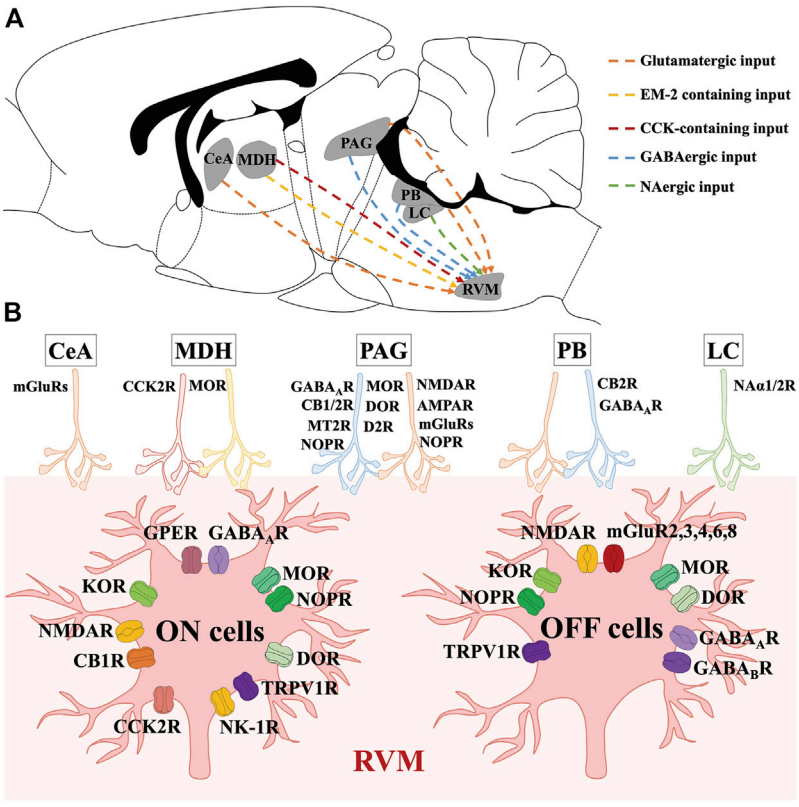

FIGURE 2
Molecular characteristics of neural circuits and transmitters modulating RVM ON and OFF cells. **(A)** shows the anatomical location of nucleus and neural circuits projecting to the RVM ON and OFF cells in the mouse brain. **(B)** shows the transmitters and receptors which participate in modulating RVM ON and OFF cells. CeA mainly act on glutamate receptors to exert modulations on RVM ON and OFF cells. By binding to MOR and CCK2R, DMH EM-2 containing inputs and CCK-containing inputs modulate RVM ON and OFF cells. Via acting on opioid, cannabinoid, GABA, glutamate, dopamine, TRPV1, and melatonin receptors, PAG GABAergic and glutamatergic inputs modulate RVM ON and OFF cells. PB GABAergic and glutamatergic neurons modulate RVM ON and OFF cells by binding to cannabinoid, and GABA receptors. LC NAergic neurons act on Naα receptors to modulate RVM ON and OFF cells.

through the central nucleus of the amygdala (CeA), and then recruited RVM OFF cells, and conducts opioid-induced analgesia under states of SIA to replenish DMH-induced SIA (Martenson et al., 2009). Despite the ineffective function of CeA under normal conditions, it is currently agreed that amygdala-mediated hyperalgesia in pain-related disorders occurs in CeA through the interactions with mGluR1/5, since there are large amounts of nociceptive neurons at this pivotal site and an increase in excitability of CeA is detected even under conditions of chronic pain (Palazzo et al., 2011). Meanwhile, CeA exerts antinociceptive effects by acting on the mGluR8. Under carrageenan-triggered inflammatory pain conditions, intra-CeA microinjections of mGluR8 agonists (S)-3,4-DCPG increase OFF cell activities while decrease ON cell activities, thus creating antinociceptive effects. (Palazzo et al., 2011). Hence, amygdala-RVM pathway, particularly CeA-RVM projections, modulate pain through acting at mGluRs (Figure 2).

4 Neural circuits and neurotransmitters modulating projections from RVM ON and OFF cells to spinal cord

4.1 Neural circuits involved in RVM-driven descending modulation

There exist RVM-spinal cord circuits modulating pain through 5-HTergic and GABAergic projections. It is generally accepted that descending projections from the RVM to the spinal cord predominantly target the laminae V dorsal horn (Martins and Tavares, 2017), although the axons of most spinal ascending projection neurons terminate in many areas of the brain, including the forebrain, pons, and midbrain, rather than in the RVM, suggesting that RVM does not receive afferents from the spinal cord (Wang et al., 2022). By injecting rabies virus into the spinal cord, Francois et al. (2017) used retrograded transsynaptic tracing to identify regions corresponding to descending pain control and found that the virus was strongly expressed in RVM neurons; thus, indicating that RVM projects to the spinal cord. Furthermore, more than 90% of the RVM spinal cord projection neurons responded to the opioid agonists DAMGO, of which a large proportion of the neurons responded only to MOR agonists (64%), while a smaller proportion responded only to KOR agonists (9%), and approximately 18% responded to both MOR and KOR agonists (Marinelli et al., 2002). In fact, the RVM descending projection neurons that participate in pain modulation mainly consist of GABAergic and 5-HTergic neurons, so how these inhibitory GABAergic neurons facilitate spinal pain transmission was previously a mystery. Francois et al. demonstrated that downstream of RVM GABAergic neurons were spinal GABAergic/enkephalinergic interneurons, and activation of the RVM GABAergic neurons would inhibit spinal inhibitory interneurons, thus inducing disinhibition of spinal pain transmission (Francois et al., 2017). The study revealed a potential circuit mechanism for ON cells-induced pain facilitation, although it is still urgent to understand how OFF cells and 5-HTergic neurons modulate spinal pain transmission and how these RVM neurons cooperate in different pain states.

4.2 Neurotransmitters mediating RVM-driven descending modulation

GABAergic projections from the RVM to the spinal cord take part in pain modulation through altering the activities of RVM ON and OFF cells. Most RVM neurons that project to the spinal cord are not 5-HTergic (60%, i.e., GABAergic), of these, 40% also express enkephalin (PENK), while the remaining 40% are 5-HTergic (Hossaini et al., 2012; Kohn et al., 2020; Talluri et al., 2022). The RVM GABAergic neurons express GAD1 and GAD2 receptors, forming axosomatic and axo-axonic inhibitory synapses, accordingly (Fink et al., 2014; Mende et al., 2016). Under physiological conditions, PENK+/GAD2+ neurons (that is, OFF cells) directly communicate with the primary afferent of DRG neurons and tonically inhibit pain responses (Francois et al., 2017), counteracting 5-HTergic-induced pronociception. When under conditions of mechanical pain, PENK/GAD1+ neurons (namely ON cells) synapse onto Penk + dorsal horn interneurons, disinhibit PENK + neurons, and facilitate the transmission of mechanical pain stimuli. Furthermore, GABAergic PENK + neurons contribute to stress-induced modulation of pain, since acute stress increases activities of GABAergic PENK + neurons, exerting analgesia while chronic stress decreases the expression of GABAergic PENK + neurons and induces hyperalgesia (Francois et al., 2017).

With regard to 5-HTergic neurons, its effects on RVM-spinal cord pathway are confirmed, however the concrete influence on RVM ON, OFF or Neutral cells remain controversial, which were discussed aftermentioned. 5-HT is produced primarily in the NRM, although retrograde labeling studies have demonstrated that 5-HTergic projections to the spinal dorsal horn simply arise from the NRM and terminate densely in the superficial laminae (laminae I and II) and in the deeper laminae (laminae IV-VI) of the dorsal horn. Meanwhile, stimulation of RVM leads to increased 5-HT release in the spinal cord, contributing to bidirectional effects on nociceptive modulation (Ossipov et al., 2010; Kort et al., 2022). In reality, there are two populations of 5-HTergic neurons in the RVM, those involved in spinal projections and in local modulation. Although some RVM 5-HTergic neurons express MOR (13.8% ± 3.9%) and GABA (8%), only about half of these project to the spinal cord, which suggests the existence of 5-HTergic neurons for local modulation (Wei et al., 2010; Lau et al., 2020). With regard to local 5-HTergic neurons in the RVM, direct microinjection of 5-HT increased the release of 5-HT in the NRM, modulating ON and OFF cells in RVM through 5-HT1R and 5-HT2R, which ultimately decrease tail flick latency, and exert an inhibitory influence on pain modulation (Brito et al., 2017; Wang et al., 2017). These findings indicate that 5-HTergic neurons could modulate the pain response by affecting the excitability of ON and OFF cells. For the spinal projection of 5-HT-ergic neurons, Sagalajev et al. (2017) explored some interesting findings in a pharmacological study involving the microinjection of NT in the RVM, which resulted in reduced ON cell discharge and facilitated OFF cell activation, thus inducing antinociceptive effects (Buhler

et al., 2005). Meanwhile, injection of EM-2 into the RVM activated MOR in spinal projection of 5-HTergic neurons and increased descending 5-HTergic facilitatory influences, although these descending 5-HTergic projections were neither necessary nor sufficient for RVM MOR- or KOR-mediated modulation of descending pain in acute pain conditions (Gu and Wessendorf, 2007; Chen and Heinricher, 2019a; Kohn et al., 2020). Hence, it is reasonable that under physiological conditions, activation of RVM 5-HTergic neurons will inhibit spinal nociceptive neurotransmission. In experimental models of diabetic neuropathy and chemotherapy-induced neuropathy, the excitability of 5-HTergic neurons in RVM increased, inducing increased recruitment of descending 5-HTergic projections to the spinal cord and resulting in pain hypersensitivity (Sikandar et al., 2012). Through molecular engineering approaches using shRNA plasmids and electroporation, RVM 5-HTergic neurons were found to function as modulators of pain in the promotion and maintenance, rather than triggering, of inflammatory or neuropathic pain (Wei et al., 2010). Taken together, the existing evidence suggests that two types of RVM 5-HTergic neurons can modulate spinal pain transmission in direct and indirect ways, which may be responsible for the bidirectional effects on modulating pain in physiology and pathophysiology conditions. Conversely, bidirectional projections in nociception also closely depend on the activation of various subtypes of the 5-HT receptor (5-HT1R-7R). Generally, 5-HT1AR, 5-HT2AR, and 5-HT4R generate bidirectional effects, while 5-HT1B/DR and 5-HT2CR are primarily antinociceptive (Bardoni, 2019; Heijmans et al., 2021; Fauss et al., 2022). In contrast, 5-HT2BR is activated by facilitating CCK2R in RVM ON cells and induces hyperalgesia (Jiang et al., 2019). Furthermore, the function of 5-HT3R and 5-HT7R remains uncertain. In neuropathic or inflammatory pain states, blocking the 5-HT3R specifically attenuates 5-HT pronociceptive actions in the RVM while activation of the 5-HT3R plays a facilitatory role in nociceptive responses. These findings were in parallel with the observations that a descending release of 5-HT from the RVM combined with the upregulation of 5-HT3R expression in spinal cord neurons was detected after inflammation and nerve injury (Wei et al., 2010; Wang et al., 2019; Liu et al., 2020). Thus, it is confirmed that spinal 5-HT3R mainly mediates descending facilitation under abnormal pain conditions. Specifically, activation of the p38 mitogen-induced protein kinase (p38MAPK) pathway in the RVM increases the expression of tryptophan hydroxylase (Tph), resulting in increased activities of ON cells and expression of 5-HT along with the silencing of OFF cells, which then act on the spinal 5-HT3R to activate ATP-gated P2X7 receptors in the microglia, and ultimately exerting pain hypersensitivity (Liu et al., 2020). As 5-HT3R is also expressed on inhibitory GABAergic interneurons, antinociceptive effects are confirmed to correspond to activation of OFF cells in subcutaneously excited RVM 5-HT3R and GABA release in the GABA spinal cord in acute pain models (Nasirinezhad et al., 2016; Kort et al., 2022). With regard to 5-HT7R, under conditions of neuropathic pain, the study conducted by Brenchat et al. (2010) showed that the spinal 5-HT7R was expressed mainly on the GABAergic and Penk + interneurons, which stimulate OFF cells, release 5-HT, GABA, and enkephalins, and therefore enhance nociceptive inhibition, in contrast to the pronociceptive effects exerted in the periphery. In healthy conditions, spinal 5-HT7R only shows antinociceptive effects, in which the exact mechanism remains to be defined (Wang et al., 2015) (Figure 3).

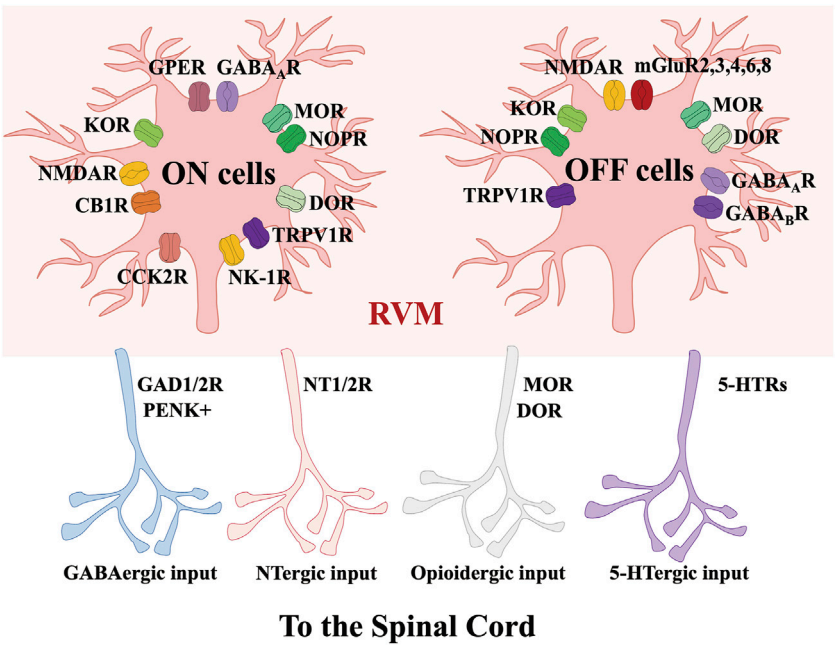

FIGURE 3
Molecular characteristics of RVM-spinal cord circuits modulating nociception. Via acting on GAD, 5-HTRs, NT and opioid receptors, the projections from RVM ON and OFF cells to the spinal cord contain GABAergic, NTergic, opioidergic and 5-HTergic inputs.

5 Conclusion

As the final relay nuclei of the descending pain modulation system, the RVM converges on the comprehensive modulation input from different nuclei like the PAG, amygdala, PB, LC, and the hypothalamus, as reviewed herein, and then integrates this information to influence the excitability status of ON, OFF, and even Neutral cells in this area, whose descending projections lead to the spinal cord, where they exert facilitation or inhibition of spinal pain transmission, and finally control the nociceptive intensity received by the brain from the periphery. In this process, GABA, 5-HT, endogenous opioids, endogenous cannabinoids, and their corresponding receptors are the main mediators involved in the facilitation and inhibition of pain. Moreover, it has been generally accepted that RVM related circuits and neurotransmitters play a pivotal role in the maintenance and persistence of chronic pain; thus, the RVM is a major therapeutic nucleus for the development of novel strategies for alleviation of pain. Conversely, in order to successfully obtain further scientific understanding of RVM or clinical pain treatment targeting RVM, we first need to identify a suitable model for specific modulation of ON and OFF cells, as well as clarify the molecular and circuit changes associated with the RVM under pathological conditions.

Author contributions

WY and YF conceptualized this study and organized the manuscript. BP and YJ co-wrote the manuscript, YZ, SL, SC, SX, and PG contributed to the critical reading and the useful comments on the manuscript.

Funding

This review was supported by The National Natural Science Foundation of China (32030043, 81971223, 82270916, and 82101287), Shanghai Science and Technology Commission Medical Innovation Research Special Fund (21Y11906000), Shanghai Municipal Key Clinical Specialty (shslczdzk03601) and Innovation Program of Shanghai Municipal Education Commission (2019-01-07-00-01-E00074). Innovative Research Team of High-level Local Universities in Shanghai (SHSMU-ZDCX20211102).

Acknowledgments

We also gratefully acknowledge support from Shanghai Engineering Research Center of Peri-operative Organ Support and Function Preservation (20DZ2254200).

Conflict of interest

The authors declare that the research was conducted in the absence of any commercial or financial relationships that could be construed as a potential conflict of interest.

Publisher's note

All claims expressed in this article are solely those of the authors and do not necessarily represent those of their affiliated organizations, or those of the publisher, the editors and the reviewers. Any product that may be evaluated in this article, or claim that may be made by its manufacturer, is not guaranteed or endorsed by the publisher.

References

Adams, J. E., and Hosobuchi, Y. (1977). Technique and technical problems. *Neurosurgery* 1, 196–199. doi:10.1097/00006123-197709000-00017

Bagley, E. E., and Ingram, S. L. (2020). Endogenous opioid peptides in the descending pain modulatory circuit. *Neuropharmacology* 173, 108131. doi:10.1016/j.neuropharm.2020.108131

Barbaro, N. M., Heinricher, M. M., and Fields, H. L. (1989). Putative nociceptive modulatory neurons in the rostral ventromedial medulla of the rat display highly correlated firing patterns. *Somatosens. Mot. Res.* 6, 413–425. doi:10.3109/08990228909144684

Bardoni, R. (2019). Serotonergic modulation of nociceptive circuits in spinal cord dorsal horn. *Curr. Neuropharmacol.* 17, 1133–1145. doi:10.2174/1570159X17666191001123900

Basbaum, A. I., and Fields, H. L. (1984). Endogenous pain control systems: Brainstem spinal pathways and endorphin circuitry. *Annu. Rev. Neurosci.* 7, 309–338. doi:10.1146/annurev.ne.07.030184.001521

Behbehani, M. M., and Fields, H. L. (1979). Evidence that an excitatory connection between the periaqueductal gray and nucleus raphe magnus mediates stimulation produced analgesia. *Brain Res.* 170, 85–93. doi:10.1016/0006-8993(79)90942-9

Beitz, A. J. (1990). Relationship of glutamate and aspartate to the periaqueductal gray-raphe magnus projection: Analysis using immunocytochemistry and microdialysis. *J. Histochem Cytochem* 38, 1755–1765. doi:10.1177/38.12.1701457

Bie, B., Fields, H. L., Williams, J. T., and Pan, Z. Z. (2003). Roles of alpha1-and alpha2-adrenoceptors in the nucleus raphe magnus in opioid analgesia and opioid abstinence-induced hyperalgesia. *J. Neurosci.* 23, 7950–7957. doi:10.1523/JNEUROSCI.23-21-07950.2003

Boadas-Vaello, P., Castany, S., Homs, J., Álvarez-Pérez, B., Deulofeu, M., and Verdú, E. (2016). Neuroplasticity of ascending and descending pathways after somatosensory system injury: Reviewing knowledge to identify neuropathic pain therapeutic targets. *Spinal Cord.* 54, 330–340. doi:10.1038/sc.2015.225

Bouchet, C. A., and Ingram, S. L. (2020). Cannabinoids in the descending pain modulatory circuit: Role in inflammation. *Pharmacol. Ther.* 209, 107495. doi:10.1016/j.pharmthera.2020.107495

Braz, J. M., Enquist, L. W., and Basbaum, A. I. (2009). Inputs to serotonergic neurons revealed by conditional viral transneuronal tracing. *J. Comp. Neurol.* 514, 145–160. doi:10.1002/cne.22003

Brenchat, A., Nadal, X., Romero, L., Ovalle, S., Muro, A., Sánchez-Arroyos, R., et al. (2010). Pharmacological activation of 5-HT7 receptors reduces nerve injury-induced mechanical and thermal hypersensitivity. *Pain* 149, 483–494. doi:10.1016/j.pain.2010.03.007

Brink, T. S., Pacharinsak, C., Khasabov, S. G., Beitz, A. J., and Simone, D. A. (2012). Differential modulation of neurons in the rostral ventromedial medulla by neurokinin-1 receptors. *J. Neurophysiol.* 107, 1210–1221. doi:10.1152/jn.00678.2011

Brito, R. G., Rasmussen, L. A., and Sluka, K. A. (2017). Regular physical activity prevents development of chronic muscle pain through modulation of supraspinal opioid and serotonergic mechanisms. *Pain Rep.* 2, e618. doi:10.1097/PR9.0000000000000618

Budai, D., Khasabov, S. G., Mantyh, P. W., and Simone, D. A. (2007). NK-1 receptors modulate the excitability of ON cells in the rostral ventromedial medulla. *J. Neurophysiol.* 97, 1388–1395. doi:10.1152/jn.00450.2006

Buhler, A. V., Choi, J., Proudfit, H. K., and Gebhart, G. F. (2005). Neurotensin activation of the NTR1 on spinally-projecting serotonergic neurons in the rostral ventromedial medulla is antinociceptive. *Pain* 114, 285–294. doi:10.1016/j.pain.2004.12.031

Buhler, A. V., Proudfit, H. K., and Gebhart, G. F. (2008). Neurotensin-produced antinociception in the rostral ventromedial medulla is partially mediated by spinal cord norepinephrine. *Pain* 135, 280–290. doi:10.1016/j.pain.2007.06.010

Bushlin, I., Gupta, A., Stockton, S. D., Miller, L. K., and Devi, L. A. (2012). Dimerization with cannabinoid receptors allosterically modulates delta opioid receptor activity during neuropathic pain. *PLoS One* 7, e49789. doi:10.1371/journal.pone.0049789

Chen, Q., and Heinricher, M. M. (2019a). Descending control mechanisms and chronic pain. *Curr. Rheumatol. Rep.* 21, 13. doi:10.1007/s11926-019-0813-1

Chen, Q., and Heinricher, M. M. (2019b). Plasticity in the link between pain-transmitting and pain-modulating systems in acute and persistent inflammation. *J. Neurosci.* 39, 2065–2079. doi:10.1523/JNEUROSCI.2552-18.2019

Chen, Q., Roeder, Z., Li, M. H., Zhang, Y., Ingram, S. L., and Heinricher, M. M. (2017). Optogenetic evidence for a direct circuit linking nociceptive transmission through the parabrachial complex with pain-modulating neurons of the rostral ventromedial medulla (RVM). *eNeuro* 4, 0202–2017. doi:10.1523/ENEURO.0202-17.2017

Cheng, Z. F., Fields, H. L., and Heinricher, M. M. (1986). Morphine microinjected into the periaqueductal gray has differential effects on 3 classes of medullary neurons. *Brain Res.* 375, 57–65. doi:10.1016/0006-8993(86)90958-3

Chiang, M. C., Bowen, A., Schier, L. A., Tupone, D., Uddin, O., and Heinricher, M. M. (2019). Parabrachial complex: A hub for pain and aversion. *J. Neurosci.* 39, 8225–8230. doi:10.1523/JNEUROSCI.1162-19.2019

Commons, K. G., Aicher, S. A., Kow, L. M., and Pfaff, D. W. (2000). Presynaptic and postsynaptic relations of mu-opioid receptors to gamma-aminobutyric acid-immunoreactive and medullary-projecting periaqueductal gray neurons. *J. Comp. Neurol.* 419, 532–542. doi:10.1002/(sici)1096-9861(20000417)419:4<532:aid-cne8>3.0.co;2-6

Commons, K. G., Beck, S. G., Rudoy, C., and Van Bockstaele, E. J. (2001). Anatomical evidence for presynaptic modulation by the delta opioid receptor in the ventrolateral periaqueductal gray of the rat. *J. Comp. Neurol.* 430, 200–208. doi:10.1002/1096-9861(20010205)430:2<200:aid-cne1025>3.0.co;2-b

Craft, R. M., Morgan, M. M., and Lane, D. A. (2004). Oestradiol dampens reflex-related activity of on- and off-cells in the rostral ventromedial medulla of female rats. *Neuroscience* 125, 1061–1068. doi:10.1016/j.neuroscience.2003.12.015

Craft, R. M. (2003). Sex differences in opioid analgesia: "from mouse to man. *Clin. J. Pain* 19, 175–186. doi:10.1097/00002508-200305000-00005

Crawford, L. S., Mills, E. P., Hanson, T., Macey, P. M., Glarin, R., Macefield, V. G., et al. (2021). Brainstem mechanisms of pain modulation: A within-subjects 7T fMRI study of placebo analgesic and nocebo hyperalgesic responses. *J. Neurosci.* 41, 9794–9806. doi:10.1523/JNEUROSCI.0806-21.2021

Da Silva, L. F., Desantana, J. M., and Sluka, K. A. (2010). Activation of NMDA receptors in the brainstem, rostral ventromedial medulla, and nucleus reticularis gigantocellularis mediates mechanical hyperalgesia produced by repeated intramuscular injections of acidic saline in rats. *J. Pain* 11, 378–387. doi:10.1016/j.jpain.2009.08.006

Dehkordi, S B, Sajedianfard, J., and Owji, A. A. (2019). The effect of intra-cerebroventricular injection of insulin on the levels of monoamines on the raphe magnus nucleus of non-diabetic and short-term diabetic rats in the formalin test. *Iran. J. Basic Med. Sci.* 22, 915–921. doi:10.22038/ijbms.2019.35580.8485

Drake, C. T., De Oliveira, A. X., Harris, J. A., Connor, D. M., Winkler, C. W., and Aicher, S. A. (2007). Kappa opioid receptors in the rostral ventromedial medulla of male and female rats. *J. Comp. Neurol.* 500, 465–476. doi:10.1002/cne.21184

Ellrich, J., Ulucan, C., and Schnell, C. (2000). Are 'neutral cells' in the rostral ventromedial medulla subtypes of on- and off-cells? *Neurosci. Res.* 38, 419–423. doi:10.1016/s0168-0102(00)00190-5

Fang, F. G., Haws, C. M., Drasner, K., Williamson, A., and Fields, H. L. (1989). Opioid peptides (DAGO-enkephalin, dynorphin A(1-13), BAM 22P) microinjected into the rat brainstem: Comparison of their antinociceptive effect and their effect on neuronal firing in the rostral ventromedial medulla. *Brain Res.* 501, 116–128. doi:10.1016/0006-8993(89)91033-0

Fauss, G. N. K., Hudson, K. E., and Grau, J. W. (2022). Role of descending serotonergic fibers in the development of pathophysiology after spinal cord injury (SCI): Contribution to chronic pain, spasticity, and autonomic dysreflexia. *Biol. (Basel)* 11, 234. doi:10.3390/biology11020234

Feng, Y. P., Wang, J., Dong, Y. L., Wang, Y. Y., and Li, Y. Q. (2015). The roles of neurotensin and its analogues in pain. *Curr. Pharm. Des.* 21, 840–848. doi:10.2174/1381612820666141027124915

Ferrari, L. F., Pei, J., Zickella, M., Rey, C., Zickella, J., Ramirez, A., et al. (2021). D2 receptors in the periaqueductal gray/dorsal raphe modulate peripheral inflammatory hyperalgesia via the rostral ventral medulla. *Neuroscience* 463, 159–173. doi:10.1016/j.neuroscience.2021.03.035

Fields, H. L., and Basbaum, A. I. (1978). Brainstem control of spinal pain-transmission neurons. *Annu. Rev. Physiol.* 40, 217–248. doi:10.1146/annurev.ph.40.030178.001245

Fields, H. L., Bry, J., Hentall, I., and Zorman, G. (1983). The activity of neurons in the rostral medulla of the rat during withdrawal from noxious heat. *J. Neurosci.* 3, 2545–2552. doi:10.1523/JNEUROSCI.03-12-02545.1983

Fields, H. L., Malick, A., and Burstein, R. (1995). Dorsal horn projection targets of ON and OFF cells in the rostral ventromedial medulla. *J. Neurophysiol.* 74, 1742–1759. doi:10.1152/jn.1995.74.4.1742

Fink, A. J., Croce, K. R., Huang, Z. J., Abbott, L. F., Jessell, T. M., and Azim, E. (2014). Presynaptic inhibition of spinal sensory feedback ensures smooth movement. *Nature* 509, 43–48. doi:10.1038/nature13276

Francois, A., Low, S. A., Sypek, E. I., Christensen, A. J., Sotoudeh, C., Beier, K. T., et al. (2017). A brainstem-spinal cord inhibitory circuit for mechanical pain modulation by GABA and enkephalins. *Neuron* 93, 822–839. doi:10.1016/j.neuron.2017.01.008

Geerling, J. C., Yokota, S., Rukhadze, I., Roe, D., and Chamberlin, N. L. (2017). Kolliker-Fuse GABAergic and glutamatergic neurons project to distinct targets. *J. Comp. Neurol.* 525, 1844–1860. doi:10.1002/cne.24164

Gu, M., and Wessendorf, M. (2007). Endomorphin-2-immunoreactive fibers selectively appose serotonergic neuronal somata in the rostral ventral medial medulla. *J. Comp. Neurol.* 502, 701–713. doi:10.1002/cne.21343

Gutstein, H. B., Mansour, A., Watson, S. J., Akil, H., and Fields, H. L. (1998). Mu and kappa opioid receptors in periaqueductal gray and rostral ventromedial medulla. *Neuroreport* 9, 1777–1781. doi:10.1097/00001756-199806010-00019

Hamity, M. V., White, S. R., and Hammond, D. L. (2010). Effects of neurokinin-1 receptor agonism and antagonism in the rostral ventromedial medulla of rats with acute or persistent inflammatory nociception. *Neuroscience* 165, 902–913. doi:10.1016/j.neuroscience.2009.10.064

Harasawa, I., Fields, H. L., and Meng, I. D. (2000). Delta opioid receptor mediated actions in the rostral ventromedial medulla on tail flick latency and nociceptive modulatory neurons. *Pain* 85, 255–262. doi:10.1016/s0304-3959(99)00280-8

Harasawa, I., Johansen, J. P., Fields, H. L., Porreca, F., and Meng, I. D. (2016). Alterations in the rostral ventromedial medulla after the selective ablation of mu-opioid receptor expressing neurons. *Pain* 157, 166–173. doi:10.1097/j.pain.0000000000000344

Heijmans, L., Mons, M. R., and Joosten, E. A. (2021). A systematic review on descending serotonergic projections and modulation of spinal nociception in chronic neuropathic pain and after spinal cord stimulation. *Mol. Pain* 17, 17448069211043965. doi:10.1177/17448069211043965

Heinricher, M M., McGaraughty, S., and Tortorici, V. (2001). Circuitry underlying antiopioid actions of cholecystokinin within the rostral ventromedial medulla. *J. Neurophysiol.* 85, 280–286. doi:10.1152/jn.2001.85.1.280

Heinricher, M. M., Cheng, Z. F., and Fields, H. L. (1987). Evidence for two classes of nociceptive modulating neurons in the periaqueductal gray. *J. Neurosci.* 7, 271–278. doi:10.1523/JNEUROSCI.07-01-00271.1987

Heinricher, M. M., McGaraughty, S., and Grandy, D. K. (1997). Circuitry underlying antiopioid actions of orphanin FQ in the rostral ventromedial medulla. *J. Neurophysiol.* 78, 3351–3358. doi:10.1152/jn.1997.78.6.3351

Heinricher, M. M., Morgan, M. M., and Fields, H. L. (1992). Direct and indirect actions of morphine on medullary neurons that modulate nociception. *Neuroscience* 48, 533–543. doi:10.1016/0306-4522(92)90400-v

Heinricher, M. M., Morgan, M. M., Tortorici, V., and Fields, H. L. (1994). Disinhibition of off-cells and antinociception produced by an opioid action within the rostral ventromedial medulla. *Neuroscience* 63, 279–288. doi:10.1016/0306-4522(94)90022-1

Heinricher, M. M., and Neubert, M. J. (2004). Neural basis for the hyperalgesic action of cholecystokinin in the rostral ventromedial medulla. *J. Neurophysiol.* 92, 1982–1989. doi:10.1152/jn.00411.2004

Heinricher, M. M., Schouten, J. C., and Jobst, E. E. (2001). Activation of brainstem N-methyl-D-aspartate receptors is required for the analgesic actions of morphine given systemically. *Pain* 92, 129–138. doi:10.1016/s0304-3959(00)00480-2

Heinricher, M. M., Tavares, I., Leith, J. L., and Lumb, B. M. (2009). Descending control of nociception: Specificity, recruitment and plasticity. *Brain Res. Rev.* 60, 214–225. doi:10.1016/j.brainresrev.2008.12.009

Heinricher, M. M., and Tortorici, V. (1994). Interference with GABA transmission in the rostral ventromedial medulla: Disinhibition of off-cells as a central mechanism in nociceptive modulation. *Neuroscience* 63, 533–546. doi:10.1016/0306-4522(94)90548-7

Hickey, L., Li, Y., Fyson, S. J., Watson, T. C., Perrins, R., Hewinson, J., et al. (2014). Optoactivation of locus ceruleus neurons evokes bidirectional changes in thermal nociception in rats. *J. Neurosci.* 34, 4148–4160. doi:10.1523/JNEUROSCI.4835-13.2014

Ho, Y. C., Cheng, J. K., and Chiou, L. C. (2013). Hypofunction of glutamatergic neurotransmission in the periaqueductal gray contributes to nerve-injury-induced neuropathic pain. *J. Neurosci.* 33, 7825–7836. doi:10.1523/JNEUROSCI.5583-12.2013

Hossaini, M., Goos, J. A. C., Kohli, S. K., and Holstege, J. C. (2012). Distribution of glycine/GABA neurons in the ventromedial medulla with descending spinal projections and evidence for an ascending glycine/GABA projection. *PLoS One* 7, e35293. doi:10.1371/journal.pone.0035293

Hosseini, M., Parviz, M., Shabanzadeh, A. P., and Zamani, E. (2021). Evaluation of the effect of (S)-3,4-Dicarboxyphenylglycine as a metabotropic glutamate receptors subtype 8 agonist on thermal nociception following central neuropathic pain. *Asian Spine J.* 15, 200–206. doi:10.31616/asj.2019.0367

Hosseini, M., Parviz, M., Shabanzadeh, A. P., Zamani, E., Mohseni-Moghaddam, P., Gholami, L., et al. (2020). The inhibiting role of periaqueductal gray metabotropic glutamate receptor subtype 8 in a rat model of central neuropathic pain. *Neurol. Res.* 42, 515–521. doi:10.1080/01616412.2020.1747730

Jiang, M., Bo, J., Lei, Y., Hu, F., Xia, Z., Liu, Y., et al. (2019). Anxiety-induced hyperalgesia in female rats is mediated by cholecystokinin 2 receptor in rostral ventromedial medulla and spinal 5-hydroxytryptamine 2B receptor. *J. Pain Res.* 12, 2009–2026. doi:10.2147/JPR.S187715

Jiao, Y., Gao, P., Dong, L., Ding, X., Meng, Y., Qian, J., et al. (2022). Molecular identification of bulbospinal ON neurons by GPER which drives pain and morphine tolerance. *J. Clin. Invest.* 133, e154588. doi:10.1172/JCI154588

Kalyuzhny, A. E., and Wessendorf, M. W. (1998). Relationship of mu- and delta-opioid receptors to GABAergic neurons in the central nervous system, including antinociceptive brainstem circuits. *J. Comp. Neurol.* 392, 528–547. doi:10.1002/(sici)1096-9861(19980323)392:4<528:aid-cne9>3.0.co;2-2

Kaplan, H., and Fields, H. L. (1991). Hyperalgesia during acute opioid abstinence: Evidence for a nociceptive facilitating function of the rostral ventromedial medulla. *J. Neurosci.* 11, 1433–1439. doi:10.1523/JNEUROSCI.11-05-01433.1991

Khasabov, S. G., Brink, T. S., Schupp, M., Noack, J., and Simone, D. A. (2012). Changes in response properties of rostral ventromedial medulla neurons during prolonged inflammation: Modulation by neurokinin-1 receptors. *Neuroscience* 224, 235–248. doi:10.1016/j.neuroscience.2012.08.029

Kohn, J. F., Trenk, A., Denham, W., Linn, J. G., Haggerty, S., Joehl, R., et al. (2020). Long-term outcomes after subtotal reconstituting cholecystectomy: A retrospective case series. *Am. J. Surg.* 220, 736–740. doi:10.1016/j.amjsurg.2020.01.030

Kort, A. R., Joosten, E. A., Versantvoort, E. M., Patijn, J., Tibboel, D., and van den Hoogen, N. J. (2022). Anatomical changes in descending serotonergic projections from the rostral ventromedial medulla to the spinal dorsal horn following repetitive neonatal painful procedures. *Int. J. Dev. Neurosci.* 82, 361–371. doi:10.1002/jdn.10185

Kovelowski, C. J., Ossipov, M. H., Sun, H., Lai, J., Malan, T. P., and Porreca, F. (2000). Supraspinal cholecystokinin may drive tonic descending facilitation mechanisms to maintain neuropathic pain in the rat. *Pain* 87, 265–273. doi:10.1016/S0304-3959(00)00290-6

Lau, B. K., Winters, B. L., and Vaughan, C. W. (2020). Opioid presynaptic disinhibition of the midbrain periaqueductal grey descending analgesic pathway. *Br. J. Pharmacol.* 177, 2320–2332. doi:10.1111/bph.14982

Li, Y., Kang, D. H., Kim, W. M., Lee, H. G., Kim, S. H., You, H. E., et al. (2021). Systemically administered neurotensin receptor agonist produces antinociception through activation of spinally projecting serotonergic neurons in the rostral ventromedial medulla. *Korean J. Pain* 34, 58–65. doi:10.3344/kjp.2021.34.1.58

Li, M H., Suchland, K. L., and Ingram, S. L. (2017). Compensatory activation of cannabinoid CB2 receptor inhibition of GABA release in the rostral ventromedial medulla in inflammatory pain. *J. Neurosci.* 37, 626–636. doi:10.1523/JNEUROSCI.1310-16.2016

Li, M M, Suchland, K. L., and Ingram, S. L. (2015). GABAergic transmission and enhanced modulation by opioids and endocannabinoids in adult rat rostral ventromedial medulla. *J. Physiol.* 593, 217–230. doi:10.1113/jphysiol.2014.275701

Li, C, Sugam, J. A., Lowery-Gionta, E. G., McElligott, Z. A., McCall, N. M., Lopez, A. J., et al. (2016). Mu opioid receptor modulation of dopamine neurons in the periaqueductal gray/dorsal raphe: A role in regulation of pain. *Neuropsychopharmacology* 41, 2122–2132. doi:10.1038/npp.2016.12

Lima, L. V., DeSantana, J. M., Rasmussen, L. A., and Sluka, K. A. (2017). Short-duration physical activity prevents the development of activity-induced hyperalgesia through opioid and serotoninergic mechanisms. *Pain* 158, 1697–1710. doi:10.1097/j.pain.0000000000000967

Liu, X., Wang, G., Ai, G., Xu, X., Niu, X., and Zhang, M. (2020). Selective ablation of descending serotonin from the rostral ventromedial medulla unmasks its pro-nociceptive role in chemotherapy-induced painful neuropathy. *J. Pain Res.* 13, 3081–3094. doi:10.2147/JPR.S275254

Lopez-Canul, M., Palazzo, E., Dominguez-Lopez, S., Luongo, L., Lacoste, B., Comai, S., et al. (2015). Selective melatonin MT2 receptor ligands relieve neuropathic pain through modulation of brainstem descending antinociceptive pathways. *Pain* 156, 305–317. doi:10.1097/01.j.pain.0000460311.71572.5f

Loyd, D. R., Morgan, M. M., and Murphy, A. Z. (2007). Morphine preferentially activates the periaqueductal gray-rostral ventromedial medullary pathway in the male rat: A potential mechanism for sex differences in antinociception. *Neuroscience* 147, 456–468. doi:10.1016/j.neuroscience.2007.03.053

Lu, N., Han, M., Yang, Z. L., Wang, Y. Q., Wu, G. C., and Zhang, Y. Q. (2010). Nociceptin/Orphanin FQ in PAG modulates the release of amino acids, serotonin and norepinephrine in the rostral ventromedial medulla and spinal cord in rats. *Pain* 148, 414–425. doi:10.1016/j.pain.2009.11.025

Maione, S., Starowicz, K., Cristino, L., Guida, F., Palazzo, E., Luongo, L., et al. (2009). Functional interaction between TRPV1 and mu-opioid receptors in the descending antinociceptive pathway activates glutamate transmission and induces analgesia. *J. Neurophysiol.* 101, 2411–2422. doi:10.1152/jn.91225.2008

Marabese, I., Rossi, F., Palazzo, E., de Novellis, V., Starowicz, K., Cristino, L., et al. (2007). Periaqueductal gray metabotropic glutamate receptor subtype 7 and 8 mediate opposite effects on amino acid release, rostral ventromedial medulla cell activities, and thermal nociception. *J. Neurophysiol.* 98, 43–53. doi:10.1152/jn.00356.2007

Marinelli, S., Vaughan, C. W., Schnell, S. A., Wessendorf, M. W., and Christie, M. J. (2002). Rostral ventromedial medulla neurons that project to the spinal cord express multiple opioid receptor phenotypes. *J. Neurosci.* 22, 10847–10855. doi:10.1523/JNEUROSCI.22-24-10847.2002

Martenson, M. E., Cetas, J. S., and Heinricher, M. M. (2009). A possible neural basis for stress-induced hyperalgesia. *Pain* 142, 236–244. doi:10.1016/j.pain.2009.01.011

Martins, I., and Tavares, I. (2017). Reticular Formation and pain: The past and the future. *Front. Neuroanat.* 11, 51. doi:10.3389/fnana.2017.00051

McGaraughty, S., and Heinricher, M. M. (2002). Microinjection of morphine into various amygdaloid nuclei differentially affects nociceptive responsiveness and RVM neuronal activity. *Pain* 96, 153–162. doi:10.1016/s0304-3959(01)00440-7

Mende, M., Fletcher, E. V., Belluardo, J. L., Pierce, J. P., Bommareddy, P. K., Weinrich, J. A., et al. (2016). Sensory-derived glutamate regulates presynaptic inhibitory terminals in mouse spinal cord. *Neuron* 90, 1189–1202. doi:10.1016/j.neuron.2016.05.008

Meng, I. D., Johansen, J. P., Harasawa, I., and Fields, H. L. (2005). Kappa opioids inhibit physiologically identified medullary pain modulating neurons and reduce morphine antinociception. *J. Neurophysiol.* 93, 1138–1144. doi:10.1152/jn.00320.2004

Meng, I. D., Manning, B. H., Martin, W. J., and Fields, H. L. (1998). An analgesia circuit activated by cannabinoids. *Nature* 395, 381–383. doi:10.1038/26481

Meyer, P. J., Morgan, M. M., Kozell, L. B., and Ingram, S. L. (2009). Contribution of dopamine receptors to periaqueductal gray-mediated antinociception. *Psychopharmacol. Berl.* 204, 531–540. doi:10.1007/s00213-009-1482-y

Micevych, P. E., Rissman, E. F., Gustafsson, J. A., and Sinchak, K. (2003). Estrogen receptor-alpha is required for estrogen-induced mu-opioid receptor internalization. *J. Neurosci. Res.* 71, 802–810. doi:10.1002/jnr.10526

Miki, K., Zhou, Q. Q., Guo, W., Guan, Y., Terayama, R., Dubner, R., et al. (2002). Changes in gene expression and neuronal phenotype in brain stem pain modulatory circuitry after inflammation. *J. Neurophysiol.* 87, 750–760. doi:10.1152/jn.00534.2001

Milligan, A. L., Szabo-Pardi, T. A., and Burton, M. D. (2020). Cannabinoid receptor type 1 and its role as an analgesic: An opioid alternative? *J. Dual Diagn* 16, 106–119. doi:10.1080/15504263.2019.1668100

Mills, E. P., Alshelh, Z., Kosanovic, D., Di Pietro, F., Vickers, E. R., Macey, P. M., et al. (2020). Altered brainstem pain-modulation circuitry connectivity during spontaneous pain intensity fluctuations. *J. Pain Res.* 13, 2223–2235. doi:10.2147/JPR.S252594

Moreau, J. L., and Fields, H. L. (1986). Evidence for GABA involvement in midbrain control of medullary neurons that modulate nociceptive transmission. *Brain Res.* 397, 37–46. doi:10.1016/0006-8993(86)91367-3

Morgan, M. M., Grisel, J. E., Robbins, C. S., and Grandy, D. K. (1997). Antinociception mediated by the periaqueductal gray is attenuated by orphanin FQ. *Neuroreport* 8, 3431–3434. doi:10.1097/00001756-199711100-00003

Morgan, M. M., Tran, A., Wescom, R. L., and Bobeck, E. N. (2020). Differences in antinociceptive signalling mechanisms following morphine and fentanyl microinjections into the rat periaqueductal gray. *Eur. J. Pain* 24, 617–624. doi:10.1002/ejp.1513

Morgan, M. M., Whittier, K. L., Hegarty, D. M., and Aicher, S. A. (2008). Periaqueductal gray neurons project to spinally projecting GABAergic neurons in the rostral ventromedial medulla. *Pain* 140, 376–386. doi:10.1016/j.pain.2008.09.009

Nasirinezhad, F., Hosseini, M., Karami, Z., Yousefifard, M., and Janzadeh, A. (2016). Spinal 5-HT3 receptor mediates nociceptive effect on central neuropathic pain; possible therapeutic role for tropisetron. *J. Spinal Cord. Med.* 39, 212–219. doi:10.1179/2045772315Y.0000000047

Neubert, M. J., Kincaid, W., and Heinricher, M. M. (2004). Nociceptive facilitating neurons in the rostral ventromedial medulla. *Pain* 110, 158–165. doi:10.1016/j.pain.2004.03.017

Nguyen, E., Smith, K. M., Cramer, N., Holland, R. A., Bleimeister, I. H., Flores-Felix, K., et al. (2022). Medullary kappa-opioid receptor neurons inhibit pain and itch through a descending circuit. *Brain* 145, 2586–2601. doi:10.1093/brain/awac189

Novellis, V d, Mariani, L., Palazzo, E., Vita, D., Marabese, I., Scafuro, M., et al. (2005). Periaqueductal grey CB1 cannabinoid and metabotropic glutamate subtype 5 receptors modulate changes in rostral ventromedial medulla neuronal activities induced by subcutaneous formalin in the rat. *Neuroscience* 134, 269–281. doi:10.1016/j.neuroscience.2005.03.014

Oliva, V., Gregory, R., Davies, W. E., Harrison, L., Moran, R., Pickering, A. E., et al. (2021). Parallel cortical-brainstem pathways to attentional analgesia. *Neuroimage* 226, 117548. doi:10.1016/j.neuroimage.2020.117548

Oliva, V., Hartley-Davies, R., Moran, R., Pickering, A. E., and Brooks, J. C. (2022). Simultaneous brain, brainstem, and spinal cord pharmacological-fMRI reveals involvement of an endogenous opioid network in attentional analgesia. *Elife* 11, e71877. doi:10.7554/eLife.71877

Ossipov, M. H., Dussor, G. O., and Porreca, F. (2010). Central modulation of pain. *J. Clin. Invest.* 120, 3779–3787. doi:10.1172/JCI43766

Palazzo, E., Boccella, S., Marabese, I., Perrone, M., Belardo, C., Iannotta, M., et al. (2022). Homo-AMPA in the periaqueductal grey modulates pain and rostral ventromedial medulla activity in diabetic neuropathic mice. *Neuropharmacology* 212, 109047. doi:10.1016/j.neuropharm.2022.109047

Palazzo, E., Marabese, I., Soukupova, M., Luongo, L., Boccella, S., Giordano, C., et al. (2011). Metabotropic glutamate receptor subtype 8 in the amygdala modulates thermal threshold, neurotransmitter release, and rostral ventromedial medulla cell activity in inflammatory pain. *J. Neurosci.* 31, 4687–4697. doi:10.1523/JNEUROSCI.2938-10.2011

Pan, Z., Hirakawa, N., and Fields, H. L. (2000). A cellular mechanism for the bidirectional pain-modulating actions of orphanin FQ/nociceptin. *Neuron* 26, 515–522. doi:10.1016/s0896-6273(00)81183-6

Park, C., Kim, J. H., Yoon, B. E., Choi, E. J., Lee, C. J., and Shin, H. S. (2010). T-type channels control the opioidergic descending analgesia at the low threshold-spiking GABAergic neurons in the periaqueductal gray. *Proc. Natl. Acad. Sci. U. S. A.* 107, 14857–14862. doi:10.1073/pnas.1009532107

Pinto, M., Sousa, M., Lima, D., and Tavares, I. (2008). Participation of mu-opioid, GABA(B), and NK1 receptors of major pain control medullary areas in pathways targeting the rat spinal cord: Implications for descending modulation of nociceptive transmission. *J. Comp. Neurol.* 510, 175–187. doi:10.1002/cne.21793

Posa, L., De Gregorio, D., Lopez-Canul, M., He, Q., Darcq, E., Rullo, L., et al. (2022). Supraspinal melatonin MT(2) receptor agonism alleviates pain via a neural circuit that recruits mu opioid receptors. *J. Pineal Res.* 73, e12825. doi:10.1111/jpi.12825

Radhakrishnan, R., and Sluka, K. A. (2009). Increased glutamate and decreased glycine release in the rostral ventromedial medulla during induction of a pre-clinical model of chronic widespread muscle pain. *Neurosci. Lett.* 457, 141–145. doi:10.1016/j.neulet.2009.03.086

Rea, K., Roche, M., and Finn, D. P. (2007). Supraspinal modulation of pain by cannabinoids: The role of GABA and glutamate. *Br. J. Pharmacol.* 152, 633–648. doi:10.1038/sj.bjp.0707440

Rempe, T., Wolff, S., Riedel, C., Baron, R., Stroman, P. W., Jansen, O., et al. (2015). Spinal and supraspinal processing of thermal stimuli: An fMRI study. *J. Magn. Reson Imaging* 41, 1046–1055. doi:10.1002/jmri.24627

Roeder, Z., Chen, Q., Davis, S., Carlson, J. D., Tupone, D., and Heinricher, M. M. (2016). Parabrachial complex links pain transmission to descending pain modulation. *Pain* 157, 2697–2708. doi:10.1097/j.pain.0000000000000688

Sagalajev, B., Viisanen, H., Wei, H., and Pertovaara, A. (2017). Descending antinociception induced by secondary somatosensory cortex stimulation in experimental neuropathy: Role of the medullospinal serotonergic pathway. *J. Neurophysiol.* 117, 1200–1214. doi:10.1152/jn.00836.2016

Schepers, R. J., Mahoney, J. L., Zapata, A., Chefer, V., and Shippenberg, T. S. (2008). The effects of local perfusion of DAMGO on extracellular GABA and glutamate concentrations in the rostral ventromedial medulla. *J. Neurochem.* 104, 806–817. doi:10.1111/j.1471-4159.2007.05017.x

Sikandar, S., Bannister, K., and Dickenson, A. H. (2012). Brainstem facilitations and descending serotonergic controls contribute to visceral nociception but not pregabalin analgesia in rats. *Neurosci. Lett.* 519, 31–36. doi:10.1016/j.neulet.2012.05.009

Silva, M., Amorim, D., Almeida, A., Tavares, I., Pinto-Ribeiro, F., and Morgado, C. (2013). Pronociceptive changes in the activity of rostroventromedial medulla (RVM) pain modulatory cells in the streptozotocin-diabetic rat. *Brain Res. Bull.* 96, 39–44. doi:10.1016/j.brainresbull.2013.04.008

Silva, M., Martins, D., Charrua, A., Piscitelli, F., Tavares, I., Morgado, C., et al. (2016). Endovanilloid control of pain modulation by the rostroventromedial medulla in an animal model of diabetic neuropathy. *Neuropharmacology* 107, 49–57. doi:10.1016/j.neuropharm.2016.03.007

Starowicz, K., Maione, S., Cristino, L., Palazzo, E., Marabese, I., Rossi, F., et al. (2007). Tonic endovanilloid facilitation of glutamate release in brainstem descending antinociceptive pathways. *J. Neurosci.* 27, 13739–13749. doi:10.1523/JNEUROSCI.3258-07.2007

Talluri, B., Hoelzel, F., Medda, B. K., Terashvili, M., Sanvanson, P., Shaker, R., et al. (2022). Identification and characterization of rostral ventromedial medulla neurons synaptically connected to the urinary bladder afferents in female rats with or without neonatal cystitis. *J. Comp. Neurol.* 530, 1129–1147. doi:10.1002/cne.25260

Tanaka, M., Matsumoto, Y., Murakami, T., Hisa, Y., and Ibata, Y. (1996). The origins of catecholaminergic innervation in the rostral ventromedial medulla oblongata of the rat. *Neurosci. Lett.* 207, 53–56. doi:10.1016/0304-3940(96)12487-3

Todd, A. J. (2010). Neuronal circuitry for pain processing in the dorsal horn. *Nat. Rev. Neurosci.* 11, 823–836. doi:10.1038/nrn2947

Tonsfeldt, K. J., Suchland, K. L., Beeson, K. A., Lowe, J. D., Li, M. H., and Ingram, S. L. (2016). Sex differences in GABAA signaling in the periaqueductal gray induced by persistent inflammation. *J. Neurosci.* 36, 1669–1681. doi:10.1523/JNEUROSCI.1928-15.2016

Vaughan, C. W., Ingram, S. L., and Christie, M. J. (1997). Actions of the ORL1 receptor ligand nociceptin on membrane properties of rat periaqueductal gray neurons *in vitro*. *J. Neurosci.* 17, 996–1003. doi:10.1523/JNEUROSCI.17-03-00996.1997

Vaughan, C. W., Ingram, S. L., Connor, M. A., and Christie, M. J. (1997). How opioids inhibit GABA-mediated neurotransmission. *Nature* 390, 611–614. doi:10.1038/37610

Verner, T. A., Pilowsky, P. M., and Goodchild, A. K. (2008). Retrograde projections to a discrete apneic site in the midline medulla oblongata of the rat. *Brain Res.* 1208, 128–136. doi:10.1016/j.brainres.2008.02.028

Viisanen, H., Lilius, T. O., Sagalajev, B., Rauhala, P., Kalso, E., and Pertovaara, A. (2020). Neurophysiological response properties of medullary pain-control neurons following chronic treatment with morphine or oxycodone: Modulation by acute ketamine. *J. Neurophysiol.* 124, 790–801. doi:10.1152/jn.00343.2020

Wagner, K. M., Roeder, Z., Desrochers, K., Buhler, A. V., Heinricher, M. M., and Cleary, D. R. (2013). The dorsomedial hypothalamus mediates stress-induced hyperalgesia and is the source of the pronociceptive peptide cholecystokinin in the rostral ventromedial medulla. *Neuroscience* 238, 29–38. doi:10.1016/j.neuroscience.2013.02.009

Wang, L H, Ding, W. Q., and Sun, Y. G. (2022). Spinal ascending pathways for somatosensory information processing. *Trends Neurosci.* 45, 594–607. doi:10.1016/j.tins.2022.05.005

Wang, C T, Feng, D. Y., Li, Z. H., Feng, B., Zhang, H., Zhang, T., et al. (2015). Activation of the mammalian target of rapamycin in the rostral ventromedial medulla contributes to the maintenance of nerve injury-induced neuropathic pain in rat. *Neural Plast.* 2015: 394820. doi:10.1155/2015/394820

WangMao, C. J., Zhang, X. Q., Zhang, C. Y., Lv, D. J., Yang, Y. P., et al. (2017). Attenuation of hyperalgesia responses via the modulation of 5-hydroxytryptamine signalings in the rostral ventromedial medulla and spinal cord in a 6-hydroxydopamine-induced rat model of Parkinson's disease. *Mol. Pain* 13, 1744806917691525. doi:10.1177/1744806917691525

Wang, W, Zhong, X., Li, Y., Guo, R., Du, S., Wen, L., et al. (2019). Rostral ventromedial medulla-mediated descending facilitation following P2X7 receptor activation is involved in the development of chronic post-operative pain. *J. Neurochem.* 149, 760–780. doi:10.1111/jnc.14650

Wei, F., Dubner, R., Zou, S., Ren, K., Bai, G., Wei, D., et al. (2010). Molecular depletion of descending serotonin unmasks its novel facilitatory role in the development of persistent pain. *J. Neurosci.* 30, 8624–8636. doi:10.1523/JNEUROSCI.5389-09.2010

Winkler, C. W., Hermes, S. M., Chavkin, C. I., Drake, C. T., Morrison, S. F., and Aicher, S. A. (2006). Kappa opioid receptor (KOR) and GAD67 immunoreactivity are found in OFF and NEUTRAL cells in the rostral ventromedial medulla. *J. Neurophysiol.* 96, 3465–3473. doi:10.1152/jn.00676.2006

Woolf, C. J. (1983). Evidence for a central component of post-injury pain hypersensitivity. *Nature* 306, 686–688. doi:10.1038/306686a0

Xu, M., Kim, C. J., Neubert, M. J., and Heinricher, M. M. (2007). NMDA receptor-mediated activation of medullary pro-nociceptive neurons is required for secondary thermal hyperalgesia. *Pain* 127, 253–262. doi:10.1016/j.pain.2006.08.020

Zhang, C., Xia, C., Zhang, X., Li, W., Miao, X., and Zhou, Q. (2020). Wrist-ankle acupuncture attenuates cancer-induced bone pain by regulating descending pain-modulating system in a rat model. *Chin. Med.* 15, 13. doi:10.1186/s13020-020-0289-y

Zhang, W., Gardell, S., Zhang, D., Xie, J. Y., Agnes, R. S., Badghisi, H., et al. (2009). Neuropathic pain is maintained by brainstem neurons co-expressing opioid and cholecystokinin receptors. *Brain* 132, 778–787. doi:10.1093/brain/awn330

Zhang, Z., and Pan, Z. Z. (2012). Signaling cascades for delta-opioid receptor-mediated inhibition of GABA synaptic transmission and behavioral antinociception. *Mol. Pharmacol.* 81, 375–383. doi:10.1124/mol.111.076307

Zhuo, M., and Gebhart, G. F. (1990). Characterization of descending inhibition and facilitation from the nuclei reticularis gigantocellularis and gigantocellularis pars alpha in the rat. *Pain* 42, 337–350. doi:10.1016/0304-3959(90)91147-B

frontiers | Frontiers in Pharmacology

TYPE Original Research
PUBLISHED 24 April 2023
DOI 10.3389/fphar.2023.1167398

OPEN ACCESS

EDITED BY
Yuan Li,
Shanghai Jiao Tong University, China

REVIEWED BY
Ping Su,
Zhejiang University, China
Wenli Chen,
The Fifth Affiliated Hospital of Sun Yat-sen University, China
Chengliang Yin,
Chinese PLA General Hospital, China

*CORRESPONDENCE
Xinmin Liu,
liuxinmin@hotmail.com

RECEIVED 16 February 2023
ACCEPTED 13 April 2023
PUBLISHED 24 April 2023

CITATION
Jiang N, Lv J, Zhang Y, Sun X, Yao C, Wang Q, He Q and Liu X (2023), Protective effects of ginsenosides Rg1 and Rb1 against cognitive impairment induced by simulated microgravity in rats. *Front. Pharmacol.* 14:1167398. doi: 10.3389/fphar.2023.1167398

Protective effects of ginsenosides Rg1 and Rb1 against cognitive impairment induced by simulated microgravity in rats

Ning Jiang[1], Jingwei Lv[1], Yiwen Zhang[1], Xinran Sun[1], Caihong Yao[1], Qiong Wang[2], Qinghu He[3] and Xinmin Liu[1,3]*

[1]Research Center for Pharmacology and Toxicology, Institute of Medicinal Plant Development (IMPLAD), Chinese Academy of Medical Sciences and Peking Union Medical College, Beijing, China, [2]Institute of Food Science and Technology, Chinese Academy of Agricultural Sciences (CAAS), Beijing, China, [3]Sino-Pakistan Center on Traditional Chinese Medicine, Hunan University of Medicine, Huaihua, China

Microgravity experienced during space flight is known to exert several negative effects on the learning ability and memory of astronauts. Few effective strategies are currently available to counteract these effects. Rg1 and Rb1, the major steroidal components of ginseng, have shown potent neuroprotective effects with a high safety profile. The present study aimed to investigate the effects of Rg1 and Rb1 on simulated microgravity-induced learning and memory dysfunction and its underlying mechanism in the hindlimb suspension (HLS) rat model. Administration of Rg1 (30 and 60 μmol/kg) and Rb1 (30 and 60 μmol/kg) for 2 weeks resulted in a significant amelioration of impaired spatial and associative learning and memory caused by 4-week HLS exposure, measured using the Morris water maze and Reward operating conditioning reflex (ROCR) tests, respectively. Furthermore, Rg1 and Rb1 administration alleviated reactive oxygen species production and enhanced antioxidant enzyme activities in the prefrontal cortex (PFC). Rg1 and Rb1 also assisted in the recovery of mitochondrial complex I (NADH dehydrogenase) activities, increased the expression of Mfn2 and decreased the fission marker dynamin-related protein (Drp)-1expression. Additionally, Rg1 and Rb1 treatment increased the SYN, and PSD95 protein expressions and decreased the ratio of Bax:Bcl-2 and reduced the expression of cleaved caspase-3 and cytochrome C. Besides these, the BDNF-TrkB/PI3K-Akt pathway was also activated by Rg1 and Rb1 treatment. Altogether, Rg1 and Rb1 treatment attenuated cognitive deficits induced by HLS, mitigated mitochondrial dysfunction, attenuated oxidative stress, inhibited apoptosis, increased synaptic plasticity, and restored BDNF-TrkB/PI3K-Akt signaling.

KEYWORDS

ginsenoside Rg1, ginsenoside Rb1, memory impairments, simulated weightlessness, rat

Abbreviations: HLS; hindlimb suspension, MWM; Morris water maze test, ROCR; Reward operating conditioning reflex test, PFC; prefrontal cortex, LTP; long-term potentiation, Rb1; ginsenoside Rb1, Rg1; ginsenoside Rg1, LPs; lever presses, NPs; nose-poke activities, SOD; superoxide dismutase, MDA; Malondialdehyde, GSH-x; glutathione peroxidase, H_2O_2; Hydrogen peroxide, Drp1; dynamin-related protein 1, Mfn2; mitofusin-2, BDNF; Brain-derived neurotrophic factor, PSD95; postsynaptic density, SYN; synaptophysin, Cyt C; Cytochrome C.

1 Introduction

During long-term space trips, astronauts are exposed to peculiar and exceedingly complicated environmental conditions, of which microgravity is considered to be one of the main hazards to human health (Yoon et al., 2017; Nordeen and Martin, 2019). Actual (spaceflight) or simulated microgravity is known to induce a variety of physiological changes, especially in the central nervous system. In particular, it affects many aspects of brain function, including cognitive performance, posture control, locomotion, and manual control (Xiang et al., 2019). Hindlimb suspension (HLS) is the most commonly used small-animal model for simulating microgravity; it was developed in the 1980s and used to reproduce a cephalad blood and fluid shift, producing the same effects as microgravity in various organ systems such as the cardiovascular, immune, and nervous systems (Globus and Morey-Holton, 2016). The HLS model is widely used to assess the effects of microgravity on learning and memory deficits. Mounting evidence from various behavioral tasks (e.g., the Morris water maze, shuttle-box test, and object recognition test) has shown that exposure to simulated microgravity using the HLS model produces cognitive impairment resulting from increased levels of ROS, reduced BDNF expression, or alterations in neurotransmitter levels as well as impaired synaptic plasticity (Wang et al., 2016; Xiang et al., 2019).

In recent years, herbal medicines have emerged as novel and attractive pharmacotherapeutic tools for the treatment of memory deficits, especially because of their effectiveness and high safety margins/profiles (Liu et al., 2016). Panax ginseng has gained immense popularity worldwide and its active ingredient is ginsenoside (Huang et al., 2015). Ginsenoside is known to exert multiple pharmacological effects on the neuronal, cardiovascular, and immune systems (Mohanan et al., 2018), especially in neurodegenerative diseases such as Alzheimer's disease (AD), and effects on memory enhancement have gained significant attention in the past few years (Jiang et al., 2020). Rb1 (diol-type ginseng saponins) and Rg1 (triol-type ginseng saponins) are regarded as the main active components that are responsible for memory enhancement (Figure 1) (Wang et al., 2010) and recent studies have demonstrated the preventive and therapeutic benefits of ginsenosides Rb1 and Rg1 on cognitive deficits. Ginsenoside Rg1 has been shown to ameliorate hippocampal long-term potentiation (LTP) and memory by facilitating the clearance of AD-associated proteins and activation of the BDNF-TrkB pathway (Li et al., 2016). A previous study from our laboratory suggested that oral administration of ginsenosides Rb1 and Rg1 could mitigate cognitive impairment in senescence-accelerated (SAMP8) mice, reducing neuroinflammation, and ameliorate cognitive deficits in rats exposed to chronic restraint stress (Kezhu et al., 2017; Yang et al., 2020; Jiang et al., 2021). However, the effects of Rb1 and Rg1 on cognitive impairment induced by simulated microgravity are still unknown. Thus, in the present study, a rat model of HLS-induced cognitive dysfunction was employed to study the potential beneficial effects of ginsenosides Rb1 and Rg1 on the prevention of impairment of spatial, associative learning and memory, and the probable underlying mechanism.

2 Materials and methods

2.1 Chemicals and reagents

Ruifensi Biological Technology Co., Ltd. (Chengdu, China) provided Ginsenoside Rg1 (Rg1, purity>98%) and ginsenoside

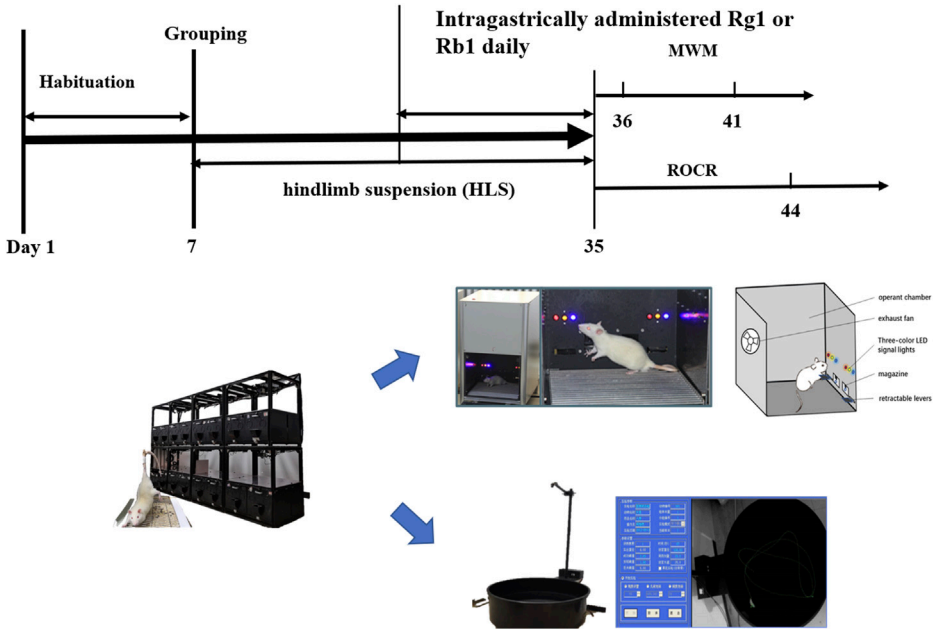

FIGURE 1
The experimental protocol of the study.

Rb1 (Rb1, purity>98%). Huperzine-A was purchased from Henan Tailong Biotech Co., Ltd. (Henan, China).

2.2 Animals

The Institute of the Chinese Academy of Medical Science Center, Beijing, donated male Wistar rats (n = 140, weight: 180–200 g). All rats were housed in standard conditions, including controlled humidity (55%) and temperature (20°C–22°C) and a 12-h:12-h light/dark cycle, with unrestricted access to water and food. The animal experiments were carried out with proper approval (Approval No. SYXK 2017-0020) following the requirements outlined by the Animal Research Committee of Peking Union Medical College's Institute of Medicinal Plant Development (China).

2.3 Drugs and treatment

The rats were randomly assigned (n = 20 per group) to seven groups, namely, the non-HLS group (control), the HLS group, the HLS + huperzine-A (0.1 mg/kg), the HLS + Rg1 group (30 and 60 μmol/kg), and the HLS + Rb1 group (30 and 60 μmol/kg). On the 14th day of HLS administration, water, Rg1, Rb1, or Huperzine-A were administered intragastrically once daily until the complete behavioral assessment.

2.4 HLS model

HLS modeling was performed as previously described with some slight adjustments to recreate microgravity in space (Qiong et al., 2016; Lv et al., 2021). The rats were suspended in individual plastic cages with a 30-degree head-down tilt for 4 weeks. At the end of 4 weeks, all the above groups were subdivided into two groups (each with 10 rats) and subjected to behavioral tests such as the Morris water maze (MWM) and the reward operating conditioning reflex (ROCR) tests (Figure 1).

2.5 Behavioral tests

2.5.1 Reward operating conditioning reflex test

2.5.1.1 Food restriction

The rats' food and water supplies were restricted until the reward training began. Sugar and water were used as a reward, and the body weights were slowly reduced to 80%–90% of the normal feeding weight over 10 days by controlling the amount of food and water given to the animals (Shi et al., 2013; Xu et al., 2017).

2.5.1.2 Magazine training

During each training cycle, an unconditioned stimulus signal (blue signal light) was shown initially, followed by reinforcement with a reward substance. The cycle was repeated 30 times during the interval, including the conditioned stimulus and rewarding activities. In other words, the blue light signal was utilized as the stimulus, and the light was switched on periodically for 10 s at an interval of 30 s. The total number of times this step was repeated was 30, and the training time was 20 min daily. The reward gadget automatically provided a drop of 8% sucrose water as a reward substance when the blue light turned on. There was no sugar pump used after the cooldown period. This phase continued for 3 consecutive days.

2.5.1.3 Lever-pressing reflex acquisition

During each training cycle, the animals pressed the left-side lever, resulting in an unconditioned stimulus that was later reinforced with a reward. The left pedal remained extended for 3 days after the rat had acquired the lever-pressing reflex. The blue signal light remained on for 10 s after the rats completed a left pedal action, activating a reward. The experiment was terminated after 30 min of training each day or 50 consecutive pedal presses during the training period.

2.5.2 Morris water maze test

On day 28 of HLS treatment, the Morris water maze (MWM) test was used to investigate the effects of Rg1 and Rb1 on spatial memory (Morris, 1984; Xu et al., 2016). The water maze was a circular pool (180 cm in diameter, 40 cm high), and black ink was added to the water (23°C–25°C) to render it opaque. The only escape was an "invisible" platform (black-colored metal, 9 cm diameter) located 1.5 cm below the water level.

To learn the escape mechanism, each rat was tested for 2 trials/day for 5 consecutive days with each trial lasting 90 s. The rats spent 10 s on the platform before testing, and an animal was considered successful if it found the platform and stayed there for more than 2 seconds. The animal was led to the platform for 10 s after the test period (post-adaptation).

For the probe trial, the platform in the circular pool was removed 24 h after the escape acquisition test, and no pre-adaptation or post-adaptation was allowed in the experiment. The rats were placed in the diagonal quadrant of the pool, where the platform was situated, facing the wall from the center point of the pool wall, and they were given 90 s to swim and explore the pool. The number of target crossings served as a test of spatial memory.

2.6 Measurement of oxidative stress

After sacrifice of the rats, the prefrontal cortices were homogenized in 10 volumes of cold saline. The total protein content of the sample was determined using bovine serum albumin as the standard and a BCA Assay kit (Pierce, United States). The H_2O_2 contents, superoxide dismutase (SOD) activity, glutathione peroxidase (GSH-Px) activity, and malondialdehyde (MDA) concentration in the cortical tissue were measured using commercial assay kits, as directed by the manufacturer (Jiancheng, Nanjing, China) (Lu et al., 2020).

2.7 Western blotting

Western blotting was conducted as previously described with minor modifications (Shi et al., 2017). Proteins were separated on SDS-PAGE and transferred to nitrocellulose membranes

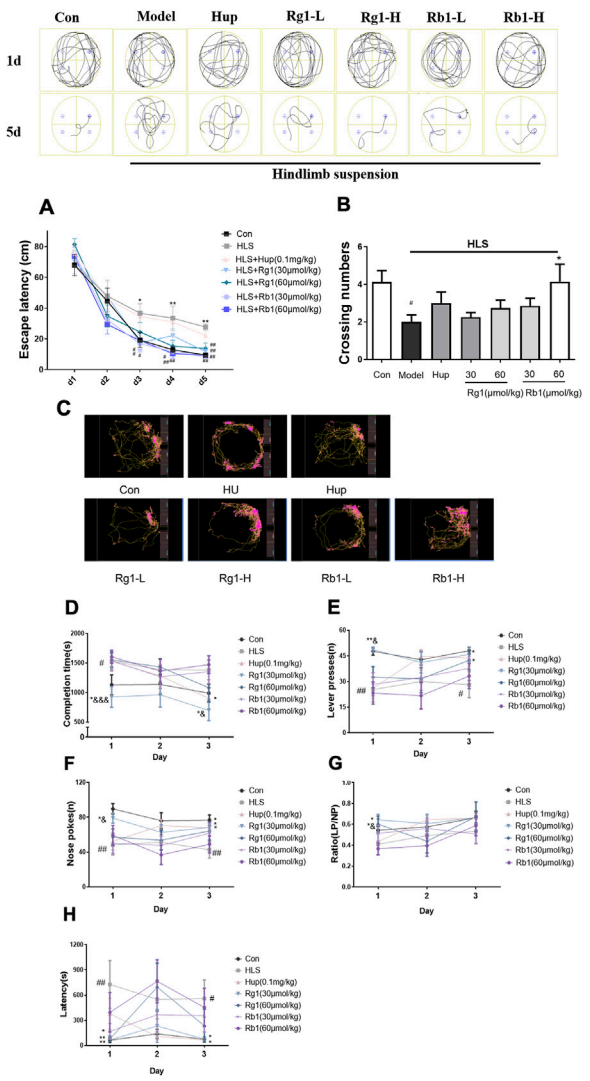

FIGURE 2
Ginsenosides Rg1 and Rb1 ameliorate cognitive dysfunction measured by behavioral tests in hindlimb suspension (HLS) model rats. **(A-B)** The Morris water maze test was used to measure escape latency and frequency of crossing the platform over 5 days. **(C–H)** Representation of moving path, Completion time, Lever presses (LPs), Nose-pokes (NPs), LP/NP ratio, and the latency on the acquisition of operant conditioning reflexes (lever-pressing) in the ROCR test. The data represent mean ± SEM; N = 10 rats per group. $^{\#}p < 0.05$, $^{\#\#}p < 0.01$, significantly different from control; $^{*}p < 0.05$, $^{**}p < 0.01$, significantly different from HLS group. $^{\&}p < 0.05$, $^{\&\&}p < 0.01$, $^{\&\&\&}p < 0.001$, significantly different from Rb1 group.

(Millipore, Bedford, MA, United States). After blocking for 2 h in 5% nonfat milk in Tris-buffered saline with Tween-20 (TBST), the membranes were incubated overnight at 4°C with primary antibodies against Phospho-Akt (ab4060, 1:2000), BDNF (ab108319, 1:2000), Cytochrome C (ab133504, 1:5000), BAX (ab32503, 1:2000), Bcl-2 (ab194583, 1:1000), PSD95 (ab18258, 1:1000), TrkB (ab187041, 1:5000), Mitofusin 2 (ab133504, 1:5000) (all from Abcam Ltd., Cambridge, United Kingdom), and GAPDH (A19056, 1:1000; ABclonal Technology Co., Ltd., Wuhan, China). The membranes were then incubated for 1 h with a horseradish peroxidase-conjugated secondary antibody. An ECL Prime Kit was used to view the protein bands, and ImageJ 1.46r software (NIH, United States, RRID: SCR_003070) was used for quantification.

2.8 Histopathological examination

After the behavioral tests, the animals were anesthetized by pentobarbital sodium injection followed by transcardial perfusion with 4% paraformaldehyde in 0.01 M phosphate buffer for 24 h (4 rats in each group) after the last session. After harvesting, the tissues were embedded in paraffin and stained with H&E following standard procedures (Shi et al., 2019; Xie et al., 2019).

2.9 Statistical analysis

SPSS 22.0 was used for data analysis, and data are represented as the mean ± _standard error of the mean (SEM). We used either one-way ANOVA or repeated-measure two-way ANOVA to assess the differences between the mean values. All one-way ANOVAs were followed by *post hoc* analysis using the LSD test. All two-way ANOVAs were followed by Bonferroni *post hoc* analysis to examine isolated comparisons. $p < 0.05$ was regarded as statistically significant, and the outcome was expressed as the mean ± standard error of the mean (±SEM).

3 Results

3.1 Effects of ginsenosides Rg1 and Rb1 on learning and memory in HLS-exposed rats

As shown in Figure 2A, in the MWM acquisition trial, the latency to reach the platform was significantly longer in the HLS group than in the CON group from days 3–5 ($p < 0.05$, $p < 0.01$, $p < 0.01$, respectively). However, treatment with Rb1 (30 and 60 μmol/kg) reduced the escape latency on days 3–5 when compared with the HLS model rats ($p < 0.05$). Administration of Rg1 (30 and 60 μmol/kg) also markedly improved HLS-induced increments in the escape latency from day 4. Moreover, the rats in the HLS group took shorter times to pass over the hidden platform than those in the control group in the probe test (Figure 2B, $p < 0.05$). These times were further reduced after treatment with high-dose Rb1 (60 μmol/kg).

On day 1 of the ROCR test (Figures 2C,D), the completion time in the model group was considerably longer than that in the control group ($p < 0.05$). Rg1 (30 μmol/kg) treatment led to significantly reduced completion times on days 1 and 3 ($p < 0.05$). On days 1 and 3 ($p < 0.05$), Rg1 considerably improved the completion time compared to the same dose of Rb1. On days 1 and 3, the number of lever presses (LPs) in the untreated model group was progressively reduced compared with the control group (Figure 2E, $p < 0.05$) while treatment with Rg1 (30 μmol/kg) raised the LP number considerably ($p < 0.05$). The number of nose-pokes (NPs) in the HLS rats was fewer compared with the control rats from day 1 to day 3 (Figure 2F, $p < 0.05$). Nevertheless, both Rg1 (30 μmol/kg) and

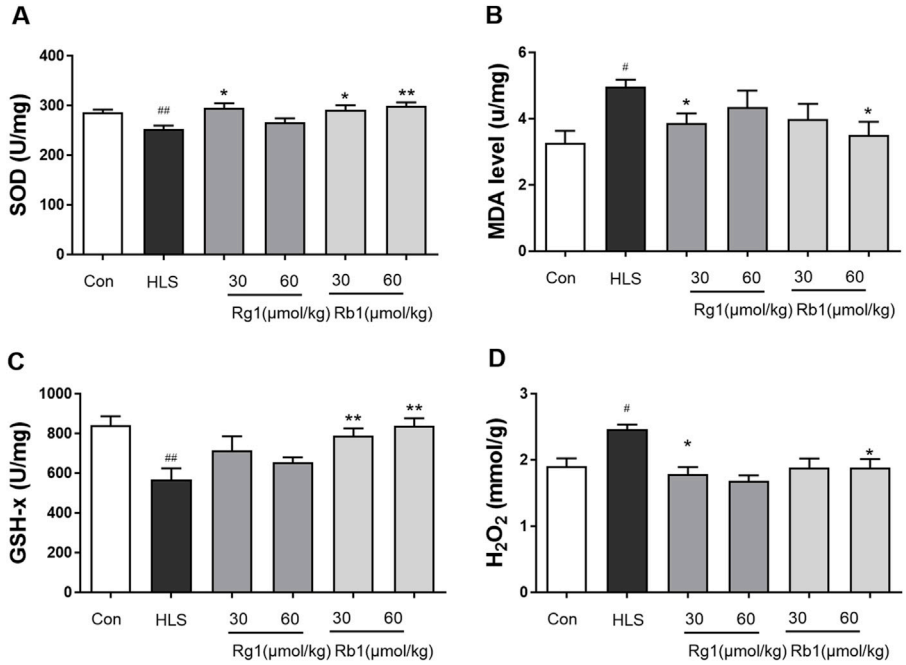

FIGURE 3
The effect of ginsenosides Rg1 and Rb1 on oxidative stress markers in hindlimb suspension (HLS) rats. **(A)** SOD activity, **(B)** MDA level, **(C)** GSH-Px activity, and **(D)** H_2O_2 contents in the prefrontal cortex. Data represent means ± SEM; $N = 6$ rats per group. $^{\#}p < 0.05$, $^{\#\#}p < 0.01$, significantly different from control; $^{*}p < 0.05$, $^{**}p < 0.01$, significantly different from HLS group.

huperzine A treatments significantly increased the NP numbers in HLS rats from day 1 to day 3. The latency of the model group was significantly increased on day 1 and day 3 (Figure 2H, $p < 0.05$). Rg1 (30 and 60 μmol/kg) treatment significantly shortened the latency on day 1 ($p < 0.01$). The latency of the Rg1 (30 μmol/kg) group on day 3 and the Rb1 low-dose group on day 1 was significantly shortened ($p < 0.05$). Furthermore, rats treated with Rg1 (30 and 60 μmol/kg) exhibited significant improvements in the LP/NP ratio on day 1, and LP/NP ratio for the low-dose Rg1 (30 μmol/kg) group was observed to be higher compared with the low-dose Rb1 group (Figure 2G, $p < 0.05$).

3.2 Effects of ginsenosides Rg1 and Rb1 on the markers of oxidative stress in the prefrontal cortex

The activities of SOD and GSH-Px in the prefrontal cortices (PFCs) of the HLS group were considerably lower in comparison with those in the control group [SOD, F (5, 30) = 4.366, $p < 0.01$; GSH-Px, F (5, 30) = 4.792, $p < 0.01$], as shown in Figures 3A, C. Rg1 (30 μmol/kg) and Rb1 (30 and 60 μmol/kg) treatment, on the other hand, led to a marked increase in SOD activity. In contrast, Rb1 (30 and 60 mol/kg) treatment significantly ameliorated the depleted GSH-Px levels in the PFC ($p < 0.05$). MDA and H_2O_2 levels in the PFC of rats exposed to HLS increased significantly [H_2O_2, Figure 3B, F (5, 30) = 3.097, $p < 0.01$; Figure 3D, MDA, F (5, 30) = 2.175, $p < 0.01$]. Treatment with Rg1 (60 μmol/kg) and Rb1 (60 μmol/kg) significantly reduced this increment ($p < 0.05$.).

3.3 Influence of ginsenosides Rg1 and Rb1 on the expression of mitochondrial OXPHOS, Drp1, and Mfn2 proteins in the prefrontal cortex

As shown in Figures 4A–E, there were no significant differences between the groups in the levels of C-V, C-III, C-IV, and C-II in the PFCs. However, the contents of C -I in the PFC of the HLS model group were significantly decreased [Figure 4F, F (5, 23) = 6.658, $p < 0.01$]. Treatment with Rg1 (30 μmol/kg) and Rb1 (30 and 60 μmol/kg), on the other hand, resulted in a substantial increase in C-I ($p < 0.05$). The HLS group had significantly higher Drp1 protein levels in the mitochondrial division [Figure 4H, F (5, 23) = 5.170, $p < 0.01$], whereas Rg1 and Rb1 treatment blocked the enhanced expression of Drp1 ($p < 0.05$). Compared to the control group, reduce expression of the fusion protein Mfn2 was observed in the PFCs of the HLS model group [Figure 4I; F (5, 23) = 6.364 $p < 0.01$]. The administration of both ginsenosides increased the expression of Mfn2 (all $p < 0.01$). The expressions of Tomm 20 were no significant difference among all groups (Figure 4J).

3.4 Influence of ginsenosides Rg1 and Rb1 on the expression of BDNF, p-Akt/AKT, TrkB, SYN, and PSD-95 in the prefrontal cortex

As shown in Figures 5A–D, the levels of p-Akt/AKT [F (5, 23) = 3.171, $p < 0.01$], TrkB [F (5, 23) = 2.701, $p < 0.01$], and BDNF [F (5,

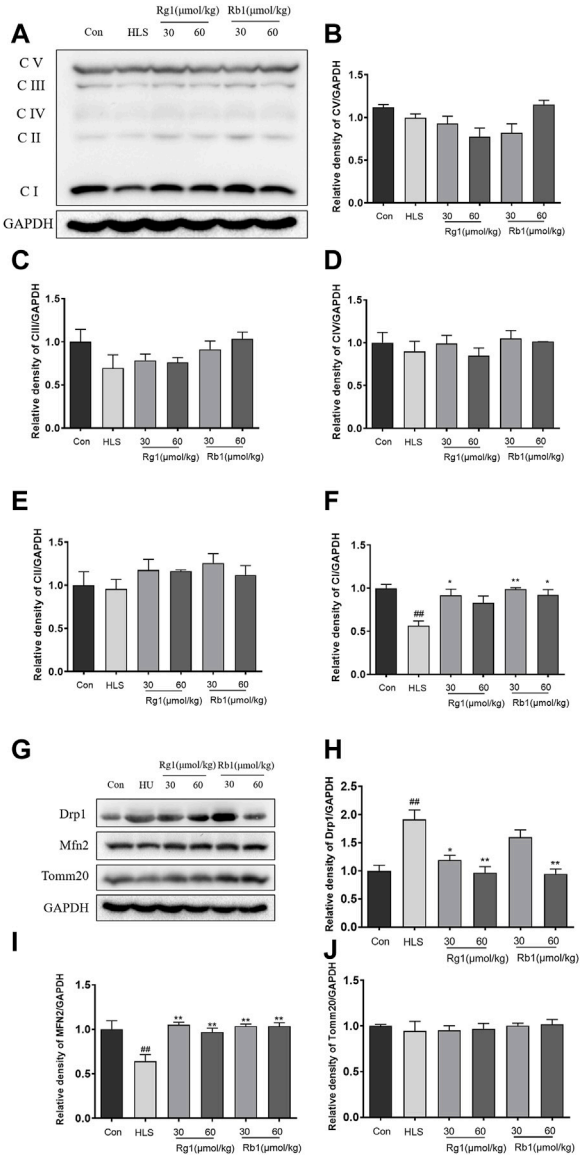

FIGURE 4
The effects of ginsenosides Rg1 and Rb1 on mitochondrial function of hindlimb suspension (HLS) rats. **(A–F)** Protein bands and relative expression levels of CV/GAPDH, CIII/GAPDH, CIV/GAPDH, C-II/GAPDH, and CV/GAPDH in the prefrontal cortex. **(G–J)** Protein bands and relative expression levels of MFN2 and Drp1. Data represent means ± SEM; $N = 4$ rats per group. $^{\#}p < 0.05$, $^{\#\#}p < 0.01$, significantly different from control; $^{*}p < 0.05$, $^{**}p < 0.01$, significantly different from HLS group.

23) = 5.439, $p < 0.01$] were markedly decreased in the HLS model group compared to the control group. Rg1 (30 μmol/kg) and Rb1 (30 μmol/kg and 60 μmol/kg) significantly increased the levels of p-Akt/AKT ($p < 0.01$, $p < 0.05$, respectively). Rg1 (30 μmol/kg) and Rb1 (60 μmol/kg) treatments significantly reversed the expression trend of BDNF ($p < 0.05$). Furthermore, Rg1 (60 μmol/kg) treatment significantly increased the TrkB level in model animals ($p < 0.05$). The expression of both SYN [Figure 5F, F (5, 23) = 3.743, $p < 0.01$] and PSD-95 [Figure 5E, F (5, 23) = 7.322, $p < 0.05$] were found to be substantially decreased in the PFCs of HLS rats compared to the control rats. Additionally, Rg1 (60 μmol/kg) treatment resulted in a substantial increment in the expression of PSD-95 and SYN, while Rb1 (30 and 60 μmol/kg) significantly reversed the observed decrease in the expression of SYN ($p < 0.05$).

3.5 Effects of ginsenosides Rg1 and Rb1 on apoptosis, apoptosis-associated proteins, and neuronal cell loss in the prefrontal cortex

The levels of Cyt C [F (5, 23) = 4.459, $p < 0.01$], cleaved-caspase 3 [F (5, 23) = 3.268, $p < 0.01$], and the Bax/Bcl-2 ratio [F (5, 23) = 2.310 $p < 0.01$], as shown in Figures 6A–D, were substantially increased in the PFCs of the HLS model group ($p < 0.01$). However, treatment with Rg1 and Rb1 significantly reduced these levels ($p < 0.05$).

Marked morphological changes were observed in both the PFC and hippocampus of HLS rats (Figure 6E), with neurons showing a loose organization and uneven cytoplasmic distribution. Neuronal cells with large nuclei were seen in the hippocampi and PFCs of rats treated with Rg1 and Rb1. These neurons adopted an ordered arrangement, suggesting that Rg1 and Rb1 treatment could notably reduce neuronal cell loss.

4 Discussion

Investigation of the effects of long-term treatment with the ginsenosides Rg1 and Rb1 on impaired spatial and associative learning and memory induced by HLS using the MWM test and reward-directed instrumental conditioning task showed that treatment with these ginsenosides led to dramatic improvements. Moreover, Rg1 and Rb1 treatment dramatically attenuated mitochondrial damage, reduced ROS production, inhibited neural cell apoptosis, and activated the BDNF-TrKB/PI3K-Akt signaling pathway in the PFCs of HLS model rats.

Deep space exploration poses risk to neural or tissue damage, cognitive function impairments, behavioral changes, and motor deficits. A recent study longitudinally compared a pair of monozygotic twin astronauts for 340-days, where one of the twins experienced the spaceflight environment on ISS, and simultaneously the other twin endures Earth environment (Mhatre et al., 2022). The results indicatesspaceflight specific effects such as altered circulating immune cytokines and metabolites levels, changes in telomere length, gene regulation at epigenetic as well as transcriptional levels, DNA damage, microbiome alterations, and attenuated cognitive performance (Garrett-Bakelman et al., 2019). In the present study, tail suspension was used (with animals angled 30° head-down), as it is the internationally recognized means of simulating weightlessness, and two types of cognitive-behavioral tests, each representing a different form of cognitive function, were conducted. Firstly, the MWM test was conducted to assess long-term spatial memory (Lu et al., 2018). Our results showed that HLS exposure generated severe neurocognitive deficits in spatial learning and memory, as indicated by the increase in escape latency during the acquisition phase and the decrease in numbers of crossings during the probing session

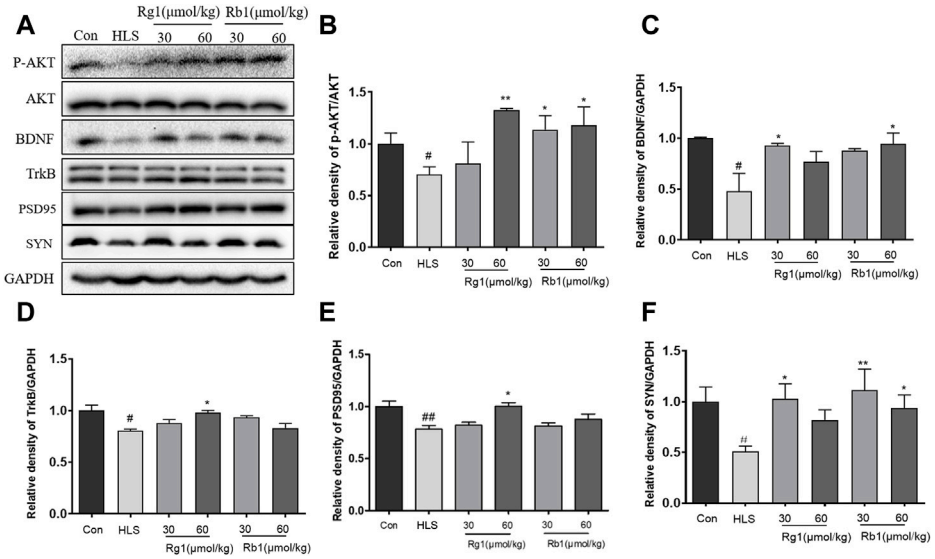

FIGURE 5
Ginsenosides Rg1 and Rb1 influence the expression of BDNF signaling pathway-related proteins in hindlimb suspension (HLS) rats. **(A–F)** Protein bands and relative expression levels of p- Akt/AKT, TrkB, BDNF, PSD-95, and SYN in the PFC. Data represent means ± SEM; $N = 4$ rats per group. $^{\#}p < 0.05$, $^{\#\#}p < 0.01$, significantly different from control; $^{*}p < 0.05$, $^{**}p < 0.01$, significantly different from HLS group.

(Zhang et al., 2018). Rg1 and Rb1 treatments enhanced MWM performance over that of the HLS model group, indicating that these ginsenosides improved spatial memory. The study found that Rb1 improved escape latency in the acquisition phase faster than Rg1 and that Rb1 therapy increased the number of crossings in the probing test. After 2 weeks of Rb1 and Rg1 treatment, Rb1 was found to have improved spatial memory more than Rg1 in HLS model rats. ROCR is a vital tool for identifying behavioral adaptation, as it allows for fast behavioral changes in response to changing conditions, offering a survival advantage (Dayan and Balleine, 2002; Shi et al., 2013). By pressing a lever, the animal receives a reward while performing the activity, making learning fun and reinforcing the activity. Two systems control instrumental behavior: the goal-directed process and the stimulus-response (S-R) habit mechanism (Balleine and Dickinson, 1998). In the current work, rats in the Rb1 and Rg1 low-dose groups could complete the task in the LP training course after 4 weeks of HLS treatment, while the former took longer. However, the other groups could not complete the task on the first day after modeling. The completion time and operation latency were higher in the model group compared to the control group, while the LP and NP values and the LP/NP ratio were decreased. These findings suggested that model rats' exploration times, executive ability, and lever pressing efficiency were reduced, and model rats could not focus on the fixed ratio response test, necessitating a longer time to adjust even to a familiar setting. Rb1 administration reduced these operational delays and improved the focus of the animals, whereas Rg1 administration reversed the changes in the five indices described above and increased the interest in exploration, attentiveness, and operational ability. A significant difference was observed in comparison with the same dose of Rb1, indicating a better improvement effect. The findings of these two behavioral tests provided evidence for Rb1 and Rg1-mediated amelioration of HLS-induced learning and memory impairment. Thus, this treatment not only resulted in a significant improvement in spatial memory but also in associative learning and memory. This manuscript is the first study of ginsenosides for cognitive impairment induced by simulated microgravity.

Chronic stress-induced memory loss has been linked to oxidative stress damage. The accumulation of excess ROS overpowers the body's antioxidant defense system, causing permanent damage to membrane lipids, proteins, and nucleic acids, intracellular damage accumulation, cognitive impairment, and cell death (Majdi et al., 2016; Ballard and Towarnicki, 2020). SOD, CAT, and GSH-Px are antioxidant enzymes that protect antioxidant systems. A recent study linked HLS-induced memory loss to increased oxidative stress (Wang et al., 2021). In agreement with these findings, HLS increased oxidative stress measured by MDA and H_2O_2 levels and decreased SOD and GSH-Px activity in the PFC. The ability of Rg1 and Rb1 to scavenge oxygen free radicals and thus enhance antioxidant functions may contribute to their protective effects against HLS-induced cognitive loss.

Mitochondrial dysfunction is a widely accepted primary cause for the development of cognitive impairment, particularly the pathogenesis of most neurodegenerative disorders, such as AD (Li J. et al., 2019). The primary purpose of mitochondria, in conjunction with cellular respiration, is to produce ATP through oxidative phosphorylation. These systems include the NADH succinic acid, CoQ reductase (complex I), and the mitochondrial respiratory chain composed of five enzyme complexes, namely, CoQ reductase (complex II), CoQcytochrome C reductase (complex III), cytochrome C oxidase (complex IV), and ATP synthase (complex V) (Stock et al., 2000). The mitochondrial complex I is the most critical of the five enzyme complexes in the respiratory chain, affecting both the respiratory chain and ATP anabolism. The Drp1 protein possesses GTPase activity and promotes fission by a chain

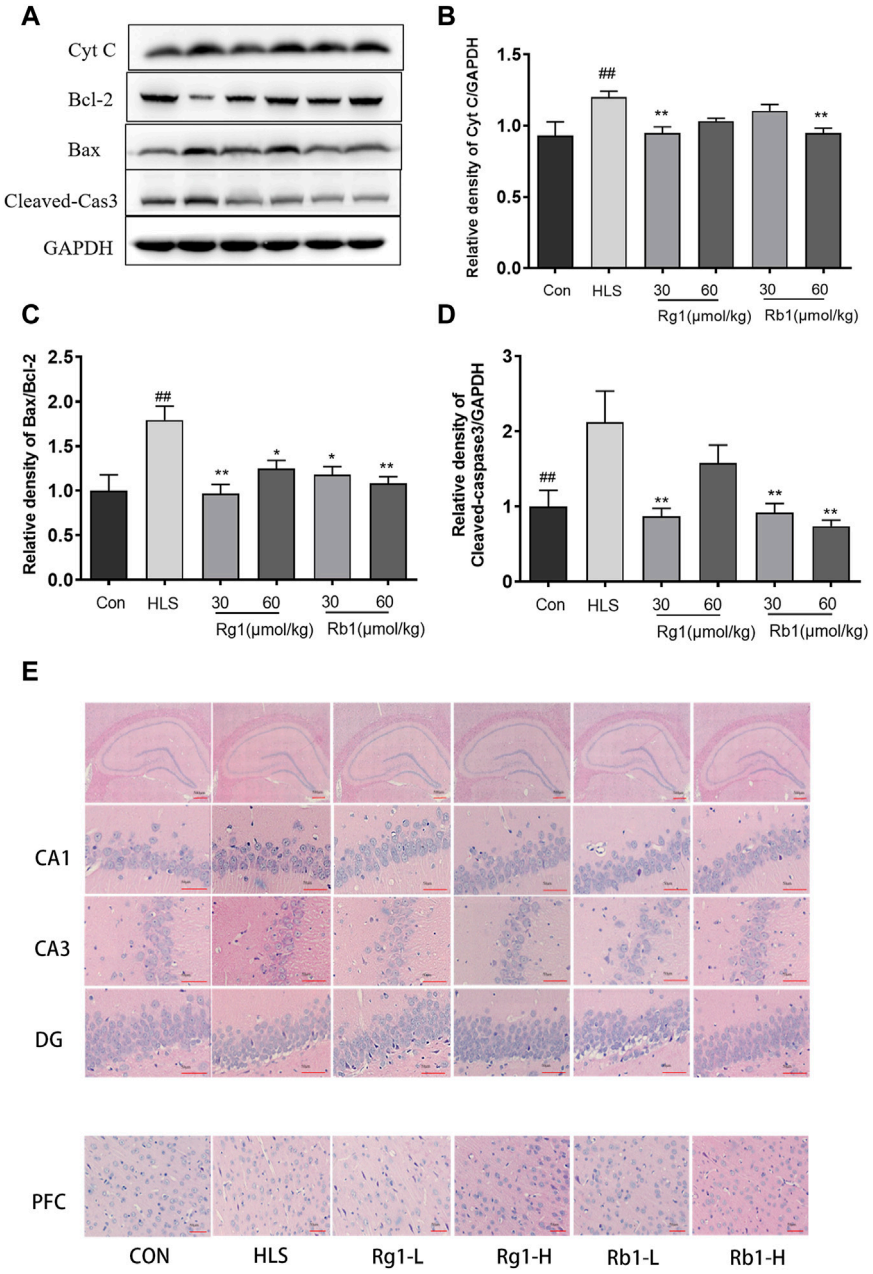

FIGURE 6
The effects of ginsenosides Rg1 and Rb1 on apoptosis, levels of apoptosis-associated proteins, and neuronal cell loss in hindlimb suspension (HLS) rats. **(A–D)** Protein bands and relative expression levels of Cyt C, Bcl-2/Bax, and cleaved-caspase 3 in the PFC. **(E)** The HLS rat hippocampal CA1, CA3, DG, and PFC regions were stained with hematoxylin-eosin (at ×400 magnification power). Data represent means ± SEM; $N = 4$ rats per group. $^{\#}p < 0.05$, $^{\#\#}p < 0.01$, significantly different from control; $^{*}p < 0.05$, $^{**}p < 0.01$, significantly different from HLS group.

formation in the mitochondrial outer membrane, which further promotes mitochondrial fission. OPA-1, Mfn1, and Mfn2, on the other hand, mediate fusion (Chan, 2020). In the current study, HLS exposure resulted in a decrease in complex I activity and Mfn2 protein levels, and an increase in the Drp1 protein expression in the rat PFCs. However, long-term Rg1 and Rb1 treatment reversed this, suggesting that Rg1 and Rb1 significantly improved mitochondrial function in HLS-exposed mice.

According to earlier research, aberrant mitochondrial dynamics influence apoptosis, and the mitotic protein Drp1 promotes Bax oligomerization and plays a role in apoptosis regulation. Overexpression of the fusion proteins Mfn2 and OPA1 reduces Bax activation while Mfn1 and Mfn2 promote sensitivity to apoptosis in cells (Camperchioli et al., 2011). Cytochrome C is an essential factor in mitochondria-mediated apoptotic pathways. The release of cytochrome C is an important indicator of mitochondrial damage. Bax and Bcl2 are members of the Bcl2 family and regulate mitochondrial cytochrome C release, caspase 3 activation, and apoptosis (Fuentealba et al., 2009; Jiang et al., 2019a). Several studies have shown that increased apoptosis

occurs in various mammalian cell types in space and simulated microgravity (SMG) (Lewis et al., 1998; Kumari et al., 2009). In agreement with these findings, HLS exposure was found to enhance the Bax/Bcl2 ratio and the expression of cleaved caspase 3 and cytochrome C. Long-term administration of Rg1 and Rb1 in HLS rats, on the other hand, significantly reversed these effects, preventing neuronal death. Considering all of the evidence, Rg1 and Rb1's neuroprotective effects in HLS rats may be partially a result of their capacity to inhibit apoptosis.

Mitochondrial insufficiency also leads to changes in synaptic density, which in turn results in significant impairment of cognitive function (D'Souza et al., 2015). SYN and PSD-95 are two key indicators and regulators of dynamic synaptic plasticity (Janz et al., 1999). Previous studies have reported that HLS exposure induced cognitive dysfunction and synaptic plasticity deficits in mice (Xiang et al., 2019). In agreement, our data showed that the expression of SYN and PSD-95 underwent a significant decline in the HLS model group, which was reversed by treatment with Rb1 and Rg1, indicating that both ginsenosides may enhance synaptic plasticity in the HLS model. In addition, a considerable amount of evidence suggests that a reduction in the level of BDNF in the PFC (presumably including the hippocampus) is strongly linked to cognitive impairment induced by simulated microgravity (Wu et al., 2017; Zhai et al., 2020). BDNF is a nutritional factor, which is known to play a major role in synaptic plasticity and neuronal stress resistance (Zhang et al., 2021). It is closely linked to various aspects of learning and memory processing (Yamada et al., 2002). Tyrosine kinase receptor B (TrkB) is a high-affinity receptor for BDNF and can trigger downstream intracellular PI3K/Akt signaling. The PI3K/Akt pathway is strongly implicated in the promotion of neuronal survival. It is also known to confer protection against apoptosis (Jiang et al., 2019b). BDNF has been previously reported to regulate the scaffolding protein PSD-95 via PI3K/Akt signaling (Li M. et al., 2019).

In the present study, HLS exposure significantly reduced the phosphorylation of TrkB, BDNF, and AKT in the PFC, together with reduced SYN expression. However, long-term administration of Rg1 and Rb1 to HLS-exposed rats significantly reversed these effects. This finding also raises the possibility that Rg1 and Rb1 treatment may affect BDNF-PI3K/Akt signaling in the PFC, which controls the expression of SYN and PSD95 and thus synaptic plasticity, thus reducing cognitive deficits in the rats.

5 Conclusion

In conclusion, the present study is the first to demonstrate that treatment with ginsenosides Rg1 and Rb1 protected against HLS-induced memory impairment. The underlying mechanism responsible for this protective influence may originate from its mitochondria-targeted antioxidant activity and regulation of the BDNF-TrkB/PI3K-Akt signaling axis, involving inhibition of apoptosis and an increase in synaptic plasticity. The present study highlights the use of ginsenosides Rg1 and Rb1 as novel candidate agents to counteract cognitive dysfunction induced by long-term spaceflight.

Data availability statement

The original contributions presented in the study are included in the article/Supplementary Materials, further inquiries can be directed to the corresponding author.

Ethics statement

The animal study was reviewed and approved by No. SYXK 2017-0020.

Author contributions

NJ and XL designed the research. NJ, JL, and YZ conducted the experiments. NJ, CY, and YZ performed the data analysis. NJ, QH, XS, QW, and XL wrote and amended the manuscript. XL and QW supervised the study and contributed to project administration. All authors approved the final version.

Funding

The Innovation Fund for Medical Sciences (CIFMS) (Grant No. 2021-1-I2M-034), the International Cooperative Project of Traditional Chinese Medicine (GZYYG2020023), National Natural Science Foundation of China (Grant No. 81773930), the Space Medical Experiment Project of the China Manned Space Program (Grant No. HYZHXM05003) the all provided funding for this project.

Conflict of interest

The authors declare that the research was conducted in the absence of any commercial or financial relationships that could be construed as a potential conflict of interest.

Publisher's note

Supplementary material

The Supplementary Material for this article can be found online at: https://www.frontiersin.org/articles/10.3389/fphar.2023.1167398/full#supplementary-material

References

Ballard, J. W. O., and Towarnicki, S. G. (2020). Mitochondria, the gut microbiome and ROS. *Cell Signal* 75, 109737. doi:10.1016/j.cellsig.2020.109737

Balleine, B. W., and Dickinson, A. (1998). Goal-directed instrumental action: Contingency and incentive learning and their cortical substrates. *Neuropharmacology* 37, 407–419. doi:10.1016/s0028-3908(98)00033-1

Camperchioli, A., Mariani, M., Bartollino, S., Petrella, L., Persico, M., Orteca, N., et al. (2011). Investigation of the bcl-2 multimerisation process: Structural and functional implications. *Biochim. Biophys. Acta* 1813, 850–857. doi:10.1016/j.bbamcr.2011.02.006

Chan, D. C. (2020). Mitochondrial dynamics and its involvement in disease. *Annu. Rev. Pathol.* 15, 235–259. doi:10.1146/annurev-pathmechdis-012419-032711

D'souza, Y., Elharram, A., Soon-Shiong, R., Andrew, R. D., and Bennett, B. M. (2015). Characterization of Aldh2 (-/-) mice as an age-related model of cognitive impairment and Alzheimer's disease. *Mol. Brain* 8, 27. doi:10.1186/s13041-015-0117-y

Dayan, P., and Balleine, B. W. (2002). Reward, motivation, and reinforcement learning. *Neuron* 36, 285–298. doi:10.1016/s0896-6273(02)00963-7

Fuentealba, R. A., Liu, Q., Kanekiyo, T., Zhang, J., and Bu, G. (2009). Low density lipoprotein receptor-related protein 1 promotes anti-apoptotic signaling in neurons by activating Akt survival pathway. *J. Biol. Chem.* 284, 34045–34053. doi:10.1074/jbc.M109.021030

Garrett-Bakelman, F. E., Darshi, M., Green, S. J., Gur, R. C., Lin, L., Macias, B. R., et al. (2019). The NASA twins study: A multidimensional analysis of a year-long human spaceflight. *Science* 364, eaau8650. doi:10.1126/science.aau8650

Globus, R. K., and Morey-Holton, E. (2016). Hindlimb unloading: Rodent analog for microgravity. *J. Appl. Physiol.* 120, 1196–1206. doi:10.1152/japplphysiol.00997.2015

Huang, Z., Lin, J., Cheng, Z., Xu, M., Huang, X., Yang, Z., et al. (2015). Production of dammarane-type sapogenins in rice by expressing the dammarenediol-II synthase gene from Panax ginseng C.A. Mey. *Plant Sci.* 239, 106–114. doi:10.1016/j.plantsci.2015.07.021

Janz, R., Südhof, T. C., Hammer, R. E., Unni, V., Siegelbaum, S. A., and Bolshakov, V. Y. (1999). Essential roles in synaptic plasticity for synaptogyrin I and synaptophysin I. *Neuron* 24, 687–700. doi:10.1016/s0896-6273(00)81122-8

Jiang, N., Lv, J., Wang, H., Huang, H., Wang, Q., Lu, C., et al. (2020). Ginsenoside Rg1 ameliorates chronic social defeat stress-induced depressive-like behaviors and hippocampal neuroinflammation. *Life Sci.* 252, 117669. doi:10.1016/j.lfs.2020.117669

Jiang, N., Lv, J. W., Wang, H. X., Lu, C., Wang, Q., Xia, T. J., et al. (2019a). Dammarane sapogenins alleviates depression-like behaviours induced by chronic social defeat stress in mice through the promotion of the BDNF signalling pathway and neurogenesis in the hippocampus. *Brain Res. Bull.* 153, 239–249. doi:10.1016/j.brainresbull.2019.09.007

Jiang, N., Lv, J. W., Wang, H. X., Wang, Q., Lu, C., Yang, Y. J., et al. (2019b). Antidepressant-like effects of 20(S)-protopanaxadiol in a mouse model of chronic social defeat stress and the related mechanisms. *Phytother. Res.* 33, 2726–2736. doi:10.1002/ptr.6446

Jiang, N., Wang, K., Zhang, Y., Huang, H., Lv, J. W., Wang, Q., et al. (2021). Protective effect of ginsenoside Rb1 against chronic restraint stress (CRS)-induced memory impairments in rats. *Behav. Brain Res.* 405, 113146. doi:10.1016/j.bbr.2021.113146

Kezhu, W., Pan, X., Cong, L., Liming, D., Beiyue, Z., Jingwei, L., et al. (2017). Effects of ginsenoside Rg1 on learning and memory in a reward-directed instrumental conditioning task in chronic restraint stressed rats. *Phytother. Res.* 31, 81–89. doi:10.1002/ptr.5733

Kumari, R., Singh, K. P., and Dumond, J. W., Jr. (2009). Simulated microgravity decreases DNA repair capacity and induces DNA damage in human lymphocytes. *J. Cell Biochem.* 107, 723–731. doi:10.1002/jcb.22171

Lewis, M. L., Reynolds, J. L., Cubano, L. A., Hatton, J. P., Lawless, B. D., and Piepmeier, E. H. (1998). Spaceflight alters microtubules and increases apoptosis in human lymphocytes (Jurkat). *Faseb J.* 12, 1007–1018. doi:10.1096/fasebj.12.11.1007

Li, F., Wu, X., Li, J., and Niu, Q. (2016). Ginsenoside Rg1 ameliorates hippocampal long-term potentiation and memory in an Alzheimer's disease model. *Mol. Med. Rep.* 13, 4904–4910. doi:10.3892/mmr.2016.5103

Li, J., Zhu, X., Yang, S., Xu, H., Guo, M., Yao, Y., et al. (2019). Lidocaine attenuates cognitive impairment after isoflurane anesthesia by reducing mitochondrial damage. *Neurochem. Res.* 44, 1703–1714. doi:10.1007/s11064-019-02799-0

Li, M., You, M., Li, S., Qiu, Z., and Wang, Y. (2019). Effects of maternal exposure to nonylphenol on learning and memory in offspring involve inhibition of BDNF-PI3K/Akt signaling. *Brain Res. Bull.* 146, 270–278. doi:10.1016/j.brainresbull.2019.01.014

Liu, Z., Qi, Y., Cheng, Z., Zhu, X., Fan, C., and Yu, S. Y. (2016). The effects of ginsenoside Rg1 on chronic stress induced depression-like behaviors, BDNF expression and the phosphorylation of PKA and CREB in rats. *Neuroscience* 322, 358–369. doi:10.1016/j.neuroscience.2016.02.050

Lu, C., Lv, J., Dong, L., Jiang, N., Wang, Y., Wang, Q., et al. (2018). Neuroprotective effects of 20(S)-protopanaxatriol (PPT) on scopolamine-induced cognitive deficits in mice. *Phytother. Res.* 32, 1056–1063. doi:10.1002/ptr.6044

Lu, C., Lv, J., Jiang, N., Wang, H., Huang, H., Zhang, L., et al. (2020). Protective effects of Genistein on the cognitive deficits induced by chronic sleep deprivation. *Phytother. Res.* 34, 846–858. doi:10.1002/ptr.6567

Lv, J., Jiang, N., Wang, H., Huang, H., Bao, Y., Chen, Y., et al. (2021). Simulated weightlessness induces cognitive changes in rats illustrated by performance in operant conditioning tasks. *Life Sci. Space Res. (Amst)* 29, 63–71. doi:10.1016/j.lssr.2021.03.004

Majdi, A., Mahmoudi, J., Sadigh-Eteghad, S., Golzari, S. E., Sabermarouf, B., and Reyhani-Rad, S. (2016). Permissive role of cytosolic pH acidification in neurodegeneration: A closer look at its causes and consequences. *J. Neurosci. Res.* 94, 879–887. doi:10.1002/jnr.23757

Mhatre, S. D., Iyer, J., Puukila, S., Paul, A. M., Tahimic, C. G. T., Rubinstein, L., et al. (2022). Neuro-consequences of the spaceflight environment. *Neurosci. Biobehav Rev.* 132, 908–935. doi:10.1016/j.neubiorev.2021.09.055

Mohanan, P., Subramaniyam, S., Mathiyalagan, R., and Yang, D. C. (2018). Molecular signaling of ginsenosides Rb1, Rg1, and Rg3 and their mode of actions. *J. Ginseng Res.* 42, 123–132. doi:10.1016/j.jgr.2017.01.008

Morris, R. (1984). Developments of a water-maze procedure for studying spatial learning in the rat. *J. Neurosci. Methods* 11, 47–60. doi:10.1016/0165-0270(84)90007-4

Nordeen, C. A., and Martin, S. L. (2019). Engineering human stasis for long-duration spaceflight. *Physiol. (Bethesda)* 34, 101–111. doi:10.1152/physiol.00046.2018

Qiong, W., Yong-Liang, Z., Ying-Hui, L., Shan-Guang, C., Jiang-Hui, G., Yi-Xi, C., et al. (2016). The memory enhancement effect of Kai Xin San on cognitive deficit induced by simulated weightlessness in rats. *J. Ethnopharmacol.* 187, 9–16. doi:10.1016/j.jep.2016.03.070

Shi, D. D., Huang, Y. H., Lai, C. S. W., Dong, C. M., Ho, L. C., Li, X. Y., et al. (2019). Ginsenoside Rg1 prevents chemotherapy-induced cognitive impairment: Associations with microglia-mediated cytokines, neuroinflammation, and neuroplasticity. *Mol. Neurobiol.* 56, 5626–5642. doi:10.1007/s12035-019-1474-9

Shi, Z., Chen, L., Li, S., Chen, S., Sun, X., Sun, L., et al. (2013). Chronic scopolamine-injection-induced cognitive deficit on reward-directed instrumental learning in rat is associated with CREB signaling activity in the cerebral cortex and dorsal hippocampus. *Psychopharmacol. Berl.* 230, 245–260. doi:10.1007/s00213-013-3149-y

Shi, Z., Ren, H., Huang, Z., Peng, Y., He, B., Yao, X., et al. (2017). Fish oil prevents lipopolysaccharide-induced depressive-like behavior by inhibiting neuroinflammation. *Mol. Neurobiol.* 54, 7327–7334. doi:10.1007/s12035-016-0212-9

Stock, D., Gibbons, C., Arechaga, I., Leslie, A. G., and Walker, J. E. (2000). The rotary mechanism of ATP synthase. *Curr. Opin. Struct. Biol.* 10, 672–679. doi:10.1016/s0959-440x(00)00147-0

Wang, Q., Dong, L., Wang, M., Chen, S., Li, S., Chen, Y., et al. (2021). Dammarane sapogenins improving simulated weightlessness-induced depressive-like behaviors and cognitive dysfunction in rats. *Front. Psychiatry* 12, 638328. doi:10.3389/fpsyt.2021.638328

Wang, Q., Sun, L. H., Jia, W., Liu, X. M., Dang, H. X., Mai, W. L., et al. (2010). Comparison of ginsenosides Rg1 and Rb1 for their effects on improving scopolamine-induced learning and memory impairment in mice. *Phytother. Res.* 24, 1748–1754. doi:10.1002/ptr.3130

Wang, Y., Javed, I., Liu, Y., Lu, S., Peng, G., Zhang, Y., et al. (2016). Effect of prolonged simulated microgravity on metabolic proteins in rat Hippocampus: Steps toward safe space travel. *J. Proteome Res.* 15, 29–37. doi:10.1021/acs.jproteome.5b00777

Wu, X., Li, D., Liu, J., Diao, L., Ling, S., Li, Y., et al. (2017). Dammarane sapogenins ameliorates neurocognitive functional impairment induced by simulated long-duration spaceflight. *Front. Pharmacol.* 8, 315. doi:10.3389/fphar.2017.00315

Xiang, S., Zhou, Y., Fu, J., and Zhang, T. (2019). rTMS pre-treatment effectively protects against cognitive and synaptic plasticity impairments induced by simulated microgravity in mice. *Behav. Brain Res.* 359, 639–647. doi:10.1016/j.bbr.2018.10.001

Xie, W., Meng, X., Zhai, Y., Ye, T., Zhou, P., Nan, F., et al. (2019). Antidepressant-like effects of the Guanxin Danshen formula via mediation of the CaMK II-CREB-BDNF

signalling pathway in chronic unpredictable mild stress-induced depressive rats. *Ann. Transl. Med.* 7, 564. doi:10.21037/atm.2019.09.39

Xu, P., Wang, K., Lu, C., Dong, L., Chen, Y., Wang, Q., et al. (2017). Effects of the chronic restraint stress induced depression on reward-related learning in rats. *Behav. Brain Res.* 321, 185–192. doi:10.1016/j.bbr.2016.12.045

Xu, P., Wang, K. Z., Lu, C., Dong, L. M., Le Zhai, J., Liao, Y. H., et al. (2016). Antidepressant-like effects and cognitive enhancement of the total phenols extract of Hemerocallis citrina Baroni in chronic unpredictable mild stress rats and its related mechanism. *J. Ethnopharmacol.* 194, 819–826. doi:10.1016/j.jep.2016.09.023

Yamada, K., Mizuno, M., and Nabeshima, T. (2002). Role for brain-derived neurotrophic factor in learning and memory. *Life Sci.* 70, 735–744. doi:10.1016/s0024-3205(01)01461-8

Yang, Y., Li, S., Huang, H., Lv, J., Chen, S., Pires Dias, A. C., et al. (2020). Comparison of the protective effects of ginsenosides Rb1 and Rg1 on improving cognitive deficits in SAMP8 mice based on anti-neuroinflammation mechanism. *Front. Pharmacol.* 11, 834. doi:10.3389/fphar.2020.00834

Yoon, N., Na, K., and Kim, H. S. (2017). Simulated weightlessness affects the expression and activity of neuronal nitric oxide synthase in the rat brain. *Oncotarget* 8, 30692–30699. doi:10.18632/oncotarget.15407

Zhai, B., Fu, J., Xiang, S., Shang, Y., Yan, Y., Yin, T., et al. (2020). Repetitive transcranial magnetic stimulation ameliorates recognition memory impairment induced by hindlimb unloading in mice associated with BDNF/TrkB signaling. *Neurosci. Res.* 153, 40–47. doi:10.1016/j.neures.2019.04.002

Zhang, W., Ou, H., Zhang, B., Zheng, M., Yan, L., Chen, Y., et al. (2021). Treadmill exercise relieves chronic restraint stress-induced cognitive impairments in mice via activating protein phosphatase 2A. *Neurosci. Bull.* 37, 1487–1492. doi:10.1007/s12264-021-00766-w

Zhang, Y., Wang, Q., Chen, H., Liu, X., Lv, K., Wang, T., et al. (2018). Involvement of cholinergic dysfunction and oxidative damage in the effects of simulated weightlessness on learning and memory in rats. *Biomed. Res. Int.* 2018, 2547532. doi:10.1155/2018/2547532

frontiers | Frontiers in Pharmacology

TYPE Original Research
PUBLISHED 03 May 2023
DOI 10.3389/fphar.2023.1173920

OPEN ACCESS

EDITED BY
Yuan Li,
Shanghai Jiao Tong University, China

REVIEWED BY
Jinxiu Li,
Chinese Academy of Sciences (CAS), China
Li Xing Xing,
Ningbo Kangning Hospital, China

*CORRESPONDENCE
Xinmin Liu,
liuxinmin@hotmail.com
Ning Jiang,
jiangning0603@163.com

RECEIVED 25 February 2023
ACCEPTED 05 April 2023
PUBLISHED 03 May 2023

CITATION
Zhang Y, Huang H, Yao C, Sun X, He Q, Choudharyc MI, Chen S, Liu X and Jiang N (2023), Fresh *Gastrodia elata* Blume alleviates simulated weightlessness-induced cognitive impairment by regulating inflammatory and apoptosis-related pathways.
Front. Pharmacol. 14:1173920.
doi: 10.3389/fphar.2023.1173920

Fresh *Gastrodia elata* Blume alleviates simulated weightlessness-induced cognitive impairment by regulating inflammatory and apoptosis-related pathways

Yiwen Zhang[1], Hong Huang[1], Caihong Yao[1], Xinran Sun[1], Qinghu He[2], Muhammad Iqbal Choudharyc[3], Shanguang Chen[4], Xinmin Liu[2,5,6]* and Ning Jiang[1]*

[1]Research Center for Pharmacology and Toxicology, Institute of Medicinal Plant Development (IMPLAD), Chinese Academy of Medical Sciences and Peking Union Medical College, Beijing, China, [2]Sino-Pakistan Center on Traditional Chinese Medicine, Hunan University of Medicine, Huaihua, China, [3]H.E.J. Research Institute of Chemistry, International Center for Chemical and Biological Sciences, University of Karachi, Karachi, Pakistan, [4]National Laboratory of Human Factors Engineering, The State Key Laboratory of Space Medicine Fundamentals and Application, China Astronaut Research and Training Center, Beijing, China, [5]Institute of Drug Discovery Technology, Ningbo University, Ningbo, China, [6]Healthy & Intelligent Kitchen Engineering Research Center of Zhejiang Province, Zhejiang, China

In aerospace medicine, the influence of microgravity on cognition has always been a risk factor threatening astronauts' health. The traditional medicinal plant and food material *Gastrodia elata* Blume has been used as a therapeutic drug for neurological diseases for a long time due to its unique neuroprotective effect. To study the effect of fresh *Gastrodia elata* Blume (FG) on cognitive impairment caused by microgravity, hindlimb unloading (HU) was used to stimulate weightlessness in mice. The fresh *Gastrodia elata* Blume (0.5 g/kg or 1.0 g/kg) was intragastrically administered daily to mice exposed to HU and behavioral tests were conducted after four weeks to detect the cognitive status of animals. The behavioral tests results showed that fresh *Gastrodia elata* Blume therapy significantly improved the performance of mice in the object location recognition test, Step-Down test, and Morris Water Maze test, including short-term and long-term spatial memory. According to the biochemical test results, fresh *Gastrodia elata* Blume administration not only reduced serum factor levels of oxidative stress but also maintained the balance of pro-inflammatory and anti-inflammatory factors in the hippocampus, reversing the abnormal increase of NLRP3 and NF-κB. The apoptosis-related proteins were downregulated which may be related to the activation of the PI3K/AKT/mTOR pathway by fresh *Gastrodia elata* Blume therapy, and the abnormal changes of synapse-related protein and glutamate neurotransmitter were corrected. These results identify the improvement effect of fresh *Gastrodia elata* Blume as a new application form of *Gastrodia elata* Blume on cognitive impairment caused by simulated weightlessness and advance our understanding of the mechanism of fresh *Gastrodia elata* Blume on the neuroprotective effect.

KEYWORDS

Gastrodia elata Blume, stimulated weightlessness, learning and memory, inflammatory, apoptosis

Introduction

Astronauts' cognitive impairment caused by weightlessness has always been an urgent problem to be solved. Evidence has proved that after experiencing the microgravity and confined environments of spaceflight, astronauts are at an increased risk of memory impairment, disorientation, and other symptoms (Casler and Cook, 1999). The pressure of long-term space flight would lead to the cognitive overload of astronauts, causing damage to the completion of the mission (Bock et al., 2010; Lv et al., 2021).

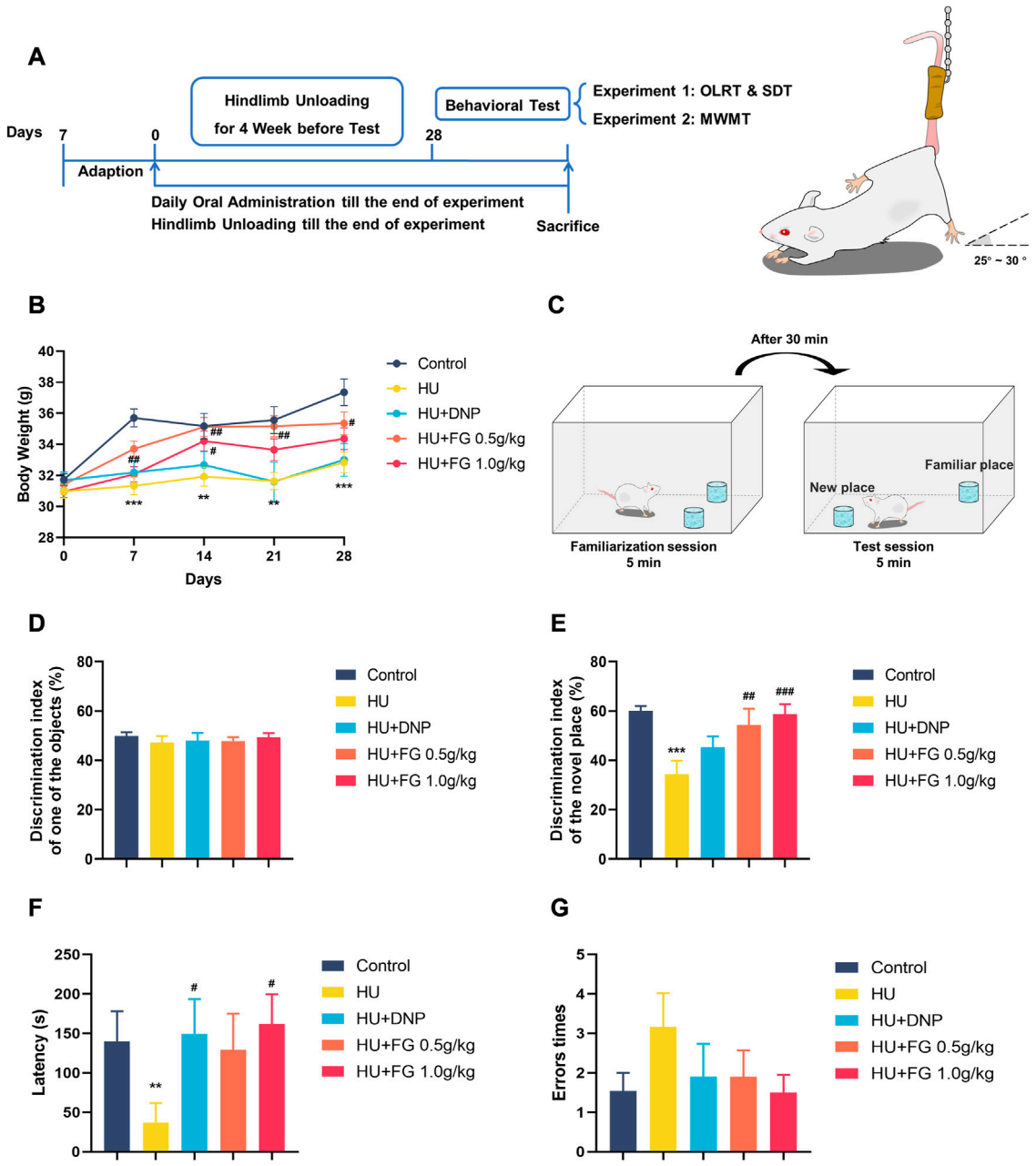

FIGURE 1
The schematic diagram of the experiment and the effect of FG on LORT and STD. **(A)** The experimental protocol of this study. **(B)** Body weight change during the HU procedure. **(C)** Schematic diagram of OLRT. **(D)** The discrimination index in the familiarization session of LORT. **(E)** The discrimination index in the test session of LORT. **(F)** The latency SDT. **(G)** The error times of SDT. Data were expressed as mean ± SEM (n = 10–12 per group). $^{*}p < 0.05$, $^{**}p < 0.01$, and $^{***}p < 0.001$ versus the control group; $^{\#}p < 0.05$, $^{\#\#}p < 0.01$, and $^{\#\#\#}p < 0.001$ versus the HU group. Note: Hindlimb unloading, HU; Object location recognition test, OLRT; Step Down test, SDT; Morris Water Maze Test, WMWT.

Especially, evidence showed that the operational tasks in space missions are more challenging for humans compared with ground missions (Fowler et al., 2000). In space experiments of animals, it was found that long-term spaceflight affects the principal regulatory factors of brain neuroplasticity and neurotrophic factors in rodents (Popova et al., 2020). Combined with these conditions, maintaining the health of astronauts in long-term space flight has become one of the main concerns of aerospace medicine. This decline in learning and memory abilities caused by specific circumstances is a functional impairment, with no clear lesion location and specific targets and no effective prevention and treatment methods. Although in 1990, NASA launched the "Neurolab Mission" hoping to find measures to protect astronauts from cognitive decline caused by aerospace stress, the progress has been slow so far (Homick et al., 1998). Finding safe and effective protective measures to improve and increase the response and decision-making abilities of astronauts in special aerospace environments remain a challenge facing the international aerospace medical community. To better study the effects of microgravity on the human body, hindlimb unloading caused by tail suspension is used as a classic modeling method to simulate weightlessness in the present pharmacological research, which has been proven to take risk of learning and memory impairment in rodents (Globus and Morey-Holton, 2016).

Traditional Chinese Medicine (TCM) places more emphasis on the holistic concept of diseases, and the concept of "treating diseases before they occur" in TCM is more suitable for preventing functional injury. *Gastrodia elata* Blume, both as a traditional medicinal plant and food material, is often used to treat dizziness, headache, and cognitive impairment caused by Alzheimer's disease, ischemic brain injury, etc. (Mao et al., 2017; Fasina et al., 2022). *In vivo* and *vitro* experiments, *Gastrodia elata* Blume shows protective effects on neuronal cells from oxidative stress, apoptosis, and inflammatory responses, thus, improving cognitive dysfunction induced by various brain injury models (Ng et al., 2016; Zhou et al., 2018; Lin et al., 2021). In this research, water extract of Fresh *Gastrodia elata* Blume (FG) was used, which is a new and original form that maintains its original nutritional value compared with the processed form and is commonly used in herbal cuisine (Huang et al., 2021). Moreover, our previous research has proved that FG has great benefits for improving cognitive impairment caused by circadian rhythm disorder and chronic restraint stress in mice, both of which are problems faced by astronauts during spaceflight (Huang et al., 2021; Huang et al., 2022). The present study was designed to investigate the effect of FG on cognitive impairment induced by a simulated weightlessness model to explore the potential application value of FG in aerospace medicine.

Materials and methods

Animals

Male ICR mice, weighing 23–25 g, were obtained from Charles River Laboratories, Beijing, China, with Qualified No. SCXK 2012-0001. All mice were housed, with a maximum of five mice per cage and a 12:12 h light/dark cycle (lights on at 8:00 a.m.). The room temperature and humidity condition were maintained at 23°C ± 2°C and 55% ± 10%. Before experiments, mice were adapted to the environment for 7 days, and all the behavioral experiments were conducted during the light phase. The animals were divided into two batches for testing different behavioral experiments, respectively, with twelve animals in each group. The protocol described in the present study was approved by the committee for the Care and Use of Laboratory Animals of the Institute of Medicinal Plant Development, Beijing, China, (NO. 20161028).

Drugs

The fresh *Gastrodia elata* Blume tuber used in this experiment was purchased from its authentic origin—Jinkouhe, Sichuan Province, China, and identified as the tuber of *Gastrodia elata* Blume by Guanghua Lu, professor at Chengdu University of Traditional Chinese Medicine, Chengdu, China. The manufacturing process of the FG sample is consistent with previous literature and the content of GAS and HBA in FG has been determined with the HPLC chromatogram of the reference material published (Huang et al., 2021; Huang et al., 2022). After being crushed by the high-speed blender, we collected the filtrate and washed the filter residue with purified water to ensure complete extraction. The collected liquid was freeze-dried and refrigerated at −20°C for later use. Donepezil hydrochloride (DNP [Aricept], Eisai Inc. [Ibaraki, Japan]) was used as a positive control.

Treatment

Animals were randomly divided into five groups, namely, the control group, model group, positive drug group (Donepezil, 1.6 mg/kg), FG low-dose group (0.5 g/kg), and high-dose group (1.0 g/kg). The dose of Donepezil was determined by previous literature (Yang et al., 2020), and the doses of FG were according to our preliminary experiments and literature reports (Huang et al., 2021; Huang et al., 2022). Oral administration was at a volume of 20 mL/kg and started at the same time as the modeling. Drugs were formulated into corresponding concentration liquids with distilled water according to the above-mentioned dosages. The control group and model group were given corresponding volumes of distilled water. Modeling and drug administration continued until the end of behavioral testing (Figure 1A).

Hindlimb unloading procedures (HU)

A simulated weightlessness apparatus was developed to keep the hindlimb of mice off the ground with the body at a 25°–30° angle for a long time, allowing free access to water and food (Chinese patent No. 201310228949.2). Briefly, mice were placed in a 26 cm × 26 cm × 30 cm black plexiglass box with their tails bound by medical adhesive tape and hung with a small hook in a stainless chain mounted at the top of the cage. Mice were isolated from each other and allowed free access to water and food. The animals remained tail-suspended for 28-day modeling except for daily drug administration.

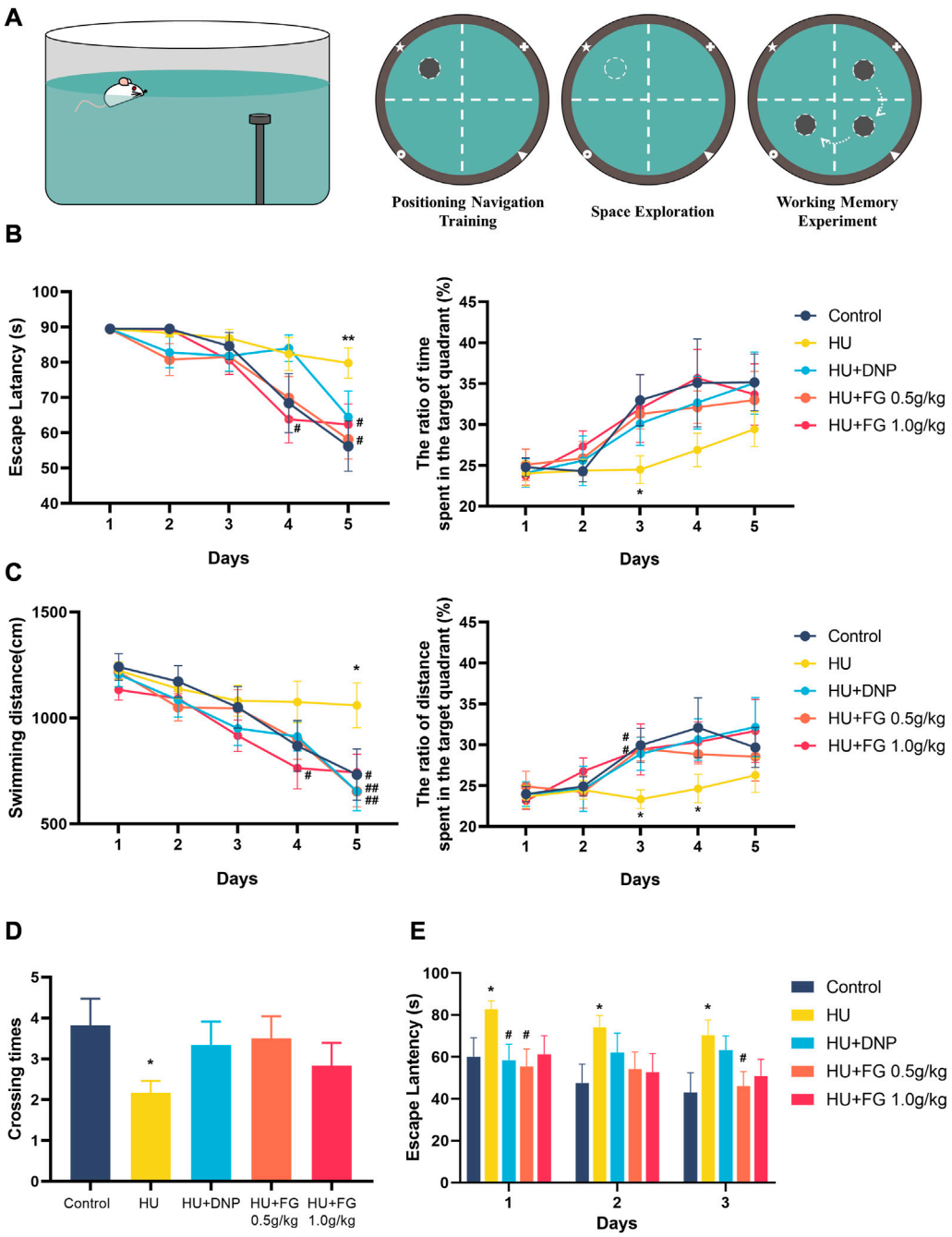

FIGURE 2
The effect of FG on Morris Water Maze test. **(A)** Schematic diagrams of MWMT. **(B)** The escape latency and the ratio of time spent in the target quadrant during the positioning navigation training session. **(C)** The swimming distance and the ratio of distance spent in the target quadrant during the positioning navigation training session. **(D)** The crossing times in the space exploration session. **(E)** The escape latency in the working memory experiment. Data were expressed as mean ± SEM (n = 10–12 per group). $^{*}p < 0.05$ and $^{**}p < 0.01$ versus the control group; $^{\#}p < 0.05$ and $^{\#\#}p < 0.01$ versus the HU group.

Behavioral tests

Object location recognition test, OLRT

The animals were allowed to explore the experimental test box (45 L × 45 W × 30 H cm) once a day (10 min for each session) for a 3-day adaptation period before familiarization period and testing period were operated. Two identical objects were put in a symmetrical position on one side of the chamber, allowing animals to explore for 5 min. After a 30-min intersession interval, one of the familiar objects was moved to the contralateral position. To avoid biasing the experimental results due to the animal's position preference, the familiar position and the new position were in balance during the test period. The memory ability of animals is evaluated by the discrimination index (DI). The

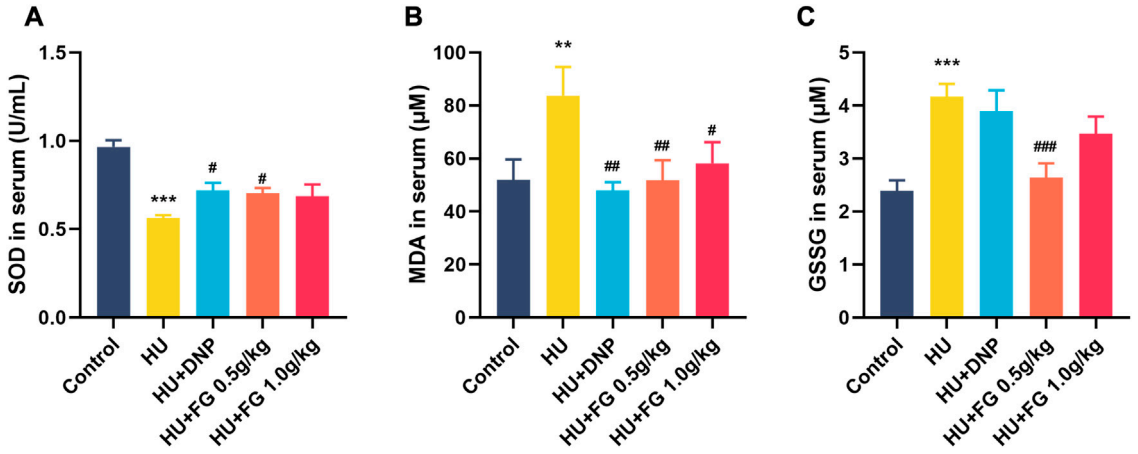

FIGURE 3
The effect of FG on oxidative stress in the serum. **(A)** The level of SOD. **(B)** The level of MDA. **(C)** The level of GSSG. Data were expressed as mean ± SEM (n = 8–9 per group). $^{**}p < 0.01$ and $^{***}p < 0.001$ versus the control group; $^{\#}p < 0.05$, $^{\#\#}p < 0.01$, and $^{\#\#\#}p < 0.001$ versus the HU group.

calculation formula is DI = $(T_N)/(T_N + T_F) \times 100\%$. T_N (new) and T_F (familiar) means the exploration time of an object in the new position and the exploration time of an object in the familiar position objects, respectively.

Step-down Test

Step-Down Test is a memory evaluation method based on the punishment principle. On the first day of the acquisition experiment, the animals acclimated for 3 min in the chamber (20 L × 12 W cm), and then the electric grid at the bottom of the chamber gave a continuous current of 0.3 mA for 5 min. Animals can escape the shock by jumping onto an insulated platform located on one side of the chamber. A retention test was conducted after 24 h lasting 5 min. Animals were placed on the insulated platform, and the power grid was immediately energized. The latency and total error times of the animals jumping off the platform were recorded.

Morris water maze test

The experiment is divided into three stages: the positioning navigation training session, the space exploration session, and the working memory experiment. In the 5-day positioning navigation training, the animals were put into the pool (120 D × 40 H cm) from different quadrants twice a day and the fixed platform was hidden 1.5 cm below the water surface. The space exploration test was carried out on the sixth day, in which the platform was removed. In the working memory experiment, the platform was placed and moved into adjacent quadrants sequentially and carried out for 3 days to test the working memory of animals.

Biochemical Analysis

Preparation of serum and brain samples

All mice were sacrificed the day after the last behavioral tests to collect the biological samples. Blood was collected from the ophthalmic veins and stood at 4°C overnight to obtain the serum. Three mice were randomly selected and transcardially perfused for Nissl staining. The hippocampi were dissected on ice and stored at −80°C until analysis.

Determination of biochemical parameters

The levels of SOD, MDA, and GSSG in the serum were detected using commercial kits from Beyotime (Shanghai, China) according to the manufacturer's protocols. The levels of TNF-α, IFN-γ, IL-4, IL-6, IL-10, and Arg-1 of the hippocampal were determined by commercial enzyme-linked immunosorbent assay (ELISA) kits from Dakewe Biotech (Shenzhen, China) according to the manufacturer's protocols.

Western blotting analysis

The hippocampus was homogenized in protein lysis buffer (Solarbio, China) and fully lysed for 30 min. After centrifuging (12 000 g, 4°C, and 30 min), the supernatant was taken. The protein concentration was detected by BCA protein assay kits (CWBIO, China) and was prepared to 5 μg/μL protein solution with the lysate solution and SDS PAGE loading buffer (×5) for use. Proteins were separated by SDS PAGE, transferred onto PVDF membrane (Merck Millipore, Germany), and then blocked with 5% non-fat milk with Tris Buffered Saline Tween (TBST) for 1.5 h at room temperature. The membranes were incubated with primary antibodies: NLRP3 (1:1,000, Abcam, United Kingdom, #ab263899), NF-κB p65 (1:1,000, Abcam, United Kingdom, #ab19870), BAX (1:1,000, Abcam, United Kingdom, #ab32503), Cyt C (1:1,000, Abcam, United Kingdom, #ab133504), Drp 1, (1:1,000, Abcam, United Kingdom, #ab184247), PI3K (1:1,000, ABclonal, CN, #A19742), AKT (1:1,000, Cell Signaling, United States, #4685); mTOR (1:1,000, Abcam, United Kingdom, #ab32028), SYP (1:1,000, Abcam, United Kingdom, #ab32127), TrkB (1:1,000, Abcam, United Kingdom, #ab187041), and GAPDH (1:1,000, ABclonal, CN, #A19056) at 4°C overnight followed by incubation with HRP-conjugated secondary antibody for 1.5 h at room temperature. The protein bands were visualized by the BeyoECL Moon kit (Beyotime, China). The gray values of band density were analyzed using the Image J software.

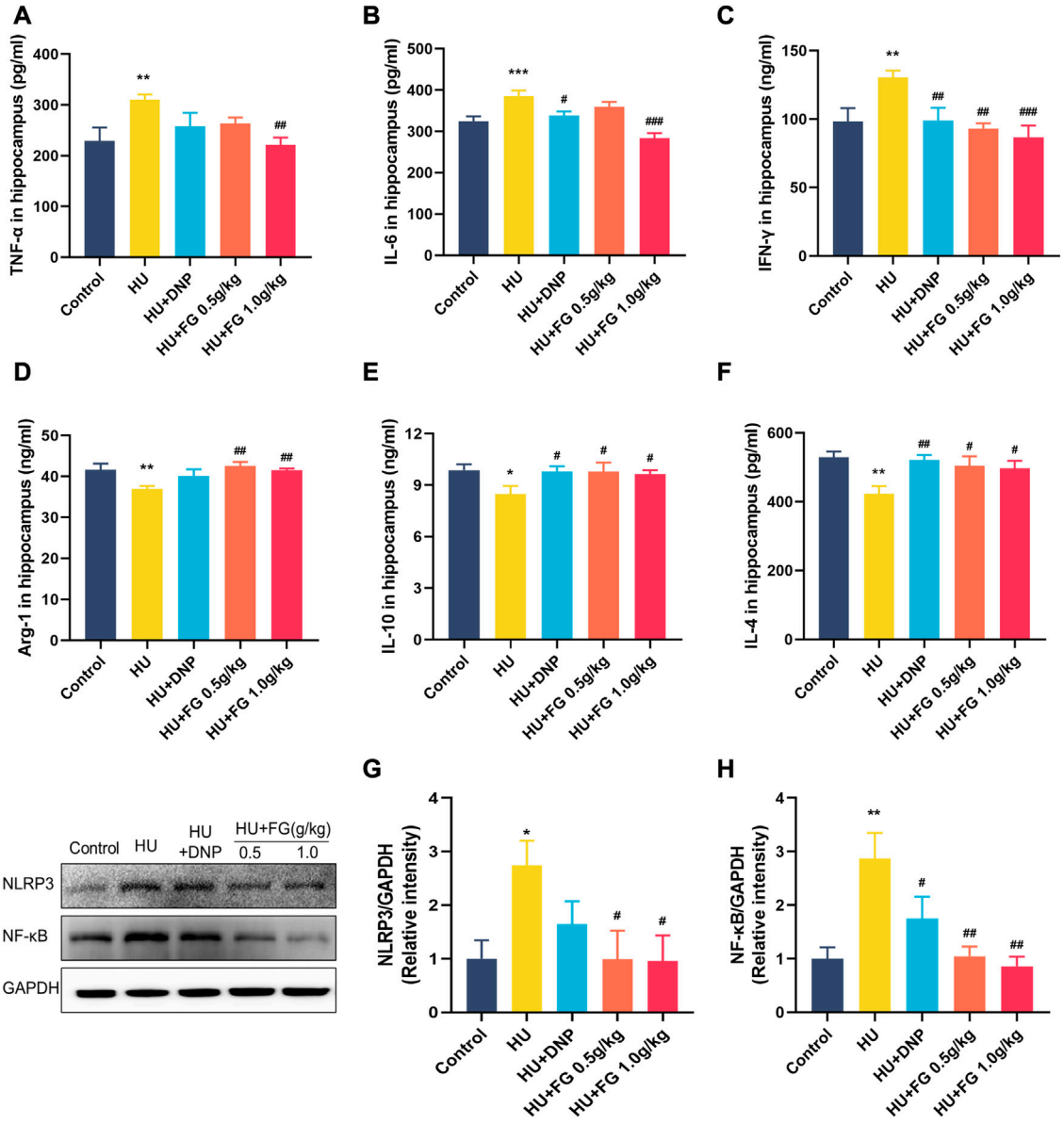

FIGURE 4
The effect of FG on inflammatory response in the hippocampus. **(A–F)** The levels of TNF-α, IL-6, INF-γ, Arg-1, IL-10, and IL-4 (n = 8–9). **(G, H)** The protein expression of NLRP3 and NF-κB (n = 3). Data were expressed as mean ± SEM. $^{*}p < 0.05$ and $^{**}p < 0.01$ versus the control group; $^{\#}p < .05$, $^{\#\#}p < 0.01$, and $^{\#\#\#}p < 0.001$ versus the HU group.

Nissl's staining

Three paraffin sections in each group were dewaxed in xylene and rehydrated with graded ethanol (70, 95, and 100%), followed by rehydration with distilled water. Staining was performed according to the Nissl staining kit (Jiancheng Biology, China). The images were obtained using a microscope slide scanner (Pannoramic 250, 3D Histech Ltd., Hungary) and the quantification of integrated optical density (IOD) of Nissl bodies in each group was analyzed with the NIH Image J Pro software (Media Cybernetics, United States).

Neurotransmitter detection

The neurotransmitter analysis method was performed as previously described but with minor modifications (Wang et al., 2019). A measurement of 2 μL of the prepared sample was taken for LC-MS/MS analysis. Glu and GABA in the hippocampus were detected by prominence ultrafast liquid chromatography (UFLC) (Shimadzu, Kyoto, Japan) coupled with a QTRAP 5500 mass spectrometer (AB SCIEX, Framingham, MA, United States). The metabolites were separated using the Restek Ultra Aqueous C18 column (100 mm × 2.1 mm, 3 μm, Bellefonte, PA, United States). Gradient elution was performed using 0.1% formic acid and acetonitrile as flow at a rate of 0.4 mL per minute.

Statistical analysis

The experimental results were analyzed by the SPSS 21.0 software and performed by the ImageJ and GraphPad Prism Software 5.0.

Differences among normally distributed values were analyzed by one-way ANOVA, and LSD was used for the post-test. The Mann-Whitney *U* test was performed to investigate whether the data unfollowed a normal distribution. Data were expressed by mean ± SEM, and it was considered to have a significant difference when $p < 0.05$.

Result

FG ameliorated the HS-induced weight loss in mice

The animals were randomly divided into groups with similar weights at the beginning of the experiment and the animals were weighed weekly (Figure 1B). During the hindlimb suspension paradigm, the model group displayed a prominent weight loss ($F(4,55) = 8.987$, $p < 0.001$). Both the low and high doses (0.5 g/kg and 1.0 g/kg) of FG groups showed significant weight increase in the second week of HU modeling compared with the model group, while DNP administration did not show weight gain effect ($F(4,55) = 4.113$, $p < 0.05$, and $p < 0.05$ in FG low and high dose group, respectively, $p < 0.05$ in DNP group).

FG improved the HU-induced position discrimination impairment in the object location recognition test

In the familiarization session, mice showed no preference for any object, while in the test session, the model group showed a significant decrease in the discrimination index compared with the control group (Figures 1C–E) ($F(4,50) = 5.615$, $p < 0.001$), indicating that the HU modeling-induced mice spent less time exploring the object in the new position than in the old position. DNP treatment increased the relative discrimination index with no significance ($p < 0.05$). A high dose of FG treatment (1.0 g/kg) showed significant improvement in ameliorating the impaired memory ability ($p < 0.01$, $p < 0.001$).

FG improved the HU-induced memory impairment in the step-down test

In the consolidation stage, compared with the control group, the latency of the HU group was significantly shortened ($p < 0.01$). The DNP group and the high dose (1.0 g/kg) of the FG group showed a significant trend of prolonging the error latency ($p < 0.05$, $p < 0.05$). In addition, compared with the control group, the times of errors in the model group tended to increase, and the number of errors in the administration group was less than that in the model group (Figures 1F, G).

FG improved the HU-induced spatial and working learning memory impairment in the Morris Water Maze test

In the positioning navigation training, the HU group had a longer latency and swimming distance for seeking the platform, and there was a significant difference on the fifth day compared with the control group ($F(4,54) = 2.332$, $p < 0.01$; $F(4,54) = 3.118$, $p < 0.05$). On the last day of training, both low and high doses (0.5 g/kg and 1.0 g/kg) of FG treatment shortened escape latency ($p < 0.05$ and $p < 0.05$) and swimming distance ($p < 0.05$ and $p < 0.05$). The DNP group also showed a reverse effect but only significantly shortened swimming distance ($p < 0.05$). In addition, the ratio of time and swim distance spent in the target quadrant (where the platform is located) in the HU group was significantly lower than that in the control group ($F(4,54) = 1.397$, $p < 0.05$, and $F(4,54) = 1.770$ of the ratio of time and distance, respectively, on the third day; $F(4,53) = 1.385$ of the ratio of the distance on the fourth day). This impairment was ameliorated by DNP and FG treatment, and on the third day, both low and high doses (0.5 g/kg and 1.0 g/kg) of FG groups showed a significant improvement effect ($p < 0.05$, $p < 0.05$). In the stage of the space exploration experiment, the number of crossing times in the model group was significantly lower than that in the control group ($F(4,54) = 1.428$, $p < 0.05$). The crossing times in the DNP group and the low and high-dose FG groups showed a higher trend than that in the HU group. During the working memory experiment, the escape latency of the HU group was significantly longer than that in the control group ($F(4,52) = 2.117$, $p < 0.05$ on the first day; $F(4,52) = 1.576$, $p < 0.05$ on the second day; and $F(4,53) = 2.278$ on the last day). The latency of the DNP group decreased significantly on the first day ($p < 0.05$) and the latency of the FG low dose 0.5 g/kg) group decreased significantly on both the first and last days ($p < 0.05$, $p < 0.05$). The others showed a shorter escape latency with no significance (Figure 2).

FG alleviated oxidative stress in the serum induced by HU

In the serum (Figure 3), the production of SOD decreased ($F(4,37) = 11.432$, $p < 0.001$) and MDA and GSSG increased ($F(4,36) = 3.665$, $p < 0.01$ in MDA; $F(4,35) = 7.312$, $p < 0.001$ in GSSG) in HU group. The administration of low-dose FG could significantly reverse the abnormal changes ($p < 0.05$ in SOD, $p < 0.01$ in MDA, and $p < 0.001$ in GSSG). DNP and the high dose FG could also ameliorate the oxidative stress with significance ($p < 0.05$ in SOD and $p < 0.01$ in SOD of the DNP group and $p < 0.05$ in the MDA of the high dose FG group).

FG reduced inflammatory response in the hippocampus and reversed the upregulation of NF-κB/NLRP3 pathways induced by HU

The expressions of three pro-inflammatory factors including TNF-α, IL-6, and IFN-γ were significantly increased in the HU group compared with the control group ($F(4,36) = 3.184$, $p < 0.01$; $F(4,36) = 10.288$, $p < 0.001$; $F(4,37) = 4.825$, $p < 0.01$). The DNP administration significantly reversed the increase of IL-6 and IFN-γ ($p < 0.05$; $p < 0.01$). FG high-dose group showed a significant decrease of TNF-α, IL-6, and IFN-γ ($p < 0.01$; $p < 0.001$; $p < 0.01$), while the low-dose FG group could decrease them as well but only showed a significant difference in the level of IFN-γ ($p < 0.01$) (Figures 4A-C).

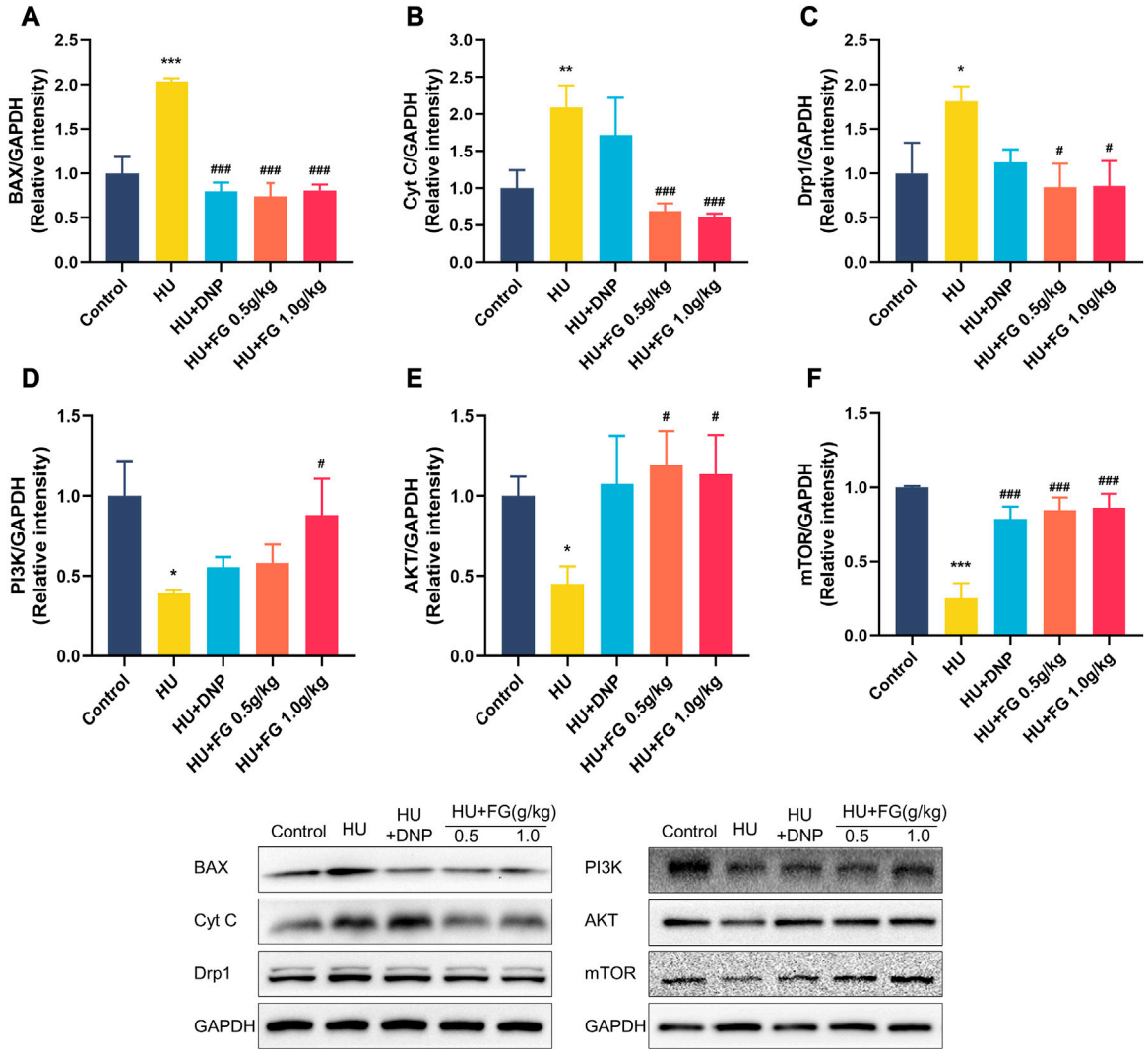

FIGURE 5
The effect of FG on the anti-apoptotic in the hippocampus. **(A–F)** The protein expression of BAX, Cyt C, Drp1 AKT, PI3K, and mTOR (n = 3). Data were expressed as mean ± SEM. *$p < 0.05$, **$p < 0.01$, and ***$p < 0.001$ versus the control group; $^{\#}p < 0.05$, $^{\#\#}p < 0.01$, and $^{\#\#\#}p < 0.001$ versus the HU group.

To better explore the effect of FG on the inflammatory response, we measured the levels of anti-inflammatory factors in the hippocampus (Figures 4D-F). The results showed that the levels of Arg-1, IL-10, and IL-4 of the model group were significantly reduced compared with the control group ($F(4,37) = 3.707$, $p < 0.01$; $F(4,37) = 2.250$, $p < 0.05$; $F(4,35) = 3.898$, $p < 0.01$). The administration of DNP significantly increased the levels of IL-10 and IL-4 in the hippocampus ($p < 0.05$; $p < 0.01$), and both low and high doses of FG administration could significantly increase the levels of Arg-1, IL-10, and IL-4 in the hippocampus of mice ($p < 0.01$, $p < 0.05$, and $p < 0.05$ of FG at low dose; $p < 0.01$, $p < 0.05$, and $p < 0.05$ of FG at high dose).

Moreover, to determine the causes of inflammation, the protein expressions of NLRP3 and NF-κB in the hippocampus were measured (Figures 4G-H). The levels of NF-κB and NLRP3 in the hippocampus increased significantly after HU ($p < 0.05$ and $p < 0.01$) and both could be decreased by DNP ($p < 0.05$ in NF-κB) and FG administration ($p < 0.05$ in NLRP3 and $p < 0.01$ in NF-κB).

FG prevents apoptosis in the hippocampus induced by HU and upregulates the PI3K/AKT signaling pathway

In the HU group, the levels of BAX, Cyt C, and Drp1 in the hippocampus were significantly increased (Figures 5A–C; $p < 0.001$, $p < 0.01$, and $p < 0.05$), while treatment with DNP decreased the level of BAX ($p < 0.001$) and FG (0.5 g/kg and 1.0 g/kg) substantially decressed these apoptosis-related proteins ($p < 0.001$, $p < 0.001$, and $p < 0.05$). Figures 5D–F showed the reduced levels of AKT, PI3K, and mTOR in the HU group ($p < 0.05$, $p < 0.05$, and $p < 0.001$), and this reduction could be reversed to varying degrees by the

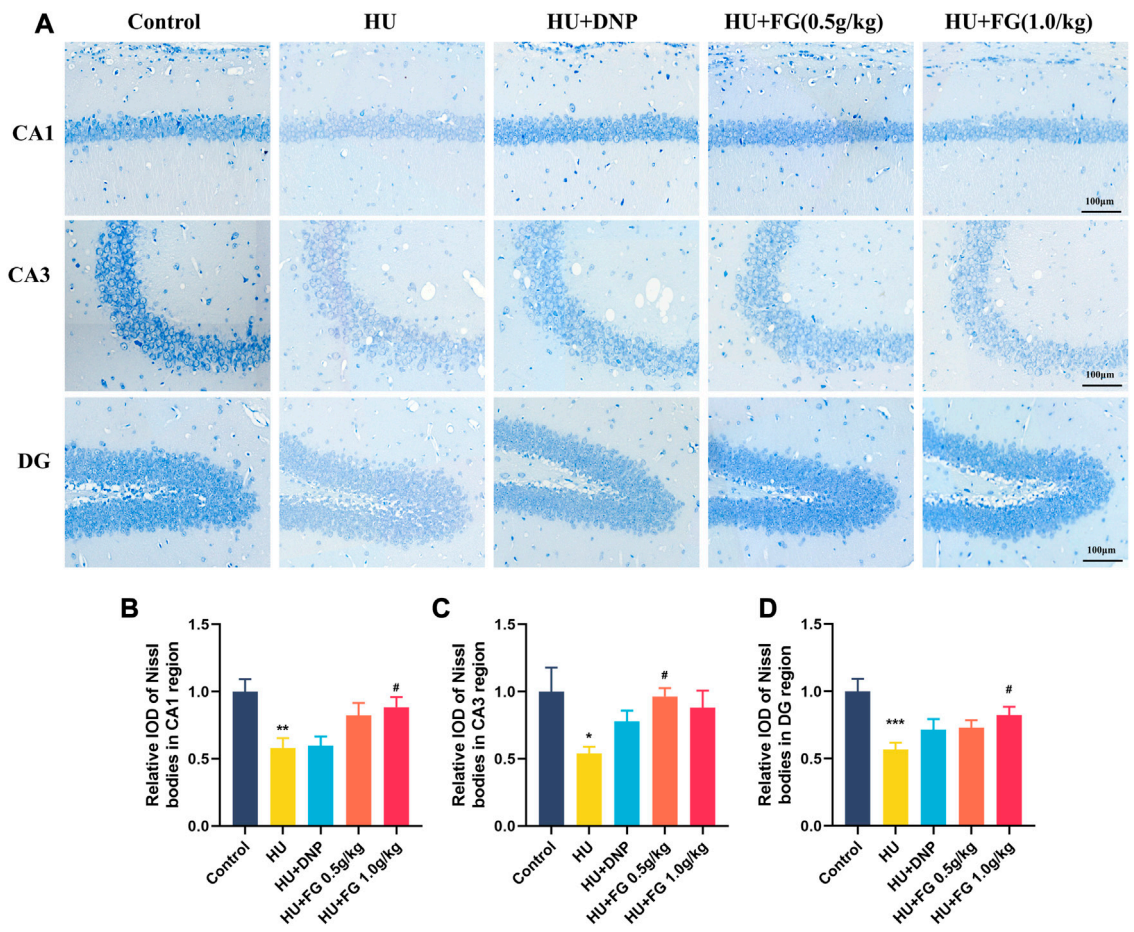

FIGURE 6
The effect of GRe on the morphological damage to neurons in mice with HU-induced memory impairment. **(A)**The representative Nissl staining photomicrographs of hippocampal CA1, CA3, and DG regions. **(B–D)** The histograms represent the relative IOD values of the Nissl bodies of hippocampal CA1, CA3, and DG regions (n = 3). Data were expressed as mean ± SEM. *$p < 0.05$, **$p < 0.01$, and ***$p < 0.001$ versus the control group; $^{\#}p < 0.05$ versus the HU group.

administration of DNP ($p < 0.001$ in mTOR), FG low dose ($p < 0.05$ in AKT; $p < 0.001$ in mTOR), and FG high dose ($p < 0.05$ in PI3K, $p < 0.05$ in AKT, and $p < 0.001$ in mTOR).

FG improved the hippocampus neuron loss induced by HU

Since the activation of inflammatory and apoptosis-related factors affects the survival of neurons, neuronal damage was next observed by Nissl's staining. Figure 6 showed that in the CA1, CA3, and DG subregions of the hippocampus, the Nissl bodies in the control group were clearly stained, and the neurons were abundant and orderly arranged. However, the HS group showed obvious cell loss and loose cell arrangement ($p < 0.01$, $p < 0.05$, and $p < 0.001$ in CA1, CA3, and DG, respectively). While the administration of FG (both low and high doses) could alleviate the neuron loss that occurred in the HU group ($p < 0.05$ and $p < 0.05$ of FG at a high dose in CA1 and DG; $p < 0.05$ of FG at low dose in CA3).

FG improved synaptic plasticity and maintained the imbalance of GABA/Glu in the hippocampal induced by HU

Figure 7 showed that the expression of SYP and TrkB in the HU group was significantly reduced ($p < 0.01$ and $p < 0.001$), while the DNP and FG (both low and high dose) administration could significantly reverse these reductions ($p < 0.01$ and $p < 0.001$). The level of Glu in the HU group was significantly increased ($F(4,35) = 6.603$, $p < 0.01$) and affected the balance of GABA/GLU ($F(4,35) = 9.749$, $p < 0.001$). After administration of DNP and FG (both low and high doses), the abnormal increase of Glu and the GABA/Glu ratio was reversed ($p < 0.001$ and $p < 0.05$).

Discussion

In the present study, we identified the cognitive improvement effect of the fresh *Gastrodia elata* Blume (FG), which alleviated hindlimb unloading (HU) and induced spatial and working cognitive

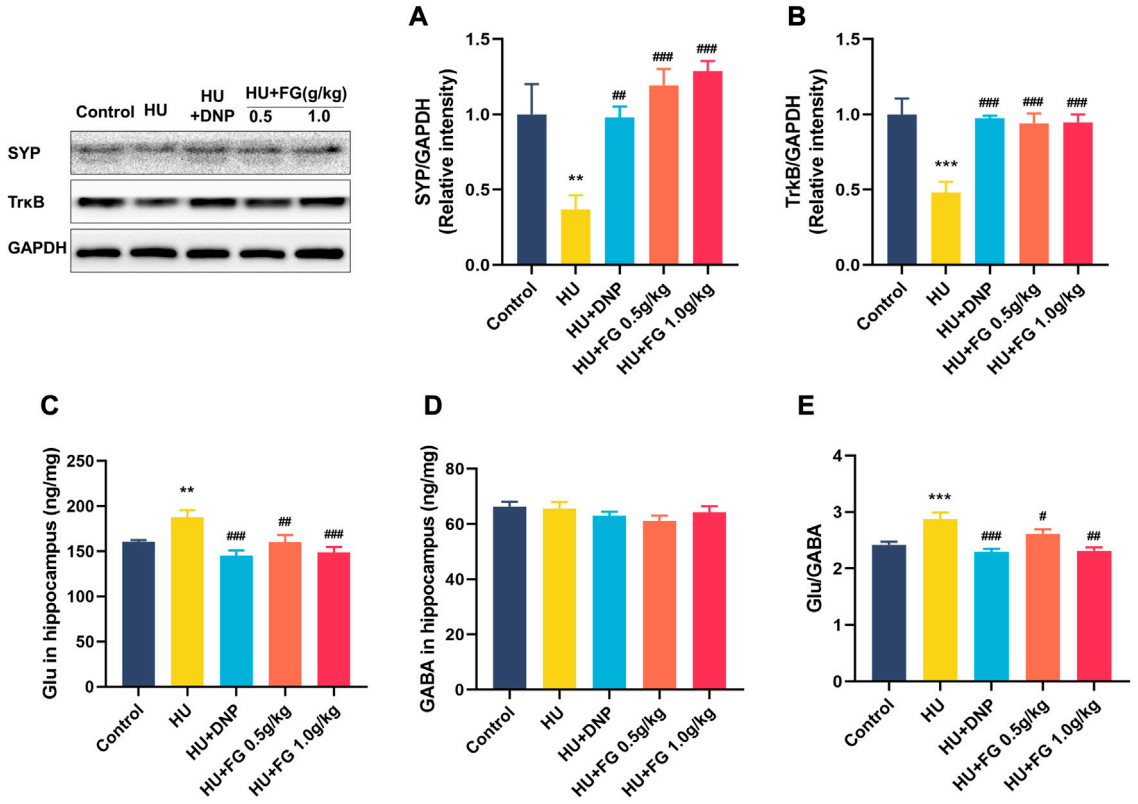

FIGURE 7
The effect of FG on the anti-apoptotic effect and maintaining the stability of neurotransmitters in the hippocampus. **(A)** The protein expression of SYP and **(B)**TrkB (n = 3). **(C)** The levels of Glu and **(D)** GABA. **(E)** The ratio of Glu/GABA (n = 8–9). Data were expressed as mean ± SEM. $^{**}p < 0.01$ and $^{***}p < 0.001$ versus the control group; $^{\#}p < 0.05$, $^{\#\#}p < 0.01$, and $^{\#\#\#}p < 0.001$ versus the HU group.

dysfunction in mice. Specifically, FG improved the performance of mice in the object location recognition test (OLRT), Step-Down test (SDT), and Morris Water Maze test (MWMT). In biochemical experiments, we found that being given FG, the oxidative stress in the serum and neuroinflammatory response in the hippocampus induced by HU were suppressed. Meanwhile, the hippocampal apoptosis-related proteins decreased with the administration of FG, which may be mediated by the upregulation of the PI3K/AKT signaling pathway. In addition, it is also found that FG played a role in improving synaptic plasticity and neurotransmitter transmission.

Gastrodia elata Blume belongs to the genus Gastrodia in the orchid family. In modern pharmacological research, it is known as a popular traditional medicine for the treatment of neurological diseases including headache, dizziness, Alzheimer's disease and Parkinson's disease, and so on, and for its distinguished neuroprotective effect (Lu et al., 2022). The application of fresh *Gastrodia elata* was first seen in the *Shennong Herbal Classic*, which is also a common edible or medicinal form for the public (Huang et al., 2022); whereas, the main research form of *Gastrodia elata* Blume is generally processed products, and the application of fresh *Gastrodia elata* Blume (FG) is less. In this research, FG is obtained from the expressed juice of fresh *Gastrodia elata* Blume and is filtered, freeze-dried, and stored as powder until used. Our previous studies have proved the remarkable effect of FG in improving cognitive impairment caused by chronic stress, including circadian rhythm disorder and restraint (Huang et al., 2021; Huang et al., 2022). Together with weightlessness, all these are characteristic of the extreme environments that astronauts are faced with during spaceflight. Therefore, it is of great meaning to study the protective effect of FG on cognitive impairment caused by stimulated weightlessness, which not only provides scientific evidence for FG to ameliorate cognitive dysfunction in special space environment but also enriches the application of *Gastrodia elata* Blum as a health product.

HU is a classic animal model simulating microgravity on Earth to study aerospace medicine. The present work shows that after 28 days of HU modeling, the short-term and long-term memory of animals is weakened. OLRT has been used extensively to detect short-term spatial memory (Arbogast et al., 2019). The perception ability of mice to the new place of the object declined, as evidenced by decreased discrimination index. In SDT, animals would actively escape to the insulated platform to avoid injuries after learning that electrical stimulation continuously exists on the ground (Hiramatsu et al., 1995). As evidenced by the decline in escape latency and error times, the HU group showed a weakened short-term spatial memory in passive conditions. In MWMT, a classic spatial learning and memory testing method, animals can only rely on spatial reference to find the location of the platform which is hidden in a fixed position under the water surface (Morris, 1984). In the positioning navigation training, mice in the HU group escaping from the aversive water displayed increased escape latency, swimming distance, and the ratio of

both time and distance spent in the target quadrant, indicating that an impairment occurred to the mice in their learning and memory abilities. At the stage of the space exploration experiment, the platform originally fixed in the target quadrant was removed, and the trained animals were expected to pass through the positions where the platform originally existed. Similarly, the cognitive impairment in the HU group was verified by the reduction of crossing times. In the working memory experiment, the platform originally fixed in the first quadrant was moved into the adjacent quadrant to detect the working memory of mice, and the prolonged escape latency showed that the working ability of mice was damaged by HU modeling. The above results suggested that HU could cause cognitive impairment in mice, which were consistent with the results reported in previous studies (Sun et al., 2009; Zhang et al., 2018; Li et al., 2021). The behavior deficits were corrected by the administration of FG (both 0.5 g/kg and 1.0 kg/kg), which indicated FG's beneficial effects on HU-induced cognitive impairment of mice.

Oxidative stress injury occurs when people suffered from exogenous acute or chronic stress, leading to cell dysfunction and apoptosis (Rohleder, 2019; Forman and Zhang, 2021; Xue et al., 2022). The level of oxidative stress-related markers in the serum is found to be altered in the serum of patients with memory impairment (Du et al., 2019; Torres et al., 2021). Studies have proved that the indicators related to oxidative stress were changed in the serum of astronauts including the peroxide oxidation of lipids (POL), oxidized low-density lipoprotein (ox-LDL), and so on (Markin et al., 1997; Lee et al., 2020). In rodent experiments in space and on earth, antioxidant defense genes such as Ehd2 and oxidative stress-related biomarkers such as superoxide dismutase (SOD) and malondialdehyde (MDA) changed significantly (Mao et al., 2014; Moustafa, 2021). SOD is the most important enzyme that protects against the damage of reactive oxygen species or free radicals in organisms (Ma et al., 2021). MDA is one of the main products of cell membrane oxidation, which is used as a biomarker of peroxidation (An et al., 2022). The present study found that the HU procedure could reduce the level of antioxidant substances SOD while increasing the level of oxidant substances including MDA and glutathione disulfide (GSSG) in mice serum. GSSG, the oxidized form of glutathione, is a tripeptide thiol antioxidant and plays an important role in cell oxidation and signal transduction (Rahman et al., 2006). The results are consistent with the previous research results, suggesting the reliability of HU modeling, while FG administration reversed these oxidative stress products and thus played an antioxidant role.

Neuroinflammation is closely associated with cognitive impairment in many pathological conditions. Studies have shown that stimulated weightlessness caused neuroinflammation in the brain and led to spatial memory disorder in mice (Qiong et al., 2016). When the body gets injured, microglia rapidly proliferate and activate, releasing a variety of pro-inflammatory factors including TNF- α, IL-6, and INF- γ, etc. (Muhammad et al., 2019), while anti-inflammatory factors such as Arg-1, IL-10, and IL-4 can antagonize inflammatory reactions and inhibit astrocyte activation (Zhang and Wei, 2020; Descalzi, 2021). Astrocytes can release nuclear factor-κB (NF-κB) triggered by inflammatory mediators, which is known as an important transcription factor in inflammation, releasing various pro-inflammatory factors and leading to neuroinflammation in its over-activation situation (Dresselhaus and Meffert, 2019; Gao et al., 2021; Peng et al., 2021). According to our result, FG therapy had the function of maintaining the balance of pro-inflammation and anti-inflammation in the hippocampus by regulating the abnormal changes of the above oxidative stress-related factors. In addition, the expressions of NF-κB and NOD-like receptor protein 3 (NLRP3), both of which are essential drivers of inflammation, were inhibited by FG administration. NLRP3 inflammasome belongs to the NLR family and is the representative component of the innate immune system, which can be activated by NF-κB. Being over-activated, NLRP3 can release inflammatory factors and mediate downstream inflammatory reactions (Jiang et al., 2022). Many studies have shown that the activation of NLRP3 has a close association with cognitive dysfunction that can be attenuated by inhibiting NLRP3 (Ye et al., 2018; Garaschuk, 2021). Inhibiting the NLRP3/NF-κB pathway plays an important role in blocking the occurrence of neuroinflammation caused by stress injury. Therefore, we suggest that FG may play an anti-inflammatory role by inhibiting the activation of NLRP3/NF-κB pathway, thereby reducing HU-induced cognitive impairment.

A notable increase in the level of apoptosis-related proteins in the hippocampus was caused by the hindlimb unloading procedure in the present study. Previous research has proved that apoptosis in the brain occurs after long-term simulated weightlessness and is accompanied by mitochondrial metabolic abnormalities (Nguyen et al., 2021). During cellular stress, the pro-apoptotic protein Bax transfers from the cytoplasm to the membrane of the mitochondria through translocation, thus improving the permeability of the outer membrane of the mitochondria (Spitz et al., 2021). As induced by Bax, Cytochrome C (Cyt C) gets released into the cytoplasm, activating the apoptosis-related cascade reaction and finally leading to programmed cell death (Kulikov et al., 2012). Mitochondria are the main place for providing energy for cells. The abnormal elevation of dynamin-related protein 1 (Drp1), which is an important protein to maintain the balance of mitochondrial fusion and division, was found in neurological diseases, leading to neuronal injury (Feng et al., 2020). Besides, it was found that preventing mitochondrial dysfunction by inhibiting Drp1 could protect neurons from damage caused by oxidative stress (Oliver and Reddy, 2019). This study found that FG can downregulate the levels of Cyt C, Bax, and Drp1 in the hippocampus increased by HU modeling, thus, inhibiting the apoptosis of nerve cells. Moreover, the results showed that HU caused an increase in the levels of phosphatidylinositol3-kinase (PI3K), protein kinase B (AKT), and mammalian target of rapamycin (mTOR) in the hippocampus, and according to the Nissl staining's results, FG therapy improved the arrangement and loss of neurons. PI3K/AKT as a classic signaling pathway plays an essential role in affecting various biological activities including the regulation of cell survival, metabolism and apoptosis, and so on due to its downstream protein participating in the transcription of a large number of genes and protein expression (Ediriweera et al., 2019). When the body receives external stimulation, PI3K phosphorylation is activated and acts on downstream targets, of which AKT is the prominent downstream effector. The activation of this PI3K/AKT pathway brings the increase of apoptosis-related proteins such as Bcl-2, Bax, etc., thus, causing programmed cell death (Wang et al., 2020). Its downstream signal molecule mTOR is considered an important protein in regulating the survival, differentiation, and maturation of neurons, and the upregulation of mTOR is proven to be beneficial to AD pathologies (Van Skike et al., 2020; Shi et al., 2022). In addition,

cell apoptosis can be induced via inhibiting the PI3K/Akt/mTOR pathway (Yang et al., 2018; Chang X. et al., 2021). Taken together, our results demonstrated that the cognitive improvement effect of FG may be achieved through the activation of the PI3K/AKT/mTOR pathway, thus, inhibiting the release of apoptotic proteins and ultimately protecting nerve cells.

An increasing number of studies have proved the connection between synaptic plasticity and cognition (Raven et al., 2018; Santello et al., 2019). Long-term space microgravity environment can affect the main mediators related to brain plasticities such as 5-HT and BDNF (Popova et al., 2020). Synaptophysin (SYP) as a major membrane protein regulates the endocytosis of synaptic vesicles and has an obvious influence on the change of synaptic transmission efficiency (Chang C.-W. et al., 2021). Research has found that SYP decreased and pro-inflammatory factors increased in mice with Alzheimer's disease, and increasing the expression of SYP can ameliorate the impairment of the synaptic transmission effect in cognitive impairment (Liu et al., 2020; Jiang et al., 2021). Tyrosine Kinase receptor B (TrkB) is located in the postsynaptic membrane and is a functional receptor of brain-derived neurotrophic factor (BDNF) (Chen et al., 2021). BDNF needs to be combined with TrkB to activate the intracellular signal transduction pathway, thus, producing corresponding molecules to protect neurons and promote regeneration (Mitre et al., 2022). The present results showed that FG therapy significantly increased the expression of SYP and TrkB. In addition, the abnormal increase of Glu in the hippocampus was suppressed by FG, thus, maintaining the balance of glutamate/GABA. Glutamate and GABA are the main excitatory and inhibitory neurotransmitters, respectively, in the brain, and maintaining their balance assists in the smooth operation of the nervous system (Sood et al., 2021). Previous studies have proved that the abnormal increase of glutamate and the imbalance of glutamate/GABA occurred in the hippocampus of chronic simulated microgravity rats, and this procedure was mediated by presynaptic proteins, which is consistent with our results (Wang et al., 2015). Therefore, we suggest that FG has beneficial effects on improving synaptic plasticity and alleviating the excitatory toxicity of glutamate.

Conclusion

The present study provides evidence for the first time that FG can effectively improve HU-induced cognitive impairment in mice. The cognitive-enhancing effect of FG may be related to the inhibition of NF-κB and NLRP3 to reduce neuroinflammation and the improvement of the PI3K/Akt/mTOR pathway to alleviate neuronal apoptosis. The above results indicate that FG, as a health food, has great therapeutic potential in protecting against cognitive impairment caused by special space environments.

Data availability statement

The raw data supporting the conclusion of this article will be made available by the authors, without undue reservation.

Ethics statement

The animal study was reviewed and approved by the Research Center for Pharmacology and Toxicology, Institute of Medicinal Plant Development (approval no. SYXK 2017-0020).

Author contributions

YZ, HH, and NJ designed the research. HH and CY conducted the experiments. YZ and XS performed the data analysis. YZ wrote and QH, MC, and XL revised this manuscript. XL and NJ supervised the study and contributed to project administration. All authors approved the final version.

Funding

The Innovation Fund for Medical Sciences (CIFMS) (Grant No. 2021-1-I2M-034), the International Cooperative Project of Traditional Chinese Medicine (GZYYG2020023), National Natural Science Foundation of China (Grant No. 81773930), the Space Medical Experiment Project of the China Manned Space Program (Grant No. HYZHXM05003) the all provided funding for this project.

Conflict of interest

The authors declare that the research was conducted in the absence of any commercial or financial relationships that could be construed as a potential conflict of interest.

Publisher's note

All claims expressed in this article are solely those of the authors and do not necessarily represent those of their affiliated organizations, or those of the publisher, the editors and the reviewers. Any product that may be evaluated in this article, or claim that may be made by its manufacturer, is not guaranteed or endorsed by the publisher.

References

An, J.-R., Su, J.-N., Sun, G.-Y., Wang, Q.-F., Fan, Y.-D., Jiang, N., et al. (2022). Liraglutide alleviates cognitive deficit in db/db mice: Involvement in oxidative stress, iron overload, and ferroptosis. *Neurochem. Res.* 47 (2), 279–294. doi:10.1007/s11064-021-03442-7

Arbogast, T., Razaz, P., Ellegood, J., McKinstry, S. U., Erdin, S., Currall, B., et al. (2019). Kctd13-deficient mice display short-term memory impairment and sex-dependent genetic interactions. *Hum. Mol. Genet.* 28 (9), 1474–1486. doi:10.1093/hmg/ddy436

Bock, O., Weigelt, C., and Bloomberg, J. J. (2010). Cognitive demand of human sensorimotor performance during an extended space mission: A dual-task study. *Aviat. Space, Environ. Med.* 81 (9), 819–824. doi:10.3357/asem.2608.2010

Casler, J. G., and Cook, J. R. (1999). Cognitive performance in space and analogous environments. *Int. J. Cognitive Ergonomics* 3 (4), 351–372. doi:10.1207/s15327566ijce0304_5

Chang, C.-W., Hsiao, Y.-T., and Jackson, M. B. (2021). Synaptophysin regulates fusion pores and exocytosis mode in chromaffin cells. *J. Neurosci. Official J. Soc. For Neurosci.* 41 (16), 3563–3578. doi:10.1523/JNEUROSCI.2833-20.2021

Chang, X., Wang, X., Li, J., Shang, M., Niu, S., Zhang, W., et al. (2021). Silver nanoparticles induced cytotoxicity in HT22 cells through autophagy and apoptosis via PI3K/AKT/mTOR signaling pathway. *Ecotoxicol. Environ. Saf.* 208, 111696. doi:10.1016/j.ecoenv.2020.111696

Chen, C., Ahn, E. H., Liu, X., Wang, Z.-H., Luo, S., Liao, J., et al. (2021). Optimized TrkB agonist ameliorates Alzheimer's disease pathologies and improves cognitive functions via inhibiting delta-secretase. *ACS Chem. Neurosci.* 12 (13), 2448–2461. doi:10.1021/acschemneuro.1c00181

Descalzi, G. (2021). Cortical astrocyte-neuronal metabolic coupling emerges as a critical modulator of stress-induced hopelessness. *Neurosci. Bull.* 37 (1), 132–134. doi:10.1007/s12264-020-00559-7

Dresselhaus, E. C., and Meffert, M. K. (2019). Cellular specificity of NF-κB function in the nervous system. *Front. Immunol.* 10, 1043. doi:10.3389/fimmu.2019.01043

Du, L., Ma, J., He, D., and Zhang, X. (2019). Serum ischaemia-modified albumin might be a potential biomarker for oxidative stress in amnestic mild cognitive impairment. *Psychogeriatrics Official J. Jpn. Psychogeriatr. Soc.* 19 (2), 150–156. doi:10.1111/psyg.12377

Ediriweera, M. K., Tennekoon, K. H., and Samarakoon, S. R. (2019). Role of the PI3K/AKT/mTOR signaling pathway in ovarian cancer: Biological and therapeutic significance. *Seminars Cancer Biol.* 59, 147–160. doi:10.1016/j.semcancer.2019.05.012

Fasina, O. B., Wang, J., Mo, J., Osada, H., Ohno, H., Pan, W., et al. (2022). Gastrodin from gastrodia elata enhances cognitive function and neuroprotection of AD mice via the regulation of gut microbiota composition and inhibition of neuron inflammation. *Front. Pharmacol.* 13, 814271. doi:10.3389/fphar.2022.814271

Feng, S.-T., Wang, Z.-Z., Yuan, Y.-H., Wang, X.-L., Sun, H.-M., Chen, N.-H., et al. (2020). Dynamin-related protein 1: A protein critical for mitochondrial fission, mitophagy, and neuronal death in Parkinson's disease. *Pharmacol. Res.* 151, 104553. doi:10.1016/j.phrs.2019.104553

Forman, H. J., and Zhang, H. (2021). Targeting oxidative stress in disease: Promise and limitations of antioxidant therapy. *Nat. Rev. Drug Discov.* 20 (9), 689–709. doi:10.1038/s41573-021-00233-1

Fowler, B., Comfort, D., and Bock, O. (2000). A review of cognitive and perceptual-motor performance in space. *Aviat. Space, Environ. Med.* 71 (9), A66–A68.

Gao, W., Ning, Y., Peng, Y., Tang, X., Zhong, S., and Zeng, H. (2021). LncRNA NKILA relieves astrocyte inflammation and neuronal oxidative stress after cerebral ischemia/reperfusion by inhibiting the NF-κB pathway. *Mol. Immunol.* 139, 32–41. doi:10.1016/j.molimm.2021.08.002

Garaschuk, O. (2021). The role of NLRP3 inflammasome for microglial response to peripheral inflammation. *Neural Regen. Res.* 16 (2), 294–295. doi:10.4103/1673-5374.290889

Globus, R. K., and Morey-Holton, E. (2016). Hindlimb unloading: Rodent analog for microgravity. *J. Appl. Physiology* 120 (10), 1196–1206. doi:10.1152/japplphysiol.00997.2015

Hiramatsu, M., Sasaki, M., and Kameyama, T. (1995). Effects of dynorphin A-(1-13) on carbon monoxide-induced delayed amnesia in mice studied in a step-down type passive avoidance task. *Eur. J. Pharmacol.* 282 (1-3), 185–191. doi:10.1016/0014-2999(95)00330-n

Homick, J. L., Delaney, P., and Rodda, K. (1998). Overview of the neurolab spacelab mission. *Acta Astronaut.* 42 (1-8), 69–87. doi:10.1016/s0094-5765(98)00107-6

Huang, H., Jiang, N., Zhang, Y. W., Lv, J. W., Wang, H. X., Lu, C., et al. (2021). Gastrodia elata blume ameliorates circadian rhythm disorder-induced mice memory impairment. *Life Sci. Space Res. (Amst)* 31, 51–58. doi:10.1016/j.lssr.2021.07.004

Huang, H., Zhang, Y., Yao, C., He, Q., Chen, F., Yu, H., et al. (2022). The effects of fresh Gastrodia elata Blume on the cognitive deficits induced by chronic restraint stress. *Front. Pharmacol.* 13, 890330. doi:10.3389/fphar.2022.890330

Jiang, N., Zhang, Y., Yao, C., Huang, H., Wang, Q., Huang, S., et al. (2022). Ginsenosides Rb1 attenuates chronic social defeat stress-induced depressive behavior via regulation of SIRT1-NLRP3/nrf2 pathways. *Front. Nutr.* 9, 868833. doi:10.3389/fnut.2022.868833

Jiang, Y., Li, K., Li, X., Xu, L., and Yang, Z. (2021). Sodium butyrate ameliorates the impairment of synaptic plasticity by inhibiting the neuroinflammation in 5XFAD mice. *Chemico-biological Interact.* 341, 109452. doi:10.1016/j.cbi.2021.109452

Kulikov, A. V., Shilov, E. S., Mufazalov, I. A., Gogvadze, V., Nedospasov, S. A., and Zhivotovsky, B. (2012). Cytochrome c: The achilles' heel in apoptosis. *Cell. Mol. Life Sci. CMLS* 69 (11), 1787–1797. doi:10.1007/s00018-011-0895-z

Lee, S. M. C., Ribeiro, L. C., Martin, D. S., Zwart, S. R., Feiveson, A. H., Laurie, S. S., et al. (2020). Arterial structure and function during and after long-duration spaceflight. *J. Appl. Physiology* 129 (1), 108–123. doi:10.1152/japplphysiol.00550.2019

Li, Q., Yan, J., Liao, J., Zhang, X., Liu, L., Fu, X., et al. (2021). Distinct effects of social stress on working memory in obsessive-compulsive disorder. *Neurosci. Bull.* 37 (1), 81–93. doi:10.1007/s12264-020-00579-3

Lin, Y. E., Lin, C. H., Ho, E. P., Ke, Y. C., Petridi, S., Elliott, C. J., et al. (2021). Glial Nrf2 signaling mediates the neuroprotection exerted by Gastrodia elata Blume in Lrrk2-G2019S Parkinson's disease. *Elife* 10, e73753. doi:10.7554/eLife.73753

Liu, B., Kou, J., Li, F., Huo, D., Xu, J., Zhou, X., et al. (2020). Lemon essential oil ameliorates age-associated cognitive dysfunction via modulating hippocampal synaptic density and inhibiting acetylcholinesterase. *Aging* 12 (9), 8622–8639. doi:10.18632/aging.103179

Lu, C., Qu, S., Zhong, Z., Luo, H., Lei, S. S., Zhong, H.-J., et al. (2022). The effects of bioactive components from the rhizome of gastrodia elata blume (Tianma) on the characteristics of Parkinson's disease. *Front. Pharmacol.* 13, 963327. doi:10.3389/fphar.2022.963327

Lv, J., Jiang, N., Wang, H., Huang, H., Bao, Y., Chen, Y., et al. (2021). Simulated weightlessness induces cognitive changes in rats illustrated by performance in operant conditioning tasks. *Life Sci. Space Res.* 29, 63–71. doi:10.1016/j.lssr.2021.03.004

Ma, X., Song, M., Yan, Y., Ren, G., Hou, J., Qin, G., et al. (2021). Albiflorin alleviates cognitive dysfunction in STZ-induced rats. *Aging* 13 (14), 18287–18297. doi:10.18632/aging.203274

Mao, X. N., Zhou, H. J., Yang, X. J., Zhao, L. X., Kuang, X., Chen, C., et al. (2017). Neuroprotective effect of a novel gastrodin derivative against ischemic brain injury: Involvement of peroxiredoxin and TLR4 signaling inhibition. *Oncotarget* 8 (53), 90979–90995. doi:10.18632/oncotarget.18773

Mao, X. W., Pecaut, M. J., Stodieck, L. S., Ferguson, V. L., Bateman, T. A., Bouxsein, M. L., et al. (2014). Biological and metabolic response in STS-135 space-flown mouse skin. *Free Radic. Res.* 48 (8), 890–897. doi:10.3109/10715762.2014.920086

Markin, A. A., Popova, I. A., Vetrova, E. G., Zhuravleva, O. A., and Balashov, O. I. (1997). Lipid peroxidation and activity of diagnostically significant enzymes in cosmonauts after flights of various durations. *Aviakosmicheskaia I Ekologicheskaia Meditsina = Aerosp. Environ. Med.* 31 (3), 14–18.

Mitre, M., Saadipour, K., Williams, K., Khatri, L., Froemke, R. C., and Chao, M. V. (2022). Transactivation of TrkB receptors by oxytocin and its G protein-coupled receptor. *Front. Mol. Neurosci.* 15, 891537. doi:10.3389/fnmol.2022.891537

Morris, R. (1984). Developments of a water-maze procedure for studying spatial learning in the rat. *J. Neurosci. Methods* 11 (1), 47–60. doi:10.1016/0165-0270(84)90007-4

Moustafa, A. (2021). Hindlimb unloading-induced reproductive suppression via Downregulation of hypothalamic Kiss-1 expression in adult male rats. *Reproductive Biol. Endocrinol. RB&E* 19 (1), 37. doi:10.1186/s12958-021-00694-4

Muhammad, T., Ikram, M., Ullah, R., Rehman, S. U., and Kim, M. O. (2019). Hesperetin, a citrus flavonoid, attenuates LPS-induced neuroinflammation, apoptosis and memory impairments by modulating TLR4/NF-κB signaling. *Nutrients* 11 (3), 648. doi:10.3390/nu11030648

Ng, C. F., Ko, C. H., Koon, C. M., Chin, W. C., Kwong, H. C., Lo, A. W., et al. (2016). The aqueous extract of rhizome of Gastrodia elata Blume attenuates locomotor defect and inflammation after traumatic brain injury in rats. *J. Ethnopharmacol.* 185, 87–95. doi:10.1016/j.jep.2016.03.018

Nguyen, H. P., Tran, P. H., Kim, K.-S., and Yang, S.-G. (2021). The effects of real and simulated microgravity on cellular mitochondrial function. *NPJ Microgravity* 7 (1), 44. doi:10.1038/s41526-021-00171-7

Oliver, D., and Reddy, P. H. (2019). Dynamics of dynamin-related protein 1 in Alzheimer's disease and other neurodegenerative diseases. *Cells* 8 (9), 961. doi:10.3390/cells8090961

Peng, Z., Li, X., Li, J., Dong, Y., Gao, Y., Liao, Y., et al. (2021). Dlg1 knockout inhibits microglial activation and alleviates lipopolysaccharide-induced depression-like behavior in mice. *Neurosci. Bull.* 37 (12), 1671–1682. doi:10.1007/s12264-021-00765-x

Popova, N. K., Kulikov, A. V., and Naumenko, V. S. (2020). Spaceflight and brain plasticity: Spaceflight effects on regional expression of neurotransmitter systems and neurotrophic factors encoding genes. *Neurosci. Biobehav. Rev.* 119, 396–405. doi:10.1016/j.neubiorev.2020.10.010

Qiong, W., Yong-Liang, Z., Ying-Hui, L., Shan-Guang, C., Jiang-Hui, G., Yi-Xi, C., et al. (2016). The memory enhancement effect of Kai Xin San on cognitive deficit induced by simulated weightlessness in rats. *J. Ethnopharmacol.* 187, 9–16. doi:10.1016/j.jep.2016.03.070

Rahman, I., Kode, A., and Biswas, S. K. (2006). Assay for quantitative determination of glutathione and glutathione disulfide levels using enzymatic recycling method. *Nat. Protoc.* 1 (6), 3159–3165. doi:10.1038/nprot.2006.378

Raven, F., Van der Zee, E. A., Meerlo, P., and Havekes, R. (2018). The role of sleep in regulating structural plasticity and synaptic strength: Implications for memory and cognitive function. *Sleep. Med. Rev.* 39, 3–11. doi:10.1016/j.smrv.2017.05.002

Rohleder, N. (2019). Stress and inflammation - the need to address the gap in the transition between acute and chronic stress effects. *Psychoneuroendocrinology* 105, 164–171. doi:10.1016/j.psyneuen.2019.02.021

Santello, M., Toni, N., and Volterra, A. (2019). Astrocyte function from information processing to cognition and cognitive impairment. *Nat. Neurosci.* 22 (2), 154–166. doi:10.1038/s41593-018-0325-8

Shi, Q., Chang, C., Saliba, A., and Bhat, M. A. (2022). Microglial mTOR activation upregulates Trem2 and enhances β-amyloid plaque clearance in the 5XFAD Alzheimer's disease model. *J. Neurosci. Official J. Soc. For Neurosci.* 42 (27), 5294–5313. doi:10.1523/JNEUROSCI.2427-21.2022

Sood, A., Preeti, K., Fernandes, V., Khatri, D. K., and Singh, S. B. (2021). Glia: A major player in glutamate-GABA dysregulation-mediated neurodegeneration. *J. Neurosci. Res.* 99 (12), 3148–3189. doi:10.1002/jnr.24977

Spitz, A. Z., Zacharioudakis, E., Reyna, D. E., Garner, T. P., and Gavathiotis, E. (2021). Eltrombopag directly inhibits BAX and prevents cell death. *Nat. Commun.* 12 (1), 1134. doi:10.1038/s41467-021-21224-1

Sun, X.-Q., Xu, Z.-P., Zhang, S., Cao, X.-S., and Liu, T.-S. (2009). Simulated weightlessness aggravates hypergravity-induced impairment of learning and memory and neuronal apoptosis in rats. *Behav. Brain Res.* 199 (2), 197–202. doi:10.1016/j.bbr.2008.11.035

Torres, M. L., Wanionok, N. E., McCarthy, A. D., Morel, G. R., and Fernández, J. M. (2021). Systemic oxidative stress in old rats is associated with both osteoporosis and cognitive impairment. *Exp. Gerontol.* 156, 111596. doi:10.1016/j.exger.2021.111596

Van Skike, C. E., Lin, A.-L., Roberts Burbank, R., Halloran, J. J., Hernandez, S. F., Cuvillier, J., et al. (2020). mTOR drives cerebrovascular, synaptic, and cognitive dysfunction in normative aging. *Aging Cell* 19 (1), e13057. doi:10.1111/acel.13057

Wang, L.-S., Zhang, M.-D., Tao, X., Zhou, Y.-F., Liu, X.-M., Pan, R.-L., et al. (2019). LC-MS/MS-based quantification of tryptophan metabolites and neurotransmitters in the serum and brain of mice. *J. Chromatogr. B, Anal. Technol. Biomed. Life Sci.* 1112, 24–32. doi:10.1016/j.jchromb.2019.02.021

Wang, M.-Y., Meng, M., Yang, C.-C., Zhang, L., Li, Y.-L., Zhang, L., et al. (2020). Cornel iridoid glycoside improves cognitive impairment induced by chronic cerebral hypoperfusion via activating PI3K/Akt/GSK-3β/CREB pathway in rats. *Behav. Brain Res.* 379, 112319. doi:10.1016/j.bbr.2019.112319

Wang, Y., Iqbal, J., Liu, Y., Su, R., Lu, S., Peng, G., et al. (2015). Effects of simulated microgravity on the expression of presynaptic proteins distorting the GABA/glutamate equilibrium--A proteomics approach. *Proteomics* 15 (22), 3883–3891. doi:10.1002/pmic.201500302

Xue, X.-J., Su, R., Li, Z.-F., Bu, X.-O., Dang, P., Yu, S.-F., et al. (2022). Oxygen metabolism-induced stress response underlies heart-brain interaction governing human consciousness-breaking and attention. *Neurosci. Bull.* 38 (2), 166–180. doi:10.1007/s12264-021-00761-1

Yang, J., Pi, C., and Wang, G. (2018). Inhibition of PI3K/Akt/mTOR pathway by apigenin induces apoptosis and autophagy in hepatocellular carcinoma cells. *Biomed. Pharmacother.* 103, 699–707. doi:10.1016/j.biopha.2018.04.072

Yang, Y., Li, S., Huang, H., Lv, J., Chen, S., Pires Dias, A. C., et al. (2020). Comparison of the protective effects of ginsenosides Rb1 and Rg1 on improving cognitive deficits in SAMP8 mice based on anti-neuroinflammation mechanism. *Front. Pharmacol.* 11, 834. doi:10.3389/fphar.2020.00834

Ye, T., Meng, X., Wang, R., Zhang, C., He, S., Sun, G., et al. (2018). Gastrodin alleviates cognitive dysfunction and depressive-like behaviors by inhibiting ER stress and NLRP3 inflammasome activation in db/db mice. *Int. J. Mol. Sci.* 19 (12), 3977. doi:10.3390/ijms19123977

Zhang, L., and Wei, W. (2020). Anti-inflammatory and immunoregulatory effects of paeoniflorin and total glucosides of paeony. *Pharmacol. Ther.* 207, 107452. doi:10.1016/j.pharmthera.2019.107452

Zhang, Y., Wang, Q., Chen, H., Liu, X., Lv, K., Wang, T., et al. (2018). Involvement of cholinergic dysfunction and oxidative damage in the effects of simulated weightlessness on learning and memory in rats. *BioMed Res. Int.* 2018, 2547532. doi:10.1155/2018/2547532

Zhou, B., Tan, J., Zhang, C., and Wu, Y. (2018). Neuroprotective effect of polysaccharides from Gastrodia elata blume against corticosterone-induced apoptosis in PC12 cells via inhibition of the endoplasmic reticulum stress-mediated pathway. *Mol. Med. Rep.* 17 (1), 1182–1190. doi:10.3892/mmr.2017.7948

frontiers | Frontiers in Pharmacology

TYPE Original Research
PUBLISHED 17 May 2023
DOI 10.3389/fphar.2023.1171665

OPEN ACCESS

EDITED BY
Weijie Xie,
Shanghai Jiao Tong University, China

REVIEWED BY
Ming Chen,
Fudan University, China
Ming-Gang Liu,
Shanghai Jiao Tong University, China
Chengliang Yin,
Chinese PLA General Hospital, China

*CORRESPONDENCE
Yuan Han,
yuan.han@fdeent.org
Wen-Xian Li,
wenxian.li@fdeent.org

†These authors have contributed equally to this work and share first authorship

RECEIVED 22 February 2023
ACCEPTED 09 May 2023
PUBLISHED 17 May 2023

CITATION
Fan B-Q, Xia J-M, Chen D-D, Feng L-L, Ding J-H, Li S-S, Li W-X and Han Y (2023), Medial septum glutamatergic neurons modulate nociception in chronic neuropathic pain via projections to lateral hypothalamus.
Front. Pharmacol. 14:1171665.
doi: 10.3389/fphar.2023.1171665

Medial septum glutamatergic neurons modulate nociception in chronic neuropathic pain via projections to lateral hypothalamus

Bing-Qian Fan†, Jun-Ming Xia†, Dan-Dan Chen†, Li-Li Feng, Jia-Hui Ding, Shuang-Shuang Li, Wen-Xian Li* and Yuan Han*

Department of Anesthesiology, The Eye and ENT Hospital of Fudan University, Shanghai, China

The medial septum (MS) contributes in pain processing and regulation, especially concerning persistent nociception. However, the role of MS glutamatergic neurons in pain and the underlying neural circuit mechanisms in pain remain poorly understood. In this study, chronic constrictive injury of the sciatic nerve (CCI) surgery was performed to induce thermal and mechanical hyperalgesia in mice. The chemogenetic activation of MS glutamatergic neurons decreased pain thresholds in naïve mice. In contrast, inhibition or ablation of these neurons has improved nociception thresholds in naïve mice and relieved thermal and mechanical hyperalgesia in CCI mice. Anterograde viral tracing revealed that MS glutamatergic neurons had projections to the lateral hypothalamus (LH) and supramammillary nucleus (SuM). We further demonstrated that MS glutamatergic neurons regulate pain thresholds by projecting to LH but not SuM, because the inhibition of MS-LH glutamatergic projections suppressed pain thresholds in CCI and naïve mice, yet, optogenetic activation or inhibition of MS-SuM glutamatergic projections had no effect on pain thresholds in naïve mice. In conclusion, our results reveal that MS glutamatergic neurons play a significant role in regulating pain perception and decipher that MS glutamatergic neurons modulate nociception via projections to LH.

KEYWORDS

glutamatergic, lateral hypothalamus, medial septum, neuropathic pain, hyperalgesia, supramammillary nucleus

Introduction

As a leading cause of years lost to disability, chronic pain imposes a massive personal and economic burden on more than 30% of people worldwide (Murray et al., 2013; Cohen et al., 2021). Neuropathic pain is chronic pain caused by primary lesions or nervous system dysfunction associated with sensory abnormalities (Baron, 2006; Lu et al., 2017; Cohen et al., 2021). Although multiple pharmacological and non-pharmacological therapies proposed a solution for reducing neuropathic pain, treating this condition remains challenging for physicians cause a sufficient number of patients failed to experience satisfactory pain relief after treatment (Baron et al., 2010; Culp et al., 2020; Fitzcharles et al., 2021; Jiang et al., 2022). Thus, exploring the neural mechanism of neuropathic pain may lead to discovering novel pharmacological therapeutic targets.

The medial septum (MS), mainly composed of cholinergic, glutamatergic, and GABAergic neurons, is implicated in a variety of functions such as sensorimotor integration, affect-motivation and cognition (Freund, 1989; Kiss et al., 1990; Dutar et al., 1995; Colom et al., 2005; Hasselmo, 2006; McNaughton et al., 2006; Calandreau et al., 2007; Braida et al., 2014; Ang et al., 2017; Danisman et al., 2022). Studies of deep brain stimulation have shown that medial septal stimulation immediately relieves chronic pain in patients (Gol, 1967; Schvarcz, 1993). Besides, MS lesion attenuated formalin-induced theta activation and pyramidal cell suppression in dorsal hippocampus field CA1, while muscimol or zolpidem microinjection into MS suppressed formalin-induced nociceptive behavior (Zheng & Khanna, 2001; Lee et al., 2011). Moreover, another study reported that muscimol microinjection into the MS reversed peripheral hypersensitivity evoked by chronic constriction injury (CCI) (Ariffin et al., 2018). These findings indicate a potential link between MS and chronic neuropathic pain providing a critical neurophysiologic basis of chronic neuropathic pain responsible for the manifestations of neuronal plasticity changes (Xia et al., 2016). Ionotropic glutamate receptors, especially N-methyl-D-aspartate receptors expressed on postsynaptic membranes and related to neuronal plasticity, are involved in pain-related processes (Hansen et al., 2014; Xia et al., 2016; Li et al., 2019). Furthermore, nonselective and selective N-methyl-D-aspartate receptor antagonists have been shown to mitigate neuropathic pain (Collins et al., 2010; Rondon et al., 2010). In line with all the evidence, we hypothesize that MS glutamatergic neurons might be involved in regulating neuropathic pain sensitization.

The current study aimed to investigate the cellular level mechanisms of MS glutamatergic neurons in regulating neuropathic pain sensitization. First, using c-Fos staining, we identified the activity changes of MS glutamatergic neurons in CCI animals. Moreover, chemogenetic manipulations demonstrated that MS glutamatergic neurons contribute in regulating pain sensitization of naïve and CCI animals. Hence, optogenetic investigations revealed that MS glutamatergic neurons regulate pain sensitization by projecting to the LH but not SuM. All this evidence was sufficient to provide and demonstrate a novel neuronal and neural circuit mechanism that modulates the perception of chronic neuropathic pain.

Materials and methods

Animals

The Vglut2-Cre mice (Vglut2, vesicular glutamate transporter 2; #028863) were obtained from Jackson Laboratory. Adult male mice (2–6 months old) were group-housed (≤ 5 per cage) on a 12 h light/dark cycle with food and water available *ad libitum*. These mice were randomly assigned to the nominated groups described in the following experiments. All procedures were performed under international guidelines on the ethical use of animals and approved by the Animal Care and Use Committee of Fudan University (Approval No. SYXK20200032). Efforts were taken to minimize animal suffering and the testing procedure adheres to principles of animal ethics and the 3Rs.

Chronic constriction injury (CCI) model

To establish a neuropathic pain model, CCI surgery (Chronic constriction injury of the sciatic nerve) was performed as described previously (Bennett and Xie, 1988; Wang et al., 2021a). In brief, mice were anesthetized with sodium pentobarbital (50 mg kg^{-1} i.p.). The left sciatic nerve was exposed at the mid-thigh level by blunt dissection. Three nonabsorbable 4–0 silks were loosely tied around the sciatic nerve at ~1.0 mm intervals. Sham procedures (sciatic nerve exposure without ligation) were performed as controls. After suturing, erythromycin ointment was applied locally to keep the wound from infection. Finally, mice were placed in a clean and warm cage to recover from the anesthesia.

AAV vectors

In this study, adenovirus-associated virus (AAV) vectors were utilized, including AAV2/9-EF1α-DIO-EGFP (PT-0795; Brain VTA, China), AAV2/9-EF1α-DIO-mCherry (PT-0013; Brain VTA, China), AAV2/9-EF1α-DIO-hM3Dq-mCherry (PT-0042; Brain VTA, China), AAV2/9-EF1α-DIO-hM4Di-mCherry (PT-0043; Brain VTA, China), AAV2/9-flex-taCasp3-TEVp (PT-0206; Brain VTA, China), AAV2/9-hSyn-DIO-mGFP-T2A-Synaptophysin-mRuby (PT-1244; Brain VTA, China), AAV2/9-EF1α-DIO-hChR2(H134R)-mCherry (PT-0002; Brain VTA, China), and AAV2/9-EF1α-DIO-NpHR3.0-mCherry (PT-0007; Brain VTA, China). The titer of all AAV vectors ranged from 1 to 5 × 10̃12 genomic copies per milliliter.

Stereotaxic surgery and microinjection

Male mice (2–3 months old, 22–28 g) were anesthetized and stabilized in a stereotaxic frame (RWD Life Technology Co., Ltd., Shenzhen, China). The eyes were protected with erythromycin ointment. After exposing the skull's cranium, 3% hydrogen peroxide was applied to remove the periosteum, and the residual was washed off by normal saline. For the microinjection, the AAV vectors (~100 nL) were injected into MS (AP = +0.88 mm; ML = +0.55 mm; DV = −3.7 mm, 8° angle) at a rate of 1 nL sec-1 via a glass pipette connected to a programmable auto-nanoliter Injector (Nanoject III, Drummond, United States), followed by a 10-min pause to minimize backflow. The optic fibers were implanted above the LH (AP = −1.35 mm; ML = ±1.05 mm; DV = −5.10 mm) or SuM (AP = −2.70 mm; ML = +0.25 mm; DV = −4.50 mm) through dental cement. Mice were kept in their home cages after fully awake. After experiments, histological analysis was performed to verify the locations of viral transduction and optical fibers. Data were excluded for analysis if viral transduction extended beyond the MS brain regions or the locations of optical fibers were out of LH or SuM.

Chemogenetic manipulation

After mCherry, hM3Dq-mCherry or hM4Di-mCherry expression in MS for 3 weeks, saline or clozapine *N*-oxide

(CNO) (Brain VTA, China) 1 mg kg^{-1} were intraperitoneally injected at least 30 min (Tang et al., 2021) before behavioral tests. Experimenters were blind to saline or CNO administered during behavioral tests.

Optogenetic stimulation

Optical fibers in LH or SuM were connected to a blue (473 nm) or yellow (589 nm) laser generator (Newdoon, Hangzhou, China) through optical cables (Aoguan, Nanjing, China). A blue laser with 5 ms width (473 nm, 3–5 mW, 10 Hz) was synchronized for optogenetic activation during behavioral measurements. For optogenetic inhibition, a constant yellow laser (589 nm, 5–7 mW, 8s-on/2s-off) was applied synchronized during behavioral measures.

Behavioral tests

50% Paw withdraw threshold (50% PWT)

A simplified up-down method with von Frey filaments was used to estimate the mechanical hyperalgesia of mice. Briefly, mice were placed in polyethylene cages separately on an elevated metallic wire mesh platform in a quiet environment. Before testing, mice were allowed to acclimatize to the environment for 1–2 h. The test started with the midrange filament of 0.16 g strength. Subsequent filaments were proceeded according to the up-down method, and 5 consecutive touches were applied at 5 min intervals for rest. The filaments were pressed against the plantar surface and held for 3 s. Positive responses were noted when mice withdrew their hind paws during this time. Finally, 50% PWTs were calculated as described previously (Bonin et al., 2014). Behavioral tests were carried out in a blinded manner. Detailed timelines for each experiment are presented in Figures.

Paw withdrawal latency

To assess thermal nociception, paw withdrawal latencies (PWLs) were measured using the Hargreaves test (Hargreaves et al., 1988) with an IITC plantar analgesia meter (IITC Life Science). Room temperature was controlled at 23°C ± 2°C. Mice were individually placed in polyethylene cages on a glass platform and allowed to accommodate the apparatus for 1–2 h. A radiant heat source beneath the glass was used to stimulate the plantar surface of the hind paw. In advance, heat intensity was adjusted to produce a baseline of 10–15 s. To prevent tissue damage, the cutoff time was set to 20 s. Flinching, flicking, and trembling were considered as positive responses. The measurements were triplicated at 10 min intervals, and the mean was calculated as the PWL.

Immunohistology and confocal imaging

The mice were deeply anesthetized using pentobarbital sodium (60 mg kg^{-1}, i.p.) and perfused transcardially with 20 mL of phosphate-buffered saline (PBS), followed by 20 mL 4% paraformaldehyde (PFA) (G1101, Servicebio, China). The brains were carefully extracted from the skull and postfixed in 4% PFA for 6 h and then dehydrated with 30% sucrose at 4°C until the brain tissue sank to the bottom of the solution. Then 30-μm-thick coronal sections were prepared by a frozen microtome (CM 1950; Leica Microsystems, Germany). Free-floating sections were washed three times with PBS for 10 min each and blocked in PBS with 1% bovine serum albumin (V900933, Sigma–Aldrich, United States of America) and 0.2% Triton X-100 (T109027, Aladdin, China) for 45 min. Sections were incubated with primary antibody diluted in PBS and 0.2% Triton X-100 at 4°C in a shaker overnight. The primary antibodies used were rabbit anti-immediate early gene expression of proteins (c-Fos) (1:1,000; Cell Signaling Technology, United States). Incubated sections were washed thrice in PBS for 10 min and incubated for 2 h with a secondary antibody in PBS. The secondary antibodies used were Alexa Fluor 594 donkey anti-rabbit (1:400; Invitrogen, United States) or Alexa Fluor 488 donkey anti-rabbit (1:400; Invitrogen, United States). The samples were subsequently washed four times with PBS for 10 min each (all at room temperature). Confocal images were acquired using an automated slide scanner system (VS. 120, Olympus, Japan) and further observed and counted using OlyVIA 3.2.1 software (Olympus).

Statistical analysis

Statistical analyses were conducted with GraphPad Prism 9.0 software (GraphPad Software). All data were presented as mean ± SEM. Unpaired *t*-tests were performed to compare the differences between the two groups, and *Welch's* correction was used when the variance was not equal. Two-way *ANOVA* was followed by Bonferroni, Tukey, or Šídák post-tests calculate p values (treatment with different virus as the between-subject factors and different drugs as the within-subjects factor). Detailed descriptions can be found in the figure legends. Statistical significance was defined as $p < 0.05$.

Results

MS glutamatergic neurons are hyperactivated in CCI mice

To study MS glutamatergic neuron activity in CCI mice, we measured the co-expression of c-Fos, a marker of neuronal activation (Dragunow and Faull, 1989) and Vglut2, a marker of glutamatergic neurons (Fremeau et al., 2004) in MS. First, CCI was performed to establish a neuropathic pain model. To ensure the stability of hyperalgesia in this pain model, we evaluated the pain behaviors of the injured hind paw at multiple time points following the sham or CCI surgery (Figure 1A). Compared with sham mice, CCI mice showed a long-lasting decreased 50% PWTs and PWLs (Figures 1B, C). Since both 50% PWTs and PWLs tended to be stable 14 days after the CCI surgery, we chose this time point in the experiments. Next, we labeled MS glutamatergic neurons by injecting an AAV vector (AAV-EF1α-DIO-EGFP) into MS of Vglut2-Cre mice (Figure 1D). After CCI surgery, pain

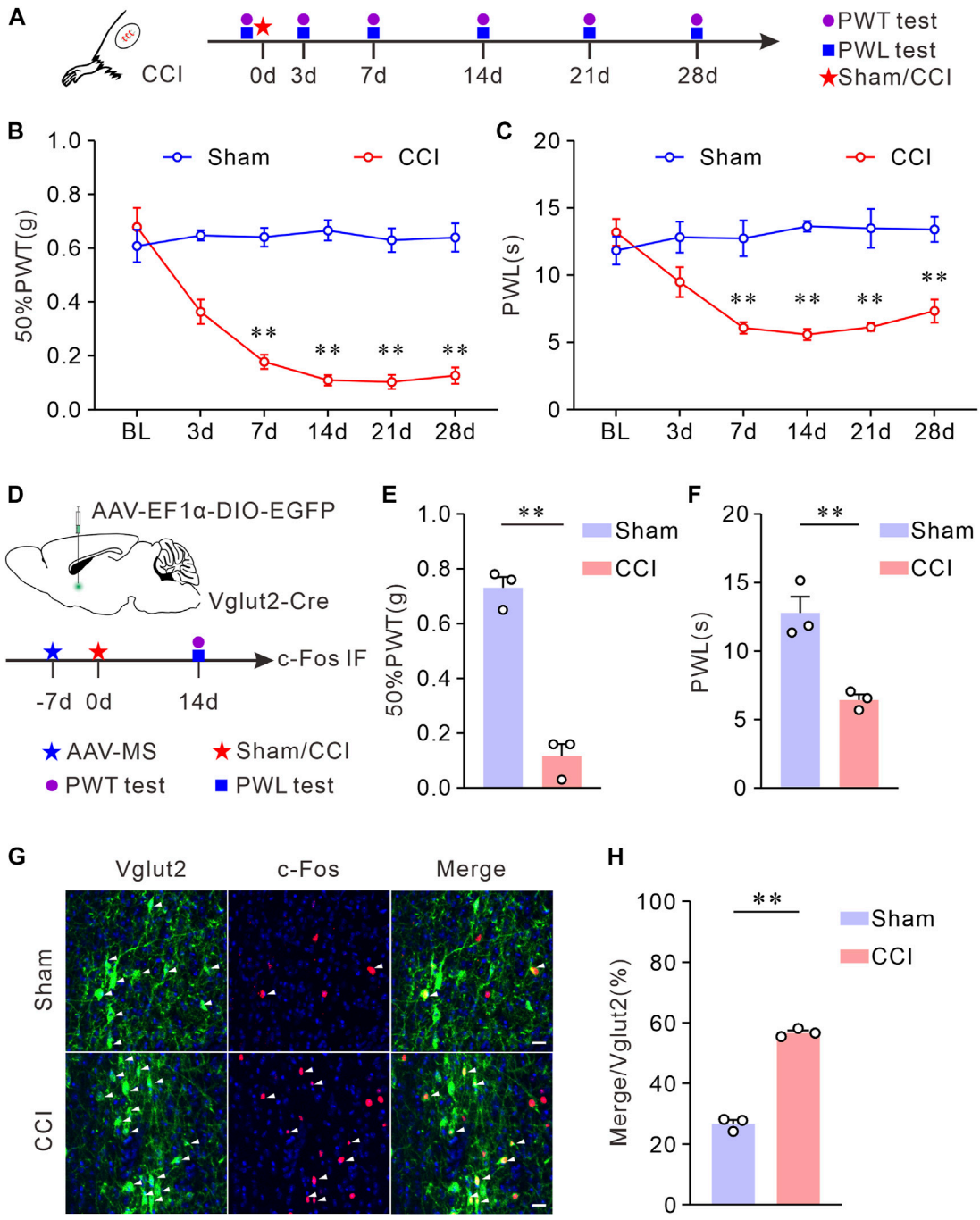

FIGURE 1
Vglut2 neurons in MS are hyperactivated on chronic neuropathic pain induced by CCI. **(A)** Schematic of CCI surgery and experimental timeline. PWTs and PWLs of the hind paws in mice were tested at day 0 before, and at days 3, 7, 14, 21, and 28 after the sham or CCI surgery. **(B,C)** The quantitative comparison of 50% PWTs **(B)** and PWLs **(C)** between the two groups. Compared with the sham mice, CCI mice exhibited a decrease in 50% PWTs and PWLs in the injured paw at days 7, 14, 21, and 28 after the CCI surgery. n = 8 mice/group. 50% PWT: sham *versus* CCI, 7 days $p < 0.0001$, 14 days $p < 0.0001$, 21 days $p < 0.0001$, 28 days $p < 0.0001$; PWL: sham *versus* CCI, 7 days $p = 0.0076$, 14 days $p < 0.0001$, 21 days $p = 0.0076$, 28 days $p = 0.0018$. Two-way *ANOVA* with *Bonferroni* post-tests. BL: baseline. **(D)** Experimental timeline and schematic of virus injection. Mice were injected with AAV-vectors into the MS at day 7 before the CCI surgery. 50% PWTs and PWLs were tested from day 14 after the CCI surgery. **(E,F)** Statistics demonstrated that, the CCI mice exhibited mechanical allodynia **(E)** and thermal hyperalgesia **(F)**. 50% PWT: Sham, 0.73 ± 0.04; CCI, 0.12 ± 0.04, $p = 0.0002$; PWL: Sham, 12.78 ± 1.19; CCI, 6.43 ± 0.40, $p = 0.0036$. Unpaired t-test: mean ± SEM. **(G)** Representative images showing Vglut2 neurons (Green) in MS of mice were co-labeled with c-Fos-positive cells (Red) at day 14 following the CCI surgery. Arrowheads indicate co-labeled neurons. Scale bar: 10 μm. **(H)** Quantification indicating that the Vglut2 neurons are hyperactivated in CCI mice. Sham: 26.71 ± 1.29, n = 6 slices from 3 mice; CCI: 56.70 ± 0.78, n = 6 slices from 3 mice, $p < 0.0001$. Unpaired t-test with *welch* correction. $^{**}p < 0.01$. Error bars indicate SEM.

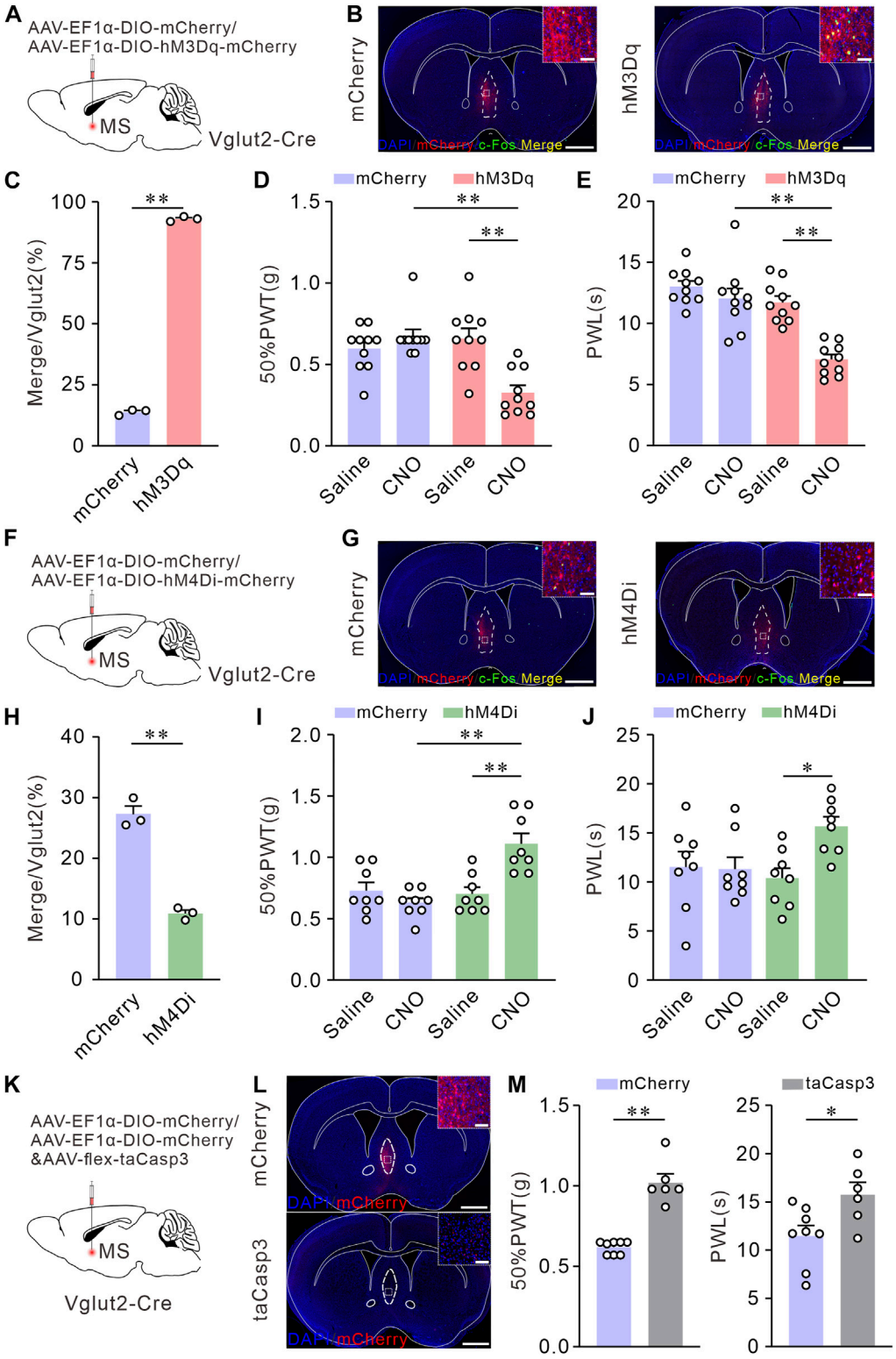

FIGURE 2
Chemogenetic activation of Vglut2 neurons in MS induces mechanical allodynia and thermal hyperalgesia, whereas inhibition or ablation of these neurons elevates mechanical and thermal pain thresholds in Naïve mice. **(A)** Schematic of virus injection. AAV-vectors were injected into the MS of Vglut2-Cre mice. **(B)** Coronal fluorescence images showing the expression of hM3Dq-mCherry in the MS Vglut2 neurons (Red). Scale bar: 1 mm. Magnified image on the top right shows the boxed area: the Vglut2 and c-Fos (Green) co-labeling neurons (Yellow) in MS in mCherry + CNO and hM3Dq + CNO groups. Scale bar: 50 μm. **(C)** Statistics showing that, the Vglut2 neurons in MS were significantly activated in hM3Dq + CNO group. n = 3 mice/group. Saline: 13.86 ± 0.69; CNO: 93.02 ± 0.58, $p < 0.0001$. Unpaired t-test: mean ± SEM. **(D,E)** Summary results showing that, compared with their control counterparts, the hM3Dq + CNO mice exhibited a decrease in 50% PWTs **(D)** and PWLs **(E)**. n = 10 mice/group. 50% PWT: mCherry *versus*
(*Continued*)

FIGURE 2 (Continued)
hM3Dq, CNO, $p < 0.0001$; Saline *versus* CNO, hM3Dq, $p = 0.0002$. PWL: mCherry *versus* hM3Dq, CNO, $p < 0.0001$; Saline *versus* CNO, hM3Dq, $p < 0.0001$. Two-way *ANOVA* with *Tukey* post-tests. **(F)** Schematic of virus injection. **(G)** Coronal fluorescence images showing the expression of hM4Di-mCherry in the MS Vglut2 neurons (Red). Scale bar: 1 mm. Magnified image on the top right shows the boxed area: the Vglut2 and c-Fos (Green) co-labeling neurons (Yellow) in MS in mCherry + CNO and hM4Di + CNO groups. Scale bar: 50 μm. **(H)** Statistics showing that, the Vglut2 neurons were inhibited in hM4Di + CNO group. $n = 3$ mice/group. Saline: 27.23 ± 1.38; CNO: 10.87 ± 0.58, $p = 0.0002$. Unpaired *t*-test: mean ± SEM. **(I,J)** Summary results showing that, compared with their control counterparts, the hM4Di + CNO mice exhibited an increase in 50% PWTs **(I)** and PWLs **(J)**. $n = 8$ mice/group. 50% PWT: mCherry *versus* hM4Di, CNO, $p < 0.0001$; Saline *versus* CNO, hM4Di, $p = 0.0005$. PWL: Saline *versus* CNO, hM4Di, $p = 0.0226$. Two-way *ANOVA* with *Tukey* post-tests. **(K)** Schematic of virus injection. **(L)** Representative confocal images of genetic ablation of the Vglut2 neurons in MS (Red). Scale bar: 1 mm. Magnified image on the top right shows the boxed area. The mCherry and taCasp3 typical confocal image indicating the efficacy of taCasp3. Scale bar: 50 μm. **(M)** Summary results showing that, compared with mCherry group, the mice with taCasp3 expression exhibited an increase in 50% PWTs and PWLs. $n = 8/6$. 50% PWTs: mCherry, 0.62 ± 0.1; taCasp3, 1.02 ± 0.05, $p < 0.0001$. PWL: mCherry, 11.49 ± 1.09; taCasp3, 15.76 ± 1.27, $p = 0.0125$. Unpaired *t*-test: mean ± SEM. $^*p < 0.05$, $^{**}p < 0.01$. Error bars indicate SEM.

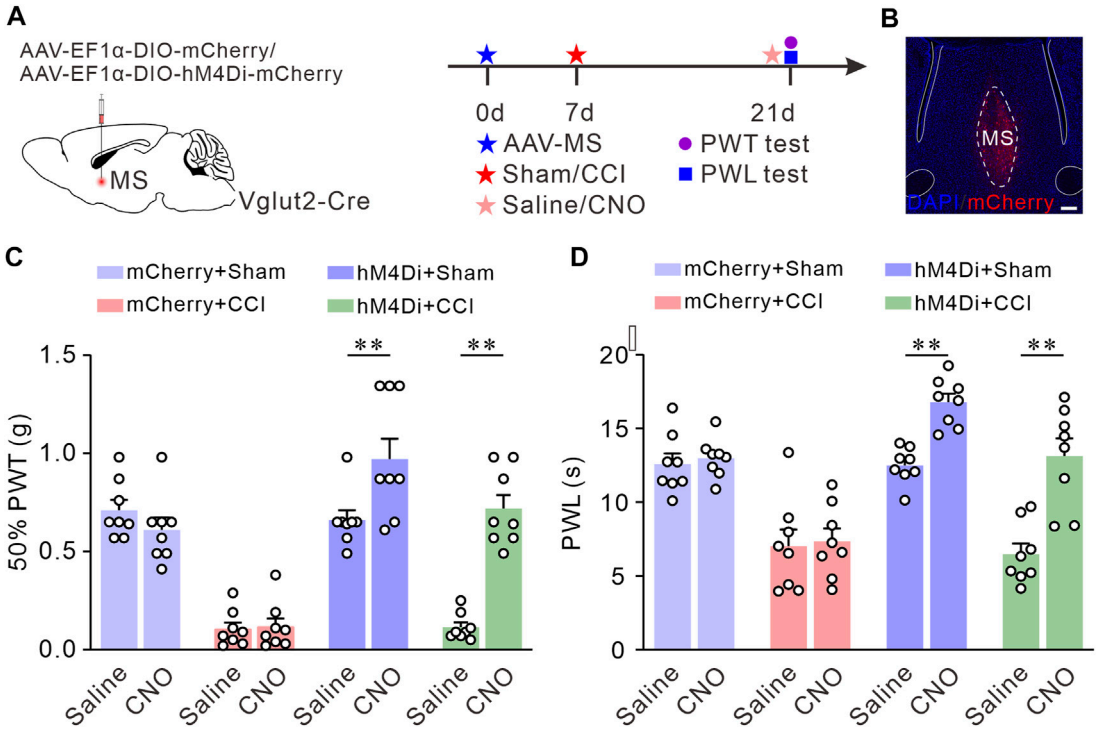

FIGURE 3
Chemogenetic inhibition of the Vglut2 neurons in MS relieves chronic neuropathic pain induced by CCI. **(A)** The diagram of virus injection and experimental timeline. **(B)** Example confocal images of hM4Di-mCherry expression in the MS Vglut2 neurons (Red). **(C,D)** Summary results showing that, compared with their control counterparts, the hM4Di + CCI + CNO mice exhibited an increase in 50% PWTs **(C)** and PWLs **(D)**. $n = 8$ mice/group. 50% PWT: Saline *versus* CNO, hM4Di + CCI, $p < 0.0001$. PWL: Saline *versus* CNO, hM4Di + CCI, $p < 0.0001$. Two-way *ANOVA* with *Bonferroni* post-tests. $^{**}p < 0.01$. Error bars indicate SEM.

behavioral tests were performed on day 14. As expected, 50% PWTs and PWLs of CCI mice declined significantly (Figures 1E, F). Then, c-Fos immunofluorescence staining was performed in MS sections of Vglut2-Cre mice to determine the neuronal activity in response to chronic neuropathic pain (Figure 1G). The staining results showed that, compared with their sham counterparts, CCI surgery induced a significant increase of c-Fos expression in MS glutamatergic neurons (Figure 1H), suggesting that these neurons were activated in CCI mice. This data indicates that the MS glutamatergic neurons are involved in chronic neuropathic pain.

Chemogenetic activation of the Vglut2 neurons in MS induces mechanical allodynia and thermal hyperalgesia, whereas inhibition or ablation of these neurons elevates mechanical and thermal pain thresholds in naïve mice

To further explore whether the activation of MS glutamatergic neurons leads to hyperalgesia, we applied chemogenetic stimulations to activate MS glutamatergic neurons specifically and assessed the pain thresholds in mice.

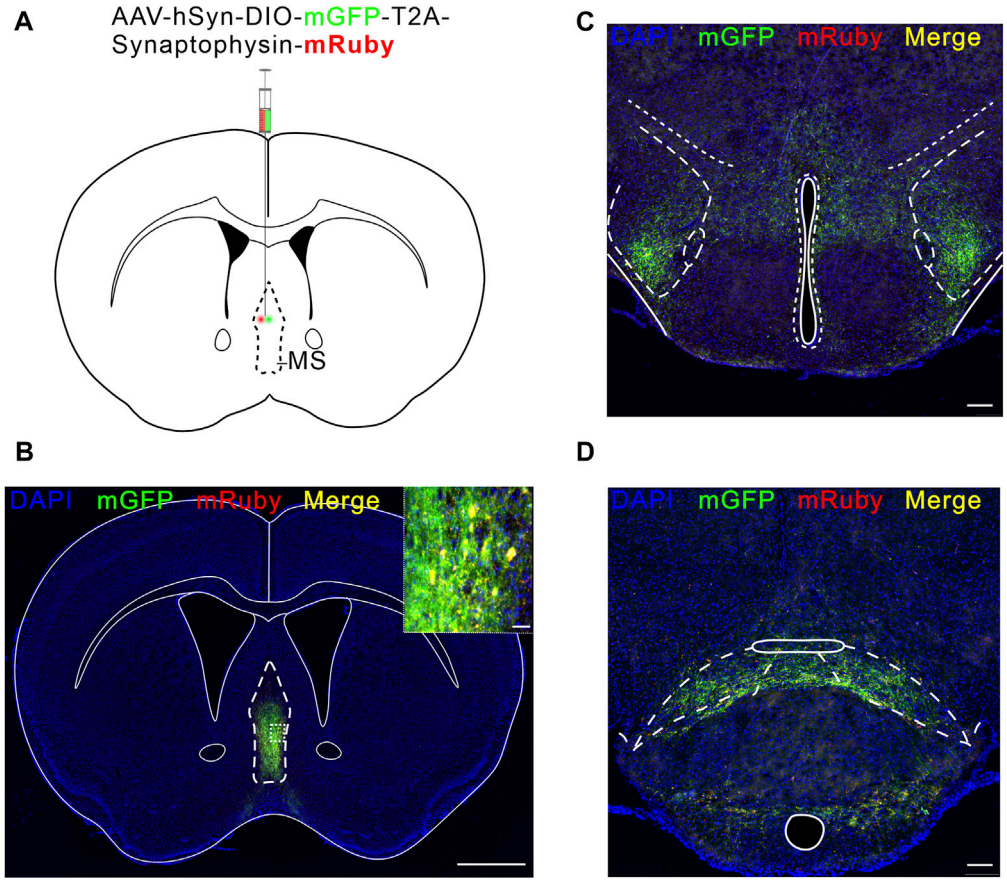

FIGURE 4
LH and SuM receive direct projections from MS Vglut2 neurons. **(A)** Schematic of AAV-hSyn-DIO-mGFP-T2A-Synaptophysin-mRuby injection into MS of Vglut2-Cre mice. **(B)** Fluorescence image of mGFP-mRuby expression in MS. Scale bar: 1 mm. The magnified image on the top right shows the expression of mGFP-mRuby (Green-Red) *in situ*. Scale bar: 50 μm. **(C,D)** Example confocal images of mGFP-mRuby expression in LH **(C)** and SuM **(D)**. Scale bar: 200 μm.

AAV-EF1α-DIO-hM3Dq-mCherry (an AAV vector that expresses mCherry and hM3Dq dependence on Cre) or AAV-EF1α-DIO-mCherry (as control) was injected into the MS of Vglut2-Cre mice. 50% PWTs and PWLs were performed on day 21 (Figure 2A). Mice were injected intraperitoneally with saline (1 mg kg^{-1}). Then the first determination of 50% PWTs and PWLs was considered as the baseline for the pain sensitivity. At least 1 h later, mice were subjected to an intraperitoneal injection of CNO (1 mg kg^{-1}). After 30 min, 50% PWTs or PWLs were examined again. To verify the efficacy of the chemogenetics strategy, the mice were sacrificed for c-Fos immunofluorescence staining of MS sections after behavioral tests. Compared to the controls, > 90% of mCherry-positive neurons were co-labeled by c-Fos in hM3Dq group mice (Figures 2B, C), suggesting that CNO does activate these glutamatergic neurons. After CNO injection, the mice injected with AAV-EF1α-DIO-hM3Dq-mCherry exhibited a decrease in 50% PWTs and PWLs (Figures 2D, E). These data indicate that chemogenetic activation of MS glutamatergic neurons induces mechanical allodynia and thermal hyperalgesia in naïve mice.

Chemogenetic inhibition or selective lesion of MS glutamatergic neurons elevates mechanical and thermal pain thresholds in naïve mice

We further wanted to investigate whether inhibition or lesion of MS glutamatergic neurons can improve pain thresholds. For specifical inhibition of MS glutamatergic neurons, AAV-EF1α-DIO-hM4Di-mCherry or AAV-EF1α-DIO-mCherry (as control) was injected into the MS of Vglut2-Cre mice and the pain behavioral tests were determined on day 21 (Figure 2F). The expression of chemogenetics virus was also confirmed by c-Fos immunofluorescence staining. A few Vglut2 neurons were co-labeled by c-Fos (Figures 2G, H). After CNO injection, the mice injected with hM4Di-mCherry exhibited the increased 50% PWTs and PWLs (Figures 2I, J), indicating that chemogenetic inhibition of MS glutamatergic neurons elevates mechanical and thermal pain thresholds in naïve mice.

In addition, we selectively lesioned the MS glutamatergic neurons by injecting the mixture of AAV-EF1α-DIO-mCherry

and AAV-flex-taCasp3-TEVp. The controls only were injected with AAV-EF1α-DIO-mCherry (Figure 2K). We confirmed cell death by confocal fluorescent imaging. Compared to the controls, less number of mCherry neurons were presented on MS with AAV-flex-taCasp3-TEVp injection (Figure 2L). 50% PWTs and PWLs were tested on day 21. Similarly, mice injected with AAV-flex-taCasp3-TEVp exhibited an increase in 50% PWTs and PWLs (Figure 2M), demonstrating that selective lesion of MS glutamatergic neurons improves mechanical and thermal pain thresholds in naïve mice.

Chemogenetic inhibition of MS glutamatergic neurons relieves chronic neuropathic pain induced by CCI

Next, we investigated the pain-relieving effect of MS glutamatergic neurons in the CCI-induced neuropathic pain model mice. We targeted MS glutamatergic neurons by injecting AAV-EF1α-DIO-hM4Di-mCherry or AAV-EF1α-DIO-mCherry (as control) into the MS of Vglut2-Cre mice. Subsequent sham or CCI surgery was performed, respectively. 50% PWTs and PWLs were measured 14 days after surgery (Figure 3A). MS sections were prepared to verify the expression of hM4Di-mCherry (Figure 3B). The results showed that the pain thresholds in CCI mice injected with AAV-EF1α-DIO-hM4Di-mCherry and CNO did not decline as much as those of CCI control mice (Figures 3C, D). These findings suggest that chemogenetic inhibition of the MS glutamatergic neurons relieves chronic neuropathic pain induced by CCI.

LH and SuM receive direct projections from MS glutamatergic neurons

We next investigated how MS glutamatergic neurons are involved in pain regulation. In this part, we explored the MS glutamatergic downstream pathways mediating neuropathic pain. We used an anterograde, viral tracing method (Knowland et al., 2017) to examine the brain regions receiving direct projections from MS glutamatergic neurons. AAV-hSyn-DIO-mGFP-T2A-Synaptophysin-mRuby was injected into the MS of Vglut2-Cre mice (Figures 4A, B). Synaptophysin-mRuby is a fusion protein of mRuby and Synaptophysin. Synaptophysin proteins are located on synaptic vesicles and are used to mark the location of synapses (Tsetsenis et al., 2021). Although mGFP-positive fibers are present in some brain regions, this does not mean MS glutamatergic neurons form synapses in these nuclei but only cross these pathways. Therefore, the co-existence of mGFP and synaptophysin-mRuby in LH and SuM suggests a direct projection relationship between MS and these two nuclei (Figures 4C, D).

MS Vglut2-LH projections bilaterally regulate mechanical and thermal pain thresholds in naïve mice

We have determined the MS glutamatergic neurons mainly project to LH and SuM. Next, we planned to confirm the functional role of these projections in mediating pain sensitivity. Here, through optogenetics, we observe the real-time effects of MS Vglut2-LH projections intervention on pain behaviors. For optogenetic activation of MS Vglut2-LH projections, AAV-EF1α-DIO-hChR2 (H134R)-mCherry or AAV-EF1α-DIO-mCherry (as controls) was injected into MS, and optical fibers were implanted above LH of Vglut2-Cre mice (Figures 5A–C). According to the previous study (An et al., 2021), to activate MS glutamatergic neurons, we randomly applied 10 Hz blue laser stimulations. 50% PWTs and PWLs were examined when the mice have subjected to the blue laser (470 nm) stimulation by optical fiber coupled with a laser generator. The data showed that the mice injected with hChR2 (H134R)-mCherry and received laser stimulation had lower 50% PWTs and PWLs than the controls (Figures 5D, E), suggesting that optogenetic activation of MS glutamatergic neurons promotes pain sensitivity. For optogenetic inhibition of MS Vglut2-LH projections, AAV-EF1α-DIO-NpHR3.0-mCherry or AAV-EF1α-DIO-mCherry (as controls) was injected into MS, and optical fibers were implanted above LH of Vglut2-Cre mice (Figures 5F–H). After 21 days, yellow light (589 nm) was delivered to LH by optical fiber connected to a laser generator. The result showed that, compared to the controls, mice injected with NpHR3.0-mCherry and received laser stimulation had an increase in 50% PWTs and PWLs (Figures 5I, J). Together, we demonstrated that MS Vglut2-LH projections bilaterally regulate pain sensitivity.

MS Vglut2-SuM projections have no effect on pain thresholds in naïve mice

According to the same procedures, we activated MS Vglut2-SuM projections by optogenetics (Figures 6A–C). Surprisingly, we found no significant difference between baseline and laser-on groups in the 50% PWTs and PWLs (Figures 6D, E). Similarly, optogenetic inhibition of MS Vglut2-SuM projections (Figures 6F–H) did not influence 50% PWTs or PWLs (Figures 6I, J). Hence, revealing that MS Vglut2-LH, but not MS Vglut2-SuM projections regulate mechanical and thermal pain thresholds in naïve mice.

Optogenetic inhibition of MS Vglut2-LH projections relieves chronic neuropathic pain induced by CCI

Since inhibition of MS Vglut2-LH projections elevated pain thresholds in naïve mice, we inferred that these projections also relieve chronic neuropathic pain induced by CCI. To test this hypothesis, we utilized optogenetic tools to inhibit MS Vglut2-LH projections in CCI mice. The mice were injected with AAV-EF1α-DIO-NpHR3.0-mCherry or AAV-EF1α-DIO-mCherry (as controls) 7 days before sham or CCI surgery. Twenty-one days after the AAV injection, 50% PWTs, and PWLs were checked (Figures 7A–C). Statistics showed that there were no differences in mCherry group mice. Compared to the laser-off mice, 50% PWTs and PWL increased in the NpHR3.0-mCherry mice with laser-on (Figures 7D, E). The results suggested that inhibition of MS Vglut2-LH projections relieves chronic neuropathic pain induced by CCI.

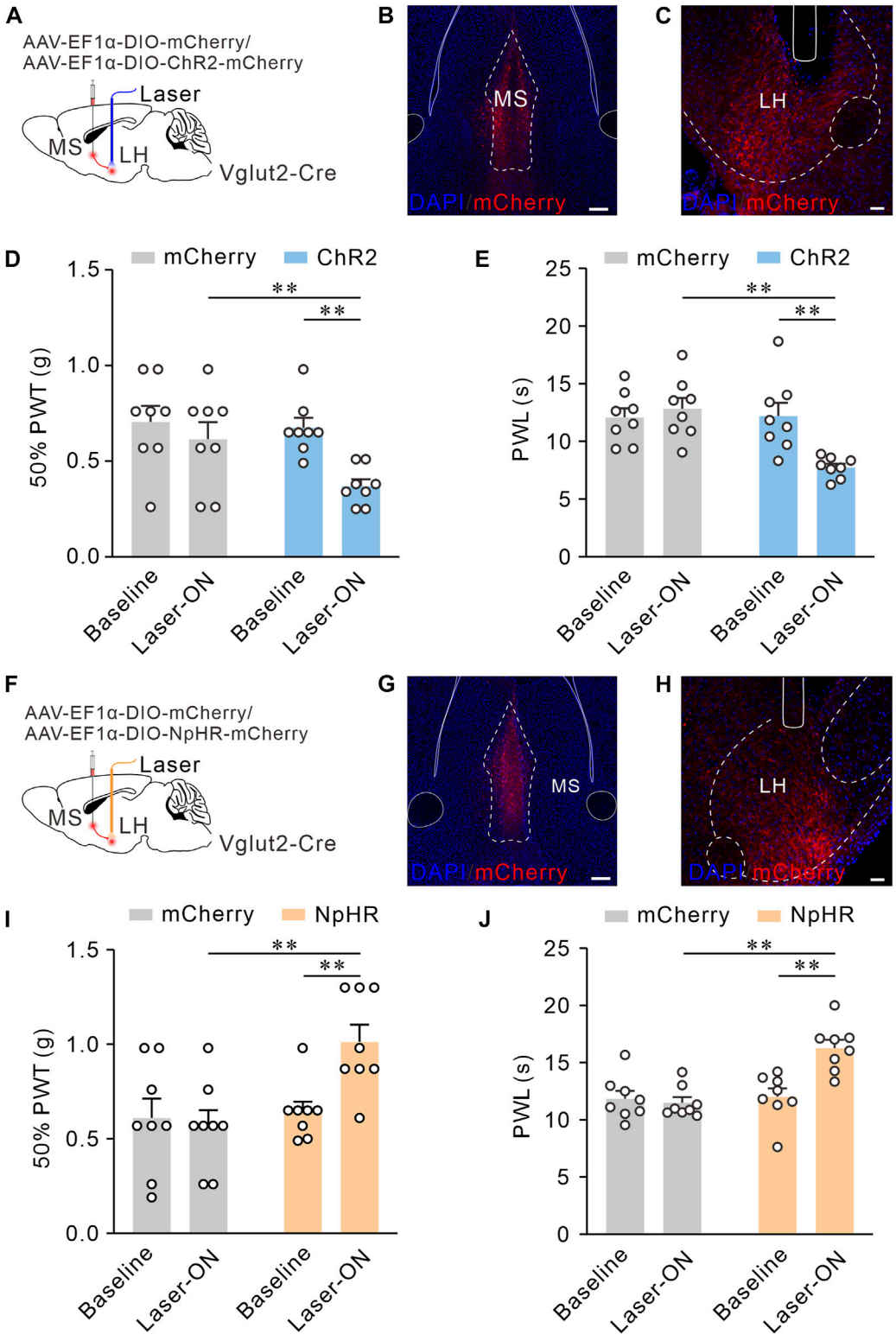

FIGURE 5
MS Vglut2-LH projections bilaterally regulate mechanical and thermal pain thresholds in naïve mice. **(A,F)** Schematic drawing of virus injection. **(B,G)** Typical confocal images of ChR2-mCherry and NpHR-mCherry expression in MS Vglut2 neurons, respectively. Scale bar: 200 μm. **(C,H)** Sample confocal images showing the terminals of MS Vglut2 neurons in LH and the tips of optical fibers above LH. Scale bar: 50 μm. **(D,E)** Statistics showing that, the ChR2 mice exhibited a decrease in 50% PWTs **(D)** and PWLs **(E)** by optogenetic activation of MS Vglut2-LH projections, $n = 8$ mice/group. 50% PWT: Baseline *versus* Laser-ON, ChR2, $p = 0.0005$. PWL: Baseline *versus* Laser-ON, ChR2, $p = 0.0006$. **(I,J)** Statistics showing that, optogenetic inhibition of MS Vglut2-LH projections increase mechanical **(I)** and thermal pain thresholds **(J)** in naïve mice. $n = 8$ mice/group. 50% PWT: Baseline *versus* Laser-ON, NpHR, $p = 0.0114$. PWL: Baseline *versus* Laser-ON, NpHR, $p < 0.0001$. Two-way *ANOVA* with Šídák post-tests. $^{**}p < 0.01$. Error bars indicate SEM.

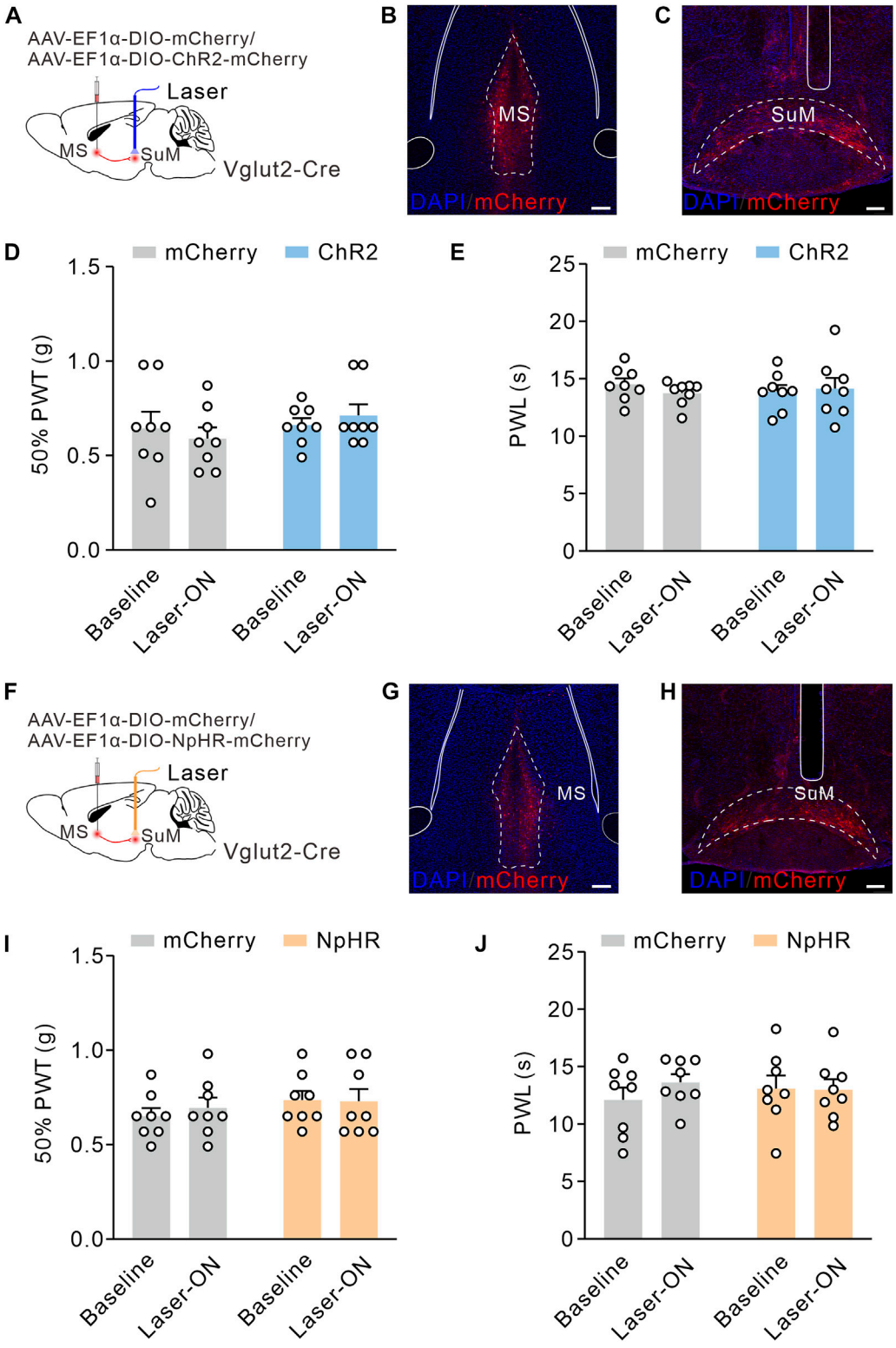

FIGURE 6
MS Vglut2-SuM projections have no effect on pain thresholds in naïve mice. **(A,F)** Schematic drawing of virus injection. **(B,G)** Typical confocal images of ChR2-mCherry and NpHR-mCherry expression in MS Vglut2 neurons, respectively. Scale bar: 200 μm. **(C,H)** Sample confocal images showing the terminals of MS Vglut2 neurons in SuM and the tips of optical fibers above SuM. Scale bar: 200 μm. **(D,E,I,J)** Statistics showing that, neither optogenetics activation **(D,E)** nor inhibition **(I,J)** of the MS Vglut2-SuM projections caused statical differences for 50% PWTs and PWLs in naïve mice, compared to their counterparts. Two-way ANOVA with Šídák post-tests. Error bars indicate SEM.

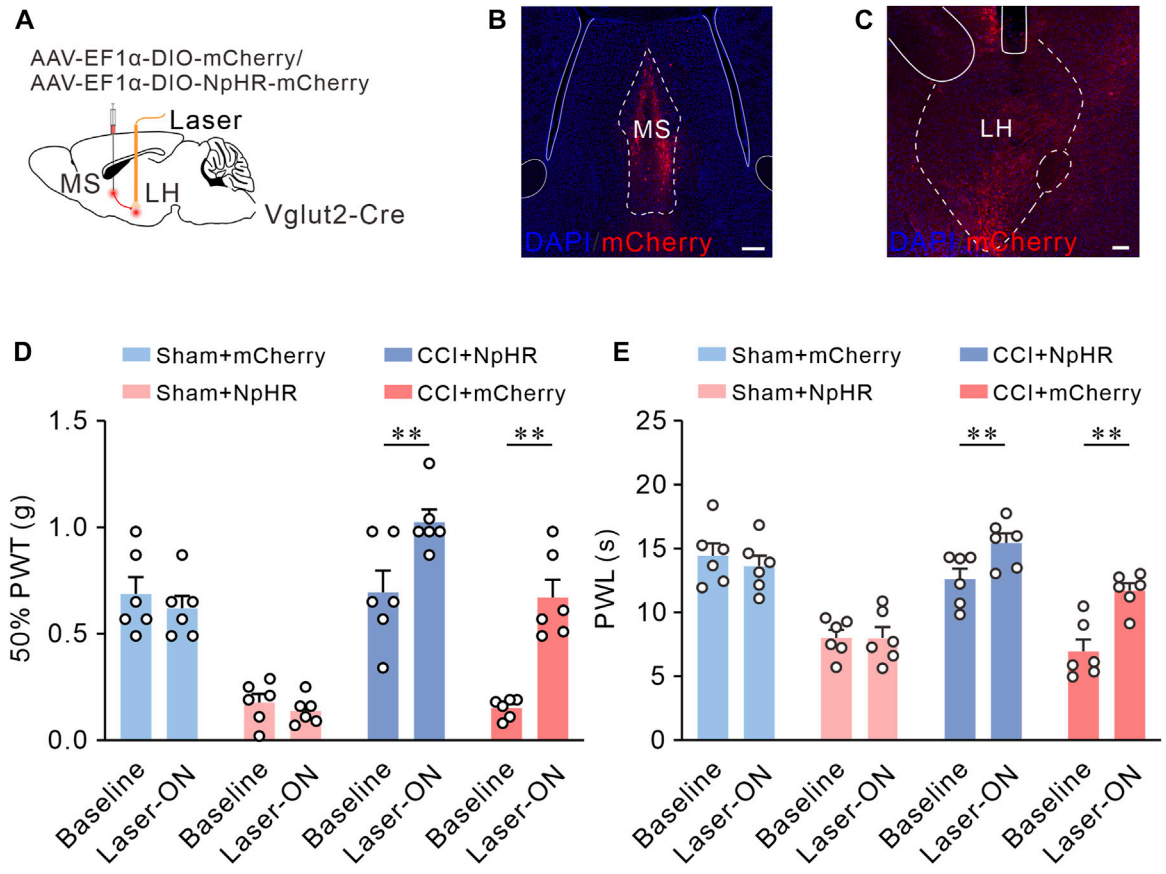

FIGURE 7
Optogenetic inhibition of MS Vglut2-LH projections relieves chronic neuropathic pain induced by CCI. **(A)** The diagram of virus injection. **(B)** Confocal image showing ChR2-mCherry expression in MS Vglut2 neurons. Scale bar: 200 μm. **(C)** Confocal images showing the terminals of MS Vglut2 neurons in LH and the tips of optical fibers above LH. Scale bar: 200 μm. **(D,E)** Summary results showing that, the NpHR + Laser-ON mice exhibited increased 50% PWTs and PWLs, compared with their control counterparts. n = 6 mice/group. 50% PWT: Baseline *versus* Laser-ON, NpHR + CCI, $p < 0.0001$. PWL: Baseline *versus* Laser-ON, NpHR + CCI, $p < 0.0001$. Two-way *ANOVA* with Šídák post-tests. $^{**}p < 0.01$. Error bars indicate SEM.

Discussion

Evidence from rodent studies suggests that MS is implicated in processing and regulation pain (Ang et al., 2017). Studies have shown that MS neurons can be activated by both acute or chronic nociceptive stimulation (Dutar et al., 1985; Burstein et al., 1987; Jiang et al., 2018a). The results of pharmacological tests demonstrated that inhibition of the MS reduced experimental neuropathic pain in mice and inhibited formalin-induced licking and flinching in rats (Lee et al., 2011; Ariffin et al., 2018). Besides, the analgesic effects of general anesthesia are prolonged by lesion or inactivation of MS (Ma et al., 2002; Leung et al., 2013). These results prove that MS is essential in the regulation of nociception. However, how the individual neuronal populations of MS regulate pain perception remains a questionable phenomenon. The MS consists of three major neuronal populations: cholinergic (about 47%), glutamatergic (about 25%), and GABAergic neurons (about 28%) (Griffith & Matthews, 1986; Markram & Segal, 1990; Dutar et al., 1995; Colom et al., 2005; Yu et al., 2022). Previous findings (Jiang et al., 2018a; Jiang, et al., 2018b) suggest that cholinergic neurons in MS are involved in encoding hyperalgesia and anxiety-like behaviors in mice with chronic pain induced by the complete Freund's adjuvant (CFA). Intraplantar injection of CFA increased the number of c-Fos-positive neurons in MS cholinergic neurons (Jiang et al., 2018a). Chemogenetic inhibition of MS cholinergic neurons attenuated perceptual (Jiang, et al., 2018b) and anxiety-like (Jiang et al., 2018a) behaviors of chronic pain induced by CFA injection in mice. Interestingly, another study (Ang et al., 2015) found that selective lesions of MS GABAergic neurons did not affect the abnormal pain-perceptual behavior but attenuated the conditioned place aversion induced by formalin injection. However, we found that chronic neuropathic pain caused by CCI activates MS glutamatergic neurons, and inhibition of MS glutamatergic neurons reverses nociceptive sensitization induced by CCI. Our results demonstrate that MS glutamatergic neurons play a critical role in perceiving and regulating nociceptive sensitization in chronic neuropathic pain.

MS is a part of the pain system in the brain (Takeuchi et al., 2021). On the one hand, the MS receives afferents from the nociceptive system, and peripheral nociceptive stimuli activate MS neurons (Dutar et al., 1985; Burstein et al., 1987; Jiang, et al., 2018b) and receives neural afferents from a cluster of nuclei that

have been shown to be involved in pain regulation (Ang et al., 2017), including LH (Fakhoury et al., 2020), the lateral septal nucleus (LS) (Wang et al., 2023), and the ventral tegmental area (VTA) (Zhang et al., 2017). On the other hand, the MS receives afferents from the nociceptive system, and peripheral nociceptive stimuli activate MS neurons. MS regulates pain by directly or indirectly innervating regions of the nociceptive system (Ang et al., 2017). Neurons in MS are known to send neural efferences to nuclei involved in sensory information transmission, including the anterior cingulate cortex (ACC), raphe nucleus (RN), LH, and SuM (Takeuchi et al., 2021). Furthermore, inhibition of the MS-rACC cholinergic pathway suppresses rACC pyramidal neuronal activities and relieves CFA-induced inflammatory pain (Jiang, et al., 2018b). Interestingly, in anesthetized animals, electrical stimulation of the MS inhibited the firing rate of wide dynamic range neurons in the spinal cord dorsal horn evoked by the peripheral noxious stimuli (Carstens et al., 1982; Hagains et al., 2011). This implies that MS might modulate pain by acting on the descending pain inhibitory system. Indeed, the evidence above suggests that MS may be a critical hub for the reception and processing of nociceptive stimulus signals. The current study demonstrates that chronic neuropathic pain increases the activity of MS glutamatergic neurons and MS glutamatergic neural population modulates the hyperalgesia of chronic neuropathic pain via their projections to LH.

LH is a heterogeneous brain region composed mainly of orexinergic, glutamatergic, GABAergic, and various neuropeptide-expressing neurons (Fakhoury et al., 2020).The LH regulates many processes, including feeding, sleep, arousal, and pain (Fakhoury et al., 2020; An et al., 2021; Xiang et al., 2022; Wang et al., 2023) and electrical stimulation of the LH region induces analgesic effects (Fakhoury et al., 2020). It has been confirmed that orexinergic neurons and parvalbumin (PV)-positive neurons of the LH play an essential role in the process of pain regulation (Inutsuka et al., 2016; Siemian et al., 2021). Specifically, activation of LH orexinergic or PV-positive neuronal population attenuated formalin-induced pain-related behaviors in mice. However, little is known about the role of other types of neurons in the LH in pain regulation. Interestingly, an *in vivo* study showed that optogenetic inhibition of MS-LH pathway neurons attenuated the firing frequency of LH glutamatergic neurons in wake-state mice (An et al., 2021). Therefore, we hypothesized that the MS-LH glutamatergic pathway might regulate pain by acting on LH glutamatergic neurons. Although it has been confirmed that the activation of LH glutamatergic neurons can cause aversion, arousal, promote-recovery from general anesthesia, escape behavior, and defensive behavior (Nieh et al., 2016; Li et al., 2018; de Jong et al., 2019; Chen et al., 2020; Wang et al., 2021b; Zhao et al., 2021). But there is still a lack of reliable evidence to confirm the regulatory role of LH glutamatergic neurons on pain, which may become a direction for future research. Furthermore, the synaptic terminals of orexinergic neurons exhibit co-localization with Vglut2 markers, indicating they are capable of rapid, synaptic glutamate release (Rosin et al., 2003; Henny et al., 2010; Bonnavion et al., 2016). Therefore, further confirmation is required to determine whether the MS-LH glutamatergic pathway targets LH orexinergic neurons.

Previous studies have found that the SuM plays a role in modulating arousal, locomotion, and feeding processes (Pedersen et al., 2017; Farrell et al., 2021; Chen et al., 2022). Besides, studies also indicate that the SuM is involved in the processing of nociceptive information (Borhegyi & Freund, 1998; Ma & Leung, 2006; Ariffin et al., 2010; Ang et al., 2017). Microinjection of nicotinic antagonists into the SuM selectively attenuated the hippocampal responses elicited by formalin-induced nociceptive stimuli (Ariffin et al., 2010), and inactivation of the SuM prolongs the duration of antinociceptive function of general anesthetics (Ma & Leung, 2006). The present study shows that MS glutamatergic neurons export numerous neuronal terminals to the SuM. Nevertheless, our results found that activation or inactivation of the MS-SuM glutamatergic pathway did not alter responses to noxious stimulation in naive mice. However, activation of the MS-LH glutamatergic pathway enhanced the sensitivity to nociceptive stimulation in naive mice. In contrast, inhibition of the MS-LH glutamatergic pathway attenuated the sensitivity to nociceptive stimulation in naive mice and reversed the hyperalgesia in CCI mice. Our results confirms that the modulation of nociception by MS glutamatergic neurons depends on their specific downstream projection target region.

Although, few researchers have made progress in studying the circuit mechanism of chronic neuropathic pain (Zhang et al., 2017; Wang et al., 2021c). But the neural circuit mechanism of MS regulating chronic neuropathic pain has been rarely reported. In the present study, we have identified an important role of MS glutamatergic neurons in regulating chronic neuropathic pain, and these MS glutamatergic neurons regulate nociception through the MS-LH pathway but not the MS-SUM pathway. Our study identifies novel cellular and neural circuit mechanisms that regulate chronic neuropathic pain, which may provide valuable therapeutic targets for chronic pain.

Data availability statement

The original contributions presented in the study are included in the article/supplementary material, further inquiries can be directed to the corresponding authors.

Ethics statement

The animal study was reviewed and approved by theAnimal Care and Use Committee of Fudan University.

Author contributions

W-XL, YH, and B-QF were responsible for conceiving, organizing, and implementing the research protocol, interpreting the data, guiding discussions of the results, and drafting the manuscript. B-QF, D-DC, and J-MX participated in the animal experiments and sampling. S-SL, L-LF and J-HD participated in laboratory experiments and data measurement. All authors listed have made a substantial, direct, and intellectual contribution to the work and approved it for publication. All authors contributed to the article and approved the submitted version.

Funding

This study was supported in part by grants-in-aid for scientific research from the National Natural Science Foundation of China (82271295), the Natural Science Foundation of Shanghai (21ZR1411300) to YH. The National Natural Science Foundation of China (82201375) to S-SL. The National Natural Science Foundation of China (82171264) to W-XL.

Acknowledgments

We thank Tian-Jie Yuan, Rui Xu, Jin-Hong Wu, Yu Zhou, Yan-Jun Liu, Yu Lu, Ya-Yue Yang, Jian-Yu Zhu, and Ying Xia (Fudan University) for technical assistance. We are grateful to Abdul Manan (Fudan University) for revising the language in our manuscript.

Conflict of interest

The authors declare that the research was conducted in the absence of any commercial or financial relationships that could be construed as a potential conflict of interest.

The reviewer MC declared a shared affiliation with the authors at the time of review.

Publisher's note

References

An, S., Sun, H., Wu, M., Xie, D., Hu, S. W., Ding, H. L., et al. (2021). Medial septum glutamatergic neurons control wakefulness through a septo-hypothalamic circuit. *Curr. Biol.* 31 (7), 1379–1392.e4. doi:10.1016/j.cub.2021.01.019

Ang, S. T., Ariffin, M. Z., and Khanna, S. (2017). The forebrain medial septal region and nociception. *Neurobiol. Learn Mem.* 138, 238–251. doi:10.1016/j.nlm.2016.07.017

Ang, S. T., Lee, A. T., Foo, F. C., Ng, L., Low, C. M., and Khanna, S. (2015). GABAergic neurons of the medial septum play a nodal role in facilitation of nociception-induced affect. *Sci. Rep.* 5, 15419. doi:10.1038/srep15419

Ariffin, M. Z., Ibrahim, K. M., Lee, A. T., Lee, R. Z., Poon, S. Y., Thong, H. K., et al. (2018). Forebrain medial septum sustains experimental neuropathic pain. *Sci. Rep.* 8 (1), 11892. doi:10.1038/s41598-018-30177-3

Ariffin, M. Z., Jiang, F., Low, C. M., and Khanna, S. (2010). Nicotinic receptor mechanism in supramammillary nucleus mediates physiological regulation of neural activity in dorsal hippocampal field CA1 of anaesthetized rat. *Hippocampus* 20 (7), 852–865. doi:10.1002/hipo.20687

Baron, R., Binder, A., and Wasner, G. (2010). Neuropathic pain: Diagnosis, pathophysiological mechanisms, and treatment. *Lancet Neurol.* 9 (8), 807–819. doi:10.1016/S1474-4422(10)70143-5

Baron, R. (2006). Mechanisms of disease: Neuropathic pain--a clinical perspective. *Nat. Clin. Pract. Neurol.* 2 (2), 95–106. doi:10.1038/ncpneuro0113

Bennett, G. J., and Xie, Y. K. (1988). A peripheral mononeuropathy in rat that produces disorders of pain sensation like those seen in man. *Pain* 33 (1), 87–107. doi:10.1016/0304-3959(88)90209-6

Bonin, R. P., Bories, C., and De Koninck, Y. (2014). A simplified up-down method (SUDO) for measuring mechanical nociception in rodents using von Frey filaments. *Mol. Pain* 10, 26. doi:10.1186/1744-8069-10-26

Bonnavion, P., Mickelsen, L. E., Fujita, A., de Lecea, L., and Jackson, A. C. (2016). Hubs and spokes of the lateral hypothalamus: Cell types, circuits and behaviour. *J. Physiol.* 594 (22), 6443–6462. doi:10.1113/JP271946

Borhegyi, Z., and Freund, T. F. (1998). Dual projection from the medial septum to the supramammillary nucleus in the rat. *Brain Res. Bull.* 46 (5), 453–459. doi:10.1016/s0361-9230(98)00038-0

Braida, D., Ponzoni, L., Martucci, R., Sparatore, F., Gotti, C., and Sala, M. (2014). Role of neuronal nicotinic acetylcholine receptors (nAChRs) on learning and memory in zebrafish. *Psychopharmacol. Berl.* 231 (9), 1975–1985. doi:10.1007/s00213-013-3340-1

Burstein, R., Cliffer, K. D., and Giesler, G. J. (1987). Direct somatosensory projections from the spinal cord to the hypothalamus and telencephalon. *J. Neurosci.* 7 (12), 4159–4164. doi:10.1523/JNEUROSCI.07-12-04159.1987

Calandreau, L., Jaffard, R., and Desmedt, A. (2007). Dissociated roles for the lateral and medial septum in elemental and contextual fear conditioning. *Learn Mem.* 14 (6), 422–429. doi:10.1101/lm.531407

Carstens, E., MacKinnon, J. D., and Guinan, M. J. (1982). Inhibition of spinal dorsal horn neuronal responses to noxious skin heating by medial preoptic and septal stimulation in the cat. *J. Neurophysiol.* 48 (4), 981–989. doi:10.1152/jn.1982.48.4.981

Chen, L., Cai, P., Wang, R. F., Lu, Y. P., Chen, H. Y., Guo, Y. R., et al. (2020). Glutamatergic lateral hypothalamus promotes defensive behaviors. *Neuropharmacology* 178, 108239. doi:10.1016/j.neuropharm.2020.108239

Chen, Z., Chen, G., Zhong, J., Jiang, S., Lai, S., Xu, H., et al. (2022). A circuit from lateral septum neurotensin neurons to tuberal nucleus controls hedonic feeding. *Mol. Psychiatry* 27 (12), 4843–4860. doi:10.1038/s41380-022-01742-0

Cohen, S. P., Vase, L., and Hooten, W. M. (2021). Chronic pain: An update on burden, best practices, and new advances. *Lancet* 397 (10289), 2082–2097. doi:10.1016/S0140-6736(21)00393-7

Collins, S., Sigtermans, M. J., Dahan, A., Zuurmond, W. W., and Perez, R. S. (2010). NMDA receptor antagonists for the treatment of neuropathic pain. *Pain Med.* 11 (11), 1726–1742. doi:10.1111/j.1526-4637.2010.00981.x

Colom, L. V., Castaneda, M. T., Reyna, T., Hernandez, S., and Garrido-Sanabria, E. (2005). Characterization of medial septal glutamatergic neurons and their projection to the hippocampus. *Synapse* 58 (3), 151–164. doi:10.1002/syn.20184

Culp, C., Kim, H. K., and Abdi, S. (2020). Ketamine use for cancer and chronic pain management. *Front. Pharmacol.* 11, 599721. doi:10.3389/fphar.2020.599721

Danisman, B., Akcay, G., Gokcek-Sarac, C., Kantar, D., Aslan, M., and Derin, N. (2022). The role of acetylcholine on the effects of different doses of sulfite in learning and memory. *Neurochem. Res.* 47 (11), 3331–3343. doi:10.1007/s11064-022-03684-z

de Jong, J. W., Afjei, S. A., Pollak Dorocic, I., Peck, J. R., Liu, C., Kim, C. K., et al. (2019). A neural circuit mechanism for encoding aversive stimuli in the mesolimbic dopamine system. *Neuron* 101 (1), 133–151. doi:10.1016/j.neuron.2018.11.005

Dragunow, M., and Faull, R. (1989). The use of c-fos as a metabolic marker in neuronal pathway tracing. *J. Neurosci. Methods* 29 (3), 261–265. doi:10.1016/0165-0270(89)90150-7

Dutar, P., Bassant, M. H., Senut, M. C., and Lamour, Y. (1995). The septohippocampal pathway: Structure and function of a central cholinergic system. *Physiol. Rev.* 75 (2), 393–427. doi:10.1152/physrev.1995.75.2.393

Dutar, P., Lamour, Y., and Jobert, A. (1985). Activation of identified septo-hippocampal neurons by noxious peripheral stimulation. *Brain Res.* 328 (1), 15–21. doi:10.1016/0006-8993(85)91317-4

Fakhoury, M., Salman, I., Najjar, W., Merhej, G., and Lawand, N. (2020). The lateral hypothalamus: An uncharted territory for processing peripheral neurogenic inflammation. *Front. Neurosci.* 14, 101. doi:10.3389/fnins.2020.00101

Farrell, J. S., Lovett-Barron, M., Klein, P. M., Sparks, F. T., Gschwind, T., Ortiz, A. L., et al. (2021). Supramammillary regulation of locomotion and hippocampal activity. *Science* 374 (6574), 1492–1496. doi:10.1126/science.abh4272

Fitzcharles, M. A., Cohen, S. P., Clauw, D. J., Littlejohn, G., Usui, C., and Hauser, W. (2021). Nociplastic pain: Towards an understanding of prevalent pain conditions. *Lancet* 397 (10289), 2098–2110. doi:10.1016/S0140-6736(21)00392-5

Fremeau, R. T., Jr., Kam, K., Qureshi, T., Johnson, J., Copenhagen, D. R., Storm-Mathisen, J., et al. (2004). Vesicular glutamate transporters 1 and 2 target to functionally distinct synaptic release sites. *Science* 304 (5678), 1815–1819. doi:10.1126/science.1097468

Freund, T. F. (1989). GABAergic septohippocampal neurons contain parvalbumin. *Brain Res.* 478 (2), 375–381. doi:10.1016/0006-8993(89)91520-5

Gol, A. (1967). Relief of pain by electrical stimulation of the septal area. *J. Neurol. Sci.* 5 (1), 115–120. doi:10.1016/0022-510x(67)90012-3

Griffith, W. H., and Matthews, R. T. (1986). Electrophysiology of AChE-positive neurons in basal forebrain slices. *Neurosci. Lett.* 71 (2), 169–174. doi:10.1016/0304-3940(86)90553-7

Hagains, C. E., He, J. W., Chiao, J. C., and Peng, Y. B. (2011). Septal stimulation inhibits spinal cord dorsal horn neuronal activity. *Brain Res.* 1382, 189–197. doi:10.1016/j.brainres.2011.01.074

Hansen, K. B., Ogden, K. K., Yuan, H., and Traynelis, S. F. (2014). Distinct functional and pharmacological properties of Triheteromeric GluN1/GluN2A/GluN2B NMDA receptors. *Neuron* 81 (5), 1084–1096. doi:10.1016/j.neuron.2014.01.035

Hargreaves, K., Dubner, R., Brown, F., Flores, C., and Joris, J. (1988). A new and sensitive method for measuring thermal nociception in cutaneous hyperalgesia. *Pain* 32 (1), 77–88. doi:10.1016/0304-3959(88)90026-7

Hasselmo, M. E. (2006). The role of acetylcholine in learning and memory. *Curr. Opin. Neurobiol.* 16 (6), 710–715. doi:10.1016/j.conb.2006.09.002

Henny, P., Brischoux, F., Mainville, L., Stroh, T., and Jones, B. E. (2010). Immunohistochemical evidence for synaptic release of glutamate from orexin terminals in the locus coeruleus. *Neuroscience* 169 (3), 1150–1157. doi:10.1016/j.neuroscience.2010.06.003

Inutsuka, A., Yamashita, A., Chowdhury, S., Nakai, J., Ohkura, M., Taguchi, T., et al. (2016). The integrative role of orexin/hypocretin neurons in nociceptive perception and analgesic regulation. *Sci. Rep.* 6, 29480. doi:10.1038/srep29480

Jiang, W., Tang, M., Yang, L., Zhao, X., Gao, J., Jiao, Y., et al. (2022). Analgesic alkaloids derived from traditional Chinese medicine in pain management. *Front. Pharmacol.* 13, 851508. doi:10.3389/fphar.2022.851508

Jiang, Y. Y., Shao, S., Zhang, Y., Zheng, J., Chen, X., Cui, S., et al. (2018a). Neural pathways in medial septal cholinergic modulation of chronic pain: Distinct contribution of the anterior cingulate cortex and ventral hippocampus. *Pain* 159 (8), 1550–1561. doi:10.1097/j.pain.0000000000001240

Jiang, Y. Y., Zhang, Y., Cui, S., Liu, F. Y., Yi, M., and Wan, Y. (2018b). Cholinergic neurons in medial septum maintain anxiety-like behaviors induced by chronic inflammatory pain. *Neurosci. Lett.* 671, 7–12. doi:10.1016/j.neulet.2018.01.041

Kiss, J., Patel, A. J., Baimbridge, K. G., and Freund, T. F. (1990). Topographical localization of neurons containing parvalbumin and choline acetyltransferase in the medial septum-diagonal band region of the rat. *Neuroscience* 36 (1), 61–72. doi:10.1016/0306-4522(90)90351-4

Knowland, D., Lilascharoen, V., Pacia, C. P., Shin, S., Wang, E. H., and Lim, B. K. (2017). Distinct ventral pallidal neural populations mediate separate symptoms of depression. *Cell* 170 (2), 284–297. doi:10.1016/j.cell.2017.06.015

Lee, A. T., Ariffin, M. Z., Zhou, M., Ye, J. Z., Moochhala, S. M., and Khanna, S. (2011). Forebrain medial septum region facilitates nociception in a rat formalin model of inflammatory pain. *Pain* 152 (11), 2528–2542. doi:10.1016/j.pain.2011.07.019

Leung, L. S., Ma, J., Shen, B., Nachim, I., and Luo, T. (2013). Medial septal lesion enhances general anesthesia response. *Exp. Neurol.* 247, 419–428. doi:10.1016/j.expneurol.2013.01.010

Li, X. H., Miao, H. H., and Zhuo, M. (2019). NMDA receptor dependent long-term potentiation in chronic pain. *Neurochem. Res.* 44 (3), 531–538. doi:10.1007/s11064-018-2614-8

Li, Y., Zeng, J., Zhang, J., Yue, C., Zhong, W., Liu, Z., et al. (2018). Hypothalamic circuits for predation and evasion. *Neuron* 97 (4), 911–924. doi:10.1016/j.neuron.2018.01.005

Lu, L., Pan, C., Chen, L., Hu, L., Wang, C., Han, Y., et al. (2017). AMPK activation by peri-sciatic nerve administration of ozone attenuates CCI-induced neuropathic pain in rats. *J. Mol. Cell Biol.* 9 (2), 132–143. doi:10.1093/jmcb/mjw043

Ma, J., and Leung, L. S. (2006). Limbic system participates in mediating the effects of general anesthetics. *Neuropsychopharmacology* 31 (6), 1177–1192. doi:10.1038/sj.npp.1300909

Ma, J., Shen, B., Stewart, L. S., Herrick, I. A., and Leung, L. S. (2002). The septohippocampal system participates in general anesthesia. *J. Neurosci.* 22 (2), RC200. doi:10.1523/JNEUROSCI.22-02-j0004.2002

Markram, H., and Segal, M. (1990). Electrophysiological characteristics of cholinergic and non-cholinergic neurons in the rat medial septum-diagonal band complex. *Brain Res.* 513 (1), 171–174. doi:10.1016/0006-8993(90)91106-q

McNaughton, N., Ruan, M., and Woodnorth, M. A. (2006). Restoring theta-like rhythmicity in rats restores initial learning in the Morris water maze. *Hippocampus* 16 (12), 1102–1110. doi:10.1002/hipo.20235

Murray, C. J., Atkinson, C., Bhalla, K., Birbeck, G., Burstein, R., Chou, D., et al. (2013). The state of US health, 1990-2010: Burden of diseases, injuries, and risk factors. *JAMA* 310 (6), 591–608. doi:10.1001/jama.2013.13805

Nieh, E. H., Vander Weele, C. M., Matthews, G. A., Presbrey, K. N., Wichmann, R., Leppla, C. A., et al. (2016). Inhibitory input from the lateral hypothalamus to the ventral tegmental area disinhibits dopamine neurons and promotes behavioral activation. *Neuron* 90 (6), 1286–1298. doi:10.1016/j.neuron.2016.04.035

Pedersen, N. P., Ferrari, L., Venner, A., Wang, J. L., Abbott, S. B. G., Vujovic, N., et al. (2017). Supramammillary glutamate neurons are a key node of the arousal system. *Nat. Commun.* 8 (1), 1405. doi:10.1038/s41467-017-01004-6

Rondon, L. J., Privat, A. M., Daulhac, L., Davin, N., Mazur, A., Fialip, J., et al. (2010). Magnesium attenuates chronic hypersensitivity and spinal cord NMDA receptor phosphorylation in a rat model of diabetic neuropathic pain. *J. Physiol.* 588 (21), 4205–4215. doi:10.1113/jphysiol.2010.197004

Rosin, D. L., Weston, M. C., Sevigny, C. P., Stornetta, R. L., and Guyenet, P. G. (2003). Hypothalamic orexin (hypocretin) neurons express vesicular glutamate transporters VGLUT1 or VGLUT2. *J. Comp. Neurol.* 465 (4), 593–603. doi:10.1002/cne.10860

Schvarcz, J. R. (1993). Long-term results of stimulation of the septal area for relief of neurogenic pain. *Acta Neurochir. Suppl. (Wien)* 58, 154–155. doi:10.1007/978-3-7091-9297-9_35

Siemian, J. N., Arenivar, M. A., Sarsfield, S., Borja, C. B., Erbaugh, L. J., Eagle, A. L., et al. (2021). An excitatory lateral hypothalamic circuit orchestrating pain behaviors in mice. *Elife* 10, e66446. doi:10.7554/eLife.66446

Takeuchi, Y., Nagy, A. J., Barcsai, L., Li, Q., Ohsawa, M., Mizuseki, K., et al. (2021). The medial septum as a potential target for treating brain disorders associated with oscillopathies. *Front. Neural Circuits* 15, 701080. doi:10.3389/fncir.2021.701080

Tang, W., Zhou, D., Wang, S., Hao, S., Wang, X., Helmy, M., et al. (2021). CRH neurons in the laterodorsal tegmentum mediate acute stress-induced anxiety. *Neurosci. Bull.* 37 (7), 999–1004. doi:10.1007/s12264-021-00684-x

Tsetsenis, T., Badyna, J. K., Wilson, J. A., Zhang, X., Krizman, E. N., Subramaniyan, M., et al. (2021). Midbrain dopaminergic innervation of the hippocampus is sufficient to modulate formation of aversive memories. *Proc. Natl. Acad. Sci. U. S. A.* 118 (40), e2111069118. doi:10.1073/pnas.2111069118

Wang, D., Pan, X., Zhou, Y., Wu, Z., Ren, K., Liu, H., et al. (2023). Lateral septum-lateral hypothalamus circuit dysfunction in comorbid pain and anxiety. *Mol. Psychiatry* 28, 1090–1100. doi:10.1038/s41380-022-01922-y

Wang, H. R., Guo, H., Jiang, S. Y., Liu, Z. L., Qu, W. M., Huang, Z. L., et al. (2021b). Control of wakefulness by lateral hypothalamic glutamatergic neurons in male mice. *J. Neurosci. Res.* 99 (6), 1689–1703. doi:10.1002/jnr.24828

Wang, H. R., Hu, S. W., Zhang, S., Song, Y., Wang, X. Y., Wang, L., et al. (2021a). KCNQ channels in the mesolimbic reward circuit regulate nociception in chronic pain in mice. *Neurosci. Bull.* 37 (5), 597–610. doi:10.1007/s12264-021-00668-x

Wang, H. R., Wang, J., Xia, S. H., Gutstein, H. B., Huang, Y. H., Schluter, O. M., et al. (2021c). Neuropathic pain generates silent synapses in thalamic projection to anterior cingulate cortex. *Pain* 162 (5), 1322–1333. doi:10.1097/j.pain.0000000000002149

Xia, T., Cui, Y., Qian, Y., Chu, S., Song, J., Gu, X., et al. (2016). Regulation of the NR2B-CREB-CRTC1 signaling pathway contributes to circadian pain in murine model of chronic constriction injury. *Anesth. Analg.* 122 (2), 542–552. doi:10.1213/ANE.0000000000000991

Xiang, X., Chen, Y., Li, K. X., Fang, J., Bickler, P. E., Guan, Z., et al. (2022). Neuroanatomical basis for the orexinergic modulation of anesthesia arousal and pain control. *Front. Cell Neurosci.* 16, 891631. doi:10.3389/fncel.2022.891631

Yu, N., Song, H., Chu, G., Zhan, X., Liu, B., Mu, Y., et al. (2022). Basal forebrain cholinergic innervation induces depression-like behaviors through ventral subiculum hyperactivation. *Neurosci. Bull.* 39, 617–630. doi:10.1007/s12264-022-00962-2

Zhang, H., Qian, Y. L., Li, C., Liu, D., Wang, L., Wang, X. Y., et al. (2017). Brain-derived neurotrophic factor in the mesolimbic reward circuitry mediates nociception in chronic neuropathic pain. *Biol. Psychiatry* 82 (8), 608–618. doi:10.1016/j.biopsych.2017.02.1180

Zhao, S., Li, R., Li, H., Wang, S., Zhang, X., Wang, D., et al. (2021). Lateral hypothalamic area glutamatergic neurons and their projections to the lateral habenula modulate the anesthetic potency of isoflurane in mice. *Neurosci. Bull.* 37 (7), 934–946. doi:10.1007/s12264-021-00674-z

Zheng, F., and Khanna, S. (2001). Selective destruction of medial septal cholinergic neurons attenuates pyramidal cell suppression, but not excitation in dorsal hippocampus field CA1 induced by subcutaneous injection of formalin. *Neuroscience* 103 (4), 985–998. doi:10.1016/s0306-4522(01)00006-9

frontiers | Frontiers in Pharmacology

TYPE Original Research
PUBLISHED 05 June 2023
DOI 10.3389/fphar.2023.1207020

OPEN ACCESS

EDITED BY
Zezhi Li,
Guangzhou Medical University, China

REVIEWED BY
Pengfei Xu,
Beijing Normal University, China
Shen Li,
Tianjin Medical University, China

*CORRESPONDENCE
Guidong Zhu,
hzzcer@126.com
Dongsheng Zhou,
wyzhouds@sina.com
Weiqian Xu,
zjttxwq@163.com

†These authors have contributed equally to this work

RECEIVED 17 April 2023
ACCEPTED 24 May 2023
PUBLISHED 05 June 2023

CITATION
Li X, Chen M, Liu Q, Zheng C, Yu C, Hou G, Chen Z, Chen Y, Chen Y, Zhu G, Zhou D and Xu W (2023), TMS-evoked potential in the dorsolateral prefrontal cortex to assess the severity of depression disease: a TMS-EEG study.
Front. Pharmacol. 14:1207020.
doi: 10.3389/fphar.2023.1207020

TMS-evoked potential in the dorsolateral prefrontal cortex to assess the severity of depression disease: a TMS-EEG study

Xingxing Li[1†], Meng Chen[1†], Qinqin Liu[2], Chao Zheng[1], Chang Yu[1], Guangwei Hou[3], Zan Chen[1], Yiqing Chen[3], Yinping Chen[3], Guidong Zhu[4*], Dongsheng Zhou[1*] and Weiqian Xu[5*]

[1]Ningbo Kangning Hospital, Ningbo, Zhejiang, China, [2]Qingdao Mental Health Center, Qingdao, Shandong, China, [3]Yu Yao Third People's Hospital, Ningbo, Zhejiang, China, [4]The Second People's Hospital of Lishui, Lishui, Zhejiang, China, [5]Taizhou Second People's Hospital, Taizhou, Zhejiang, China

Objective: The combined use of transcranial magnetic stimulation and electroencephalography (TMS-EEG), as a powerful technique that can non-invasively probe the state of the brain, can be used as a method to study neurophysiological markers in the field of psychiatric disorders and discover potential diagnostic predictors. This study used TMS-evoked potentials (TEPs) to study the cortical activity of patients with major depressive disorder depression (MDD) and the correlation with clinical symptoms to provide an electrophysiological basis for the clinical diagnosis.

Methods: A total of 41 patients and 42 healthy controls were recruited to study. Using TMS-EEG techniques to measure the left dorsolateral prefrontal cortex (DLPFC) 's TEP index and evaluate the clinical symptoms of MDD patients using the Hamilton Depression Scale-24 (HAMD-24).

Results: MDD subjects performing TMS-EEG on the DLPFC showed lower cortical excitability P60 index levels than healthy controls. Further analysis revealed that the degree of P60 excitability within the DLPFC of MDD patients was significantly negatively correlated with the severity of depression.

Conclusion: The low levels of P60 exhibited in DLPFC reflect low excitability in MDD; the P60 component can be used as a biomarker for MDD in clinical assessment tools.

KEYWORDS

tmseeg, depression, psychology, DLPFC (dorsolateral prefrontal cortex), TEPS, HAMD, hamilton depression rating scale

1 Introduction

Depression is a mood disorder characterized by persistent depression and varying degrees of cognitive and behavioral changes (McCarron et al., 2021). Its high prevalence, high recurrence rate, high suicide rate, low recognition rate, and low cure rate have caused a severe burden to the patients themselves, their families, and society (Touloumis, 2021). Seeking potential biomarkers of depression patients can provide new strategies for early recognition and intervention of depression.

The dorsolateral prefrontal cortex (DLPFC) is considered the control center of emotion and cognition (Segal and Elkana, 2023). Patients with depression are believed to have functional and structural abnormalities in DLPFC, such as reduced volume, abnormal activity patterns, or abnormal available connection networks (Koenigs and Grafman, 2009). Repetitive transcranial magnetic stimulation (rTMS) is widely used to treat depression. The stimulation site is also selected for the left DLPFC, which is believed to effectively improve patients' clinical symptoms with depression (Kan et al., 2023). In most depression patients, the left DLPFC has shown low activity and low metabolism in functional neuroimaging studies, leading to the disturbance of neurotransmitter levels, such as glutamate and γ- Aminobutyric acid (Duman et al., 2019). Therefore, studying the EEG signals of left DLPFC has important significance for depression.

TMS generates a transient time-varying magnetic field, producing a transient electric field in the brain through electromagnetic conduction to depolarize or polarize neurons (Klomjai et al., 2015). TMS-EEG, which is formed by the combination of synchronous TMS and electroencephalography (EEG), has become a powerful tool for the non-invasive detection of human brain circuits, thus evaluating several cortical characteristics such as excitability and connectivity (Cao et al., 2021). Sun used TMS-EEG to assess whether baseline cortical inhibition in depression patients can predict the effect of treatment on suicidal ideation. Voneskos used TMS-EEG to compare the difference between DLPFC inhibition and excitation in depression and healthy controls (Sun et al., 2018; Voineskos et al., 2019). This technology has been applied to different clinical populations in recent years (C. T. Li et al., 2022; Strafella et al., 2023). Disease-related predictors can be found through this technology, providing markers for the pathophysiology of brain diseases.

As far as we know, few previous studies have used TMS-EEG to study depression, and the sample size is small. We want to find TEP in DLPFC induced by TMS-EEG as a potential biomarker to distinguish depression from healthy controls, and further clarify the relationship between this marker and the severity of depression, providing the theoretical basis for the clinical diagnosis and treatment of depression.

2 Materials and methods

2.1 Subject and assessment

The project recruited a total of 41 depression patients (9 male/32 female) in Ningbo Kangning Hospital from November 2021 to October 2022. Two psychiatrists evaluated all patients as assessed by the Structured Clinical Interview for the Diagnostic and Statistical Manual of Mental Disorders (DSM-V). Additional inclusion criteria were: 1) Age 16–65 years, 2) Hamilton Depression Scale-24 score (HAMD-24) ≥ 20 points; 3) All patients or guardians know the purpose of the experiment and sign an informed consent form.

Exclusion criteria: 1) Patients with severe somatic diseases, infectious diseases, and immune system diseases; 2) Accompany with other mental illnesses or severe neurological diseases.

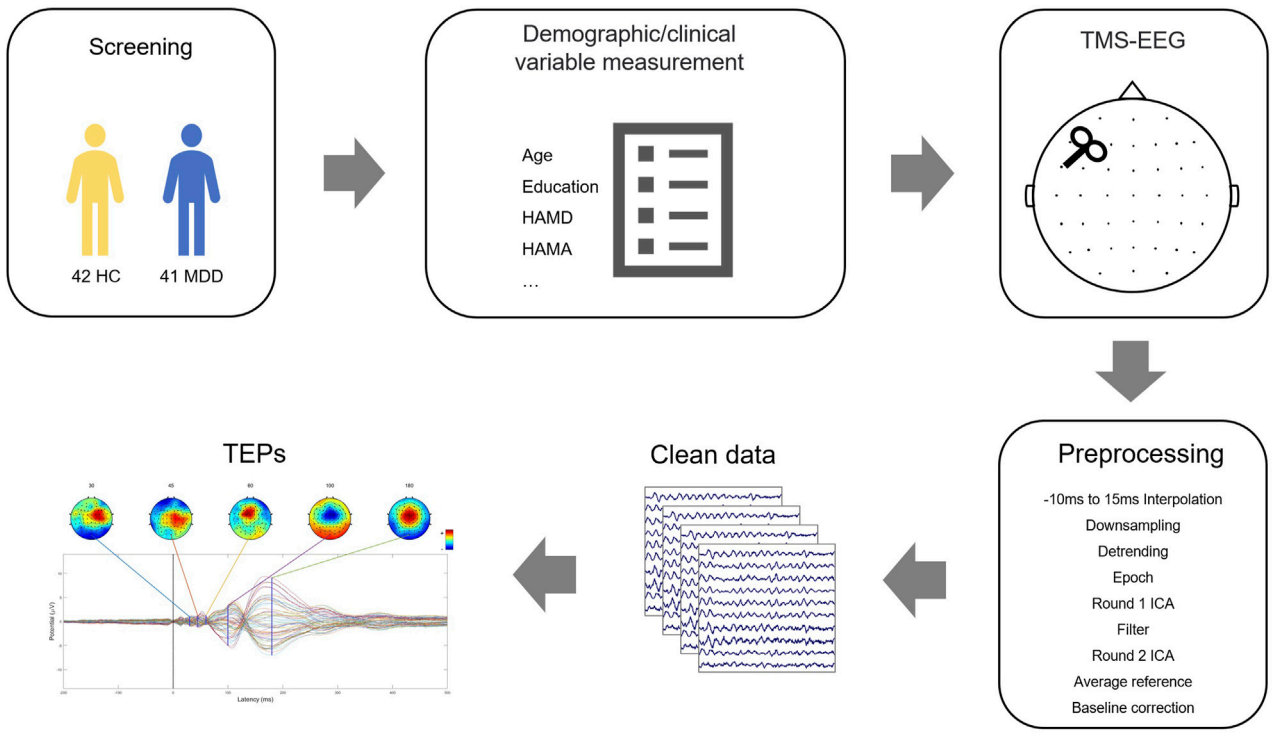

FIGURE 1
Schematic diagram of the experimental process and TMS-EEG data processing framework.

TABLE 1 Demographic and clinical information of the HC and MDD group.

	HC[a] (*n* = 42)	MDD[b] (*n* = 41)	*t* (*χ2*)	*p*
	M(SE)	*M(SE)*		
Gender			0.21	0.65
male	11	9		
female	31	32		
Age	31.48 (1.35)	29.29 (2.51)	0.77	0.44
Education (years)	15.67 (0.53)	10.95 (0.51)	6.42	<0.001***
HAMD-24	5.02 (0.31)	24.49 (0.10)	−20.22	<0.001***
HAMA-14	4.02 (0.30)	17.27 (1.02)	−12.46	<0.001***

[a]*HC*, healthy controls.
[b]*MDD*, individuals with major depressive disorder.
HDRS-24, Hamilton Depression Rating Scale-24; HAMA-14, Hamilton Anxiety Scale-14.

At the same time, we recruited 42 healthy controls in the community and matched them with MDD patients in terms of gender and age. We also excluded people with other mental diseases, basic diseases (such as stroke, diabetes, etc.), or alcohol disorders. The flow is shown in Figure 1.

The ethics committee of Ningbo Kangning Hospital approved the project, and all experimental procedures were conducted in accordance with the guidelines for human medical research (Helsinki Declaration). Before enrollment, the research protocol was registered at Chictr.org.cn (ChiCTR2100052007).

2.2 Assessment

The HAMD-24 items evaluated the depressive symptoms. The participants participated in the evaluation training of the scale before the study and re-evaluated each month to ensure that their correlation coefficient (ICC) remained above 0.8 to keep their scores consistent and reliable. The scores of HAMD-24 ≥ 20 points are classified as a depression group. The HAMD-24 scale can better reflect the severity of the condition. The more severe the condition, the higher the total score. Demographic information is a form of information collected through self-designed demographic statistics. Structured clinical interviews are used to process medical history.

2.3 TMS-EEG testing

TMS-EEG research collects data from TMS (Magstim Ltd, Oxford, United Kingdom) and TMS-compatible 64-channel EEG (Easycap, Germany). The figure-of-eight coil (Coil—D70-air film coil, Magstim) was placed over the F3 (roughly used to represent the left DLPFC brain region). The splay lock is tangent to the scalp and the handle points rearward at a 45° angle. Before TMS-EEG recording, all patients underwent a resting motion threshold (RMT) test to determine the stimulation intensity. RMT uses the necessary minimum stimulus intensity to determine the apparent motor response of the right abductor pollicis brevis (APB). Generally, at least five of the ten stimuli have an amplitude of ≥ 50 mV.

FCz and AFz are used as recording reference and ground electrodes, respectively. Use BrainVision Recorder software (BrainProducts, Germany) to record the EEG signal at a sampling rate of 25 kHz during the acquisition process. During the experiment, ensure the electrode impedance is kept below 5 k Ω. During TMS-EEG recording, 100 single TMS pulse stimuli were performed at F3 using a 100% RMT intensity. The interval between the individual stimuli was randomly generated over 5 s, and the patient kept their eyes open during the recording period. We also put earplugs on patients to prevent related auditory evoked potentials from being generated during stimulation.

2.4 TMS-EEG analysis

TMS-EEG data were analyzed offline using Matlab R2016b (MathWorks, United States) and in combination with the EEGLAB (Delorme and Makeig, 2004) and ARTIST (Wu et al., 2018) toolboxes. The preprocessing code was adapted from the fully automated artifact suppression algorithm for monopulse TMS-EEG (spTMS-EG), which consists of the following steps. The time window containing TMS pulse artifacts was first removed and replaced with an interpolation (−5–15 ms). Then the EEG data were downsampled to 1 kHz to reduce the file size. After data segmentation of TMS pulses (−2000–2000 ms), large fading artifacts are automatically removed using the first ICA based on thresholding. Band-pass filtering (1–100 Hz) is performed for slow drift and high-frequency noise. 50 Hz Alternating Current line noise artifacts are removed by a trap filter (48–52 Hz). Bad trials with signal amplitudes exceeding 3 standard deviations from the test mean are rejected. Bad channels were identified and interpolated by adjacent trials. Remaining artifacts, such as scalp muscle artifacts and eye artifacts, were automatically removed using a second ICA. Clean EEG data were then re-referenced to the common mean and corrected to the pre-TMS pulse baseline (−550 ms−−50 ms).

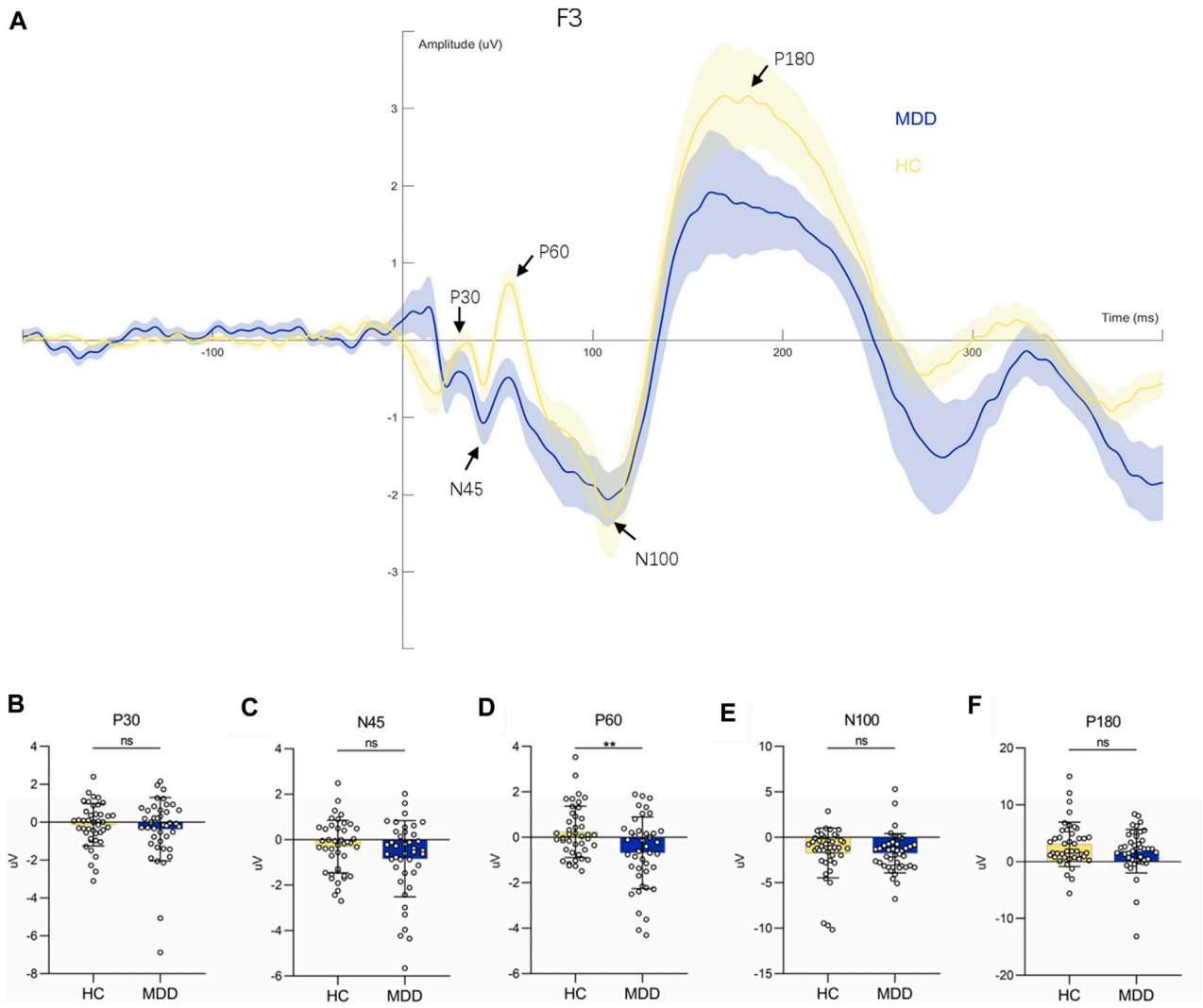

FIGURE 2
Waveform diagram at F3 electrode and comparison of each component. **(A)**: TEPs induced by stimulation of F3 electrodes. **(B–F)**: Comparison of P30, N45, P60, N100 and P180 components between HC and MDD respectively.

2.5 Statistical analysis

All of the data analyses used the Statistical Package for the Social Sciences (SPSS version 23, IBM). All data are expressed as mean ± SD; The data were tested for normality using Kolmogorov–Smirnov. For continuous variables, two-sample t-tests were used when comparing baseline (i.e., HC vs. MDD), but the Wilcoxon signed-rank test was used if the normality assumption was not satisfied. For categorical variables, chi-square tests were used. Analysis of covariance was used where necessary to control for the effect of covariates on the results.

In MDD patients, the Pearson correlation was used to analyze the correlation between the TEP index and the severity of depression. In addition, a linear logistic regression analysis was conducted to determine the factors related to depression. The statistically significant difference was set to $p < 0.05$; all tests were two-tailed.

3 Results

3.1 Demographic and clinical assessments

The demographic and clinical information of the participants is listed in Table 1. There was no significant difference between the MDD and HC groups in age and gender (all $p > 0.05$) except educational attainment ($p < 0.001$). Moreover, MDD exhibited higher depression and anxiety scores than healthy controls (all $p < 0.001$).

3.2 TEP differences between MDD and HC control in DLPFC

We investigated the potentials evoked by TMS pulses at the stimulation target, i.e., F3 (see Figure 2A). The P60 amplitude in individuals with MDD was significantly lower than that of the

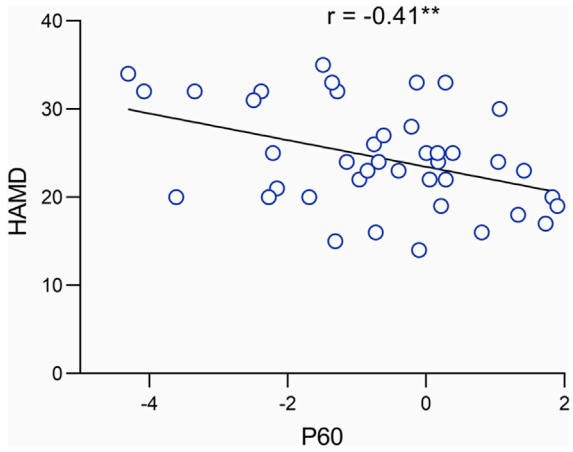

FIGURE 3
Correlation of P60 component with depression severity.

healthy controls (F = 7.44, p = 0.008**. see Figure 2D). The amplitudes of the other components did not reach significant differences between the two groups (for P30 amplitude, F = 0.40, p = 0.53; for N45 amplitude, F = 1.91, p = 0.17; for N100 amplitude, F = 0.05, p = 0.83; for P180 amplitude, F = 0.66, p = 0.42) see Figures 2B, C, E, F. Covariates in the RM MANOVA analysis included educational attainment.

3.3 Association between depressive symptoms and P60

We performed a Pearson correlation analysis to investigate further the role of P60 abnormalities in the neuropathology of MDD. The results indicated that the amplitude of the P60 component was significantly and negatively correlated with the severity of depression (r = −0.41, p = 0.008**. See Figure 3).

3.4 Regression analysis

To investigate whether P60 could be used as a biomarker to examine depressive symptoms, we created a regression model of depression severity. Considering the mismatch in education attainment between the individuals with MDD and HC, it was necessary to control for educational attainment as a covariate. The results indicated that the P60 could significantly predict depressive symptoms (B = −1.5, CI -2.61—−0.40, t = −2.75, p = 0.009**).

4 Discussion

Compared to previous studies using TMS-EEG techniques to assess cortical inhibition. This study provides evidence for abnormal DLPFC excitability in MDD patients compared with healthy control. The results showed that the cortical excitability index (P60) measured by TMS-EEG was lower in MDD. More importantly, this decreased cortical excitability in DLPFC correlates with the severity of depressive symptoms. Taken together, the P60 index induced by TMS may be of great significance for the diagnosis of depression.

Abnormal DLPFC excitability is an important neural mechanism of depression. Previous experiments have reportedly typically used TMS-evoked motor potentials (MEPs) to study abnormal cortical excitability and inhibition in MDD patients (Oliveira-Maia et al., 2017; Khedr et al., 2020; Castricum et al., 2022; Li et al., 2023). However. the non-motor cortex has been less studied (mostly using TMS-evoked potentials (TEPs), and previous studies have mostly been based on global mean field amplitudes used to reveal changes in cortical excitability at the whole brain level (Cao et al., 2021). Furthermore, TEPs are more sensitive than MEPs in studying cortical excitability. this can be recorded in local and distal electrodes, allowing the study of the spread of activation in cortical areas. And TEPs are evoked only after stimulation of intact functional areas of the cortex, providing direct evidence that TEPs reflect cortical activity rather than electrical or physiological artifacts (Jannati et al., 2023). The DLPFC is particularly important in the neuropathology of MDD, and TMS-EEG allows direct assessment of its excitatory and inhibitory properties, with hypoexcitability of the DLPFC associated with impaired emotion regulation and cognitive control, thereby increasing the risk of undesirable behaviors in response to negative stimuli (Koenigs and Grafman, 2009). Previous studies have identified abnormal expression of DLPFC in MDD patients, mainly in the form of low activity and hypometabolism of DLPFC in neuroimaging studies (Ma, 2015; Zhang et al., 2021). Moreover, improved clinical symptoms in depressed patients after treatment with antidepressants are associated with increased activity of the left DLPFC (George and Post, 2011). Our findings are consistent with the above conclusion that depressed patients with DLPFC exhibit hypoactivation, i.e., low amplitude of p60, which is thought to correlate with excitability and inhibition.

Some evidence suggests that the balance of inhibition and excitation in the DLPFC is altered in patients with major depression. Animal models of major depression show a decrease in GABAergic interneurons, mainly in the DLPFC region, while human imaging studies using magnetic resonance spectroscopy have also shown altered GABA levels in the DLPFC (Rajkowska et al., 2007; Godfrey et al., 2018). These studies support that prefrontal inhibition is an important feature of major depression, but little has been done to link altered prefrontal excitability to the neuropathological mechanisms of MDD. Previous studies have shown that P60 reflects cortical excitatory mechanisms involving NMDA and glutamatergic-mediated neurotransmission processes (Gordon et al., 2023). Noda et al. found a correlation between P60 and N100 in healthy individuals induced using a short-interval intracortical inhibition paradigm. This correlation was suggested to be explained by a correlation with glutamate and GABA receptor-mediated excitation-inhibition balance (Cash et al., 2017). Belardinelli et al. investigated the effects of anti-glutamatergic drugs on TMS-evoked potentials and showed that the effects of AMPA receptor antagonists on TMS-evoked potentials reduced the amplitude of P60, reflecting that P60 may be associated with AMPA receptor activation-mediated glutamatergic signal propagation. It is further suggested that P60 may reflect glutamatergic-mediated cortical excitability (Belardinelli et al., 2021). Glutamate is a

central factor in mood disorders. It has been found that the excitatory neurotransmitter glutamate levels are generally reduced in MDD, especially in the prefrontal cortex (Abdallah et al., 2014; Henter et al., 2021; Kantrowitz et al., 2021). Also, glutamate receptor antagonists are more effective in combination with transcranial magnetic therapy for MDD (Best et al., 2019; Elkrief et al., 2022). In the present study, we found that the amplitude of P60 in depressed patients was positively correlated with the severity of depressive symptoms. This suggests a possible significant intrinsic association of P60 with clinical depressive symptoms. This study suggests that there may be a significant intrinsic association between prefrontal cortex excitability and clinical depressive symptoms. And based on previous studies, this cortical excitability is associated with glutamatergic activity. Therefore, we hypothesize that restoring glutamate-related cortical excitability in DLPFC may be one of the potential neural mechanisms for treating depression, and further research is necessary to verify this in the future. The above findings may help clinicians objectively measure patients' conditions, facilitate the implementation of individualized treatment plans and improve the treatment success rate.

There are several limitations to this study. Firstly, the small sample size makes our sample more susceptible to random factors. Therefore, increasing the sample size would have produced more stable results. Secondly, it can be due to the nature of the cross-sectional study design that the present study could not confirm whether P60 amplitude recovers with symptom improvement, and furthermore, a causal relationship between DLPFC excitability and depression severity could not be obtained. Future longitudinal studies are needed to explore this aspect more. Thirdly, each patient was taking antidepressants during the clinical trial and we cannot exclude that medication may have an effect on TEPs, which is not conducive to exploring the true predictive effect of P60. In the future, further studies are needed to verify whether group differences in P60 persist in the absence of antidepressants. In addition, this study used the F3 electrode point location of the EEG cap to refer to the DLPFC, which was not accurate for every participant. Therefore, it is necessary to use MRI-based neuronavigation systems to identify precise targets in future studies.

Finally, the study lacked serum or cerebrospinal fluid examinations to identify potential molecular biomarkers (such as BDNF levels) and to explain the relationship between neurotransmitters, and the TMS-EEG indicators may have new findings.

In summary, this report applied TMS-EEG to confirm that prefrontal cortex excitability is decreased in patients with major depressive disorder and that there is a correlation between this diminished DLPFC excitability and the severity of depressive symptoms. TMS-EEG objectively and directly assesses the excitatory properties of the cortex without relying on the subjective involvement of the participant and has excellent retest reliability. This study provides evidence for an association between P60 and depression severity, which is expected to be integrated into clinical assessment tools in the future.

Data availability statement

The raw data supporting the conclusion of this article will be made available by the authors, without undue reservation.

Ethics statement

The studies involving human participants were reviewed and approved by the ethics committee of Ningbo Kangning Hospital. The patients/participants provided their written informed consent to participate in this study. Written informed consent was obtained from the individual(s) for the publication of any potentially identifiable images or data included in this article.

Author contributions

DZ, XL, GZ, and WX were responsible for the study concept and design. DZ, XL, ZC, CY, YnC, YqC, and MC contributed to the data collection and experimental procedures. XL, WX, and MC assisted with data analysis and interpretation of findings. XL and MC drafted the manuscript. XL, GZ, and DZ provided critical manuscript revision for important intellectual content. All authors contributed to the article and approved the submitted version.

Funding

This research was supported by the Basic Public Welfare Project of Zhejiang Province (LGF22H090055), the Medical Health Science and Technology Project of the Zhejiang Provincial Health Commission (2019RC079), Ningbo Medical and health brand discipline (PPXK2018-08), the Ningbo Natural Science Foundation of China(202003N4263, 2021J275) Ningbo Medical Science and Technology Project (2019Y24, 2020Y19, 2020Y70, 2022Y52), the Ningbo Top Medical and Health Research Program (No.2022030410) and the Taizhou Science and Technology Plan Project (20ywa56).

Acknowledgments

The authors thank the lab members for their technical support.

Conflict of interest

The authors declare that the research was conducted in the absence of any commercial or financial relationships that could be construed as a potential conflict of interest.

Publisher's note

References

Abdallah, C. G., Jiang, L., De Feyter, H. M., Fasula, M., Krystal, J. H., Rothman, D. L., et al. (2014). Glutamate metabolism in major depressive disorder. *Am. J. Psychiatry* 171 (12), 1320–1327. doi:10.1176/appi.ajp.2014.14010067

Belardinelli, P., König, F., Liang, C., Premoli, I., Desideri, D., Müller-Dahlhaus, F., et al. (2021). TMS-EEG signatures of glutamatergic neurotransmission in human cortex. *Sci. Rep.* 11 (1), 8159. doi:10.1038/s41598-021-87533-z

Best, S. R. D., Pavel, D. G., and Haustrup, N. (2019). Combination therapy with transcranial magnetic stimulation and ketamine for treatment-resistant depression: A long-term retrospective review of clinical use. *Heliyon* 5 (8), e02187. doi:10.1016/j.heliyon.2019.e02187

Cao, K. X., Ma, M. L., Wang, C. Z., Iqbal, J., Si, J. J., Xue, Y. X., et al. (2021). TMS-EEG: An emerging tool to study the neurophysiologic biomarkers of psychiatric disorders. *Neuropharmacology* 197, 108574. doi:10.1016/j.neuropharm.2021.108574

Cash, R. F., Noda, Y., Zomorrodi, R., Radhu, N., Farzan, F., Rajji, T. K., et al. (2017). Characterization of glutamatergic and GABA(A)-Mediated neurotransmission in motor and dorsolateral prefrontal cortex using paired-pulse TMS-EEG. *Neuropsychopharmacology* 42 (2), 502–511. doi:10.1038/npp.2016.133

Castricum, J., Birkenhager, T. K., Kushner, S. A., Elgersma, Y., and Tulen, J. H. M. (2022). Cortical inhibition and plasticity in major depressive disorder. *Front. Psychiatry* 13, 777422. doi:10.3389/fpsyt.2022.777422

Delorme, A., and Makeig, S. (2004). Eeglab: An open source toolbox for analysis of single-trial EEG dynamics including independent component analysis. *J. Neurosci. methods* 134 (1), 9–21. doi:10.1016/j.jneumeth.2003.10.009

Duman, R. S., Sanacora, G., and Krystal, J. H. (2019). Altered connectivity in depression: GABA and glutamate neurotransmitter deficits and reversal by novel treatments. *Neuron* 102 (1), 75–90. doi:10.1016/j.neuron.2019.03.013

Elkrief, L., Payette, O., Foucault, J. N., Longpré-Poirier, C., Richard, M., Desbeaumes Jodoin, V., et al. (2022). Transcranial magnetic stimulation and intravenous ketamine combination therapy for treatment-resistant bipolar depression: A case report. *Front. Psychiatry* 13, 986378. doi:10.3389/fpsyt.2022.986378

George, M. S., and Post, R. M. (2011). Daily left prefrontal repetitive transcranial magnetic stimulation for acute treatment of medication-resistant depression. *Am. J. Psychiatry* 168 (4), 356–364. doi:10.1176/appi.ajp.2010.10060864

Godfrey, K. E. M., Gardner, A. C., Kwon, S., Chea, W., and Muthukumaraswamy, S. D. (2018). Differences in excitatory and inhibitory neurotransmitter levels between depressed patients and healthy controls: A systematic review and meta-analysis. *J. Psychiatr. Res.* 105, 33–44. doi:10.1016/j.jpsychires.2018.08.015

Gordon, P. C., Song, Y. F., Jovellar, D. B., Rostami, M., Belardinelli, P., and Ziemann, U. (2023). Untangling TMS-EEG responses caused by TMS versus sensory input using optimized sham control and GABAergic challenge. *J. Physiol.* 601, 1981–1998. doi:10.1113/jp283986

Henter, I. D., Park, L. T., and Zarate, C. A. (2021). Novel glutamatergic modulators for the treatment of mood disorders: Current status. *CNS Drugs* 35 (5), 527–543. doi:10.1007/s40263-021-00816-x

Jannati, A., Oberman, L. M., Rotenberg, A., and Pascual-Leone, A. (2023). Assessing the mechanisms of brain plasticity by transcranial magnetic stimulation. *Neuropsychopharmacology* 48 (1), 191–208. doi:10.1038/s41386-022-01453-8

Kan, R. L. D., Padberg, F., Giron, C. G., Lin, T. T. Z., Zhang, B. B. B., Brunoni, A. R., et al. (2023). Effects of repetitive transcranial magnetic stimulation of the left dorsolateral prefrontal cortex on symptom domains in neuropsychiatric disorders: A systematic review and cross-diagnostic meta-analysis. *Lancet Psychiatry* 10, 252–259. doi:10.1016/s2215-0366(23)00026-3

Kantrowitz, J. T., Dong, Z., Milak, M. S., Rashid, R., Kegeles, L. S., Javitt, D. C., et al. (2021). Ventromedial prefrontal cortex/anterior cingulate cortex Glx, glutamate, and GABA levels in medication-free major depressive disorder. *Transl. Psychiatry* 11 (1), 419. doi:10.1038/s41398-021-01541-1

Khedr, E. M., Elserogy, Y., Fawzy, M., Elnoaman, M., and Galal, A. M. (2020). Global cortical hypoexcitability of the dominant hemisphere in major depressive disorder: A transcranial magnetic stimulation study. *Neurophysiol. Clin.* 50 (3), 175–183. doi:10.1016/j.neucli.2020.02.005

Klomjai, W., Katz, R., and Lackmy-Vallée, A. (2015). Basic principles of transcranial magnetic stimulation (TMS) and repetitive TMS (rTMS). *Ann. Phys. Rehabil. Med.* 58 (4), 208–213. doi:10.1016/j.rehab.2015.05.005

Koenigs, M., and Grafman, J. (2009). The functional neuroanatomy of depression: Distinct roles for ventromedial and dorsolateral prefrontal cortex. *Behav. Brain Res.* 201 (2), 239–243. doi:10.1016/j.bbr.2009.03.004

Li, C. T., Juan, C. H., Lin, H. C., Cheng, C. M., Wu, H. T., Yang, B. H., et al. (2022). Cortical excitatory and inhibitory correlates of the fronto-limbic circuit in major depression and differential effects of left frontal brain stimulation in a randomized sham-controlled trial. *J. Affect. Disord.* 311, 364–370. doi:10.1016/j.jad.2022.05.107

Li, X., Yu, C., Ding, Y., Chen, Z., Zhuang, W., Liu, Z., et al. (2023). Motor cortical plasticity as a predictor of treatment response to high frequency repetitive transcranial magnetic stimulation (rTMS) for cognitive function in drug-naive patients with major depressive disorder. *J. Affect Disord.* 334, 180–186. doi:10.1016/j.jad.2023.04.085

Ma, Y. (2015). Neuropsychological mechanism underlying antidepressant effect: A systematic meta-analysis. *Mol. Psychiatry* 20 (3), 311–319. doi:10.1038/mp.2014.24

McCarron, R. M., Shapiro, B., Rawles, J., and Luo, J. (2021). Depression. *Ann. Intern Med.* 174 (5), Itc65–itc80. doi:10.7326/aitc202105180

Oliveira-Maia, A. J., Press, D., and Pascual-Leone, A. (2017). Modulation of motor cortex excitability predicts antidepressant response to prefrontal cortex repetitive transcranial magnetic stimulation. *Brain Stimul.* 10 (4), 787–794. doi:10.1016/j.brs.2017.03.013

Rajkowska, G., O'Dwyer, G., Teleki, Z., Stockmeier, C. A., and Miguel-Hidalgo, J. J. (2007). GABAergic neurons immunoreactive for calcium binding proteins are reduced in the prefrontal cortex in major depression. *Neuropsychopharmacology* 32 (2), 471–482. doi:10.1038/sj.npp.1301234

Segal, O., and Elkana, O. (2023). The ventrolateral prefrontal cortex is part of the modular working memory system: A functional neuroanatomical perspective. *Front. Neuroanat.* 17, 1076095. doi:10.3389/fnana.2023.1076095

Strafella, R., Momi, D., Zomorrodi, R., Lissemore, J., Noda, Y., Chen, R., et al. (2023). Identifying neurophysiological markers of intermittent theta-burst stimulation in treatment-resistant depression using transcranial magnetic stimulation-electroencephalography. *Biol. Psychiatry* doi:10.1016/j.biopsych.2023.04.011

Sun, Y., Blumberger, D. M., Mulsant, B. H., Rajji, T. K., Fitzgerald, P. B., Barr, M. S., et al. (2018). Magnetic seizure therapy reduces suicidal ideation and produces neuroplasticity in treatment-resistant depression. *Transl. Psychiatry* 8 (1), 253. doi:10.1038/s41398-018-0302-8

Touloumis, C. (2021). The burden and the challenge of treatment-resistant depression. *Psychiatriki* 32, 11–14. doi:10.22365/jpsych.2021.046

Voineskos, D., Blumberger, D. M., Zomorrodi, R., Rogasch, N. C., Farzan, F., Foussias, G., et al. (2019). Altered transcranial magnetic stimulation-electroencephalographic markers of inhibition and excitation in the dorsolateral prefrontal cortex in major depressive disorder. *Biol. Psychiatry* 85 (6), 477–486. doi:10.1016/j.biopsych.2018.09.032

Wu, W., Keller, C. J., Rogasch, N. C., Longwell, P., Shpigel, E., Rolle, C. E., et al. (2018). Artist: A fully automated artifact rejection algorithm for single-pulse TMS-EEG data. *Hum. Brain Mapp.* 39 (4), 1607–1625. doi:10.1002/hbm.23938

Zhang, L., Verwer, R. W. H., Zhao, J., Huitinga, I., Lucassen, P. J., and Swaab, D. F. (2021). Changes in glial gene expression in the prefrontal cortex in relation to major depressive disorder, suicide and psychotic features. *J. Affect Disord.* 295, 893–903. doi:10.1016/j.jad.2021.08.098

frontiers | Frontiers in Neuroscience

TYPE Original Research
PUBLISHED 09 June 2023
DOI 10.3389/fnins.2023.1177214

OPEN ACCESS

EDITED BY
Yuwei Wang,
SingHealth, Singapore

REVIEWED BY
Yumei Wu,
Zunyi Medical University, China
Mehreen Arif,
COMSATS University Islamabad, Pakistan

*CORRESPONDENCE
Jing Zhao
✉ maggy-1978@163.com
Bin Long
✉ longbin903@aliyun.com

†These authors have contributed equally to this work

RECEIVED 01 March 2023
ACCEPTED 25 May 2023
PUBLISHED 09 June 2023

CITATION
Zhu C, Wang X-Y, Zhao J, Long B, Xiao X, Pan L-Y, Yuan T-F and Chen J-H (2023) Effect of transdermal drug delivery therapy on anxiety symptoms in schizophrenic patients. *Front. Neurosci.* 17:1177214. doi: 10.3389/fnins.2023.1177214

Effect of transdermal drug delivery therapy on anxiety symptoms in schizophrenic patients

Cuifang Zhu[1,2†], Xin-Yue Wang[1†], Jing Zhao[1,2*], Bin Long[1,2*], Xudong Xiao[1,2], Ling-Yi Pan[1], Ti-Fei Yuan[1] and Jian-Hua Chen[1,2]

[1]Shanghai Mental Health Center, Shanghai Jiao Tong University School of Medicine, Shanghai, China, [2]Shanghai Institute of Traditional Chinese Medicine for Mental Health, Shanghai, China

Objective: To evaluate the efficacy and safety of transdermal drug delivery therapy for schizophrenia with anxiety symptoms.

Methods: A total of 80 schizophrenic patients (34 males and 56 females) with comorbid anxiety disorders were randomly assigned to the treatment group (n=40) and the control group (n=40) with 6weeks of follow-up. The patients in the treatment group received the standard antipsychotic drug treatment along with transdermal drug delivery therapy. The evaluation of the patients included the Hamilton Anxiety Scale (HAMA), Hamilton Depression Scale (HAMD-17), and treatment emergent symptom scale (TESS) at baseline, 3weeks, and 6weeks after transdermal drug delivery therapy. The Positive and Negative Symptom Scale (PANSS) was assessed at baseline and after 6weeks of treatment.

Results: After 3 and 6weeks of treatment, the HAMA scale scores in the treatment group were lower than those in the control group (p<0.001). However, there were no significant differences in the HAMD-17 scale scores, PANSS total scores, and subscale scores between the two groups (p>0.05). Additionally, no significant differences in adverse effects were observed between the two groups during the intervention period (p>0.05). After 6weeks of penetration therapy, there was a low negative correlation between total disease duration and the change in HAMA scale score (pretreatment-posttreatment) in the treatment group.

Conclusion: Combined traditional Chinese medicine directed penetration therapy can improve the anxiety symptoms of patients with schizophrenia and has a safe profile.

KEYWORDS

schizophrenia, anxiety disorder, transdermal drug delivery therapy, efficacy, psychiatry

Introduction

The importance of anxiety in schizophrenia has been recognized for a long time, and up to 65% of schizophrenic patients experience anxiety symptoms (Temmingh and Stein, 2015; Buonocore et al., 2017). Meta-analyzes and systematic reviews have demonstrated a considerable prevalence of social phobia, obsessive–compulsive disorder, posttraumatic stress disorder, panic attacks, and generalized anxiety disorder in schizophrenic patients (Achim et al., 2011; Braga et al., 2013); meanwhile, anxiety symptoms may be associated with depression, suicide, and cognitive impairment in patients and lead to increased consumption of healthcare resources (Temmingh and Stein, 2015). Sigmund Freud identified the emergence of psychotic symptoms

as a defense against a potentially heightened state of anxiety, while Bluler similarly emphasized the role of affective disorders in the basic symptoms of schizophrenia. A growing body of research has highlighted the important role of anxiety in the development and recurrence of psychosis (Gomes et al., 2019) and emphasized that interventions for anxiety and emotional symptoms can play a role in the primary and secondary prevention of psychiatric disorders (Hall, 2017; Xi et al., 2021). A recent meta-analysis showed that in schizophrenic patients, the combination of antidepressants and antipsychotic medication was beneficial not only regarding affective symptoms but also psychotic symptoms (Helfer et al., 2016).

Clinical treatment of schizophrenia with anxiety disorders is still dominated by antidepressant medications, anxiolytics, and benzodiazepines (Emsley et al., 1999; Temmingh and Stein, 2015). Meta-analysis showed that second-generation antidepressants had a higher incidence of gastrointestinal adverse effects than placebo, including nausea/vomiting, diarrhoea, constipation, abdominal pain, indigestion, anorexia, increased appetite, and xerostomia (Oliva et al., 2021), and headache adverse reactions may occur with the antidepressant bupropion (Telang et al., 2018). An online investigation of the responses of 1,431 adult patients in 38 countries showed that 61% of patients reported the presence of adverse effects after using antidepressants, including drowsiness (63%) and sexual dysfunction (66%) (Read and Williams, 2018). Thus, the rate of adverse effects of antidepressants is much higher than we previously appreciated, severely affecting the quality of life of patients and often explaining their withdrawal from treatment. As a 5-hydroxytryptamine 1A receptor partial agonist, buspirone is also known to cause many adverse effects, including dizziness, nausea, fatigue, tremors, and insomnia (Strawn et al., 2018). Benzodiazepines are associated with the adverse effects of dizziness, fatigue, decreased concentration, and even addiction (Ashton, 1994; O'Brien, 2005). Neurostimulation techniques are an alternative to medication or adjunct to medication to enhance the therapeutic effect for psychiatric disorders (Gault et al., 2018; Hyde et al., 2022). Among them, transcranial magnetic stimulation (TMS) and theta burst stimulation (TBS) are noninvasive neurostimulation techniques, while deep brain stimulation (DBS) is an invasive treatment method in which stimulation electrodes are implanted in certain brain areas to send electrical stimulation (Ashton, 1994; O'Brien, 2005). A preliminary study found that TMS and TBS were effective for anxiety treatment (Chung et al., 2015). Even with the noninvasive TMS treatment method, due to the direct action on local regions, adverse effects such as the increased risk of epilepsy, headache, dizziness, and facial muscle twitching may occur, with an overall incidence of 16.7% (Stultz et al., 2020; Rossi et al., 2021). Epilepsy was the most serious complication, with an incidence of 0.16% (3/1815) (Muller et al., 2012). These factors also affect the patient's compliance with treatment, and concerns about brain stimulation influence patients' choice of treatment. Therefore, clinical treatments that can improve anxiety symptoms without significant adverse effects are urgently needed to improve the accompanying anxiety symptoms in schizophrenic patients.

The vine stem of *polygonum multiflorum* thunb has the functions of nourishing blood and calming the mind, dispelling wind, and promoting blood circulation. With the addition and subtraction of other drugs, many Chinese herbal formulas can be formed, which are boiled in water and taken orally. It can be used to treat insomnia, blood deficiency, body pain, rheumatism, and can also be boiled in water and applied to the affected area to treat skin itching (Liu et al., 2004). Studies have found that its effective components include stilbenes, anthraquinones, flavonoids, lecithin, tannic acid, and various trace elements (Lin et al., 2015), which have multiple pharmacological effects, including regulating the nervous system, antioxidant, immune modulation, lowering blood sugar, and reducing blood lipids (Lin et al., 2015). The main components of vine stem of *polygonum multiflorum* thunb are metabolized by the liver and kidney. Long-term use can cause a heavy burden on the liver and affect its detoxification function. Some patients may experience drug-induced liver damage (Dong et al., 2014). Transdermal drug delivery therapy is a method of external treatment in traditional Chinese medicine. Transdermal drug delivery therapy is an external Chinese medicine treatment method that uses body electrodes containing the volatile oil of the vine stem of *Polygonum multiflorum* Thunb as a substrate for drug penetration by selecting appropriate acupoints under the guidance of meridian doctrine. By means of skin administration, it avoids both the irritation of oral drugs to the gastrointestinal tract and the side effects of hepatic and renal injury and is painless and free of toxic side effects.

Materials and methods

Participation

Patients with schizophrenia were recruited from the inpatient department of Shanghai Mental Health Center from September 2021 to January 2022 and were randomly divided into treatment and control groups, with 40 cases in each group (with 36 male and 64 female patients, see Table 1). The inclusion criteria were as follows: (1) meeting the diagnostic criteria of ICD-10 schizophrenia and generalized anxiety disorder, (2) both patient groups received the second-generation antipsychotic medication, Olanzapine, at a dose of 10-25 mg, for 2 weeks and the dosage remained unchanged throughout the intervention period, (3) PANSS scale total score > 60, anxiety symptoms remained stable for more than 2 weeks after treatment, medication regimen remained unchanged during the intervention

TABLE 1 Comparison of general characteristics.

	Treatment group	Control group	t/x^2	*p* value
Gender				
Male	18	16	0.205	0.651
Female	22	24		
Marital status				
Married	25	21	1.035	0.793
Single	12	14		
Divorced	2	3		
Widowed	1	2		
Mean age	50.80 ± 10.99	48.90 ± 11.84	0.744	0.459
Education	10.73 ± 2.89	10.95 ± 2.855	−0.350	0.727
Course of disease	26.38 ± 10.272	25.65 ± 8.123	0.350	0.727

period, 14 points < HAMA ≤21 points, (4) 18–70 years old; (5) have more than 5 years of education; (6) determined to be free of severe physical or mental disasters, history of alcohol or drug abuse, or recent major psychological stress; and (7) signed a written informed consent form before participating in this study.

Study design

Based on the original second-generation antipsychotic medication and routine care, patients in the treatment group were treated with transdermal drug delivery therapy (Directional drug delivery instrument: Nanjing Ding Shi Medical Equipment Co. No. DS-MF2B, Figure 1). Each session is performed at the ST36 (Zusanli) and SP6 (Sanyinjiao) acupuncture points, and a body electrode containing volatile oil of the vine stem of *Polygonum multiflorum* Thunb is used to penetrate the herbal medicine and introduce it through the bioelectricity of the instrument. Twelve consecutive sessions were considered 1 course of treatment, with a 3-day interval between each course, for a total of 3 courses of treatment, and the entire intervention was 6 weeks. Patients in the control group were administered the original second-generation antipsychotic medication regimen and given routine care. The study was approved by the Ethics Committee of Shanghai Mental Health Center (ethical approval number: 2017-35). All patients signed an informed consent form to participate in the study.

Treatmental index

The Hamilton Anxiety Inventory (HAMA), Hamilton Depression Inventory (HAMD-17 items), and TESS were assessed at baseline and at 3 weeks and 6 weeks of treatment. The PANSS scale consists of 7 items on the positive scale, 7 items on the negative scale, and 16 items on the general psychopathology scale to assess the severity of psychiatric symptoms. The PANSS score was assessed at baseline and 6 weeks. The TESS scale consists of 3 parts, including symptom severity, relationship with medication, and management measures,

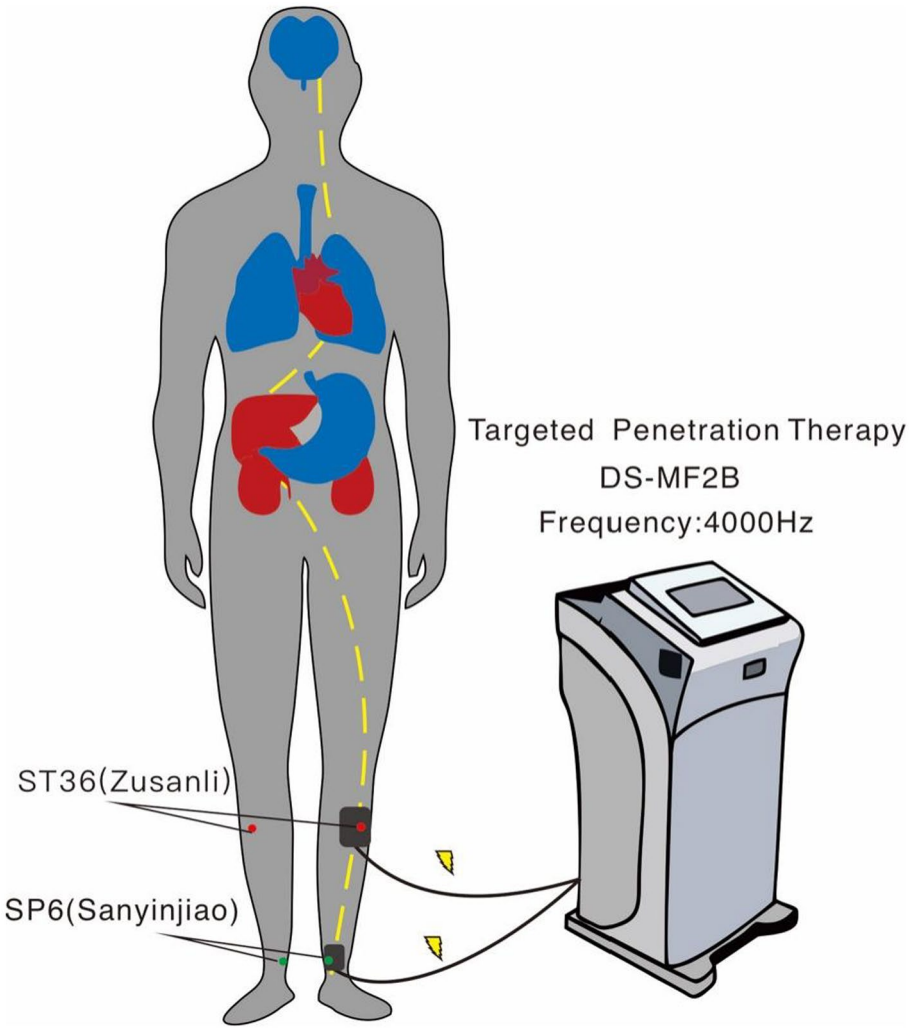

FIGURE 1
Schematic diagram of transdermal drug delivery therapy. Two acupuncture points were administered on one side of the body for 20min; this was repeated on the other side the next day to prevent skin damage.

and the frequency of symptoms observed in this study. The HAMA scale was developed by Hamilton in 1959; it is one of the most commonly used scales in psychiatric practice and consists of 14 items, with all options rated on a 5-point scale from 0 to 4. The HAMD-17 was developed by Hamilton in 1960 and is the most commonly used scale to assess depressive states in clinical treatment. A total score of ≤7 is normal; a total score of 8–17 indicates mild depression; a total score of 18–24 indicates moderate depression; and a total score of ≥25 indicates major depression.

Data statistics

SPSS 23.0 statistical software was applied for descriptive analysis and general statistics of the data. Descriptive analysis was performed for each efficacy indicator at each follow-up time point. The measurement data are expressed as the mean ± standard deviation, and the count data are expressed as percentages. The general demographic data of patients in both groups at baseline were statistically analysed by chi-square and t-tests, and the patients' HAMA and HAMD scale scores were analysed by repeated-measures ANOVA at baseline and at weeks 3 and 6 after enrolment. The t test was used for comparison between groups, and the chi-square test was used for comparison of the incidence of adverse reactions between the two groups. Differences were considered statistically significant for values of $p < 0.05$.

Results

General statistics

In this study, we included 80 patients who were randomly divided into the treatment group and the control group. The treatment group was comprised of 18 male and 22 female patients, who were aged from 30 to 69 years, with 6–15 years of education and a total disease course lasting 5–49 years; additionally, 25 of the patients were married, 12 were unmarried, 2 were divorced, and 1 was widowed. The control group was comprised of 16 male and 24 female patients, who were aged 30–69 years, with 6–15 years of education and a total disease course lasting 12–39 years; additionally, 21 of the patients were married, 14 were unmarried, 3 were divorced, and 2 were widowed. No significant differences were found between the two groups in terms of age, education, total duration of illness, marital status or sex composition ratio ($p > 0.05$) (see Table 1).

Comparison of HAMA scale scores between the two groups

At baseline, the difference between the two groups was not statistically significant ($p > 0.05$). By repeated-measures ANOVA, there was a significant difference between the group main effect ($F = 9.270$, $p = 0.003$) and a statistically significant time main effect ($F = 61.365$, $p < 0.001$) between the two groups, and there was an interaction effect ($F = 40.957$, $p < 0.001$), so simple effects analysis was used. A two-sample t-test was performed at each time point, and the HAMA scale scores of the study group were considerably lower than those of the control group after 3 weeks and 6 weeks of transdermal drug treatment (all $p < 0.001$); repeated-measures ANOVA was performed at different time points for each group with fixed grouping factors, and the statistical results showed a significant decrease in HAMA scores after treatment in the study group (all $p < 0.05$), as shown in Table 2.

Comparison of HAMD-17 scale scores between the two groups

At baseline, the difference in HAMD-17 scale scores between the treatment and control groups was not statistically significant ($p > 0.05$). By repeated-measures ANOVA, the group main effect was not significantly different between the transdermal permeation treatment and control groups ($F = 0.310$, $p = 0.579$), and the main effect of time was significantly different ($F = 7.583$, P < =0.005), with no interaction ($F = 1.083$, $p = 0.311$), see Table 3.

The HAMA scale has 14 factors; items 7–13 represent somatic anxiety, while items 1–6 and 14 represent psychogenic anxiety. The change in each factor of the HAMA scale can be calculated by the change from the scores at baseline and after treatment. The changes in HAMA scores did not conform to normal distribution, so a nonparametric test (Mann–Whitney) was applied. Statistical results showed that psychogenic anxiety behaviors (tension, insomnia, behavioral manifestations during talks) and somatic anxiety behaviors (muscular system symptoms and genitourinary system symptoms) were significantly alleviated after the intervention (Z = −3.617, −5.925, −3.342, −3.087, −2.961; $p < 0.01$), see Table 4.

Comparison of PANSS between the two groups

At baseline, no statistically significant differences were seen between the two groups in the PANSS scale total score and each subscale score ($p > 0.05$), while the comparison did not show statistically significant differences between the groups after being treated for 6 weeks ($p > 0.05$) (see Table 5).

We also evaluated the factors affecting the effectiveness of Chinese medicine targeted penetration therapy. As shown in Figure 2, after 6 weeks of penetration therapy, there was a low negative correlation between total disease duration and the change in HAMA scale score (pretreatment-posttreatment) in the treatment group (R = -0.512, $p = 0.001$, Figure 2A). Additionally, a low positive correlation was found between the baseline HAMA scale score and the change in HAMA scale score in the treatment group (R = 0.483, $p = 0.002$, Figure 2B).

Comparison of side effect incidence between the two groups

There was no significant difference in the incidence of adverse effects within the TESS scale between the two groups ($p > 0.05$) (see Table 6).

TABLE 2 Comparison of HAMA scale scores ($\bar{x}\pm s$).

	Cases	Baseline	3weeks	6weeks	*F* value (*p* value)			
					Group Main Effect	Time Main Effect	Interaction Effect	Simple Effects
Treatment group	40	17.80 ± 1.539	16.10 ± 1.676	15.38 ± 1.764	9.270 (0.003)	61.365 (0.000)	40.957 (0.000)	54.901 (0.000)
Control group	40	17.58 ± 1.615	17.58 ± 1.615	17.28 ± 1.797				11.323 (0.002)
t		0.638	−4.007	−4.772				
P		0.526	0.000	0.000				

TABLE 3 Comparison of HAMD-17 scale scores ($\bar{x}\pm s$).

	Cases	Baseline	3weeks	6weeks	F value (*p* value)		
					Group main effect	Time main effect	Interaction effect
Treatment group	40	10.05 ± 1.037	9.93 ± 0.917	9.88 ± 0.883	0.310 (0.579)	7.583 (0.005)	1.083 (0.311)
Control group	40	10.13 ± 1.137	10.05 ± 1.061	10.05 ± 1.061			

Discussion

The present research investigated the efficacy of external Chinese medicine treatment methods for patients with schizophrenia with anxiety disorders. The results of this study showed that 1. At baseline, there were no significant differences in demographic and clinical parameters between the observation group and the control group ($p > 0.05$). 2. At the end of the 3rd and 6th week of intervention, patients treated with transdermal drug delivery therapy had lower HAMA scale scores compared to the control group ($p < 0.001$), indicating that transdermal drug delivery therapy can improve anxiety symptoms in patients. 3. There were no significant differences in the occurrence and frequency of adverse reactions between the two groups after intervention ($p > 0.05$), suggesting that transdermal drug delivery therapy has a high level of safety. 4. There were no significant differences between the two groups in the PANSS total score, subscale scores, and HAMD-17 scores before and after the intervention ($p > 0.05$), indicating that the 6-week transdermal drug delivery therapy had no impact on psychotic symptoms and depressive symptoms. The results of this study suggest that transdermal drug delivery therapy can improve anxiety symptoms in patients with schizophrenia and has a high level of safety.

Regarding mild anxiety disorders, psychotherapy, exercise therapy and internal and external Chinese medicine can be considered as first-line treatment to relieve anxiety while ensuring sufficient sleep and consumption of vegetables and fruits, performing more aerobic exercises, etc. For moderate and severe anxiety disorders, a combination of Chinese and Western medicinal regimens can be used to decrease drug onset time and achieve better clinical efficacy with a lower dose of drugs and fewer adverse effects. In this study, we selected Chinese medicine targeted transdermal therapy as the intervention method, which is a method of physically enhancing the delivery of topical drugs (Raphael et al., 2015) using heat therapy, bionic massage and bioelectric conduction. In the past 20 years, this technology has displayed promising performance in physiotherapy and transdermal drug delivery; for instance, its therapeutic effects have been demonstrated in dysmenorrhea, uterine cold and gynecological inflammation in obstetrics and gynecology; enlarged prostate and urinary frequency and urgency in males; adjuvant treatment in diabetes; stomach pain, diarrhoea, insomnia and other diseases. Thus, traditional Chinese targeted transdermal therapy can be used as a supplementary treatment for various ailments. In recent years, several studies have shown that Chinese medicine targeted transdermal therapy can improve the therapeutic effect of insomnia (Chen et al., 2017; Xie et al., 2019); furthermore, it has been shown that in the clinical treatment of depression, the combination of traditional Chinese targeted transdermal therapy with pharmacotherapy is highly effective and safe in improving patients' anxiety symptoms with high efficiency and safety (Su and Huang, 2019). A study by Zhuang concluded that Chinese medicine-targeted transdermal therapy could improve anxiety in patients with somatization disorder (Zhuang, 2019). Shang et al. showed that psychological care could alleviate patients' anxiety and improve their quality of life (Shang and Jiang, 2016). Similar results were obtained in the present study. After 3 weeks of intervention using Chinese medicine-directed transdermal therapy, the patients' HAMA scale scores were significantly lower than those of the control group ($p < 0.001$), and no significant difference was observed in the frequency of adverse effects ($p > 0.05$), suggesting that this therapy can improve the anxiety symptoms of patients with schizophrenia and has a good safety profile. There was no significant difference between the PANSS scale total score and subscale subgroups of the two groups before and after the intervention, which suggests that Chinese medicine-directed transdermal treatment has no effect on psychiatric symptoms.

Chinese medicine classifies anxiety disorders into three types: heart deficiency and timidity, phlegm-heat disturbing the mind, and liver and kidney yin deficiency. The heart deficiency and timidity disorders may manifest as restlessness, frequent dreaming and waking up, palpitations and less food, and aversion to hearing sounds. By nourishing the heart, tranquilizing the mind, dispelling wind, and

TABLE 4 The change in each factor of the HAMA scale [M (P25, P75)].

	Cases	Tension	Insomnia	Muscular system	Genitourinary system	Behavioral manifestations during talk
Treatment group	40	0 (0,1)	1 (0,1)	0 (0,1)	0 (0,1)	1 (0,1)
Control group	40	0 (0,0)	0 (0,0)	0 (0,0)	0 (0,0)	0 (0,0)

TABLE 5 Comparison of PANSS scale total score and each subscale score ($\bar{x}\pm s$).

Groups	Cases	Positive scale score		Negative scale score		General psychopathological scales		PANSS total score	
		Baseline	6weeks	Baseline	6weeks	Baseline	6weeks	Baseline	6weeks
Treatment	40	16.30 ± 1.757	15.93 ± 1.730	30.88 ± 2.151	30.18 ± 2.049	38.25 ± 4.174	37.98 ± 4.197	85.43 ± 5.022	84.40 ± 5.148
Control	40	16.20 ± 1.800	15.70 ± 1.522	31.48 ± 2.439	30.58 ± 2.218	39.00 ± 4.326	38.85 ± 4.246	86.68 ± 5.749	85.65 ± 5.596
t		0.251	0.617	−1.167	−0.838	−0.789	−0.927	−1.036	−1.04
P		0.802	0.539	0.247	0.405	0.432	0.357	0.304	0.302

clearing ligaments, the vine stem of *Polygonum multiflorum* Thunb, as the active ingredient of transdermal drug delivery therapy can improve symptoms such as fatigue, insomnia and dreaminess and therefore can be used in the treatment of anxiety disorders. In 2020, meta-analysis researchers conducted a review of the literature on Chinese herbal medicine for insomnia with anxiety from 2000 to September 2017and concluded that the vine stem of *Polygonum multiflorum* Thunb was among the top 10 most frequently used prescribed medicines for the clinical treatment of insomnia with anxiety (Liu and Wang, 2018). For example, Danzhi Xiaoyao powder (Liu C. et al., 2021; Shi et al., 2021), which contains the vine stem of *Polygonum multiflorum* Thunb in its composition, has been shown to improve anxiety and insomnia symptoms in patients. It was also reported that extracts of the vine stem of *Polygonum multiflorum* Thunb depress the central nervous system and prolong sleep time in animals, suggesting that nightshade extracts may alleviate anxiety symptoms the next day by improving sleep quality (Sun and Wen, 2008). The inflammatory response is a major mechanism of anxiety behaviors, and studies have found that patients with anxiety disorders have significantly elevated levels of proinflammatory cytokines compared to healthy individuals (Duivis et al., 2013), meanwhile, the stem of *Polygonum multiflorum* Thunb, which has been shown to have inhibitory activities against COX-1, COX-2, and 5-LO, indicating its anti-inflammatory benefits (Li et al., 2003).

In the present study, we selected the ST36 and SP6 acupoints exert anxiolytic effects and our results demonstrate that targeted penetration therapy significantly alleviates anxiety symptoms in schizophrenic patients. ST36 (Zusanli) is a very famous acupuncture point with excellent tonic effects for treating stomach pain, indigestion, gastric distension, and hypertension and is one of Sun Simiao's Thirteen Ghost Acupuncture Points for treating neurological disorders such as depression, anxiety, and schizophrenia (Le et al., 2016). A study found that electroacupuncture at acupoint ST36 could moderate anxiety-like behaviors in a rat model of PTSD (Liu et al., 2019). SP6 (Sanyinjiao) is the meeting point of the Spleen Meridian of ZuTaiyin, Kidney Meridian of Zushaoyin and Liver Meridian of ZuJueyin. Targeting it clinically can treat a variety of diseases, such as genital and urinary disorders (diarrhoea, bloating, dysmenorrhea, enuresis), palpitation, insomnia, hypertension, etc. A study by Du et al. (2022) indicated that electroacupuncture of SP6 could improve insomnia, anxiety, and depression symptoms in patients. The mechanisms underlying this targeted penetration therapy are currently the subject of several ongoing studies. Xing Yushuang et al. showed that acupuncture (ST36 + SP6) could alleviate anxiety in rats with alcohol withdrawal anxiety, and its anxiolytic mechanism of action was shown to be related to the regulation of cAMP-CRH interaction in hippocampal tissue in the rat brain (Xing et al., 2019). An acupuncture treatment acting on ST36 and SP6 acupoints attenuated anxiety-like behavior in rats by modulating the hippocampal inflammatory response and metabolic disorders as well as the HPA axis through effects on the gut microbiome (Zhou et al., 2022). Electroacupuncture stimulation of the ST36 acupuncture point to activate the vagal-adrenal axis to suppress systemic inflammation depends on NPY+ adrenal chromaffin cells and PROKR2^{Cre}-marked sensory neurons (Liu et al., 2020; Liu S. et al., 2021). The stem of *Polygonum multiflorum* Thunb extract has anti-inflammatory activity, and stimulation of the ST36 and SP6 acupoints modulates the hippocampal inflammatory response and activates the vagus-adrenergic axis and the HPA axis; when used together, the two may jointly play an effective role in alleviating anxiety behavior in schizophrenic patients. In our subsequent studies, emphasis will be placed on the biological mechanisms of traditional Chinese medicine permeation therapy to better facilitate its application in clinical treatment.

The current study conducted a correlation analysis of the potential factors influencing the effectiveness of targeted penetration therapy, revealing that the longer the duration of schizophrenia, the worse the treatment effect. In traditional Chinese medicine theory, the initial stage of anxiety disorder is mostly characterized by mental symptoms such as nervousness and insomnia, and as the disease progresses, somatic anxiety becomes the main symptom, manifesting as the muscular system and genitourinary system symptoms, which increases the difficulty of treatment. This is also consistent with the literature reports that a longer duration of untreated psychosis and relapses are modestly related to worse outcomes, and early antipsychotic treatment in the prodromal stage can achieve better results (Sarotar et al., 2008; Fountoulakis et al., 2020). This study also

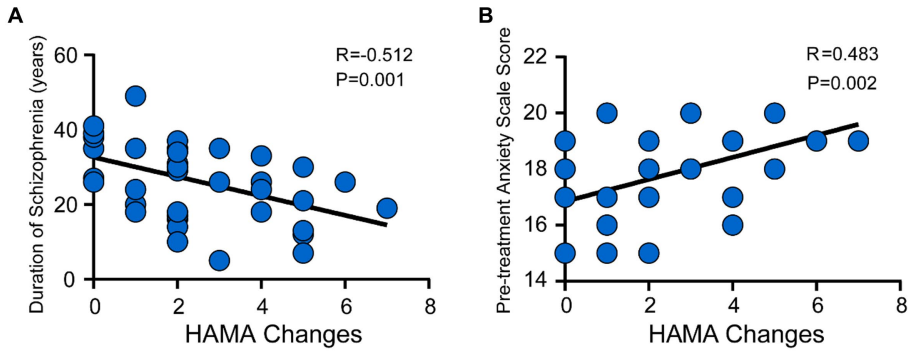

FIGURE 2
Correlation between the change in HAMA scale score with disease duration and baseline score after the intervention in the treatment group. **(A)** The correlation between total disease duration and the change in HAMA scale score (pretreatment-posttreatment) in the treatment group (R=−0.512, p=0.001). **(B)** The correlation between the baseline HAMA scale score and the change in HAMA scale score (R=0.483, p=0.002).

TABLE 6 Comparison of the incidence of side effects.

	Cases	Hypopraxia	Insomnia	Myotonia	Tremor
Treatment group	40	2 (5.0)	3 (7.5)	2 (5.0)	3 (7.5)
Control group	40	3 (7.5)	5 (12.5)	3 (7.5)	4 (10.0)
X^2		0.213	0.556	0.213	0.157
P		0.500	0.712	0.500	0.692

	Cases	Xerostomia	Akathisia	Diarrhoea	Dizziness
Treatment group	40	4 (10.0)	4 (10.0)	1 (2.5)	1 (2.5)
Control group	40	4 (10.0)	6 (15.0)	2 (5.0)	0 (0)
X^2		0.00	0.457	0.346	1.013
P		1.00	0737	1.000	1.000

found that the higher the baseline HAMA scale (i.e., the more severe the underlying anxiety symptoms), the more obvious the improvement in anxiety after traditional Chinese Medicine treatment. In conclusion, our results suggest a correlation between the improvement effect of treatment on anxiety disorders in patients with schizophrenia and the duration of illness and baseline anxiety level, providing a theoretical basis for large-scale clinical implementation. Patients with schizophrenia with a short duration of disease and significant anxiety symptoms should be targeted for treatment.

In conclusion, transdermal drug delivery therapy, as a simple and convenient method of external Chinese medicine treatment, using vine stem of *polygonum multiflorum* thunb as the penetrant and acupoints of ST36 + SP6, significantly improves the anxiety symptoms of patients with schizophrenia, with minimal adverse effects and a good safety profile. However, this study had a small sample size and was conducted as a preliminary exploratory study. There was no testing of inflammatory factors, serotonin, dopamine, or other biomarkers that may be related to anxiety before and after intervention, nor was there a breakdown of the active ingredients in the vine stem of *polygonum multiflorum* thunb. These limitations are regrettable for identifying the effective components of the treatment and the biological markers. Nevertheless, our study provides a new approach to improving anxiety in patients with schizophrenia, and future studies need to be conducted on a larger scale in multiple centers with more comprehensive research designs, including a group treated with "body electrode with bioelectricity of the instrument" as a control and further clarification of the biological mechanisms of targeted transdermal drug delivery through animal experiments.

Data availability statement

The raw data supporting the conclusions of this article will be made available by the authors, without undue reservation.

Ethics statement

The studies involving human participants were reviewed and approved by the Ethics Committee of Shanghai Mental Health Center (ethical approval number: 2017-35). The patients/participants provided their written informed consent to participate in this study.

Author contributions

JZ and BL formulated the design of the studies. CZ and X-YW performed the experiments and analysis of the studies

and drafted the manuscript. CZ, X-YW, XX, and L-YP performed the experiments and collected data. J-HC reanalysis the data and helped revise manuscripts and draw tables. All authors contributed to the article and approved the submitted version.

Funding

This study was supported by Shanghai Municipal Health Commission Key Training Program of Traditional Chinese Medicine (No: AB83180002019021); Three-year Action Plan Project of Shanghai Traditional Chinese Medicine Development (grant ZY-(2021–2023)-0207-01); "Scientific and technological innovation action plan" of Shanghai Science and Technology Commission of China (grant 21Y11921100), the special project of integrated Chinese and western medicine in Shanghai General Hospital (ZHYY-ZXYJHZX-202004).

Acknowledgments

Many thanks to T-FY for refining the experimental design.

Conflict of interest

The authors declare that the research was conducted in the absence of any commercial or financial relationships that could be construed as a potential conflict of interest.

Publisher's note

References

Achim, A. M., Maziade, M., Raymond, E., Olivier, D., Mérette, C., and Roy, M. A. (2011). How prevalent are anxiety disorders in schizophrenia? A meta-analysis and critical review on a significant association. *Schizophr. Bull.* 37, 811–821. doi: 10.1093/schbul/sbp148

Ashton, H. (1994). Guidelines for the rational use of benzodiazepines. When and what to use. *Drug* 48, 25–40. doi: 10.2165/00003495-199448010-00004

Braga, R. J., Reynolds, G. P., and Siris, S. G. (2013). Anxiety comorbidity in schizophrenia. *Psychiatry Res.* 210, 1–7. doi: 10.1016/j.psychres.2013.07.030

Buonocore, M., Bosia, M., Bechi, M., Spangaro, M., Cavedoni, S., Cocchi, F., et al. (2017). Targeting anxiety to improve quality of life in patients with schizophrenia. *Eur. Psychiatry* 45, 129–135. doi: 10.1016/j.eurpsy.2017.06.014

Chen, D. F., Hu, M., Li, H., Ke, X. W., Zhang, Y. C., Zhang, W. J., et al. (2017). Clinical study of modified Buyang Huanwu decoction combined with TCM directed medicine penetration instrument in the treatment of cervical insomnia. *China Modern Med.* 24:52.

Chung, S. W., Hoy, K. E., and Fitzgerald, P. B. (2015). Theta-burst stimulation: a new form of TMS treatment for depression? *Depress. Anxiety* 32, 182–192. doi: 10.1002/da.22335

Dong, H., Slain, D., Cheng, J., Ma, W., and Liang, W. (2014). Eighteen cases of liver injury following ingestion of *Polygonum multiflorum*. *Complement. Ther. Med.* 22, 70–74. doi: 10.1016/j.ctim.2013.12.008

Du, L., Song, X.-J., Li, Z.-W., Liao, L.-X., and Zhu, Y.-H. (2022). Combined use of Shenmen (HT 7) and Sanyinjiao (SP 6) to improve the anxiety and depression in patients with insomnia: a randomized controlled trial. *Zhongguo Zhen Jiu* 42, 13–17. doi: 10.13703/j.0255-2930.20210113-k0002

Duivis, H. E., Vogelzangs, N., Kupper, N., de Jonge, P., and Penninx, B. W. J. H. (2013). Differential association of somatic and cognitive symptoms of depression and anxiety with inflammation: findings from the Netherlands study of depression and anxiety (NESDA). *Psychoneuroendocrinology* 38, 1573–1585. doi: 10.1016/j.psyneuen.2013.01.002

Emsley, R. A., Oosthuizen, P. P., Joubert, A. F., Roberts, M. C., and Stein, D. J. (1999). Depressive and anxiety symptoms in patients with schizophrenia and schizophreniform disorder. *J. Clin. Psychiatry* 60, 747–751. doi: 10.4088/JCP.v60n1105

Fountoulakis, K. N., Moeller, H. J., Kasper, S., Tamminga, C., Yamawaki, S., Kahn, R., et al. (2020). The report of the joint WPA/CINP workgroup on the use and usefulness of antipsychotic medication in the treatment of schizophrenia. *CNS Spectr.* 26, 562–586. doi: 10.1017/S1092852920001546

Gault, J. M., Davis, R., Cascella, N. G., Saks, E. R., Corripio-Collado, I., Anderson, W. S., et al. (2018). Approaches to neuromodulation for schizophrenia. *J. Neurol. Neurosurg. Psychiatry* 89, 777–787. doi: 10.1136/jnnp-2017-316946

Gomes, F. V., Zhu, X., and Grace, A. A. (2019). Stress during critical periods of development and risk for schizophrenia. *Schizophr. Res.* 213, 107–113. doi: 10.1016/j.schres.2019.01.030

Hall, J. (2017). Schizophrenia - an anxiety disorder? *Br. J. Psychiatry* 211, 262–263. doi: 10.1192/bjp.bp.116.195370

Helfer, B., Samara, M. T., Huhn, M., Klupp, E., Leucht, C., Zhu, Y., et al. (2016). Efficacy and safety of antidepressants added to antipsychotics for schizophrenia: a systematic review and Meta-analysis. *Am. J. Psychiatry* 173, 876–886. doi: 10.1176/appi.ajp.2016.15081035

Hyde, J., Carr, H., Kelley, N., Seneviratne, R., Reed, C., Parlatini, V., et al. (2022). Efficacy of neurostimulation across mental disorders: systematic review and meta-analysis of 208 randomized controlled trials. *Mol. Psychiatry* 27, 2709–2719. doi: 10.1038/s41380-022-01524-8

Le, J. J., Yi, T., Qi, L., Li, J., Shao, L., and Dong, J. C. (2016). Electroacupuncture regulate hypothalamic-pituitary-adrenal axis and enhance hippocampal serotonin system in a rat model of depression. *Neurosci. Lett.* 615, 66–71. doi: 10.1016/j.neulet.2016.01.004

Li, R. W., David Lin, G., Myers, S. P., and Leach, D. N. (2003). Anti-inflammatory activity of Chinese medicinal vine plants. *J. Ethnopharmacol.* 85, 61–67. doi: 10.1016/S0378-8741(02)00339-2

Lin, L., Ni, B., Lin, H., Zhang, M., Li, X., Yin, X., et al. (2015). Traditional usages, botany, phytochemistry, pharmacology and toxicology of *Polygonum multiflorum* Thunb.: a review. *J. Ethnopharmacol.* 159, 158–183. doi: 10.1016/j.jep.2014.11.009

Liu, Z.-J., Li, L., and Ye, C.-F. (2004). The effects of tetrahydroxylstilbene on learning and memory ability and NMDA-receptor binding to [H] MK801 in forebrain of ischemia-reperfusion gerbils. *Chinese New Drugs J.* 13, 224–226.

Liu, L., Liu, H., Hou, Y., Shen, J., Qu, X., and Liu, S. (2019). Temporal effect of electroacupuncture on anxiety-like behaviors and c-Fos expression in the anterior cingulate cortex in a rat model of post-traumatic stress disorder. *Neurosci. Lett.* 711:134432. doi: 10.1016/j.neulet.2019.134432

Liu, P., and Wang, H. P. (2018). Medication rule of Chinese traditional medicine for insomnia and anxiety based on data mining. *World Latest Med. Inform.* 18, 168–169.

Liu, S., Wang, Z., Su, Y., Qi, L., Yang, W., Fu, M., et al. (2021). A neuroanatomical basis for electroacupuncture to drive the vagal-adrenal axis. *Nature* 598, 641–645. doi: 10.1038/s41586-021-04001-4

Liu, S., Wang, Z. F., Su, Y. S., Ray, R. S., Jing, X. H., Wang, Y. Q., et al. (2020). Somatotopic organization and intensity dependence in driving distinct NPY-expressing sympathetic pathways by Electroacupuncture. *Neuron* 108, 436–50.e7. doi: 10.1016/j.neuron.2020.07.015

Liu, C., Ying, Z., Li, Z., Zhang, L., Li, X., Gong, W., et al. (2021). Danzhi Xiaoyao powder promotes neuronal regeneration by downregulating notch signaling pathway in the treatment of generalized anxiety disorder. *Front. Pharmacol.* 12:772576. doi: 10.3389/fphar.2021.772576

Muller, P. A., Pascual-Leone, A., and Rotenberg, A. (2012). Safety and tolerability of repetitive transcranial magnetic stimulation in patients with pathologic positive sensory phenomena: a review of literature. *Brain Stimul.* 5, 320–9.e27. doi: 10.1016/j.brs.2011.05.003

O'Brien, C. P. (2005). Benzodiazepine use, abuse, and dependence. *J. Clin. Psychiatry* 66, 28–33.

Oliva, V., Lippi, M., Paci, R., Del Fabro, L., Delvecchio, G., Brambilla, P., et al. (2021). Gastrointestinal side effects associated with antidepressant treatments in patients with major depressive disorder: a systematic review and meta-analysis. *Prog. Neuro-Psychopharmacol. Biol. Psychiatry* 109:110266. doi: 10.1016/j.pnpbp.2021.110266

Raphael, A. P., Wright, O. R., Benson, H. A., and Prow, T. W. (2015). Recent advances in physical delivery enhancement of topical drugs. *Curr. Pharm. Des.* 21, 2830–2847. doi: 10.2174/1381612821666150428144852

Read, J., and Williams, J. (2018). Adverse effects of antidepressants reported by a large international cohort: emotional blunting, suicidality, and withdrawal effects. *Curr. Drug Saf.* 13, 176–186. doi: 10.2174/1574886313666180605095130

Rossi, S., Antal, A., Bestmann, S., Bikson, M., Brewer, C., Brockmöller, J., et al. (2021). Safety and recommendations for TMS use in healthy subjects and patient populations, with updates on training, ethical and regulatory issues: expert guidelines. *Clin. Neurophysiol.* 132, 269–306. doi: 10.1016/j.clinph.2020.10.003

Sarotar, B. N., Pesek, M. B., Agius, M., Pregelj, P., and Kocmur, M. (2008). Duration of untreated psychosis and it's effect on the functional outcome in schizophrenia - preliminary results. *Psychiatr. Danub.* 20, 179–183.

Shang, D., and Jiang, Y. (2016). Observation of the effect of TCM directed dialytic therapy combined with psychological care on alleviating limb pain in the elderly. *Chin. J. Geriatr. Care.* 14, 121–122.

Shi, X.-J., Fan, F.-C., Liu, H., Ai, Y.-W., Liu, Q.-S., Jiao, Y.-G., et al. (2021). Traditional Chinese medicine decoction combined with antipsychotic for chronic schizophrenia treatment: a systematic review and Meta-analysis. *Front. Pharmacol.* 11:616088. doi: 10.3389/fphar.2020.616088

Strawn, J. R., Mills, J. A., Cornwall, G. J., Mossman, S. A., Varney, S. T., Keeshin, B. R., et al. (2018). Buspirone in children and adolescents with anxiety: a review and Bayesian analysis of abandoned randomized controlled trials. *J. Child Adolesc. Psychopharmacol.* 28, 2–9. doi: 10.1089/cap.2017.0060

Stultz, D. J., Osburn, S., Burns, T., Pawlowska-Wajswol, S., and Walton, R. (2020). Transcranial magnetic stimulation (TMS) safety with respect to seizures: a literature review. *Neuropsychiatr. Dis. Treat.* 16, 2989–3000. doi: 10.2147/NDT.S276635

Su, G. Q., and Huang, R. Q. (2019). Observation of treatment effect of antidepressants combined with traditional Chinese medicine for patients with depression. China modern. *Doctor* 57, 97–99.

Sun, Z. L., and Wen, L. (2008). Comparison of anti-anxiety effects of different extracts of nocturnal vine. *chin. J. Hos. Pharm.* 28, 164–165.

Telang, S., Walton, C., Olten, B., and Bloch, M. H. (2018). Meta-analysis: second generation antidepressants and headache. *J. Affect. Disord.* 236, 60–68. doi: 10.1016/j.jad.2018.04.047

Temmingh, H., and Stein, D. J. (2015). Anxiety in patients with schizophrenia: epidemiology and management. *CNS Drugs* 29, 819–832. doi: 10.1007/s40263-015-0282-7

Xi, S. J., Shen, M. X., Wang, Y., Zhou, W., Xiao, S. Y., Tebes, J. K., et al. (2021). Depressive symptoms, anxiety symptoms, and their co-occurrence among people living with schizophrenia in China: prevalence and correlates. *J. Clin. Psychol.* 77, 2137–2146. doi: 10.1002/jclp.23141

Xie, T. L., Hu, J., and Shi, M. A. (2019). The application of chinese medicine directional dialysis therapy combined with Chinese medicine foot bath in insomnia in patients with Xiang palsy. *Chin. Foreign Med. Res.* 17, 23–25.

Xing, Y. S., Lin, N., Liang, Q. C., Yang, Z., and Wu, Y. Y. (2019). Effect of acupuncture on anxiety of ethanol withdrawal in rats. *Acta Chin. Med. Pharmacol.* 47, 85–88.

Zhou, F., Jiang, H., Kong, N., Lin, J., Zhang, F., Mai, T., et al. (2022). Electroacupuncture attenuated anxiety and depression-like behavior via inhibition of hippocampal inflammatory response and metabolic disorders in TNBS-induced IBD rats. *Oxidative Med. Cell. Longev.* 2022, 1–19. doi: 10.1155/2022/8295580

Zhuang, X. M. (2019). Effects of targeted psychological nursing combined with Chinese medicine targeted drug permeation therapy on sleep and anxiety of patients with somatization disorder. *World J. Sleep Med.* 6, 1566–1567.

frontiers | Frontiers in Pharmacology

TYPE Original Research
PUBLISHED 20 June 2023
DOI 10.3389/fphar.2023.1210393

OPEN ACCESS

EDITED BY
Yuan Li,
Shanghai Jiao Tong University, China

REVIEWED BY
Lourdes Franco,
University of Extremadura, Spain
Junhua Yang,
Guangdong Pharmaceutical University, China
Ling-Yan Su,
Yunnan Agricultural University, China

*CORRESPONDENCE
Qi Chang,
qchang@implad.ac.cn
Li-Da Du,
l.du@utoronto.ca
Ming-Zhu Yan,
mzyan@implad.ac.cn

RECEIVED 22 April 2023
ACCEPTED 09 June 2023
PUBLISHED 20 June 2023

CITATION
Xia T-J, Wang Z, Jin S-W, Liu X-M, Liu Y-G, Zhang S-S, Pan R-L, Jiang N, Liao Y-H, Yan M-Z, Du L-D and Chang Q (2023), Melatonin-related dysfunction in chronic restraint stress triggers sleep disorders in mice.
Front. Pharmacol. 14:1210393.
doi: 10.3389/fphar.2023.1210393

Melatonin-related dysfunction in chronic restraint stress triggers sleep disorders in mice

Tian-Ji Xia[1], Zhi Wang[1], Su-Wei Jin[1], Xin-Min Liu[2], Yong-Guang Liu[1], Shan-Shan Zhang[1], Rui-Le Pan[1], Ning Jiang[1], Yong-Hong Liao[1], Ming-Zhu Yan[1]*, Li-Da Du[3,4]* and Qi Chang[1]*

[1]Institute of Medicinal Plant Development, Chinese Academy of Medical Sciences and Peking Union Medical College, Beijing, China, [2]Institute of Drug Discovery Technology, Ningbo University, Ningbo, China, [3]Institute of Molecular Medicine and Innovative Pharmaceutics, Qingdao University, Qingdao, China, [4]Department of Surgery, University of Toronto, Toronto, TO, Canada

Stress may trigger sleep disorders and are also risk factors for depression. The study explored the melatonin-related mechanisms of stress-associated sleep disorders on a mouse model of chronic stress by exploring the alteration in sleep architecture, melatonin, and related small molecule levels, transcription and expression of melatonin-related genes as well as proteins. Mice undergoing chronic restraint stress modeling for 28 days showed body weight loss and reduced locomotor activity. Sleep fragmentation, circadian rhythm disorders, and insomnia exhibited in CRS-treated mice formed sleep disorders. Tryptophan and 5-hydroxytryptamine levels were increased in the hypothalamus, while melatonin level was decreased. The transcription and expression of melatonin receptors were reduced, and circadian rhythm related genes were altered. Expression of downstream effectors to melatonin receptors was also affected. These results identified sleep disorders in a mice model of chronic stress. The alteration of melatonin-related pathways was shown to trigger sleep disorders.

KEYWORDS

chronic restraint stress, sleep disorders, melatonin, sleep fragmentation, circadian rhythm, insomnia

1 Introduction

Sleep affects various physiological homeostasis and has a pivotal role in regulating the central nervous system functions (Tononi and Cirelli, 2014; Cuddapah et al., 2019). Sleep disorders are commonly associated with neurological pathogenesis and may indicate some neurodegenerative processes (Musiek and Holtzman, 2016). Sleep disorders include insomnia, narcolepsy, sleep apnea syndrome, circadian rhythm disorders, etc., affecting up to 40.49% population during 2019–2021 and becoming a significant public health concern (Jahrami et al., 2022). Insomnia, the most prevalent type of sleep disorder, is characterized by difficulty in sleep initiation and maintenance (Riemann et al., 2020). Circadian rhythm disorders include advanced or delayed sleep phase disorder and irregular sleep-wake rhythm (Allega et al., 2018). Sleep disorders are tightly linked with functional consequences like decreased attention and concentration, an increased risk of disease, lower work productivity, etc (Battle, 2013). Sleep is sensitive and can easily be affected. Predisposing factors for sleep disorders include age, sex, environment, stress, irregular sleep-wake schedule, etc (Billings et al., 2020; Meyer et al., 2022). A study has indicated that

poorer sleep is associated with elevated feelings of stress in both individuals with sleep disorders and individuals from the general population (Demichelis et al., 2022). Increased levels of stress at night lead to decreases in slow wave sleep, sleep efficiency, and general sleep quality (Kim and Dimsdale, 2007). Stressful life events, related to work/school living, family, health, or indeterminate with negative emotional valence, are the most frequent triggers of insomnia (Bastien et al., 2004; Drake et al., 2014). In addition, many neuropsychiatric disorders, especially depression, can lead to sleep disorders. Sleep disorders are the most prominent symptom in depressive patients (Fang et al., 2019).

Sleep is regulated by circadian and homeostatic processes (Saper et al., 2005; Borbély, 2022). Melatonin (N-acetyl-5-methoxytryptamine) is an endogenous hormone that interacts with membrane melatonin receptors MT1 and MT2, two different types of G-protein-coupled receptors expressed both in brain regions and peripheral tissues (Pandi-Perumal et al., 2008; Pohanka, 2022). Melatonin regulates the circadian rhythm and affects sleep architecture. The central actions of melatonin on circadian rhythms focus on the hypothalamus, especially the suprachiasmatic nucleus (SCN) (Slominski et al., 2012). Melatonin also functions on the cortex, cerebellum, hippocampus, substantia nigra, and ventral tegument. Melatonin provides feedback signals to the SCN, having two distinct actions on the suprachiasmatic circadian clock, an acute inhibitory effect on neuronal firing and a phase-shifting effect on rhythm to regulate sleep (Liu et al., 1997; Cruz-Sanabria et al., 2023). The SCN neurons exhibit spontaneous circadian rhythms by interacting with positive and negative transcriptional-translational feedback loops (TTFLs), which contain clock genes and proteins. The positive transcriptional part of TTFLs consists of brain and muscle ARNT-like 1 (Bmal1) and circadian locomotor output kaput (Clock). Bmal1/Clock heterodimers bind to E-box components of the promoters of the Period (Per1-3), Cryptochrome (Cry1, 2), and Reverb (Nr1d1, Nr1d2) genes, whose proteins suppress the positive part of the loop (Musiek and Holtzman, 2016). At the molecular level, melatonin affects the circadian expression of clock genes. The mRNA transcription patterns of Per1 and Bmal1 in the rat SCN are phase shifted during the second night after 1 mg/kg melatonin injection (Poirel et al., 2003).

The function of melatonin is related to its central and peripheral concentrations. It has been proved that exogenous melatonin administration during the daytime increases subjective sleepiness (Lok et al., 2019). Melatonin synthesis and secretion occur in the pineal gland (Klein and Moore, 1979). The synthesis of melatonin involves several enzymes and small molecular compounds. Firstly, tryptophan (Trp) is transported into the cell and forms serotonin (5-hydroxytryptamine, 5-HT) by tryptophan-5-hydroxylase and 5-hydroxytryptophan decarboxylase. Then, 5-HT is acetylated by aralkylamine-N-acetyltransferase and methylated by N-acetylserotonin-O-methyltransferase to form melatonin (Acuña-Castroviejo et al., 2014).

It has been widely agreed that sleep disorders are linked to stress (Åkerstedt et al., 2012; Veeramachaneni et al., 2019). In clinical observations, chronic stress is one of the key risk factors for depression (Cruz-Pereira et al., 2020). Sleep disorder is a symptom of depression (Steiger and Pawlowski, 2019). The potential mechanisms between depression and sleep disorders have been associated with several pathways, including inflammation, neurotransmitters, and circadian rhythm, but the precise molecular mechanism of how depression induces sleep disorders remained unclear (Fang et al., 2019). Therefore, to elucidate the specific mechanism underlying the sleep disorders caused by chronic stress, we used a chronic restraint stress (CRS) mouse model to simulate chronic daily stress in humans.

Numerous studies have shown that CRS treatment can cause physiological and psychological stress in rodents by restricting movement in narrow spaces (Campos et al., 2013). CRS is a commonly used model of depression, and 28 days of such treatment causes depression in animals (Lin et al., 2021; Zhou et al., 2021). Some articles have studied the effects of short-term (<2 weeks) restraint stress on sleep in mice, but no long-term studies. (Meerlo et al., 2001; Koehl et al., 2006; Tang et al., 2007; Xu et al., 2023). In the present study, we built a mouse model by CRS 10 h each day for 28 days mimicking chronic stress, long-term stress-associated sleep structure, and disrupted circadian rhythm in patients. We then focused on melatonin, a key sleep regulator, including its content, synthesis, interaction with receptors, and regulation of circadian rhythm genes and proteins. Our study aims to provide a route for developing better treatment for sleep disorders.

2 Materials and methods

2.1 Animals modeling

Male ICR mice (4-week-old, weighing 20–22 g) were purchased from Beijing Vital River Laboratory Animal Technology Co., Ltd. (Beijing, China) and randomly assigned into different groups by weight to equalize the average weight in each group. Four mice were housed per cage, maintained at a constant temperature (25°C ± 0.5°C) and humidity (50% ± 10%) under an automatically controlled 12 h light/dark cycle, with *ad libitum* access to food and water. The light started at 9:00, defined as zeitgeber time (ZT) 0. All animal procedures were approved by the Animal Ethics Committee of the Institute of Medicinal Plant Development, Chinese Academy of Medical Sciences (approved No. SLXD-20210826023) and maintained adherence to the National Institutes of Health (NIH) guidelines for the care and use of laboratory animals.

After 3 days of acclimatization, the mice in the CRS-treated group were individually placed into a plastic cylinder (width: 3 cm) with holes at the bottom to allow free breathing (Wang et al., 2022), for 10 h (9:00–19:00) per day, for 14, 21, or 28 consecutive days (Figure 1A). The cylinder length was adjusted according to the mouse size to ensure complete restraint. The control mice did not receive food and water during the time the CRS-treated groups were subjected to stress. After CRS completion, the mice were returned to their cages with free access to food and water. The body weight (BW) of the animals was recorded every 3–4 days (Figure 1A).

2.2 Open field test

The open field test (OFT) was conducted on day 29 after modeling. The mice were placed individually in the center of Plexiglas boxes (30 × 28 × 35 cm) to record locomotor behaviors within 10 min after adapting to the new environment for 3 min.

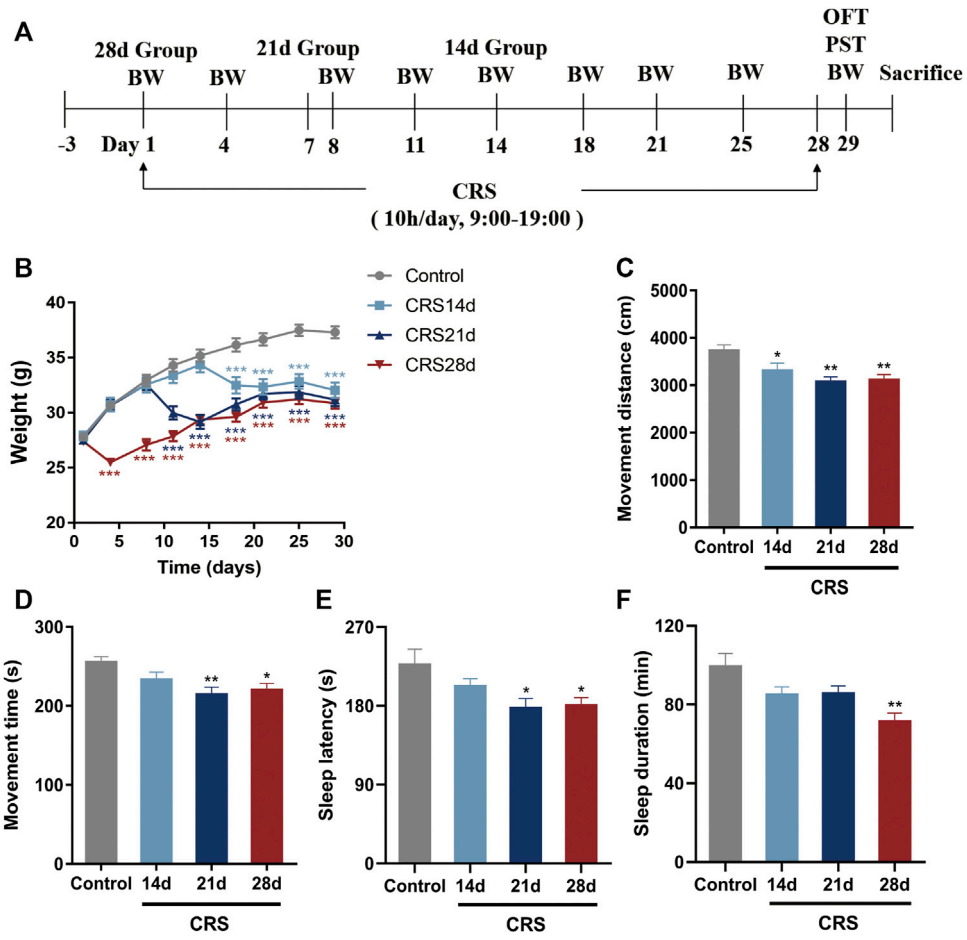

FIGURE 1
Effects of CRS on weight, locomotor activity, and sleep in mice (n = 10–12). **(A)** Experimental design of CRS-induced sleep disorders. Group CRS (28 days) was restrained on day 1 while group CRS (21 days) and group CRS (14 days) were restrained on day 8 and 15, respectively. **(B)** Body weight. **(C)** Movement distance of OFT. **(D)** Movement time of OFT. **(E)** Sleep latency. **(F)** Sleep duration. Data are presented as mean ± SEM. Compared with control group, $*p < 0.05$, $**p < 0.01$, $***p < 0.001$.

Locomotor activity was expressed as movement time (s) and distance (cm) using a video-tracking and analysis system (KSYY-OP-V4.0, Beijing, China).

2.3 Pentobarbital-induced sleep test

After the OFT, the pentobarbital-induced sleep test (PST) was performed between ZT 4.0–8.0 on day 29. The mice were moved to the testing room to adapt for 1 h, after which mice were injected intraperitoneally with 40 mg/kg (subthreshold dose) pentobarbital sodium to observe and record the number of mice falling asleep in each group within 30 min (Zhong et al., 2021). When the mice lost the righting reflex for about 1 min, they were considered asleep. Other mice were treated with pentobarbital (65 mg/kg, i.p.) to measure the sleep latency (time between pentobarbital injection and sleep onset) and duration (time between righting reflex loss and recovery) (Dong et al., 2021). The observers scoring these variables were blinded to grouping.

2.4 Electrode implantation

Mice in the control (n = 6) and CRS 28 d ($n = 6$) groups were anesthetized with 70 mg/kg pentobarbital and placed in a stereotaxic frame (RWD Life science Co., Ltd, Shenzhen, China). For electroencephalogram (EEG) monitoring, three stainless steel recording screws were implanted epidurally over the right frontal cortex (ML + 1.0 mm, AP + 1.5 mm from lambda) and the right parietal cortex (ML + 2.0 mm, AP—3.0 mm from lambda), and the cerebellum (ML 0.0 mm, AP—2.0 mm from bregma) as a reference electrode. For electromyography (EMG) monitoring, two flexible stainless-steel wire electrodes were placed bilaterally into the neck muscles to record postural tone. All screws were fixed on the skull surface with a dental base acrylic resin by connecting to a mini-connector to provide insulation and structural stability. Mice were allowed to recover in their cage for ≥10–14 days before EEG/EMG recordings. CRS-treated animals started with restraint on the second day after surgery.

2.5 EEG/EMG recording and analysis

Mice in the control (n = 6) and CRS 28 d (n = 6) groups were recorded individually in each chamber for 24 h (starting at ZT 0 on day 29) after acclimation. EEG/EMG signals were filtered (band passes EEG 0.5–49 Hz, EMG 10–100 Hz) and digitized at a sampling rate of 512 Hz using Sirenia Acquisition (Pinnacle Technology, Michigan, United States). EEG and EMG signals were subjected to spectral analysis by fast Fourier transformation using Sirenia Sleep Pro (Pinnacle Technology, Michigan, United States). Vigilance states were classified as wake, NREMS (non-rapid eye movement sleep), and REMS (rapid eye movement sleep) for each 10 s epoch according to EEG patterns of delta power (0.5–4 Hz), theta power (4.0–8.0 Hz), and the integral of EMG signals as previously described (Yasugaki et al., 2019). For each epoch, we first determined the brain state using a threshold algorithm. The state of wake included states with high EMG power or low delta power without elevated EMG activity. A state was classified as NREM if the delta power was larger than the delta threshold with low EMG power. A state was assigned as REM if the delta power was lower than the delta threshold with high theta power and low EMG power. Then, we manually verified the automatic sorting to ensure that all states were assigned correctly. Every epoch contained several states (wake, NREMS, REMS), defined as the state that lasted the longest time. The standard for one count of any state was ≥2 consecutive epochs having the same state.

2.6 Transcriptomic analysis

Mice in the control (n = 4) and CRS 28 d (n = 4) groups were anesthetized and sacrificed parallelly during ZT 2.0–3.0 on day 29. Total RNA from the hypothalamus was by Trizol Reagent (Solarbio, Beijing, China) and RNA-Seq analysis was performed. RNA quality was measured using NanoDrop 2000and8000, Agilent 2100 Bioanalyzer, Agilent RNA 6000 Nano Kit, and RNA was sequenced using Illumina NovaSeq 6000 platform. The per kilobase of exon model per million mapped fragments of gene expression for each sample was calculated using HTSeq. To obtain and adjust the p-values between samples, a negative binomial distribution test and false discovery rate estimation were used. Differentially expressed genes (DEGs) were defined as those having adjusted p-values <0.05.

2.7 Real-time quantitative PCR

Mice in the control (n = 6) and CRS 28 d (n = 6) groups were anesthetized and sacrificed in parallel during ZT 2.0–5.0 on day 29. Total RNA was extracted from the hypothalamus using Trizol Reagent (CW0580A; CWBIO, Beijing, China) according to the manufacturer's protocol and cDNA was generated by reverse transcription using the All-in-One First-Stand cDNA Synthesis Kit (P31012, TransGen Biotech, Beijing, China) with 2 μg of RNA as template. Real-time quantitative PCR (qRT-PCR) was performed using the TransStart Top Green qPCR SuperMix Kit (O21225, TransGen Biotech, Beijing, China). Each sample was tested in triplicate, and the results of relative mRNA levels were calculated using the $2^{-\Delta\Delta CT}$ method and normalized to the expression of the housekeeping gene β-actin. qPCR primers were synthesized by Sango Biotech (Shanghai, China); sequences are shown in Table 1.

2.8 Liquid chromatography-tandem mass spectrometry analysis

The levels of Trp and γ-aminobutyric acid (GABA) in the hypothalamus and cortex were measured by liquid chromatography-tandem mass spectrometry (LC-MS/MS) by using a Prominence LC system (SHIMADZU, Kyoto, Japan) connected with a QTRAP 5500 mass spectrometer (AB SCIEX, Foster City, CA). A Restek Ultra Aqueous C18 column (3 μm, 100 mm × 2.1 mm, Bellefonte, PA, United States) was used for chromatographic separation. Acetonitrile and water containing 0.1% formic acid constituted the mobile phase at an eluting rate of 0.4 mL/min. The hypothalamus and cortex samples were homogenized with 100 μL water and then the 50 μL homogenate was spiked with 20 μL 500 ng/mL acetaminol as internal standard and 10 μL trifluoroacetic acid to precipitate the protein. The mixture was blended and centrifuged at 4°C, 21,000 ×g for 20 min. Then, the supernatant was collected and a 2 μL aliquot was injected into the system.

2.9 Enzyme-linked immunosorbent assay (ELISA)

5-HT concentrations in the hypothalamus and cortex were detected using a Serotonin Assay Kit (H104-1-2, Nanjing Jiancheng Bioengineering Institute, Nanjing, China). The melatonin concentration in the hypothalamus and serum was measured with a Mouse Melatonin ELISA Kit (D721190, Sango Biotech, Shanghai, China). The process was carried out according to the manufacturer's instructions.

2.10 Western blotting

Mice in the control (n = 6) and CRS 28 d (n = 6) groups were anesthetized and sacrificed in parallel during ZT 2.0–6.0 on day 29. Brain tissues were immediately removed on ice and frozen at −80°C until homogenization. First, the hypothalamus and cortex tissues were lysed in ice-cold RIPA buffer (Solarbio, Beijing, China) containing 1% protease and phosphatase inhibitor cocktail (CWBIO, Beijing, China) with a mechanical homogenizer (Sonics, Newton, United States). Samples were then centrifuged for 20 min at 4°C and 15,000 g. Total protein concentrations were measured using a BCA protein assay kit (Solarbio, Beijing, China) and normalized on the basis. An equivalent of 30–50 μg protein was subjected to 10% tris-glycine SDS-PAGE and transferred to nitrocellulose membranes (Pall Corporation, New York, United States). The membranes were blocked with 5% BSA or non-fat milk in TBST for 1 h at room temperature and incubated in specific primary antibodies at 4°C overnight. After washing with TBST three times, the membranes were incubated with HRP-labeled goat anti-mouse or anti-rabbit IgG (1:5000 dilution, CWBIO, Beijing, China) for 2 h at room temperature. Protein bands were visualized using a gel

TABLE 1 Primer sequences for qRT-PCR.

Genes (mouse)	Forward primer (5′-3′)	Reverse primer (5′-3′)
Mtnr1a	ACCGCAACAAGAAGCTCAGGAAC	GATGTCAGCACCAAGGGATAAGGG
Mtnr1b	TCCGCAGGGAGTACAAGAGG	CACCTTCCTTGACAGGCACG
Clock	AGACGGCGAGAACTTGGCATTG	AACCTTTCCAGTGCTTCCTTGAGAC
Arntl	GGACTTCGCCTCTACCTGTTCAAAG	TCGTTGTCTGGCTCATTGTCTTCG
Per1	CTCCTCCTCCTACACTGCCTCTTC	TTGCTGACGACGGATCTTTCTTGG
Per2	CTGCGGATGCTCGTGGAATCTTC	GGTTGTGCTCTGCCTCTGTCATC
Per3	AAAGATCCTGACCTCGCCCTACG	TTTGTGCTTCTGCCTCTCGCTTC
Cry1	GCCAGCAGACACCATCACATCAG	CCAGGGAAGGAACGCCATATTTCTC
Cry2	TGGACAAGCACTTGGAACGGAAG	GTAGAAGAGGCGGCAGGAGAGG
Nr1d1	CGTCATCCTCTTCATCCTCCTCCTC	CTTGGTAATGTTGCTTGTGCCCTTG
Bhlhe40	CAGTACCTGGCGAAGCATGAGAAC	TCCGAGACCACACGATGGAGATG

TABLE 2 The effect of CRS on the falling asleep rate of mice (n = 11–12).

Group	Number of groups	Number of mice falling asleep	Falling asleep rate (%)
Control	12	7	58.33
CRS 14d	12	9	75.00
CRS 21d	12	3	25.00
CRS 28d	11	2	18.18*

Compared with the control group, *$p < 0.05$.

imaging system (Bio-Rad, Hercules, United States) with an enhanced ECL substrate (CWBIO, Beijing, China) and analyzed with ImageJ software.

Antibodies used were as follows: ß-actin (1:2000, AC006, ABclonal), Melatonin receptor 1A (1:100, SC-390328, Santa Cruz), Melatonin receptor 1B (1:500, ab203346, Abcam), PKCα (1:1,000, 2056T, Cell Signaling Technology), CREB (1:1,000, ab32515, Abcam), Phospho-CREB (Ser133) (1:1,000, 9198S, Cell Signaling Technology), CaMKII (1:1,000, #3362, Cell Signaling Technology), Phospho-CaMKII (1:200, sc-32289, Santa Cruz), Bmal1 (1:500, ET1705-5, HUABIO), Clock (1:500, T1704-82, HUABIO), Cry1 (1:1,000, ab104736, Abcam), Cry2 (1:500, 13997-1-AP, Proteintech), Per1 (1:500, HA500097, HUABIO), Per2 (1:1,000, 67513-1-Ig, Proteintech), and Per3 (1:500, HA500072, HUABIO).

2.11 Statistical analysis

All results are represented as the mean ± standard error of the mean (SEM) and analyzed using SPSS version 18.0 statistical software (SPSS, Inc., Chicago, United States). The normality and homogeneity were checked by Shapiro-Wilk test and Levene's test. Differences in multiple groups were statistically analyzed with One-way ANOVA followed by least significant difference or Dunnett's T3 test. The data in the two groups were compared using Student's t-test. The Mann-Whitney test was used for data following a non-parametric distribution. Significance was expressed as *$p < 0.05$, **$p < 0.01$ or ***$p < 0.001$. Figures were created using GraphPad Prism version 7.0 software (San Diego, United States).

3 Results

3.1 Impacts of repeated CRS treatments on mice behavior

To explore the effect of CRS treatment on weight, locomotor activity, and sleep, as well as to determine the time required by CRS treatment to cause sleep disorders in mice, the mouse body weight was recorded every 3–4 days, and an OFT and pentobarbital-induced sleep test were conducted on day 29 (Figure 1A). Compared with mice in the control group, the weight of CRS-treated mice decreased significantly in the first 3–4 days of the restraint process ($p < 0.001$) (Figure 1B). The movement distance and time decreased significantly, especially in the mice treated with CRS for 21 and 28 days, indicating that the locomotor activity was impaired (Figures 1C,D). The falling asleep rate, sleep latency, and sleep duration in the CRS groups were decreased in comparison with the controls. All these indexes in the CRS 28 d group were significantly different

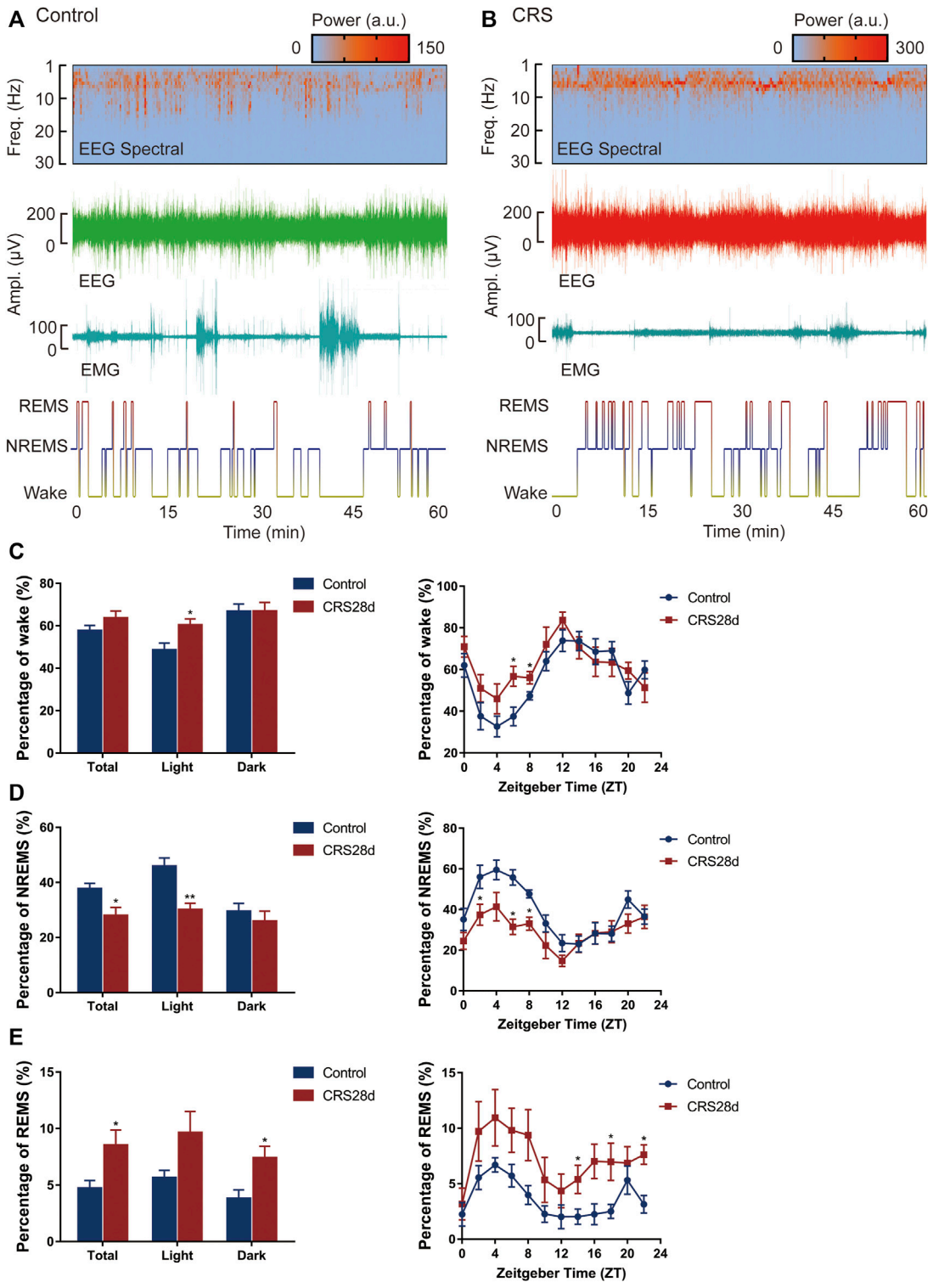

FIGURE 2
Effect of CRS 28 d on the sleep/wake cycle in mice (n = 6). **(A)** Example experiment. The EEG power spectrogram, EEG and EMG amplitude, and hypnogram of control mouse. **(B)** Example experiment. The EEG power spectrogram, EEG and EMG amplitude, and hypnogram of CRS mouse. **(C)** The percentage of wake amount. **(D)** The percentage of NREMS amount. **(E)** The percentage of REMS amount. Data were presented as mean ± SEM. Compared with control group, *p < 0.05.

from the control group (Table 2; Figures 1C–F). Particularly, the sleep duration decreased to 85.5%, 86.3%, and 71.9% that of control mice after CRS treatment for 14, 21, and 28 days, respectively. Thus, CRS treatment for 28 days induced sleep disorders in mice and was selected to study the underlying mechanism.

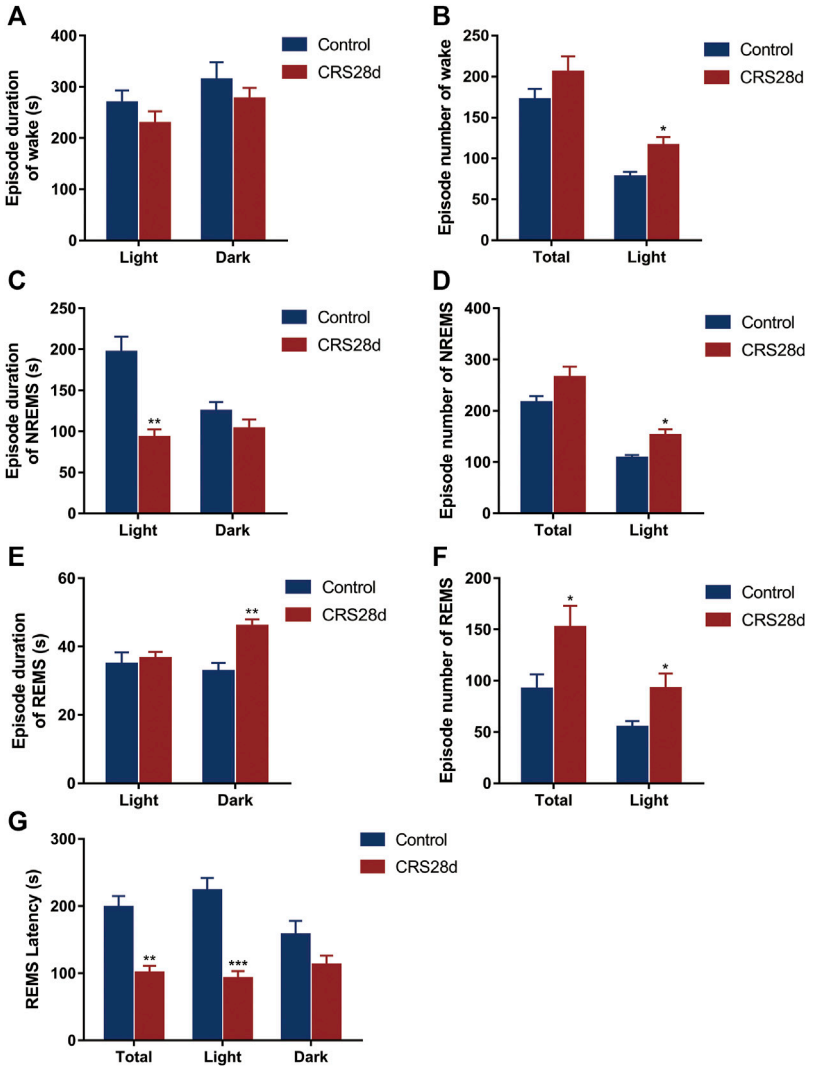

FIGURE 3
Effect of CRS 28 d on the episode duration and number of sleep/wake cycle in mice (n = 6). **(A)** Episode duration of wake time in light and dark phases. **(B)** Episode number of wake time in total and light phase. **(C)** Episode duration of NREMS time in light and dark phases. **(D)** Episode number of NREMS time in total and light phase. **(E)** Episode duration of REMS time in light and dark phases. **(F)** Episode number of REMS time in total and light phase. **(G)** Mean REMS latency in 24 h, light phase, and dark phase. Data were presented as mean ± SEM, $*p < 0.05$, $**p < 0.01$, $***p < 0.001$.

3.2 CRS treatment caused sleep disorders in mice

The effect of CRS treatment on the sleep/wake architecture of the mice was investigated by consecutive EEG/EMG recordings for 24 h (started at ZT 0 on day 29). Brain states were classified from EEG and EMG recordings, including wake, REMS, and NREMS. REMS was observed at a high probability in CRS-treated mice. A tendency of increased wake frequency was also displayed in the CRS group (Figures 2A,B). Wake and NREMS are complementary in proportional changes in 24 h, the percentage of wakefulness was increased, especially during the light (Figure 2C). The percentage of NREMS was decreased significantly both in light and total. NREMS was mainly reduced in ZT 2–8, while wakefulness was significantly increased in ZT 6–8 (Figures 2C,D). In contrast to NREMS, the REMS percentage was increased significantly at ZT 14,18, and 22, mainly in the dark phase (Figure 2E). The alternations of percentage in each phase demonstrated disrupted circadian rhythm and insomnia in CRS-treated mice.

Brain states and sleep structures are varied during light and dark phases (Figure 3). The mean duration of wake episodes was tended to decrease, and the episode numbers were increased significantly in the light phase (Figures 3A,B). Reversed episode duration changes were shown in NREMS and REMS episodes. The duration of NREMS was decreased significantly in the light phase, while REMS duration was increased significantly in the dark phase (Figures 3C,E). However, the number of NREMS and REMS episodes was increased significantly in light (Figures 3D,F). No alteration was found in the episode number of wake, NREMS, and REMS in dark. The increase in episode number in each phase explained that sleep in CRS-modeled mice was fragmented.

The REMS latency, i.e., duration of the NREMS episode immediately preceding a REMS episode, was examined from all

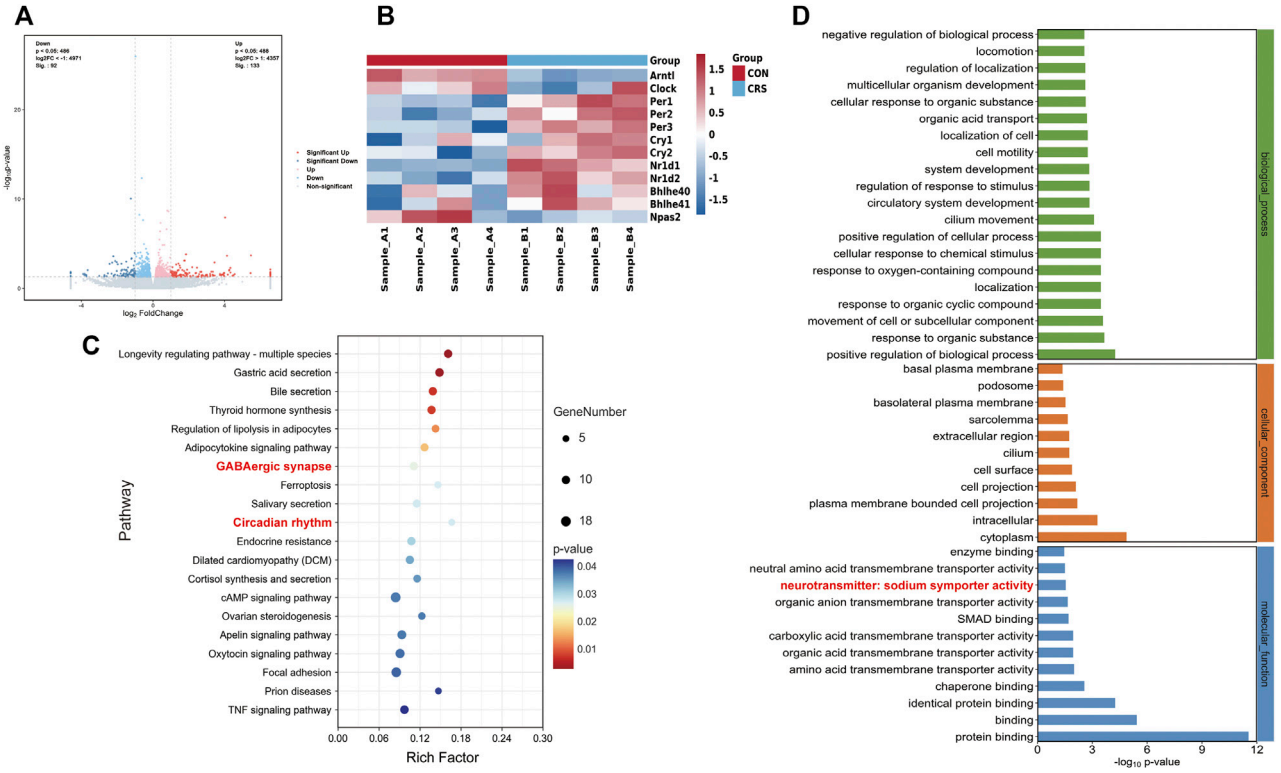

FIGURE 4
Effect of CRS 28 d on gene expression profile in the mouse hypothalamus (n = 4). **(A)** Volcano map of transcriptome. **(B)** Heatmap of the circadian rhythm signaling pathway-related DEG expression. **(C)** KEGG (Top 20 of the total pathway, $p < 0.05$). **(D)** Significantly enriched GO biological process, cellular component, and molecular function for DEGs.

groups. Accordingly, the REMS latency decreased not only over 24 h but also in the light phase (Figure G). Our EEG/EMG results indicated sleep fragmentation, circadian rhythm disorders, and insomnia in the CRS-treated mice.

3.3 Impacts of CRS treatment on hypothalamic gene expression profile

Hypothalamic RNA sequencing was performed after 28 d-CRS treatment to gain insights into the molecular mechanisms whereby CRS treatment caused sleep disorders. We identified 225 DEGs between the control and CRS 28 d groups, including 92 genes significantly downregulated and 133 genes significantly upregulated (Figure 4A). Kyoto Encyclopedia of Genes and Genomes (KEGG) enrichment analysis showed the top 20 pathways of these DEGs (Figure 4C). In which, the pathways involved in sleep regulation were GABAergic synapse and circadian rhythm signaling pathways. The main alternation in GABAergic synapses was neurotransmitter symporter activity as shown in Figure 4D. GABA symporters were more relative to epilepsy and other neurological disorders than sleep. Therefore, we focused on circadian rhythm signaling pathways; the heatmap of circadian rhythm genes was highly regulated by CRS treatment (Figure 4B). GABA and circadian rhythms were both regulated by melatonin. Therefore, our transcriptome results indicated that melatonin was a key regulator in the sleep disorder caused by CRS treatment, and the GABA and melatonin levels were probably altered in the brain.

3.4 CRS treatment changed transcription and expression of hypothalamic circadian rhythm genes

To verify the transcriptome results, we detected the mRNA transcription of the main circadian rhythm genes forming TTFLs in the hypothalamus by qRT-PCR. The hypothalamic tissues were sampled in parallel at ZT 6.0–7.0. The relative mRNA level of *Bmal1* was significantly decreased (p = 0.044) while *Clock* only slightly decreased (Figures 5A,B). The results revealed a significant main effect of CRS treatment on *Per2*, *Per3*, and *Cry2* mRNA levels, which were increased in the hypothalamus (Figures 5D,E,G). The mRNA transcription of *Cry1* in CRS-treated mice was higher than in controls but not significantly so (Figure 5F). Further analysis indicated that *Per1* was unchanged (Figure 5C).

According to the results of the qRT-PCR, we then studied the protein levels of the main genes in TTFLs. Given light's strong Zeitgeber, TTFL proteins were changed inconspicuously. There was no significant increase in Bmal1 and Clock levels in CRS-treated mice (Figures 5I,J). As described in Figure 5K–M,

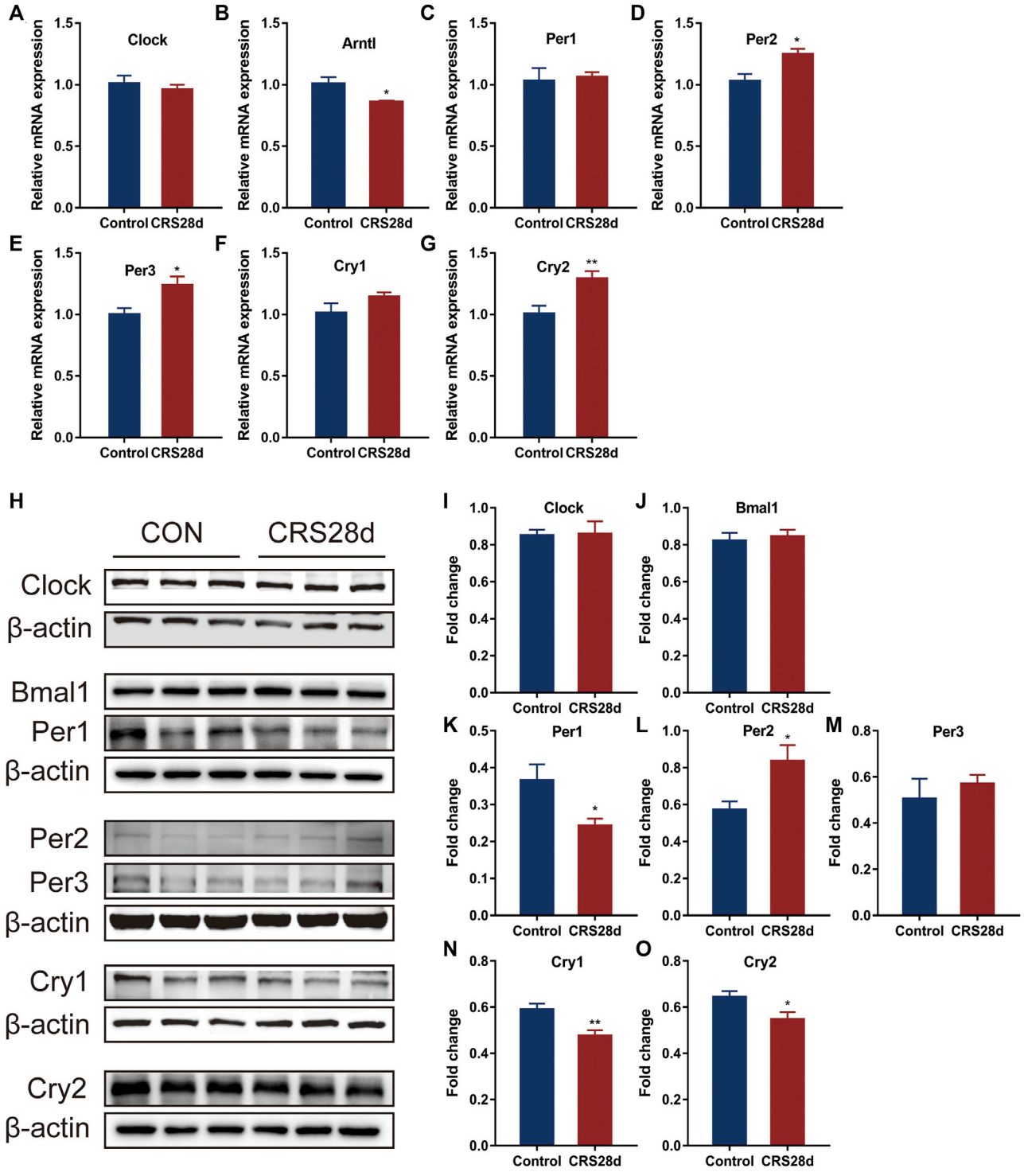

FIGURE 5
Effect of CRS 28 d on mRNA and protein expression levels of circadian rhythm genes in the mouse hypothalamus (n = 5–6). mRNA levels of *Clock* **(A)**, *Bmal1* **(B)**, *Per1* **(C)**, *Per2* **(D)**, *Per3* **(E)**, *Cry1* **(F)**, *Cry2* **(G)** circadian rhythm genes were examined by Real-time PCR (n = 5–6). **(H)** Immunoblotting of Clock, Bmal1, Per1, Per2, Per3, Cry1 and Cry2 in the hypothalamus. Quantification of Bmal1 **(I)**, Clock **(J)**, Per1 **(K)**, Per2 **(L)**, Per3 **(M)**, Cry1 **(N)**, Cry2 **(O)** protein abundance (n = 6). Data are presented as mean ± SEM, $^{*}p < 0.05$, $^{**}p < 0.01$.

in response to CRS treatment, Per1–3 had different alternations. Per1 protein levels decreased significantly while those of Per2 and Per3 increased. Additional quantification analysis showed that treatment with CRS resulted in significant Cry1 and Cry2 downregulation (Figures 5N,O). These results indicated that CRS treatment influenced more the downstream factors of TTFLs, Per1–3 and Cry1–2, so we focused on their upstream regulator, melatonin.

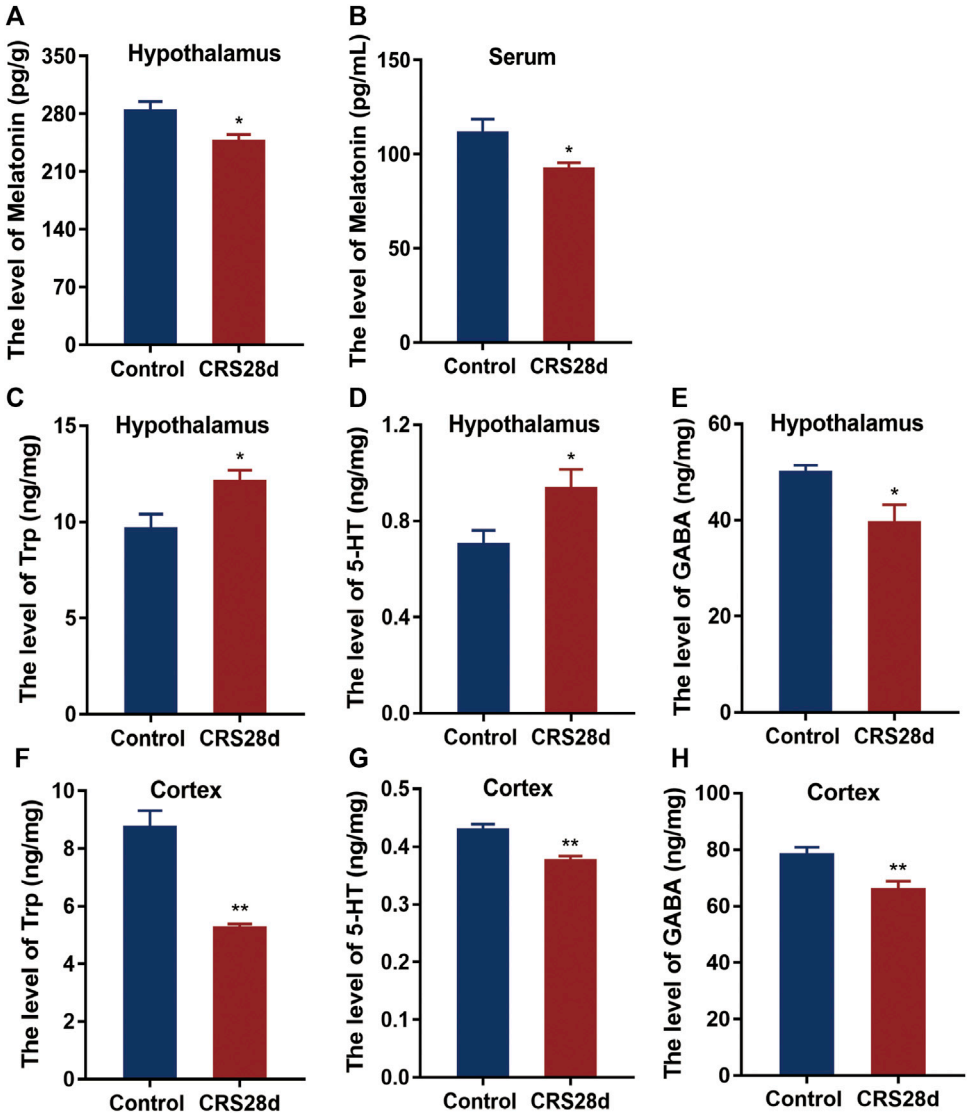

FIGURE 6
Effect of CRS 28 d on the concentrations of melatonin, 5-HT, Trp, and GABA in mice. **(A)** Melatonin in the hypothalamus (n = 9). **(B)** Melatonin in the serum (n = 10). **(C)** Trp in the hypothalamus (n = 10–12). **(D)** 5-HT in the hypothalamus (n = 8–9). **(E)** GABA in the hypothalamus (n = 10–11). **(F)** Trp in the cortex (n = 10–11). **(G)** 5-HT in the cortex (n = 11). **(H)** GABA in the cortex (n = 11–12). Data are presented as mean ± SEM, *p < 0.05, **p < 0.01.

3.5 CRS treatment downregulates melatonin concentration and melatonin related Trp, 5-HT and GABA

As the circadian rhythm signaling pathway is regulated by melatonin, we measured the levels of melatonin in the brain and in the periphery. Melatonin levels were significantly lower in CRS-treated mice than in controls both in the hypothalamus and sera (Figures 6A,B). Since melatonin is synthesized from Trp and 5-HT, their concentrations in the hypothalamus and cerebral cortex were also detected. Many wake-sleep projections are sent to the cortex through different neurons to regulate sleep (Saper et al., 2010). Trp and 5-HT levels in the hypothalamus were significantly increased but dramatically decreased in the cortex (Figures 6C,D,F,G). Melatonin could increase GABA level after pinealectomy and potentiate the GABA neuronal activity (Acuña-Castroviejo et al., 1995). As described in Figures 6A,E,H significant reduction of GABA levels was observed in both the hypothalamus and cortex. These results suggest that both melatonin synthesis and maintenance were altered by CRS treatment.

3.6 CRS treatment decreased the transcription and expression of melatonin receptors and altered melatonin receptors' downstream effectors

We also investigated mRNA transcription and protein levels of the melatonin receptors MT1 and MT2 in the hypothalamus. Both were significantly downregulated by CRS treatment (Figures 7B–D). In the

10.3389/fphar.2023.1210393

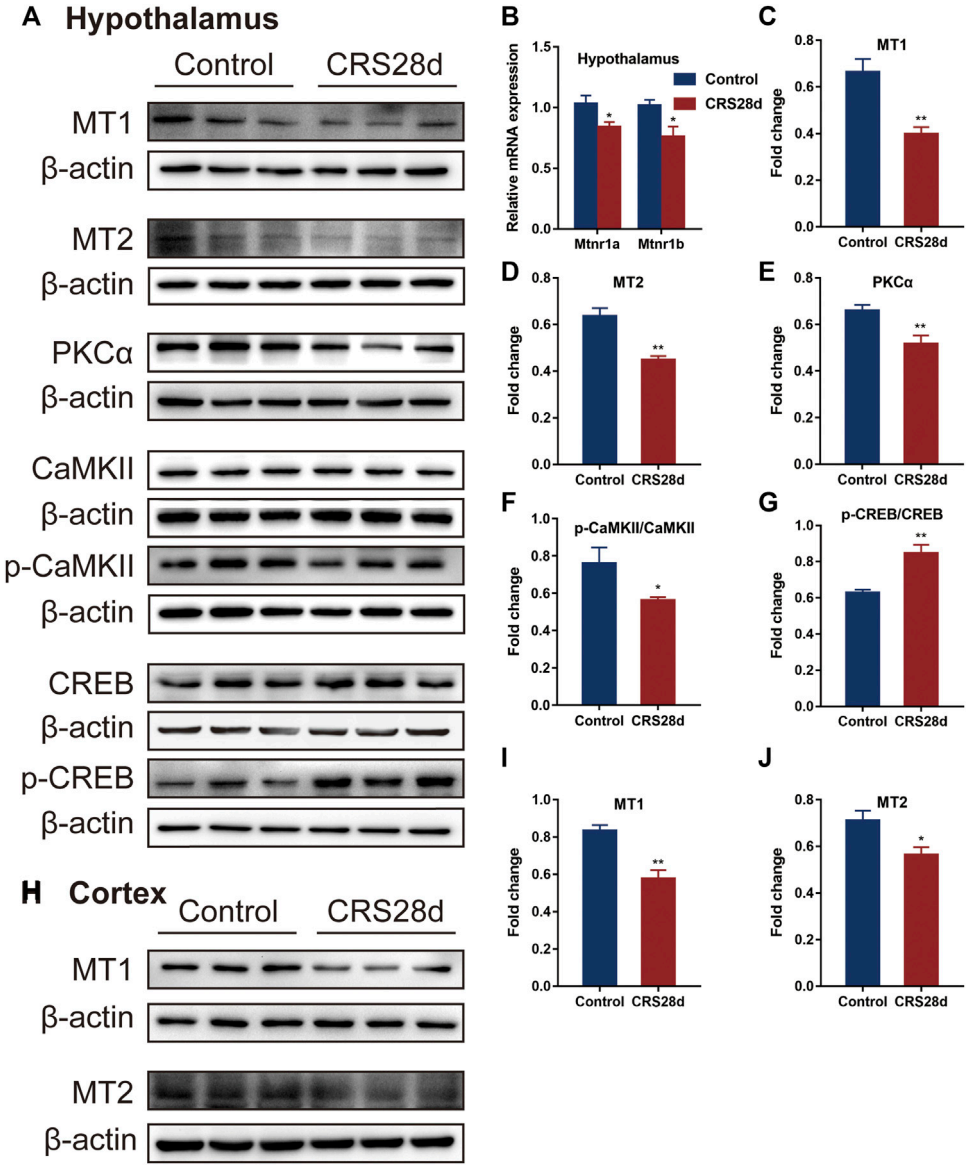

FIGURE 7
Effect of CRS 28 d on melatonin receptors and their related proteins in mice. **(A)** Immunoblotting of melatonin receptors and their related proteins in the hypothalamus. **(B)** mRNA levels of melatonin receptors (n = 4–6). Quantification of MT1 **(C)**, MT2 **(D)**, PKCα **(E)**, p-CAMKII/CAMKII **(F)**, p-CREB/CREB **(G)** protein abundance (n = 4–6) in the hypothalamus. **(H)** Immunoblotting of melatonin receptors in the cortex. Quantification of MT1 **(I)**, MT2 **(J)** protein abundance (n = 6) in the cortex. Data are presented as mean ± SEM, *p < 0.05, **p < 0.01.

cortex, MT1 and MT2 protein levels were also lower compared with the control (Figures 7H–J). Further, the expression of MT downstream proteins in the hypothalamus such as protein kinase C alpha type (PKCα) and phosphorylated calcium/calmodulin-dependent protein kinase II (p-CaMKII) was significantly decreased by CRS treatment but the total CaMKII remained unaffected (Figures 7E,F). With respect to the downstream signals of MT1 and MT2, CRS treatment upregulated the phosphorylation level of cyclic adenosine monophosphate (cAMP)-responsive element binding (p-CREB) protein but CREB levels remained unchanged (Figure 7G). These data demonstrated that CRS treatment affected the MT1 and MT2 signaling pathways and that melatonin and its receptors are the major targets in the mice of sleep disorders by CRS treatment.

4 Discussion

In the present study, we have simulated clinically observed chronic physiological and psychological stress in mice and explored changes in sleep architecture and molecular mechanisms underlying said sleep disorders. With the increasing CRS-modeling period, the symptoms of sleep disorders are gradually aggravated in mice. Although mice modeled by CRS for 21 days showed reduced locomotor activity and decrease in falling asleep rate and sleep duration in PST, at 28 days we observed significant sleep disorders. To our knowledge, this is the first study to examine the effects of chronic stress on mouse sleep by applying CRS for up to 28 days. Not only did the stress alter sleep architecture, but modeling for 10 h a day disrupted the mice's circadian

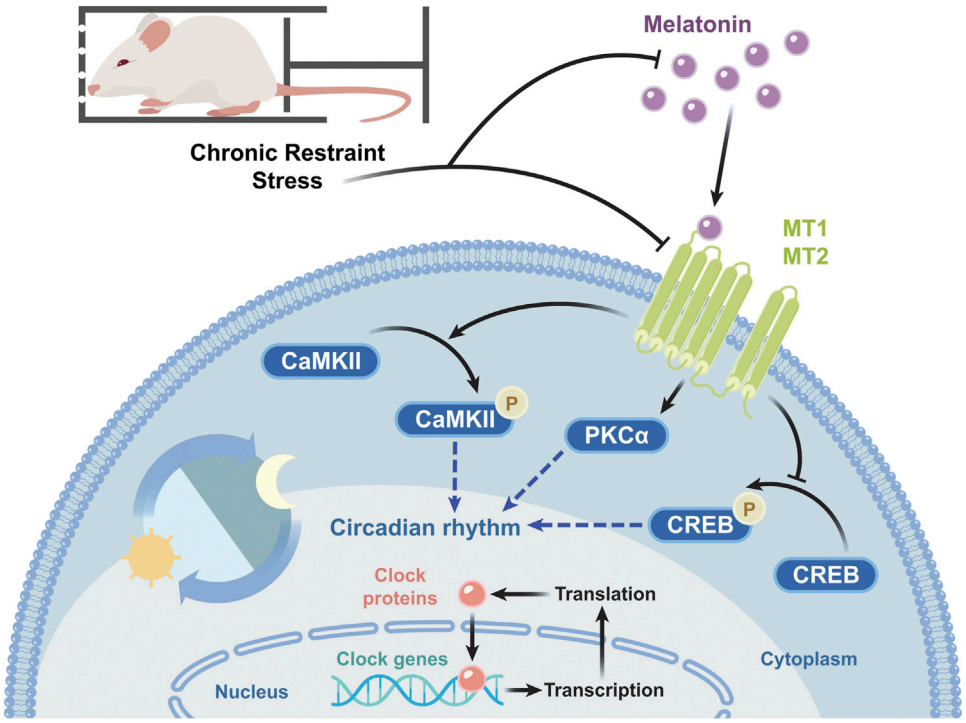

FIGURE 8
Schematic diagram of the molecular target pathways involved in CRS-induced sleep disorders. CRS decreases the melatonin level and the mRNA and protein levels of melatonin receptors, in turn reducing PKCα expression and p-CaMKII/CaMKII levels, increasing p-CREB/CREB levels, and changing the mRNA transcription and protein expression of circadian rhythm genes.

rhythms regulated by melatonin. Both the levels of melatonin and melatonin receptors were decreased in CRS-treated mice. The expression of melatonin-related receptors and circadian rhythm genes was affected as well. The molecular target pathways of CRS-induced sleep disorders are summarized in Figure 8.

In this study, we first found weight loss and decreased locomotor activity in mice with CRS treatment, similar to previous reports (Wang et al., 2021). The effect of CRS-treatment on sleep was evaluated by PST which preliminarily revealed reduced falling asleep rate, and shortened sleep latency and sleep duration (Table 2; Figures 1E,F). With increased CRS-treated time, sleep problems gradually intensified. Since 28 d-CRS mice showed the most obvious changes in various indexes, we chose this modeling intensity for the study of sleep architecture.

The corresponding polysomnographic of depressed patients is usually marked by a deficit in total sleep and slow wave sleep, shortened REM sleep onset latency, increased REM duration and density, sleep continuity disruption, and early morning awakening (Gillin et al., 1979; Pandi-Perumal et al., 2020). In our study, compared with the control, the CRS-treated mice had increased wakefulness in the light phase, especially during ZT 6–8 (Figure 2C). Recently, prolonged (about 4 w) chronic sleep disorders induced by psychophysiological stress have been shown to lead to increased arousal in mice (Oishi et al., 2020). The higher episode numbers of wake and NREM led to greater NREM sleep fragmentation during the light phase (Figures 3B,D). It was also confirmed by shorter average duration of NREM bouts in CRS-treated mice (Figure 3C). Correspondingly, the percentage of NREMS declined significantly during the light (ZT 2, 6–8). The alternation in these indexes indicated that CRS-treated mice had obvious symptoms of insomnia. In contrast to NREMS, the percentage, episode duration, and episode number of REMS dramatically increased (Figure 2E; Figures 3E,F). The increase in REMS was most evident in ZT14, 18–22 during the dark phase. Compared with the control mice, model mice were found to have reduced NREMS in the light phase and increased REMS in the dark phase, which demonstrated circadian rhythm disorders in CRS-treated mice (Figures 2C–E). The REMS amount and episode number also increased in the model of water immersion and restraint (2 h/d) for 1 w, 2 w, and 3 w. However, the model of water immersion and restraint showed increased wakefulness and NREMS, which is not consistent with our results because of the differences in stress factors, stimulating strength, and EEG/EMG detection period (Yasugaki et al., 2019). Another study found that 9 weeks of unpredictable chronic mild stress caused increased REMS variables in mice, which is the earliest marker of a stress response (Nollet et al., 2019). In addition, shortened REM latency has been considered a biological marker of depression in human (Palagini et al., 2013). In our study, the REMS latency was reduced totally in CRS-treated mice but more significantly during the dark phase (Figure 3G). The REMS latency was also decreased in the mice under social defeat stress for 10 days (Wells et al., 2017). In summary, CRS treatment caused sleep fragmentation, circadian rhythm disorders, and insomnia in mice is consistent with clinical observations from depressive patients and demonstrated typical stress-associated sleep disorders (Crouse et al., 2021).

Melatonin inputs to sleep controlling neurons reduce the time to sleep onset and increase sleep duration, also increasing NREMS (Holmes and Sugden, 1982). Research demonstrated that melatonin levels were significantly reduced at the peak of secretion in depression patients (Ogłodek et al., 2016). In our results, melatonin levels were reduced not only in the hypothalamus but also in the serum, indicating an overall decrease in central and peripheral melatonin levels. Trp and 5-HT levels were increased in the hypothalamus but decreased in the cortex, suggesting an issue with melatonin synthesis, which may be related to the activity of aralkylamine-N-acetyltransferase and N-acetylserotonin-O-methyltransferase enzymes. Studies over the past three decades has shown that 5-HT functions predominantly to promote wake (Monti, 2011). Increased hypothalamic 5-HT levels explained the increased wakefulness in model mice. Cortical 5-HT decline has been reported in CRS model (Geng et al., 2021; Sahoo et al., 2021), but its association with sleep needs further investigation. Melatonin increases GABA concentration by stimulating glutamic acid decarboxylase (Rosenstein and Cardinali, 1990), the enzyme that synthesizes GABA from glutamic acid. The ventrolateral preoptic nuclei is the main sleep-promoting center and contains plenty of GABAergic neurons, which inhibit the major wake-promoting centers in the hypothalamus and brain stem by GABA to induce sleep (Riemann et al., 2020). In our study, the significant decrease in GABA levels in the hypothalamus and cortex, which affect sleep in CRS-treated mice, may be related to the decreased melatonin levels in the brain.

The mRNA transcription of *MT1* and *MT2* is not only decreased in the hypothalamus, but the protein expressions are also decreased in the hypothalamus and cortex. In mice with genetic inactivation of both MT1/MT2 (*MT1*−/−/*MT2*−/−) receptors, wakefulness time increased. Mice with single inactivation of MT1 receptors showed a decrease in REMS time whereas those with inactivated MT2 receptors displayed a decrease in NREMS time (Comai et al., 2013). Therefore, MT1 receptors are mainly involved in REM sleep regulation while MT2 receptors are in NREM sleep (Gobbi and Comai, 2019). In our study, aside from the lower NREMS time in CRS-treated mice, we found significantly lower levels of both MT1 and MT2 receptors. Between *MT1*−/−/*MT2*−/− and wild-type mice, the total time of NREMS showed a downward trend but no statistical difference (Comai et al., 2013). Therefore, our study found a tendency that CRS treatment affected not only the expression of MT1 and MT2 receptors but other factors regulating sleep.

Downstream effectors of MT receptors play important roles in circadian rhythms and sleep regulation. In fact, melatonin receptors are coupled to pertussis toxin-sensitive G proteins. Pertussis toxin blocked melatonin-induced phase shifts in MT1 receptor-deficient mice (Liu et al., 1997). Melatonin can selectively activate PKC in the SCN inducing phase shift. For instance, 12-O-Tetradecanoylphorbol 13-acetate, a specific and direct PKC activator, could mimic the effect of melatonin, while a PKC inhibitor blocked this effect (McArthur et al., 1997). In our study, the reduction of PKCα proteins in the hypothalamus was decreased. Furthermore, the activation of MT2 receptors increases intracellular calcium ion and CaMKII expression and reduces CREB phosphorylation to recover the delayed sleep phase (Wang et al., 2020). CRS-treated mice showed decreased p-CaMKII levels and increased p-CREB levels. These results indicated impaired melatonin receptor function and downstream signal transduction that eventually affects the circadian rhythm.

Melatonin, melatonin receptors, and downstream proteins affect mRNA transcription and protein expression of circadian rhythm genes. Dardente et al. demonstrated that *Cry1* mRNA transcription (with diminished Per1) was directly induced by melatonin in the pars tuberalis (Dardente et al., 2003). Melatonin affects classical receptor-mediated pathways, regulating the circadian rhythm proteins via phosphorylation (Von Gall et al., 2002) and proteasome pathway (Vriend and Reiter, 2015). In addition, PKCα overexpression suppresses Bmal1-Clock transcriptional activity (Robles et al., 2010). The expression of circadian factors Bmal1, Clock, Per, and Cry is mainly regulated by the CaMK-CREB signaling pathway in the SCN (Yokota et al., 2001). Melatonin pretreatment can restore the circadian process by regulating circadian factors expressions through the CaMK-CREB pathway and post-translational modulation (Yin et al., 2022). With respect to mRNA, the transcription of *Per1–3* and *Cry1–2* was increased. The protein levels of Per1, Cry1, and Cry2 significantly decreased in the hypothalamus whereas those of Per2 increased after CRS treatment. Another research showed the relationship between melatonin and the rhythmic pattern of clock genes and their proteins in the pars tuberalis (Jilg et al., 2005). The mRNA transcriptions and protein expressions of clock genes have their own rhythm, and there is no clear expression correspondence. The changes in circadian rhythm genes between the CRS-treated and control mice suggested that CRS treatment induced circadian rhythm disorders, related to sleep disorders.

In conclusion, our results indicate that chronic CRS treatment induces typical stress-associated sleep disorders in mice which is consistent with observations from patients. All observed sleep disorders are related to impaired melatonin pathways and manifested by decreased levels of ligands, receptors, and relative downstream effectors. This study accessed the cause of stress-associated sleep symptoms. This study will also help us better understand the sleep characteristics and the pathogenesis of insomnia in depressed patients and provide a firm basis for future research. However, the changes in melatonin-related pathways may not fully explain the cause of CRS-induced sleep disorders; in the future, more targets need to be explored to dissect the complete mechanisms.

Data availability statement

The data presented in the study are deposited in the Figshare Dryad Digital Repository, and can be found online at: https://figshare.com/s/e19f30e8328125580863. Further inquiries can be directed to the corresponding authors.

Ethics statement

The animal study was reviewed and approved by Animal Ethics Committee of the Institute of Medicinal Plant Development, Chinese Academy of Medical Sciences.

Author contributions

T-JX conceived the project, analyzed the data, prepared the figures, and wrote the manuscript. T-JX, ZW, S-WJ, Y-GL, and S-SZ

performed the experiments. X-ML, R-LP, NJ, Y-HL, and M-ZY provided resources for the study and joined data discussion. L-DD revised the manuscript. M-ZY and QC achieved funding support, revised the manuscript and supervision. All authors contributed to the article and approved the submitted version.

Funding

This work was supported by the CAMS Innovation Fund for Medical Sciences (CIFMS, 2021-I2M-1-048), the National Key R&D Program of China (No. 2018YFC1602105), and the National Natural Science Foundation of China (82204739).

Acknowledgments

We thank Enago (www.enago.cn) for providing language editing service and Shandong Yikang Pharmaceutical Co. Ltd. for supporting on conference.

Conflict of interest

The authors declare that the research was conducted in the absence of any commercial or financial relationships that could be construed as a potential conflict of interest.

Publisher's note

Supplementary material

The Supplementary Material for this article can be found online at: https://www.frontiersin.org/articles/10.3389/fphar.2023.1210393/full#supplementary-material

References

Acuña-Castroviejo, D., Escames, G., Macías, M., Muñóz Hoyos, A., Molina Carballo, A., Arauzo, M., et al. (1995). Cell protective role of melatonin in the brain. *J. Pineal Res.* 19 (2), 57–63. doi:10.1111/j.1600-079x.1995.tb00171.x

Acuña-Castroviejo, D., Escames, G., Venegas, C., Díaz-Casado, M. E., Lima-Cabello, E., López, L. C., et al. (2014). Extrapineal melatonin: Sources, regulation, and potential functions. *Cell Mol. Life Sci.* 71 (16), 2997–3025. doi:10.1007/s00018-014-1579-2

Åkerstedt, T., Orsini, N., Petersen, H., Axelsson, J., Lekander, M., and Kecklund, G. (2012). Predicting sleep quality from stress and prior sleep--a study of day-to-day covariation across six weeks. *Sleep. Med.* 13 (6), 674–679. doi:10.1016/j.sleep.2011.12.013

Allega, O. R., Leng, X., Vaccarino, A., Skelly, M., Lanzini, M., Hidalgo, M. P., et al. (2018). Performance of the biological rhythms interview for assessment in neuropsychiatry: An item response theory and actigraphy analysis. *J. Affect Disord.* 225, 54–63. doi:10.1016/j.jad.2017.07.047

Bastien, C. H., Vallières, A., and Morin, C. M. (2004). Precipitating factors of insomnia. *Behav. Sleep. Med.* 2 (1), 50–62. doi:10.1207/s15402010bsm0201_5

Battle, B. E. (2013). Diagnostic and statistical manual of mental disorders. *Codas* 25, 191. doi:10.1590/s2317-17822013000200017

Billings, M. E., Hale, L., and Johnson, D. A. (2020). Physical and social environment relationship with sleep health and disorders. *Chest* 157 (5), 1304–1312. doi:10.1016/j.chest.2019.12.002

Borbély, A. (2022). The two-process model of sleep regulation: Beginnings and outlook. *J. Sleep. Res.* 31 (4), e13598. doi:10.1111/jsr.13598

Campos, A. C., Fogaça, M. V., Aguiar, D. C., and Guimarães, F. S. (2013). Animal models of anxiety disorders and stress. *Braz J. Psychiatry* 35 (2), S101–S111. doi:10.1590/1516-4446-2013-1139

Comai, S., Ochoa-Sanchez, R., and Gobbi, G. (2013). Sleep-wake characterization of double MT_1/MT_2 receptor knockout mice and comparison with MT_1 and MT_2 receptor knockout mice. *Behav. Brain Res.* 243, 231–238. doi:10.1016/j.bbr.2013.01.008

Crouse, J. J., Carpenter, J. S., Song, Y. J. C., Hockey, S. J., Naismith, S. L., Grunstein, R. R., et al. (2021). Circadian rhythm sleep-wake disturbances and depression in young people: Implications for prevention and early intervention. *Lancet Psychiatry* 8 (9), 813–823. doi:10.1016/s2215-0366(21)00034-1

Cruz-Pereira, J. S., Rea, K., Nolan, Y. M., O'Leary, O. F., Dinan, T. G., and Cryan, J. F. (2020). Depression's unholy trinity: Dysregulated stress, immunity, and the microbiome. *Annu. Rev. Psychol.* 71, 49–78. doi:10.1146/annurev-psych-122216-011613

Cruz-Sanabria, F., Carmassi, C., Bruno, S., Bazzani, A., Carli, M., Scarselli, M., et al. (2023). Melatonin as a chronobiotic with sleep-promoting properties. *Curr. Neuropharmacol.* 21 (4), 951–987. doi:10.2174/1570159x20666220217152617

Cuddapah, V. A., Zhang, S. L., and Sehgal, A. (2019). Regulation of the blood-brain barrier by circadian rhythms and sleep. *Trends Neurosci.* 42 (7), 500–510. doi:10.1016/j.tins.2019.05.001

Dardente, H., Menet, J. S., Poirel, V. J., Streicher, D., Gauer, F., Vivien-Roels, B., et al. (2003). Melatonin induces Cry1 expression in the pars tuberalis of the rat. *Brain Res. Mol. Brain Res.* 114 (2), 101–106. doi:10.1016/s0169-328x(03)00134-7

Demichelis, O. P., Grainger, S. A., McKay, K. T., Bourdaniotis, X. E., Churchill, E. G., and Henry, J. D. (2022). Sleep, stress and aggression: Meta-analyses investigating associations and causality. *Neurosci. Biobehav Rev.* 139, 104732. doi:10.1016/j.neubiorev.2022.104732

Dong, Y. J., Jiang, N. H., Zhan, L. H., Teng, X., Fang, X., Lin, M. Q., et al. (2021). Soporific effect of modified Suanzaoren Decoction on mice models of insomnia by regulating Orexin-A and HPA axis homeostasis. *Biomed. Pharmacother.* 143, 112141. doi:10.1016/j.biopha.2021.112141

Drake, C. L., Pillai, V., and Roth, T. (2014). Stress and sleep reactivity: A prospective investigation of the stress-diathesis model of insomnia. *Sleep* 37 (8), 1295–1304. doi:10.5665/sleep.3916

Fang, H., Tu, S., Sheng, J., and Shao, A. (2019). Depression in sleep disturbance: A review on a bidirectional relationship, mechanisms and treatment. *J. Cell Mol. Med.* 23 (4), 2324–2332. doi:10.1111/jcmm.14170

Geng, X., Wu, H., Li, Z., Li, C., Chen, D., Zong, J., et al. (2021). Jie-Yu-He-Huan capsule ameliorates anxiety-like behaviours in rats exposed to chronic restraint stress via the cAMP/PKA/CREB/BDNF signalling pathway. *Oxid. Med. Cell Longev.* 2021, 1703981. doi:10.1155/2021/1703981

Gillin, J. C., Duncan, W., Pettigrew, K. D., Frankel, B. L., and Snyder, F. (1979). Successful separation of depressed, normal, and insomniac subjects by EEG sleep data. *Arch. Gen. Psychiatry* 36 (1), 85–90. doi:10.1001/archpsyc.1979.01780010091010

Gobbi, G., and Comai, S. (2019). Differential function of melatonin MT (1) and MT (2) receptors in REM and NREM sleep. *Front. Endocrinol. (Lausanne)* 10, 87. doi:10.3389/fendo.2019.00087

Holmes, S. W., and Sugden, D. (1982). Effects of melatonin on sleep and neurochemistry in the rat. *Br. J. Pharmacol.* 76 (1), 95–101. doi:10.1111/j.1476-5381.1982.tb09194.x

Jahrami, H. A., Alhaj, O. A., Humood, A. M., Alenezi, A. F., Fekih-Romdhane, F., AlRasheed, M. M., et al. (2022). Sleep disturbances during the COVID-19 pandemic: A systematic review, meta-analysis, and meta-regression. *Sleep. Med. Rev.* 62, 101591. doi:10.1016/j.smrv.2022.101591

Jilg, A., Moek, J., Weaver, D. R., Korf, H. W., Stehle, J. H., and von Gall, C. (2005). Rhythms in clock proteins in the mouse pars tuberalis depend on MT1 melatonin receptor signalling. *Eur. J. Neurosci.* 22 (11), 2845–2854. doi:10.1111/j.1460-9568.2005.04485.x

Kim, E. J., and Dimsdale, J. E. (2007). The effect of psychosocial stress on sleep: A review of polysomnographic evidence. *Behav. Sleep. Med.* 5 (4), 256–278. doi:10.1080/15402000701557383

Klein, D. C., and Moore, R. Y. (1979). Pineal N-acetyltransferase and hydroxyindole-O-methyltransferase: Control by the retinohypothalamic tract and the suprachiasmatic nucleus. *Brain Res.* 174 (2), 245–262. doi:10.1016/0006-8993(79)90848-5

Koehl, M., Battle, S., and Meerlo, P. (2006). Sex differences in sleep: The response to sleep deprivation and restraint stress in mice. *Sleep* 29 (9), 1224–1231. doi:10.1093/sleep/29.9.1224

Lin, S., Li, Q., Jiang, S., Xu, Z., Jiang, Y., Liu, L., et al. (2021). Crocetin ameliorates chronic restraint stress-induced depression-like behaviors in mice by regulating MEK/ERK pathways and gut microbiota. *J. Ethnopharmacol.* 268, 113608. doi:10.1016/j.jep.2020.113608

Liu, C., Weaver, D. R., Jin, X., Shearman, L. P., Pieschl, R. L., Gribkoff, V. K., et al. (1997). Molecular dissection of two distinct actions of melatonin on the suprachiasmatic circadian clock. *Neuron* 19 (1), 91–102. doi:10.1016/s0896-6273(00)80350-5

Lok, R., van Koningsveld, M. J., Gordijn, M. C. M., Beersma, D. G. M., and Hut, R. A. (2019). Daytime melatonin and light independently affect human alertness and body temperature. *J. Pineal Res.* 67 (1), e12583. doi:10.1111/jpi.12583

McArthur, A. J., Hunt, A. E., and Gillette, M. U. (1997). Melatonin action and signal transduction in the rat suprachiasmatic circadian clock: Activation of protein kinase C at dusk and dawn. *Endocrinology* 138 (2), 627–634. doi:10.1210/endo.138.2.4925

Meerlo, P., Easton, A., Bergmann, B. M., and Turek, F. W. (2001). Restraint increases prolactin and REM sleep in C57BL/6J mice but not in BALB/cJ mice. *Am. J. Physiol. Regul. Integr. Comp. Physiol.* 281 (3), R846–R854. doi:10.1152/ajpregu.2001.281.3.R846

Meyer, N., Harvey, A. G., Lockley, S. W., and Dijk, D. J. (2022). Circadian rhythms and disorders of the timing of sleep. *Lancet* 400 (10357), 1061–1078. doi:10.1016/s0140-6736(22)00877-7

Monti, J. M. (2011). Serotonin control of sleep-wake behavior. *Sleep. Med. Rev.* 15 (4), 269–281. doi:10.1016/j.smrv.2010.11.003

Musiek, E. S., and Holtzman, D. M. (2016). Mechanisms linking circadian clocks, sleep, and neurodegeneration. *Science* 354 (6315), 1004–1008. doi:10.1126/science.aah4968

Nollet, M., Hicks, H., McCarthy, A. P., Wu, H., Möller-Levet, C. S., Laing, E. E., et al. (2019). REM sleep's unique associations with corticosterone regulation, apoptotic pathways, and behavior in chronic stress in mice. *Proc. Natl. Acad. Sci. U. S. A.* 116 (7), 2733–2742. doi:10.1073/pnas.1816456116

Ogłodek, E. A., Just, M. J., Szromek, A. R., and Araszkiewicz, A. (2016). Melatonin and neurotrophins NT-3, BDNF, NGF in patients with varying levels of depression severity. *Pharmacol. Rep.* 68 (5), 945–951. doi:10.1016/j.pharep.2016.04.003

Oishi, K., Okauchi, H., Yamamoto, S., and Higo-Yamamoto, S. (2020). Dietary natural cocoa ameliorates disrupted circadian rhythms in locomotor activity and sleep-wake cycles in mice with chronic sleep disorders caused by psychophysiological stress. *Nutrition* 75-76, 110751. doi:10.1016/j.nut.2020.110751

Palagini, L., Baglioni, C., Ciapparelli, A., Gemignani, A., and Riemann, D. (2013). REM sleep dysregulation in depression: State of the art. *Sleep. Med. Rev.* 17 (5), 377–390. doi:10.1016/j.smrv.2012.11.001

Pandi-Perumal, S. R., Monti, J. M., Burman, D., Karthikeyan, R., BaHammam, A. S., Spence, D. W., et al. (2020). Clarifying the role of sleep in depression: A narrative review. *Psychiatry Res.* 291, 113239. doi:10.1016/j.psychres.2020.113239

Pandi-Perumal, S. R., Trakht, I., Srinivasan, V., Spence, D. W., Maestroni, G. J., Zisapel, N., et al. (2008). Physiological effects of melatonin: Role of melatonin receptors and signal transduction pathways. *Prog. Neurobiol.* 85 (3), 335–353. doi:10.1016/j.pneurobio.2008.04.001

Pohanka, M. (2022). New uses of melatonin as a drug; A review. *Curr. Med. Chem.* 29 (20), 3622–3637. doi:10.2174/0929867329666220105115755

Poirel, V. J., Boggio, V., Dardente, H., Pevet, P., Masson-Pevet, M., and Gauer, F. (2003). Contrary to other non-photic cues, acute melatonin injection does not induce immediate changes of clock gene mRNA expression in the rat suprachiasmatic nuclei. *Neuroscience* 120 (3), 745–755. doi:10.1016/s0306-4522(03)00344-0

Riemann, D., Krone, L. B., Wulff, K., and Nissen, C. (2020). Sleep, insomnia, and depression. *Neuropsychopharmacology* 45 (1), 74–89. doi:10.1038/s41386-019-0411-y

Robles, M. S., Boyault, C., Knutti, D., Padmanabhan, K., and Weitz, C. J. (2010). Identification of RACK1 and protein kinase Calpha as integral components of the mammalian circadian clock. *Science* 327 (5964), 463–466. doi:10.1126/science.1180067

Rosenstein, R. E., and Cardinali, D. P. (1990). Central gabaergic mechanisms as targets for melatonin activity in brain. *Neurochem. Int.* 17 (3), 373–379. doi:10.1016/0197-0186(90)90019-p

Sahoo, S., Kharkar, P. S., Sahu, N. U., and S, B. (2021). Anxiolytic activity of Psidium guajava in mice subjected to chronic restraint stress and effect on neurotransmitters in brain. *Phytother. Res.* 35 (3), 1399–1415. doi:10.1002/ptr.6900

Saper, C. B., Fuller, P. M., Pedersen, N. P., Lu, J., and Scammell, T. E. (2010). Sleep state switching. *Neuron* 68 (6), 1023–1042. doi:10.1016/j.neuron.2010.11.032

Saper, C. B., Scammell, T. E., and Lu, J. (2005). Hypothalamic regulation of sleep and circadian rhythms. *Nature* 437 (7063), 1257–1263. doi:10.1038/nature04284

Slominski, R. M., Reiter, R. J., Schlabritz-Loutsevitch, N., Ostrom, R. S., and Slominski, A. T. (2012). Melatonin membrane receptors in peripheral tissues: Distribution and functions. *Mol. Cell Endocrinol.* 351 (2), 152–166. doi:10.1016/j.mce.2012.01.004

Steiger, A., and Pawlowski, M. (2019). Depression and sleep. *Int. J. Mol. Sci.* 20 (3), 607. doi:10.3390/ijms20030607

Tang, X., Yang, L., and Sanford, L. D. (2007). Interactions between brief restraint, novelty and footshock stress on subsequent sleep and EEG power in rats. *Brain Res.* 1142, 110–118. doi:10.1016/j.brainres.2007.01.029

Tononi, G., and Cirelli, C. (2014). Sleep and the price of plasticity: From synaptic and cellular homeostasis to memory consolidation and integration. *Neuron* 81 (1), 12–34. doi:10.1016/j.neuron.2013.12.025

Veeramachaneni, K., Slavish, D. C., Dietch, J. R., Kelly, K., and Taylor, D. J. (2019). Intraindividual variability in sleep and perceived stress in young adults. *Sleep. Health* 5 (6), 572–579. doi:10.1016/j.sleh.2019.07.009

Von Gall, C., Stehle, J. H., and Weaver, D. R. (2002). Mammalian melatonin receptors: Molecular biology and signal transduction. *Cell Tissue Res.* 309 (1), 151–162. doi:10.1007/s00441-002-0581-4

Vriend, J., and Reiter, R. J. (2015). Melatonin feedback on clock genes: A theory involving the proteasome. *J. Pineal Res.* 58 (1), 1–11. doi:10.1111/jpi.12189

Wang, Q., Zhu, D., Ping, S., Li, C., Pang, K., Zhu, S., et al. (2020). Melatonin recovers sleep phase delayed by MK-801 through the melatonin MT (2) receptor- Ca (2+) -CaMKII-CREB pathway in the ventrolateral preoptic nucleus. *J. Pineal Res.* 69 (3), e12674. doi:10.1111/jpi.12674

Wang, Z., Jin, S., Xia, T., Liu, Y., Zhou, Y., Liu, X., et al. (2022). Nelumbinis stamen ameliorates chronic restraint stress-induced muscle dysfunction and fatigue in mice by decreasing serum corticosterone levels and activating Sestrin2. *J. Agric. Food Chem.* 70 (51), 16188–16200. doi:10.1021/acs.jafc.2c06318

Wang, Z., Xia, T., Jin, S., Liu, X., Pan, R., Yan, M., et al. (2021). Chronic restraint stress-induced muscle atrophy leads to fatigue in mice by inhibiting the AMPK signaling pathway. *Biomedicines* 9 (10), 1321. doi:10.3390/biomedicines9101321

Wells, A. M., Ridener, E., Bourbonais, C. A., Kim, W., Pantazopoulos, H., Carroll, F. I., et al. (2017). Effects of chronic social defeat stress on sleep and circadian rhythms are mitigated by kappa-opioid receptor antagonism. *J. Neurosci.* 37 (32), 7656–7668. doi:10.1523/jneurosci.0885-17.2017

Xu, Y. X., Liu, G. Y., Ji, Z. Z., Li, Y. Y., Wang, Y. L., Wu, X. Y., et al. (2023). Restraint stress induced anxiety and sleep in mice. *Front. Psychiatry* 14, 1090420. doi:10.3389/fpsyt.2023.1090420

Yasugaki, S., Liu, C. Y., Kashiwagi, M., Kanuka, M., Honda, T., Miyata, S., et al. (2019). Effects of 3 Weeks of water immersion and restraint stress on sleep in mice. *Front. Neurosci.* 13, 1072. doi:10.3389/fnins.2019.01072

Yin, X. L., Li, J. C., Xue, R., Li, S., Zhang, Y., Dong, H. J., et al. (2022). Melatonin pretreatment prevents propofol-induced sleep disturbance by modulating circadian rhythm in rats. *Exp. Neurol.* 354, 114086. doi:10.1016/j.expneurol.2022.114086

Yokota, S., Yamamoto, M., Moriya, T., Akiyama, M., Fukunaga, K., Miyamoto, E., et al. (2001). Involvement of calcium-calmodulin protein kinase but not mitogen-activated protein kinase in light-induced phase delays and Per gene expression in the suprachiasmatic nucleus of the hamster. *J. Neurochem.* 77 (2), 618–627. doi:10.1046/j.1471-4159.2001.00270.x

Zhong, Y., Zheng, Q., Hu, P., Huang, X., Yang, M., Ren, G., et al. (2021). Sedative and hypnotic effects of Perilla frutescens essential oil through GABAergic system pathway. *J. Ethnopharmacol.* 279, 113627. doi:10.1016/j.jep.2020.113627

Zhou, Y., Yan, M., Pan, R., Wang, Z., Tao, X., Li, C., et al. (2021). Radix Polygalae extract exerts antidepressant effects in behavioral despair mice and chronic restraint stress-induced rats probably by promoting autophagy and inhibiting neuroinflammation. *J. Ethnopharmacol.* 265, 113317. doi:10.1016/j.jep.2020.113317

frontiers | Frontiers in Neuroscience

TYPE Mini Review
PUBLISHED 24 July 2023
DOI 10.3389/fnins.2023.1237153

OPEN ACCESS

EDITED BY
Song Zhang,
Shanghai Jiao Tong University, China

REVIEWED BY
Barnali Ray Basu,
University of Calcutta, India

*CORRESPONDENCE
Osama A. Abulseoud
✉ Abulseoud.osama@Mayo.edu

RECEIVED 08 June 2023
ACCEPTED 10 July 2023
PUBLISHED 24 July 2023

CITATION
Sousa RAL, Yehia A and Abulseoud OA (2023) Attenuation of ferroptosis as a potential therapeutic target for neuropsychiatric manifestations of post-COVID syndrome. *Front. Neurosci.* 17:1237153. doi: 10.3389/fnins.2023.1237153

Attenuation of ferroptosis as a potential therapeutic target for neuropsychiatric manifestations of post-COVID syndrome

Ricardo A. L. Sousa[1], Asmaa Yehia[1,2] and Osama A. Abulseoud[1,3]*

[1]Department of Psychiatry and Psychology, Mayo Clinic Arizona, Phoenix, AZ, United States, [2]Department of Medical Physiology, Faculty of Medicine, Mansoura University, Mansoura, Egypt, [3]Department of Neuroscience, Graduate School of Biomedical Sciences, Mayo Clinic College of Medicine, Phoenix, AZ, United States

Coronavirus disease-19 (COVID-19), caused by severe acute respiratory syndrome coronavirus type 2 (SARS-CoV-2), is associated with the persistence of pre-existing or the emergence of new neurological and psychiatric manifestations as a part of a multi-system affection known collectively as "post-COVID syndrome." Cognitive decline is the most prominent feature among these manifestations. The underlying neurobiological mechanisms remain under intense investigation. Ferroptosis is a form of cell death that results from the excessive accumulation of intracellular reactive iron, which mediates lipid peroxidation. The accumulation of lipid-based reactive oxygen species (ROS) and the impairment of glutathione peroxidase 4 (GPX4) activity trigger ferroptosis. The COVID-19-associated cytokine storm enhances the levels of circulating pro-inflammatory cytokines and causes immune-cell hyper-activation that is tightly linked to iron dysregulation. Severe COVID-19 presents with iron overload as one of the main features of its pathogenesis. Iron overload promotes a state of inflammation and immune dysfunction. This is well demonstrated by the strong association between COVID-19 severity and high levels of ferritin, which is a well-known inflammatory and iron overload biomarker. The dysregulation of iron, the high levels of lipid peroxidation biomarkers, and the inactivation of GPX4 in COVID-19 patients make a strong case for ferroptosis as a potential mechanism behind post-COVID neuropsychiatric deficits. Therefore, here we review the characteristics of iron and the attenuation of ferroptosis as a potential therapeutic target for neuropsychiatric post-COVID syndrome.

KEYWORDS

ferroptosis, post-COVID syndrome, SARS-CoV-2, therapeutic target, long COVID

Introduction

Ferroptosis is defined as a controlled form of cell death driven by excess intracellular labile iron and loss of the anti-oxidant enzyme glutathione peroxidase 4 (GPX4) activity, with consequent accumulation of lipid-based reactive oxygen species (ROS), especially lipid hydroperoxides (Yang and Stockwell, 2016). Interestingly, a knockout of GPX4 in mice led to lethality before embryonic day 9 (E9), which indicates a vital role for GPX4 in mouse development (Matsui, 1996; Yant et al., 2003). In the absence of GPX4, lipid peroxidation *in vivo* has a lethal nature,especially in neurons (Seiler et al., 2008). Alongside the unfavorable effect of

GPX4 activity loss, iron overload contributes to the pathogenesis of coronavirus disease-19 (COVID-19), inciting inflammation, hypercoagulation, and immune dysfunction. Iron overload fosters an environment with free, unbound reactive iron, which triggers ROS generation (Habib et al., 2021). Ferritin, an iron storage protein, is a well-known inflammatory and iron overload biomarker, and is considered a direct mediator of the immune system in COVID-19 (Kappert et al., 2020; Kaushal et al., 2022; Lee et al., 2022). Iron overload is strongly suggested to contribute to the development of post-COVID neurological deficits (Fratta Pasini et al., 2021; Pandey et al., 2021; Zhang et al., 2022).

The post-COVID progressive and intense neurological clinical deterioration seems to occur due to the cytokine storm in COVID-19 patients (Para et al., 2022), which could create a vicious cycle with ferroptosis. Patients with COVID-19 presenting with high serum ferritin levels are usually in a severe condition (Abulseoud et al., 2022; Para et al., 2022). In addition, COVID-19 patients with comorbidities such as severe acute liver injury, diabetes, thrombotic complications, and cancer present with significantly higher levels of ferritin than those without (Cheng et al., 2020; Li et al., 2021).

A recent study analyzed COVID-19 effects over a 2-year retrospective cohort of 1,248,437 patients and revealed that cognitive decline, brain fog, and dementia are increasing over a 2-year follow-up period (Taquet et al., 2022). Another recent study by Wang et al. analyzed 6,245,282 older adults (over 65 years old), and the authors showed that older people infected by severe acute respiratory syndrome coronavirus 2 (SARS-CoV-2) were at significantly higher risk for a new diagnosis of Alzheimer's disease (Wang et al., 2022). Post-COVID neurological consequences are tightly linked to other systems, including changes in the cardiovascular and immune systems, as well as higher levels of stress, anxiety, and depression (Campos et al., 2019; Salari et al., 2020; Zubair et al., 2020; Improta-Caria et al., 2021; Júnior et al., 2021; Sousa et al., 2021). The enigmatic nature of the post-COVID syndrome's underlying mechanism necessitates intense investigation in order to achieve effective management strategy. Uncovering the role of iron as a potential therapeutic target is a critical step in pursuing better management of the post-COVID neurological consequences. Here, we review the characteristics of iron, and the attenuation of ferroptosis as a potential therapeutic target for neurological post-COVID syndrome.

Iron chemistry

Iron is the 26th element in the periodic table and is located in the transition metals group. It can exist in different oxidation states and possess catalytic properties (Neyens and Baeyens, 2003). Ferrous (Fe^{+2}) and ferric (Fe^{+3}) irons are the two most common iron states in biological systems (Cabantchik, 2014). From an atomic orbital energy standpoint, a ferrous iron atom has a total of 26 electrons distributed in the following manner: two electrons in 1 s (the least energy orbit), 2 electrons in 2 s, 6 electrons in 2p, 2 electrons in 3 s, 6 electrons in 3p, 2 electrons in 4 s, and 6 electrons in the 4d orbit (Fe: $1s^2 2s^2 2p^6 3s^2 3p^6 3d^6 4s^2$). The position energy in the 3rd orbit (3d) is slightly higher than the position energy in the 4th orbit (4 s). This means that electrons will fill the 4 s position first before filling the 3d position, and also that the 4 s electrons will be lost first before the 3d electrons (Sherry and Fürstner, 2008). That is why ferrous iron [(Fe^{2+}): $1s^2 2s^2 2p^6 3s^2 3p^6 3d^6$] has lost two electrons from the 4 s position, while ferric iron [(Fe^{3+}): $1s^2 2s^2 2p^6 3s^2 3p^6 3d^5$] has lost a total of three electrons (two from the 4 s and one from the 3d position). As such, ferric iron (Fe^{3+}) is relatively more stable than ferrous iron (Fe^{2+}). Stability means the balance between positive and negative charges in the atom. Changing the number of electrons disturbs this balance. The atom holds electrons through electron binding energy, which is the minimum energy required to remove an electron from an atom. This energy is directly proportional to the atomic number (heavier atoms have more energy) and inversely proportional to the distance from the nucleus (electrons in outer orbits require less energy to be removed from the atom). As stated, ferrous iron has lost two electrons from 4 s, leaving six electrons in 3d, while ferric iron has lost two electrons from 4 s and one from 3d leaving five electrons in 3d. Electrons in partially filled orbits require more energy to remove from the orbit compared to electrons in fully filled orbits, which is why ferric iron is more stable compared to ferrous iron. The ability of ferric iron (Fe^{3+}) to accept an electron and become ferrous iron (Fe^{2+}) is called reduction, and the ability of ferrous iron (Fe^{2+}) to donate an electron and become ferric iron (Fe^{3+}) is called oxidation (Figure 1).

This reduction–oxidation or Redox, is what makes iron a catalyst for reactions that require electron transfer (Hosseinzadeh and Lu, 2016). In the Fenton reaction, for example, iron catalyzes the decomposition of hydrogen peroxide (H_2O_2) to produce hydroxyl radicals ($^{\bullet}OH$) at an acidic PH with high oxidizing properties (Neyens and Baeyens, 2003) [see the reaction below. The unpaired electron of a free radical is represented with a dot ($^{\bullet}$)].

$$H_2O_2 + Fe^{3+} \rightarrow Fe^{2+} + H^+ + HO^{\bullet}{}_2$$

$$H_2O_2 + Fe^{2+} \rightarrow Fe^{3+} + OH^- + {}^{\bullet}OH$$

Numerous key enzymes rely on iron redox properties such as the mitochondrial respiratory chain enzymes (Gille and Reichmann, 2011), the aconitase enzyme in the tri-carboxylic acid cycle, which facilitates the conversion of citrate to iso-citrate via cis-aconitate (Kennedy et al., 1983; Robbins and Stout, 1989), and tyrosine hydroxylase, which is the rate-limiting enzyme in catecholamine synthesis (Ramsey et al., 1996; Daubner et al., 2011). Moreover, the serotonergic system may require ferrous iron (Fe^{2+}) for binding serotonin to serotonin-binding proteins (Tamir and Liu, 1982). As such, iron is beneficial in regulating energy production and neurotransmitter synthesis, such as glutamate (McGahan et al., 2005; Lall et al., 2008) and dopamine (Ramsey et al., 1996). However, the same inherent "pro-oxidant" ability of ferrous iron (Fe^{2+}) to donate an electron and catalyze enzymatic reactions also causes hydrogen peroxide (H_2O_2) to breakdown into hydroxyl radicals ($^{\bullet}OH$) causing lipid peroxidation and oxidative damage to proteins, deoxyribonucleic acid (DNA), and ribonucleic acid (RNA) (Graham et al., 2007). For this reason, the oxidative property of ferrous iron (Fe^{2+}) must be managed by transforming it into a more stable ferric iron (Fe^{3+}) and shielding this ferric iron (Fe^{2+}) from water by transporting ferric iron into protein transporters.

The liver is the major organ involved in iron homeostasis. The liver produces iron transporters, including transferrin and divalent metal transporter-1 (DMT1). Transferrin transports ferric iron in the

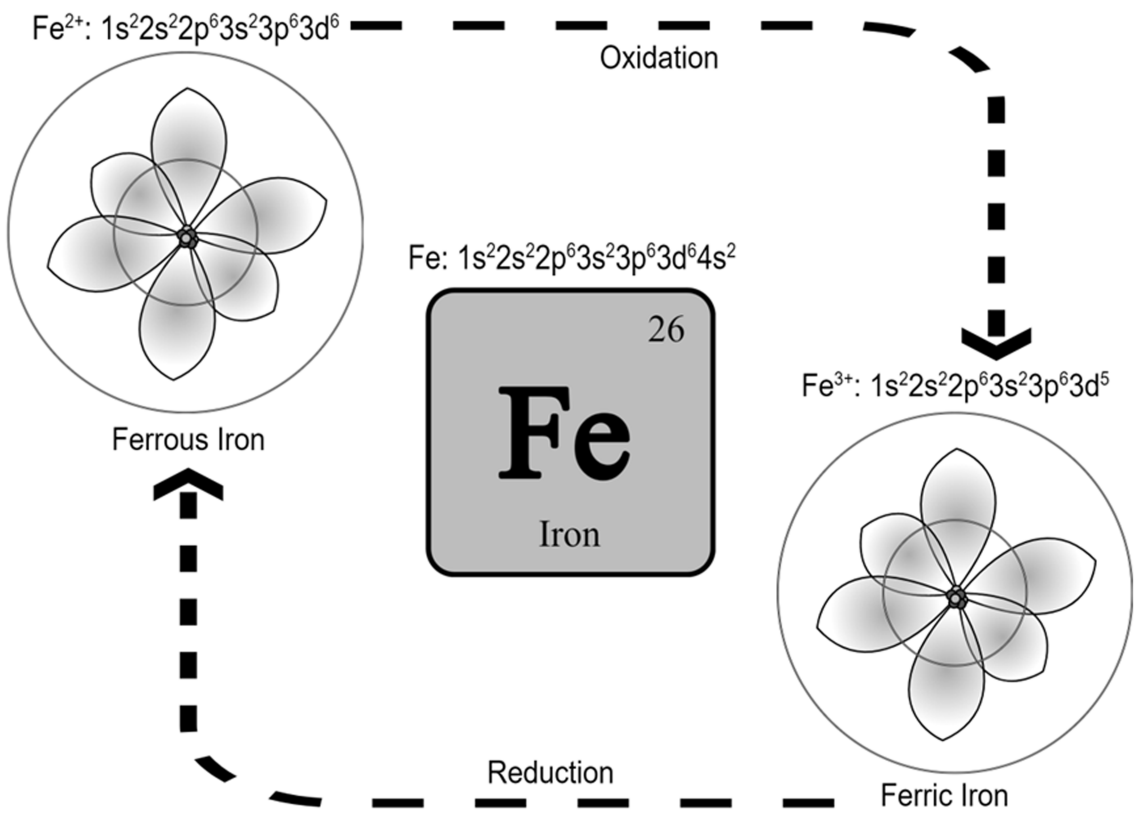

FIGURE 1
Iron and the two most common iron states in biological systems. It is called reduction when Fe^{3+} accepts an electron and becomes Fe^{2+}, and it is called oxidation when Fe^{2+} donates an electron and becomes Fe^{3+}. Schrodinger atom model is represented in the figures for ferrous and ferric iron.

intestinal lumen and plasma, while DMT1 transports ferrous iron from the interior of the endosome to the cytosol. The liver also produces ferritin and hepcidin, which serve as the iron storage protein, and the only iron hormonal regulator, respectively. Furthermore, it produces transferrin receptor 1 (TfR1) and the iron responsive element binding proteins, which act as iron sensors and regulate the mRNA iron responsive element to enhance transferrin receptor translation and to down-regulate ferritin translation (Winterbourn, 1995). Moreover, the liver controls the oxidative state of iron by producing ferrireductase and ferroxidase enzymes. Ferrireductase reduces endosomal ferric iron, at low PH, within endocytosis vesicles into ferrous iron before it is released from the transferrin and reduces stored ferric iron into ferrous iron before release from ferritin, while ferroxidase oxidizes ferrous iron into ferric iron to be stored in ferritin (Graham et al., 2007).

Iron absorption and fate within the cell

Dietary ferric iron uptake by the intestinal mucosa depends on hepatic transferrin, Transferrin Receptor 1 (TfR1), and iron content within enterocytes. Transferrin is synthesized by hepatocytes and excreted through the biliary system into the intestinal lumen. Transferrin binds two atoms of iron per protein molecule and brings them into the cells by endocytosis (Bezkorovainy, 1989b). Duodenal and upper jejunal (low PH), but not ileal (Huebers et al., 1983), enterocyte crypts express TfR1 at the basolateral border (Barisani and Conte, 2002). These cells uptake iron from plasma transferrin by receptor-mediated endocytosis (Morgan and Oates, 2002). TfR1 is involved in sensing body iron stores. TfR1 expression increases with iron deficiency and decreases with iron overload (Barisani and Conte, 2002). Within endosomes, transferrin, TfR1, and ferric iron (Fe^{3+}) are subject to low PH to separate ferric iron (Fe^{3+}) from transferrin and TfR1. Transferrin and TfR1 are cycled back to the cell surface or plasma, while ferric iron (Fe^{3+}) is reduced by the ferrireductase enzyme into ferrous iron (Fe^{2+}). DMT1 transports ferrous iron (Fe^{2+}) out of the endosome and into the cytoplasm, where it enters a transient pool of metabolically active iron known as the labile iron pool (LIP). LIP iron can be utilized for cellular processes such as DNA synthesis, repair, and cell cycling. Alternatively, excess LIP iron can be stored in ferritin (Paul et al., 2017) or exit the cell through ferroportin. Iron storage as ferric iron (Fe^{3+}) within ferritin protein may occur (Ponka et al., 1998; Zandman-Goddard and Shoenfeld, 2007; Finazzi and Arosio, 2014). However, iron must be in the ferrous state (Fe^{2+}) to enter and exit the ferritin molecule (Crichton, 1973; Bezkorovainy, 1989a; Hintze and Theil, 2006). The enzymes ferroxidase and ferrireductase change the state of iron back and forth between ferric (Fe^{3+}) and ferrous (Fe^{2+}). Ferritin synthesis is up regulated by several factors, including high toxic oxygen radical or cytokine concentrations, typically seen during infections. High ferritin production reduces the bioavailability of iron which leads to less reactive oxygen radical production (Koorts and Viljoen, 2007; Zandman-Goddard and Shoenfeld, 2007).

On the other hand, rapid degradation of ferritin could be toxic due to the uncontrolled release of free reactive iron. However,

degradation within membrane-encapsulated "secondary lysosomes' may avoid this problem through the formation of hemosiderin, which is another form of iron storage protein (Harrison and Arosio, 1996). Iron exit depends on the iron export channel ferroportin expression and the hepatic hormone hepcidin concentration. Ferroportin is an iron transporter on the surface of absorptive enterocytes, hepatocytes, and other cells. The main function of ferroportin is to export ferrous iron from iron-containing cells into plasma transferrin as ferric iron (Fe^{3+}). The ferroxidase enzyme oxidizes ferrous iron into ferric iron (Nemeth et al., 2004; Ganz, 2005, 2006, 2007; Drakesmith et al., 2015). Hepcidin is an iron-regulatory hormone synthesized in hepatocytes. Hepcidin binds, internalizes, and degrades the cellular iron exporter ferroportin and thereby decreases iron efflux into plasma. Hepcidin synthesis is stimulated by high plasma iron and iron stores and inhibited by erythropoietic activity (Ganz, 2007). Hepcidin deficiency causes iron overload in hereditary hemochromatosis and ineffective erythropoiesis (Ganz and Nemeth, 2012; Ginzburg, 2019).

Brain iron uptake

Blood transferrin binds to transferrin receptors on epithelial cells of the choroid plexus and oligodendrocytes. Among glial cells, oligodendrocytes synthesize 90% of brain transferrin since iron plays a significant role in their development and in myelin formation (Todorich et al., 2009). Neurons and glial cells take up iron released into the brain interstitium, and apo-transferrin is recycled back to the blood (Bloch et al., 1987; Crowe and Morgan, 1992; Moos, 2002). This process increases during the period of rapid brain growth and iron deficiency and declines with age (Taylor and Morgan, 1990). It also can be reversed (from the brain interstitium back to the blood) during brain iron overload (Broadwell, 1989). Most iron entering the brain across the capillary endothelium finally leaves the system with the bulk outflow of the cerebrospinal fluid (CSF) through the arachnoid villi and other channels (Bradbury, 1997). Interestingly, approximately half of the transferrin in the CSF is derived from the choroid plexus, while the other half comes from the blood in the adult brain (Crowe and Morgan, 1992). Neuronal function is iron-dependent because of the high energy demand, oxidative metabolism, and cytochrome participation in the respiratory chain. The function of oligodendrocytes is also iron-dependent since iron is involved in lipid synthesis needed for myelin synthesis (Connor and Menzies, 1996). Microglial iron is essential for the inflammatory release of hydrolytic enzymes and free radicals via the oxidation of ferrous iron. Microglial iron also participates in the formation of nitric oxide, where iron acts as a co-factor for the nitric oxide synthase enzyme that catalyzes the formation of nitric oxide from the amino acid L-arginine (Moos, 2002). Several iron-related molecular pathways have been reported to be involved in COVID-19 (Farahani et al., 2022).

Iron-related molecular mechanisms in COVID-19

Uncovering the molecular mechanisms involved in SARS-CoV-2 infection is crucial for a better understanding and management of COVID-19's consequences. The angiotensin converting enzyme 2 (ACE2)/Angiotensin 1–7 Mas receptor pathway is an important part of the renin-angiotensin system (RAS), which converts angiotensin II into a heptapeptide (Angiotensin 1–7) and angiotensin I into a nonapeptide (Angiotensin 1–9). ACE2 works as a cell surface receptor through which SARS-CoV-2 can enter the cell (De Sousa et al., 2021; Farahani et al., 2022). Viral brain invasion occurs through the olfactory nerve, infection of the vascular endothelium, or migrating leukocytes crossing the blood–brain barrier (Zubair et al., 2020). SARS-CoV-2 infection leads to higher levels of ROS that will cause harmful effects on proteins, lipids, and DNA, creating a similar state to cell necrosis (Kouhpayeh et al., 2021). Ferroptosis is considered a novel type of cell death that shares some aspects with cell necrosis (Anthonymuthu et al., 2021). The excess of iron in the plasma and body organs is tightly related to COVID-19 (Liu P. et al., 2020; Habib et al., 2021; Li et al., 2021; Zhang et al., 2022).

Among the COVID-19 related molecular pathways, there are 22 pathways identified (RAS, NF-kappa B, mTOR, Notch, HIF-1, MAPK, JAK–STAT, TNF signaling pathway, autophagy, apoptosis, necroptosis, B cell receptor signaling pathway, chemokine signaling pathway, IL-17 signaling pathway, natural killer cell mediated cytotoxicity, NOD-like receptor signaling pathway, T cell receptor signaling pathway, Th1 and Th2 cell differentiation, Th17 cell differentiation, toll-like receptor signaling pathway, complement and coagulation cascades, and cytokine-cytokine receptor interaction pathway) with non-cross-talk genes and cross-talk genes making up 561 genes. The cytokine-cytokine receptor interaction pathway is the most significant pathway, presenting 197 crosstalk genes of the 561 total genes (Farahani et al., 2022). ADAM17 is also identified as an important mediator of the major signaling pathways involved in the deleterious consequences of COVID-19 since it processes various substrates, like membrane-anchored cytokines, growth factors, cell adhesion molecules, receptors, and other proteins. The reported damage to body organs and brain regions in COVID-19 results mainly from the cytokine storm, one of the main SARS-CoV-2 infection harmful consequences (Li et al., 2020).

Greater levels of inflammatory cytokines combined with a hypoxic state resulting from pulmonary dysfunction can lead to a reduction in blood flow and oxygen supply (Fratta Pasini et al., 2021). The cytokine storm is a prominent feature of the SARS-CoV-2 infection, instigating systemic flooding with pro-inflammatory cytokines such as interleukin-6 (IL-6), IL-1β, IL-8, interferon-γ (IFN-γ), tumor necrosis factor-alpha (TNF-α), monocyte chemo-attractant protein-1 (MCP-1), and macrophage inflammatory protein-1A (MIP-1A) (Fara et al., 2020; Kempuraj et al., 2020). Moreover, the cytokine storm co-exists with a massive increase in coagulopathies and acute phase reactants such as C-reactive protein (CRP) and serum ferritin which correlate with the severity of the disease (Cheng et al., 2020; Lino et al., 2021; Savla et al., 2021). High levels of peripheral pro-inflammatory cytokines compromise the blood brain barrier (BBB) integrity, cross over to the brain vicinity, and activate its resident immune cells, causing microglial activation which in turn creates a medium of neuroinflammation (Almutairi et al., 2021). Interleukin-6 (IL-6) stimulates the synthesis of ferritin and hepcidin in a cytokine storm (Daher et al., 2017; Bessman et al., 2020). Hepcidin and hepcidin-like proteins bind to ferroportin, the cellular iron exporter, which prevents iron outflow and contributes to enhanced LIP, posing the risk of the Fenton reaction and ferroptosis when GPX4 does not eliminate the excess lipid ROS (Frazer and Anderson, 2014; Ganz, 2018). Hoarding iron into the cell as in cases of iron overload could be detrimental since SARS-CoV-2 replication requires iron (Liu W. et al., 2020). Furthermore, SARS-CoV-2 attacks hemoglobin, leading to iron release into the circulation (Zhang et al.,

2022). Therefore, the interaction between the cytokine storm and iron dysregulation, with potential subsequent ferroptosis in COVID-19, could activate molecular mechanisms that result in brain damage. In that case, brain damage could heavily rely on higher hepcidin levels, excessive iron influx through transferrin receptors, and the release of free iron into the circulation due to infection. In addition, during ferroptosis, mitochondria stop elongating, condense, and reduce in size and number. Microglia get activated, engulf synapses, and are polarized to a pro-inflammatory phenotype, flooding the brain with pro-inflammatory cytokines such as tumor necrosis factor alpha (TNF-α), leading to changes in cognition and behavior (Figure 2; Zhang et al., 2022).

Ferroptosis inhibition: a possible therapeutic target for neurological post-COVID syndrome

Ferroptosis can be classified as a new type of cell death that is dependent on lipid peroxidation and characterized by mitochondrial shrinkage (Liu P. et al., 2020). Ferroptosis contributes to the development of several pathologic processes, including inflammation and neurodegenerative diseases (Zhang et al., 2022). Multiple neurodegenerative diseases present with iron accumulation and lipid peroxidation in the brain (Farahani et al., 2022). Hambright et al. tested the efficacy of tamoxifen-induced deletion of forebrain neuronal GPx4 gene (Gpx4BIKO mice) as a model of ferroptosis. Gpx4BIKO mice exhibited significant deficits in spatial learning and memory function associated with lipid peroxidation and hippocampal neurodegeneration. Treatment with the ferroptosis inhibitor liproxstatin-1 ameliorated neurodegeneration (Hambright et al., 2017). Recent studies have also documented the role of ferroptosis in mediating cognitive dysfunction in animal models of Alzheimer's disease (AZ). Using the 5xFAD mouse model (has low GPx4 and cognitive impairment), Chen et al. generated a 5xFAD mice that overexpress Gpx4 (5xFAD/GPX4). These mice with overexpressed GPx4 performed significantly better in memory and learning tasks compared to the control 5xFAD mice and had reduced neurodegeneration (Chen et al., 2022). Bao et al. showed that selective genetic deletion of ferroportin 1 led to ferroptosis, hippocampal atrophy and memory deficits, while restoring ferroportin 1 ameliorated ferroptosis and memory impairment in the APPswe/PS1dE9 mouse

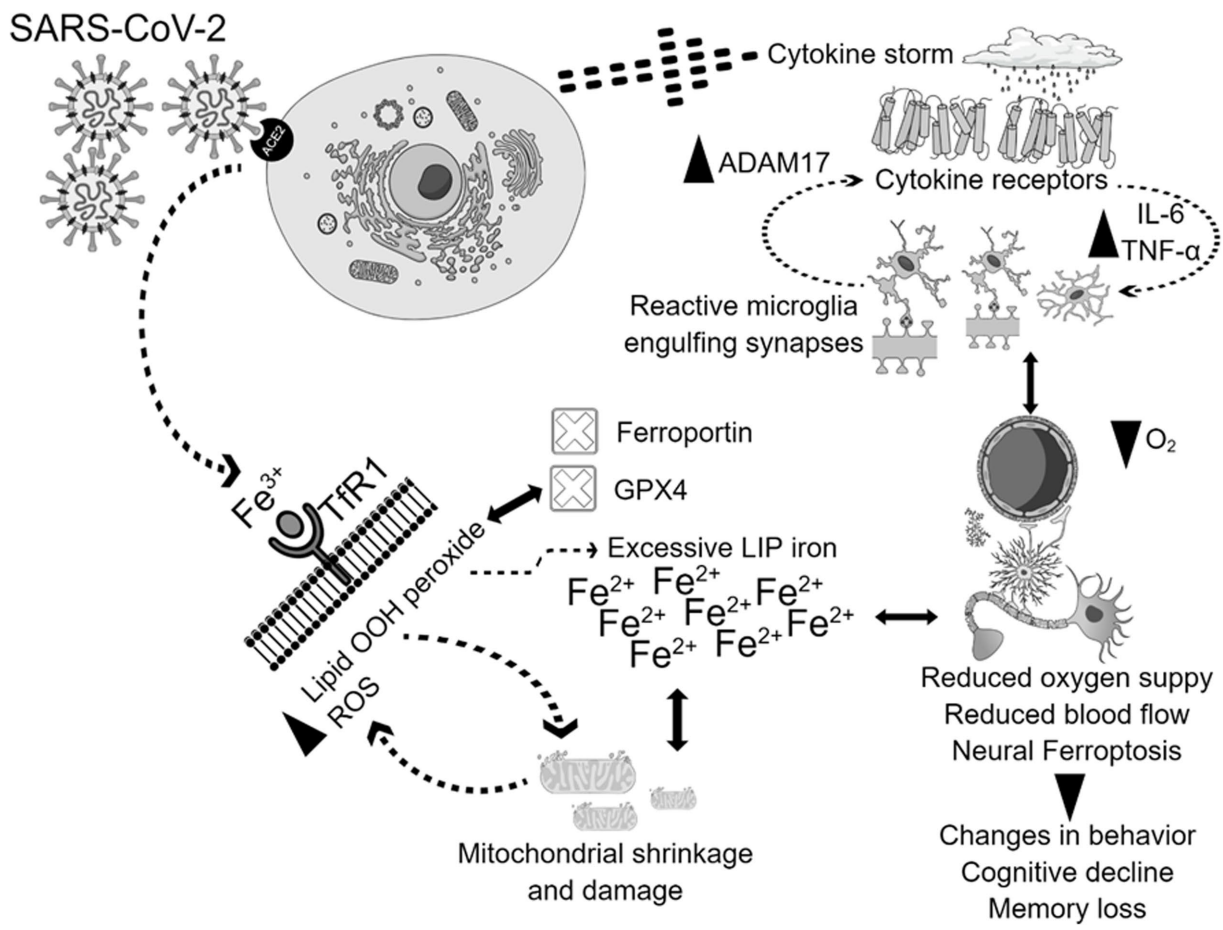

FIGURE 2
Potential mechanisms of physiological and neurological ferroptosis-associated changes due to SARS-CoV-2 infection. SARS-CoV-2 virus enters the cells through the ACE2 receptor, and triggers cytokine storm, and ferroptosis, which together contributes to mitochondrial damage, and microglial activation. The activation of all these mechanisms together contribute to the enhancement of ADAM17, TNF-, IL-6, with simultaneous inhibition of GPX4, ferroportin, reduction of oxygen supply, and blood flow. These physiological and neurological changes will lead to behavioral disturbances, cognitive decline, and memory loss.

model of AZ (Bao et al., 2021). Along the same lines, Hao et al. showed that cognitive dysfunction in the streptozotocin rat model of type 1 diabetes is related to hippocampal iron overload and ferroptosis mediated by down regulation of ferroportin 1 gene (Hao et al., 2021). A growing body of evidence suggests ferroptosis as a plausible mechanism behind the SARS-CoV-2-associated neuropsychiatric symptoms, cognitive decline, and memory loss (Zhang et al., 2022). In an ischemic stroke model, Acyl-coenzyme A synthase long-chain family member 4 (ACSL4), which is crucial to ferroptosis-related lipid peroxidation, promoted ferroptosis-induced brain injury and neuroinflammation with similar findings to neuro-COVID-19 events, such as infarct size increase, reduced neurological function, microglial activation, and increased pro-inflammatory cytokines (Cui et al., 2021). In the context of COVID 19, we can see glimpses of potential iron perturbation along with

TABLE 1 Ferroptosis inhibitors/ROS scavengers.

Ferroptosis inhibitors/ROS scavengers	Animal model	Effect	Reference
Liproxtatin-1	Tamoxifen-induced deletion of GPx4 gene (Gpx4BIKO mice), model of ferroptosis	Ameliorated spatial learning and memory function along with lipid peroxidation and hippocampal neurodegeneration.	Hambright et al. (2017)
Liproxtatin-1	Endovascular perforation model of sub arachnoid hemorrhage in Male C57BL/6 mice.	Attenuated the neurological deficits and brain edema, reduced neuronal cell death, restored the redox equilibrium, and preserved GPX4. It also decreased the activation of microglia and the release of IL-6, IL-1β, and TNF-α.	Cao et al. (2021)
Liproxtatin-1	LPS-Induced Cognitive Impairment in male C57BL/6 mice.	Ameliorated memory impairment induced by LPS. It decreased the microglial activation and the production of IL-6 and TNF-α, attenuated oxidative stress and lipid peroxidation, and alleviated mitochondrial injury and neuronal damage after LPS exposure. It decreased iron deposition and regulated the ferroptosis-related proteins; transferrin, heavy ferritin, mitochondrial ferritin and Gpx4.	Li et al. (2022)
Liproxtatin-1	Complete Freund's adjuvant (CFA)-induced inflammatory pain in male adult Sprague–Dawley (SD) rats	Intrathecal liproxstatin-1 improved mechanical and thermal hypersensitivities in CFA rats. It inhibited ferroptosis in the spinal cord and dorsal root ganglion tissues of CFA rats. It alleviated lipid peroxidation, disorders of anti-acyl-coenzyme A synthetase long-chain family member 4 (ACSL4) and GPX4.	Deng et al. (2023)
Liproxtatin-1	Type 2 diabetes (T2D)-associated cognitive dysfunction in HFD-fed C57BL/6 mice injected with low-dose streptozotocin.	Attenuated iron accumulation and oxidative stress response, resulting in better cognitive function.	Xie et al. (2023)
Ferrostatin-1	Kainic-acid model of temporal lobe epilepsy in adult male Sprague–Dawley rats	It improved cognitive functions in epileptic rats by inhibiting P38 MAPK and in turn increasing the expression of synaptophysin (SYP) and postsynaptic density protein 95 (PSD-95) in the hippocampus.	Ye et al. (2020)
Ferrostatin-1	Angiotensin II-induced inflammation in mouse primary cortical astrocytes isolated from CD-1 mice.	It suppressed the Ag II-induced increase of angiotensin 1 receptors, IL-6, IL-1β, and GFAP in the astrocytes. It upregulated the decreased GPx4, GSH, Nrf2, and HO-1 in the astrocytes induced by Ang II, denoting decreased inflammation and ROS production.	Li et al. (2021)
Ferrostatin-1	Amyloid beta (25–35)-injected Wistar rats model of Alzheimer's disease	It reversed the Aβ-induced spatial learning and memory impairment and enhanced the neuropathological changes such as better cell survival and less intracellular Aβ deposits. Levels of GPX4 and SLC7A11 were improved.	Naderi et al. (2023)
Ferrostatin-1	Middle cerebral artery occlusion (MCAO) model of cerebral ischemia/reperfusion injury in male C57BL/6 mice	It reduced high iron levels demonstrated in the stroke model. It also decreased lipid peroxidation with lower levels of malondialdehyde. It increased the levels of GSH and the expression of SLC7A11 and GPX 4. It reduced the infarct size and improved the neurobehavioral outcomes.	Liu et al. (2023)
Ferrostatin-1	Bupivacaine (BUP)-Induced spinal neurotoxicity in Sprague–Dawley male rats	Intrathecal ferrostatin-1 improved rats functional recovery, histopathological outcomes, and neural survival. It reversed the e BUP-induced ferroptosis-related mitochondrial shrinkage. It decreased lipid peroxidation products such as malondialdehyde (MDA) and 4-hydroxynonenal (4HNE). It inhibited the ROS accumulation and restored normal levels of GPX4, GSH, and SLC7A11.	Zhao et al. (2023)
GPX4	5xFAD Alzheimer's mouse model	Mice with overexpressed GPx4 performed significantly better in memory and learning tasks and had reduced neurodegeneration	Chen et al. (2022)

neuroinflammation in several forms. High serum ferritin (Cheng et al., 2020) and hepcidin levels (Hortová-Kohoutková et al., 2023), low serum iron levels (Gaiatto et al., 2023), and low transferrin saturation (Claise et al., 2022) have been significantly correlated with COVID-19 severity, hospitalization, and mortality (Zhou et al., 2020; Kaushal et al., 2022; Suriawinata and Mehta, 2022). In COVID-19 patients, altered iron metabolism, depletion of glutathione (GSH) (Kumar et al., 2022), inactivation of GPX4 (Muhammad et al., 2021), and up regulation of lipid peroxidation biomarkers strongly propose ferroptosis as a plausible mechanism for COVID-19 multi-organ affection, including neuropsychiatric sequelae (Yang and Lai, 2020).

It is repeatedly reported that the use of multiple iron chelators such as deferoxamine prevents the formation of ROS by averting electron donation from iron to oxygen, which could minimize ferroptosis (Ren et al., 2020; Anthonymuthu et al., 2021). To prevent ferroptosis, ferrostatin-1 plays a role as a lipid ROS scavenger (Yang and Stockwell, 2016). Ferrostatin-1 alleviates angiotensin II-induced inflammation and ferroptosis by inhibiting the enhancement of ROS levels in astrocytes and the subsequent reactive gliosis (Li et al., 2021). Another recent study showed that ferrostatin-1 diminishes the levels of ROS and malondialdehyde and enhances superoxide dismutase activity in HT-22 cells, revealing a protective effect of this ferroptosis inhibitor (Chu et al., 2020). Curiously, a recent study reported that ferrostatin-1, in the presence of reduced iron levels, eliminates lipid hydroperoxides, presenting a similar effect as GPX4 (Miotto et al., 2020). The use of deferoxamine as a ferroptosis inhibitor showed success in reducing inflammation and improving memory in different models of neurodegenerative diseases (Xue et al., 2016; Fine et al., 2020; Lee et al., 2021). These results propose ferroptosis inhibition as a plausible approach to managing the post-COVID neurological disturbances (Table 1).

Conclusion

The attenuation of ferroptosis as a potential therapeutic target for neurological post-COVID syndrome is not yet fully established. However, inactivation of GPX4 and up regulation of lipid peroxidation and ROS are constitutive components of both SARS-CoV-2 infection and ferroptosis, suggesting a potentially major role for ferroptosis inhibitors. Identifying the possible beneficial molecular changes in the brain caused by these inhibitors in the context of COVID-19 would provide a great insight into managing post-COVID neuropsychiatric manifestations.

Author contributions

OA: concept and design, drafting of the manuscript, and supervision. All authors: critical revision of the manuscript for important intellectual content.

Funding

This work was funded by the Department of Psychiatry and Psychology at the Mayo Clinic Arizona.

Conflict of interest

The authors declare that the research was conducted in the absence of any commercial or financial relationships that could be construed as a potential conflict of interest.

Publisher's note

References

Abulseoud, O. A., Yehia, A., Egol, C. J., Nettey, V. N., Aly, M., Qu, Y., et al. (2022). Attenuated initial serum ferritin concentration in critically ill coronavirus disease 2019 geriatric patients with comorbid psychiatric conditions. *Front. Psych.* 13:1035986. doi: 10.3389/fpsyt.2022.1035986

Almutairi, M. M., Sivandzade, F., Albekairi, T. H., Alqahtani, F., and Cucullo, L. (2021). Neuroinflammation and its impact on the pathogenesis of COVID-19. *Front. Med.* 8:745789. doi: 10.3389/fmed.2021.745789

Anthonymuthu, T. S., Tyurina, Y. Y., Sun, W. Y., Mikulska-Ruminska, K., Shrivastava, I. H., Tyurin, V. A., et al. (2021). Resolving the paradox of ferroptotic cell death: Ferrostatin-1 binds to 15LOX/PEBP1 complex, suppresses generation of peroxidized ETE-PE, and protects against ferroptosis. *Redox Biol.* 38:101744. doi: 10.1016/j.redox.2020.101744

Bao, W.-D., Pang, P., Zhou, X.-T., Fan, H., Xiong, W., Chen, K., et al. (2021). Loss of ferroportin induces memory impairment by promoting ferroptosis in Alzheimer's disease. *Cell Death Different.* 28, 1548–1562. doi: 10.1038/s41418-020-00685-9

Barisani, D., and Conte, D. (2002). Transferrin receptor 1 (TfR1) and putative stimulator of Fe transport (SFT) expression in iron deficiency and overload: an overview. *Blood Cells Mol. Dis.* 29, 498–505. doi: 10.1006/bcmd.2002.0588

Bessman, N. J., Mathieu, J. R. R., Renassia, C., Zhou, L., Fung, T. C., Fernandez, K. C., et al. (2020). Dendritic cell-derived hepcidin sequesters iron from the microbiota to promote mucosal healing. *Science* 368, 186–189. doi: 10.1126/science.aau6481

Bezkorovainy, A. (1989a). Biochemistry of nonheme iron in man. I. Iron proteins and cellular iron metabolism. *Clin. Physiol. Biochem.* 7, 1–17.

Bezkorovainy, A. (1989b). Biochemistry of nonheme iron in man. II. Absorption of iron. *Clin. Physiol. Biochem.* 7, 53–69.

Bloch, B., Popovici, T., Chouham, S., Levin, M. J., Tuil, D., and Kahn, A. (1987). Transferrin gene expression in choroid plexus of the adult rat brain. *Brain Res. Bull.* 18, 573–576. doi: 10.1016/0361-9230(87)90122-5

Bradbury, M. W. (1997). Transport of iron in the blood-brain-cerebrospinal fluid system. *J. Neurochem.* 69, 443–454.

Broadwell, R. D. (1989). Transcytosis of macromolecules through the blood-brain barrier: a cell biological perspective and critical appraisal. *Acta Neuropathol.* 79, 117–128. doi: 10.1007/BF00294368

Cabantchik, Z. I. (2014). Labile iron in cells and body fluids: physiology, pathology, and pharmacology. *Front. Pharmacol.* 5:45. doi: 10.3389/fphar.2014.00045

Campos, B. P. e. S., dos Santos Gomes, G. D., de Sousa Braz, A., and de Vilela, A. T. (2019). Cardiovascular risk factors and risk measurement in patients with psoriatic arthritis in a university hospital. *Int. J. Cardiovasc. Sci.* 33, 112–118.

Cao, Y., Li, Y., He, C., Yan, F., Li, J.-R., Hang-Zhe, X., et al. (2021). Selective ferroptosis inhibitor liproxstatin-1 attenuates neurological deficits and neuroinflammation after subarachnoid hemorrhage. *Neurosci. Bull.* 37, 535–549. doi: 10.1007/s12264-020-00620-5

Chen, L., Dar, N. J., Na, R., McLane, K. D., Yoo, K., Han, X., et al. (2022). Enhanced defense against ferroptosis ameliorates cognitive impairment and reduces neurodegeneration in 5xFAD mice. *Free Radic. Biol. Med.* 180, 1–12. doi: 10.1016/j.freeradbiomed.2022.01.002

Cheng, L., Li, H., Li, L., Liu, C., Yan, S., Chen, H., et al. (2020). Ferritin in the coronavirus disease 2019 (COVID-19): a systematic review and meta-analysis. *J. Clin. Lab. Anal.* 34:e23618. doi: 10.1002/jcla.23618

Chu, J., Liu, C. X., Song, R., and Li, Q. L. (2020). Ferrostatin-1 protects HT-22 cells from oxidative toxicity. *Neural Regen. Res.* 15, 528–536. doi: 10.4103/1673-5374.266060

Claise, C., Saleh, J., Rezek, M., Vaulont, S., Peyssonnaux, C., and Edeas, M. (2022). Low transferrin levels predict heightened inflammation in patients with COVID-19: new insights. *Int. J. Infect. Dis.* 116, 74–79. doi: 10.1016/j.ijid.2021.12.340

Connor, J. R., and Menzies, S. L. (1996). Relationship of iron to oligodendrocytes and myelination. *Glia* 17, 83–93. doi: 10.1002/(SICI)1098-1136(199606)17:2<83::AID-GLIA1>3.0.CO;2-7

Crichton, R. R. (1973). Structure and function of ferritin. *Angew. Chem. Int. Ed. Engl.* 12, 57–65. doi: 10.1002/anie.197300571

Crowe, A., and Morgan, E. H. (1992). Iron and transferrin uptake by brain and cerebrospinal fluid in the rat. *Brain Res.* 592, 8–16. doi: 10.1016/0006-8993(92)91652-U

Cui, Y., Zhang, Y., Zhao, X., Shao, L., Liu, G., Sun, C., et al. (2021). ACSL4 exacerbates ischemic stroke by promoting ferroptosis-induced brain injury and neuroinflammation. *Brain Behav. Immun.* 93, 312–321. doi: 10.1016/j.bbi.2021.01.003

Daher, R., Manceau, H., and Karim, Z. (2017). Iron metabolism and the role of the iron-regulating hormone hepcidin in health and disease. *Presse Med.* 46, e272–e278. doi: 10.1016/j.lpm.2017.10.006

Daubner, S. C., Le, T., and Wang, S. (2011). Tyrosine hydroxylase and regulation of dopamine synthesis. *Arch. Biochem. Biophys.* 508, 1–12. doi: 10.1016/j.abb.2010.12.017

Deng, Y.-F., Xiang, P., Jing-Yi, D., Liang, J.-F., and Li, X. (2023). Intrathecal liproxstatin-1 delivery inhibits ferroptosis and attenuates mechanical and thermal hypersensitivities in rats with complete Freund's adjuvant-induced inflammatory pain. *Neural Regen. Res.* 18, 456–462. doi: 10.4103/1673-5374.346547

Drakesmith, H., Nemeth, E., and Ganz, T. (2015). Ironing out Ferroportin. *Cell Metab.* 22, 777–787. doi: 10.1016/j.cmet.2015.09.006

Fara, A., Mitrev, Z., Rosalia, R. A., and Assas, B. M. (2020). Cytokine storm and COVID-19: a chronicle of pro-inflammatory cytokines. *Open Biol.* 10:200160. doi: 10.1098/rsob.200160

Farahani, M., Niknam, Z., Mohammadi Amirabad, L., Amiri-Dashatan, N., Koushki, M., Nemati, M., et al. (2022). Molecular pathways involved in COVID-19 and potential pathway-based therapeutic targets. *Biomed. Pharmacother.* 145:112420. doi: 10.1016/j.biopha.2021.112420

Finazzi, D., and Arosio, P. (2014). Biology of ferritin in mammals: an update on iron storage, oxidative damage and neurodegeneration. *Arch. Toxicol.* 88, 1787–1802. doi: 10.1007/s00204-014-1329-0

Fine, J. M., Kosyakovsky, J., Baillargeon, A. M., Tokarev, J. V., Cooner, J. M., Svitak, A. L., et al. (2020). Intranasal deferoxamine can improve memory in healthy C57 mice, suggesting a partially non-disease-specific pathway of functional neurologic improvement. *Brain Behav.* 10:e01536. doi: 10.1002/brb3.1536

Fratta Pasini, A. M., Stranieri, C., Girelli, D., Busti, F., and Cominacini, L. (2021). Is Ferroptosis a key component of the process leading to multiorgan damage in COVID-19? *Antioxidants* 10:1677. doi: 10.3390/antiox10111677

Frazer, D. M., and Anderson, G. J. (2014). The regulation of iron transport. *Biofactors* 40, 206–214. doi: 10.1002/biof.1148

Gaiatto, A. C., Macedo, T. A., Bibo, N. D. G. M., Raimundo, J. R. S., da Costa Aguiar Alves, B., Gascón, T., et al. (2023). COVID-19 compromises iron homeostasis: transferrin as a target of investigation. *J. Trace Elem. Med. Biol.* 76:127109. doi: 10.1016/j.jtemb.2022.127109

Ganz, T. (2005). Hepcidin--a regulator of intestinal iron absorption and iron recycling by macrophages. *Best Pract. Res. Clin. Haematol.* 18, 171–182. doi: 10.1016/j.beha.2004.08.020

Ganz, T. (2006). Hepcidin--a peptide hormone at the interface of innate immunity and iron metabolism. *Curr. Top. Microbiol. Immunol.* 306, 183–198. doi: 10.1007/3-540-29916-5_7

Ganz, T. (2007). Molecular control of iron transport. *J. Am. Soc. Nephrol.* 18, 394–400. doi: 10.1681/ASN.2006070802

Ganz, T. (2018). Iron and infection. *Int. J. Hematol.* 107, 7–15. doi: 10.1007/s12185-017-2366-2

Ganz, T., and Nemeth, E. (2012). Hepcidin and iron homeostasis. *Biochim. Biophys. Acta* 1823, 1434–1443. doi: 10.1016/j.bbamcr.2012.01.014

Gille, G., and Reichmann, H. (2011). Iron-dependent functions of mitochondria--relation to neurodegeneration. *J. Neural Transm. (Vienna)* 118, 349–359. doi: 10.1007/s00702-010-0503-7

Ginzburg, Y. Z. (2019). Hepcidin-ferroportin axis in health and disease. *Vitam. Horm.* 110, 17–45. doi: 10.1016/bs.vh.2019.01.002

Graham, R. M., Chua, A. C., Herbison, C. E., Olynyk, J. K., and Trinder, D. (2007). Liver iron transport. *World J. Gastroenterol.* 13, 4725–4736. doi: 10.3748/wjg.v13.i35.4725

Habib, H. M., Ibrahim, S., Zaim, A., and Ibrahim, W. H. (2021). The role of iron in the pathogenesis of COVID-19 and possible treatment with lactoferrin and other iron chelators. *Biomed. Pharmacother.* 136:111228. doi: 10.1016/j.biopha.2021.111228

Hambright, W. S., Fonseca, R. S., Chen, L., Na, R., and Ran, Q. (2017). Ablation of ferroptosis regulator glutathione peroxidase 4 in forebrain neurons promotes cognitive impairment and neurodegeneration. *Redox Biol.* 12, 8–17. doi: 10.1016/j.redox.2017.01.021

Hao, L., Mi, J., Song, L., Guo, Y., Li, Y., Yin, Y., et al. (2021). SLC40A1 mediates ferroptosis and cognitive dysfunction in type 1 diabetes. *Neuroscience* 463, 216–226. doi: 10.1016/j.neuroscience.2021.03.009

Harrison, P. M., and Arosio, P. (1996). The ferritins: molecular properties, iron storage function and cellular regulation. *Biochim. Biophys. Acta* 1275, 161–203. doi: 10.1016/0005-2728(96)00022-9

Hintze, K. J., and Theil, E. C. (2006). Cellular regulation and molecular interactions of the ferritins. *Cell. Mol. Life Sci.* 63, 591–600. doi: 10.1007/s00018-005-5285-y

Hortová-Kohoutková, M., Skotáková, M., Onyango, I. G., Slezáková, M., Panovský, R., Opatřil, L., et al. (2023). Hepcidin and ferritin levels as markers of immune cell activation during septic shock, severe COVID-19 and sterile inflammation. *Front. Immunol.* 14:1110540. doi: 10.3389/fimmu.2023.1110540

Hosseinzadeh, P., and Lu, Y. (2016). Design and fine-tuning redox potentials of metalloproteins involved in electron transfer in bioenergetics. *Biochim. Biophys. Acta* 1857, 557–581. doi: 10.1016/j.bbabio.2015.08.006

Huebers, H. A., Huebers, E., Csiba, E., Rummel, W., and Finch, C. A. (1983). The significance of transferrin for intestinal iron absorption. *Blood* 61, 283–290. doi: 10.1182/blood.V61.2.283.283

Improta-Caria, A. C., Soci, Ú. P. R., Pinho, C. S., Júnior, R. A., De Sousa, R. A. L., and Bessa, T. C. B. (2021). Physical exercise and immune system: perspectives on the COVID-19 pandemic. *Rev. Assoc. Med. Bras.* 67, 102–107. doi: 10.1590/1806-9282.67.suppl1.20200673

Júnior, R. A., Durães, A., Roever, L., Macedo, C., Aras, M. G., Nascimento, L., et al. (2021). The impact of COVID-19 on the cardiovascular system. *Rev. Assoc. Med. Bras.* 67, 163–167. doi: 10.1590/1806-9282.67.suppl1.20201063

Kappert, K., Jahic, A., and Tauber, R. (2020). Assessment of serum ferritin as a biomarker in COVID-19: bystander or participant? Insights by comparison with other infectious and non-infectious diseases. *Biomarkers* 25, 616–625. doi: 10.1080/1354750X.2020.1797880

Kaushal, K., Kaur, H., Sarma, P., Bhattacharyya, A., Sharma, D. J., Prajapat, M., et al. (2022). Serum ferritin as a predictive biomarker in COVID-19. A systematic review, meta-analysis and meta-regression analysis. *J. Crit. Care* 67, 172–181. doi: 10.1016/j.jcrc.2021.09.023

Kempuraj, D., Selvakumar, G. P., Ahmed, M. E., Raikwar, S. P., Thangavel, R., Khan, A., et al. (2020). COVID-19, mast cells, cytokine storm, psychological stress, and neuroinflammation. *Neuroscientist* 26, 402–414. doi: 10.1177/1073858420941476

Kennedy, M. C., Emptage, M. H., Dreyer, J. L., and Beinert, H. (1983). The role of iron in the activation-inactivation of aconitase. *J. Biol. Chem.* 258, 11098–11105. doi: 10.1016/S0021-9258(17)44390-0

Koorts, A. M., and Viljoen, M. (2007). Ferritin and ferritin isoforms II: protection against uncontrolled cellular proliferation, oxidative damage and inflammatory processes. *Arch. Physiol. Biochem.* 113, 55–64. doi: 10.1080/13813450701422575

Kouhpayeh, S., Shariati, L., Boshtam, M., Rahimmanesh, I., Mirian, M., Esmaeili, Y., et al. (2021). The molecular basis of COVID-19 pathogenesis, conventional and nanomedicine therapy. *Int. J. Mol. Sci.* 22:5438. doi: 10.3390/ijms22115438

Kumar, P., Osahon, O., Vides, D. B., Hanania, N., Minard, C. G., and Sekhar, R. V. (2022). Severe glutathione deficiency, oxidative stress and oxidant damage in adults hospitalized with COVID-19: implications for GlyNAC (glycine and N-acetylcysteine) supplementation. *Antioxidants* 11:50. doi: 10.3390/antiox11010050

Lall, M. M., Ferrell, J., Nagar, S., Fleisher, L. N., and McGahan, M. C. (2008). Iron regulates L-cystine uptake and glutathione levels in lens epithelial and retinal pigment epithelial cells by its effect on cytosolic aconitase. *Invest. Ophthalmol. Vis. Sci.* 49, 310–319. doi: 10.1167/iovs.07-1041

Lee, J. X., Chieng, W. K., Abdul Jalal, M. I., Tan, C. E., and Lau, S. C. D. (2022). Role of serum ferritin in predicting outcomes of COVID-19 infection among sickle cell disease patients: a systematic review and meta-analysis. *Front. Med.* 9:919159. doi: 10.3389/fmed.2022.919159

Lee, K. E., Mo, S., Lee, H. S., Jeon, M., Song, J. S., Choi, H. J., et al. (2021). Deferoxamine reduces inflammation and osteoclastogenesis in avulsed teeth. *Int. J. Mol. Sci.* 22:8225. doi: 10.3390/ijms22158225

Li, Z., Liu, T., Yang, N., Han, D., Mi, X., Li, Y., et al. (2020). Neurological manifestations of patients with COVID-19: potential routes of SARS-CoV-2 neuroinvasion from the periphery to the brain. *Front. Med.* 14, 533–541. doi: 10.1007/s11684-020-0786-5

Li, Y., Sun, M., Fuyang Cao, Y., Chen, L. Z., Li, H., Cao, J., et al. (2022). The ferroptosis inhibitor liproxstatin-1 ameliorates LPS-induced cognitive impairment in mice. *Nutrients* 14:4599. doi: 10.3390/nu14214599

Li, S., Zhou, C., Zhu, Y., Chao, Z., Sheng, Z., Zhang, Y., et al. (2021). Ferrostatin-1 alleviates angiotensin II (Ang II)- induced inflammation and ferroptosis in astrocytes. *Int. Immunopharmacol.* 90:107179. doi: 10.1016/j.intimp.2020.107179

Lino, K., Guimarães, G. M. C., Alves, L. S., Oliveira, A. C., Faustino, R., Fernandes, C. S., et al. (2021). Serum ferritin at admission in hospitalized COVID-19 patients as a predictor of mortality. *Braz. J. Infect. Dis.* 25:101569. doi: 10.1016/j.bjid.2021.101569

Liu, P., Feng, Y., Li, H., Chen, X., Wang, G., Xu, S., et al. (2020). Ferrostatin-1 alleviates lipopolysaccharide-induced acute lung injury via inhibiting ferroptosis. *Cell. Mol. Biol. Lett.* 25:10. doi: 10.1186/s11658-020-00205-0

Liu, X., Yue, D., Liu, J., Cheng, L., He, W., and Zhang, W. (2023). Ferrostatin-1 alleviates cerebral ischemia/reperfusion injury through activation of the AKT/GSK3β signaling pathway. *Brain Res. Bull.* 193, 146–157. doi: 10.1016/j.brainresbull.2022.12.009

Liu, W., Zhang, S., Nekhai, S., and Liu, S. (2020). Depriving Iron supply to the virus represents a promising adjuvant therapeutic against viral survival. *Curr. Clin. Microbiol. Rep.* 7, 13–19. doi: 10.1007/s40588-020-00140-w

Matsui, M. (1996). Early embryonic lethality caused by targeted disruption of the mouse thioredoxin gene. *Dev. Biol.* 178, 179–185. doi: 10.1006/dbio.1996.0208

McGahan, M. C., Harned, J., Mukunnemkeril, M., Goralska, M., Fleisher, L., and Ferrell, J. B. (2005). Iron alters glutamate secretion by regulating cytosolic aconitase activity. *Am. J. Physiol. Cell Physiol.* 288, C1117–C1124. doi: 10.1152/ajpcell.00444.2004

Miotto, G., Rossetto, M., Di Paolo, M. L., Orian, L., Venerando, R., Roveri, A., et al. (2020). Insight into the mechanism of ferroptosis inhibition by ferrostatin-1. *Redox Biol.* 28:101328. doi: 10.1016/j.redox.2019.101328

Moos, T. (2002). Brain iron homeostasis. *Dan. Med. Bull.* 49, 279–301.

Morgan, E. H., and Oates, P. S. (2002). Mechanisms and regulation of intestinal iron absorption. *Blood Cells Mol. Dis.* 29, 384–399. doi: 10.1006/bcmd.2002.0578

Muhammad, Y., Kani, Y. A., Iliya, S., Muhammad, J. B., Binji, A., Ahmad, A. E.-F., et al. (2021). Deficiency of antioxidants and increased oxidative stress in COVID-19 patients: a cross-sectional comparative study in Jigawa, Northwestern Nigeria. *SAGE Open Med.* 9:205031212199124. doi: 10.1177/2050312121991246

Naderi, S., Khodagholi, F., Pourbadie, H. G., Naderi, N., Rafiei, S., Janahmadi, M., et al. (2023). Role of amyloid beta (25− 35) neurotoxicity in the ferroptosis and necroptosis as modalities of regulated cell death in Alzheimer's disease. *Neurotoxicology* 94, 71–86. doi: 10.1016/j.neuro.2022.11.003

Nemeth, E., Tuttle, M. S., Powelson, J., Vaughn, M. B., Donovan, A., Ward, D. M., et al. (2004). Hepcidin regulates cellular iron efflux by binding to ferroportin and inducing its internalization. *Science* 306, 2090–2093. doi: 10.1126/science.1104742

Neyens, E., and Baeyens, J. (2003). A review of classic Fenton's peroxidation as an advanced oxidation technique. *J. Hazard. Mater.* 98, 33–50. doi: 10.1016/S0304-3894(02)00282-0

Pandey, K., Thurman, M., Johnson, S. D., Acharya, A., Johnston, M., Klug, E. A., et al. (2021). Mental health issues during and after COVID-19 vaccine era. *Brain Res. Bull.* 176, 161–173. doi: 10.1016/j.brainresbull.2021.08.012

Para, O., Caruso, L., Pestelli, G., Tangianu, F., Carrara, D., Maddaluni, L., et al. (2022). Ferritin as prognostic marker in COVID-19: the FerVid study. *Postgrad. Med.* 134, 58–63. doi: 10.1080/00325481.2021.1990091

Paul, B. T., Manz, D. H., Torti, F. M., and Torti, S. V. (2017). Mitochondria and Iron: current questions. *Expert. Rev. Hematol.* 10, 65–79. doi: 10.1080/17474086.2016.1268047

Ponka, P., Beaumont, C., and Richardson, D. R. (1998). Function and regulation of transferrin and ferritin. *Semin. Hematol.* 35, 35–54.

Ramsey, A. J., Hillas, P. J., and Fitzpatrick, P. F. (1996). Characterization of the active site iron in tyrosine hydroxylase. Redox states of the iron. *J. Biol. Chem.* 271, 24395–24400.

Ren, J. X., Sun, X., Yan, X. L., Guo, Z. N., and Yang, Y. (2020). Ferroptosis in neurological diseases. *Front. Cell. Neurosci.* 14:218. doi: 10.3389/fncel.2020.00218

Robbins, A. H., and Stout, C. D. (1989). The structure of aconitase. *Proteins* 5, 289–312. doi: 10.1002/prot.340050406

Salari, N., Hosseinian-Far, A., Jalali, R., Vaisi-Raygani, A., Rasoulpoor, S., Mohammadi, M., et al. (2020). Prevalence of stress, anxiety, depression among the general population during the COVID-19 pandemic: a systematic review and meta-analysis. *Glob. Health* 16, 1–11. doi: 10.1186/s12992-020-00589-w

Savla, S. R., Prabhavalkar, K. S., and Bhatt, L. K. (2021). Cytokine storm associated coagulation complications in COVID-19 patients: pathogenesis and management. *Expert Rev. Anti-Infect. Ther.* 19, 1397–1413. doi: 10.1080/14787210.2021.1915129

Seiler, A., Schneider, M., Forster, H., Roth, S., Wirth, E. K., Culmsee, C., et al. (2008). Glutathione peroxidase 4 senses and translates oxidative stress into 12/15-lipoxygenase dependent- and AIF-mediated cell death. *Cell Metab.* 8, 237–248. doi: 10.1016/j.cmet.2008.07.005

Sherry, B. D., and Fürstner, A. (2008). The promise and challenge of Iron-catalyzed cross coupling. *Acc. Chem. Res.* 41, 1500–1511. doi: 10.1021/ar800039x

Sousa, D., Leoni, R. A., Improta-caria, A. C., Aras-júnior, R., De Oliveira, E. M., Soci, Ú. P. R., et al. (2021). Physical exercise effects on the brain during COVID-19 pandemic: links between mental and cardiovascular health. *Neurol. Sci.* 42, 1325–1334. doi: 10.1007/s10072-021-05082-9

Suriawinata, E., and Mehta, K. J. (2022). Iron and iron-related proteins in COVID-19. *Clin. Exp. Med.* 1591–9528. doi: 10.1007/s10238-022-00851-y

Tamir, H., and Liu, K.-P. (1982). On the nature of the interaction between serotonin and serotonin binding protein: effect of nucleotides, ions, and sulfhydryl reagents. *J. Neurochem.* 38, 135–141. doi: 10.1111/j.1471-4159.1982.tb10864.x

Taquet, M., Sillett, R., Zhu, L., Mendel, J., Camplisson, I., Dercon, Q., et al. (2022). Neurological and psychiatric risk trajectories after SARS-CoV-2 infection: an analysis of 2-year retrospective cohort studies including 1 284 437 patients. *Lancet Psychiatry* 9, 815–827. doi: 10.1016/S2215-0366(22)00260-7

Taylor, E. M., and Morgan, E. H. (1990). Developmental changes in transferrin and iron uptake by the brain in the rat. *Brain Res. Dev. Brain Res.* 55, 35–42. doi: 10.1016/0165-3806(90)90103-6

Todorich, B., Pasquini, J. M., Garcia, C. I., Paez, P. M., and Connor, J. R. (2009). Oligodendrocytes and myelination: the role of iron. *Glia* 57, 467–478. doi: 10.1002/glia.20784

Wang, L., Davis, P. B., Volkow, N. D., Berger, N. A., Kaelber, D. C., and Xu, R. (2022). Association of COVID-19 with new-onset Alzheimer's disease. *J. Alzheimers Dis.* 89, 411–414. doi: 10.3233/JAD-220717

Winterbourn, C. C. (1995). Toxicity of iron and hydrogen peroxide: the Fenton reaction. *Toxicol. Lett.* 82-83, 969–974. doi: 10.1016/0378-4274(95)03532-X

Xie, Z., Wang, X., Luo, X., Yan, J., Zhang, J., Sun, R., et al. (2023). Activated AMPK mitigates diabetes-related cognitive dysfunction by inhibiting hippocampal ferroptosis. *Biochem. Pharmacol.* 207:115374. doi: 10.1016/j.bcp.2022.115374

Xue, H., Chen, D., Zhong, Y. K., Zhou, Z. D., Fang, S. X., Li, M. Y., et al. (2016). Deferoxamine ameliorates hepatosteatosis via several mechanisms in Ob/Ob mice. *Ann. N. Y. Acad. Sci.* 1375, 52–65. doi: 10.1111/nyas.13174

Yang, M., and Lai, C. L. (2020). SARS-CoV-2 infection: can ferroptosis be a potential treatment target for multiple organ involvement? *Cell Death Discovery* 6:130. doi: 10.1038/s41420-020-00369-w

Yang, W. S., and Stockwell, B. R. (2016). Ferroptosis: death by lipid peroxidation. *Trends Cell Biol.* 26, 165–176. doi: 10.1016/j.tcb.2015.10.014

Yant, L. J., Ran, Q., Rao, L., Van Remmen, H., Shibatani, T., Belter, J. G., et al. (2003). The selenoprotein GPX4 is essential for mouse development and protects from radiation and oxidative damage insults. *Free Radic. Biol. Med.* 34, 496–502. doi: 10.1016/S0891-5849(02)01360-6

Ye, Q., Zeng, C., Luo, C., and Yuan, W. (2020). Ferrostatin-1 mitigates cognitive impairment of epileptic rats by inhibiting P38 MAPK activation. *Epilepsy Behav.* 103:106670. doi: 10.1016/j.yebeh.2019.106670

Zandman-Goddard, G., and Shoenfeld, Y. (2007). Ferritin in autoimmune diseases. *Autoimmun. Rev.* 6, 457–463. doi: 10.1016/j.autrev.2007.01.016

Zhang, R., Sun, C., Chen, X., Han, Y., Zang, W., Jiang, C., et al. (2022). COVID-19-related brain injury: the potential role of ferroptosis. *J. Inflamm. Res.* 15, 2181–2198. doi: 10.2147/JIR.S353467

Zhao, Y., Luo, Y., Liu, Z., Chen, Y., Wei, L., Luo, X., et al. (2023). Ferrostatin-1 ameliorates bupivacaine-induced spinal neurotoxicity in rats by inhibiting ferroptosis. *Neurosci. Lett.* 809:137308. doi: 10.1016/j.neulet.2023.137308

Zhou, C., Chen, Y., Ji, Y., He, X., and Xue, D. (2020). Increased serum levels of hepcidin and ferritin are associated with severity of COVID-19. *Med. Sci. Monit.* 26:e926178. doi: 10.12659/MSM.926178

Zubair, A. S., McAlpine, L. S., Gardin, T., Farhadian, S., Kuruvilla, D. E., and Spudich, S. (2020). Neuropathogenesis and neurologic manifestations of the coronaviruses in the age of coronavirus disease 2019: a review. *JAMA* 77, 1018–1010. doi: 10.1001/jamaneurol.2020.2065

frontiers | Frontiers in Neuroscience

TYPE Review
PUBLISHED 07 August 2023
DOI 10.3389/fnins.2023.1230404

OPEN ACCESS

EDITED BY
Zezhi Li,
Guangzhou Medical University, China

REVIEWED BY
Ning Jiang,
Chinese Academy of Medical Sciences and Peking Union Medical College, China
Jolanta Dorszewska,
Poznan University of Medical Sciences, Poland

*CORRESPONDENCE
Wenzhou Zhang
✉ hnzzzwzx@sina.com

RECEIVED 28 May 2023
ACCEPTED 24 July 2023
PUBLISHED 07 August 2023

CITATION
Chen J, Song W and Zhang W (2023) The emerging role of copper in depression. *Front. Neurosci.* 17:1230404. doi: 10.3389/fnins.2023.1230404

The emerging role of copper in depression

Jinhua Chen, Wenping Song and Wenzhou Zhang*

Department of Pharmacy, Affiliated Cancer Hospital of Zhengzhou University and Henan Cancer Hospital, Henan Engineering Research Center for Tumor Precision Medicine and Comprehensive Evaluation, Henan Provincial Key Laboratory of Anticancer Drug Research, Zhengzhou, China

Copper (Cu) is an essential trace element in the brain and serves as an important cofactor for numerous enzymes involved in a wide range of biochemical processes including neurobehavioral, mitochondrial respiration, and antioxidant effects. Recent studies have demonstrated that copper dyshomeostasis is tightly associated with the development of depression by inducing oxidative stress and inflammatory responses. However, these findings have remained controversial so far. Cumulative studies have shown a positive association, while some other studies showed no association and even a negative association between serum/plasma copper level and depression. Based on these conflicted results, the association was speculated to be due to the clinical features of the population, stages of the disease, severity of copper excess, and types of specimens detected in these studies. In addition, there was an inverse association between dietary copper intake and depression. Furthermore, increasing copper intake could influence dietary zinc and iron intake to prevent and treat depression. Thus, copper supplementation may be a good measure to manage depression. This review provided a deeper understanding of the potential applicability of copper in the prevention and treatment of depression.

KEYWORDS

copper, depression, homeostasis, oxidative stress, inflammatory response, dietary supplementation

1. Introduction

Depression is one of the leading mental disorders, and the number of people with depression has reached approximately 280 million worldwide from World Health Organization (WHO) statistics, making it a major contributor to the overall global burden of diseases (World Health Organization, 2023a,b). Given the deleterious effect of depression on human health, WHO's Mental Health Gap Action Programme (mhGAP) has listed it as a priority condition in its Mental health action plan 2013–2030 (Institute of Health Metrics and Evaluation, 2023). There are many etiologies involved in depression including social, psychological, and biological factors (Ferrari et al., 2016). It is characterized by several symptoms such as depressed mood, hopelessness about the future, and thoughts of dying or suicide (World Health Organization, 2023a,b). Depression can be categorized as mild, moderate, and severe on the basis of the number and severity of symptoms, as well as the impact on the individual's functioning. Depending on the severity and pattern of depressive episodes, different treatments are recommended, including psychological treatment and antidepressant medications (Shusharina et al., 2023), but a significant proportion of people who received treatment still fail to achieve remission (Mauskopf et al., 2009; Moriarty et al., 2020) and more than 75% of people in low and middle-income countries do not receive any treatment (Evans-Lacko et al., 2018). Hence, it is

imperative to look for new risk factors and effective treatments to prevent and treat depression.

Copper (Cu) is an essential trace element and the third most abundant trace metal after iron and zinc in the human body (Barceloux, 1999). It is almost entirely absorbed in the gastrointestinal tract, stored in the liver, and eliminated through biliary excretion (Halliwell and Gutteridge, 1984). It is a vital cofactor of numerous important enzymes, such as dopamine monooxygenase, cytochrome oxidase, and the free radical scavenger superoxide dismutase (Uauy et al., 1998; Turnlund, 2000), and is involved in a wide range of biochemical processes including neurobehavioral, mitochondrial respiration, and antioxidant effects (Uriu-Adams and Keen, 2005). The roles of copper in mental diseases have attracted the attention of researchers due to its high levels in the brain (Rihel, 2018). An imbalance in copper levels in the brain has been reported to be associated with many neuropathic diseases, such as depression, Alzheimer's disease, Menkes disease, and Wilson's disease (An et al., 2022). Several studies have explored the association between copper levels in the human body and depression, but their conclusions remain controversial. Cumulative studies have shown a positive association between serum/plasma copper levels and depression (Russo, 2011; Habibi et al., 2017; Islam et al., 2018; Ni et al., 2018; Ullas Kamath et al., 2019; Wu et al., 2022), while some other studies showed that there were no associations (Styczeń et al., 2016; Siwek et al., 2017) and even negative associations between serum/plasma copper level and depression (Styczeń et al., 2016; Li et al., 2018; Twayej et al., 2020; Ding and Zhang, 2022). Given these conflicting results, we focused on the role of copper in depression and its underlying mechanisms in this review, aiming to provide a better understanding of its potential applicability in preventing and treating depression.

2. Regulation of copper homeostasis

Copper homeostasis, namely, the dynamic balance in copper levels, is a tightly regulated process by various key molecules, including copper chaperones, transmembrane transporters, and transcriptional regulators (Chen et al., 2022, 2023). These molecules cooperatively regulate the import, intracellular distribution, and export of copper to maintain homeostasis. As shown in Figure 1, copper is a redox-active metal ion that exists in two oxidation states: Cu^{+} and Cu^{2+} (Ge et al., 2022). Extracellular Cu^{2+} binding to ceruloplasmin is reduced by the metalloreductase six-transmembrane epithelial antigen of the prostate (SETAP) to Cu^{+}, and copper transporter 1 (CTR1) (also known as solute carrier family 31 member 1, SLC31A1) transports Cu^{+} into cells (Ohgami et al., 2006). Once it enters the cytoplasm, a part of Cu^{+} binds to glutathione (GSH) and is delivered to metallothionein 1/2 (MT1/2) to be restored, and other parts of Cu^{+} are either transferred to the nucleus or ATP7A/7B located in the trans-Golgi network (TGN) by the chaperone antioxidant-1(ATOX1) to facilitate the synthesis of cuproenzymes (Lutsenko et al., 2007) or delivered to superoxide dismutase 1 (SOD1) in the cytoplasm and mitochondrial intermembrane space by a copper chaperone for superoxide dismutase (CCS) to detoxify reactive oxygen species (ROS). In addition, Cu^{+} in the cytoplasm can be transported to the mitochondrial intermembrane space, in which Cu^{+} binds to chaperone cytochrome oxidase 17 (COX17) and is delivered to either the chaperone synthesis of cytochrome oxidase 1 (SCO1) or COX11, ultimately delivering to the cytochrome C oxidase (CCO) I (COX1) or II (COX2) subunits to involve them in the respiratory chain (Horng et al., 2004).

Because of the alteration of physiological or pathological conditions in the human body, the cellular copper content changes, resulting in the disturbance of copper homeostasis, namely, copper excess or copper deficiency. Based on the cellular copper status, the expression of some molecules involved in copper homeostasis is regulated. For example, CTR1 and CCS are down-regulated when intracellular copper overloads and up-regulated when intracellular copper is deficient (Bertinato and L'Abbé, 2003; Liang et al., 2012). Moreover, ATP7A and ATP7B, as the major transporters for exporting cellular copper, are commonly located in the TGN. However, when intracellular copper overloads, ATP7A and ATP7B translocate from the TGN to the plasma membrane to export copper. When intracellular copper recovers to the physiological condition, ATP7A and ATP7B return to the TGN (La Fontaine and Mercer, 2007). It is important to note that the expression of ATP7A and ATP7B is tissue-specific. ATP7A is expressed in various tissues and organs, whereas ATP7B is predominantly expressed in the liver, suggesting that ATP7A, but not ATP7B, is primarily involved in the exporting of copper into the brain cell (Lutsenko et al., 2007).

3. The role of copper in oxidative stress and inflammation

Some of the molecular mechanisms underlying copper-induced depression included oxidative stress, neurotransmitter imbalance, and impaired synaptic plasticity. Among these mechanisms, oxidative stress is regarded as a mainstay because of its effect on other depression-associated mechanisms (Bhatt et al., 2020; Correia et al., 2023). Oxidative stress is a biological process caused by a disturbance between production and accumulation of ROS in cells and tissues and is responsible for some diseases such as neuropathic diseases and cancer due to its deleterious effects (Pizzino et al., 2017). The redox activity of copper induces oxidative stress via redox and Fenton reactions (Pereira et al., 2016; Ruizs et al., 2021). A positive association was observed between copper level in the serum or brain and oxidative stress (Maes et al., 1997; Frey et al., 2007; Ozcelik and Uzun, 2009; Salustri et al., 2010; Lee et al., 2013; Bajpai et al., 2014; Liu et al., 2015; Kumar et al., 2019). Copper has been revealed as a key regulator in various cell signaling pathways such as membrane receptor-associated pathways and growth factor-associated pathways (Grubman and White, 2014). The signaling pathways associated with copper-induced oxidative stress have been explored mainly based on *in vitro* cell experiments and *in vivo* animal studies. These studies demonstrated that a large amount of copper intake can result in oxidative damage by activating the antioxidant protection signals mitogen-activated protein kinase 14 (MAPK14)/the nuclear factor erythroid 2-related factor 2 (Nrf2)/heme oxygenase-1 (HO-1)/NAD(P)H:quinone oxidoreductase 1 (NQO1) pathway, inhibiting cAMP-response element binding protein (CREB)/Brain-derived neurotrophic factor (BDNF) pathway or PI3K/AKT/mTOR pathway to induce apoptosis or autophagy (Figure 2; Filomeni et al., 2011; Boilan et al., 2013; Zhong et al., 2014; Wang Y. et al., 2018; Xie et al., 2020; Zou et al., 2021; Li et al., 2022; Lu et al., 2022; Zhong et al., 2022). Kim et al. also found that the autophagy kinase ULK1 can induce the autophagic

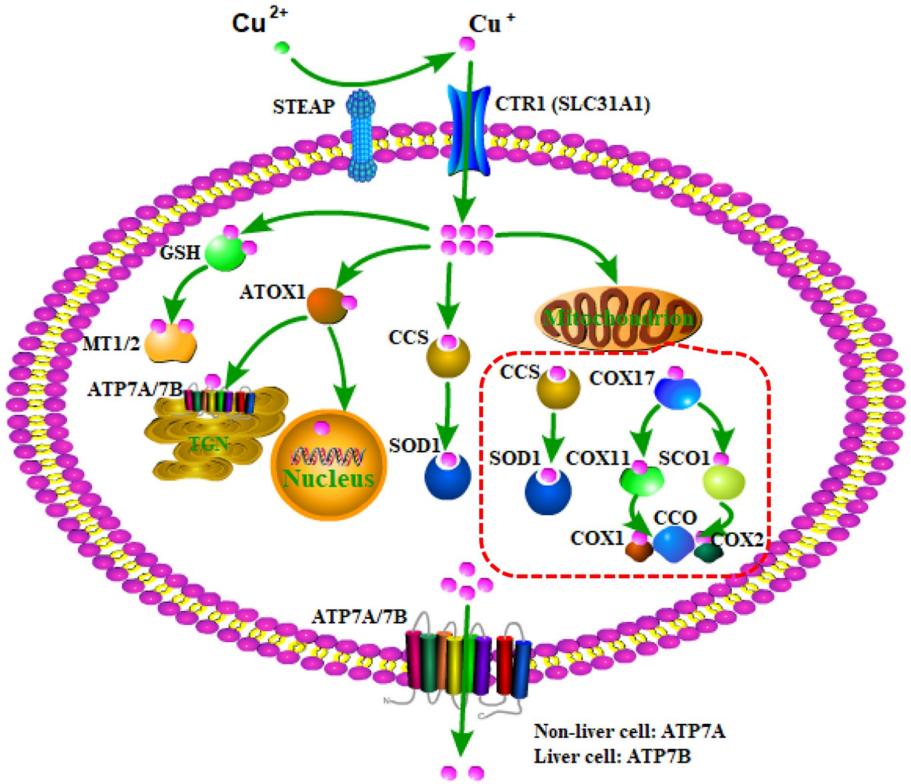

FIGURE 1
The regulation process of copper homeostasis. SETAP, metalloreductase six-transmembrane epithelial antigen of the prostate; CTR1, copper transporter 1; SLC31A1, solute carrier family 31 member 1; GSH, glutathione; MT1/2, metallothionein 1/2; ATOX1, the chaperone antioxidant-1; CCS, copper chaperone for superoxide dismutase; SOD1, superoxide dismutase 1; COX17, chaperone cytochrome oxidase 17; SCO1, chaperone synthesis of cytochrome oxidase 1; CCO, cytochrome C oxidase; COX1, cytochrome C oxidase (CCO) I; COX2, cytochrome C oxidase (CCO) II.

degradation of mitochondria by phosphorylating the ser-73 and ser-254 residues of Sestrin 2 under copper-induced oxidative stress conditions (Kim et al., 2020). In addition, copper can destroy the antioxidant defense system by decreasing antioxidant enzyme activities (SOD, CAT, and GSH-Px) to induce toxicity (Lai et al., 1996; West and Prohaska, 2004; Sun et al., 2018; Jian et al., 2020).

In addition to oxidative stress, accumulating evidence suggested that copper can exert toxicity, resulting in depression by triggering an inflammatory process. A number of studies revealed that high serum copper levels were associated with decreased levels of anti-inflammatory cytokines (IL4 and IL-10) and increased levels of pro-inflammatory cytokines (TNF-a, IL-6, IL-2, IL-8, and IL-1β) to trigger the pathogenesis of depression (Maes et al., 1995; Cattaneo et al., 2015; Habibi et al., 2017; Xu et al., 2021). Furthermore, there are various pathways that are involved in copper-regulated inflammation, including the nuclear factor kappa-B (NF-KB), MAPKs, JAK–STAT, and NLRP3 pathways (Deng et al., 2023). In addition, an alteration in the microbial richness and diversity of feces in Sprague–Dawley rats fed a high level of copper was associated with copper-regulated inflammatory responses (Zhang et al., 2017). Oxidative stress was deemed to be an important factor for the inflammatory response in the central nervous system (Ruiz et al., 2022). Consistent with it, increasing evidence suggested that copper-induced oxidative stress contributed to cellular inflammatory responses (Yang et al., 2020; Kouadri et al., 2021). Therefore, understanding copper-induced oxidative stress and inflammatory responses would be beneficial for the prevention and treatment of copper-related diseases.

4. Dysregulation of copper homeostasis and depression

Copper is abundant in the brain, especially in the cerebellum, hippocampus, basal ganglia, numerous synaptic membranes, cell bodies of cortical pyramidal, and cerebellar granular neurons (Desai and Kaler, 2008). It is regarded as an important cofactor for many enzymes that affect a variety of brain functions. Because the brain is a highly metabolizing organ, a small imbalance in copper levels may cause detrimental effects on the brain. Disturbance of copper homeostasis in the brain can cause copper excess or copper deficiency, leading to an array of diseases (Chakravarty and Chowdhury, 1984). This is because copper excess may result in injury, while copper deficiency may cause incomplete development (Sharma et al., 2014).

Copper excess has a higher incidence than copper deficiency in humans. It is toxic to many organs, especially the brain (Winge and Mehra, 1990). Multiple studies have suggested that copper levels in patients with depression were significantly higher than the control without depression (Narang et al., 1991; Butterworth, 2010; Russo, 2011; Habibi et al., 2017; Islam et al., 2018; Ullas Kamath et al., 2019;

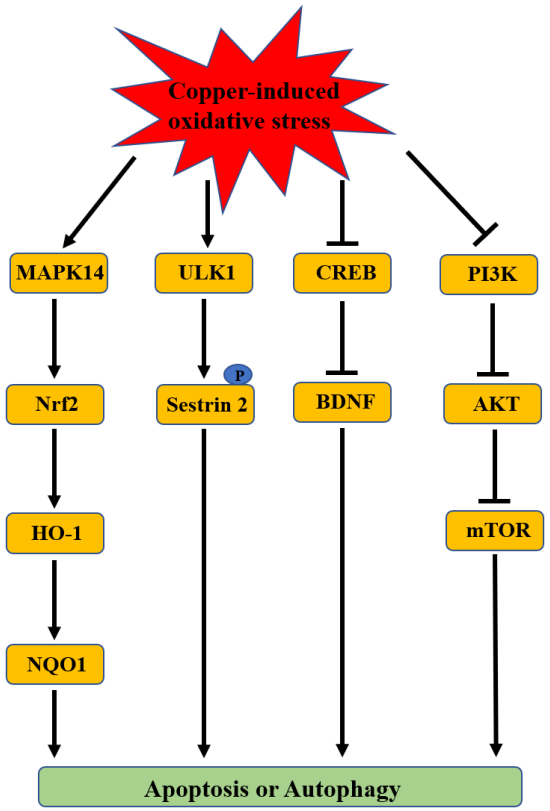

FIGURE 2
The associated signaling pathways of copper-induced oxidative stress.

Wu et al., 2022). Additionally, copper content in the human body gradually increased in pregnant women, which may be related to the elevated levels of circulatory progesterone and estrogens; thus, it can easily cause depression (Gernand et al., 2016). In a study of 574 women aged 30–60 years with various mental and behavioral disorders, the serum copper levels were significantly higher in women with a history of post-partum depression (PPD) than in non-depressed women and depressed women without a history of PPD (Crayton and Walsh, 2007). This is consistent with a study showing that the mean level of copper in the serum was higher in pregnant Iranian adolescents with depression than in those without depression (Bahramy et al., 2020). As aforementioned, this may be because an elevated concentration of cellular copper can cause neuronal injury, resulting in depression by inducing oxidative stress and inflammatory responses. However, an inverse relationship was observed between copper serum level and depression (Styczeń et al., 2016; Li et al., 2018; Twayej et al., 2020; Ding and Zhang, 2022) even though there were no associations between copper serum level and depression in several studies (Styczeń et al., 2016; Siwek et al., 2017). Based on these conflicted results, the association was speculated to be related to the clinical features of the population, stages of the disease, severity of copper excess, and types of detected specimens in these studies (Table 1). For example, the epidemiology data suggested that the incidence of depression is about twice as common in women than in men (Kessler, 2003; World Health Organization, 2023a,b). Obesity was also a risk factor for depressive symptoms in individuals with high serum copper levels (Wu et al., 2022). However, the role of age as a risk factor for depression remains controversial. A study by Clark et al. showed that there was no association between blood copper and age, but two other studies demonstrated that they were correlated (Clark et al., 2007; Ma et al., 2014; Ni et al., 2018). Siwek et al. found that serum copper concentrations in patients with stage 1 bipolar disorder (including depression) were significantly higher than those of patients in advanced stages (2 + 3 + 4) of bipolar disorder (including depression) (Siwek et al., 2017). Moreover, a systematic review and meta-analysis of observational studies demonstrated that blood levels of copper in patients with depression were higher than those of patients without depression, while there was no difference in copper content in the hair between the two groups, suggesting that copper levels in the blood may be more sensitive to pathological changes in patients compared to those in the hair (Harvey et al., 2009; Ni et al., 2018). Thus, the level of plasma copper is currently the most widely used criterion for detecting copper content. Further systematic studies are needed to better understand the association between copper excess and depression.

Although the incidence of copper deficiency is relatively lower than that of copper excess, it cannot be ignored because it results in some diseases. In humans, Menkes syndrome is a main manifestation of copper deficiency and causes serious neurological disorders (Danks et al., 1972; Mercer, 1998). The mechanism may be that copper deficiency affects brain functioning by impairing brain mitochondrial function to damage energy metabolism (Munakata et al., 2005). In addition, increasing evidence reveals that copper deficiency results in decreased levels of plasma iron, which may be due to a decrease in the absorption and inhibition of iron released from the liver (Reeves and Demars, 2006; Pyatskowit and Prohask, 2008). Iron deficiency can induce depression, and thus copper deficiency may result in depression by decreasing the iron levels in the human body. Iron deficiency in the brain can be reversed by iron injections (Pyaskowit and Prohaska, 2008).

5. Copper supplementation for the prevention and treatment of depression

Increasing evidence has indicated that nutrients played a vital role in preventing and managing depression (Lai et al., 2014; Marx et al., 2017; Salehi-Abargouei et al., 2019). For example, there was an inverse relationship between dietary patterns rich in fruits and vegetables and high depressive symptoms (Xia et al., 2017; Wang C. J. et al., 2018; Cheng et al., 2019). Thus, the identification of the dietary factors involved in depression has attracted researchers' attention in recent years. As aforementioned, copper is an essential dietary component in the human body. The adult human body contains approximately 75–100 mg of copper, and the recommended daily dosage is 0.9 mg/day in adults (Food and Nutrition Board, Institute of Medicine, 2001). Food is the primary source of daily copper intake (National Academy of Sciences, 2000). There is rich copper in various foods, such as shellfish, seeds, nuts, meats, and chocolate (Ma and Betts, 2000; Institute of Medicine (US) Panel on Micronutrients, 2001).

A number of studies have demonstrated that an imbalance in dietary copper intake contributed to the development of depression.

TABLE 1 The influencing factors for studies on the association between copper levels and depression.

	Type of study	Countries	Results	References
Clinical features				
Sex	Epidemiology data	Worldwide	Incidence of depression was about twice as common in women than in men	World Health Organization (2023a,b)
Obesity	Cross-sectional study	America	Obesity (BMI ≥ 30 kg/m^2) was a risk factor for people with high serum copper levels to develop depression symptoms	Wu et al. (2022)
Age	Clinical study	Canada	No relationship in people aged 30–65 years old	Clark et al. (2007)
	Clinical study	China	A relationship in children aged 3–12 years old	Ma et al. (2014)
	A systematic review and meta-analysis of observational studies	–	A relationship between blood copper and depression in people under 50 years old, but not in people over 50 years old	Ni et al. (2018)
The severity of the disease	Clinical study	Poland	Serum copper concentrations in patients with stage 1 bipolar disorder (including depression) were obviously higher than that of patients in advanced stages (2 + 3 + 4) of bipolar disorder (including depression)	Siwek et al. (2017)
Types of detected specimen	A systematic review	–	Serum copper appears to be a useful biomarker of copper status at the population level	Harvey et al. (2009)
	A systematic review and meta-analysis of observational studies	–	Blood levels of copper in patients with depression were higher than that of patients without depression, while there was no difference in copper content in the hair between the two groups	Ni et al. (2018)

A cross-sectional study of 14,834 US adults (7,399 men and 7,435 women) aged 18 years or older suggested that total copper intake may be an inverse association with depression, and these enrolled people given the Recommended Dietary Allowance had an obviously lower incidence of depression compared to those given less than the Recommended Dietary Allowance (Li et al., 2018). Consistent with this result, a negative association was observed between dietary copper intake and depression in two cross-sectional Japanese studies and a meta-analysis (Nakamura et al., 2019; Thi Thu Nguyen et al., 2019; Ding and Zhang, 2022). Additionally, a case–control study of 849 Korean adolescent girls aged 12–18 years also indicated that there was a high risk of depression in participants who ate more instant and processed foods and that dietary copper intake was negatively related to depression, suggesting that a reasonable dietary pattern played an important role in preventing and managing depression (Kim et al., 2015). Furthermore, an inverse association between dietary copper intake and depression was observed to be more relevant in women than in men (Thi Thu Nguyen et al., 2019; Ding and Zhang, 2022). Therefore, adequate intake of copper and reasonable dietary pattern was very important in preventing depression.

In addition to a dietary pattern that results in the dysregulation of copper intake, an imbalance of other metal ions in the human body can also influence copper to be involved in the pathogenesis of depression. In a cross-sectional study of 139 men and women aged ≥60 years in Australia, copper concentrations and copper/zinc ratios were found to be negatively associated with depressive symptoms (Mravunac et al., 2019). This is because zinc can compete with copper for absorption in the small intestine (Mravunac et al., 2019). It has been suggested that a high-iron diet might result in copper deficiency; in turn, increasing copper intake would correct many of the notable high iron-related physiological perturbations (Klevay, 2001, 2016; Reeves and Demars, 2005; Ha et al., 2017; Wang T. et al., 2018). A negative association has been observed between depression and dietary zinc and iron intake (Li et al., 2017). Thus, copper supplementation may be an effective measure to prevent and treat depression by interfering with the metabolic processes of zinc and iron.

6. Conclusion

In summary, copper is an essential trace element in the brain, and serves as an important cofactor for numerous enzymes involved in a wide series of biochemical processes, including neurobehavioral, mitochondrial respiration, and antioxidant effects. Thus, a trace dyshomeostasis of copper may cause serious brain diseases such as depression. Recent research has demonstrated that copper dyshomeostasis was tightly associated with the development of depression by inducing oxidative stress and inflammatory responses. However, the conclusion had remained controversial so far. Cumulative studies tended to show a positive association between serum/plasma copper level and depression, whereas some other studies showed no association and even negative associations between serum/plasma copper level and depression. Based on these conflicted results, the association was speculated to be related to the clinical features of the population, stages of the disease, severity of copper excess, and types of detected specimens in these studies. Further systematic studies are needed to better understand the association between copper excess and depression.

Furthermore, there was an inverse association between dietary copper intake and depression. Food is the primary source of daily copper intake. Thus, adequate intake of copper and a reasonable dietary pattern is very important for preventing depression. Additionally, increasing copper intake can influence dietary zinc and iron intake and is involved in the pathogenesis of depression.

Therefore, copper supplementation may be a good strategy to prevent and treat depression.

Author contributions

JC reviewed these works of literature and drafted the manuscript. WS and WZ revised the manuscript. All authors contributed to the article and approved the submitted version.

Funding

This work was supported by the Tackling-plan Project of Henan Department of Science and Technology (No. 212102310325).

Conflict of interest

The authors declare that the research was conducted in the absence of any commercial or financial relationships that could be construed as a potential conflict of interest.

Publisher's note

All claims expressed in this article are solely those of the authors and do not necessarily represent those of their affiliated organizations, or those of the publisher, the editors and the reviewers. Any product that may be evaluated in this article, or claim that may be made by its manufacturer, is not guaranteed or endorsed by the publisher.

References

An, Y., Li, S., Huang, X., Chen, X., Shan, H., and Zhang, M. (2022). The role of copper homeostasis in brain disease. *Int. J. Mol. Sci.* 23:13850. doi: 10.3390/ijms232213850

Bahramy, P., Mohammad-Alizadeh-Charandabi, S., Ramezani-Nardin, F., and Mirghafourvand, M. (2020). Serum levels of vitamin D, calcium, magnesium, and copper, and their relations with mental health and sexual function in pregnant Iranian adolescents. *Biol. Trace Elem. Res.* 198, 440–448. doi: 10.1007/s12011-020-02109-8

Bajpai, A., Verma, A. K., Srivastava, M., and Srivastava, R. (2014). Oxidative stress and major depression. *J. Clin. Diagn. Res.* 8:CC04-7. doi: 10.7860/JCDR/2014/10258.5292

Barceloux, D. G. (1999). Copper. *J. Toxicol. Clin. Toxicol.* 37, 217–230. doi: 10.1081/clt-100102421

Bertinato, J., and L'Abbé, M. R. (2003). Copper modulates the degradation of copper chaperone for cu,Zn superoxide dismutase by the 26S proteosome. *J. Biol. Chem.* 278, 35071–35078. doi: 10.1074/jbc.M302242200

Bhatt, S., Nagappa, A. N., and Patil, C. R. (2020). Role of oxidative stress in depression. *Drug Discov. Today* 25, 1270–1276. doi: 10.1016/j.drudis.2020.05.001

Boilan, E., Winant, V., Dumortier, E., Piret, J. P., Bonfitto, F., Osiewacz, H. D., et al. (2013). Role of p38MAPK and oxidative stress in copper-induced senescence. *Age* 35, 2255–2271. doi: 10.1007/s11357-013-9521-3

Butterworth, R. F. (2010). Metal toxicity, liver disease and neurodegeneration. *Neurotox. Res.* 18, 100–105. doi: 10.1007/s12640-010-9185-z

Cattaneo, A., Macchi, F., Plazzotta, G., Veronica, B., Bocchio-Chiavetto, L., Riva, M. A., et al. (2015). Inflammation and neuronal plasticity: a link between childhood trauma and depression pathogenesis. *Front. Cell. Neurosci.* 9:40. doi: 10.3389/fncel.2015.00040

Chakravarty, P. K., and Chowdhury, J. R. (1984). Serum copper in malignant neoplasia with special reference to the cervix uteri. *J. Cancer Res. Clin. Oncol.* 108, 312–315. doi: 10.1007/BF00390464

Chen, X., Cai, Q., Liang, R., Zhang, D., Liu, X., Zhang, M., et al. (2023). Copper homeostasis and copper-induced cell death in the pathogenesis of cardiovascular disease and therapeutic strategies. *Cell Death Dis.* 14:105. doi: 10.1038/s41419-023-05639-w

Chen, L., Min, J., and Wang, F. (2022). Copper homeostasis and cuproptosis in health and disease. *Signal Transduct. Target. Ther.* 7:378. doi: 10.1038/s41392-022-01229-y

Cheng, H. Y., Shi, Y. X., Yu, F. N., Zhao, H. Z., Zhang, J. H., and Song, M. (2019). Association between vegetables and fruits consumption and depressive symptoms in a middle-aged Chinese population: an observational study. *Medicine* 98:e15374. doi: 10.1097/MD.0000000000015374

Clark, N. A., Teschke, K., Rideout, K., and Copes, R. (2007). Trace element levels in adults from the west coast of Canada and associations with age, gender, diet, activities, and levels of other trace elements. *Chemosphere* 70, 155–164. doi: 10.1016/j.chemosphere.2007.06.038

Correia, A. S., Cardoso, A., and Vale, N. (2023). Oxidative stress in depression: the link with the stress response, neuroinflammation, serotonin, neurogenesis and synaptic plasticity. *Antioxidants* 12:470. doi: 10.3390/antiox12020470

Crayton, J. W., and Walsh, W. J. (2007). Elevated serum copper levels in women with a history of post-partum depression. *J. Trace Elem. Med. Biol.* 21, 17–21. doi: 10.1016/j.jtemb.2006.10.001

Danks, D. M., Campbell, P. E., Stevens, B. J., Mayne, V., and Cartwright, E. (1972). Menkes's kinky hair syndrome. An inherited defect in copper absorption with widespread effects. *Pediatrics* 50, 188–201. doi: 10.1542/peds.50.2.188

Deng, H., Zhu, S., Yang, H., Cui, H., Guo, H., Deng, J., et al. (2023). The dysregulation of inflammatory pathways triggered by copper exposure. *Biol. Trace Elem. Res.* 201, 539–548. doi: 10.1007/s12011-022-03171-0

Desai, V., and Kaler, S. G. (2008). Role of copper in human neurological disorders. *Am. J. Clin. Nutr.* 88, 855S–858S. doi: 10.1093/ajcn/88.3.855S

Ding, J., and Zhang, Y. (2022). Associations of dietary copper, selenium, and manganese intake with depression: a meta-analysis of observational studies. *Front. Nutr.* 9:854774. doi: 10.3389/fnut.2022.854774

Evans-Lacko, S., Aguilar-Gaxiola, S., Al-Hamzawi, A., Alonso, J., Benjet, C., Bruffaerts, R., et al. (2018). Socio-economic variations in the mental health treatment gap for people with anxiety, mood, and substance use disorders: results from the WHO world mental health (WMH) surveys. *Psychol. Med.* 48, 1560–1571. doi: 10.1017/S0033291717003336

Ferrari, A. J., Stockings, E., Khoo, J. P., Erskine, H. E., Degenhardt, L., Vos, T., et al. (2016). The prevalence and burden of bipolar disorder: findings from the global burden of disease study 2013. *Bipolar Disord.* 18, 440–450. doi: 10.1111/bdi.12423

Filomeni, G., Cardaci, S., Da Costa Ferreira, A. M., Rotilio, G., and Ciriolo, M. R. (2011). Metabolic oxidative stress elicited by the copper(II) complex [cu(isaepy)2] triggers apoptosis in SH-SY5Y cells through the induction of the AMP-activated protein kinase/p38MAPK/p53 signalling axis: evidence for a combined use with 3-bromopyruvate in neuroblastoma treatment. *Biochem. J.* 437, 443–453. doi: 10.1042/BJ20110510

Food and Nutrition Board, Institute of Medicine (2001). *Dietary reference intakes: Vitamin a, vitamin K, arsenic, boron, chromium, copper, iodine, iron, manganese, molybdenum, nickel, silicon, vanadium, and zinc*. Washington, DC: National Academy Press.

Frey, B. N., Andreazza, A. C., Kunz, M., Gomes, F. A., Quevedo, J., Salvador, M., et al. (2007). Increased oxidative stress and DNA damage in bipolar disorder: a twin-case report. *Prog. Neuro-Psychopharmacol. Biol. Psychiatry* 31, 283–285. doi: 10.1016/j.pnpbp.2006.06.011

Ge, E. J., Bush, A. I., Casini, A., Cobine, P. A., Cross, J. R., DeNicola, G. M., et al. (2022). Connecting copper and cancer: from transition metal signalling to metalloplasia. *Nat. Rev. Cancer* 22, 102–113. doi: 10.1038/s41568-021-00417-2

Gernand, A. D., Schulze, K. J., Stewart, C. P., West, K. P., and Christian, P. (2016). Micronutrient deficiencies in pregnancy worldwide: health effects and prevention. *Nat. Rev. Endocrinol.* 12, 274–289. doi: 10.1038/nrendo.2016.37

Grubman, A., and White, A. R. (2014). Copper as a key regulator of cell signalling pathways. *Expert Rev. Mol. Med.* 16:e11. doi: 10.1017/erm.2014.11

Ha, J. H., Doguer, C., and Collins, J. F. (2017). Consumption of a high-iron diet disrupts homeostatic regulation of intestinal copper absorption in adolescent mice. *Am. J. Physiol. Gastrointest. Liver Physiol.* 313, G353–G360. doi: 10.1152/ajpgi.00169.2017

Habibi, L., Tafakhori, A., Hadiani, R., Maserat-Mashhadi, M., Kafrash, Z., Torabi, S., et al. (2017). Molecular changes in obese and depressive patients are similar to neurodegenerative disorders. *Iran. J. Neurol.* 16, 192–200.

Halliwell, B., and Gutteridge, J. M. (1984). Oxygen toxicity, oxygen radicals, transition metals and disease. *Biochem. J.* 219, 1–14. doi: 10.1042/bj2190001

Harvey, L. J., Ashton, K., Hooper, L., Casgrain, A., and Fairweather-Tait, S. J. (2009). Methods of assessment of copper status in humans: a systematic review. *Am. J. Clin. Nutr.* 89, 2009S–2024S. doi: 10.3945/ajcn.2009.27230E

Horng, Y. C., Cobine, P. A., Maxfield, A. B., Carr, H. S., and Winge, D. R. (2004). Specific copper transfer from the Cox17 metallochaperone to both Sco1 and Cox11 in the assembly of yeast cytochrome C oxidase. *J. Biol. Chem.* 279, 35334–35340. doi: 10.1074/jbc.M404747200

Institute of Health Metrics and Evaluation (2023). *Global health data exchange (GHDx)*. Available at: https://vizhub.healthdata.org/gbd-results/ (Accessed March 4, 2023).

Institute of Medicine (US) Panel on Micronutrients (2001). *Dietary reference intakes for vitamin a, vitamin K, arsenic, boron, chromium, copper, iodine, iron, manganese, molybdenum, nickel, silicon, vanadium, and zinc*. Washington, DC: National Academies Press.

Islam, M. R., Islam, M. R., Shalahuddin Qusar, M. M. A., Islam, M. S., Kabir, M. H., Mustafizur Rahman, G. K. M., et al. (2018). Alterations of serum macro-minerals and trace elements are associated with major depressive disorder: a case-control study. *BMC Psychiatry* 18:94. doi: 10.1186/s12888-018-1685-z

Jian, Z., Guo, H., Liu, H., Cui, H., Fang, J., Zuo, Z., et al. (2020). Oxidative stress, apoptosis and inflammatory responses involved in copper-induced pulmonary toxicity in mice. *Aging* 12, 16867–16886. doi: 10.18632/aging.103585

Kessler, R. C. (2003). Epidemiology of women and depression. *J. Affect. Disord.* 74, 5–13. doi: 10.1016/s0165-0327(02)00426-3

Kim, T. H., Choi, J. Y., Lee, H. H., and Park, Y. (2015). Associations between dietary pattern and depression in Korean adolescent girls. *J. Pediatr. Adolesc. Gynecol.* 28, 533–537. doi: 10.1016/j.jpag.2015.04.005

Kim, H., Jeon, B. T., Kim, I. M., Bennett, S. J., Lorch, C. M., Viana, M. P., et al. (2020). Sestrin2 phosphorylation by ULK1 induces autophagic degradation of mitochondria damaged by copper-induced oxidative stress. *Int. J. Mol. Sci.* 21:6130. doi: 10.3390/ijms21176130

Klevay, L. M. (2001). Iron overload can induce mild copper deficiency. *J. Trace Elem. Med. Biol.* 14, 237–240. doi: 10.1016/S0946-672X(01)80009-2

Klevay, L. M. (2016). IHD from copper deficiency: a unified theory. *Nutr. Res. Rev.* 29, 172–179. doi: 10.1017/S0954422416000093

Kouadri, A., Cormenier, J., Gemy, K., Macari, L., Charbonnier, P., Richaud, P., et al. (2021). Copper-associated oxidative stress contributes to cellular inflammatory responses in cystic fibrosis. *Biomedicine* 9:329. doi: 10.3390/biomedicines9040329

Kumar, J., Sathua, K. B., and Flora, S. J. S. (2019). Chronic copper exposure elicit neurotoxic responses in rat brain: assessment of 8-hydroxy-2-deoxyguanosine activity, oxidative stress and neurobehavioral parameters. *Cell. Mol. Biol.* 65, 27–35. doi: 10.14715/cmb/2019.65.1.5

La Fontaine, S., and Mercer, J. F. (2007). Trafficking of the copper-ATPases, ATP7A and ATP7B: role in copper homeostasis. *Arch. Biochem. Biophys.* 463, 149–167. doi: 10.1016/j.abb.2007.04.021

Lai, J. S., Hiles, S., Bisquera, A., Hure, A. J., McEvoy, M., and Attia, J. (2014). A systematic review and meta-analysis of dietary patterns and depression in community-dwelling adults. *Am. J. Clin. Nutr.* 99, 181–197. doi: 10.3945/ajcn.113.069880

Lai, C. C., Huang, W. H., Klevay, L. M., Gunning, W. T. III, and Chiu, T. H. (1996). Antioxidant enzyme gene transcription in copper-deficient rat liver. *Free Radic. Biol. Med.* 21, 233–240. doi: 10.1016/0891-5849(96)00029-9

Lee, S. Y., Lee, S. J., Han, C., Patkar, A. A., Masand, P. S., and Pae, C. U. (2013). Oxidative/nitrosative stress and antidepressants: targets for novel antidepressants. *Prog. Neuropsychopharmacol. Biol. Psychiatry* 46, 224–235. doi: 10.1016/j.pnpbp.2012.09.008

Li, Z., Li, B., Song, X., and Zhang, D. (2017). Dietary zinc and iron intake and risk of depression: a meta-analysis. *Psychiatry Res.* 251, 41–47. doi: 10.1016/j.psychres.2017.02.006

Li, Q., Liao, J., Zhang, K., Hu, Z., Zhang, H., Han, Q., et al. (2022). Toxicological mechanism of large amount of copper supplementation: effects on endoplasmic reticulum stress and mitochondria-mediated apoptosis by Nrf2/HO-1 pathway-induced oxidative stress in the porcine myocardium. *J. Inorg. Biochem.* 230:111750. doi: 10.1016/j.jinorgbio.2022.111750

Li, Z., Wang, W., Xin, X., Song, X., and Zhang, D. (2018). Association of total zinc, iron, copper and selenium intakes with depression in the US adults. *J. Affect. Disord.* 228, 68–74. doi: 10.1016/j.jad.2017.12.004

Liang, Z. D., Tsai, W. B., Lee, M. Y., Savaraj, N., and Kuo, M. T. (2012). Specificity protein 1 (sp1) oscillation is involved in copper homeostasis maintenance by regulating human high-affinity copper transporter 1 expression. *Mol. Pharmacol.* 81, 455–464. doi: 10.1124/mol.111.076422

Liu, T., Zhong, S., Liao, X., Chen, J., He, T., Lai, S., et al. (2015). A meta-analysis of oxidative stress markers in depression. *PLoS One* 10:e0138904. doi: 10.1371/journal.pone.0138904

Lu, Q., Zhang, Y., Zhao, C., Zhang, H., Pu, Y., and Yin, L. (2022). Copper induces oxidative stress and apoptosis of hippocampal neuron via pCREB/BDNF/ and Nrf2/HO-1/NQO1 pathway. *J. Appl. Toxicol.* 42, 694–705. doi: 10.1002/jat.4252

Lutsenko, S., Barnes, N. L., Bartee, M. Y., and Dmitriev, O. Y. (2007). Function and regulation of human copper-transporting ATPases. *Physiol. Rev.* 87, 1011–1046. doi: 10.1152/physrev.00004.2006

Ma, J., and Betts, N. M. (2000). Zinc and copper intakes and their major food sources for older adults in the 1994-96 continuing survey of food intakes by individuals (CSFII). *J. Nutr.* 130, 2838–2843. doi: 10.1093/jn/130.11.2838

Ma, D. F., Zhang, Y. M., Wang, P. Y., Yang, T. T., Tuo, Y., and Sheng, Q. H. (2014). Analysis for the blood mineral content of children aged 3 to 12 years in 7 cities and 2 towns in China. *Beijing Da Xue Xue Bao* 46, 379–382.

Maes, M., Meltzer, H. Y., Bosmans, E., Bergmans, R., Vandoolaeghe, E., Ranjan, R., et al. (1995). Increased plasma concentrations of interleukin-6, soluble interleukin-6, soluble interleukin-2 and transferrin receptor in major depression. *J. Affect. Disord.* 34, 301–309. doi: 10.1016/0165-0327(95)00028-l

Maes, M., Vandoolaeghe, E., Neels, H., Demedts, P., Wauters, A., Meltzer, H. Y., et al. (1997). Lower serum zinc in major depression is a sensitive marker of treatment resistance and of the immune/inflammatory response in that illness. *Biol. Psychiatry* 42, 349–358. doi: 10.1016/S0006-3223(96)00365-4

Marx, W., Moseley, G., Berk, M., and Jacka, F. (2017). Nutritional psychiatry: the present state of the evidence. *Proc. Nutr. Soc.* 76, 427–436. doi: 10.1017/S0029665117002026

Mauskopf, J. A., Simon, G. E., Kalsekar, A., Nimsch, C., Dunayevich, E., and Cameron, A. (2009). Nonresponse, partial response, and failure to achieve remission: humanistic and cost burden in major depressive disorder. *Depress. Anxiety* 26, 83–97. doi: 10.1002/da.20505

Mercer, J. F. (1998). Menkes syndrome and animal models. *Am. J. Clin. Nutr.* 67, 1022S–1028S. doi: 10.1093/ajcn/67.5.1022S

Moriarty, A. S., Castleton, J., Gilbody, S., McMillan, D., Ali, S., Riley, R. D., et al. (2020). Predicting and preventing relapse of depression in primary care. *Br. J. Gen. Pract.* 70, 54–55. doi: 10.3399/bjgp20X707753

Mravunac, M., Szymlek-Gay, E. A., Daly, R. M., Roberts, B. R., Formica, M., Gianoudis, J., et al. (2019). Greater circulating copper concentrations and copper/zinc ratios are associated with lower psychological distress, but not cognitive performance, in a sample of Australian older adults. *Nutrients* 11:2503. doi: 10.3390/nu11102503

Munakata, M., Sakamoto, O., Kitamura, T., Ishitobi, M., Yokoyama, H., Haginoya, K., et al. (2005). The effects of copper-histidine therapy on brain metabolism in a patient with Menkes disease: a proton magnetic resonance spectroscopic study. *Brain and Development* 27, 297–300. doi: 10.1016/j.braindev.2004.08.002

Nakamura, M., Miura, A., Nagahata, T., Shibata, Y., Okada, E., and Ojima, T. (2019). Low zinc, copper, and manganese intake is associated with depression and anxiety symptoms in the Japanese working population: findings from the eating habit and well-being study. *Nutrients* 11:847. doi: 10.3390/nu11040847

Narang, R. L., Gupta, K. R., Narang, A. P., and Singh, R. (1991). Levels of copper and zinc in depression. *Indian J. Physiol. Pharmacol.* 35, 272–274.

National Academy of Sciences. (2000). *Copper in drinking water. Prepared by the Board of Environmental Studies and Toxicology, Commission on Life Sciences, National Research Council*. Washington, DC: National Academy Press.

Ni, M., You, Y., Chen, J., and Zhang, L. (2018). Copper in depressive disorder: a systematic review and meta-analysis of observational studies. *Psychiatry Res.* 267, 506–515. doi: 10.1016/j.psychres

Ohgami, R. S., Campagna, D. R., McDonald, A., and Fleming, M. D. (2006). The Steap proteins are metalloreductases. *Blood* 108, 1388–1394. doi: 10.1182/blood-2006-02-003681

Ozcelik, D., and Uzun, H. (2009). Copper intoxication; antioxidant defenses and oxidative damage in rat brain. *Biol. Trace Elem. Res.* 127, 45–52. doi: 10.1007/s12011-008-8219-3

Pereira, T. C., Campos, M. M., and Bogo, M. R. (2016). Copper toxicology, oxidative stress and inflammation using zebrafish as experimental model. *J. Appl. Toxicol.* 36, 876–885. doi: 10.1002/jat.3303

Pizzino, G., Irrera, N., Cucinotta, M., Pallio, G., Mannino, F., Arcoraci, V., et al. (2017). Oxidative stress: harms and benefits for human health. *Oxidative Med. Cell. Longev.* 2017:8416763. doi: 10.1155/2017/8416763

Pyaskowit, J. W., and Prohaska, J. R. (2008). Multiple mechanisms account for lower plasma iron in young copper deficient rats. *Biometals* 21, 343–352. doi: 10.1007/s10534-007-9123-6

Pyatskowit, J. W., and Prohask, J. R. (2008). Iron injection restores brain iron and hemoglobin deficits in perinatal copper-deficient rats. *J. Nutr.* 138, 1880–1886. doi: 10.1093/jn/138.10.1880

Reeves, P. G., and Demars, L. C. (2005). Repletion of copper-deficient rats with dietary copper restores duodenal hephaestin protein and iron absorption. *Exp. Biol. Med.* 230, 320–325. doi: 10.1177/153537020523000505

Reeves, P. G., and Demars, L. C. (2006). Signs of iron deficiency in copper-deficient rats are not affected by iron supplements administered by diet or by injection. *J. Nutr. Biochem.* 17, 635–642. doi: 10.1016/j.jnutbio.2006.04.004

Rihel, J. (2018). Copper on the brain. *Nat. Chem. Biol.* 14, 638–639. doi: 10.1038/s41589-018-0089-1

Ruiz, N. A. L., Del Ángel, D. S., Brizuela, N. O., Peraza, A. V., Olguín, H. J., Soto, M. P., et al. (2022). Inflammatory process and immune system in major depressive disorder. *Int. J. Neuropsychopharmacol.* 25, 46–53. doi: 10.1093/ijnp/pyab072

Ruizs, L. M., Libedinsky, A., and Elorza, A. A. (2021). Role of copper on mitochondrial function and metabolism. *Front. Mol. Biosci.* 8:711227. doi: 10.3389/fmolb.2021.711227

Russo, A. J. (2011). Analysis of plasma zinc and copper concentration, and perceived symptoms, in individuals with depression, post zinc and anti-oxidant therapy. *Nutr. Metab. Insights.* 4, 19–27. doi: 10.4137/NMI.S6760

Salehi-Abargouei, A., Esmaillzadeh, A., Azadbakht, L., Keshteli, A. H., Afshar, H., Feizi, A., et al. (2019). Do patterns of nutrient intake predict self-reported anxiety, depression and psychological distress in adults? SEPAHAN study. *Clin. Nutr.* 38, 940–947. doi: 10.1016/j.clnu.2018.02.002

Salustri, C., Squitti, R., Zappasodi, F., Ventriglia, M., Bevacqua, M. G., Fontana, M., et al. (2010). Oxidative stress and brain glutamate-mediated excitability in depressed patients. *J. Affect. Disord.* 127, 321–325. doi: 10.1016/j.jad.2010.05.012

Sharma, S. K., Sood, S., Sharma, A., and Gupta, I. D. (2014). Estimation of serum zinc and copper levels patients with schizophrenia: a preliminary study. *Sri. Lanka. J. Psyc.* 5, 14–17. doi: 10.4038/sljpsyc.v5i1.7076

Shusharina, N., Yukhnenko, D., Botman, S., Sapunov, V., Savinov, V., Kamyshov, G., et al. (2023). Modern methods of diagnostics and treatment of neurodegenerative diseases and depression. *Diagnostics* 13:573. doi: 10.3390/diagnostics13030573

Siwek, M., Styczeń, K., Sowa-Kućma, M., Dudek, D., Reczyński, W., Szewczyk, B., et al. (2017). The serum concentration of copper in bipolar disorder. *Psychiatr. Pol.* 51, 469–481. doi: 10.12740/PP/OnlineFirst/65250

Styczeń, K., Sowa-Kućma, M., Siwek, M., Dudek, D., Reczyński, W., Misztak, P., et al. (2016). Study of the serum copper levels in patients with major depressive disorder. *Biol. Trace Elem. Res.* 174, 287–293. doi: 10.1007/s12011-016-0720-5

Sun, X., Li, J., Zhao, H., Wang, Y., Liu, J., Shao, Y., et al. (2018). Synergistic effect of copper and arsenic upon oxidative stress, inflammation and autophagy alterations in brain tissues of Gallus gallus. *J. Inorg. Biochem.* 178, 54–62. doi: 10.1016/j.jinorgbio.2017.10.006

Thi Thu Nguyen, T., Miyagi, S., Tsujiguchi, H., Kambayashi, Y., Hara, A., Nakamura, H., et al. (2019). Association between lower intake of minerals and depressive symptoms among elderly Japanese women but not men: findings from Shika study. *Nutrients* 11:389. doi: 10.3390/nu11020389

Turnlund, J. R. (2000). "Copper status and metabolism studied with isotopic tracers" in *Advances in isotope methods for the analysis of trace elements in man*. eds. M. Jackson and N. Lowe (Boca Raton: CRC Press)

Twayej, A. J., Al-Hakeim, H. K., Al-Dujaili, A. H., and Maes, M. (2020). Lowered zinc and copper levels in drug-naïve patients with major depression: effects of antidepressants, ketoprofen and immune activation. *World J. Biol. Psychiatry* 21, 127–138. doi: 10.1080/15622975.2019.1612090

Uauy, R., Olivares, M., and Gonzalez, M. (1998). Essentiality of copper in humans. *Am. J. Clin. Nutr.* 67, 952S–959S. doi: 10.1093/ajcn/67.5.952S

Ullas Kamath, S., Chaturvedi, A., Bhaskar Yerrapragada, D., Kundapura, N., Amin, N., and Devaramane, V. (2019). Increased levels of acetylcholinesterase, paraoxonase 1, and copper in patients with moderate depression-a preliminary study. *Rep. Biochem. Mol. Biol.* 7, 174–180.

Uriu-Adams, J. Y., and Keen, C. L. (2005). Copper, oxidative stress, and human health. *Mol. Asp. Med.* 26, 268–298. doi: 10.1016/j.mam.2005.07.015

Wang, T., Xiang, P., Ha, J. H., Wang, X., Doguer, C., Flores, S. R. L., et al. (2018). Copper supplementation reverses dietary iron overload-induced pathologies in mice. *J. Nutr. Biochem.* 59, 56–63. doi: 10.1016/j.jnutbio.2018.05.006

Wang, C. J., Yang, T. F., Wang, G. S., Zhao, Y. Y., Yang, L. J., and Bi, B. N. (2018). Association between dietary patterns and depressive symptoms among middle-aged adults in China in 2016-2017. *Psychiatry Res.* 260, 123–129. doi: 10.1016/j.psychres.2017.11.052

Wang, Y., Zhao, H., Shao, Y., Liu, J., Li, J., Luo, L., et al. (2018). Copper or/and arsenic induces autophagy by oxidative stress-related PI3K/AKT/mTOR pathways and cascaded mitochondrial fission in chicken skeletal muscle. *J. Inorg. Biochem.* 188, 1–8. doi: 10.1016/j.jinorgbio.2018.08.001

West, E. C., and Prohaska, J. R. (2004). Cu,Zn-superoxide dismutase is lower and copper chaperone CCS is higher in erythrocytes of copper-deficient rats and mice. *Exp. Biol. Med.* 229, 756–764. doi: 10.1177/153537020422900807

Winge, D. R., and Mehra, R. K. (1990). Host defenses against copper toxicity. *Int. Rev. Exp. Pathol.* 31, 47–83. doi: 10.1016/b978-0-12-364931-7.50007-0

World Health Organization. (2023a). *Depressive disorder (depression)*. Available at: https://www.who.int/news-room/fact-sheets/detail/depression (Accessed March 31, 2023).

World Health Organization. (2023b). *Depression*. Available at: https://www.who.int/news-room/fact-sheets/detail/depression (Accessed January13, 2023).

Wu, H. R., Li, Q. Q., Gao, R., Tang, S. Y., Zhang, K. F., and Zhao, J. F. (2022). BMI modifies the association between depression symptoms and serum copper levels. *Biol. Trace Elem. Res.* 201, 4216–4229. doi: 10.1007/s12011-022-03505-y

Xia, Y., Wang, N., Yu, B., Zhang, Q., Liu, L., Meng, G., et al. (2017). Dietary patterns are associated with depressive symptoms among Chinese adults: a case-control study with propensity score matching. *Eur. J. Nutr.* 56, 2577–2587. doi: 10.1007/s00394-016-1293-y

Xie, J., He, X., Fang, H., Liao, S., Liu, Y., Tian, L., et al. (2020). Identification of heme oxygenase-1 from golden pompano (*Trachinotus ovatus*) and response of Nrf2/HO-1 signaling pathway to copper-induced oxidative stress. *Chemosphere* 253:126654. doi: 10.1016/j.chemosphere.2020.126654

Xu, J., He, K., Zhang, K., Yang, C., Nie, L., Dan, D., et al. (2021). Low-dose copper exposure exacerbates depression-like behavior in ApoE4 transgenic mice. *Oxidative Med. Cell. Longev.* 2021:6634181. doi: 10.1155/2021/6634181

Yang, F., Liao, J., Yu, W., Pei, R., Qiao, N., Han, Q., et al. (2020). Copper induces oxidative stress with triggered NF-κB pathway leading to inflammatory responses in immune organs of chicken. *Ecotoxicol. Environ. Saf.* 200:110715. doi: 10.1016/j.ecoenv.2020.110715

Zhang, F., Zheng, W., Guo, R., and Yao, W. (2017). Effect of dietary copper level on the gut microbiota and its correlation with serum inflammatory cytokines in Sprague-Dawley rats. *J. Microbiol.* 55, 694–702. doi: 10.1007/s12275-017-6627-9

Zhong, C. C., Zhao, T., Hogstrand, C., Chen, F., Song, C. C., and Luo, Z. (2022). Copper (cu) induced changes of lipid metabolism through oxidative stress-mediated autophagy and Nrf2/PPARγ pathways. *J. Nutr. Biochem.* 100:108883. doi: 10.1016/j.jnutbio.2021.108883

Zhong, W., Zhu, H., Sheng, F., Tian, Y., Zhou, J., Chen, Y., et al. (2014). Activation of the MAPK11/12/13/14 (p38 MAPK) pathway regulates the transcription of autophagy genes in response to oxidative stress induced by a novel copper complex in HeLa cells. *Autophagy* 10, 1285–1300. doi: 10.4161/auto.28789

Zou, L., Cheng, G., Xu, C., Liu, H., Wang, Y., Li, N., et al. (2021). Copper nanoparticles induce oxidative stress via the heme oxygenase 1 signaling pathway in vitro studies. *Int. J. Nanomedicine* 16, 1565–1573. doi: 10.2147/IJN.S292319

frontiers | Frontiers in Pharmacology

TYPE Original Research
PUBLISHED 17 August 2023
DOI 10.3389/fphar.2023.1255501

OPEN ACCESS

EDITED BY
Weijie Xie,
Shanghai Jiao Tong University, China

REVIEWED BY
Xiang Dong Du,
Suzhou Psychiatric Hospital, China
Shen Li,
Tianjin Medical University, China

*CORRESPONDENCE
Shuyun Li,
jiujiang1996@163.com

RECEIVED 08 July 2023
ACCEPTED 04 August 2023
PUBLISHED 17 August 2023

CITATION
Zhao L, Liu H, Wang W, Wang Y, Xiu M and Li S (2023), Carnitine metabolites and cognitive improvement in patients with schizophrenia treated with olanzapine: a prospective longitudinal study.
Front. Pharmacol. 14:1255501.
doi: 10.3389/fphar.2023.1255501

Carnitine metabolites and cognitive improvement in patients with schizophrenia treated with olanzapine: a prospective longitudinal study

Lei Zhao[1], Hua Liu[1], Wenjuan Wang[1], Youping Wang[2,3,4], Meihong Xiu[5] and Shuyun Li[2,3,4]*

[1]Qingdao Mental Health Center, Qingdao, Shandong, China, [2]Department of Nutritional and Metabolic Psychiatry, The Affiliated Brain Hospital of Guangzhou Medical University, Guangzhou, China, [3]Guangdong Engineering Technology Research Center for Translational Medicine of Mental Disorders, Guangzhou, China, [4]Key Laboratory of Neurogenetics and Channelopathies of Guangdong Province and the Ministry of Education of China, Guangzhou Medical University, Guangzhou, China, [5]Beijing HuiLongGuan Hospital, Peking University HuiLongGuan Clinical Medical School, Beijing, China

Objective: Cognitive impairment is one of the core symptoms of schizophrenia, which is stable and lifelong. L-carnitine has been shown to improve cognitive function and decrease the rate of cognitive deterioration in patients with Alzheimer's disease. However, it remains unclear regarding the role of L-carnitine and its metabolites in cognitive functions in schizophrenia after treatment with olanzapine. The purpose of this study was to evaluate the relationship between changes in plasma levels of L-carnitine metabolites and cognitive improvement after olanzapine treatment.

Methods: This was a prospective longitudinal study. In this study, we recruited 25 female patients with first episode schizophrenia (FES) who were drug naïve at baseline and received 4 weeks of olanzapine monotherapy. Cognitive function was assessed at baseline and 4-week follow-up using the RBANS. Plasma L-carnitine metabolite levels were determined by a metabolomics technology based on untargeted ultra-performance liquid chromatography-mass spectrometry (UPLC-MS).

Results: We found that the immediate memory index, delayed memory index and RBANS composite score were significantly increased at the 4-week follow-up after treatment. A total of 7 differential L-carnitine metabolites were identified in FES patients after olanzapine monotherapy. In addition, we found that changes in butyrylcarnitine were positively correlated with improvements in language index and RBANS composite score. Further regression analyses confirmed the association between reduced butyrylcarnitine levels and cognitive improvement after olanzapine monotherapy in FES patients.

Conclusion: Our study shows that cognitive improvement after olanzapine treatment was associated with changes in L-carnitine metabolite levels in patients with FES, suggesting a key role of L-carnitine in cognition in schizophrenia.

KEYWORDS

schizophrenia, carnitines, cognitive improvement, olanzapine, longitudinal study

1 Introduction

Patients with schizophrenia are characterized by modest to severe impairments in verbal learning, working memory, executive function and processing speed (Barnett, 2018; Harvey and Isner, 2020; Xiu et al., 2020; Xiu et al., 2021; Zhu et al., 2022). Cognitive impairment is present throughout the course of the disorder, from prodromal to more severe stages. Large retrospective cohort studies showed that cognitive impairment is the first sign and a trait marker in individuals later diagnosed with schizophrenia (Häfner et al., 1992; Rund, 1998). In addition, evidence of cognitive impairment in the prodromal stage and throughout the course of schizophrenia demonstrates a close relationship between cognitive impairment and independent living, social and community cognitive function, and functional outcomes (Green and Nuechterlein, 1999; Bilder et al., 2000; Green et al., 2000; Fett et al., 2011).

Carnitine, biosynthesized from an amino acid, is present in nearly all cells of the body (Flanagan et al., 2010). There are two forms of carnitine, known as D-carnitine and L-carnitine, and only L-carnitine is active in the body. L-carnitine is found in mammalian cells as free carnitine and acylcarnitines. *In vivo*, carnitine can be transferred with the acyl group by carnitine palmitoyltransferase 1 to produce acylcarnitine (Bonnefont et al., 2004). L-carnitine has various biological functions, such as in the metabolism of fatty acids as energy to keep the body's cells powered and working efficiently and in anti-inflammatory and antioxidant defense (Moghaddas and Dashti-Khavidaki, 2016; Traina, 2016). For example, the L-carnitine system is known for its role in the transport of fatty acids into the mitochondrial matrix and β-oxidation of fatty acids (Noland et al., 2009). Cellular energy production is primarily derived from mitochondrial β-oxidation of fatty acids, especially when carbohydrate stores are exhausted after exercise. L-carnitine can improve mitochondrial and peroxisomal metabolism in neurons (Jones et al., 2010). Abnormal levels of L-carnitine or its metabolites may decrease fatty acid β-oxidation and reduce the production of mitochondrial energy in mental disorders (Kępka et al., 2021). In addition, L-carnitine maintains the integrity of cell membranes and stabilizes the physiological CoA-SH/acetyl-CoA ratio in mitochondria (Siliprandi et al., 1990). Its deficiency causes the structural swells of astrocytes and the expansion of mitochondria in nerve cells. Noteworthy, impaired mitochondrial function in schizophrenia is supported by converging evidence from genetic, post-mortem and peripheral studies (Clay et al., 2011; Rajasekaran et al., 2015). Interestingly, compounds containing L-carnitine substructures did show neuroprotective effects, which were reported to be related to the protection of mitochondria accompanied by improved energy supply (Spagnoli et al., 1991; Wang et al., 2017).

Antipsychotics are the first-line treatment for patients with schizophrenia and there is evidence that olanzapine (OLA) improves cognitive function in patients with schizophrenia (Ljubin et al., 2000; Sergi et al., 2007; Baldez et al., 2021), although the effect size was small and some prospective cohort studies have reported inconsistent results (Baldez et al., 2021). For example, the Clinical Antipsychotic Trials of Intervention Effectiveness (CATIE), a clinical trial with one of the largest neuropsychological tests in schizophrenia, showed moderate improvements in patients following antipsychotic drugs (Keefe et al., 2007). On the contrary, a naturalistic sub-group analysis demonstrated that discontinuation of antipsychotic medication was not associated with a negative effect on cognitive function, but with a better effect on it (Albert et al., 2019). Cognitive impairments in schizophrenia have been shown to be related to abnormalities in several biological pathways (Xiu et al., 2019; Wu et al., 2020; Xiu et al., 2020; Su et al., 2021). Of particular interest is the accumulating evidence of carnitine deficiency in cognitive deficits in general populations, which may also be a possible pathological mechanism of cognitive impairments in schizophrenia. Given the fundamental role of L-carnitine in mitochondrial functions and energy production, a growing body of evidence supports its dysfunctions in cognitive declines, such as Alzheimer's disease (AD) (Signorelli et al., 2006; Ciacci et al., 2007; Wesnes and Reynolds, 2019; Pennisi et al., 2020; Kępka et al., 2021).

Moreover, abnormal L-carnitine levels may be associated with certain mental illnesses, including schizophrenia and depression (Wang et al., 2014; Kriisa et al., 2017). Current evidence supports an imbalance in the oxidative stress status or inflammatory status involved in the pathogenesis of schizophrenia, which is also related to β-oxidation in the mitochondrion of L-carnitines (Cuturic et al., 2016). In addition, acetyl-carnitine supplementation to clozapine therapy has been shown to improve positive symptoms in patients with schizophrenia. Together, all these studies suggest that carnitine or its metabolites play a pivotal role in the treatment response of schizophrenia.

We hypothesized that abnormal levels of L-carnitine metabolites are associated with cognitive impairments and that changes in them after OLA monotherapy are associated with cognitive improvement in FES patients. Therefore, to test this hypothesis, we recruited unmedicated FES patients and conducted a comprehensive analysis of L-carnitine metabolites in a 4-week OLA-treatment population with schizophrenia. We tested the following questions in schizophrenia: a) differences in L-carnitine metabolite levels in patients after OLA monotherapy relative to baseline; b) the relationship between changes in L-carnitine metabolites levels and cognitive improvement; and c) the predictive role of baseline L-carnitine metabolites levels for cognitive improvement.

2 Methods

2.1 Patients

This study was conducted from July 2011 to January 2013. The study protocol was reviewed and approved by the Institutional Review Board of Beijing Huilongguan Hospital. Patients signed the written informed consent forms.

A total of 25 FES patients were recruited at Beijing Huilongguan Hospital. The definition of FES was as a previous study (Lieberman et al., 2003). The inclusion criteria included: 1) diagnosis of schizophrenia by the Chinese version of the Structured Clinical Interview (SCID) for Diagnostic and Statistical Manual of Mental Disorders IV (Phillips and Liu, 2011); 2) medication naïve; 3) age between 18 and 45 years old; and 4) experiencing a first episode of

TABLE 1 Demographic and clinical variables of patients at baseline and at follow-up.

Variables, mean ± SD	First-episode	After 4 weeks	
	n = 25	n = 25	t(p)
Age (ys)	27.4 ± 7.6		
Education (ys)	9.1 ± 3.5		
BMI (kg/m2)	21.0 ± 3.6		
Age of onset	26.4 ± 8.9		
PANSS total score	81.8 ± 13.9	63.9 ± 13.8	5.4 (<0.001)
P subscore	25.0 ± 6.0	16.4 ± 5.2	7.6 (<0.001)
N subscore	17.1 ± 4.7	15.6 ± 4.3	1.2 (0.23)
G subscore	39.7 ± 7.5	32.0 ± 6.0	4.2 (<0.001)

Abbreviations: ys years; BMI, body mass index; PANSS, positive and negative syndrome scale; P subscore, positive symptom subscore; N subscore, negative symptom subscore; G subscore, general psychopathology subscore.

TABLE 2 Carnitines of the FES patients at baseline and after 4 weeks.

Carnitine, median (IQR)	First-episode (10^4)	After 4 weeks (10^4)	Z(p)
Linoelaidyl carnitine	9.2 (3.1, 327.4)	54.0 (39.2, 71.8)	−0.3 (0.82)
2-Octenoylcarnitine	164.9 (83.5, 321.5)	4.9 (2.7, 10.9)	−3.8 (<0.001)
Butyrylcarnitine	94.9 (58.7, 230.5)	125.3 (69.6, 224.5)	−1.3 (0.20)
11Z-Octadecenylcarnitine	14.9 (2.3, 189.1)	203.4 (129.2, 317.3)	−2.2 (0.03)
9-Decenoylcarnitine	3.2 (2.2, 4.5)	14.5 (1.8, 194.8)	−2.9 (0.004)
Propionylcarnitine	38.5 (14.0, 72.8)	30.0 (13.2, 55.1)	−1.4 (0.17)
L-Palmitoylcarnitine	89.0 (35.4, 279.3)	3.5 (2.8, 4.0)	−4.4 (<0.001)

psychosis. The exclusion criteria included: 1) abuse or substance dependence obtained through the questions we asked participants verbally; 2) suicide ideation; 3) pregnancy or breastfeeding; 4) serious neurological or major medical illnesses; and 5) receiving antidiabetic, antihyperlipidemic, and/or antihypertensive drugs.

2.2 Study procedures

A prospective, observational, cohort study with a 4-week follow-up was conducted on patients with schizophrenia. A questionnaire was designed to collect demographic and clinical data. Over the course of 4weeks of treatment, FES patients received a flexible-dosage, oral OLA monotherapy as prescribed by the psychiatrists based on clinical response. The oral dose of OLA for FES patients ranges from 10 mg/day to 30 mg/day. During the 4 weeks, all patients were hospitalized and nurses monitored OLA medication adherence.

2.3 Assessment

The Repeatable Battery for the Assessment of Neuropsychological Status (RBANS, Form A) was used to assess the cognitive functioning of patients (Randolph et al., 1998). The index score of the RBANS includes immediate memory, visuoconstructional, attention, language, and delayed memory. All these index scores are combined to form a composite score. In addition, the Positive and Negative Syndrome Scales (PANSS) were evaluated to determine the severity of clinical symptoms (Kay et al., 1987). After a brief standardized training, repeated assessments showed that the inter-rater reliability of the PANSS total score maintained greater than 0.8. Cognitive functions and clinical symptoms were assessed at baseline and at the end of 4 weeks.

2.4 Plasma collection and metabolomics processing

Fasting blood was collected by the research nurse at 7: 00 a.m. at baseline and at the 4-week follow-up. Plasma samples were separated and 200 μl was ground into powder in liquid nitrogen. As reported in our previous study, an LC-HRMS system, Q-Exactive Focus equipped with a heated electrospray ionization source was used for untargeted metabolomics (Liu J et al., 2021; Liu J H et al., 2021).

TABLE 3 Correlations of baseline lysophosphatidylcholine levels and the improvement in cognitive functions in patients.

Baseline carnitines	Immediate memory (r/p)	Visuoconstructional (r/p)	Language (r/p)	Attention (r/p)	Delayed memory (r/p)	Total score (r/p)
Linoelaidyl carnitine	−0.16 (0.44)	0.13 (0.54)	0.04 (0.84)	−0.19 (0.37)	−0.12 (0.55)	−0.21 (0.31)
2-Octenoylcarnitine	0.36 (0.08)	0.39 (0.05)	−0.06 (0.78)	−0.06 (0.77)	0.11 (0.61)	−0.05 (0.80)
Butyrylcarnitine	0.14 (0.50)	0.22 (0.29)	0.30 (0.15)	−0.04 (0.85)	0.31 (0.14)	0.20 (0.34)
11Z-Octadecenylcarnitine	−0.15 (0.48)	0.17 (0.41)	0.24 (0.26)	−0.28 (0.18)	0.02 (0.94)	0.06 (0.78)
9-Decenoylcarnitine	0.15 (0.48)	0.11 (0.61)	0.20 (0.33)	0.14 (0.49)	**0.43(0.03)**	0.30 (0.15)
Propionylcarnitine	0.27 (0.19)	0.36 (0.08)	0.17 (0.43)	0.02 (0.93)	0.14 (0.50)	0.10 (0.64)
L-Palmitoylcarnitine	0.05 (0.81)	0.23 (0.26)	0.03 (0.89)	−0.22 (0.28)	−0.004 (0.9)	−0.10 (0.62)

Note: The bold p value means less than 0.05.

2.5 Statistical analysis

The concentrations of L-carnitine metabolites were not normally distributed, thus, we performed the non-parametric tests in this study. Non-parametric analyses of paired sample t-test were used to compare clinical symptoms and cognitive functions at baseline and 4-week follow-up. Spearman rank correlation analysis was used to evaluate the association between L-carnitine metabolites and cognitive improvements in patients. In addition, we divided the original α-values by the number of analyses performed on the variables to obtain Bonferroni-corrected/adjusted p values. The new α = 0.05/7 = 0.007 for metabolite analysis and α = 0.05/6 = 0.008 for cognitive function analysis. Multiple linear regression analysis was performed to investigate the influencing factors for cognitive improvement in FES patients, by limiting the effects of confounding factors, such as age, education and baseline BMI. Improvements in RBANS total score or its subscores served as dependent variables and changes in L-carnitine levels or baseline L-carnitine levels served as independent variables in the current study.

Data were analyzed using statistical software (IBM SPSS 22.0). The significance threshold was set at $p < 0.05$.

3 Results

The demographic and clinical characteristics of the FES patients are shown in Sup Table 1. As reported in our previous study, OLA treatment for 4 weeks significantly improved clinical symptoms and cognitive functions in patients with FES ($p_{Bonferroni} < 0.05$).

3.1 L-carnitine metabolites determination

Plasma metabolomics analysis identified abnormalities in lipids, organic acids, bilirubin, carnitine, ammonium salts, proline, olanzapine and its metabolites after treatment. Among these compounds, we identified 7 differential L-carnitine metabolites with a VIP value >1 and $p < 0.05$. Further analysis showed that 2-Octenoylcarnitine, 11Z-Octadecenylcarnitine, 9-Decenoylcarnitine and L-Palmitoylcarnitine levels were significantly decreased after OLA monotherapy relative to baseline levels (all $p < 0.05$) (Table 2). In contrast, there were no significant differences in the levels of other 3 L-carnitine metabolites between baseline and follow-up (all $p > 0.05$). There was no significant association between plasma levels of L-carnitine metabolites and RBANS total score or its five subscores at baseline.

3.2 Association of baseline L-carnitine metabolites with cognitive improvement

Spearman correlation analysis showed that baseline 9-Decenoylcarnitine levels were significantly associated with improvements in the delayed memory index (r = 0.43, $p = 0.031$) (Table 3). However, this association did not pass the Bonferroni correction. After controlling for onset age, education and baseline BMI, multiple regression analysis also did not find a significant association between baseline metabolite levels and cognitive improvement with cognitive improvement as the independent variable and baseline 9-Decenoylcarnitine level as the dependent variable ($p > 0.05$).

3.3 Association between changes in plasma L-carnitine metabolite levels and cognitive improvement

As shown in Table 4, we found that the decrease in 2-octenoylcarnitine levels was associated with the improvement in immediate memory index (r = −0.43, $p = 0.033$). In addition, the decrease in butyrylcarnitine was positively correlated with improvements in language performance (r = 0.47, $p = 0.017$) and RBANS composite score (r = 0.42, $p = 0.039$). Further regression analysis also showed a significant association between a decrease in butyrylcarnitine and improvement in language index (β= 0.49, t = 2.5, $p = 0.021$) or RBANS composite score (β= 0.45, t = 2.3, $p = 0.034$) after controlling for onset age, education and baseline BMI.

4 Discussion

In this cohort study, we found that 1) OLA monotherapy significantly decreased plasma levels of four L-carnitine

TABLE 4 Correlations of the changes in carnitine levels and cognitive improvement in FES patients.

Decreases in carnitines	Immediate memory (r/p)	Visuoconstructional (r/p)	Language (r/p)	Attention (r/p)	Delayed memory (r/p)	Total score (r/p)
Linoelaidyl carnitine	−0.16 (0.45)	0.15 (0.49)	0.04 (0.85)	−0.19 (0.35)	−0.12 (0.55)	−0.21 (0.32)
2-Octenoylcarnitine	**0.43(0.03)**	0.28 (0.17)	−0.11 (0.61)	−0.04 (0.84)	0.22 (0.30)	−0.01 (0.97)
Butyrylcarnitine	0.10 (0.64)	0.07 (0.74)	**0.47(0.017)**	0.26 (0.22)	0.36 (0.08)	**0.42(0.04)**
11Z-Octadecenylcarnitine	−0.23 (0.27)	0.06 (0.76)	0.11 (0.60)	−0.35 (0.09)	−0.27 (0.20)	−0.09 (0.66)
9-Decenoylcarnitine	0.19 (0.37)	0.08 (0.71)	−0.03 (0.90)	0.25 (0.22)	0.22 (0.29)	0.19 (0.36)
Propionylcarnitine	−0.12 (0.58)	0.23 (0.28)	0.26 (0.22)	−0.02 (0.92)	−0.35 (0.09)	−0.02 (0.95)
L-Palmitoylcarnitine	0.05 (0.81)	0.24 (0.26)	0.03 (0.88)	0.22 (0.29)	−0.003 (0.9)	−0.10 (0.62)

Note: The bold *p* value means less than 0.05.

metabolites in FES patients; 2) reduced plasma levels of 2-octenoylcarnitine and butyrylcarnitine were correlated with the cognitive improvement after treatment; and 3) baseline L-carnitine metabolite levels were not associated with cognitive improvement.

We found that OLA significantly decreased several L-carnitine metabolites levels in FES patients, including 2-octenoylcarnitine, 11z-octadecenylcarnitine, 9-decenoylcarnitine and L-palmitoylcarnitine. All of these metabolites are known to be medium- or long-chain acylcarnitines with six or more carbons. More specifically, they are all acyl fatty acid derivative esters. In the body, acylcarnitines can be divided into nine categories based on the size and type of acyl group: 1) short-chain ACs; 2) medium-chain ACs; 3) long-chain ACs; 4) very long-chain ACs; 5) hydroxy ACs; 6) branched chain ACs; 7) unsaturated ACs; 8) dicarboxylic ACs and 9) miscellaneous ACs. Medium- and long-chain acylcarnitines are slightly less abundant in the body than short-chain acylcarnitines and are involved in the mitochondrial β-oxidation pathway in mitochondria. More specifically, 2-Octenoylcarnitine is an acylcarnitine having (2E)-octenoyl as the acyl substituent. 9-Decenoylcarnitine is an acyl fatty acid derivative ester formed by carnitine and arachidonic acid. L-palmitoylcarnitine is formed via palmitoyl-CoA reacts with L-carnitine, which is then moved into the mitochondrial intermembrane space. L-palmitoylcarnitine can react with the carnitine o-palmitoyltransferase 2 enzyme present in the mitochondrial inner membrane to once again form palmitoyl-CoA and L-carnitine. Palmitoyl-CoA then enters into the β-oxidation pathway to form acyl coenzyme A (aceytl-CoA). We found that levels of these three L-carnitine metabolites were decreased after treatment, which was in line with a previous study (Cao et al., 2019a), suggesting that OLA can downregulate acylcarnitine levels in patients with FES. However, given that no controls were recruited in this study, we do not know whether the decreased acylcarnitine levels normalized to those found in healthy controls, Acylcarnitine plays a fundamental role in the transfer of fatty acid to mitochondria for subsequent β-oxidation. Consistent with our findings, some studies have also reported abnormal levels of acylcarnitine in various diseases. For example, 9-decenoylcarnitine has been shown to be increased the plasma of overweight individuals (Kang et al., 2018). Metabolite profiling of the 1946 British birth cohort also found a relationship between a module consisting of acylcarnitine and processing speed after controlling for life course, showing L-palmitoylcarnitine to be a hub (Green et al., 2022). Prior studies have also found acylcarnitines levels with abnormalities in the plasma of patients with schizophrenia and familial Mediterranean fever (Kiykim et al., 2016; Cao et al., 2020). Moreover, the regulation of L-carnitine metabolites by antipsychotic drugs has been reported in clinical studies (Lheureux and Hantson, 2009; Molina et al., 2021; Yi et al., 2021), and in animal studies (Albaugh et al., 2012; Jiang et al., 2019), particularly in two early studies in patients with schizophrenia after treatment (Kriisa et al., 2017; Cao et al., 2019b). All these findings support our finding that the carnitine pathway can be regulated by OLA.

The second finding was that cognitive improvement after OLA treatment was significantly associated with decreased levels of 2-octenoylcarnitine and butyrylcarnitine in schizophrenia. And the lower the levels of 2-octenoylcarnitine and butyrylcarnitine, the better the cognitive improvement. This finding is the first report in patients with schizophrenia, but is consistent with recent findings in AD patients. Studies in AD and preclinical AD have shown that some medium- or long-chain acylcarnitines involved in fatty acid transportation and metabolism were associated with cognitive decline (Fiandaca et al., 2015; Ciavardelli et al., 2016). For example, plasma acylcarnitines have been found to decrease aging and have been shown to predict conversion to mild cognitive impairment or AD. In addition, altered metabolism of medium-chain acylcarnitines and impaired ketogenesis may be metabolic features of AD (Ciavardelli et al., 2016). We cannot give an exact explanation for the close relationship between the two special acylcarnitines and cognitive improvement. However, it is known that the carnitine shuttle pathway is responsible for the transport of long-chain fatty acids from the cytoplasm into the mitochondria for subsequent β-oxidation, a process that requires aceytl-CoA and leads to the esterification of L-carnitine to form acylcarnitine derivatives (Sharma and Black, 2009). It is possible that perturbation of the carnitine shuttle leads to compromised mitochondrial function, which could decrease cellular capacity to handle reactive oxygen species and increase the levels of the inflammatory cytokine, resulting in increased cellular dysfunction and cell death (Mitchell et al., 2018).

The brain is highly dependent on oxidative metabolism. In the absence of carnitine, fatty acid metabolism and energy production in the brain are impaired, leading to cognitive impairment. A previous review has supported the critical role of acylcarnitine in fatty acid metabolism, ketosis and buffering the concentration ratio of acyl-CoA to free CoA in brain metabolism in neurological disorders

(Jones et al., 2010). Considering the close relationship between metabolic disturbances and acylcarnitine, we further analyzed the relationship between acylcarnitine and cognitive impairment after controlling for weight gain and found that the association between decreased acylcarnitine levels and cognitive improvement remained significant. Therefore, the association of cognitive improvement with acylcarnitine is reliable and robust, suggesting its role in schizophrenia.

There were several limitations to note in this study. First, only female patients were recruited in our study, as the majority of patients in our research center are female. Only female patients may limit generalizations to the broader population with FES schizophrenia. Second, we did not collect data on the levels of L-carnitine metabolites in the cerebro-spinal fluid (CSF). Further studies should include this data, which would lend consistency to the findings in this study.

In summary, we found that OLA treatment significantly decreased L-carnitine metabolite levels and improved cognitive functions in patients with schizophrenia. In addition, decreased carnitine metabolite levels were significantly associated with cognitive improvements after treatment. Our study provides new evidence for the involvement of L-carnitine metabolite levels in cognitive improvement after the treatment with OLA. However, due to the small sample size and the short-term OLA monotherapy, our findings should be interpreted with great caution. Moreover, only female patients may limit generalizations to the broader population with DNFE schizophrenia. Further longitudinal studies using larger samples with longer antipsychotic treatment are warranted to understand the exact mechanism of L-carnitine metabolites in cognitive improvement in schizophrenia.

Data availability statement

The raw data supporting the conclusion of this article will be made available by the authors, without undue reservation.

Ethics statement

The studies involving humans were approved by Ethics committee of Beijing huilongguan hospital. The studies were conducted in accordance with the local legislation and institutional requirements. The participants provided their written informed consent to participate in this study. No potentially identifiable images or data are presented in this study.

Author contributions

MX: Writing–original draft. LZ: Conceptualization, data curation, investigation, writing–original draft. HL: Investigation, writing–original draft. WW: Data curation, Investiagtion, Writing–original draft. YW: Data curation, Investiagtion, Writing–original draft. SL: Data curation, supervision, validation, writing–original draft.

Funding

This study was funded by the Guangzhou Municipal Health Commission (2023C-TS26), Traditional Chinese Medicine Bureau of Guangdong Province (No. 20222178), Opening Foundation of Jiangsu Key Laboratory of Neurodegeneration, Nanjing Medical University (KF202202), Open Project Program of State Key Laboratory of Virtual Reality Technology and Systems, Beihang University (VRLAB2022 B02), and Shanghai Key Laboratory of Psychotic Disorders Open Grant (21-K03), Guangzhou High-level Clinical Key Specialty, and Guangzhou Research-oriented Hospital. All funding had no role in study design, data analysis, paper submission and publication.

Acknowledgments

We would like to thank the participants in the study and their families.

Conflict of interest

The authors declare that the research was conducted in the absence of any commercial or financial relationships that could be construed as a potential conflict of interest.

Publisher's note

References

Albaugh, V. L., Vary, T. C., Ilkayeva, O., Wenner, B. R., Maresca, K. P., Joyal, J. L., et al. (2012). Atypical antipsychotics rapidly and inappropriately switch peripheral fuel utilization to lipids, impairing metabolic flexibility in rodents. *Schizophr. Bull.* 38 (1), 153–166. doi:10.1093/schbul/sbq053

Albert, N., Randers, L., Allott, K., Jensen, H. D., Melau, M., Hjorthøj, C., et al. (2019). Cognitive functioning following discontinuation of antipsychotic medication. A naturalistic sub-group analysis from the OPUS II trial. *A Nat. sub-group analysis OPUS II trial* 49 (7), 1138–1147. doi:10.1017/S0033291718001836

Baldez, D. P., Biazus, T. B., Rabelo-da-Ponte, F. D., Nogaro, G. P., Martins, D. S., Kunz, M., et al. (2021). The effect of antipsychotics on the cognitive performance of individuals with psychotic disorders: network meta-analyses of randomized controlled trials. *Neurosci. Biobehav Rev.* 126, 265–275. doi:10.1016/j.neubiorev.2021.03.028

Barnett, R. (2018). Schizophrenia. *Lancet* 391 (10121), 648. doi:10.1016/S0140-6736(18)30237-X

Bilder, R. M., Goldman, R. S., Robinson, D., Reiter, G., Bell, L., Bates, J. A., et al. (2000). Neuropsychology of first-episode schizophrenia: initial characterization and clinical correlates. *Am. J. Psychiatry* 157 (4), 549–559. doi:10.1176/appi.ajp.157.4.549

Bonnefont, J. P., Djouadi, F., Prip-Buus, C., Gobin, S., Munnich, A., and Bastin, J. (2004). Carnitine palmitoyltransferases 1 and 2: biochemical, molecular and medical aspects. *Mol. Asp. Med.* 25 (5-6), 495–520. doi:10.1016/j.mam.2004.06.004

Cao, B., Jin, M., Brietzke, E., McIntyre, R. S., Wang, D., Rosenblat, J. D., et al. (2019a). Serum metabolic profiling using small molecular water-soluble metabolites in

individuals with schizophrenia: a longitudinal study using a pre–post-treatment design. *Psychiatry Clin. Neurosci.* 73 (3), 100–108. doi:10.1111/pcn.12779

Cao, B., Wang, D., Pan, Z., Brietzke, E., McIntyre, R. S., Musial, N., et al. (2019b). Characterizing acyl-carnitine biosignatures for schizophrenia: a longitudinal pre- and post-treatment study. *Transl. Psychiatry* 9 (1), 19. doi:10.1038/s41398-018-0353-x

Cao, B., Wang, D., Pan, Z., McIntyre, R. S., Brietzke, E., Subramanieapillai, M., et al. (2020). Metabolic profiling for water-soluble metabolites in patients with schizophrenia and healthy controls in a Chinese population: a case-control study. *World J. Biol. Psychiatry* 21 (5), 357–367. doi:10.1080/15622975.2019.1615639

Ciacci, C., Peluso, G., Iannoni, E., Siniscalchi, M., Iovino, P., Rispo, A., et al. (2007). L-carnitine in the treatment of fatigue in adult celiac disease patients: a pilot study. *Dig. Liver Dis.* 39 (10), 922–928. doi:10.1016/j.dld.2007.06.013

Ciavardelli, D., Piras, F., Consalvo, A., Rossi, C., Zucchelli, M., Di Ilio, C., et al. (2016). Medium-chain plasma acylcarnitines, ketone levels, cognition, and gray matter volumes in healthy elderly, mildly cognitively impaired, or Alzheimer's disease subjects. *Neurobiol. Aging* 43, 1–12. doi:10.1016/j.neurobiolaging.2016.03.005

Clay, H. B., Sillivan, S., and Konradi, C. (2011). Mitochondrial dysfunction and pathology in bipolar disorder and schizophrenia. *Int. J. Dev. Neurosci.* 29 (3), 311–324. doi:10.1016/j.ijdevneu.2010.08.007

Cuturic, M., Abramson, R. K., Breen, R. J., Edwards, A. C., and Levy, E. E. (2016). Comparison of serum carnitine levels and clinical correlates between outpatients and acutely hospitalised individuals with bipolar disorder and schizophrenia: a cross-sectional study. *World J. Biol. Psychiatry* 17 (6), 475–479. doi:10.1080/15622975.2016.1178803

Fett, A. K., Viechtbauer, W., Dominguez, M. D., Penn, D. L., van Os, J., and Krabbendam, L. (2011). The relationship between neurocognition and social cognition with functional outcomes in schizophrenia: a meta-analysis. *Neurosci. Biobehav Rev.* 35 (3), 573–588. doi:10.1016/j.neubiorev.2010.07.001

Fiandaca, M. S., Zhong, X., Cheema, A. K., Orquiza, M. H., Chidambaram, S., Tan, M. T., et al. (2015). Plasma 24-metabolite panel predicts preclinical transition to clinical stages of alzheimer's disease. *Front. Neurol.* 6, 237. doi:10.3389/fneur.2015.00237

Flanagan, J. L., Simmons, P. A., Vehige, J., Willcox, M. D., and Garrett, Q. (2010). Role of carnitine in disease. *Nutr. Metab. (Lond)* 7, 30. doi:10.1186/1743-7075-7-30

Green, M. F., Kern, R. S., Braff, D. L., and Mintz, J. (2000). Neurocognitive deficits and functional outcome in schizophrenia: are we measuring the "right stuff. *Schizophr. Bull.* 26 (1), 119–136. doi:10.1093/oxfordjournals.schbul.a033430

Green, M. F., and Nuechterlein, K. H. (1999). Should schizophrenia be treated as a neurocognitive disorder? *Schizophr. Bull.* 25 (2), 309–319. doi:10.1093/oxfordjournals.schbul.a033380

Green, R., Lord, J., Xu, J., Maddock, J., Kim, M., Dobson, R., et al. (2022). Metabolic correlates of late midlife cognitive outcomes: findings from the 1946 British birth cohort. *Brain Commun.* 4 (1), fcab291. doi:10.1093/braincomms/fcab291

Häfner, H., Riecher-Rössler, A., Hambrecht, M., Maurer, K., Meissner, S., Schmidtke, A., et al. (1992). Iraos: an instrument for the assessment of onset and early course of schizophrenia. *Schizophr. Res.* 6 (3), 209–223. doi:10.1016/0920-9964(92)90004-o

Harvey, P. D., and Isner, E. C. (2020). Cognition, social cognition, and functional capacity in early-onset schizophrenia. *Child. Adolesc. Psychiatr. Clin. N. Am.* 29 (1), 171–182. doi:10.1016/j.chc.2019.08.008

Jiang, T., Zhang, Y., Bai, M., Li, P., Wang, W., Chen, M., et al. (2019). Up-regulation of hepatic fatty acid transporters and inhibition/down-regulation of hepatic OCTN2 contribute to olanzapine-induced liver steatosis. *Toxicol. Lett.* 316, 183–193. doi:10.1016/j.toxlet.2019.08.013

Jones, L. L., McDonald, D. A., and Borum, P. R. (2010). Acylcarnitines: role in brain. *Prog. Lipid Res.* 49 (1), 61–75. doi:10.1016/j.plipres.2009.08.004

Kang, M., Yoo, H. J., Kim, M., Kim, M., and Lee, J. H. (2018). Metabolomics identifies increases in the acylcarnitine profiles in the plasma of overweight subjects in response to mild weight loss: a randomized, controlled design study. *Lipids Health Dis.* 17 (1), 237. doi:10.1186/s12944-018-0887-1

Kay, S. R., Fiszbein, A., and Opler, L. A. (1987). The positive and negative syndrome scale (PANSS) for schizophrenia. *Schizophr. Bull.* 13 (2), 261–276. doi:10.1093/schbul/13.2.261

Keefe, R. S., Bilder, R. M., Davis, S. M., Harvey, P. D., Palmer, B. W., Gold, J. M., et al. (2007). Neurocognitive effects of antipsychotic medications in patients with chronic schizophrenia in the CATIE Trial. *Arch. Gen. Psychiatry* 64 (6), 633–647. doi:10.1001/archpsyc.64.6.633

Kępka, A., Ochocińska, A., Chojnowska, S., Borzym-Kluczyk, M., Skorupa, E., Knaś, M., et al. (2021). Potential role of L-carnitine in autism spectrum disorder. *J. Clin. Med.* 10 (6), 1202. doi:10.3390/jcm10061202

Kiykim, E., Aktuğlu Zeybek, A., Barut, K., Zübarioğlu, T., Cansever, M., Alsancak, Ş., et al. (2016). Screening of free carnitine and acylcarnitine status in children with familial mediterranean fever. *Arch. Rheumatol.* 31 (2), 133–138. doi:10.5606/ArchRheumatol.2016.5696

Kriisa, K., Leppik, L., Balõtšev, R., Ottas, A., Soomets, U., Koido, K., et al. (2017). Profiling of acylcarnitines in first episode psychosis before and after antipsychotic treatment. *J. Proteome Res.* 16 (10), 3558–3566. doi:10.1021/acs.jproteome.7b00279

Lheureux, P. E., and Hantson, P. (2009). Carnitine in the treatment of valproic acid-induced toxicity. *Clin. Toxicol. (Phila)* 47 (2), 101–111. doi:10.1080/15563650902752376

Lieberman, J. A., Phillips, M., Gu, H., Stroup, S., Zhang, P., Kong, L., et al. (2003). Atypical and conventional antipsychotic drugs in treatment-naive first-episode schizophrenia: a 52-week randomized trial of clozapine vs chlorpromazine. *Neuropsychopharmacology* 28 (5), 995–1003. doi:10.1038/sj.npp.1300157

Liu J H, J. H., Chen, N., Guo, Y. H., Guan, X. N., Wang, J., Wang, D., et al. (2021). Metabolomics-based understanding of the olanzapine-induced weight gain in female first-episode drug-naïve patients with schizophrenia. *J. Psychiatr. Res.* 140, 409–415. doi:10.1016/j.jpsychires.2021.06.001

Liu J, J., Xiu, M., Liu, H., Wang, J., and Li, X. (2021). Plasma lysophosphatidylcholine and lysophosphatidylethanolamine levels were associated with the therapeutic response to olanzapine in female antipsychotics-naïve first-episode patients with schizophrenia. *Front. Pharmacol.* 12, 735196. doi:10.3389/fphar.2021.735196

Ljubin, T., Zakić Milas, D., Mimica, N., Folnegović-Smalc, V., and Makarić, G. (2000). A preliminary study of the comparative effects of olanzapine and fluphenazine on cognition in schizophrenic patients. *Hum. Psychopharmacol.* 15 (7), 513–519. doi:10.1002/1099-1077(200010)15:7<513:AID-HUP213>3.0.CO;2-Y

Mitchell, S. L., Uppal, K., Williamson, S. M., Liu, K., Burgess, L. G., Tran, V., et al. (2018). The carnitine shuttle pathway is altered in patients with neovascular age-related macular degeneration. *Invest. Ophthalmol. Vis. Sci.* 59 (12), 4978–4985. doi:10.1167/iovs.18-25137

Moghaddas, A., and Dashti-Khavidaki, S. (2016). Potential protective effects of l-carnitine against neuromuscular ischemia-reperfusion injury: from experimental data to potential clinical applications. *Clin. Nutr.* 35 (4), 783–790. doi:10.1016/j.clnu.2015.07.001

Molina, J. D., Avila, S., Rubio, G., and López-Muñoz, F. (2021). Metabolomic connections between schizophrenia, antipsychotic drugs and metabolic syndrome: a variety of players. *Curr. Pharm. Des.* 27, 4049–4061. doi:10.2174/1381612827666210804110139

Noland, R. C., Koves, T. R., Seiler, S. E., Lum, H., Lust, R. M., Ilkayeva, O., et al. (2009). Carnitine insufficiency caused by aging and overnutrition compromises mitochondrial performance and metabolic control. *J. Biol. Chem.* 284 (34), 22840–22852. doi:10.1074/jbc.M109.032888

Pennisi, M., Lanza, G., Cantone, M., D'Amico, E., Fisicaro, F., Puglisi, V., et al. (2020). Acetyl-L-carnitine in dementia and other cognitive disorders: a critical update. *Nutrients* 12 (5), 1389. doi:10.3390/nu12051389

Phillips, M. R., and Liu, X. H. (2011). *Translated and adapted Chinese version of structured clinical interview for DSM-IV-TR Axis I disorders, research version, patient edition (SCID-I/P) byby Michael B. First, Robert L. Spitzer, Miriam Gibbon, and Janet B.W. Williams.*

Rajasekaran, A., Venkatasubramanian, G., Berk, M., and Debnath, M. (2015). Mitochondrial dysfunction in schizophrenia: pathways, mechanisms and implications. *Neurosci. Biobehav Rev.* 48, 10–21. doi:10.1016/j.neubiorev.2014.11.005

Randolph, C., Tierney, M. C., Mohr, E., and Chase, T. N. (1998). The repeatable Battery for the assessment of neuropsychological status (RBANS): preliminary clinical validity. *J. Clin. Exp. Neuropsychol.* 20 (3), 310–319. doi:10.1076/jcen.20.3.310.823

Rund, B. R. (1998). A review of longitudinal studies of cognitive functions in schizophrenia patients. *Schizophr. Bull.* 24 (3), 425–435. doi:10.1093/oxfordjournals.schbul.a033337

Sergi, M. J., Green, M. F., Widmark, C., Reist, C., Erhart, S., Braff, D. L., et al. (2007). Social cognition and neurocognition: effects of risperidone, olanzapine, and haloperidol. *Am. J. Psychiatry* 164 (10), 1585–1592. doi:10.1176/appi.ajp.2007.06091515

Sharma, S., and Black, S. M. (2009). Carnitine homeostasis, mitochondrial function, and cardiovascular disease. *Drug Discov. Today Dis. Mech.* 6 (1-4), e31–e39. doi:10.1016/j.ddmec.2009.02.001

Signorelli, S. S., Fatuzzo, P., Rapisarda, F., Neri, S., Ferrante, M., Oliveri Conti, G., et al. (2006). A randomised, controlled clinical trial evaluating changes in therapeutic efficacy and oxidative parameters after treatment with propionyl L-carnitine in patients with peripheral arterial disease requiring haemodialysis. *Drugs Aging* 23 (3), 263–270. doi:10.2165/00002512-200623030-00008

Siliprandi, N., Di Lisa, F., and Menabó, R. (1990). Clinical use of carnitine. Past, present and future. *Adv. Exp. Med. Biol.* 272, 175–181. doi:10.1007/978-1-4684-5826-8_11

Spagnoli, A., Lucca, U., Menasce, G., Bandera, L., Cizza, G., Forloni, G., et al. (1991). Long-term acetyl-L-carnitine treatment in Alzheimer's disease. *Neurology* 41 (11), 1726–1732. doi:10.1212/wnl.41.11.1726

Su, X., Qiao, L., Liu, Q., Shang, Y., Guan, X., Xiu, M., et al. (2021). Genetic polymorphisms of BDNF on cognitive functions in drug-naive first episode patients with schizophrenia. *Sci. Rep.* 11 (1), 20057. doi:10.1038/s41598-021-99510-7

Traina, G. (2016). The neurobiology of acetyl-L-carnitine. *Front. Biosci. (Landmark Ed.* 21, 1314–1329. doi:10.2741/4459

Wang, S. M., Han, C., Lee, S. J., Patkar, A. A., Masand, P. S., and Pae, C. U. (2014). A review of current evidence for acetyl-l-carnitine in the treatment of depression. *J. Psychiatr. Res.* 53, 30–37. doi:10.1016/j.jpsychires.2014.02.005

Wang, Z., Zhou, Z., Wei, X., Wang, M., Wang, B. O., Zhang, Y., et al. (2017). Therapeutic potential of novel twin compounds containing tetramethylpyrazine and carnitine substructures in experimental ischemic stroke. *Oxid. Med. Cell Longev.* 2017, 7191856. doi:10.1155/2017/7191856

Wesnes, K. A., and Reynolds, J. (2019). The effects on the cognitive function of healthy volunteers of a combination of acetyl-L-carnitine, vinpocetine and huperzine A administered over 28 days. *Int. J. Neurology Neurother.* 6. doi:10.23937/2378-3001/1410089

Wu, Z. W., Shi, H., Chen, D. C., Chen, S., Xiu, M. H., and Zhang, X. Y. (2020). BDNF serum levels and cognitive improvement in drug-naive first episode patients with schizophrenia: a prospective 12-week longitudinal study. *Psychoneuroendocrinology* 122, 104879. doi:10.1016/j.psyneuen.2020.104879

Xiu, M. H., Lang, X., Chen, D. C., Cao, B., Kosten, T. R., Cho, R. Y., et al. (2021). Cognitive deficits and clinical symptoms with hippocampal subfields in first-episode and never-treated patients with schizophrenia. *Cereb. Cortex* 31 (1), 89–96. doi:10.1093/cercor/bhaa208

Xiu, M. H., Li, Z., Chen, D. C., Chen, S., Curbo, M. E., Wu, H. E., et al. (2020). Interrelationships between BDNF, superoxide dismutase, and cognitive impairment in drug-naive first-episode patients with schizophrenia. *Schizophr. Bull.* 46, 1498–1510. doi:10.1093/schbul/sbaa062

Xiu, M. H., Wang, D. M., Du, X. D., Chen, N., Tan, S. P., Tan, Y. L., et al. (2019). Interaction of BDNF and cytokines in executive dysfunction in patients with chronic schizophrenia. *Psychoneuroendocrinology* 108, 110–117. doi:10.1016/j.psyneuen.2019.06.006

Yi, W., Sylvester, E., Lian, J., and Deng, C. (2021). Kidney plays an important role in ketogenesis induced by risperidone and voluntary exercise in juvenile female rats. *Psychiatry Res.* 305, 114196. doi:10.1016/j.psychres.2021.114196

Zhu, M. H., Liu, Z. J., Hu, Q. Y., Yang, J. Y., Jin, Y., Zhu, N., et al. (2022). Amisulpride augmentation therapy improves cognitive performance and psychopathology in clozapine-resistant treatment-refractory schizophrenia: a 12-week randomized, double-blind, placebo-controlled trial. *Mil. Med. Res.* 9 (1), 59. doi:10.1186/s40779-022-00420-0

frontiers | Frontiers in Pharmacology

TYPE Original Research
PUBLISHED 21 September 2023
DOI 10.3389/fphar.2023.1257617

OPEN ACCESS

EDITED BY
Song Zhang,
Shanghai Jiao Tong University, China

REVIEWED BY
Dalinda Isabel Sánchez-Vidaña,
Hong Kong Polytechnic University, Hong Kong SAR, China
Opeyemi Iwaloye,
Federal University of Technology, Nigeria

*CORRESPONDENCE
Jianxiang Li,
ljx029504@njucm.edu.cn
Weifeng Guo,
gwfwfg2003@njucm.edu.cn

†These authors have contributed equally to this work and shared the first authorship

RECEIVED 12 July 2023
ACCEPTED 05 September 2023
PUBLISHED 21 September 2023

CITATION
Zhao Y, Xu D, Wang J, Zhou D, Liu A, Sun Y, Yuan Y, Li J and Guo W (2023), The pharmacological mechanism of chaihu-jia-longgu-muli-tang for treating depression: integrated meta-analysis and network pharmacology analysis. *Front. Pharmacol.* 14:1257617. doi: 10.3389/fphar.2023.1257617

The pharmacological mechanism of chaihu-jia-longgu-muli-tang for treating depression: integrated meta-analysis and network pharmacology analysis

Yang Zhao[1†], Dan Xu[2,3†], Jing Wang[4], Dandan Zhou[1], Anlan Liu[1], Yingying Sun[1], Yuan Yuan[1], Jianxiang Li[5*] and Weifeng Guo[1*]

[1]First Clinical Medical College, Nanjing University of Chinese Medicine, Nanjing, China, [2]Taicang TCM Hospital Affiliated to Nanjing University of Chinese Medicine, Taicang, China, [3]Taicang Hospital of Traditional Chinese Medicine, Taicang, China, [4]Department of Respiratory and Critical Care Medicine, Jiangsu Province Hospital of Chinese Medicine, Affiliated Hospital of Nanjing University of Chinese Medicine, Nanjing, China, [5]School of Chinese Medicine School of Integrated Chinese and Western Medicine, Nanjing University of Chinese Medicine, Nanjing, China

Aim: Chaihu-jia-Longgu-Muli-tang (CLM) is derived from "Shang Han Lun" and is traditionally prescribed for treating depression. However, there is still a lack of evidence for its antidepressant effects, and the underlying mechanism is also unclear. This study aimed to assess clinical evidence on the efficacy of CLM in patients with depression using a meta-analysis and to explore its underlying antidepressant molecular mechanisms via network pharmacology.

Methods: Eight open databases were searched for randomized controlled trials (RCTs) comparing the effects of CLM alone or combined with serotonin-norepinephrine reuptake inhibitors (SNRIs) and selective serotonin reuptake inhibitors (SSRIs) in patients with depression, evaluating the total effective rate of the treatment group (CLM alone or combined with SSRIs/SNRIs) and the control group (SNRIs or SSRIs), and comparing changes in depression scale, anxiety scale, sleep scale, inflammation indicators and adverse effects. Subsequently, the active ingredients and target genes of CLM were screened through six databases. Then Gene Ontology (GO) and Kyoto Encyclopedia of Genes and Genomes (KEGG) analysis and protein-protein interaction (PPI) network and topology analysis were performed. Finally, Molecular docking was applied to evaluate the binding affinity between components and predicted targets.

Results: Twenty-four RCTs with a total of 2,382 patients were included. For the efficacy of antidepression and adverse effects, whether CLM alone or in combination with SSRIs/SNRIs, the treatment group has no inferior to that of the control group. Additionally, the intervention of CLM + SSRI significantly improved the symptoms of anxiety and insomnia, and reduced serum IL-6 and TNF-α levels. For network pharmacology, a total of 129 compounds and 416 intersection targets in CLM were retrieved. The interaction pathway between CLM and depression is mainly enriched in PI3K-Akt, JAK-STAT, and NF-κB signaling pathway, PIK3R1, MAPK3, and AKT1 may be the potential targets of Stigmasterol, β-stiosterol, coumestrol.

Conclusion: Compared to SSRIs/SNRIs alone, CLM is more effective and safe in treating depression. It not only significantly alleviates depressive mood, but

improves symptoms such as anxiety and insomnia, with fewer side effects, especially in combination with SSRI. Its antidepressant mechanism may be correlated with the regulation of the PI3K/Akt signaling pathway and inhibiting inflammatory response.

KEYWORDS

depression, chaihu-jia-longgu-muli-tang, meta-analysis, network pharmacology, inflammation

1 Introduction

Depression is a debilitating neuropsychological disorder that impairs daily functioning and is characterized by a constant sense of melancholy, loss of interest, and intellectual disability. Globally, major depression disorder (MDD) and dysthymia are responsible for approximately 46.9 million disabilities annually, with over 800,000 suicidal deaths mostly accompanied by neurological and psychiatric disorders such as MDD (Li et al., 2022a; Moitra et al., 2022). The number of patients with depression reached 542 million in 2015, with an 18.4% global increase between 2005 and 2015 (Disease and Prevalence, 2016). Due to the effects of coronavirus disease 2019, the number of patients with depression worldwide increased by 27.6% and depression is estimated to become the leading cause of death by 2030 (COVID-19 Mental Disorders Collaborators, 2021). Therefore, discovering efficient and safe treatment modalities is currently highly needed. There are three main interventions for treating depression that are currently used: 1) pharmaceutical antidepressants, such as SNRIs and SSRIs, among others; 2) research-based psychotherapy, such as cognitive behavioral therapy and interpersonal psychotherapy; and 3) physical therapy, such as vagus nerve stimulation or repeated transcranial magnetic stimulation. However, about one-third of patients still do not achieve remission after four consecutive antidepressant trials, and at least 50%–80% of patients still exist recurrence, with a progressive increase in severity and frequency, this mainly attributed to increased resistance in depression (Borbely et al., 2022). Furthermore, patients' resistance to antidepressants is often accompanied by high levels of serum inflammatory factors such as interleukin-6 (IL-6) and tumor necrosis factor-α (TNF-α) (Beurel et al., 2020). Heightened inflammation can also exacerbate mood disorders such as anxiety and anhedonia, as well as somatic symptoms such as insomnia and gastrointestinal disorders (Kiecolt-Glaser et al., 2015). Thus, it is still necessary to find or develop antidepressant treatments with high-efficiency and fewer side effects.

Traditional Chinese Medicine (TCM) operates on the understanding that the human body is an organic whole, and the viscera coordinate with each other in function and influence each other in pathology (Xiang-yu et al., 2021). The pathogenesis of depression as viewed in TCM is a disorder of the Shao Yang pivot and dysfunction of Yin and Yang. Shao Yang is the pivot for the rise and fall of the Qi movement; Shao Yang dysfunction leads to depression and insomnia. When the Shao Yang channel restrains the Qi, the body will feel cold and physically heavy and patients will show appetite loss (Hanying et al., 2022). CLM is a TCM prescription derived from "Shang Han Lun" that is prescribed to treat mental diseases caused by the imbalance of the pivot of Shao Yang and the loss of Yin and Yang. It has the effects of mediating the Shao Yang pivot and tranquilizing the mind (Wan et al., 2021). Numerous studies have shown that CLM contributes to improvements in dementia, insomnia, anxiety, and depression (Yuanwen et al., 2022). Although the efficacy and safety of CLM for the treatment of depression have been evaluated in many studies, determining a reliable basis for evidence-based medicine is difficult due to deviations in the included studies, literature updates, and inconsistencies in patient grouping and comorbidities (Li et al., 2018; Wan et al., 2021). The potential mechanism behind CLM's antidepressant effect may be related to the inhibition of N-methyl-D-aspartate (NMDA) receptors to increase hippocampal synaptic plasticity, positively regulation of neuronal apoptosis, and inhibition of neuroinflammation (Liu et al., 2010; Wang et al., 2018; Lizhi et al., 2021). However, owing to the intricacy of the compound constituents, particularly the molecular target mechanisms of its active substances, the mechanisms associated with its antidepressant effect remain unclear. As a novel discipline, network pharmacology can effectively and systematically explore correlations between traditional Chinese medicine substances, targets, and diseases by constructing a variety of network models comprehensively using multiple platforms and technologies to help explore potential mechanisms (Chen et al., 2018).

Based on the above background, CLM has a wide range of antidepressant efficacy, but with still a lack of clinical evidence, and its antidepressant mechanism is still unclear due to the complexity of TCM compound ingredients. Therefore, this study aimed to assess clinical evidence on the efficacy of CLM in patients with depression using a meta-analysis and to explore its underlying antidepressant molecular mechanisms via network pharmacology.

2 Materials and methods

2.1 Meta-analysis

2.1.1 Data sources and searches

Clinical trials were searched in the PubMed, Web of Science, MEDLINE, Cochrane Library, China National Knowledge Internet, VIP, Wanfang, and SinoMed databases from the inception of each database until December 2022. This meta-analysis complied with the Preferred Reporting Items for Systematic Reviews and Meta-Analyses (Page et al., 2021) (protocol shown in Figure 1). The search strategy is shown in Supplementary Table S1.

2.1.2 Inclusion and exclusion criteria

Due to the limited exact treatment methods for depression at present, physical therapy has the disadvantage of

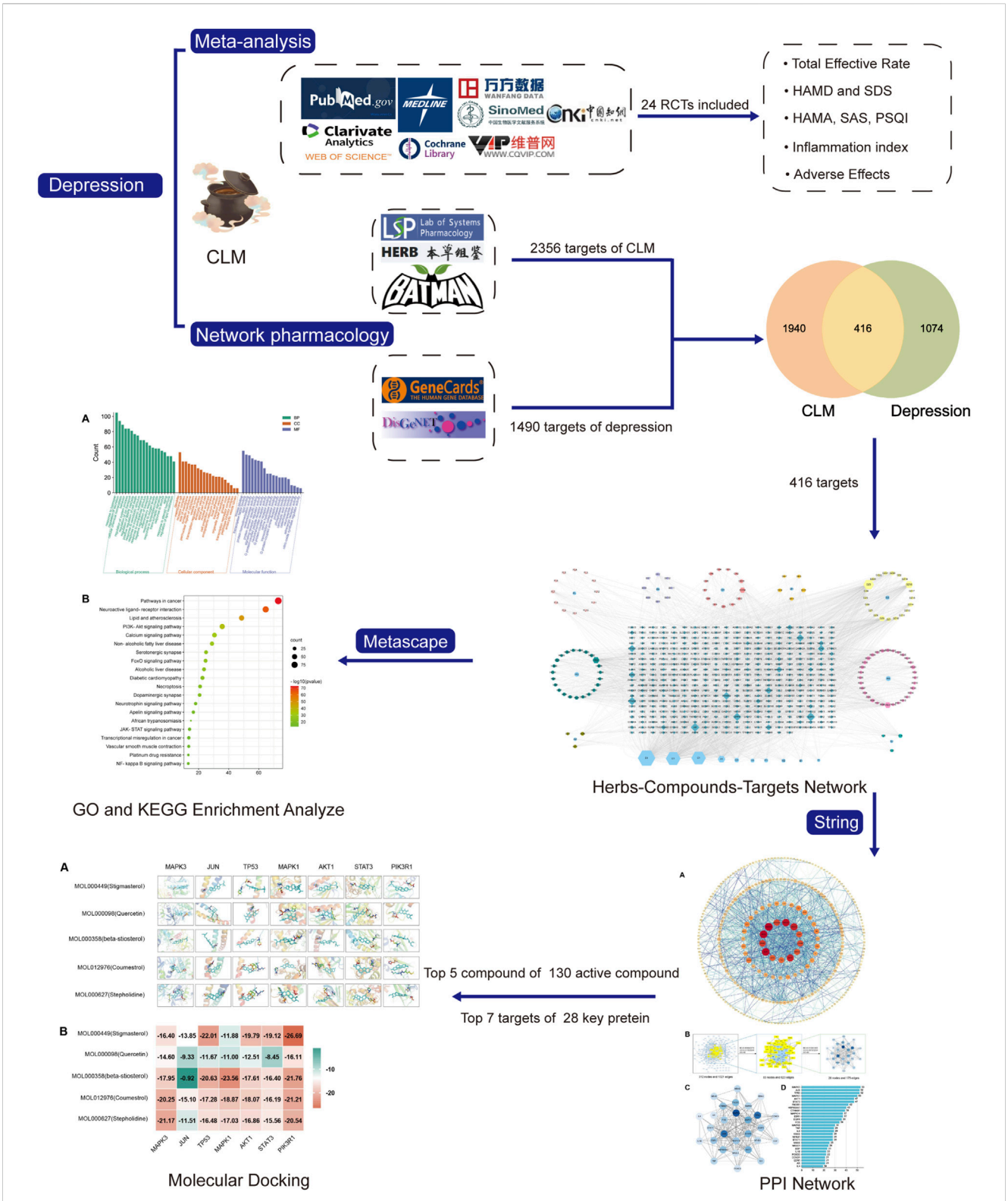

FIGURE 1
Flow chart of the investigation of CLM in the treatment of depression.

large side effects and poor compliance (e.g., repeated transcranial magnetic stimulation), and uneven efficacy (e.g., Acupuncture, massage, music, etc.). Although mainstream antidepressants (e.g., SSRIs and SNRIs) have exact therapeutic effects and are widely accepted, there are still some limitations we mentioned above, so we have made the following provisions in the inclusion and exclusion criteria.

The inclusion criteria were as follows: 1) randomized controlled trials retrieval was limited to published in Chinese and English; 2) studies including participants clearly diagnosed with major depression disorder according to the Chinese Classification of Mental Disorders Third Edition (CCMD-3) or the Diagnostic and Statistical Manual of Mental Disorders (DSM-IV) (Regier et al., 2013); 3) Studies including at least one depression related outcome indicator such as Hamilton Anxiety Rating Scale (HAMD) or Self-rating Depression Scale (SDS); 4)the treatment group received CLM or a combination of CLM and SSRIs or SNRIs, the control group treated SSRIs/SNRIs alone. In addition, the intervention of CLM was added or subtracted according to syndrome differentiation, and the botanical drugs mainly including Radix Bupleuri [Chai Hu], Fossilia Ossia Mastodi [Longgu], Radix Scutellariae [Huang Qin], Zingiber rhizoma [Shengjiang], Ginseng radix [Renshen], Cinnamomi cortex [Guizhi], Hoelen [Fuling], Pinelliae Tuber [Banxia], Radix et Rhizoma Rhei [Dahuang], Ostreae Testa [Muli], and Zizyphi fructus [Dazao]. The composition of CLM is shown in Supplementary Table S2.

The exclusion criteria were as follows: 1) incomplete data; 2) inclusion of drug-induced secondary depression, somatic or psychiatric disease-induced secondary depression, *postpartum* depression, or menopausal depression; 3) other comorbid conditions, 4) interventions combining other traditional Chinese medicine formulas or physical therapy (e.g., acupuncture, massage, music, etc.).

2.1.3 Data extraction and quality assessment

The search terms and their common synonyms in each database were as follows: "Depression OR Depressive" AND "chaihu jia longgu muli decoction OR CLM." All retrieved studies were imported into Endnote20 software for screening and eliminating duplicates according to abstracts. Two researchers (YS. and YY.) extracted the information trial characteristics (study, sample size, gender, average age, interventions, duration, average course, and outcomes (Total Effective Rate, HAMD, Hamilton Anxiety Rating Scale (HAMA), Self-rating Anxiety Scale (SAS), SDS, Pittsburgh Sleep Quality Index (PSQI), Adverse effects and serum inflammatory factors: TNF-α and IL-6). Two assessors (JW and DZ.) independently evaluated study quality and risk of bias and extracted data using the Cochrane Collaboration Assessment Tool. Discrepancies between the assessors were resolved by a third assessor.

2.1.4 Data analysis

STATA software (v16.0) to analyze this meta-analysis. For continuous outcomes (change in HAMD, SDS, HAMA, SAS, TNF-α, IL-6) and dichotomous outcomes (Total Effective Rate and Adverse Effects), the standardized mean difference (SMD) and risk ratios (RR) were represented, respectively. The 95% confidence interval (CI) was used to analyze the effects of secondary variables. When heterogeneity was high (I^2 > 50% or p < 0.05), a random effects model was used; otherwise, a fixed effects model was used. The subgroup analysis was based on the type of treatment group which included CLM + SSRI (CLM + SSRI vs. SSRI), CLM + SNRI (CLM + SNRI vs SNRI), and CLM (CLM vs. SSRI). Egger's test and funnel plots were used to assess publication bias.

2.2 Network pharmacology

2.2.1 Screening for compounds and corresponding targets of CLM

According to the 11 Chinese herbs included in CLM as recorded in the "Shang Han Lun", the compounds and corresponding targets of each drug were screened from three databases TCMSP (https://tcmspw.com/tcmsp.php) (Zeng et al., 2022), the HERB database (http://herb.ac.cn/) (Fang et al., 2021), and the BATMAN-TCM database (http://bionet.ncpsb.org/batman-tcm/; score ≥20, p-value ≤0.05) (Gao et al., 2021). Subsequently, all screened ingredients were imported into the TCMSP for normalization according to ADME (absorption, distribution, metabolism, excretion) criteria. In addition, oral bioavailability ≥30% and drug-likeness ≥0.18 as the most commonly used pharmacokinetic parameters to measure drug properties.

2.2.2 Target prediction for depression

The keyword "depression" was searched to obtain potential targets related to depression from the GeneCards (Stelzer et al., 2016) and DisGeNET (Pinero et al., 2017) databases. To forecast CLM's therapeutic targets for treating depression, the common targets of compounds and depression were sorted out, and a Venn diagram was obtained using the Venn 2.1.0 platform (Heberle et al., 2015). The intersection targets were entered into Cytoscape software (v 3.8.2) to construct Herb-Compound-Target (H-C-T) networks.

2.2.3 Gene ontology and kyoto encyclopedia of genes and genomes enrichment analyses

For KEGG and GO enrichment analyses, we uploaded intersection targets into the Metascape platform (http://metascape.org/*Homo sapiens*, p < 0.05, and p-values were corrected by the Benjamini–Hochberg procedure) (Zhou et al., 2019).

2.2.4 Construction of protein-protein interaction network and topological analysis

To further evaluate the core of regulatory targets in the treatment of depression and discover potential connections, intersection targets were uploaded to the STRING database (*H. sapiens*, minimum required interaction score: 0.9) to construct a PPI network (Szklarczyk et al., 2019). Subsequently, to evaluate the topological characteristics of the nodes, the three parameters of "betweenness centrality" (BC), "closeness centrality" (CC), and "degree centrality" (DC) were computed.

2.2.5 Molecular docking verification

To assess the binding affinity of components with predicted targets, the active components of CLM were docked with core targets. The selection of active ingredients and core targets were as follows: 1) the degree values of H-C-T and PPI; 2) the correlation of enriched signal pathways according to GO and KEGG analysis. First, the core targets' three-dimensional structure "PDB" files were retrieved from the PDB database (O'Boyle et al., 2011). Autodock Tools (v1.5.7) was used to

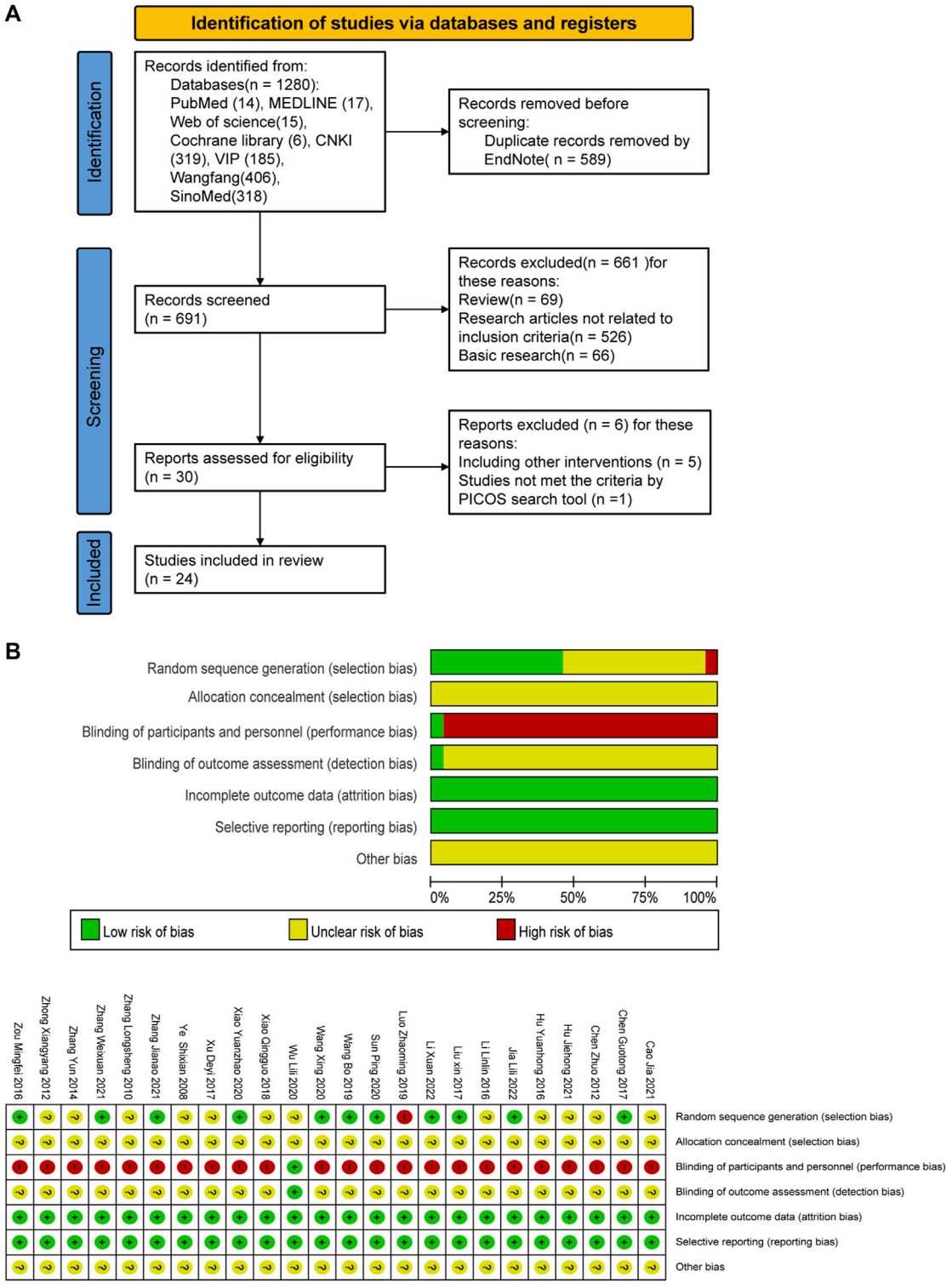

FIGURE 2
PRISMA flow diagram and risk-of-bias assessment; **(A)** literature screening process; **(B)** risk-of-bias summary.

remove the water molecules, original ligands, add hydrogens, calculate Gasteiger partial charges, and set atom types. The "SDF" format of the CLM bioactive component was obtained from the PubChem database (https://www.rcsb.org/), and the torsion angles in the ligand were identified, the solvent model was added, and the Kollman atomic charges were assigned to the protein using Autogrid4 and Autodock4. The "Local Search Parameters" algorithm was used for the docking operation. Finally, we constructed the docking interaction pattern diagram and displayed the docking findings via PyMoL (v2.4.0).

TABLE 1 Basic characteristics of included studies

Study	Sample (T/C)	Male/female	Average age/years (T/C)	Interventions		Duration/weeks	Average course/years (T/C)	Outcomes measures
				T	C			
Jia and Li (2022)	51/51	55/47	40.12 ± 6.32/41.73 ± 6.79	CLM + SSRI	SSRI	6	1.53 ± 1.16/1.81 ± 1.57	①②⑦
Li X et al. (2022)	48/48	54/42	56.45 ± 4.56/57.01 ± 4.38	CLM	SSRI	8	6.32 ± 3.24/6.41 ± 2.32	①②⑤
Zhang et al. (2021)	20/20	23/17	35.48/36.24	CLM	SSRI	4	0.86/0.89	①②⑥⑦
Cao and Guo (2021)	61/61	57/56	-	CLM	SNRI	8	-	①②⑥
Hu (2021)	49/49	37/61	36.42 ± 6.93/37.82 ± 7.56	CLM + SSRI	SSRI	8	3.16 ± 1.09/3.62 ± 0.85	②
Zhang (2021)	55/55	23/32 20/35	46.59 ± 2.91/47.26 ± 2.74	CLM + SSRI	SSRI	4	-	④⑤⑦
Wang et al. (2020)	30/28	17/41	50.2/50.6	CLM	SSRI	2	3.11/3.46	①②⑥
Xiao and Han (2020)	64/64	63/65	43.15/43.46	CLM	SSRI	4	0.14/0.14	①④⑤⑦
Wu et al. (2020)	40/40	40/40	38.96/40.41	CLM	SSRI	4	6.03/5.81	①②⑤⑦
Sun (2020)	40/40	43/37	55.21 ± 2.74/55.41 ± 2.21	CLM + SNRI	SNRI	8	0.47 ± 0.03/0.47 ± 0.02	①②④⑤⑦
Wang et al. (2019)	100/100	84/116	39.5/39.5	CLM	SSRI	8	4.94/5.13	①②⑤
Luo et al. (2019)	42/38	36/44	39.5/39.6	CLM	SSRI	8	1.0/1.0	①②⑦
Xiao et al. (2018)	40 /38	34/44	35.24/37.56	CLM	SNRI	8	2.5/2.6	①②③
Xu and Zhao (2017)	40/40	20/60	42.5/41.1	CLM	SSRI	4	2.6/2.4	①⑧⑨
Liu et al. (2017)	34/34	31/37	42.1 ± 12.7/41.7 ± 13.1	CLM + SSRI	SSRI	6	-	①②⑧⑨⑦
Chen et al. (2017)	150/150	80/70 82/68	36.29 ± 3.72/37.07 ± 3.20	CLM + SSRI	SSRI	12	2.70 ± 1.01/2.82 ± 1.02	①④⑤
Li et al. (2016)	55/55	36/74	37.4/36.8	CLM	SSRI	8	3.4/3.2	②
Zou (2016)	42/41	46/37	37.34/37.02	CLM	SSRI	8	3.67/3.61	①②⑦
Hu et al. (2016)	30/30	-	-	CLM	SSRI	6	-	①②⑤⑦
Zhang (2014)	36/36	34/32	48.7	CLM	SSRI	8	4.65 ± 2.51	①②⑤
Chen and Ding (2012)	40/40	26/54	43.15 ± 11.74/44.25 ± 12.53	CLM	SSRI	8	0.5/0.5	①
Zhong et al. (2012)	50/50	42/58	51.34 ± 5.12/53.42 ± 4.31	CLM	SSRI	8	4.21 ± 2.16/3.86 ± 1.94	①②⑤
Zhang (2010)	31/32	24/39	36/39	CLM	SSRI	6	0.25/0.3	①②④⑤⑦
Ye and Luo (2008)	50/50	47/53	36.21 ± 16.03/34.78 ± 15.87	CLM	SSRI	4	0.5/0.5	①②③⑦

Note: T: treatment group; C: control group; CLM: Chaihu-jia-Longgu-Muli-tang; ①Clinical efficacy rate; ②HAMD Scores ; ③HAMA Scores; ④SAS Scores; ⑤SDS Scores; ⑥PSQI Scores; ⑦Adverse Effects; ⑧TNF-α; ⑨IL-6.

10.3389/fphar.2023.1257617

3 Results of meta-analysis

3.1 Study screening

A total of 1280 relevant original studies were retrieved from eight databases including PubMed (14 studies), MEDLINE (17), Web of Science (15), Cochrane Library (6), China National Knowledge Internet (319), VIP (185), Wan Fang (406), and Sino Med (318). There were 589 duplicates that were eliminated. Primary screening was then performed on the remaining 691 articles, and 661 trials were removed based on the abstracts and titles. Out of the remaining 30 articles, 24 items were included in this study. (Figure 2; Table 1).

3.2 Characteristics and quality of study

Twenty-four RCTs with a total of 2,382 patients with depression were included (1195 cases in the treatment group, 1187 cases in the control group), involving five interventions, mainly including (SSRI, SNRI, CLM, CLM + SSRI, CLM + SNRI). According to the intervention in the treatment group, 13 trials on CLM + SSRI included 1337 patients, 3 trials on CLM + SNRI included 280 patients, and 8 trials on CLM alone included 765 patients. The treatment duration varies from 2 to 12 weeks.

A total of 21 trials discussed the total effective rate, of which 8 trials were for CLM alone, 10 trials were for CLM + SSRI, and 3 trials were for CLM + SNRI; 19 trials reported HAMD scores, among which 7 trials were for CLM alone, 10 trials were for CLM + SSRI, and 2 trials were for CLM + SNRI; 11 trials reported SDS scores, of which 6 trials were for CLM alone, 4 trials were for CLM + SSRI, and 1 trial was for CLM + SNRI; 2 trials reported HAMA scores, of which was for CLM and CLM + SNRI respectively; 5 trials reported SAS scores, among which 1 trial was for CLM alone, 3 trials were for CLM + SSRI, and 1 trial was for CLM + SNRI; 3 trials reported PSQI scores, all of included were for CLM + SSRI; 2 trials detected the serum levels of IL-6 and TNF-α for CLM + SSRI; and 12 trials assessed adverse effects after treatment, among which 2 trials were for CLM alone, 9 trials were for CLM + SSRI, and 1 trial were for CLM + SNRI. Additionally, Table 1 and Figure 2 show the basic characteristics of the studies and results of the risk-of-bias assessment.

3.3 Total effective rate

21 studies discussed the effective rate of CLM for treating depression. According to heterogeneity testing (p = 0.062, I^2 = 34.5%), the fixed effects model was applied. The results indicated that the effective rate of the treatment group was significantly higher than that of the control group (RR = 1.17%, 95% CI [1.13, 1.22]; Figure 3A). For the subgroup analysis, the anti-depressive effect on CLM + SSRI, CLM, and CLM + SNRI is significantly better than that of SSRI or SNRI alone (RR = 1.23%, 95% CI [1.16, 1.30], p = 0.339, I^2 = 11.3%; RR = 1.10%, 95% CI [1.04, 1.17], p = 0.241, I^2 = 23.6%; RR = 1.17%, 95% CI [1.06, 1.29], p = 0.470, I^2 = 0.0%; Figure 3A). Moreover, the funnel plot symmetry indicated no publication bias (Egger's test: p = 0.280, Figure 3B).

3.4 HAMD and self-rating depression scale scores

19 trials reported the post-treatment HAMD scores. According to heterogeneity testing (p = 0.000, I^2 = 94.7%), the random effects model was applied. Results indicated that the CLM treatment group showed more reduction in HAMD scores than the control group (SMD = −1.40%, 95% CI [−1.88, −0.92], Figure 4A). For the subgroup analysis, the CLM + SSRI, CLM, and CLM + SNRI showed significant reduction in HAMD scores comparing SSRI or SNRI alone (RR = −1.94%, 95% CI [−2.68, −1.19], p = 0.000, I^2 = 95.0%; RR = −0.54%, 95% CI [−0.101, −0.08], p = 0.000, I^2 = 88.1%; RR = −1.93%, 95% CI [−4.71, 0.86], p = 0.000, I^2 = 97.8%; Figure 4A).

Regarding SDS, 11 trials had high heterogeneity (p = 0.000, I^2 = 97.6%), and the random effects model was adopted. The results showed that the treatment group significantly improved negative emotions compared to the control group (SMD = −2.12%, 95% CI [−3, −1.23], Figure 4B). For the subgroup analysis, the CLM, CLM + SSRI, and CLM + SNRI showed significant reduction in SDS scores comparing SSRI or SNRI alone (RR = −0.56%, 95% CI [−1.08, −0.04], p = 0.000, I^2 = 88.7%; RR = −2.99%, 95% CI [−4.82, −1.17], p = 0.000, I^2 = 98.3%; RR = −2.12, 95% CI [−3.00, −1.23], p = Not applicable, I^2 = Not applicable; Figure 4B)

3.5 HAMA, self-rating anxiety scale, pittsburgh sleep quality index scores

Two trials reported HAMA scores for CLM and CLM + SNRI respectively. According to heterogeneity testing (p = 0.387, I^2 = 0.0%), the fixed effects model was applied. The HAMA scores of the group of patients receiving CLM or combined with antidepressant drugs were significantly lower than those of the control group (SMD = −0.37%, 95% CI [−0.66, −0.07], Figure 4C).

11 trials reported SAS scores. According to heterogeneity testing (p = 0.000, I^2 = 98.5%), the random effects model was performed. The SAS scores of the treatment group were significantly lower than those of the control group (SMD = −3.17%, 95% CI [−5.06, −1.28], Figure 4D). For the subgroup analysis, the CLM + SSRI, CLM + SNRI, and CLM showed marked reduction in SAS scores comparing SSRI or SNRI alone (RR = −3.76%, 95% CI [−6.70, −0.81], p = 0.000, I^2 = 99.0%; RR = −4.52%, 95% CI [−5.36, −3.69], p = Not applicable, I^2 = Not applicable; RR = −0.18%, 95% CI [−0.67, −0.32], p = Not applicable, I^2 = Not applicable; Figure 4B)

Three trials reported PSQI scores, all of included were for CLM + SSRI. According to heterogeneity testing (p = 0.930, I^2 = 0.0%), the fixed effects model was applied. The PSQI scores of the treatment group were significantly lower than those of the control group (SMD = −2.53, 95% CI [−2.89, −2.18], Figure 4E).

3.6 Inflammation index

There were 2 studies both for CLM + SSRI that assessed serum levels of TNF-α and IL-6. For TNF-α, according to heterogeneity testing (p = 0.002, I^2 = 89.6%), the random effects model was applied, which in the treatment group were significantly lower than those in the control group (SMD = −1.82%, 95% CI [−3.03, −0.61],

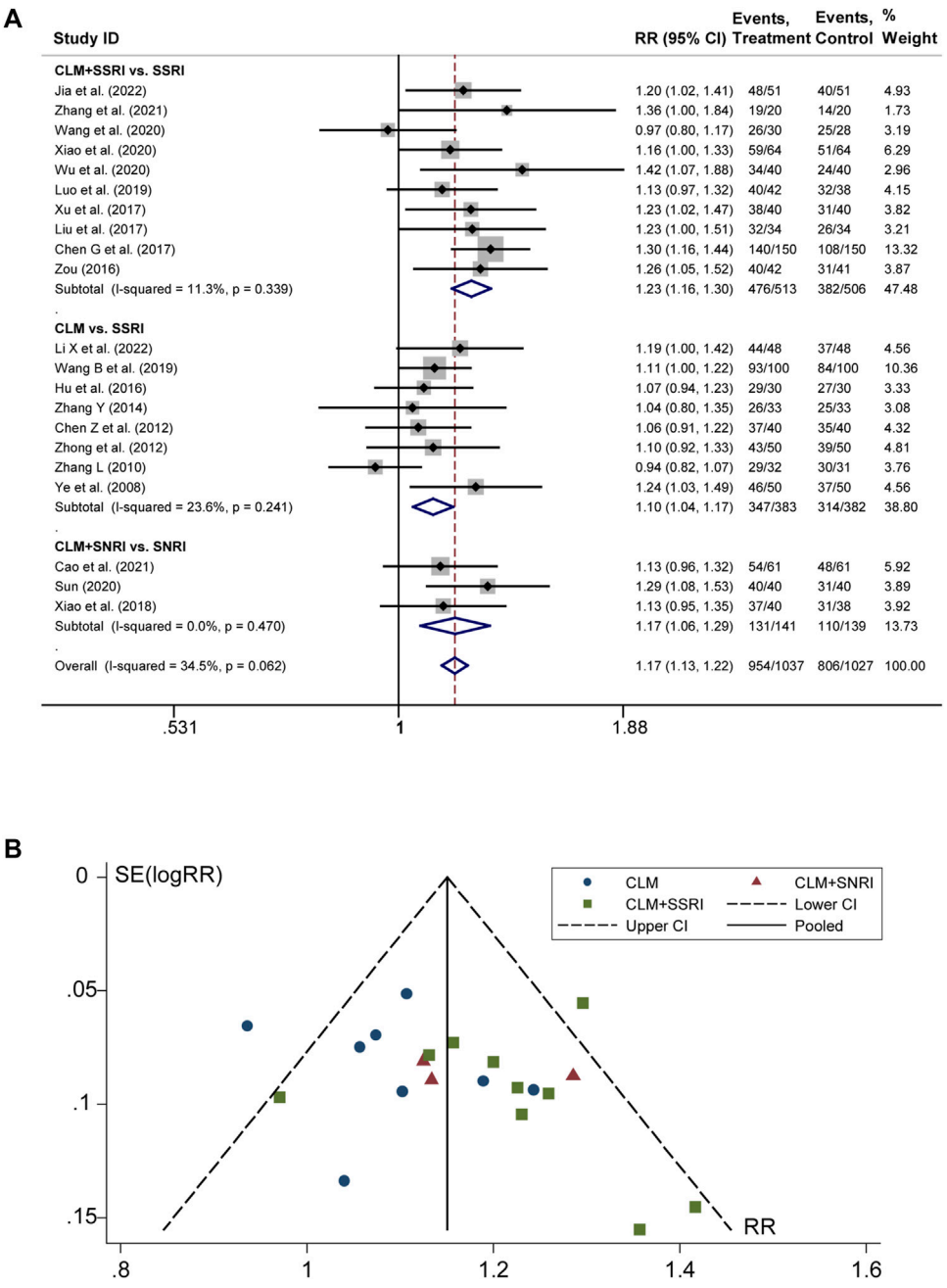

FIGURE 3
Comparative forest plots of total effective rate; **(A)** forest plot showing the total effective rate of CLM alone or anti-depressant drug therapy on depression; Treatment: CLM alone or combined with pharmaceutical anti-depressants; Control: pharmaceutical anti-depressants; **(B)** funnel plot of total effective rates.

Figure 5A). For IL-6, according to heterogeneity testing (p = 0.601, I^2 = 0.0%), the fixed effects model was applied. Compared with the control group, the treatment group showed significantly lower levels (SMD = −1.19%, 95% CI [−1.54, −0.84], Figure 5B).

3.7 Adverse effects

There were 12 trials that assessed adverse occurrences in the 24 included studies, covering neurological symptoms such as dizziness, headache, sleep disorders, hyperactivity, blurred vision, and fatigue, as well as gastrointestinal symptoms such as dry mouth, diarrhea, anorexia, nausea, vomiting, and constipation. The most common adverse reactions were dizziness, blurred vision, dry mouth, anorexia, and vomiting. According to heterogeneity testing (p = 0.250, I^2 = 13.2%), the fixed effects model was applied. The treatment group showed better safety in treating depression than the control group (RR = 0.36%, 95% CI [0.23, 0.54], Figure 6). For the subgroup analysis, CLM + SSRI and CLM alone showed fewer adverse effects compared the SSRI alone

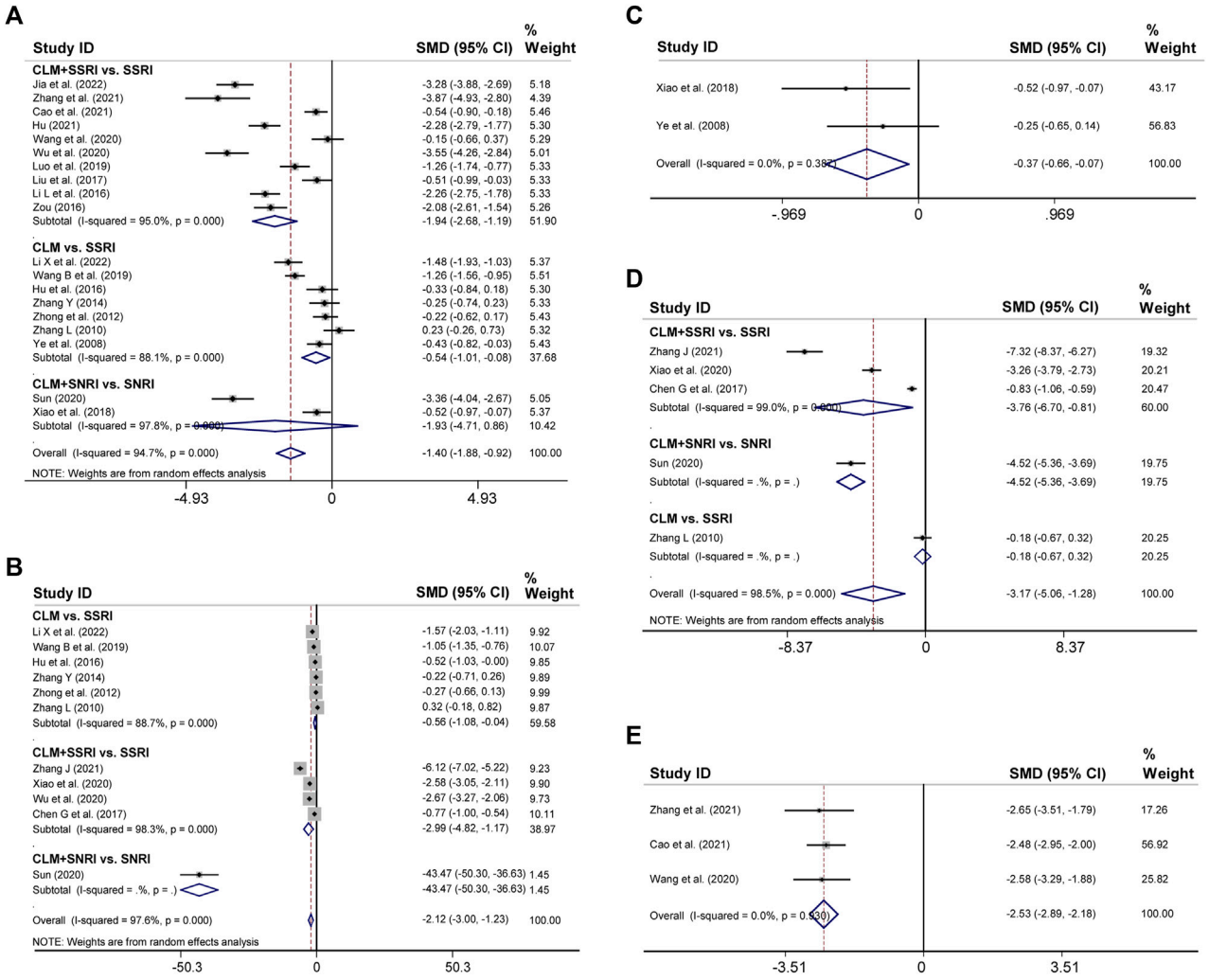

FIGURE 4
Comparative forest plots of HAMD, SDS, HAMA, SAS, and PSQI scores; **(A)** HAMD scores; **(B)** SDS scores; **(C)** HAMA scores; **(D)** SAS scores; **(E)** PSQI scores.

(RR = 0.36%, 95% CI [0.21, 0.59], Figure 6), however, there was no statistical significance between CLM + SNRI and SNRI alone.

4 Results of network pharmacology analysis

4.1 Active compounds and treatment targets of CLM

We obtained 129 active compounds from the four databases, including Radix Bupleuri (16 compounds), Radix Scutellariae (29 compounds), Pinelliae Tuber (10 compounds), Ginseng radix (35 compounds), Hoelen (12 compounds), Zingiber rhizoma (5 compounds), Zizyphi fructus (25 compounds), Radix et Rhizoma Rhei (7 compounds), and Cinnamomi cortex (7 compounds). The primary active components of CLM are listed in Supplementary Table S3.

There were 2356 targets screened from the 129 active compounds CLM using the Swiss, TCMSP, HERB, and BATMAN-TCM databases. In addition, 1490 depression-related targets were identified using the DisGeNET and GeneCards databases. The intersection of drug targets and depression targets resulted in a total of 416 CLM treatment depression targets, as shown in the Venn diagram (Figure 7A).

4.2 The construction of the H-C-T network

The H-C-T network included 555 nodes and 2480 edges and contained nine herbs, 130 compounds, and 416 genes (Figure 7B). Larger nodes have higher statistical significance. The top five compounds, as determined by degree analysis, were MOL000449 (stigmasterol), MOL000098 (quercetin), MOL000358 (β-stigmasterol), MOL012976 (coumestrol), and MOL000627 (stepholidine), with

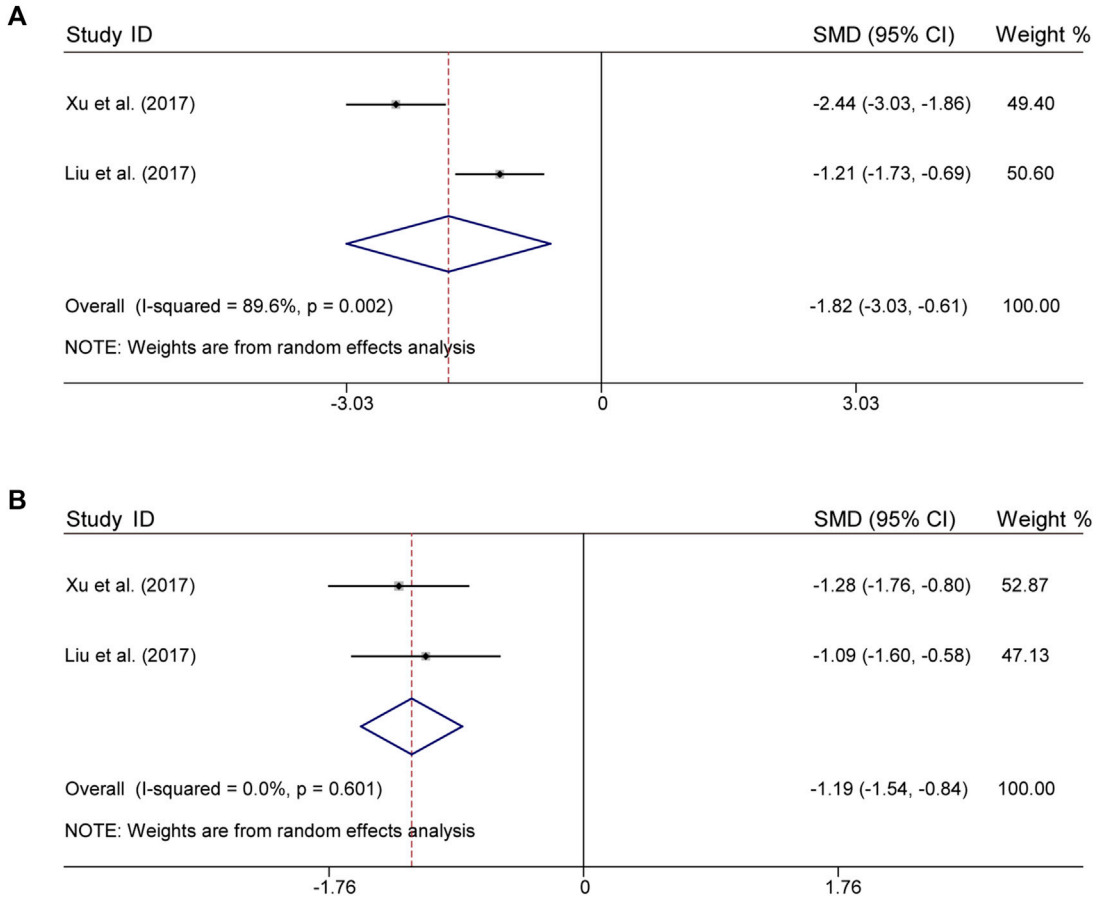

FIGURE 5
Comparative forest plots of indicators of inflammation; **(A)** TNF-α; **(B)** IL-6.

respective degrees of 245°, 199°, 196°, 130°, and 85°. More details are given in Table 2.

4.3 Gene ontology and kyoto encyclopedia of genes and genomes enrichment analyze

For GO enrichment analysis, a total of 3516 items were selected, and the top 20 significant terms in the BP, CC, and MF categories are shown in Figure 8A. The intersected target proteins in the BP category mainly included responses to hormones, behavior, positive regulation of cell death, inflammatory response, and synaptic signaling. The CC category mainly included dendrite, cell body, membrane raft, perinuclear region of cytoplasm, and side of membrane. The MF category mainly included kinase binding, transcription factor binding, protein domain-specific binding, signaling receptor regulator activity, and neurotransmitter receptor activity.

For KEGG enrichment analysis, the top 20 items were selected for visualization according to the criteria above (Figure 8B). The results mainly involved neuroactive ligand-receptor interactions, the PI3K-Akt signaling pathway, serotonergic synapses, the JAK-STAT signaling pathway, and the NF-κB signaling pathway.

4.4 Protein-protein interaction network analysis

In the PPI network analysis, 416 predicted targets were submitted to the STRING platform, and interactions with high confidence (>0.9) were chosen. Isolated nodes were removed, and the remaining targets were visualized in Cytoscape 3.8.2. The PPI relationship network, which consisted of 312 nodes and 1321 edges, is shown in Figure 9A. In addition, to further screen for key targets for CLM in the treatment of depression, we conducted topology analysis based on BC, CC, and DC. Ultimately, 28 core targets were obtained and ranked by degree values (Figures 9B–D; Table 3). The top seven core targets were MAPK3, JUN, TP53, MAPK1, AKT1, STAT3, and PIK3R1.

4.5 Molecular docking

Based on the above results in H-C-T, GO, and PPI network analysis, molecular docking analysis was performed between the top five compounds of CLM and the top seven key targets. The docking visualizations and scores are shown in Figures 10A,B. The stronger

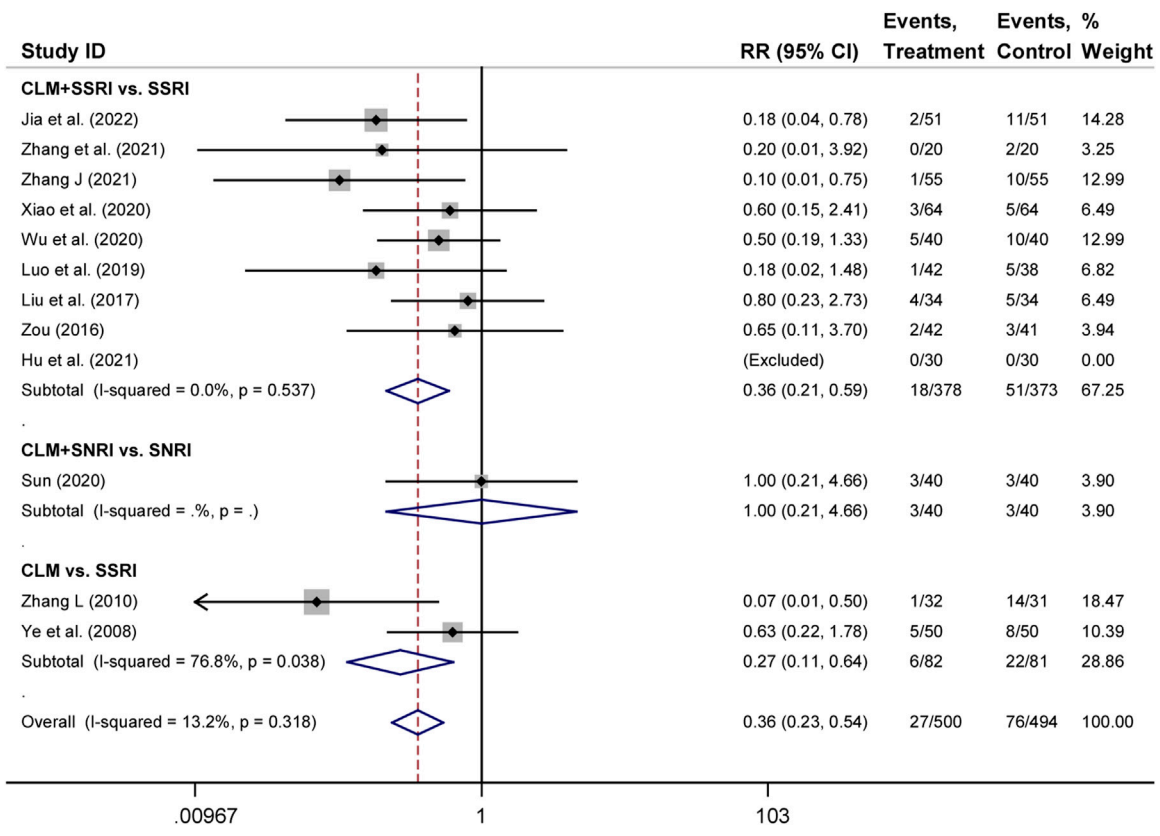

FIGURE 6
Comparative forest plots of adverse effects; Treament: CLM alone or combined with pharmaceutical anti-depressants; Control: pharmaceutical anti-depressants.

the binding force between the compound and the protein, the lower the docking score (the higher the negative number). When the docking score is ≤ −5.0 kJ/mol, the exertion of a strong binding effect is suggested. The results showed that 35 pairs of active compounds and ligands were relatively stable. PIK3R1 (PDB: 2IUG), MAPK3 (PDB: 4QTB), and AKT1 (PDB: 1UNP) might be potential therapeutic targets for depression using CLM, among which stigmasterol (MOL000449) had the highest binding energy with PIK3R1.

5 Discussion

At present, the pathological mechanisms of depression mainly involve the monoamine hypothesis, hypothalamus–pituitary–adrenal axis hyperactivity, neuroplasticity and neurogenesis, structural and functional brain changes, and inflammation (Malhi and Mann, 2018). However, due to the unclear pathophysiological mechanisms of depression, one-third of patients face treatment resistance or adverse reactions to common treatments, and the treatment of depression still faces challenges (Dodd et al., 2021). CLM is derived from "Shang Han Lun" and has a significant effect on depression. However, due to the complexity of its components, the mechanism of action of this prescription has not been fully clarified. The results of present study indicated that the antidepressant efficacy of CLM, whether administered alone or in combination with antidepressants, was significantly higher than that of antidepressants alone. In addition, whether in CLM alone or CLM + SSRI/SNRI, the symptoms of depression, anxiety, and insomnia in patients with depression were significantly improved comparing antidepressants alone. CLM and CLM + SSRI also showed fewer adverse reactions than SSRI alone. Five compounds in CLM and seven of its key targets were shown to be related to antidepressant activity in the present analysis.

CLM has extensive neural activities in the treatment of depression, anxiety, insomnia, and neurocognitive disorders (Niitsu et al., 2013). A meta-analysis of CLM's efficiency and safety in treating post-stroke depression revealed that, regardless of the length of the treatment period, CLM showed better efficacy than an antidepressant group. Additionally, in the group receiving CLM combined with pharmaceutical antidepressants, the incidence of adverse reactions such as abnormal blood or urine routine tests, abnormal liver function, sleeplessness, and digestive tract pain was dramatically decreased (Wan et al., 2021). In addition, a correlation has been shown between depression, anxiety, and insomnia; the association between insomnia and feelings of self-disgust was fully mediated by anxiety and depression (Ypsilanti et al., 2018). This means that a good treatment strategy for patients with depression seems to be relieving anxiety and insomnia while adjusting mood. In the

present findings, compared with antidepressants, both CLM alone and combined with SSRI/SNRI markedly reduced the scores of HAMD and SDS. For anxiety and insomnia, we conducted a meta-analysis of HAMA, SAS, and PSQI scores, results indicated that the synergistic effect of CLM and SSRI was significantly better than that of SSRI alone. In addition, due to the limited literature on CLM alone and CLM + SNRI, the synergistic effect of CLM alone or with SNRI may need further exploration. However, for overall efficacy in anxiety, CLM alone or in combination is not inferior to antidepressants alone. In terms of adverse reactions, whether CLM alone or in combination with SSRI, the incidence of adverse reactions is significantly fewer than that of SSRI alone. It is worth noting that the incidence of adverse reactions in CLM combined with SNRI is the same as that of SNRI alone, which may be the reason for only including one trial. Therefore, CLM could not only improve the symptoms of depression, anxiety, and insomnia, but can also reduce the incidence of adverse responses caused by commonly used antidepressants, especially in combination with SSRI.

Depression and inflammation are intertwined; heightened inflammation exacerbates not only physical symptoms such as pain sensitivity, fatigue, and anhedonia but also psychological symptoms such as negative mood, loss of appetite, and feelings of inferiority (Kiecolt-Glaser et al., 2015). Levels of proinflammatory cytokines in peripheral blood were shown to be significantly increased in patients with major depressive disorder, such as IL-6, TNF-α and IL-1β (Howren et al., 2009; Dowlati et al., 2010; Liu et al., 2012). Moreover, nonsteroidal anti-inflammatory drugs could significantly reduce depressive symptoms compared to placebo treatment (Kohler et al., 2014). Therefore, anti-inflammatory treatments may be effective for depression. The present results indicated that CLM dramatically decreased the levels of TNF-α and IL-6 in the peripheral blood of patients with depression compared to antidepressant treatment groups.

In order to further investigate the aforementioned putative mechanisms of CLM's anti-depressant effects, network pharmacology was conducted. We intersected 416 therapeutic targets from 1490 depression targets and 2356 targets of CLM compound components. According to the H-C-T network, the top five active ingredients were stigmasterol, quercetin, β-stiosterol, coumestrol, and stepholidine. Recent research has shown that oral and intraperitoneal treatment of stigmasterol and β-stiosterol significantly reduced immobility time in tail suspension and forced swimming tests in rat models of depression, and its antidepressant activity might be mediated by the glutamatergic systems (Zhao et al., 2016; Ghosh et al., 2022). Quercetin has been reported to inhibit inflammation and attenuate depression-like behavior by regulating PI3K/AKT/NF-κB and promoting mitophagy in a lipopolysaccharide-induced mouse model of depression (Han et al., 2021; Sun et al., 2021). Monoamine oxidase A inhibitors, as third-line antidepressants, are widely used in clinics, and coumestrol has been proven to be a selective and competitive monoamine oxidase A inhibitor (Seong et al., 2022). As a specific dopamine receptor D1 agonist, stepholidine could activate the PKA/mTOR pathway to upregulate the expression of synaptogenesis-related proteins and exert antidepressant effects (Zhang et al., 2017). The above research provides a pharmacological basis for the clinical efficacy of CLM in depression, although the effect of CLM on depression has been revealed directly or indirectly through the above ingredients, due to the complexity of the ingredients, the specific mechanisms have not been clarified. Therefore, we assessed the relevant pathways for CLM in the treatment of depression using KEGG and GO enrichment analyses.

Research has confirmed that inflammation induced by glial cells is an important mechanism leading to depression. Neuroglial cells can regulate neuron electrical activity and even death by adjusting synaptic plasticity and integrating and transmitting synaptic information (Perez-Catalan et al., 2021). This may explain the anti-inflammatory and antidepressant mechanism of CLM, where GO analysis showed that the antidepressant effect of CLM mainly plays a protective role by regulating the inflammatory response. In addition, at the level of CC and MF, CLM mainly plays a role in synaptic spines, synapses, membrane rafts, and nuclear envelope by combining with enzymes and neurotransmitters. The present KEGG analysis of CLM also pointed to neuroinflammation, which involves the PI3K/Akt, JAK-STAT, and NF-κB signaling pathways. The PI3K/Akt signaling pathway is involved in synaptic plasticity, learning and memory, and inflammation, which are important in the pathogenesis of depression (Matsuda et al., 2019). Enzymatic activity of PI3K and Akt was shown to be decreased in patients with depression, which may lead to neuron loss, decreased neuroplasticity, and dysregulation of neurotrophic factors (Karege et al., 2011). Evidence has also shown that activation of Akt signaling can alleviate stress-induced depressive behaviors in mice by inhibiting neuroinflammation and increasing neurotrophic factors (Xian et al., 2019). Accordingly, by activating Akt signaling, CLM was shown to reverse the abnormal expression of AMPA and NMDA receptors in the prefrontal cortex of depressed mice (Wang et al., 2018). The JAK-STAT and NF-κB signaling pathways are downstream cascade signals of the PI3K/Akt pathway and both play key roles in cell proliferation, differentiation, migration, and apoptosis. The involvement of the JAK/STAT pathway in synaptic plasticity has been confirmed to depend on the activation of NMDA receptors in the hippocampal CA1 region (Nicolas et al., 2012). Therefore, we speculate that the antidepressant effect of CLM may be related to the activation of PI3K/Akt and its downstream signaling pathways, inhibition of inflammatory storms, and protection of neurons.

Notably, the therapeutic efficacy of ketamine, an NMDA receptor antagonist, has highlighted the emerging data linking the regulation of NMDA to the etiology of depression. More significantly, increases in proinflammatory cytokines (such as IL-1, IL-6, and TNF-α) have been directly associated with JAK-STAT activation. Antidepressants may work by decreasing proinflammatory cytokines via modulation of the JAK/STAT pathway, and they may also improve somatic symptoms, anhedonia, and low energy levels (Malemud and Miller, 2008). The NF-κB signaling pathway contributes to the pathogenesis of neurodegenerative diseases, with the PI3K/Akt pathway as its major upstream component (Dong et al., 2016). Activation of the PI3K/Akt signaling pathway has been

10.3389/fphar.2023.1257617

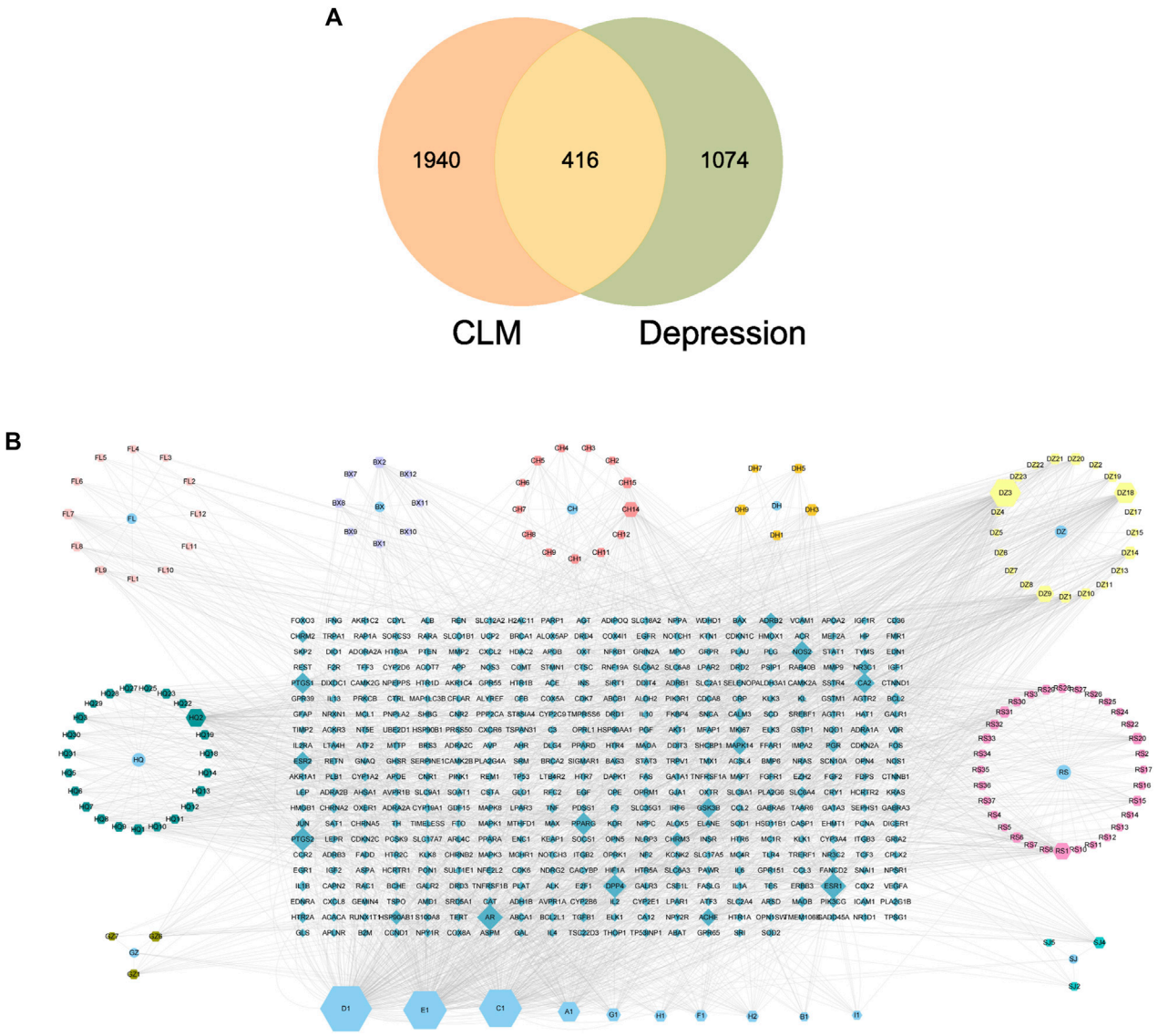

FIGURE 7
Venn diagram and H-C-T network; **(A)** Venn diagram of the active ingredients of CLM and potential treatment targets; 2356 predicted targets of CLM, 1490 therapeutic targets for depression, and 416 targets intersected; **(B)** H-C-T network of CLM; BX: Ban Xia, CH: Chai Hu, DZ: Da Zao, FL: Fu Ling, SJ: Sheng Jiang, GZ: Gui Zhi, DH: Da Huang, HQ: Sheng Jiang, RS: Ren Shen; A–H: Common components of different drugs.

TABLE 2 Basic information of the top five degree of the compounds.

MOL ID	Compound	CAS	Molecular formula	MW
MOL000449	Stigmasterol	83–48–7	$C_{29}H_{48}O$	412.77
MOL000098	Quercetin	117–39–5	$C_{15}H_{10}O_7$	302.23
MOL000358	beta-stiosterol	83–46–5	$C_{29}H_{50}O$	414.79
MOL012976	coumestrol	479–13–0	$C_{15}H_8O_5$	268.22
MOL000627	Stepholidine	16,562–13–3	$C_{19}H_{21}NO_4$	327.41

reported to significantly reduce the nuclear translocation of NF-κB and the activation of microglia, thus inhibiting neuronal apoptosis and inflammation (Zhu et al., 2018). Although CLM likely exerts anti-depressant effects via the PI3K/Akt, JAK/STAT, NF-κB, or apoptosis signaling pathways, it remains urgently necessary to clarify the therapeutic targets of CLM,

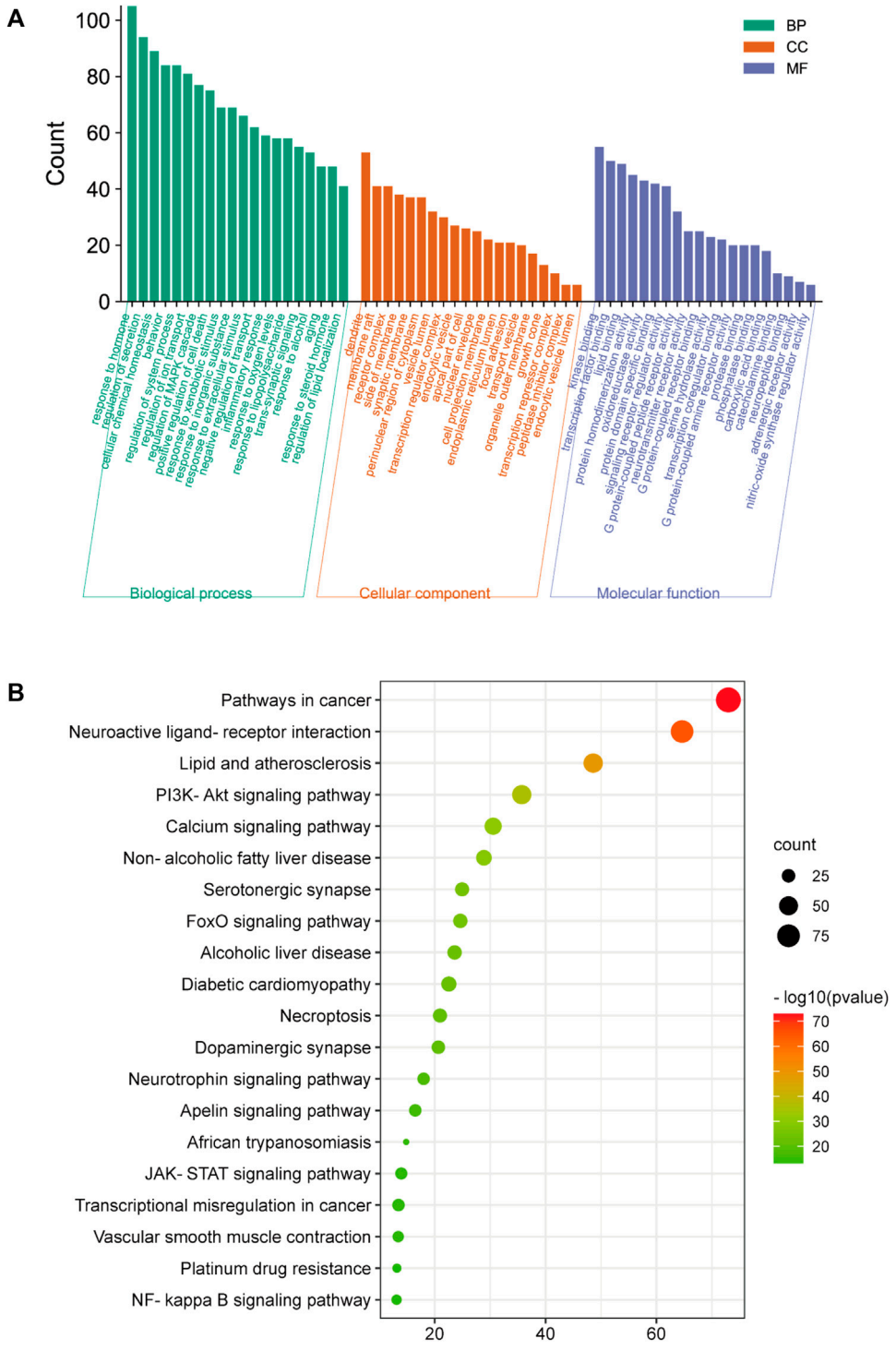

FIGURE 8
GO and KEGG analysis; **(A)** BP, MF, and CC categories in GO analysis of 416 intersection targets; **(B)** top 20 signaling pathways in KEGG enrichment analysis of 416 intersected targets.

which may contribute to the development of novel therapeutic strategies.

Next, according to the PPI network and molecular docking analyses, MAPK3, TP53, MAPK1, STAT3, and PI3KR1 were potential antidepressant targets of CLM. Similar to the above results from the network pharmacology analysis, stigmasterol showed high binding energy with PI3KR1, suggesting that CLM alleviates depression via modulation of the PI3K/Akt signaling pathway. In summary, the above evidence suggests that CLM is a safe and effective antidepressant prescription with multiple pathways

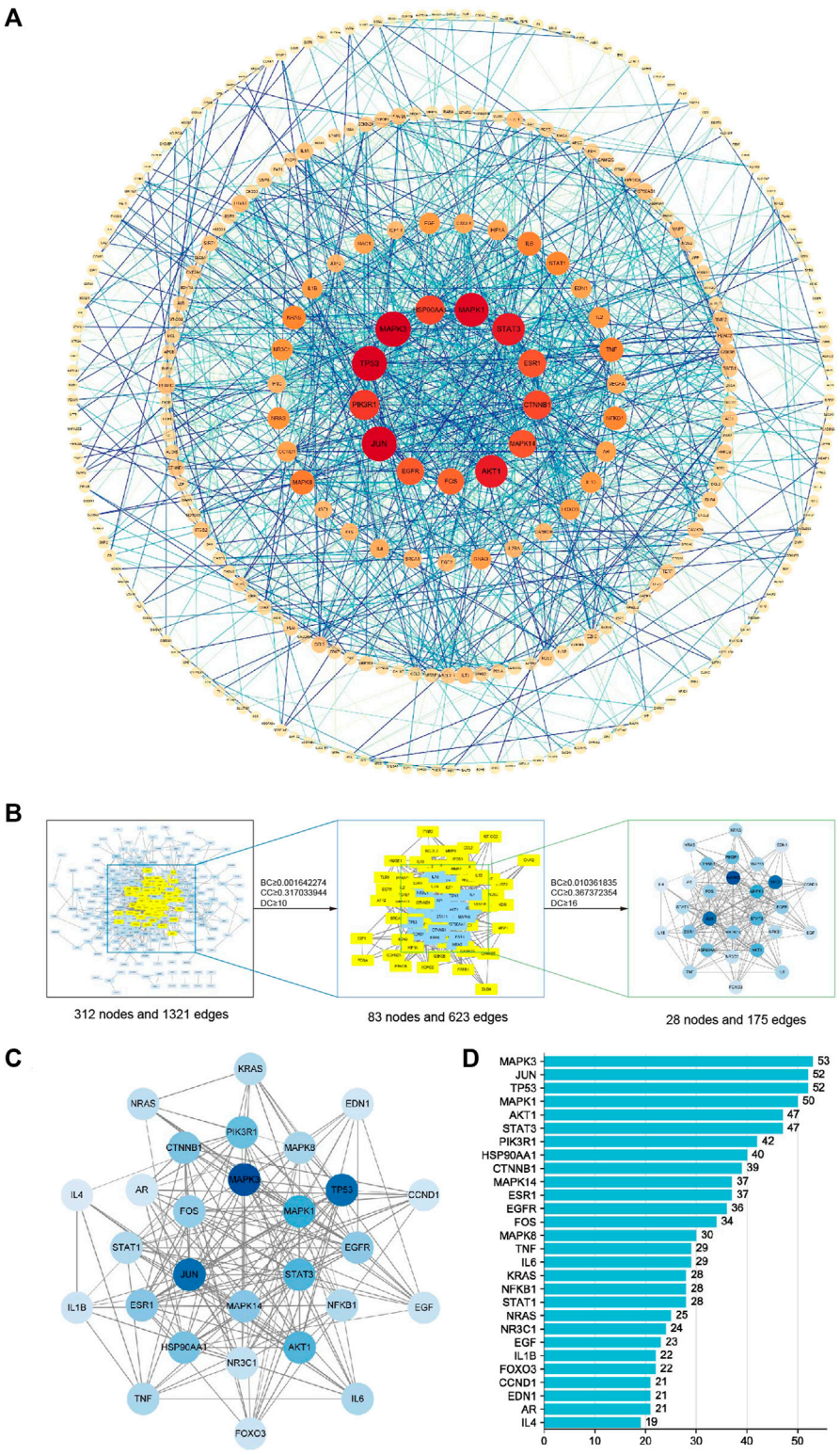

FIGURE 9
Interaction network diagram of 416 predicted targets and topology analysis; **(A)** PPI network of 416 predicted targets; **(B)** topology analysis; BC: betweenness centrality; CC: closeness centrality; DC: degree centrality; **(C)** network of the top 28 core proteins; **(D)** top 28 targets ranked by degree values.

TABLE 3 Specifc information of the 28 key target genes.

Uniprot ID	Name	Description	Degree	Betweenness centrality	Closeness centrality
P27361	MAPK3	Mitogen-activated protein kinase 3	53	0.045746269	0.435103245
P05412	JUN	Transcription factor Jun	52	0.084722588	0.44494721
P04637	TP53	Cellular tumor antigen p53	52	0.120920491	0.435745938
P28482	MAPK1	Mitogen-activated protein kinase 1	50	0.038943892	0.431918009
P40763	STAT3	Signal transducer and activator of transcription 3	47	0.058421284	0.421428571
P31749	AKT1	RAC-alpha serine/threonine-protein kinase	47	0.071162417	0.43318649
P27986	PIK3R1	Phosphatidylinositol 3-kinase regulatory subunit alpha	42	0.046009982	0.416666667
P07900	HSP90AA1	Heat shock protein HSP 90-alpha	40	0.0405667	0.411436541
P35222	CTNNB1	Catenin beta-1	39	0.059706312	0.411436541
Q16539	MAPK14	Mitogen-activated protein kinase 14	37	0.069980098	0.431918009
P03372	ESR1	Estrogen receptor	37	0.081274348	0.43255132
P00533	EGFR	Epidermal growth factor receptor	36	0.033559803	0.412011173
P01100	FOS	Protein c-Fos	34	0.024626294	0.408587258
P45983	MAPK8	Mitogen-activated protein kinase 8	30	0.032364484	0.409722222
P05231	IL6	Interleukin-6	29	0.01798382	0.380645161
P01375	TNF	Tumor necrosis factor	29	0.027560775	0.387139108
P19838	NFKB1	Nuclear factor NF-kappa-B p105 subunit	28	0.032042801	0.402455662
P42224	STAT1	Signal transducer and activator of transcription 1-alpha/beta	28	0.015860428	0.398648649
P01116	KRAS	GTPase KRas	28	0.017076325	0.39021164
P01111	NRAS	GTPase NRas	25	0.024069906	0.37966538
P04150	NR3C1	Glucocorticoid receptor	24	0.014751511	0.399188092
P01133	EGF	Pro-epidermal growth factor	23	0.014372036	0.380154639
O43524	FOXO3	Forkhead box protein O3	22	0.02241392	0.397039031
P01584	IL1B	Interleukin-1 beta	22	0.012354862	0.380645161
P24385	CCND1	G1/S-specific cyclin-D1	21	0.014984121	0.383615085
P10275	AR	Androgen receptor	21	0.016074494	0.392287234
P05305	EDN1	Endothelin-1	21	0.020720848	0.386125654
P05112	IL4	Interleukin-4	19	0.037711426	0.381630013

and targets. Its mechanism is likely related to the regulation of neuronal synaptic plasticity, inflammation, and apoptosis.

6 Limitations

This study still exist limitations. The treatment time was not explored on anti-depression efficacy. Secondly, it is still shallow that the evidence for selecting serum IL-6 and TNF-α as inflammation indicators. On the one hand, it is limited by available studies, on the other hand, other indicators such as serum IL-1β and CRP also affect the resistance to antidepressants. Meanwhile, the increase in these indicators also indicates more severe disease course outcomes and more extensive somatization symptoms (Kiecolt-Glaser et al., 2015). Furthermore, the number of trials included in this study was insufficient to clearly state the specific efficacy of some subgroup analyses such as HAMA and SAS, so part results have to be roughly concluded by assessing the comprehensive efficacy of CLM alone or in combination with antidepressants. Then, part of literature included by allocation concealment and blinding is not yet clear. TCM has the characteristics of personalized treatment, which is limited to the unique odor and color, making it difficult to implement blind methods. In addition, screening the active ingredients based on OB and DL may exist inconsistency with the precise ingredients, and the predicted targets

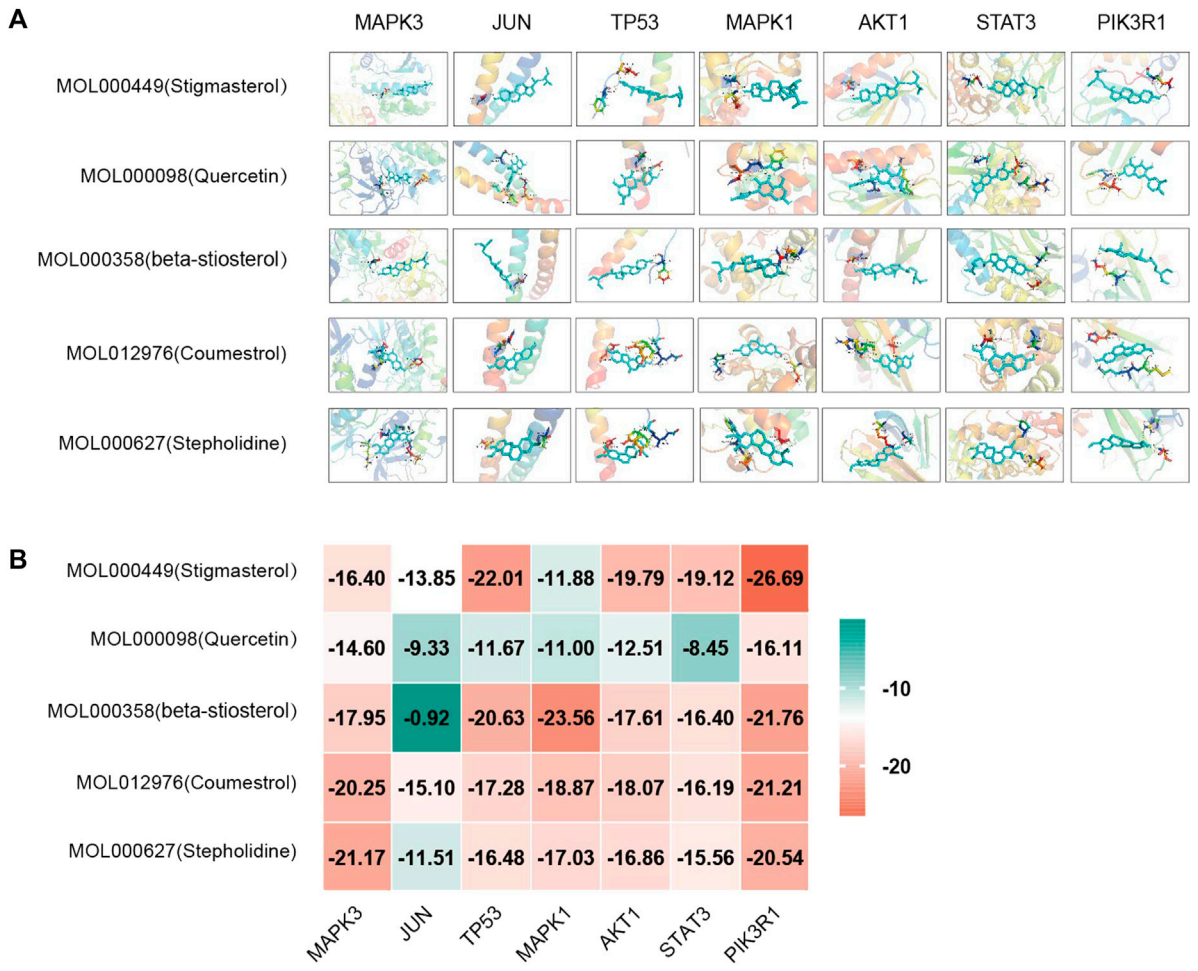

FIGURE 10
Molecular docking analysis of main compounds binding to key targets; **(A)** molecular docking models of main chemical components; **(B)** heat map showing values of docking affinity.

are likely to be limited by the hot spots of current research. Finally, the specific mechanism in this study still needs to be verified by further vivo and vitro experiments.

7 Conclusion

This study analyzed the effectiveness and mechanism of CLM in the treatment of depression. Our findings revealed that compared to antidepressants, CLM had better clinical efficacy and fewer side effects, especially in combination with SSRI. Its mechanism in treating depression may be related to regulating neuronal synaptic plasticity, inhibiting neuroinflammation, and improving neuronal damage. Stigmasterol, β-stiosterol, and coumestrol, three components of CLM. may play antidepressant roles via the targets of PIK3R1, MAPK3, and AKT1. The PI3K/Akt signaling pathway may be one of the main pathways for CLM to achieve its antidepressant effect.

Data availability statement

The original contributions presented in the study are included in the article/Supplementary Materials, further inquiries can be directed to the corresponding authors.

Author contributions

YZ: Formal Analysis, Writing–original draft, Writing–review and editing. DX: Funding acquisition, Resources, Writing–review and editing. JW: Data curation, Investigation, Writing–review and editing. DZ: Data curation, Methodology, Software, Writing–review and editing. AL: Data curation, Formal Analysis, Software, Writing–review and editing. YS: Data curation, Formal Analysis, Software, Writing–review and editing. YY: Formal Analysis, Software, Writing–review and editing. JL: Supervision,

Writing–review and editing. WG: Supervision, Writing–review and editing.

Funding

DX was supported by the Project of Taicang Science and Technology Bureau of Jiangsu Province (TC2021JCYL07).

Conflict of interest

The authors declare that the research was conducted in the absence of any commercial or financial relationships that could be construed as a potential conflict of interest.

Publisher's note

Supplementary material

The Supplementary Material for this article can be found online at: https://www.frontiersin.org/articles/10.3389/fphar.2023.1257617/full#supplementary-material

References

Beurel, E., Toups, M., and Nemeroff, C. B. (2020). The bidirectional relationship of depression and inflammation: Double trouble. *Neuron* 107 (2), 234–256. doi:10.1016/j.neuron.2020.06.002

Borbely, E., Simon, M., Fuchs, E., Wiborg, O., Czeh, B., and Helyes, Z. (2022). Novel drug developmental strategies for treatment-resistant depression. *Br. J. Pharmacol.* 179 (6), 1146–1186. doi:10.1111/bph.15753

Cao, J., and Guo, Y. (2021). Clinical observation on the treatment of depressive insomnia with modified Chaihu longgu oyster soup and mirtazapine. *World Latest Med. Inf.* 21 (88), 227–229. doi:10.3969/j.issn.1671-3141.2021.88.070

Chen, G., He, Y., and Wang, B. (2017). Curative effect and mechanism analysis of modified Chaihu longgu muli decoction combined with anti-anxiety medication for somatization, depression and anxiety state. *Chin. Archives Traditional Chin. Med.* 35 (3), 758–760. doi:10.13193/j.issn.1673-7717.2017.03.070

Chen, L., Cao, Y., Zhang, H., Lv, D., Zhao, Y., Liu, Y., et al. (2018). Network pharmacology-based strategy for predicting active ingredients and potential targets of Yangxinshi tablet for treating heart failure. *J. Ethnopharmacol.* 219, 359–368. doi:10.1016/j.jep.2017.12.011

Chen, Z., and Ding, L. (2012). Clinical observation on treating 40 cases of depression with the Chaihu plus Longgu Muli decoction and lily anemarrhena decoction. *Clin. J. Chin. Med.* 4 (3), 38–39.

COVID-19 Mental Disorders Collaborators (2021). Global prevalence and burden of depressive and anxiety disorders in 204 countries and territories in 2020 due to the COVID-19 pandemic. *Lancet* 398 (10312), 1700–1712. doi:10.1016/S0140-6736(21)02143-7

Dodd, S., Bauer, M., Carvalho, A. F., Eyre, H., Fava, M., Kasper, S., et al. (2021). A clinical approach to treatment resistance in depressed patients: What to do when the usual treatments don't work well enough? *World J. Biol. Psychiatry* 22 (7), 483–494. doi:10.1080/15622975.2020.1851052

Dong, L., Li, Y. Z., An, H. T., Wang, Y. L., Chen, S. H., Qian, Y. J., et al. (2016). The E3 ubiquitin ligase c-cbl inhibits microglia-mediated CNS inflammation by regulating PI3K/akt/NF-κB pathway. *CNS Neurosci. Ther.* 22 (8), 661–669. doi:10.1111/cns.12557

Dowlati, Y., Herrmann, N., Swardfager, W., Liu, H., Sham, L., Reim, E. K., et al. (2010). A meta-analysis of cytokines in major depression. *Biol. Psychiatry* 67 (5), 446–457. doi:10.1016/j.biopsych.2009.09.033

Fang, S., Dong, L., Liu, L., Guo, J., Zhao, L., Zhang, J., et al. (2021). Herb: A high-throughput experiment- and reference-guided database of traditional Chinese medicine. *Nucleic Acids Res.* 49 (D1), D1197–D1206. doi:10.1093/nar/gkaa1063

Gao, Q., Han, Z. Y., Tian, D. F., Liu, G. L., Wang, Z. Y., Lin, J. F., et al. (2021). Xinglou Chengqi Decoction improves neurological function in experimental stroke mice as evidenced by gut microbiota analysis and network pharmacology. *Chin. J. Nat. Med.* 19 (12), 881–899. doi:10.1016/S1875-5364(21)60079-1

GBD 2015 Disease and Injury Incidence and Prevalence Collaborators (2016). Global, regional, and national incidence, prevalence, and years lived with disability for 310 diseases and injuries, 1990-2015: A systematic analysis for the global burden of disease study 2015. *Lancet* 388 (10053), 1545–1602. doi:10.1016/S0140-6736(16)31678-6

Ghosh, S., Kumar, A., Sachan, N., and Chandra, P. (2022). Evaluation of the antidepressant-like effect of total sterols fraction and Stigmasterol isolated from leaves of aegle marmelos and possible mechanism(s) of action involved. *Curr. Drug Discov. Technol.* 19 (2), e290721195144. doi:10.2174/1570163818666210729165310

Han, X., Xu, T., Fang, Q., Zhang, H., Yue, L., Hu, G., et al. (2021). Quercetin hinders microglial activation to alleviate neurotoxicity via the interplay between NLRP3 inflammasome and mitophagy. *Redox Biol.* 44, 102010. doi:10.1016/j.redox.2021.102010

Hanying, F., Xinxia, G., Yaqi, L., Siqi, L., and Weifeng, G. (2022). Thoughts and methods of treating emotional diseases from mental disorders. *J. Hubei Univ. Chin. Med.* 24 (5), 61–64. doi:10.3969/j.issn.1008987x.2022.05.14

Heberle, H., Meirelles, G. V., da Silva, F. R., Telles, G. P., and Minghim, R. (2015). InteractiVenn: A web-based tool for the analysis of sets through venn diagrams. *BMC Bioinforma.* 16 (1), 169. doi:10.1186/s12859-015-0611-3

Howren, M. B., Lamkin, D. M., and Suls, J. (2009). Associations of depression with C-reactive protein, IL-1, and IL-6: A meta-analysis. *Psychosom. Med.* 71 (2), 171–186. doi:10.1097/PSY.0b013e3181907c1b

Hu, J. (2021). Clinical observation on the combination of Chinese and western medicines in the treatment of depression. *J. Pract. Traditional Chin. Med.* 37 (8), 1366–1367.

Hu, Y., Yang, Y., and Wang, X. (2016). Clinical observation and theoretical discussion of Chaihu plus Longgu Oyster soup in the treatment of depression. *World Latest Med. Inf.* 16 (8), 204–205. doi:10.3969/j.issn.1671-3141.2016.08.129

Jia, L., and Li, X. (2022). Analysis of the efficacy and safety of modified Chaihu plus Longgu Muli Decoction in the treatment of depression. *China Pract. Med.* 17 (10), 30–33. doi:10.14163/j.cnki.11-5547/r.2022.10.009

Karege, F., Perroud, N., Burkhardt, S., Fernandez, R., Ballmann, E., La Harpe, R., et al. (2011). Alterations in phosphatidylinositol 3-kinase activity and PTEN phosphatase in the prefrontal cortex of depressed suicide victims. *Neuropsychobiology* 63 (4), 224–231. doi:10.1159/000322145

Kiecolt-Glaser, J. K., Derry, H. M., and Fagundes, C. P. (2015). Inflammation: Depression fans the flames and feasts on the heat. *Am. J. Psychiatry* 172 (11), 1075–1091. doi:10.1176/appi.ajp.2015.15020152

Kohler, O., Benros, M. E., Nordentoft, M., Farkouh, M. E., Iyengar, R. L., Mors, O., et al. (2014). Effect of anti-inflammatory treatment on depression, depressive symptoms, and adverse effects: A systematic review and meta-analysis of randomized clinical trials. *JAMA Psychiatry* 71 (12), 1381–1391. doi:10.1001/jamapsychiatry.2014.1611

Li, G., Chunhua, J., Cuilan, M., Hui-wen, H., Zhang, X., Yang, Z., et al. (2018). Mouse macrophages capture and kill Giardia lamblia by means of releasing extracellular trap. *Henan Tradit. Chin. Med.* 38 (2), 206–212. doi:10.1016/j.dci.2018.07.024

Li, L., Liu, X., and Xu, B. (2016). Fifty-five cases with depression treated with supplemented longgu muli decoction combined with paroxetine. *Henan Tradit. Chin. Med.* 36 (5), 770–772. doi:10.16367/j.issn.1003-5028.2016.05.0329

Li, Q. F., Lu, W. T., Zhang, Q., Zhao, Y. D., Wu, C. Y., and Zhou, H. F. (2022a). Proprietary medicines containing bupleurum chinense DC. (Chaihu) for depression: Network meta-analysis and network pharmacology prediction. *Front. Pharmacol.* 13, 773537. doi:10.3389/fphar.2022.773537

Li, X., Jia, L., Lu, Y., Wang, J., and Yao, W. (2022b). Genetic analysis of platelet-related genes in hepatocellular carcinoma reveals a novel prognostic signature and determines PRKCD as the potential molecular bridge. *China Prac. Med.* 17 (12), 22–25. doi:10.1186/s12575-022-00185-9

Liu, X., Kong, Y., Feng, Y., and Yang, W. (2017). Effects of traditional Chinese medicine and sertraline on clinical efficacy and serum cytokines levels in first-episode depression patients. *J. Int. psychiatry* 44 (6), 1018–1020. doi:10.13479/j.cnki.jip.2017.06.017

Liu, Y., Ho, R. C., and Mak, A. (2012). Interleukin (IL)-6, tumour necrosis factor alpha (TNF-alpha) and soluble interleukin-2 receptors (sIL-2R) are elevated in patients with major depressive disorder: A meta-analysis and meta-regression. *J. Affect Disord.* 139 (3), 230–239. doi:10.1016/j.jad.2011.08.003

Liu, Y., Ma, S., and Qu, R. (2010). SCLM, total saponins extracted from Chaihu-jia-longgu-muli-tang, reduces chronic mild stress-induced apoptosis in the hippocampus in mice. *Pharm. Biol.* 48 (8), 840–848. doi:10.3109/13880200903296154

Lizhi, S., Mengdi, M., Erping, X., Mingyuan, Z., Chunyu, Z., Guoqiang, W., et al. (2021). Immunoregulatory effect of Chaihu jia longgu mulitang modified with bupleuri radix on hippocampal NLRP3 pathway in depressed rats. *Chin. J. Exp. Traditional Med. Formulae* 27 (24), 33–39. doi:10.13422/j.cnki.syfjx.20202303

Luo, Z., Lv, X., and Xie, W. (2019). Clinical study on 42 cases of depressive disorder treated with chaihu-jia-longgu-muli-tang combined with western medicine. *Chin. J. Ethnomedicine Ethnopharmacy* 28 (3), 104–105.

Malemud, C. J., and Miller, A. H. (2008). Pro-inflammatory cytokine-induced SAPK/MAPK and JAK/STAT in rheumatoid arthritis and the new anti-depression drugs. *Expert Opin. Ther. Targets* 12 (2), 171–183. doi:10.1517/14728222.12.2.171

Malhi, G. S., and Mann, J. J. (2018). Depression. *Lancet* 392 (10161), 2299–2312. doi:10.1016/S0140-6736(18)31948-2

Matsuda, S., Ikeda, Y., Murakami, M., Nakagawa, Y., Tsuji, A., and Kitagishi, Y. (2019). Roles of PI3K/AKT/GSK3 pathway involved in psychiatric illnesses. *Diseases* 7 (1), 22. doi:10.3390/diseases7010022

Moitra, M., Santomauro, D., Collins, P. Y., Vos, T., Whiteford, H., Saxena, S., et al. (2022). The global gap in treatment coverage for major depressive disorder in 84 countries from 2000-2019: A systematic review and bayesian meta-regression analysis. *PLoS Med.* 19 (2), e1003901. doi:10.1371/journal.pmed.1003901

Nicolas, C. S., Peineau, S., Amici, M., Csaba, Z., Fafouri, A., Javalet, C., et al. (2012). The Jak/STAT pathway is involved in synaptic plasticity. *Neuron* 73 (2), 374–390. doi:10.1016/j.neuron.2011.11.024

Niitsu, T., Okamoto, H., and Iyo, M. (2013). Behavioural and psychological symptoms of dementia in an alzheimer's disease case successfully treated with natural medicine: Association with gonadotropins. *Psychogeriatrics* 13 (2), 124–127. doi:10.1111/psyg.12010

O'Boyle, N. M., Banck, M., James, C. A., Morley, C., Vandermeersch, T., and Hutchison, G. R. (2011). Open Babel: An open chemical toolbox. *J. Cheminform* 3, 33. doi:10.1186/1758-2946-3-33

Page, M. J., McKenzie, J. E., Bossuyt, P. M., Boutron, I., Hoffmann, T. C., Mulrow, C. D., et al. (2021). The PRISMA 2020 statement: An updated guideline for reporting systematic reviews. *BMJ* 372, n71. doi:10.1136/bmj.n71

Perez-Catalan, N. A., Doe, C. Q., and Ackerman, S. D. (2021). The role of astrocyte-mediated plasticity in neural circuit development and function. *Neural Dev.* 16 (1), 1. doi:10.1186/s13064-020-00151-9

Pinero, J., Bravo, A., Queralt-Rosinach, N., Gutierrez-Sacristan, A., Deu-Pons, J., Centeno, E., et al. (2017). DisGeNET: A comprehensive platform integrating information on human disease-associated genes and variants. *Nucleic Acids Res.* 45 (D1), D833–D839. doi:10.1093/nar/gkw943

Regier, D. A., Kuhl, E. A., and Kupfer, D. J. (2013). The DSM-5: Classification and criteria changes. *World Psychiatry* 12 (2), 92–98. doi:10.1002/wps.20050

Seong, S. H., Kim, B. R., Cho, M. L., Kim, T. S., Im, S., Han, S., et al. (2022). Phytoestrogen coumestrol selectively inhibits monoamine oxidase-A and amyloid beta self-aggregation. *Nutrients* 14 (18), 3822. doi:10.3390/nu14183822

Stelzer, G., Rosen, N., Plaschkes, I., Zimmerman, S., Twik, M., Fishilevich, S., et al. (2016). The GeneCards suite: From gene data mining to disease genome sequence analyses. *Curr. Protoc. Bioinforma.* 54, 1.30.1–1.30.33. doi:10.1002/cpbi.5

Sun, P. (2020). Evaluation of the effect of chaihulonggumuli decoction in the auxiliary treatment of depression. *World J. Complex Med.* 6 (8), 136–138. doi:10.11966/j.issn.2095-994X.2020.06.08.46

Sun, Y., Zhang, H., Wu, Z., Yu, X., Yin, Y., Qian, S., et al. (2021). Quercitrin rapidly alleviated depression-like behaviors in lipopolysaccharide-treated mice: The involvement of PI3K/AKT/NF-κB signaling suppression and CREB/BDNF signaling restoration in the Hippocampus. *ACS Chem. Neurosci.* 12 (18), 3387–3396. doi:10.1021/acschemneuro.1c00371

Szklarczyk, D., Gable, A. L., Lyon, D., Junge, A., Wyder, S., Huerta-Cepas, J., et al. (2019). STRING v11: Protein-protein association networks with increased coverage, supporting functional discovery in genome-wide experimental datasets. *Nucleic Acids Res.* 47 (D1), D607–D613. doi:10.1093/nar/gky1131

Wan, R., Song, R., Fan, Y., Li, L., Zhang, J., Zhang, B., et al. (2021). Efficacy and safety of Chaihu jia longgu muli decoction in the treatment of poststroke depression: A systematic review and meta-analysis. *Evid. Based Complement. Altern. Med.* 2021, 7604537. doi:10.1155/2021/7604537

Wang, B., Xia, Y., Li, R., Fu, W., and Dai, H. (2019). Clinical observation of Chaihu plus Longgu Oyster soup in the treatment of depression. *Chin. Archives Traditional Chin. Med.* 59 (20), 62–64. doi:10.3969/j.issn.1002-266X.2019.20.017

Wang, X., Chen, J., Yang, N., and Qiao, H. (2020). Clinical study on 30 cases of major depressive disorder with insomnia treated by chaihu-jia-longgu-muli-tang combined with western medicine. *Jiangsu J. Traditional Chin. Med.* 52 (10), 27–29. doi:10.19844/j.cnki.1672-397X.2020.10.009

Wang, X., Zou, Z., Shen, Q., Huang, Z., Chen, J., Tang, J., et al. (2018). Involvement of NMDA-AKT-mTOR signaling in rapid antidepressant-like activity of chaihu-jia-longgu-muli-tang on olfactory bulbectomized mice. *Front. Pharmacol.* 9, 1537. doi:10.3389/fphar.2018.01537

Wu, L., Pan, K., and Wu, A. (2020). Clinical study of Chaihu longgu oyster soup combined with paroxetine in the treatment of depression. *Chin. J. Integr. Med. Cardio-Cerebrovascular Dis.* 18 (12), 1994–1996. doi:10.12102/j.issn.1672-1349.2020.12.041

Xian, Y. F., Ip, S. P., Li, H. Q., Qu, C., Su, Z. R., Chen, J. N., et al. (2019). Isorhynchophylline exerts antidepressant-like effects in mice via modulating neuroinflammation and neurotrophins: Involvement of the PI3K/Akt/GSK-3β signaling pathway. *FASEB J.* 33 (9), 10393–10408. doi:10.1096/fj.201802743RR

Xiang-yu, M., Peng, S., Ling, X., Ying-hui, G., Dong-mei, G., Jie-qiong, W., et al. (2021). Discussion on the research progress of proteomics in traditional Chinese medicine based on holistic concept. *China J. Traditional Chin. Med. Pharm.* 36 (11), 6585–6588.

Xiao, Q., Li, S., Wang, L., and Guo, N. (2018). Clinical observation of Chaihu-jia-Longgu-Muli-tang plus duloxetine hydrochloride in the treatment of anxiety depression. *Chin. J. Clin. Ration. Drug Use* 11 (6B), 35–36. doi:10.15887/j.cnki.13-1389/r.2018.17.021

Xiao, Y., and Han, G. (2020). Clinical effect of Chaihu-jia-Longgu-Muli-tang combined with droperithiazide and melitracen tablets in the treatment of anxiety and depression patients. *Henan Med. Res.* 29 (7), 1286–1288. doi:10.3969/j.issn.1004-437X.2020.07.070

Xu, D., and Zhao, J. (2017). The efficacy of Jiayichaihu Longgu Oyster soup combined with paroxetine in the treatment of depression and its influence on serum inflammatory factors and quality of life of patients. *Mod. J. Integr. Traditional Chin. West. Med.* 26 (12), 1303–1305. doi:10.3969/j.issn.1008-8849.2017.12.016

Ye, S., and Luo, B. (2008). A clinical observation on treating 50 case of depression syndrome with TCM medicine. *Chin. J. Pract. Chin. Mod. Med.* 21 (3), 239–240.

Ypsilanti, A., Lazuras, L., Robson, A., and Akram, U. (2018). Anxiety and depression mediate the relationship between self-disgust and insomnia disorder. *Sleep. Health* 4 (4), 349–351. doi:10.1016/j.sleh.2018.06.001

Yuanwen, Z., Tianhui, Y., Jianlue, P., Pangning, H., and Rongfa, H. (2022). Meta-analysis of Chaihu plus longgu muli decoction in the treatment of coronary heart disease complicated with anxiety and depression. *Traditional Chin. Drug Res. Clin. Pharmacol.* 33 (10), 1435–1444. doi:10.19378/j.issn.1003-9783.2022.10.019

Zeng, P., Su, H. F., Ye, C. Y., Qiu, S. W., Shi, A., Wang, J. Z., et al. (2022). A tau pathogenesis-based network pharmacology approach for exploring the protections of chuanxiong rhizoma in alzheimer's disease. *Front. Pharmacol.* 13, 877806. doi:10.3389/fphar.2022.877806

Zhang, B., Guo, F., Ma, Y., Song, Y., Lin, R., Shen, F. Y., et al. (2017). Activation of D1R/PKA/mTOR signaling cascade in medial prefrontal cortex underlying the antidepressant effects of l-SPD. *Sci. Rep.* 7 (1), 3809. doi:10.1038/s41598-017-03680-2

Zhang, J. (2021). Effect of Chaihu longgu oyster soup on negative emotion of patients with depression. *Mod. Med. Health Res. Electron. J.* 5 (13), 91–93.

Zhang, L. (2010). Clinical observation of Chaihu longgu oyster soup on depression. *Hebei Med. J.* 32 (22), 3185–3186.

Zhang, W., and Lin, Y. (2021). Clinical effectiveness of Chaihu plus Longgu Oyster soup in the treatment of depression. *Word Latest Med. Inf.* 21 (92), 149–151. doi:10.3969/j.issn.1671-3141.2021.92.050

Zhang, Y. (2014). Analysis on the effect of Chaihu plus Longgu Oyster soup in the treatment of depression. *Contemp. Med. Symp.* 12 (15), 21.

Zhao, D., Zheng, L., Qi, L., Wang, S., Guan, L., Xia, Y., et al. (2016). Structural features and potent antidepressant effects of total sterols and beta-sitosterol extracted from sargassum horneri. *Mar. Drugs* 14 (7), 123. doi:10.3390/md14070123

Zhong, X., Li, X., and Miao, X. (2012). Chaihu-jia-Longgu-Muli-tang in the treatment of 50 cases of depression. *China Health Care & Nutr.* 22 (20), 4746–4747. doi:10.3969/j.issn.1004-7484X.2012.11.629

Zhou, Y., Zhou, B., Pache, L., Chang, M., Khodabakhshi, A. H., Tanaseichuk, O., et al. (2019). Metascape provides a biologist-oriented resource for the analysis of systems-level datasets. *Nat. Commun.* 10 (1), 1523. doi:10.1038/s41467-019-09234-6

Zhu, Q., Enkhjargal, B., Huang, L., Zhang, T., Sun, C., Xie, Z., et al. (2018). Aggf1 attenuates neuroinflammation and BBB disruption via PI3K/Akt/NF-κB pathway after subarachnoid hemorrhage in rats. *J. Neuroinflammation* 15 (1), 178. doi:10.1186/s12974-018-1211-8

Zou, M. (2016). 42 cases of depression treated with paroxetine combined with Chaihu and longgu oyster soup. *Chin. J. Ethnomedicine Ethnopharmacy* 25 (22), 68–69.

frontiers | Frontiers in Pharmacology

TYPE Original Research
PUBLISHED 28 September 2023
DOI 10.3389/fphar.2023.1279512

OPEN ACCESS

EDITED BY
Song Zhang,
Shanghai Jiao Tong University, China

REVIEWED BY
Yi Dong,
East China Normal University, China
Xuenan Wang,
Shandong First Medical University, China

*CORRESPONDENCE
Yihan Gao,
yhgao17@hotmail.com
Jiexiong Ru,
rujx@sh.tobacco.com.cn
Ming Chen,
ming_chen@fudan.edu.cn

RECEIVED 18 August 2023
ACCEPTED 18 September 2023
PUBLISHED 28 September 2023

CITATION
Li X, Lu L, He Y, Zhang H, Zhang Y, Sheng H, Chen M, Ru J and Gao Y (2023), Pharmacological effects of nicotine salts on dopamine release in the nucleus accumbens.
Front. Pharmacol. 14:1279512.
doi: 10.3389/fphar.2023.1279512

Pharmacological effects of nicotine salts on dopamine release in the nucleus accumbens

Xiaonan Li[1], Lehua Lu[1], Ying He[1], Hui Zhang[1], Yihui Zhang[1], Huaquan Sheng[1], Ming Chen[2,3]*, Jiexiong Ru[1]* and Yihan Gao[1]*

[1]Shanghai New Tobacco Product Research Institute Co., Ltd, Shanghai, China, [2]School of Life Science and Technology, ShanghaiTech University, Shanghai, China, [3]MOE Frontier Center for Brain Science, Institutes of Brain Science, Fudan University, Shanghai, China

With the growing number of individuals regularly using e-cigarettes, it has become increasingly important to understand the psychobiological effects of nicotine salts. Nicotine increases the release of dopamine (DA) into the nucleus accumbens (NAc), causing feelings of satisfaction. However, the differences in the DA-increasing effects of different nicotine salts have not been reported. In this study, we used a G protein-coupled receptor-activated DA fluorescent probe (GRABDA1m) and optical fiber photometric recording equipment to monitor the dynamic changes and kinetics of DA release in the NAc of mice exposed to different e-cigarette aerosols, including nicotine, nicotine benzoate, nicotine tartrate, nicotine lactate, nicotine levulinic acid, nicotine malate, and nicotine citrate. The results of this study were as follows: 1) Different types of nicotine salts could increase the release of DA in the NAc. 2) The slopes and half-effective concentrations of the fitted curves were different, suggesting that each nicotine salt had a difference in the efficiency of increasing DA release with concentration changes. 3) The absorption rates of different nicotine salts containing the same original nicotine concentration were significantly different by measuring the blood nicotine content. The effect of nicotine salts on increasing DA was directly proportional to the blood nicotine level. In conclusion, by observing the effects of nicotine salts on DA release in real time *in vivo*, differences in the pharmacological effects of nicotine salts are revealed to better understand the mechanism underlying the regulatory effects of nicotine salts on the brain.

KEYWORDS

nicotine, nicotine salts, dopamine, nucleus accumbens, satisfaction

1 Introduction

In recent years, nicotine salt technology has been widely used in new tobacco products, which form protonated nicotine using organic acid–nicotine complexes, and nicotine exists mainly in the protonated form (Duell et al., 2020; Robichaud et al., 2020). The addition of nicotine salts improves throat irritation caused by high release amounts of free-state nicotine, resulting in a softer, smoother sensory experience and greater physiological satisfaction (Gades et al., 2022; Lu et al., 2022).

The production of satisfaction is mainly related to the effect of nicotine on the dopamine (DA) reward system in the brain, which produces euphoric and pleasurable sensory effects (Balfour et al., 2000; Benowitz, 2010). Nicotine stimulates the release of DA from dopaminergic neurons in the ventral tegmental area and acts on the nucleus accumbens (NAc) brain region by activating nicotinic acetylcholine receptors in different brain regions

(Di Chiara, 2000), resulting in a feeling of pleasure and the ability to improve attention and learning memory (Benowitz, 1996; Benowitz, 2010). Nicotine administration or smoking causes the release of DA from the NAc (Wonnacott et al., 2005; Tizabi et al., 2007). In animal studies, microdialysis has revealed nicotine-induced DA release in the Nac (Berrendero et al., 2005). In nonhuman primates, positron emission tomography scans have confirmed that intravenous nicotine administration induces DA release (Gallezot et al., 2014). Similarly, studies in human smokers have demonstrated that smoking induces DA release and that nicotine intake is an important factor in DA release from smoking. A significant association between DA release and behavioral responses to smoking, such as enhanced pleasure, has been demonstrated in human smokers (Balfour, 2004; Barrett et al., 2004). Therefore, measuring the release of the reward neurotransmitter DA in the brain is one of the most important objective indicators for evaluating satisfaction produced by tobacco.

Compared with traditional methods, in recent years, *in vivo* fluorescence imaging methods for monitoring changes in DA release have been developed in the field of neuroscience (Sun et al., 2018). The advantages of this method are that the animal is awake and freely moving, avoiding the effects of some anesthetized states on physiological effects. Second, it has higher spatial and temporal resolution and is less invasive, making it more suitable for measuring dynamic changes in neurotransmitters. Third, it is a genetically encoded fluorescent probe that can be expressed in specific brain regions and used for long-term imaging (Sych et al., 2019). The DA probe, developed using the G protein-coupled receptor as a backbone, has advantages in affinity, selectivity, kinetics, and pharmacological properties. It is designed to fluoresce upon binding to DA, thus providing a powerful tool for the fine detection of the dynamic modulation of DA neurotransmission *in vivo* (Sun et al., 2018; Skirzewski et al., 2022).

In this study, we aimed to investigate the effects of exposure to various nicotine salts on the release of DA in the NAc, the reward center of the brain, using a photometric recording method to compare the pharmacological differences in the effects of different nicotine salts.

2 Materials and methods

2.1 Experimental animals

This study comprised adult male C57BL/6 mice (aged 8–10 weeks) weighing 22–28 g (Shanghai Jihui Experimental Animal Breeding Co., Ltd.), which were housed for at least 1 week in advance in an animal room with alternating cycles of 12 h of light and 12 h of darkness (lights on at 7:00 a.m. and off at 7:00 p.m.) at 22°C–26°C temperature and 40%–60% humidity. All the mice had free access to food and water. All experimental procedures were approved by the Animal Ethics and Use Committee of ShanghaiTech University (approval number: 20221020003) and were performed in accordance with the National Institutes of Health guidelines. The mice were randomly divided into cages and labeled according to the experimental groups.

2.2 Drugs

Nicotine and nicotine salts were obtained from (Shanghai Yunyi Biotechnology Co., Ltd.). Both nicotine formulations were mixed with propylene glycol and vegetable glycerin in a 50:50 ratio (weight ratio) at a final concentration of 10–60 mg/mL. For the different formulations, the nicotine content was based on the molecular weight of the free base to ensure that equal amounts of nicotine were present.

2.3 Drug administration

Vaping machine: Vaping aerosol was produced using an ethylene carbonate (EC) atomizer coupled to a variable voltage EC battery. The specific EC battery had a 1,300 mA-h capacity with a nominal voltage range of 3.3–4.8 V direct current. The e-cigarette puffing curve was trapezoidal, determining a vaping capacity of 55 mL, vaping time of 2 s, and vaping interval of 30 s (Farsalinos and Gillman, 2017). Each animal was administered 60 puffs of aerosols for 30 min.

Oral and nasal exposure towers: The temperature and humidity of the equipment environment were kept relatively stable at 20°C–24°C and 60% ± 5% humidity. The flow rate of diluted air was calculated according to the number of exposure ports, with the aerosol exposure tower having 12 smoke exposure ports, as follows: air flow rate (L/min) = minimum respiratory volume (RMV) of mice/min × number of exposure ports—smoke production/min and RMV = 0.608 × body weight (kg) 0.852. Adult mice weighed approximately 25 g, therefore, the minimum dilution of air was set as follows: 0.608 × 0.0250.852 × 12–0.055 × 2 (2 mouths/min) = 0.204 L/min (Dawkins and Corcoran, 2014).

2.4 Stereotaxic surgery

The surgical procedures were as follows: the mice were anesthetized with isoflurane; the surgery was performed under a continuous gas mixture of oxygen and isoflurane. The mouse head was adjusted to a horizontal position using the Bregma and Lambda points on a stereotaxic instrument. Small holes were drilled above the NAc brain region (anteroposterior, 1.54; mediolateral, 0.55; dorsoventral, 4.05), and bleeding was promptly stopped if it occurred. The virus was injected as a DA neurotransmitter probe, rAAV-hSyn-DA1m-WPRE-pA, with an injection volume of 300 nL and an injection rate of 30–50 nL/min, and the needle was stopped for 10 min after the injection to allow complete virus diffusion. The optical fiber was buried above the NAc of the mice using a specific optical fiber holder, and the optical fiber was fixed with dental cement. After the dental cement was completely dried, the mice were removed from the operating table, and when they awakened, they were marked and returned to the feeding cage.

2.5 Fiber photometry recording

After 3 weeks of virus expression, the fiber-optic patch cord of the fiber-optic recording system was fixedly connected to the

ceramic insert to test the fluorescent signal, and animals that responded well were prepared for smoke exposure. Similarly, the animals were placed in the smoke exposure tower for 3 days before the smoke exposure test, from 9 to 11 a.m. each day for 3 consecutive days, and exposed to air to allow them to adapt to the smoke exposure tower environment and reduce the effects of stress. On the fourth day, DA signals were observed in mice before and after exposure to e-cigarettes and heated cigarettes. The value of ΔF/F = (F-F0)/F0 was used to characterize the change in fluorescence intensity around the event in response to the change in DA neurotransmission under smoke exposure. The recorded data were exported as MAT files for further analysis using the MATLAB software and first preprocessed using the following steps: 1) baseline calibration, 2) downsampling, and 3) smoothing. The change in the neurotransmitter probe signal was calculated using the following formula: F/F = (F-F0)/(F0-Foffset). The significance of the parameters in this formula is as follows: F represents the current signal value; F0 represents the mean signal value 15 min before drug administration; F offset represents the background noise value of the instrument; ΔF/F represents the relative signal change value, expressed as a percentage; and the percentage signal change before and after stimulation was plotted for a single mouse using the MATLAB software plot function.

Experimental fiber-optic mice were anesthetized and perfused with heart after completion of the experiment, 4% paraformaldehyde-fixed mouse brain tissue, and 30% sucrose dehydrated. Mouse brains were frozen, sectioned, and coronally cut (50 μm). It was rinsed with 1 × phosphate-buffered saline, sealed with 50% glycerol, and then photographed using Olympus VS120 sweeper, and data with large deviations in position were discarded.

2.6 Nicotine content in plasma and Cambridge filter

We used high-performance liquid chromatography (HPLC) to examine concentrations after vapor inhalation. The mice were then immediately removed from the chambers and anesthetized with CO_2. Plasma was drawn via cardiac puncture and placed on ice. Immediately after, the plasma was separated via centrifugation (1.5 rpm for 15 min at 4°C). We followed the HPLC protocol to assay plasma or Cambridge filter nicotine levels (Peace et al., 2018; Lu et al., 2022). Identification and quantitation of nicotine was performed using a 3200 Q Trap (Applied Biosystems, Foster City CA) attached to a SCL HPLC system (Shimadzu, Kyoto Japan). Chromatographic separation was performed on a Hypersil® Gold 3 mm × 50 mm, 5 μm column (Thermo Scientific, Waltham MA). The injection volume was 10 μL with a flow rate of 0.5 mL/min, with an isocratic mobile phase consisting of 90:10 Methanol: 10 mmol ammonium formate in water. The ion spray voltage was set to 5,000 V with a declustering potential of 35 eV and the source temperature was 600°C with 30 mL/min curtain gas flow, with the ion source gas 1 at 50 mL/min and ion source Gas 2 at 30 mL/min. Total runtime for this method was 2 min, and the instrument was operated in multiple reaction monitoring mode monitoring the following m/z transitions: nicotine, 163 > 130 and 163 > 117; and nicotine-d4, 167 > 134. A seven-point calibration curve was constructed with nicotine concentrations of 10, 25, 50, 100, 250, 500, and 1,000 ng/mL with 250 ng/mL of nicotine-d4 as internal standard. Aliquots were fortified with internal standard post-collection from the aerosol trap. A linear regression was generated using the peak area ratio of nicotine to internal standard versus nicotine concentration and r2 > 0.9985 for all curves. The limit of quantitation was administratively set at 10 ng/mL and signal-to-noise ratio was greater than 10 times the baseline. All determined sample concentrations were bracketed within the calibration range 10–1,000 ng/mL. Six controls were included with each analytical batch: a blank, a double blank, limit of quantitation quality control (10 ng/mL), low-quality control (30 ng/mL), mid-quality control (300 ng/mL) and high-quality control (900 ng/mL). Intra-day (within-run) accuracy and precision were determined by taking the largest percent coefficient of variation (%CV) and most extreme accuracies for each control concentration out of each of the three runs ($n = 6$). Carryover on the instrument was assessed by running a nicotine-free negative control immediately following the highest concentration calibrator (1,000 ng/mL).

2.7 Statistical analyses

Numerical data are expressed as mean ± standard error of the mean. Offline data analysis was performed using the GraphPad Prism version 6 software (GraphPad Software, United States). Statistical significance was determined by analysis of variance (ANOVA) followed by Bonferroni post-tests for multiple comparisons among more than two groups, where n denotes the number of mice. Every group of mice in each experiment was from at least three animals. For all results, $p < 0.05$ was considered statistically significant.

3 Results

3.1 Effects of nicotine salts on dopamine (DA) release in the nucleus accumbens (NAc)

Nicotine increases the release of DA from the NAc. To better simulate the state of daily smoking, mice with good DA signaling in the NAc were administered different concentrations of various nicotine salts by oral and nasal exposure using a smoke tower to observe the effect of nicotine salts on DA release (Figures 1A–D). Under different concentrations of e-cigarette aerosol exposure (10, 20, 30, 40, and 60 mg/mL), a significant increase in the DA signal curve in the NAc of mice could be observed (Figure 1E), with most nicotine or nicotine salts reaching a peak signal and gradually falling back after approximately 40 min of exposure, after calculating the highest point peak and counting the intensity of the effect of different nicotine salts (Table 1; Figure 1F). Each value represents the percentage increase in DA signal. The statistical results showed elevated and statistically significant DA signaling responses at different concentration gradients (10, 20, 30, 40, and 60 mg/mL) (two-way ANOVA, concentration factor, $F_{[7, 108]} = 34.14$, $p < 0.0001$; different nicotine salt factors, $F_{[4, 108]} = 62.51$, $p < 0.0001$). This indicates that all seven nicotine salts increase DA release in the NAc and show concentration-dependent effects.

10.3389/fphar.2023.1279512

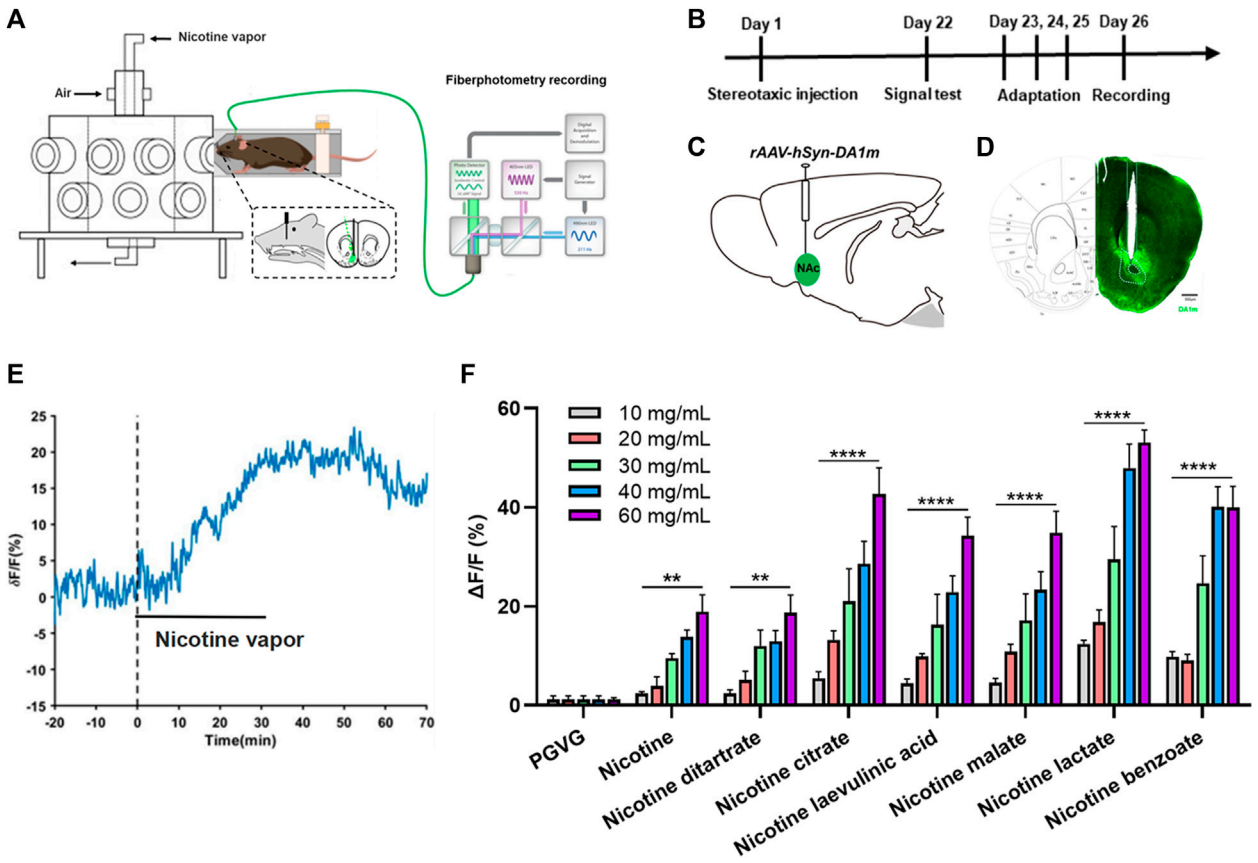

FIGURE 1
Effects of nicotine salts on dopamine release in the nucleus accumbens **(A)** Experimental diagram. **(B)** Experimental timeline. **(C)** Schematic diagram of virus injection. **(D)** Representative graph of virus injection. Scale bar: 500 μM. **(E)** Representative curve of dopamine signal. **(F)** Average ΔF/F in different groups (two-way analysis of variance, concentration factor, $F_{[7, 108]} = 34.14$, $p < 0.0001$; different nicotine salt factors, $F_{[4, 108]} = 62.51$, $p < 0.0001$). $^{**}p < 0.01$, $^{***}p < 0.001$, $^{****}p < 0.0001$. Data are shown as the mean ± standard error of the mean.

TABLE 1 Dopamine signal changes in the nucleus accumbens under different concentrations of nicotine salts exposure.

	10 (mg/mL)	20 (mg/mL)	30 (mg/mL)	40 (mg/mL)	60 (mg/mL)
Nicotine	2.37 ± 0.34	2.37 ± 1.53	9.52 ± 0.74	13.87 ± 1.11	18.91 ± 4.87
Nicotine benzoate	9.82 ± 0.85	9.05 ± 1.00	24.64 ± 4.53	40.11 ± 3.32	39.95 ± 6.05
Nicotine lactate	12.40 ± 0.60	16.82 ± 2.00	29.45 ± 5.42	47.93 ± 3.96	53.08 ± 3.57
Nicotine malate	4.60 ± 0.69	10.81 ± 1.23	17.16 ± 4.39	23.35 ± 3.00	34.85 ± 6.18
Nicotine levulinic acid	4.43 ± 0.72	9.86 ± 0.45	16.3 ± 5.02	22.90 ± 2.64	34.22 ± 5.43
Nicotine ditartrate	2.36 ± 0.64	5.08 ± 1.45	12.10 ± 2.61	12.92 ± 1.80	18.70 ± 5.03
Nicotine citrate	5.47 ± 1.07	13.23 ± 1.50	21.00 ± 5.36	28.58 ± 3.67	42.65 ± 7.56

3.2 Dose–response curve of DA signal changes and nicotine salts in the NAc

The above results suggest that nicotine salts can increase DA release in a concentration-dependent manner. We further analyzed the concentration-dependent increasing curves to compare the pharmacological action characteristics of different nicotine salts. The peak values of DA signal changes obtained from the above seven datasets were non-linearly fitted with the Boltzmann equation to further analyze and summarize the law of biological effects. The concentration effects of each substance were well fitted, in accordance with the general law of non-linearity of biological effects. The different nicotine and nicotine salt groups showed a nonlinear curve characteristic of stronger DA with increasing

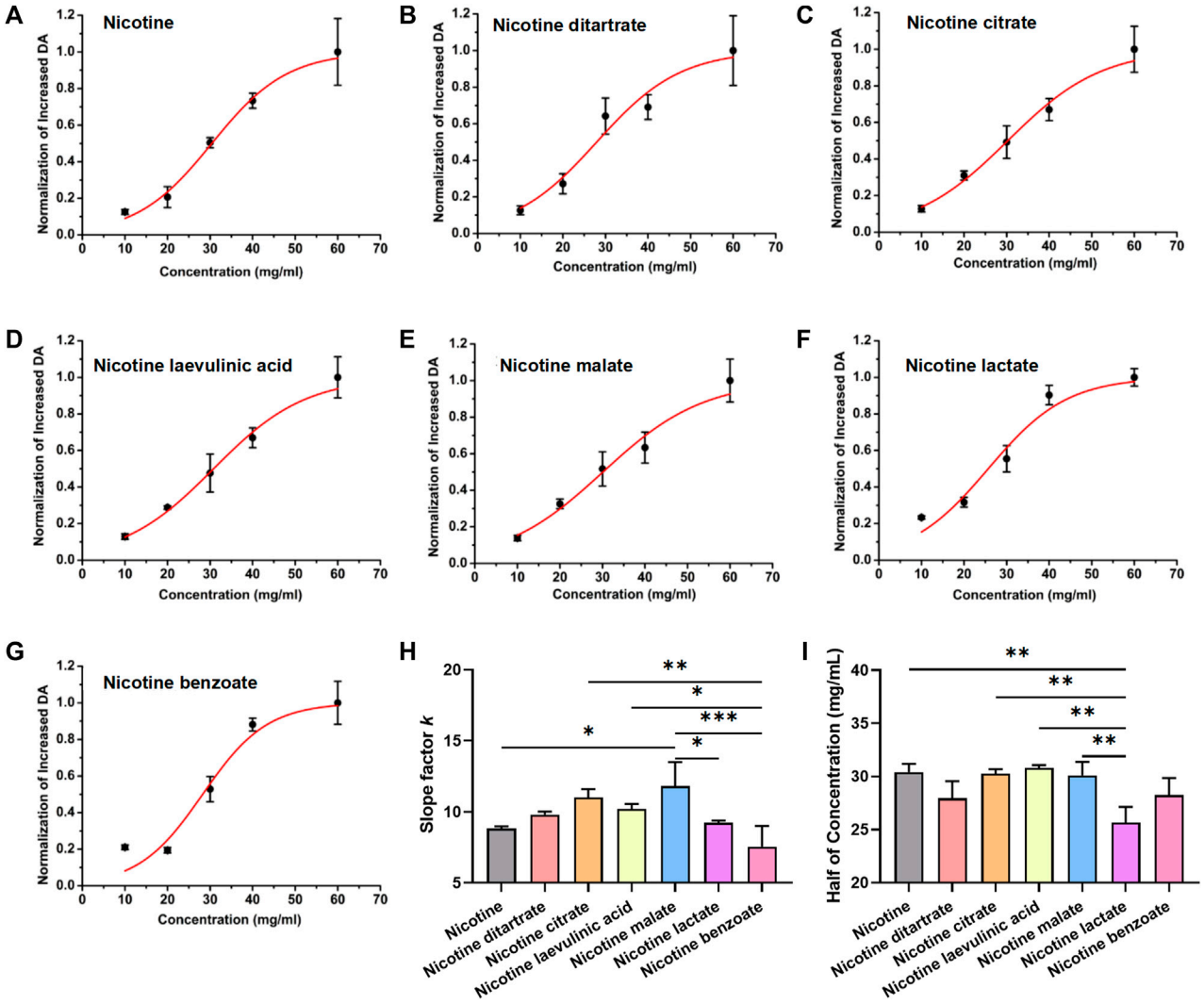

FIGURE 2
Dose–response curve of dopamine signal changes and nicotine salts in the nucleus accumbens **(A)** Boltzmann fitting concentration effect curve of nicotine. **(B)** Boltzmann fitting concentration effect curve of nicotine ditartrate. **(C)** Boltzmann fitting concentration effect curve of nicotine citrate. **(D)** Boltzmann fitting concentration effect curve of nicotine levulinic acid. **(E)** Boltzmann fitting concentration effect curve of nicotine malate. **(F)** Boltzmann fitting concentration effect curve of nicotine lactate. **(G)** Boltzmann fitting concentration effect curve of nicotine benzoate. **(H)** Average slope factor in different group [$n = 3$, one-way analysis of variance (ANOVA), $F_{[6, 14]} = 7.61$, $p = 0.0009$]. **(I)** Average half of concentration in different groups ($n = 3$, one-way ANOVA, $F_{[6, 14]} = 7.43$, $p = 0.001$). $^{**}p < 0.01$, $^{***}p < 0.001$, $^{****}p < 0.0001$. Data are shown as the mean ± standard error of the mean.

concentration (Figures 2A–G), and the slope factor of each fitted curve was statistically significant [Figure 2H, $n = 3$, one-way ANOVA, F (Balfour, 2004; Benowitz, 2010) = 7.61, $p = 0.0009$], indicating that each nicotine salt has a significant effect on the efficiency of concentration change to enhance the release of DA. However, there was a difference in the half-effective concentration for each nicotine salt [Figure 2I, $n = 3$, one-way ANOVA, F (Balfour, 2004; Benowitz, 2010) = 7.43, $p = 0.001$]. These results indicate differences in the pharmacokinetic effects of nicotine salts. The slope for nicotine malate was the largest, indicating that the DA signal was more sensitive to changes in the concentration under the action of this substance. The half-effective concentration of nicotine lactate was the lowest, indicating that this substance was the most potent at increasing DA release.

3.3 Absorption efficiency among different nicotine salts

Previous studies have shown differences in the absorption of different nicotine salts into the blood via the mouth and nose. To better assess the pharmacological effects of nicotine salts on DA release, we further examined the nicotine content at the exit of the smoke exposure tower and in the blood of the animals to determine whether there were differences in the absorption rates of different nicotine salts into the animals. We used multiple outlets of the exposure tower to collect fumes simultaneously at one of the outlets through a Cambridge filter while the animals were exposed to e-cigarette aerosol. Blood was collected from the heart 30 min after aerosol exposure. The total nicotine content of the Cambridge filter and blood was measured using HPLC.

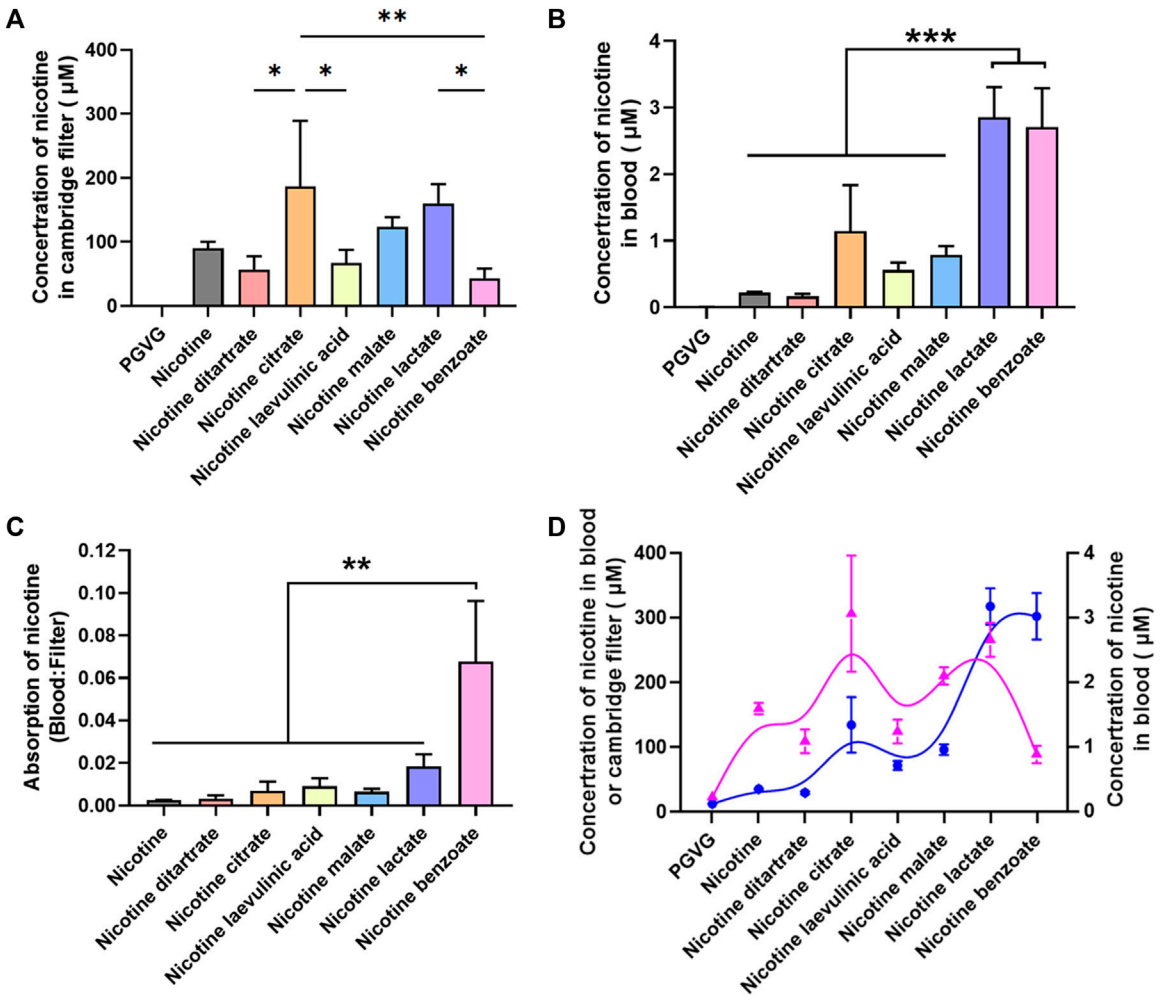

FIGURE 3
Absorption efficiency among different nicotine salts **(A)** Average concentration of nicotine in Cambridge filter in different groups [n = 3, one-way analysis of variance (ANOVA), $F_{[7, 16]} = 7.27$, $p = 0.0005$]. **(B)** Average concentration of nicotine in blood in different groups (n = 3, one-way ANOVA, $F_{[7, 16]} = 28.88$, $p < 0.0001$). **(C)** Average absorption of nicotine in different groups (n = 3, one-way ANOVA, $F_{[6, 14]} = 12.75$, $p < 0.0001$, $p < 0.0001$). **(D)** The Kendall rank correlation coefficient between Cambridge filters and blood [*p-value Sig.(two-tailed)* < 0.05]. *$p < 0.05$, **$p < 0.01$, ***$p < 0.001$. Data are shown as the mean ± standard error of the mean.

The results showed that there were differences in the total nicotine content of Cambridge filters with 60 mg/mL nicotine salt, with nicotine citrate having the highest total nicotine content [Figure 3A, n = 3, one-way ANOVA, F (Di Chiara, 2000; Sych et al., 2019) = 7.27, p = 0.0005], suggesting that there may be differences in the ability of different nicotine salts to produce nicotine after vaporization. The total nicotine content of nicotine lactate and nicotine benzoate in the blood was significantly higher than that of several other nicotine salts [Figure 3B, n = 3, one-way ANOVA, F (Di Chiara, 2000; Sych et al., 2019) = 28.88, $p < 0.0001$]. By comparing the total nicotine in the blood with that in the filter, we observed that the absorption rate of nicotine benzoate was significantly greater than that of several other nicotine salts [Figure 3C, n = 3, one-way ANOVA, F (Balfour, 2004; Benowitz, 2010) = 12.75, $p < 0.0001$]. Subsequently, we assessed the association of strength and direction in nicotine levels between Cambridge filters and blood using the Kendall rank correlation coefficient (Figure 3D, n = 2, Kendall rank correlation coefficient, $p < 0.05$). The results showed a strong correlation between the two variables [*p-value Sig.(two-tailed)* < 0.05], indicating that the final absorbed nicotine concentration in the blood was positively correlated with the original concentration provided.

3.4 Relationship between nicotine levels and DA release

Based on the fact that there was a difference in the absorption rate of different nicotine salts, the difference in the ability of different nicotine salts to increase DA release was correlated with the nicotine content in the blood. To further investigate the pharmacological effects of the different nicotine salts, we compared the correlation of the DA signal with the filter and blood nicotine content at a concentration of 60 mg/mL.

First, from the results of the increase in DA by different nicotine salts at a concentration of 60 mg/mL, the ability of all nicotine salts

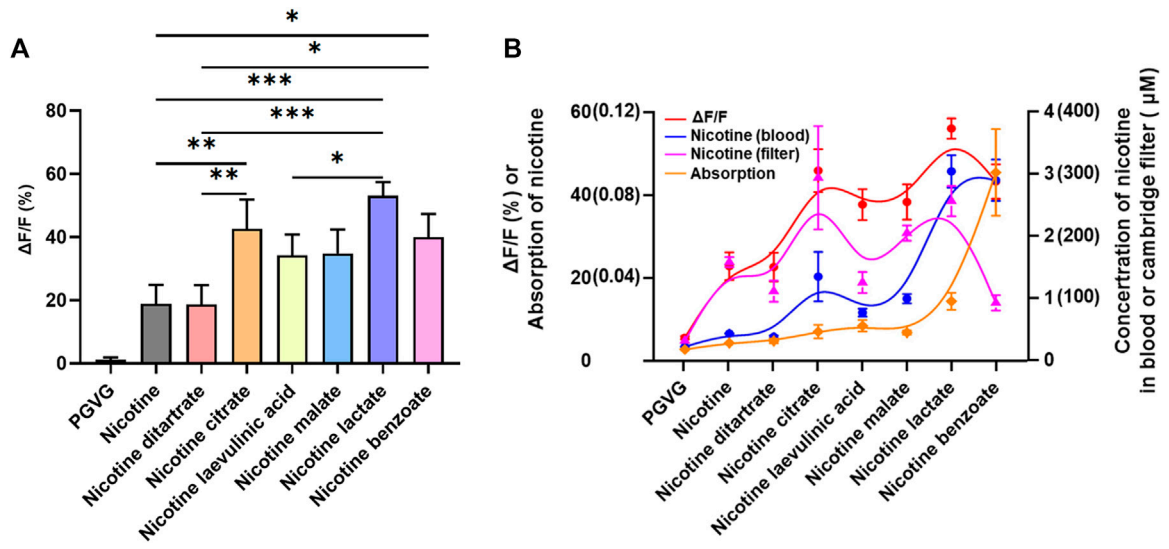

FIGURE 4
Relationship between nicotine levels and dopamine release **(A)** Average ΔF/F in different groups at 60 mg/mL (n = 3, one-way analysis of variance, $F_{[7, 16]} = 19.56$, $p < 0.0001$). **(B)** The Kendall rank correlation coefficient among ΔF/F, Cambridge filters, blood, and absorption [*p-value Sig.(two-tailed)* < 0.05]. *$p < 0.05$, **$p < 0.01$, ***$p < 0.001$. Data are shown as the mean ± standard error of the mean.

to increase DA was higher than that of nicotine, and there were differences in the ability of different nicotine salts to release DA, among which nicotine citrate, nicotine lactate, and nicotine benzoate were stronger than the other nicotine salts [Figure 4A, n = 3, one-way ANOVA, F (Di Chiara, 2000; Sych et al., 2019) = 19.56, $p < 0.0001$]. By analyzing the Kendall rank correlation coefficient to determine the correlation between the Cambridge filter and blood nicotine content, absorption rate, and increased DA signal, the results suggest that increased DA signal has a good positive correlation with nicotine salt in the Cambridge filter and blood nicotine content, whereas there was no correlation with absorption rate [Figure 4B, *p-value Sig.(two-tailed)* < 0.05].

4 Discussion

The main findings of the present study were as follows: 1) Different types of nicotine salts increased the release of DA in the NAc. 2) The slopes and half-effective concentrations of the fitted curves were different, suggesting that each nicotine salt had a difference in the efficiency of increasing DA release with concentration changes. 3) The absorption rates of different nicotine salts containing the same original nicotine concentration were significantly different by measuring the blood nicotine content. The effect of nicotine salts on increasing DA was directly proportional to the blood nicotine level.

This study has the following strength: this is the first study to perform a more comprehensive comparison of the differences in the real-time effects of multiple nicotinic salts on DA in awake animals using a DA receptor fluorescent probe. Our results showed that different nicotine salts both increased NAc DA release, and their ability to increase it was higher than nicotine alone, which is consistent with previous reports (Wickham et al., 2018). However, at the same nicotine concentration, nicotine salts induced more DA release, providing new neurobiological evidence for the previous reports that nicotine salts have stronger satisfaction compared with nicotine (O'Connell et al., 2019). In addition, our technique has a unique advantage in that previous studies mainly utilized methods, such as HPLC, which has a lower temporal resolution. We observed in real time that the DA signal would synchronously increase to the highest point after giving half-hour smoke vapor, and the DA signal would fall back to the baseline level a few minutes after smoke vapor has stopped. This is closely related to the timing of nicotine metabolism, providing new experimental evidence to further understand the interrelationship between nicotine metabolism and DA signaling. In future studies, we will also further focus on the kinetic alterations of DA signaling changes under the action of nicotine salts.

By analyzing the drug action concentration profiles, we also found differences in the kinetics of the pharmacological effects of different nicotine salts. The slope for nicotine malate was the largest, indicating that the DA signal was more sensitive to changes in the concentration under the action of this substance. The half-effective concentration of nicotine lactate was the lowest, indicating that this substance was the most potent at increasing DA release. These results reveal the pharmacological kinetics of different nicotine salts, which have not been reported in previous studies, and provide new experimental evidence for an in-depth understanding of the pharmacological effects of nicotine salts.

Nicotine salt formulations can accommodate high nicotine concentrations without causing discomfort to the user. This is particularly beneficial for individuals seeking a stronger nicotine hit or for those trying to satisfy their nicotine cravings more effectively. Nicotine salts are easily absorbed by the body, allowing faster delivery of nicotine to the bloodstream compared

with freebase nicotine (Gholap et al., 2020; Taylor et al., 2021). Previous studies have used serum nicotine or cotinine levels in e-cigarette smokers to conduct nicotine exposure assessments (Flouris et al., 2013; Marsot and Simon, 2016; Rapp et al., 2020). In this study, we selected five concentration gradients of nicotine or nicotine salts. In the pre-pre-experiment, the blood nicotine levels measured at the low concentration (20 mg/ml) for half an hour of vaping were similar to the blood nicotine levels in humans after smoking the same concentration of e-cigarettes for half an hour, and we believe that this concentration better mimics the reality of human smoking. In order to have a more comprehensive understanding of the pharmacological properties, we therefore set up five concentration gradients. We also measured the amount of nicotine in the blood of mice and the amount of nicotine released from the exposed tower after 30 min of exposure to comprehensively assess the pharmacological effects of nicotine salt exposure. The total nicotine content of nicotine lactate and nicotine benzoate in the blood was significantly higher than that of several other nicotine salts, and the absorption rate of nicotine benzoate was remarkably higher than that of several other nicotine salts. Recent clinical studies evaluating nicotine salt-based e-liquids have shown that nicotine salts lead to higher and faster nicotine absorption compared with nicotine (Mobarrez et al., 2020; Han et al., 2022a). A study by O'Connell et al. (2019) demonstrated that using the same device and vaping conditions, nicotine salts provided higher maximum plasma nicotine concentrations than similar concentrations of nicotine. Our study was conducted at only one time point and could not indicate whether and when the different nicotinate salts reached their highest blood concentrations. This will be further improved in future experiments. However, using the Kendall rank correlation coefficient, we determined that the final absorbed nicotine concentration in the blood was positively correlated with the original concentration.

Furthermore, our results suggest that the effect of nicotinic salts on increasing DA release is positively correlated with blood and filter nicotine levels; however, the strength of the increase varies among nicotinic salts. Nicotine satisfaction is closely related to the protonated and free states of nicotine in the blood (El-Hellani et al., 2015; Talih et al., 2020), and different pH values and organic acid nicotine salts have important effects on the protonated state and stability of nicotine (Han et al., 2022b; Pennings et al., 2023). Our study found that nicotine benzoate and nicotine lactate had a greater ability to increase DA release, and the relationship between their stronger ability and the protonated and free states of nicotine requires further exploration.

In conclusion, we observed the pharmacological effects of multiple nicotine salt e-cigarette exposures on brain DA release using animal models that partially simulate human smoking behavior using *in vivo* fluorescence imaging techniques and found differences in the effects of multiple nicotine salts, providing a new experimental basis for understanding the pharmacological effects of nicotine salts. Notably, the changes reflect only the immediate effects of acute exposure, whereas the clinical population may reflect long-term use. Future studies should investigate the effects of different nicotine salt formulations and concentrations on DA release after long-term e-cigarette use.

Data availability statement

The raw data supporting the conclusion of this article will be made available by the authors, without undue reservation.

Ethics statement

The animal study was approved by the Animal Ethics and Use Committee of ShanghaiTech University. The study was conducted in accordance with the local legislation and institutional requirements.

Author contributions

XL: Conceptualization, Writing–original draft, Data curation, Formal Analysis, Methodology, Project administration. LL: Data curation, Formal Analysis, Methodology, Investigation, Writing–review and editing. YH: Data curation, Formal Analysis, Methodology, Writing–review and editing. HZ: Data curation, Formal Analysis, Methodology, Writing–review and editing. YZ: Data curation, Formal Analysis, Methodology, Writing–review and editing. HS: Data curation, Formal Analysis, Methodology, Writing–review and editing. MC: Conceptualization, Investigation, Supervision, Writing–original draft. JR: Resources, Supervision, Writing–review and editing, Conceptualization, Funding acquisition. YG: Conceptualization, Investigation, Project administration, Resources, Supervision, Writing–review and editing.

Funding

The author(s) declare that no financial support was received for the research, authorship, and/or publication of this article.

Acknowledgments

We thank Dr. Ji Hu (ShanghaiTech University) for helpful discussions and providing the powerful tool for monitoring dopamine release.

Conflict of interest

Authors XL, LL, YH, HZ, YZ, HS, JR, and YG were employed by Shanghai New Tobacco Product Research Institute Co., Ltd.

The remaining author declares that the research was conducted in the absence of any commercial or financial relationships that could be construed as a potential conflict of interest.

Publisher's note

References

Balfour, D. J. (2004). The neurobiology of tobacco dependence: a preclinical perspective on the role of the dopamine projections to the nucleus accumbens [corrected]. *Nicotine Tob. Res.* 6 (6), 899–912. doi:10.1080/14622200412331324965

Balfour, D. J., Wright, A. E., Benwell, M. E., and Birrell, C. E. (2000). The putative role of extra-synaptic mesolimbic dopamine in the neurobiology of nicotine dependence. *Behav. Brain Res.* 113 (1-2), 73–83. doi:10.1016/s0166-4328(00)00202-3

Barrett, S. P., Boileau, I., Okker, J., Pihl, R. O., and Dagher, A. (2004). The hedonic response to cigarette smoking is proportional to dopamine release in the human striatum as measured by positron emission tomography and [11C]raclopride. *Synapse* 54 (2), 65–71. doi:10.1002/syn.20066

Benowitz, N. L. (2010). Nicotine addiction. *N. Engl. J. Med.* 362 (24), 2295–2303. doi:10.1056/NEJMra0809890

Benowitz, N. L. (1996). Pharmacology of nicotine: addiction and therapeutics. *Annu. Rev. Pharmacol. Toxicol.* 36, 597–613. doi:10.1146/annurev.pa.36.040196.003121

Berrendero, F., Mendizabal, V., Robledo, P., Galeote, L., Bilkei-Gorzo, A., Zimmer, A., et al. (2005). Nicotine-induced antinociception, rewarding effects, and physical dependence are decreased in mice lacking the preproenkephalin gene. *J. Neurosci.* 25 (5), 1103–1112. doi:10.1523/JNEUROSCI.3008-04.2005

Dawkins, L., and Corcoran, O. (2014). Acute electronic cigarette use: nicotine delivery and subjective effects in regular users. *Psychopharmacol. Berl.* 231 (2), 401–407. doi:10.1007/s00213-013-3249-8

Di Chiara, G. (2000). Role of dopamine in the behavioural actions of nicotine related to addiction. *Eur. J. Pharmacol.* 393 (1-3), 295–314. doi:10.1016/s0014-2999(00)00122-9

Duell, A. K., Pankow, J. F., and Peyton, D. H. (2020). Nicotine in tobacco product aerosols: 'It's deja vu all over again. *Tob. Control* 29 (6), 656–662. doi:10.1136/tobaccocontrol-2019-055275

El-Hellani, A., El-Hage, R., Baalbaki, R., Salman, R., Talih, S., Shihadeh, A., et al. (2015). Free-base and protonated nicotine in electronic cigarette liquids and aerosols. *Chem. Res. Toxicol.* 28 (8), 1532–1537. doi:10.1021/acs.chemrestox.5b00107

Farsalinos, K. E., and Gillman, G. (2017). Carbonyl emissions in E-cigarette aerosol: A systematic review and methodological considerations. *Front. Physiol.* 8, 1119. doi:10.3389/fphys.2017.01119

Flouris, A. D., Chorti, M. S., Poulianiti, K. P., Jamurtas, A. Z., Kostikas, K., Tzatzarakis, M. N., et al. (2013). Acute impact of active and passive electronic cigarette smoking on serum cotinine and lung function. *Inhal. Toxicol.* 25 (2), 91–101. doi:10.3109/08958378.2012.758197

Gades, M. S., Alcheva, A., Riegelman, A. L., and Hatsukami, D. K. (2022). The role of nicotine and flavor in the abuse potential and appeal of electronic cigarettes for adult current and former cigarette and electronic cigarette users: A systematic review. *Nicotine Tob. Res.* 24 (9), 1332–1343. doi:10.1093/ntr/ntac073

Gallezot, J. D., Kloczynski, T., Weinzimmer, D., Labaree, D., Zheng, M. Q., Lim, K., et al. (2014). Imaging nicotine- and amphetamine-induced dopamine release in rhesus monkeys with [(11)C]PHNO vs [(11)C]raclopride PET. *Neuropsychopharmacology* 39 (4), 866–874. doi:10.1038/npp.2013.286

Gholap, V. V., Kosmider, L., Golshahi, L., and Halquist, M. S. (2020). Nicotine forms: Why and how do they matter in nicotine delivery from electronic cigarettes? *Expert Opin. Drug Deliv.* 17 (12), 1727–1736. doi:10.1080/17425247.2020.1814736

Han, S., Chen, H., Su, Y., Cui, L., Feng, P., Fu, Y., et al. (2022b). Simultaneous quantification of nicotine salts in e-liquids by LC-MS/MS and GC-MS. *Anal. Methods* 14 (42), 4185–4192. doi:10.1039/d2ay00799a

Han, S., Liu, C., Chen, H., Fu, Y., Zhang, Y., Miao, R., et al. (2022a). Pharmacokinetics of freebase nicotine and nicotine salts following subcutaneous administration in male rats. *Drug Test. Anal.* 2022. doi:10.1002/dta.3363

Lu, L., Xiang, M., Lu, H., Tian, Z., and Gao, Y. (2022). Progress in quantification of nicotine content and form distribution in electronic cigarette liquids and aerosols. *Anal. Methods* 14 (4), 359–377. doi:10.1039/d1ay01679b

Marsot, A., and Simon, N. (2016). Nicotine and cotinine levels with electronic cigarette: A review. *Int. J. Toxicol.* 35 (2), 179–185. doi:10.1177/1091581815618935

Mobarrez, F., Antoniewicz, L., Hedman, L., Bosson, J. A., and Lundback, M. (2020). Electronic cigarettes containing nicotine increase endothelial and platelet derived extracellular vesicles in healthy volunteers. *Atherosclerosis* 301, 93–100. doi:10.1016/j.atherosclerosis.2020.02.010

O'Connell, G., Pritchard, J. D., Prue, C., Thompson, J., Verron, T., Graff, D., et al. (2019). A randomised, open-label, cross-over clinical study to evaluate the pharmacokinetic profiles of cigarettes and e-cigarettes with nicotine salt formulations in US adult smokers. *Intern Emerg. Med.* 14 (6), 853–861. doi:10.1007/s11739-019-02025-3

Peace, M. R., Mulder, H. A., Baird, T. R., Butler, K. E., Friedrich, A. K., Stone, J. W., et al. (2018). Evaluation of nicotine and the components of e-liquids generated from e-cigarette aerosols. *J. Anal. Toxicol.* 42 (8), 537–543. doi:10.1093/jat/bky056

Pennings, J. L. A., Havermans, A., Pauwels, C., Krusemann, E. J. Z., Visser, W. F., and Talhout, R. (2023). Comprehensive Dutch market data analysis shows that e-liquids with nicotine salts have both higher nicotine and flavour concentrations than those with free-base nicotine. *Tob. Control* 32 (1), e78–e82. doi:10.1136/tobaccocontrol-2021-056952

Rapp, J. L., Alpert, N., Flores, R. M., and Taioli, E. (2020). Serum cotinine levels and nicotine addiction potential of e-cigarettes: an NHANES analysis. *Carcinogenesis* 41 (10), 1454–1459. doi:10.1093/carcin/bgaa015

Robichaud, M. O., Seidenberg, A. B., and Byron, M. J. (2020). Tobacco companies introduce 'tobacco-free' nicotine pouches. *Tob. Control* 29 (1), e145–e146. doi:10.1136/tobaccocontrol-2019-055321

Skirzewski, M., Princz-Lebel, O., German-Castelan, L., Crooks, A. M., Kim, G. K., Tarnow, S. H., et al. (2022). Continuous cholinergic-dopaminergic updating in the nucleus accumbens underlies approaches to reward-predicting cues. *Nat. Commun.* 13 (1), 7924. doi:10.1038/s41467-022-35601-x

Sun, F., Zeng, J., Jing, M., Zhou, J., Feng, J., Owen, S. F., et al. (2018). A genetically encoded fluorescent sensor enables rapid and specific detection of dopamine in flies, fish, and mice. *Cell* 174 (2), 481–496. doi:10.1016/j.cell.2018.06.042

Sych, Y., Chernysheva, M., Sumanovski, L. T., and Helmchen, F. (2019). High-density multi-fiber photometry for studying large-scale brain circuit dynamics. *Nat. Methods* 16 (6), 553–560. doi:10.1038/s41592-019-0400-4

Talih, S., Salman, R., El-Hage, R., Karaoghlanian, N., El-Hellani, A., Saliba, N., et al. (2020). Effect of free-base and protonated nicotine on nicotine yield from electronic cigarettes with varying power and liquid vehicle. *Sci. Rep.* 10 (1), 16263. doi:10.1038/s41598-020-73385-6

Taylor, A., Dunn, K., and Turfus, S. (2021). A review of nicotine-containing electronic cigarettes-Trends in use, effects, contents, labelling accuracy and detection methods. *Drug Test. Anal.* 13 (2), 242–260. doi:10.1002/dta.2998

Tizabi, Y., Bai, L., Copeland, R. L., Jr., and Taylor, R. E. (2007). Combined effects of systemic alcohol and nicotine on dopamine release in the nucleus accumbens shell. *Alcohol Alcohol* 42 (5), 413–416. doi:10.1093/alcalc/agm057

Wickham, R. J., Nunes, E. J., Hughley, S., Silva, P., Walton, S. N., Park, J., et al. (2018). Evaluating oral flavorant effects on nicotine self-administration behavior and phasic dopamine signaling. *Neuropharmacology* 128, 33–42. doi:10.1016/j.neuropharm.2017.09.029

Wonnacott, S., Sidhpura, N., and Balfour, D. J. (2005). Nicotine: from molecular mechanisms to behaviour. *Curr. Opin. Pharmacol.* 5 (1), 53–59. doi:10.1016/j.coph.2004.12.002

frontiers | Frontiers in Pharmacology

TYPE Original Research
PUBLISHED 09 November 2023
DOI 10.3389/fphar.2023.1264591

OPEN ACCESS

EDITED BY
Song Zhang,
Shanghai Jiao Tong University, China

REVIEWED BY
Xi Wu,
Shanghai Jiao Tong University, China
Shaojia Lu,
Zhejiang University, China

*CORRESPONDENCE
Shuyun Li,
jiujiang1996@163.com

RECEIVED 21 July 2023
ACCEPTED 20 October 2023
PUBLISHED 09 November 2023

CITATION
Chen X, Fan Y, Ren W, Sun M, Guan X, Xiu M and Li S (2023), Baseline BMI is associated with clinical symptom improvements in first-episode schizophrenia: a longitudinal study. *Front. Pharmacol.* 14:1264591. doi: 10.3389/fphar.2023.1264591

Baseline BMI is associated with clinical symptom improvements in first-episode schizophrenia: a longitudinal study

Xiaofang Chen[1], Yong Fan[2], Wenchao Ren[2], Maodi Sun[3], Xiaoni Guan[1], Meihong Xiu[1] and Shuyun Li[4,5,6]*

[1]Beijing Huilongguan Hospital, Peking University Huilongguan Clinical Medical School, Beijing, China, [2]Qingdao Mental Health Center, Qingdao, China, [3]North University of China, Taiyuan, China, [4]Department of Nutritional and Metabolic Psychiatry, The Affiliated Brain Hospital of Guangzhou Medical University, Guangzhou, China, [5]Guangdong Engineering Technology Research Center for Translational Medicine of Mental Disorders, Guangzhou, China, [6]Key Laboratory of Neurogenetics and Channelopathies of Guangdong Province and the Ministry of Education of China, Guangzhou Medical University, Guangzhou, China

Background: There is sufficient evidence of the high prevalence of obesity in schizophrenia (SZ) compared to the general population. Previous studies have reported that weight gain correlated with the response to antipsychotics in patients with SZ. Nonetheless, the relationship between body mass index (BMI) and therapeutic benefits remains unclear. This study was designed to investigate the association between baseline BMI and improvements in clinical symptoms after treatment with antipsychotics in first-episode and medication-naïve SZ (FEMNS).

Methods: A total of 241 FEMNS patients were enrolled and received risperidone over 12 weeks. The severity of symptoms was assessed by the Positive and Negative Syndrome Scale (PANSS) and BMI was measured at baseline and 12-week follow-up.

Results: We found that risperidone treatment raised the body weight of FEMNS patients and baseline BMI was negatively correlated with the improvement in negative symptoms ($r = -0.14$, $p = 0.03$) after 12-week treatment. Linear regression analysis indicated that baseline BMI was an independent predictor of response to risperidone in the early stage of SZ.

Conclusion: The current study suggests a close relationship between baseline BMI and improvement in negative symptoms in SZ.

KEYWORDS

schizophrenia, weight, improvements, negative symptoms, risperidone

1 Introduction

Atypical antipsychotics are reported to be associated with severe side effects like weight gain, obesity, and metabolic dysfunction (Li et al., 2018; Luckhoff et al., 2019; Li et al., 2021). It is reported that the prevalence of obesity ranges from 10% to 60% in SZ patients (Naslund et al., 2016; Annamalai et al., 2017). Weight gain/obesity impacts the quality of life and adherence to antipsychotic drugs in SZ (Dibonaventura et al., 2012; Pillinger et al., 2020).

A large of evidence has identified weight gain as a prognosis biomarker of the response to antipsychotic drugs (Ascher-Svanum et al., 2005; Bai et al., 2006; Sharma et al., 2014), underscoring the need for early monitoring of weight in SZ patients. Even in adolescents with SZ, substantial

decreases in global psychopathology have been reported to be associated with weight gain after taking antipsychotic medications (Sharma et al., 2014). Studies have demonstrated that risperidone was associated with intermediate weight gain (1.76 kg), compared with olanzapine with the highest (3.45 kg) (De Hert et al., 2011). It is reported that individuals who were younger, female and first-episode and were less exposed to antipsychotics previously were more likely to increase the risk of obesity.

Antipsychotics have different treatment outcomes for patients with SZ (Zhu et al., 2022). Some studies have revealed the prognostic role of weight gain after treatment with antipsychotics in favorable treatment outcomes (Chen et al., 2021). However, considering the independence from confounding factors, such as treatment adherence and duration, the clinical significance of such a relationship has been questioned (Correll et al., 2011; De Hert et al., 2011; Hermes et al., 2011). Notably, a previous study has reported that baseline BMI correlated with antipsychotic-induced weight gain, and it was a predictive biomarker in the therapeutic response to antipsychotics (Verma et al., 2009). Another study in adolescents with SZ revealed that olanzapine-associated weight gain was not independently correlated with therapeutic response to olanzapine, but baseline obesity was related to more olanzapine-associated weight gain and symptomatic outcome (Kemp et al., 2013).

Studies have shown that the first-episode and medication-naive SZ (FEMNS) patients display the advantage of reducing the possible impacts of the use of antipsychotics, the duration of illness, and the impact of comorbidities associated with chronic illness (Xiu et al., 2020). In exploring the link between BMI and response to antipsychotics, thus, we recruited FEMNS patients in the current study. This study was designed to determine the predictive role of baseline BMI in the symptom improvements after 12-week treatment with risperidone in SZ.

2 Materials and methods

2.1 Patients

FEMNS patients were recruited from Beijing Hui-long-guan Hospital and Zhu-ma-dian Hospital. Patients were diagnosed with SZ as the Structured Clinical Interview for DSM-IV (SCID). The inclusion criteria were: 1) male and female inpatients; 2) first onset of psychosis; 3) between the ages of 18 and 45; 4) duration of illness less than 5 years; 5) previous antipsychotics exposure less than 14 days; 6) without substance abuse except for tobacco; 7) without major medical illness, such as diabetes, metabolic syndrome, hypertension, and cardiovascular disease; and 8) without taking weight-loss drug.

FEMNS patients received a flexible dose of risperidone for 12 weeks. During this 12-week study, all participants were hospitalized and nurses monitored compliance with risperidone. The protocol was approved by the ethical committee of Beijing Hui-long-guan Hospital (Ethic No.: 2011-4). Written informed consent was obtained from each patient.

2.2 BMI measurement

Height was determined by a metric stadiometer after removing the shoes. Weight was determined following overnight fasting at baseline and 12-week follow-up. Weight was measured in a hospital uniform with the pocket empty and without shoes. BMI was calculated using the weight divided by the height. All measurements were taken twice for each patient, and the mean was recorded.

In the present study, patients were classified into a high-BMI group when their BMI was 24 kg/m^2 or higher and a low BMI group when their BMI was lower than 24 kg/m^2, as in previous studies (An et al., 2018; Chen et al., 2023).

2.3 Clinical symptoms

The severity of symptoms was evaluated using the Positive and Negative Syndrome Scale (PANSS). The interviewers were trained before the assessment. After training, the inter-observer correlation coefficient for the PANSS total score was maintained at >0.8 during repeated assessments. PANSS scales were assessed at baseline and the end of 12 weeks. Improvement in clinical symptoms was calculated as the changes in PANSS score between baseline and 12-week follow-up after treatment with risperidone.

2.4 Statistical analysis

All statistical analyses were conducted using SPSS version 20.0. Statistical significance was defined as $p < 0.05$.

As described previously, the Last-observation-carried-forward (LOCF) was used for the data of the last time point of patients who dropped out (Wang et al., 2014; Raven et al., 2020; Wimms et al., 2020). ANOVA and X^2 test were used to investigate whether there was a difference in demographic and clinical characteristics, body weight and BMI between the groups at baseline. If there were differences between the two groups, then the analysis of covariance (ANCOVA) was performed after controlling for the confounding variables. Then, Pearson correlation analysis was used to explore the relationship between BMI and PANSS scores at baseline, and further the relationship between baseline BMI and reductions in PANSS scores after treatment. Further regression analysis was performed to assess the association of BMI at baseline with the decrease in PANSS scores after 12 weeks of treatment after adjusting for various confounding factors.

3 Results

The sample included 241 FEMNS patients (128 men, 113 women). Thirty-eight participants were lost before the 2-month follow-up and 53 patients were lost after 2 months of treatment with risperidone. Finally, a total of 91 patients were lost. Table 1 shows the differences between completers and those who dropped out in the follow-up. There were no significant differences in the demographic characteristics and clinical data between completers and drop-outs (all $p > 0.05$).

After treatment, the mean changes in weight were 2.7 kg (SD = 3.8). According to the criteria of obesity, we identified 34 patients in the high BMI group and 207 patients in the low BMI group. Comparisons of demographic characteristics and clinical data between the high BMI and low BMI groups are shown in Table 1. The mean changes in weight were 0.4 (95% CI: −0.7–1.5) in the high BMI subgroup and 3.1 (95% CI: 2.5–3.6) in the low BMI subgroup. Significant differences were observed in weight gain between the low BMI and high BMI subgroups ($p < 0.01$).

TABLE 1 Demographic characteristics and clinical data.

Variable	Completers (n = 150)	Dropouts (n = 91)	F or χ^2 (p-value)	Low BMI group (n = 207)	High BMI group (n = 34)	F or χ^2 (p-value)
Sex (M/F)	80/70	48/43	0.01 (0.93)	109/98	19/15	0.1 (0.73)
Age (y)	28.1 ± 9.3	26.8 ± 9.0	1.1 (0.31)	27.1 ± 9.3	30.8 ± 8.3	4.8 (0.03)
Weight (kg)	59.6 ± 11.9	57.1 ± 9.8	2.9 (0.09)	56.1 ± 8.3	78.2 ± 10.3	<0.001
BMI (kg/m^2)	21.6 ± 3.6	20.9 ± 3.0	2.1 (0.15)	20.3 ± 2.1	27.7 ± 2.8	<0.001
Age of onset (y)	26.3 ± 9.2	25.7 ± 9.1	0.3 (0.59)	26.0 ± 9.3	28.2 ± 8.5	1.5 (0.23)
PANSS score						
Positive	21.6 ± 6.3	22.3 ± 6.2	0.8 (0.38)	22.0 ± 6.8	22.8 ± 5.3	0.4 (0.55)
Negative	19.1 ± 6.5	18.3 ± 7.2	0.8 (0.37)	18.9 ± 7.2	18.1 ± 6.2	0.3 (0.58)
General	35.1 ± 10.0	36.1 ± 8.9	0.6 (0.44)	35.7 ± 10.3	37.0 ± 8.9	0.4 (0.52)
Total	75.6 ± 17.7	76.5 ± 16.8	0.1 (0.70)	76.4 ± 18.7	78.0 ± 14.9	0.2 (0.67)

Abbreviations: *y*, years; *ms*, months; *BMI*, body mass index.

TABLE 2 Reduction of symptoms after 12-week treatment with risperidone in the low BMI and high BMI groups.

	Changes in PANSS and weight (95% CI)[a]	
	High BMI group	Low BMI group
	n = 34	n = 207
Positive subscore	10.2 (7.8–12.6)**	8.5 (7.6–9.5)**
Negative subscore	2.9 (1.3–4.5)**	4.1 (3.2–4.9)**
General subscore	10.7 (8.2–13.3)**	9.1 (7.7–10.4)**
PANSS total score	28.0 (23.1–32.9)**	21.5 (18.7–24.2)**

[a]Paired t-test to compare the changes of PANSS, and its subscores after treatment with risperidone between baseline and week 12 after treatment. **$p < 0.01$, *$p < 0.05$.

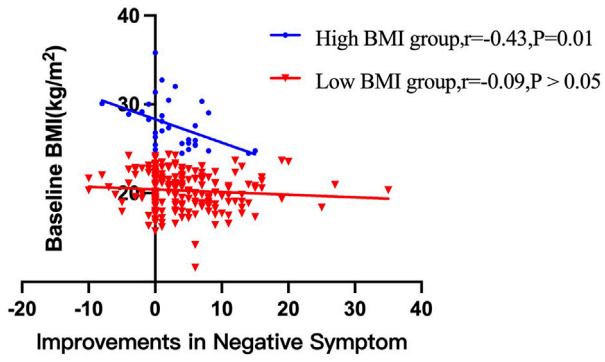

FIGURE 1
There were significant associations between baseline BMI and improvements in negative symptom improvements after 12 weeks of treatment with risperidone in high BMI group ($p < 0.05$), but not in low BMI group.

After treatment with risperidone, clinical symptoms were significantly improved (Bonferroni corrected all $p < 0.05$) (Table 2). Pearson correlation analysis revealed that baseline BMI was negatively correlated with the improvement in negative symptoms ($r = -0.14$, $p = 0.03$). After subgroup analysis, we found that the negative association was only present in the high BMI group ($r = -0.43$, $p = 0.01$), but not in the low BMI group (Figure 1). Moreover, baseline BMI was not associated with the improvement in positive symptoms, general psychopathology, and PANSS total score (all $p > 0.05$). Further linear regression analysis confirmed that baseline BMI ($\beta = -0.15$, $t = -2.2$, $p = 0.027$) was a predictive factor for negative symptom improvements, while sex, age and years of education were not associated with negative symptom improvement (all $p > 0.05$).

Further, among those with low BMI, we found 28 patients were underweight or with undernutrition. To rule out their influence on the results, we reanalyzed the data without these 28 patients and there was no difference in the result (Supplementary Tables S1).

4 Discussion

We here found that baseline BMI was associated with weight gain and negative symptom improvements in this relatively large sample of FEMNS patients on 12-week treatment with risperidone. However, we did not find an association between female sex, younger age education levels, and symptom improvements.

This study found that baseline BMI was significantly associated with weight gain after 3 months of risperidone monotherapy. Patients with a lower baseline BMI gained more weight after risperidone

medication than those with a higher baseline BMI. Our findings are in line with most previous studies (Jones et al., 2001; Leucht et al., 2013; Huhn et al., 2019) and the recent longitudinal cohort study in FEMN patients with SCZ (Vázquez-Bourgon et al., 2022), providing further evidence for a relationship between baseline BMI/bodyweight and antipsychotic-induced weight gain in SCZ (Gentile, 2009; Verma et al., 2009). Notably, previous evidence-based data reveal that a variety of other risk factors, including ethnicity, young age, recent onset of psychotic symptoms, unemployment, unhealthy lifestyle and low income, may contribute to the rate or magnitude of antipsychotic-induced weight gain during long-term treatments (Gentile, 2009). However, in this study, we did not find an association between weight gain and education years, which was well-known to be strongly associated with unemployment, unhealthy diet and low income. This may be due to the differences between the patients with SCZ we recruited in this study and those in previous studies, considering that a majority of previous studies have investigated weight gain in outpatients on long-term antipsychotic medication.

We further found that baseline BMI was an independent predictor for the improvement of negative symptoms after treatment, after controlling for age, sex, and education years. Indeed, there is evidence to show a close relationship between negative symptoms in SZ patients and BMI at baseline (Jones et al., 2001; Leucht et al., 2013; Sharma et al., 2014; Raben et al., 2017; Huhn et al., 2019), which is consistent with our findings. The findings in the current study were also in line with the studies on FEMNS patients (Zipursky et al., 2005; Venkatasubramanian et al., 2010; Kemp et al., 2013). Importantly, the abovementioned studies have all controlled for confounding factors, such as sex, age, antipsychotic medications, and duration of illness.

However, the exact mechanism remains unclear. It may be due to the shared mechanistic pathway between body weight regulation and negative symptom improvements after antipsychotics. Risperidone has been reported to have a relatively high affinity for D_2, 5-HT_2, histamine H_1 receptors, and NE alpha-2 receptors (Nasrallah, 2008). Animal studies also revealed that obesity induced by a high-fat diet and increased food intake correlated with 5-HT_2 deficiency (Mercer et al., 1994). In particular, the use of antipsychotics may lead to the preferential metabolism of carbohydrates over fats and further lead to increased fat storage (Tiwari et al., 2018; Kaar et al., 2019). Leptin, a key signal for determining the size of fat depots in the brain, was found to be increased following atypical antipsychotic medication (Brömel et al., 1998; Kraus et al., 1999). On the other hand, dopamine D_2 receptors play an important role in the reward circuit and in mediating both obesity and therapeutic response to antipsychotics, which may explain the association between BMI and therapeutic benefits in SZ.

Higher BMI was associated with fewer negative symptom changes in this study. It is reported that in patients with higher BMI in the early phase of SZ, brain functional connectivity associated with food cravings and weight control was decreased (Homan et al., 2019). Additionally, the prefrontal cortex of obese patients exhibited altered insulin and DA gene expression, resulting in relatively poorer outcomes than those with lower BMI (Mansur et al., 2018). Altogether, this study suggests that BMI at baseline may be a more sensitive indicator of the therapeutic benefits in the early stage of SZ, as most of the reported correlations between weight gain and therapeutic responses to antipsychotics are mixed.

Some strengths should be mentioned in this study. This is a prospective and longitudinal study examining a well-characterized group of FEMNS patients. Standardized treatment with a single antipsychotic excluded the different impacts of antipsychotic drugs. However, this study has several limitations. First, in this study, obesity-related biomarkers such as glucose, cholesterol, insulin resistance, and lipids were not recorded. Additionally, other metabolic parameters, such as food preference, dietary record, and caloric intake were also not collected. Second, only risperidone was assessed in our study. Therefore, the results of this study may not be generalized to other types of antipsychotics that may be different in metabolic disturbance. Third, the criteria for obesity in our study are only for Chinese, thus the conclusions in this study cannot be generalized to other populations. Fourth, the regulation of body weight may overlap with the pharmacological mechanisms of antipsychotic drugs. Genetic factors are known to be associated with the pharmacodynamics, pharmacokinetics, and adverse effects of antipsychotics. Additional pharmacogenetic analyses may provide new insights into the current findings. Fifth, considering the role of lifestyle, diet, and exercise in explaining the contradictory findings across studies, we did not collect the detailed diet and exercise in the present study.

In conclusion, the current study found that BMI was negatively correlated with the improvements in negative symptoms after treatment with risperidone for 12 weeks in FEMNS patients. In addition, we identified baseline BMI as an independent predictor for negative symptom improvements in SZ. Our study underscores the key role of BMI in the clinical management of patients in the early stage of SZ. These findings provide further evidence that greater efforts should be made to prevent obesity in clinical practice from the early phase of SZ.

Data availability statement

The raw data supporting the conclusion of this article will be made available by the authors, without undue reservation.

Ethics statement

The studies involving humans were approved by the ethics committee of Beijing Huilongguan Hospital. The studies were conducted in accordance with the local legislation and institutional requirements. The participants provided their written informed consent to participate in this study.

Author contributions

YF: Conceptualization, Writing–original draft, Investigation. XG: Conceptualization, Investigation, Writing–original draft. MX: Conceptualization, Writing–original draft. SL: Data curation, Writing–original draft. XC: Writing-original draft, review and editing. MS: Data curation. WR: Investigation, review and editing.

Funding

The authors declare financial support was received for the research, authorship, and/or publication of this article. This study was funded by the Guangzhou Municipal Health Commission (2023C-TS26), Opening

Foundation of Jiangsu Key Laboratory of Neurodegeneration, Nanjing Medical University (KF202202), Open Project Program of State Key Laboratory of Virtual Reality Technology and Systems, Beihang University (VRLAB2022 B02), and Shanghai Key Laboratory of Psychotic Disorders Open Grant (21-K03), Guangzhou High-level Clinical Key Specialty, and Guangzhou Research-oriented Hospital.

Acknowledgments

We would like to thank the participants in the study and their families.

Conflict of interest

The authors declare that the research was conducted in the absence of any commercial or financial relationships that could be construed as a potential conflict of interest.

Supplementary material

The Supplementary Material for this article can be found online at: https://www.frontiersin.org/articles/10.3389/fphar.2023.1264591/full#supplementary-material

References

An, H., Du, X., Huang, X., Qi, L., Jia, Q., and Yin, G., (2018). Obesity, altered oxidative stress, and clinical correlates in chronic schizophrenia patients. *Transl. Psychiatry* 8 (1), 258. doi:10.1038/s41398-018-0303-7

Annamalai, A., Kosir, U., and Tek, C. (2017). Prevalence of obesity and diabetes in patients with schizophrenia. *World J. Diabetes* 8 (8), 390–396. doi:10.4239/wjd.v8.i8.390

Ascher-Svanum, H., Stensland, M. D., Kinon, B. J., and Tollefson, G. D. (2005). Weight gain as a prognostic indicator of therapeutic improvement during acute treatment of schizophrenia with placebo or active antipsychotic. *J. Psychopharmacol.* 19 (6), 110–117. doi:10.1177/0269881105058978

Bai, Y. M., Lin, C. C., Chen, J. Y., Lin, C. Y., Su, T. P., and Chou, P. (2006). Association of initial antipsychotic response to clozapine and long-term weight gain. *Am. J. Psychiatry* 163 (7), 1276–1279. doi:10.1176/appi.ajp.163.7.1276

Brömel, T., Blum, W. F., Ziegler, A., Schulz, E., Bender, M., and Fleischhaker, C., (1998). Serum leptin levels increase rapidly after initiation of clozapine therapy. *Mol. Psychiatry* 3 (1), 76–80. doi:10.1038/sj.mp.4000352

Chen, K., Shen, Z., Gu, W., Lyu, Z., Qi, X., and Mu, Y., (2023). Prevalence of obesity and associated complications in China: a cross-sectional, real-world study in 15.8 million adults. *Diabetes Obes. Metab.* 25, 3390–3399. doi:10.1111/dom.15238

Chen, Y. Q., Li, X. R., Zhang, L., Zhu, W. B., Wu, Y. Q., and Guan, X. N., (2021). Therapeutic response is associated with antipsychotic-induced weight gain in drug-naive first-episode patients with schizophrenia: an 8-week prospective study. *J. Clin. Psychiatry* 82 (3), 20m13469. doi:10.4088/JCP.20m13469

Correll, C. U., Lencz, T., and Malhotra, A. K. (2011). Antipsychotic drugs and obesity. *Trends Mol. Med.* 17 (2), 97–107. doi:10.1016/j.molmed.2010.10.010

De Hert, M., Detraux, J., van Winkel, R., Yu, W., and Correll, C. U. (2011). Metabolic and cardiovascular adverse effects associated with antipsychotic drugs. *Nat. Rev. Endocrinol.* 8 (2), 114–126. doi:10.1038/nrendo.2011.156

De Hert, M., Dobbelaere, M., Sheridan, E. M., Cohen, D., and Correll, C. U. (2011). Metabolic and endocrine adverse effects of second-generation antipsychotics in children and adolescents: a systematic review of randomized, placebo controlled trials and guidelines for clinical practice. *Eur. Psychiatry* 26 (3), 144–158. doi:10.1016/j.eurpsy.2010.09.011

Dibonaventura, M., Gabriel, S., Dupclay, L., Gupta, S., and Kim, E. (2012). A patient perspective of the impact of medication side effects on adherence: results of a cross-sectional nationwide survey of patients with schizophrenia. *BMC Psychiatry* 12, 20. doi:10.1186/1471-244X-12-20

Gentile, S. (2009). Contributing factors to weight gain during long-term treatment with second-generation antipsychotics. A systematic appraisal and clinical implications. *Obes. Rev.* 10 (5), 527–542. doi:10.1111/j.1467-789X.2009.00589.x

Hermes, E., Nasrallah, H., Davis, V., Meyer, J., McEvoy, J., and Goff, D., (2011). The association between weight change and symptom reduction in the CATIE schizophrenia trial. *Schizophr. Res.* 128 (1-3), 166–170. doi:10.1016/j.schres.2011.01.022

Homan, P., Argyelan, M., Fales, C. L., Barber, A. D., DeRosse, P., and Szeszko, P. R., (2019). Striatal volume and functional connectivity correlate with weight gain in early-phase psychosis. *Neuropsychopharmacology* 44 (11), 1948–1954. doi:10.1038/s41386-019-0464-y

Huhn, M., Nikolakopoulou, A., Schneider-Thoma, J., Krause, M., Samara, M., and Peter, N., (2019). Comparative efficacy and tolerability of 32 oral antipsychotics for the acute treatment of adults with multi-episode schizophrenia: a systematic review and network meta-analysis. *Lancet* 394 (10202), 939–951. doi:10.1016/S0140-6736(19)31135-3

Jones, B., Basson, B. R., Walker, D. J., Crawford, A. M., and Kinon, B. J. (2001). Weight change and atypical antipsychotic treatment in patients with schizophrenia. *J. Clin. Psychiatry* 62 (2), 41–44.

Kaar, S. J., Natesan, S., McCutcheon, R., and Howes, O. D. (2019). Antipsychotics: mechanisms underlying clinical response and side-effects and novel treatment approaches based on pathophysiology. *Neuropharmacology* 172, 107704. doi:10.1016/j.neuropharm.2019.107704

Kemp, D. E., Correll, C. U., Tohen, M., Delbello, M. P., Ganocy, S. J., and Findling, R. L., (2013). Associations among obesity, acute weight gain, and response to treatment with olanzapine in adolescent schizophrenia. *J. Child. Adolesc. Psychopharmacol.* 23 (8), 522–530. doi:10.1089/cap.2012.0099

Kraus, T., Haack, M., Schuld, A., Hinze-Selch, D., Kühn, M., and Uhr, M., (1999). Body weight and leptin plasma levels during treatment with antipsychotic drugs. *Am. J. Psychiatry* 156 (2), 312–314. doi:10.1176/ajp.156.2.312

Leucht, S., Cipriani, A., Spineli, L., Mavridis, D., Orey, D., and Richter, F., (2013). Comparative efficacy and tolerability of 15 antipsychotic drugs in schizophrenia: a multiple-treatments meta-analysis. *Lancet* 382 (9896), 951–962. doi:10.1016/S0140-6736(13)60733-3

Li, S., Chen, D., Xiu, M., Li, J., and Zhang, X. Y. (2021). Diabetes mellitus, cognitive deficits and serum BDNF levels in chronic patients with schizophrenia: a case-control study. *J. Psychiatr. Res.* 134, 39–47. doi:10.1016/j.jpsychires.2020.12.035

Li, S., Gao, Y., Lv, H., Zhang, M., Wang, L., and Jiang, R., (2018). T(4) and waist:hip ratio as biomarkers of antipsychotic-induced weight gain in Han Chinese inpatients with schizophrenia. *Psychoneuroendocrinology* 88, 54–60. doi:10.1016/j.psyneuen.2017.11.010

Luckhoff, H., Phahladira, L., Scheffler, F., Asmal, L., Du Plessis, S., and Chiliza, B., (2019). Weight gain and metabolic change as predictors of symptom improvement in first-episode schizophrenia spectrum disorder patients treated over 12 months. *Schizophr. Res.* 206, 171–176. doi:10.1016/j.schres.2018.11.031

Mansur, R. B., Fries, G. R., Subramaniapillai, M., Frangou, S., De Felice, F. G., and Rasgon, N., (2018). Expression of dopamine signaling genes in the post-mortem brain of individuals with mental illnesses is moderated by body mass index and mediated by insulin signaling genes. *J. Psychiatr. Res.* 107, 128–135. doi:10.1016/j.jpsychires.2018.10.020

Mercer, L. P., Kelley, D. S., Humphries, L. L., and Dunn, J. D. (1994). Manipulation of central nervous system histamine or histaminergic receptors (H1) affects food intake in rats. *J. Nutr.* 124 (7), 1029–1036. doi:10.1093/jn/124.7.1029

Naslund, J. A., Aschbrenner, K. A., Scherer, E. A., Pratt, S. I., Wolfe, R. S., and Bartels, S. J. (2016). Lifestyle intervention for people with severe obesity and serious mental illness. *Am. J. Prev. Med.* 50 (2), 145–153. doi:10.1016/j.amepre.2015.07.012

Nasrallah, H. A. (2008). Atypical antipsychotic-induced metabolic side effects: insights from receptor-binding profiles. *Mol. Psychiatry* 13 (1), 27–35. doi:10.1038/sj.mp.4002066

Pillinger, T., McCutcheon, R. A., Vano, L., Mizuno, Y., Arumuham, A., and Hindley, G., (2020). Comparative effects of 18 antipsychotics on metabolic function in patients with schizophrenia, predictors of metabolic dysregulation, and association with psychopathology: a systematic review and network meta-analysis. *Lancet Psychiatry* 7 (1), 64–77. doi:10.1016/S2215-0366(19)30416-X

Raben, A. T., Marshe, V. S., Chintoh, A., Gorbovskaya, I., Müller, D. J., and Hahn, M. K. (2017). The complex relationship between antipsychotic-induced weight gain and therapeutic benefits: a systematic review and implications for treatment. *Front. Neurosci.* 11, 741. doi:10.3389/fnins.2017.00741

Raven, S. F. H., Hoebe, C., Vossen, A., Visser, L. G., Hautvast, J. L. A., and Roukens, A. H. E., (2020). Serological response to three alternative series of hepatitis B revaccination (Fendrix, Twinrix, and HBVaxPro-40) in healthy non-responders: a multicentre, open-label, randomised, controlled, superiority trial. *Lancet Infect. Dis.* 20 (1), 92–101. doi:10.1016/S1473-3099(19)30417-7

Sharma, E., Rao, N. P., and Venkatasubramanian, G. (2014). Association between antipsychotic-induced metabolic side-effects and clinical improvement: a review on the Evidence for "metabolic threshold. *Asian J. Psychiatr.* 8, 12–21. doi:10.1016/j.ajp.2013.11.017

Tiwari, A. K., Zhang, D., Pouget, J. G., Zai, C. C., Chowdhury, N. I., and Brandl, E. J., (2018). Impact of histamine receptors H1 and H3 polymorphisms on antipsychotic-induced weight gain. *World J. Biol. Psychiatry* 19 (3), S97-S105–S105. doi:10.1080/15622975.2016.1262061

Vázquez-Bourgon, J., Ortiz-García de la Foz, V., Gómez-Revuelta, M., Mayoral-van Son, J., Juncal-Ruiz, M., and Garrido-Torres, N., (2022). Aripiprazole and risperidone present comparable long-term metabolic profile; data from a pragmatic randomized controlled trial in drug-naïve first episode psychosis. *Int. J. Neuropsychopharmacol.* doi:10.1093/ijnp/pyac033

Venkatasubramanian, G., Chittiprol, S., Neelakantachar, N., Shetty, T., and Gangadhar, B. N. (2010). Effect of antipsychotic treatment on Insulin-like Growth Factor-1 and cortisol in schizophrenia: a longitudinal study. *Schizophr. Res.* 119 (1-3), 131–137. doi:10.1016/j.schres.2010.01.033

Verma, S., Liew, A., Subramaniam, M., and Poon, L. Y. (2009). Effect of treatment on weight gain and metabolic abnormalities in patients with first-episode psychosis. *Aust. N. Z. J. Psychiatry* 43 (9), 812–817. doi:10.1080/00048670903107609

Wang, K., Birring, S. S., Taylor, K., Fry, N. K., Hay, A. D., and Moore, M., (2014). Montelukast for postinfectious cough in adults: a double-blind randomised placebo-controlled trial. *Lancet Respir. Med.* 2 (1), 35–43. doi:10.1016/S2213-2600(13)70245-5

Wimms, A. J., Kelly, J. L., Turnbull, C. D., McMillan, A., Craig, S. E., and O'Reilly, J. F., (2020). Continuous positive airway pressure versus standard care for the treatment of people with mild obstructive sleep apnoea (MERGE): a multicentre, randomised controlled trial. *Lancet Respir. Med.* 8 (4), 349–358. doi:10.1016/S2213-2600(19)30402-3

Xiu, M. H., Li, Z., Chen, D. C., Chen, S., Curbo, M. E., and Wu, H. E., (2020). Interrelationships between BDNF, superoxide dismutase, and cognitive impairment in drug-naive first-episode patients with schizophrenia. *Schizophr. Bull.* 46, 1498–1510. doi:10.1093/schbul/sbaa062

Zhu, M. H., Liu, Z. J., Hu, Q. Y., Yang, J. Y., Jin, Y., and Zhu, N., (2022). Amisulpride augmentation therapy improves cognitive performance and psychopathology in clozapine-resistant treatment-refractory schizophrenia: a 12-week randomized, double-blind, placebo-controlled trial. *Mil. Med. Res.* 9 (1), 59. doi:10.1186/s40779-022-00420-0

Zipursky, R. B., Gu, H., Green, A. I., Perkins, D. O., Tohen, M. F., and McEvoy, J. P., (2005). Course and predictors of weight gain in people with first-episode psychosis treated with olanzapine or haloperidol. *Br. J. Psychiatry* 187, 537–543. doi:10.1192/bjp.187.6.537

Frontiers in Pharmacology

Explores the interactions between chemicals and living beings

The most cited journal in its field, which advances access to pharmacological discoveries to prevent and treat human disease.

Discover the latest Research Topics

See more →

Frontiers

Avenue du Tribunal-Fédéral 34
1005 Lausanne, Switzerland
frontiersin.org

Contact us

+41 (0)21 510 17 00
frontiersin.org/about/contact